OL.
7
59/60

THE INTERNATIONAL JOURNAL OF

Applied Radiation and Isotopes

Volume 7 1960

Editorial Board

P. C. AEBERSOLD
Washington

A. H. W. ATEN, Jr.
Amsterdam

M. BRUCER
Oak Ridge

J. COURSAGET
Saclay

V. N. KONDRATIEV
Moscow

M. MAGAT
Paris

B. MANOWITZ
New York

J. L. PUTMAN
Wantage

H. SELIGMAN
Vienna

Editorial Advisory Board

Austria
B. Karlik, Vienna

Argentina
E. E. Galloni, Buenos Aires

Belgium
Z. M. Bacq, Liége
P. C. Capron, Louvain

France
L. Bugnard, Paris
C. H. Fischer, Saclay
B. Goldschmidt, Paris
M. Haissinsky, Paris

Germany
H. Langendorff, Freiburg
M. Maier-Leibnitz, Munich
F. Strassmann, Mainz
F. Weygand, Berlin

Israel
I. Dostrovsky, Rehovoth

Italy
E. B. Chain, Rome
A. Perussia, Milan
G. Trabacchi, Rome

Japan
Masao Tsuzuki, Tokyo

Portugal
H. de Carvalho, Lisbon

Scandinavia
G. C. de Hevesy, Stockholm

Switzerland
H. H. Staub, Zürich

U.N.E.S.C.O.
P. Auger, Paris

United Kingdom and Commonwealth
J. S. Anderson, Victoria
R. H. Betts, Chalk River, Ontario
A. Charlesby, Shrivenham
Sir John Cockcroft, Cambridge
V. R. Khanolkar, Bombay
Sir Hans Krebs, Oxford
C. P. LeBlond, Montreal
D. R. Llewellyn, Auckland
A. S. McFarlane, London
Sir E. Rock Carling, London

U.S.A.
J. C. Bugher, New York
V. Conquest, Chicago
R. D. Evans, Cambridge
M. Harris, Spokane, Wash.
W. F. Libby, Los Angeles
W. B. Mann, Washington
H. F. Mark, New York
H. R. Nelson, Columbus, Ohio
S. Warren, Boston

U.S.S.R.
N. A. Bach, Moscow
G. M. Frank, Moscow
G. V. Kurdiumov, Moscow.

Pergamon Press New York • London • Paris • Los Angeles

CONTENTS OF VOLUME 7

NUMBER 1

W. S. Broecker, C. S. Tucek and E. A. Olson: Radio-carbon analysis of oceanic CO_2 1
Robert L. Bell and George J. Hertsch: Automatic contour scanner for myelography 19
Milton G. Crane, John E. Holloway, Ralph Adams and Ivor C. Woodward: The relative flow rates of red cells and plasma. Peripheral and central circulation studies in the dog 23
J. S. Robertson, V. P. Bond and E. P. Cronkite: Resolution and image spread in autoradiographs of tritium-labeled cells 33
R. A. Oppermann, R. F. Nystrom, W. O. Nelson and R. E. Brown: Use of tertiary alkyl primary C_{12}–C_{14} amines for the assay of $C^{14}O_2$ by liquid scintillation counting 38
Technical Notes
T. Fields, E. Kaplan and A. A. Imperato: Precision blood volume procedure using RIHSA 43
Henry Lanz and Mary Sue McCall: Nomogram for estimating tissue dose from internally deposited β-emitting radioisotopes 44
Book Reviews 46
Report of Meeting
International Atomic Energy Agency Conference on the Application of Large Radiation Sources in Industry and Especially to Chemical Processes, Warsaw, Poland, September, 1959 49
Forthcoming Papers 76

NUMBER 2

F. J. Domingues, K. J. Gildner, R. R. Baldwin and J. R. Lowry: An instrument and technique for the continuous measurement of respiratory CO_2 patterns in metabolic tracer studies 77
M. Anbar, S. Guttmann and Z. Lewitus: The mode of action of perchlorate ions on the iodine uptake of the thyroid gland 87
Milton G. Crane, John E. Holloway, Charles Sears, James McEachen and Ralph Adams: The effect of recirculation on the shape of the arterial concentration curve after an instantaneous injection of indicator . 97
N. M. Emanuel, Z. K. Maizus and L. G. Privalova: Use of the kinetic tracer method for investigations on the mechanism of *n*-decane liquid-phase oxidation 111
A. M. Brodsky, R. A. Kalinenko and K. P. Lavrovsky: On the kinetic isotope effect in cracking . . 118
S. M. Makin and A. E. Nunley: An autoradiographic method for determining the distribution of iron on recording tape 123
R. M. Black and A. Charlesby: The oxidation of irradiated polyethylene—I. Radio-oxidation . . . 126
R. M. Black and A. Charlesby: The oxidation of irradiated polyethylene—II. Thermal oxidation . . 134
D. J. Chleck and C. A. Ziegler: The preparation and some properties of radioactive quinol–krypton clathrate compounds 141
G. A. Ovezall-Klaasen and J. Halberstadt: The preparation of S^{35}- and/or Cl^{36}-labelled SO_2Cl_2. A simple technique for the quantitative preparation of micro- as well as macro-quantities 145
Technical Notes
M. Lubran and G. Corsini: The preparation and use of Br^{82}-labelled triolein and oleic acid 148
Emil Kleemann and Günter Herrmann: Abtrennung von Sb^{125} aus Sn^{113} durch galvanische Abscheidung des Antimons 149
N. A. Dyson and P. E. Francois: The preparation of potassium-43 using an interrupted cyclotron beam . 150
A. Bill, K. J. Öbrink and H. R. Ulfendahl: An easy way of calculating the composition of a two-component system from two-channel spectrometry 152
Letters to the Editors
M. A. Greenfield and Ismael Mena: Total-count technique for flow measurement 155
D. E. Hull: Reply to letter of 20 May from M. A. Greenfield and I. Mena 156
M. A. Greenfield and Ismael Mena: Reply to D. E. Hull's letter of 3 July 159
Book Reviews 160
Further abstracts of papers presented at the International Atomic Energy Agency Conference on the Application of Large Radiation Sources in Industry and Especially to Chemical Processes, Warsaw, Poland, September, 1959 163
Forthcoming Papers 168

NUMBER 3

I. P. Alimarin and G. N. Bilimovitch: The isotope dilution method and its application to analysis of inorganic substances 169
D. J. Chleck, F. J. Brousaides, W. Sullivan and C. A. Ziegler: Lithium aluminum tritide in active hydrogen analysis 182
Joel R. Gutmann: Use of the isotope effect in the study of heterogeneous catalytic reactions 186
E. A. Halevi: The secondary hydrogen isotope effect 192

VOL. 7 1959/

Joshua Jortner and Gabriel Stein: Hydrogen isotope effects in the photo- and radiation chemistry of aqueous solutions . . . 198
P. R. Hills, R. Roberts and M. W. Spindler: The radiation-induced synthesis of the insecticide "Gammexane" —I. Synthesis by ultra-violet light . . . 207
P. R. Hills, R. Roberts and M. W. Spindler: The radiation-induced synthesis of the insecticide "Gammexane" —II. Synthesis by high-energy radiation . . . 217
J. C. N. Wakeley, Brenda Moffatt, Ann Crook and J. R. Mallard: The distribution and radiation dosimetry of zinc-65 in the rat . . . 225
M. Lainé-Böszörményi, P. Fallot, J. Masson et P. Calvet: Étude de l'absorption digestive de l'eau chez les malades atteints de cirrhose du foie à l'aide de deux indicateurs de l'hydrogène . . . 233
J. F. Cameron and J. R. Rhodes: Beta-excited characteristic X-rays as energy reference sources . . . 244
A. R. G. Lang and S. G. Mason: A counter for solid samples containing labile tritium . . . 251
Technical Note
S. M. Makin: The use of irradiated extraction replicas to identify inclusions and precipitates in metals: A preliminary note . . . 258
Letter to the Editors
D. E. Hull: Tracing of water flow by means of radioactive isotopes and scintillation counters . . . 260

NUMBER 4

H. J. M. Bowen: Biological fractionation of isotopes . . . 261
George V. LeRoy, George T. Okita, Edward C. Tocus and Donald Charleston: Continuous measurement of specific activity of $C^{14}O_2$ in expired air . . . 273
Jeanne C. Bateman, Harry N. Carlton, Ralph C. Calvert and Gordon E. Lindenblad: Investigation of distribution and excretion of C^{14} tagged triethylene thiophosphoramide following injection by various routes . 287
Tien-Cheng Kao, Kuang-Chu Wang, Sheh-Fang Yang and Jui-San Chen: Iodine-131 thyroid uptake study of endemic goiter patients in Taiwan . . . 299
P. A. Osinski: Detection and determination of tritium labelled compounds on paper chromatograms . . . 306
M. L. Sazonov and L. A. Schwarzman: Use of radioactive isotopes of arsenic and niobium for investigations on metallurgical reactions . . . 311
P. Hayden and R. Roberts: The synthesis of non-random copolymers by the gamma irradiation of emulsion systems—II . . . 317
M. Lefort et X. Tarrago: Dosimétrie des rayonnements au moyen de matières plastiques—I . . . 323
Albert E. Johnson Jr. and Alvin S. Blum: Radioactive ion exchange surfaces, versatile radiation sources . 327
Technical Notes
A. H. W. Aten Jr. and A. C. Pieterse: Dose distribution of gamma radiation in cylindrical volumes of water 330
Torbjörn Westermark, Hans Lindroth and Bengt Enander: Isotope labelling by means of electrical gaseous discharges . . . 331
Book Reviews . . . 335

OL.
7
9/60

AUTHOR INDEX

Adams, Ralph 23, 97
Alimarin, I. P. 169
Anbar, M. 87
Aten Jr., A. H. W. 330
Baldwin, R. R. 77
Bateman, Jeanne C. 287
Bell, Robert L. 19
Bilimovitch, G. N. 169
Bill, A. 152
Black, R. M. 126, 134
Blum, Alvin S. 327
Bond, V. P. 33
Bowen, H. J. M. 261
Brodsky, A. M. 118
Broecker, W. S. 1
Brousaides, F. J. 182
Brown, R. E. 38
Calvert, Ralph C. 287
Calvet, P. 233
Cameron, J. F. 244
Carlton, Harry N. 287
Charlesby, A. 126, 134
Charleston, Donald 273
Chen, Jui-San 299
Chleck, D. J. 141, 182
Corsini, G. 148
Crane, Milton G. 23, 97
Cronkite, E. P. 33
Crook, Ann 225
Domingues, F. J. 77
Dyson, N. A. 150
Emanuel, N. M. 111
Enander, Bengt 331
Fallot, P. 233
Fields, T. 43
Francois, P. E. 150
Gildner, K. J. 77
Greenfield, M. A. 155, 159
Gutmann, Joel R. 186
Guttmann, S. 87
Halberstadt, J. 145
Halevi, E. A. 192
Hayden, P. 317
Herrmann, Günter 149
Hertsch, George J. 19
Hills, P. R. 207, 217
Holloway, John E. 23, 97
Hull, D. E. 156, 260
Imperato, A. A. 43
Johnson Jr., Albert E. 327
Jortner, Joshua 198
Kalinenko, R. A. 118
Kao, Tien-Cheng 299
Kaplan, E. 43
Kleemann, Emil 149
Lainé-Böszörményi, M. 233
Lang, A. R. G. 251
Lanz, Henry 44
Lavrovsky, K. P. 118
Lefort, M. 323
Leroy, George V. 273
Lewitus, Z. 87
Lindenblad, Gordon E. 287
Lindroth, Hans 331
Lowry, J. R. 77
Lubran, M. 148
McCall, Mary Sue 44
McEachen, James 97
Maizus, Z. K. 111
Makin, S. M. 123, 258
Mallard, J. R. 225
Mason, S. G. 251
Masson, J. 233
Mena, Ismael 155, 159
Moffatt, Brenda 225
Nelson, W. O. 38
Nunley, A. E. 123
Nystrom, R. F. 38
Öbrink, K. J. 152
Okita, George T. 273
Olson, E. A. 1
Oppermann, R. A. 38
Osinski, P. A. 306
Ovesall-Klaasen, G. A. 145
Pieterse, A. C. 330
Privalova, L. G. 111
Rhodes, J. R. 244
Roberts, R. 207, 217, 317
Robertson, J. S. 33
Sazonov, M. L. 311
Schwarzman, 311
Sears, Charles 97
Spindler, M. W. 207, 217
Stein, Gabriel 198
Sullivan, W. 182
Tarrago, X. 323
Tocus, Edward C. 273
Tucek, C. S. 1
Ulfendahl, H. R. 152
Wakeley, J. C. N. 225
Wang, Kuang-Chu 299
Westermark, Torbjörn 331
Woodward, Ivor C. 23
Yang, Sheh-Fang 299
Ziegler, C. A. 141, 182

VOL.
7
1959/6

International Journal of Applied Radiation and Isotopes, 1959, Vol. 7, pp. 1–18. Pergamon Press Ltd. Printed in Northern Ireland

Radio-carbon Analysis of Oceanic CO_2*

W. S. BROECKER, C. S. TUCEK,† and E. A. OLSON
Lamont Geological Observatory, Columbia University, Palisades, New York

(*Received* 18 *February* 1959)

Variations in the radio-carbon concentration of oceanic bicarbonate offer clues to large-scale ocean circulation patterns as well as to operation of the terrestrial CO_2 cycle. Samples for C^{14} analysis are processed aboard ship where CO_2 gas is stripped from 100 gal of acidified ocean water and absorbed in two small containers of KOH solution. In the laboratory the regenerated CO_2 is purified and its C^{14} activity is directly measured in one of two 5 l. gas proportional counters. These are surrounded by 1 in. of mercury and an anti-coincidence ring of 23 Geiger counters and are permanently mounted within an iron shield 8 in. thick. Backgrounds approximate 15 counts/min; net contemporary counts are about 30 and 60 counts/min at one and two atmospheres filling pressure. Each sample is counted for at least two 1000 min periods. The results, now representing over 100 deep and surface water samples, are expressed as per mil difference from a standard rather than in absolute units. For a given water mass, sample variations are consistent with those stemming from counting statistics alone (between 0·5 and 1·0 per cent). By mass spectrometrically analyzing the C^{13}/C^{12} ratio of the CO_2 assayed for radio-carbon, corrections are made for isotopic fractionation during shipboard processing of the samples.

MESURE DE LA RADIOACTIVITÉ DU C^{14} DANS LE BICARBONATE OCÉANIQUE

L'analyse des variations de la concentration du C^{14} dans le bicarbonate océanique est importante pour l'étude des grands courants de circulation océanique et celle du fonctionnement du cycle CO_2 terrestre. Le traitement des échantillons commence à bord du navire avec l'extraction du gaz CO_2 de 400 l. d'eau de mer acidifiée. Le gaz est ensuite transféré dans deux récipients contenant une solution de KOH. Le gaz CO_2 régénéré est purifié au laboratoire et sa radioactivité mesurée directement dans un des deux compteurs à gaz proportionnels de 5 l. Les compteurs sont entourés de 2,5 cm de mercure, d'un écran de 23 compteurs Geiger et d'un blindage de fer d'une épaisseur de 20 cm. L'activité résiduelle est d'environ 15 cpm. Les mesures nettes d'échantillons contemporains sont de 30 à 60 cpm sous une pression intérieure d' une à deux atmosphères. Chaque échantillon est mesuré pendant au moins deux périodes de 1000 min. Les résultats qui se rapportent à plus de cent échantillons d'eau de surface et de profondeur ne sont pas présentés en valeur absolue mais en millième d'une valeur arbitraire unique. Les variations des échantillons pour une quantité d'eau donnée sont compatibles avec les variations statistiques (entre 0,5 et 1,0 pour cent). Des analyses spectrométriques du rapport C^{13}/C^{12} dans les échantillons mesurés ont été effectuées afin de corriger les effets du fractionnement isotopique pendant le traitement des échantillons à bord du navire.

АНАЛИЗЫ РАДИОАКТИВНОГО УГЛЕРОДА В ОКЕАНСКОМ УГЛЕКИСЛОМ ГАЗЕ

Изменения в концентрации радиоактивного углерода в океанском бикарбонате дают нам представление о схеме океанской циркуляции большого масштаба и о ходе CO_2 цикла в земной коре.

Пробы, предназначенные для определения C^{14}, были обработаны в судне, а именно CO_2 каждой пробы объемом в 100 галлонов (378 литров) подкисленной океанской воды были извлечены и абсорбированы в двух маленьких сосудах с раствором KOH. Вновь освобожденный CO_2 был затем очищен в лаборатории и радиоактивность содержащегося в нем C^{14} была непосредственно определена в одном из двух пятилитровых газо-измери-

* Lamont contribution No. 359.

† Present address: Department of Physics, Bethel College, St. Paul, Minnesota.

телей. Последние, постоянно монтированные внутри восьмидюймовой железной плиты, окруженной однодюймовой оболочкой ртути, помещаются в противо-случайном кольце из 23 счетчиков Гейгера. На фоне примерно 15 срт локальной радиоактивности местности, чистые отсчеты во время измерения равнялись примерно 30 и 60 срт при соответственно одно- и двух-атмосферном давлениях заполнения. Каждая проба испытывалась в счетчике по меньшей мере в течении двух 1000 минут периодов. Результаты измерений в уже имеющихся свыше 100 пробах глубинных и поверхностных вод даны не в обсолютных единицах, а в тысячных долях стандарта. Вариации проб из конкретной массы воды соизмеримы с теми различиями, которые случаются уже в самих статистиках отсчетов (0,5–1,0%). При массовом спектральном определении соотношения C^{13} : C^{12} в CO_2, анализированном на радиоактивность, поправки внесены на изотопный распад, произшедший во время обработки проб в судне.

ANALYSE VON RADIOAKTIVEM KOHLENSTOFF IN OZEANISCHEM CO_2

Konzentrationsschwankungen von radioaktivem Kohlenstoff in ozeanischem Bikarbonat bieten Anhaltspunkte für das Schema der grossangelegten Ozeanzirkulation wie auch für den Ablauf des terrestrischen CO_2-Zyklus. Proben für die C^{14} Analyse wurden an Bord des Schiffes bearbeitet, wo CO_2-Gas aus 100 Gallon angesäuertem Ozeanwasser entzogen und in zwei kleine Behälter mit KOH-Lösung absorbiert wurde. Das regenerierte CO_2 wurde im Laboratorium gereinigt und seine C^{14}-Aktivität direkt in einem von den zwei zu 5 l. Gas proportionalen Zählern gemessen. Diese sind permanent innerhalb eines 8 in. dicken Eisenschildes aufmontiert und von einem inch Quecksilber und einem Anti-Koinzidenz-Ring von 23 Geigerzählern umgeben. Die NormAktivität ist um 15 cpm; Nettoablesungen während der Messungen sind ungefähr 30 und 60 cpm bei einem Fülldruck von einer und zwei Atmosphären. Jede Probe wurde mindestens zwei 1000-Min-Perioden lang gemessen. Die Resultate von nun über 100 Tief- und Oberflächenwasserproben sind als Promille-Unterschiede von einer Standardprobe anstatt in absoluten Einheiten ausgedrückt. Für eine gegebene Wassermenge stimmen die Mess-Schwankungen mit denen, die sich rein aus Statistiken entnehmen lassen, überein (zwischen 0,5 und 1,0 Prozent). Im Falle spektrometrischer Reihenanalysen, die das Verhältnis C^{13}/C^{12} des CO_2, welches auf radioaktiven Kohlenstoff untersucht wurde, bestimmten, wurden Korrekturen für den isotopischen Zerfall während der Bearbeitung der Proben an Bord des Schiffes vorgenommen.

VOL 7 1959/

INTRODUCTION

DATA on the C^{14} concentration in the dissolved bicarbonate of ocean water samples have proven valuable in understanding large scale circulation of the oceans and the operation of the CO_2 cycle.[1–5] In order to survey the variations of the C^{14}/C^{12} ratio in the Atlantic Ocean and adjacent seas, a system for the precise assay of oceanic CO_2 has been developed at the Lamont Geological Observatory. During the past 3 yr over 100 samples have been analyzed using the system described below.

The procedure used can be conveniently divided into four steps:

(1) shipboard release and collection of CO_2 from a sea water sample,

(2) laboratory purification of the CO_2 gas,

(3) assay of the C^{14} concentration in the CO_2 gas, and

(4) determination of the C^{13}/C^{12} ratio in the CO_2 gas for use in monitoring isotopic fractionation.

SHIPBOARD RELEASE AND COLLECTION OF SEA WATER CO_2

1. *Sample collection from depth*

Details of the method used to obtain sea water samples will be published separately in an oceanographic journal. In brief, a 100 gal barrel is lowered from the ship* along with the coring apparatus. Water continuously flushes through the barrel as it descends. When the desired depth has been

* Research vessel VEMA operated by the Lamont Geological Observatory under the direction of MAURICE EWING.

reached, the barrel is sealed off and raised back to the surface. Experiments with dyed water indicate that flushing is sufficiently rapid so that contamination from overlying water masses is negligible.

2. CO_2 *Release and absorption*

Once on deck the water sample is immediately transferred to a 165 gal polyvinyl chloride plastic tank (7 ft long × 2 ft diameter); the open space in the upper part of the tank together with two gas outlets at the top permits processing in rolling seas without liquid carry-over. Half the contents of a standard 9 lb bottle of concentrated sulfuric acid are added to the water in the tank. Such acidification drives the various carbonate equilibria toward the dissolved CO_2 state and thus makes possible complete removal of dissolved inorganic CO_2 regardless of whether it was initially as bicarbonate or carbonate ions. It then remains only to strip out the released CO_2 by bubbling a CO_2-free gas through the water and finally to reabsorb the extracted CO_2 in a KOH solution. Such a procedure obviates returning bulky 100 gal samples to the laboratory by transferring the CO_2 to convenient KOH containers, each the size of a quart milk bottle. Fig. 1, the flow sheet, shows the recovery equipment used.

3. *Quantity of* CO_2 *available per unit of sea water*

From data in SVERDRUP[6], the total concentration of CO_2 in all inorganic chemical forms is essentially uniform both as to depth and geographic distribution. This concentration is about 0·1 g of carbon (or 0·37 g of CO_2) per gal of sea water. Since the Lamont counters which measure C^{14} content are 5 l. in size, 2·5 g of carbon as CO_2 gas are needed for filling to one atmosphere pressure and twice this amount for two atmospheres pressure. Based on the latter amount, a minimum of 50 gal of water is needed. In practice, approximately 100 gal of water are treated for CO_2 removal in case the per cent recovery is lowered by adverse circumstances.

4. *Factors influencing per cent* CO_2 *recovery*

The per cent recovery obtained is influenced by a number of factors of varying importance:

(1) the amount of acid added to the water,
(2) the concentration, amount, and physical arrangement of the KOH absorbing solution, and
(3) the time and rate of flow of stripping gas.

These are considered in turn.

Acid added. At a pH of 4 or less, over 99 per cent of the CO_2 in sea water is present as molecular CO_2 or H_2CO_3. As such, it is subject to removal by bubbling a CO_2-free gas through the water. Although 65 g of acid are sufficient to achieve a pH of 3 in 100 gal of sea water, about 2000 g are routinely added. The difference between the theoretical and practical amounts results mainly from a desire to accelerate the CO_2 release as well as to assure that a sufficient amount of acid reaches every part of the water sample in a reasonable time. When distributed uniformly, the actual acid used brings the pH close to 1.

Concentration, amount, and physical arrangement of the KOH *absorbing solution.* Assuming, as before, 0·37 g of CO_2 per gal of sea water, a 100 gal sample would provide 37 g of CO_2, equivalent to 0·84 moles. When absorbed in KOH to form the carbonate, this CO_2 would require 1·68 moles of KOH. The problem, then, is to distribute this amount of KOH (plus excess) throughout the optimum quantity of water. Since the effects of gas flow rate and solution normality on absorption rates are not great enough to be significant in design of small-scale equipment,[7] the bubbler-type design specified here was essentially an arbitrary one. Normality was fixed at 8, and three 1 l. steel bubblers (see the inset in Fig. 1 for design), each half full of KOH solution, were arranged in series. With this arrangement there is more than enough KOH in the first bubbler to absorb all the CO_2 from a 100 gal sample. Experience has shown, however, that about 10 per cent of the CO_2 escapes the first bubbler and is picked up in the second. Since the third bubbler picks up essentially no CO_2, its use has been discontinued.

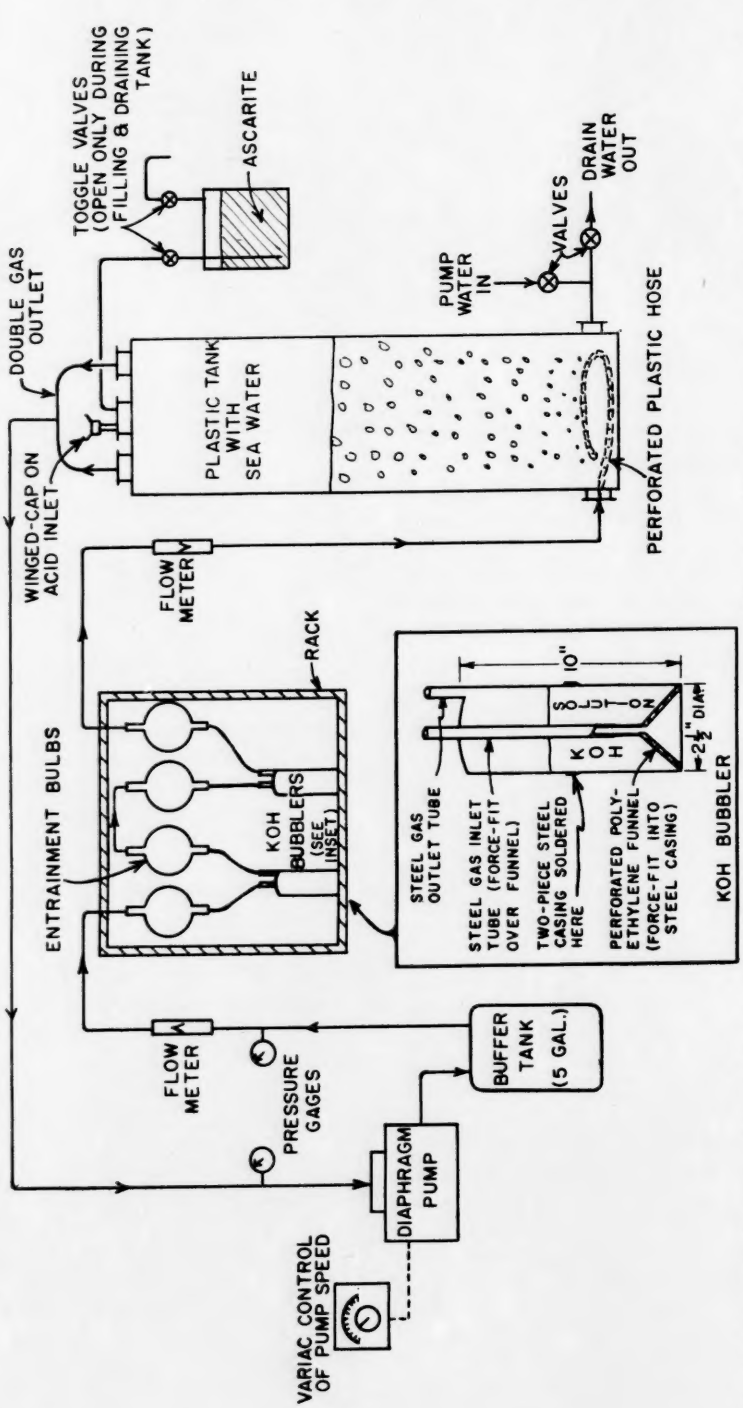

FIG. 1. Schematic diagram of the shipboard system for the release and collection of CO_2 from 100 gal ocean water samples. CO_2-free air is cycled through the acidified water. The CO_2 extracted from the water in each cycle is absorbed in the KOH bubblers.

VOL 7 1959/

Rate and time of flow of stripping gas. The rate at which stripping gas can be passed through a sea water sample is limited by the absorbing bubblers. At rates exceeding about 12 l. per min, carry-over of the KOH solution occurs. Hence, the flow is kept in the range of 10 l. per min. With this rate it has been found by experience that essentially all the CO_2 is removed from the sea water at the end of 3 hr. The total quantity of gas passed through the water is then 1800 l., which is about five times the open volume of the system. In other words, the recycled air carrying the CO_2 gas from the tank to the bubblers makes approximately five circuits in the course of processing one sample. Previous to the use of recycled air in a closed system, tank nitrogen was used as the stripping gas.

5. *Shipboard estimate of* CO_2 *recovery*

At the completion of a 3 hr run aboard ship, it is well to know whether the CO_2 recovered is sufficient for a radio-carbon measurement. This shipboard analysis is made by acidifying a small amount of bubbler KOH solution in a closed system of known volume; the CO_2 released causes a slight pressure rise that can be measured by a manometer filled with colored water. With an analyzer volume of 0·56 l. and withdrawal of 1 ml from the 500 ml KOH solution in a bubbler, the manometer deflection and the total quantity of bubbler CO_2 are approximately related by the equation: $Q = 0{\cdot}53M$ where Q is in grams and M is in centimeters. Since there is a thermal effect when acid neutralizes KOH, a blank of about 6 cm is obtained; this must be subtracted from each reading. Variations in the blank as well as practical problems resulting from ship movement limit the accuracy of the analysis. Checks between the CO_2 actually recovered in the Lamont laboratory and that expected from the shipboard analysis show that 6 out of 7 samples fall within ± 30 per cent of the analyzer predictions. Such accuracy is usually sufficient to enable detection of the faulty operating condition causing low CO_2 recovery.

6. *Sample contamination problems*

Because analyses of oceanic CO_2 are intended to show small differences in point-to-point C^{14} concentrations, it is essential that the CO_2 measured be without significant contamination. Two questions then arise:

(1) what is the critical level of contamination? and

(2) how can extraneous CO_2 be kept below this critical level?

The critical level of contamination. In determining the radio-carbon concentration of a CO_2 sample, the statistical uncertainty of radioactive decay together with certain other non-statistical variations sets a limit of $\pm 0{\cdot}5$ per cent on the measured activity. On the basis that systematic errors up to $\pm 0{\cdot}1$ per cent are tolerable, it is possible to calculate the maximum acceptable amount of contaminating radio-carbon and to equate this to corresponding amounts of CO_2 of given C^{14} concentrations. Since experience has shown that at least 13 g of CO_2 are collected in a bubbler containing 500 ml KOH solution, the equation relating maximum permissible CO_2 contamination and the C^{14} concentration of the contaminant is as follows:

$$W = \frac{0{\cdot}013}{|1 - R|}$$

where W is the maximum permissible weight in grams of CO_2 contamination per 500 ml KOH in one bubbler, R is the ratio of C^{14} concentration of contaminant to that of sample, and $|1 - R|$ is the absolute value of $(1 - R)$.

For the extreme case where $R = 0$ (i.e., a contaminant free of C^{14}) W is 13 mg. Measurements on CO_2 extracted from raw KOH yield C^{14}/C^{12} ratios about 75 per cent that in surface ocean water. Since any additional contamination would be atmospheric CO_2, $|1 - R|$ probably does not exceed 0·25. In this case 50 mg of CO_2 can be tolerated.

Keeping contamination below critical level. The following 6-step purification allows production of a solution meeting the requirement stated above:

(1) Make up a saturated KOH solution from distilled water and KOH pellets.

(2) Add about 10 g of $BaCl_2 \cdot 2H_2O$ (in solution form) per liter of KOH solution, precipitating $BaCO_3$.
(3) Filter off the precipitated $BaCO_3$, collecting the KOH solution in a vacuum flask. From this point on the solution is kept from atmospheric contact.
(4) Add H_2SO_4 in stoichiometric equivalence to the $BaCl_2$ added, precipitating any excess $BaCl_2$ as $BaSO_4$.
(5) After the solution sits for a day, decant and discard the bottom residue containing the $BaSO_4$ precipitate.
(6) Dilute to the desired normality with *boiled* distilled water.

Measurements of the residual CO_2 content of KOH prepared in this manner indicate that less than 50 mg are present in each bubbler.

Since the bubblers are stoppered and taped when not in use, contamination during use aboard ship is about the only possibility once the bubblers have left the laboratory. There are two potential sources of extraneous CO_2 during shipboard absorption of the ocean water CO_2: first, air in the open volume of the absorption system; and second, inward air leakage (during processing) at points of the system below atmospheric pressure. Since air contains approximately 0·6 mg of CO_2 per standard l. and since its C^{14} concentration is about 25 per cent higher than the ocean water sample with the lowest C^{14}/C^{12} ratio measured so far, it takes about 100 l. of air to exceed the critical limit set above. Because the open volume of the absorption system (about 350 l.) is large enough for the contained CO_2 to be significant, the air which enters the system during drainage of spent ocean water samples is filtered through Ascarite for CO_2 removal. As to air leakage during the processing of a sample, this is unlikely to occur since the only part of the system below atmospheric pressure is a continuous line from the top of the processing tank to the inlet of the circulating pump. For leakage to be important, a leak would have to let air in at 5 per cent of the stripping gas flow rate.

VOL. 7 1959/6

LABORATORY RECOVERY AND PURIFICATION OF CO_2

1. *Introduction*

Upon arrival at the Lamont radio-carbon laboratory, oceanic CO_2 is in the form of potassium carbonate dissolved in an excess of KOH solution. After release by acidification, the CO_2 is purified to the high degree required for C^{14} activity measurement in a gas proportional counter.

2. *Acidification*

The system for releasing CO_2 from KOH bubbler solutions is shown in Fig. 2. In order to minimize gaseous contamination, an acid of low volatility (H_3PO_4) is used to neutralize the solution. After evacuation of the system, acid (50% by volume) is slowly added to the sample, CO_2 escaping as soon as the excess KOH is neutralized. The CO_2 passes through a condenser to remove part of its moisture, then through finely granular magnesium perchlorate to take out the remainder. It is frozen out in glass traps which are immersed in Dewar flasks filled with liquid nitrogen. An additional passage through magnesium perchlorate precedes the final purification. At this point, it may be well to state that all movements of CO_2 gas are made by evaporation of dry ice either into evacuated bulbs or into freeze-out traps cooled by liquid nitrogen. Various purifying columns can then be placed at intermediate positions along the flow path.

3. *Final purification*

With respect to its counting characteristics in a gas proportional counter, carbon dioxide is extremely sensitive to even minute amounts of so-called electronegative impurities—specifically, water vapor, oxygen, nitrogen oxides, sulfur dioxide, and halogens.[8] Inside the counter these impurities pick up secondary electrons produced by the β-particles which are ejected in C^{14} decay; the sluggish heavy ions formed lengthen the pulses received at the counter center wire, sometimes reducing the pulse height enough to prevent detection. According to DeVries[8] and Fergusson[9] the toleration limit for oxygen is 1 p.p.m., while Fergusson sets 0·1 p.p.m. as the limit for chlorine. In addition, radioactive radon-222 may occasionally be present as an impurity.

In order to remove residual trace impurities the general method of DeVries and Barendsen[10] and of Rafter[11] is used. This involves reacting the CO_2

with radium-free* CaO at about 700°C, cooling the $CaCO_3$ so formed down to 450°C, and pumping away the non-reacting gaseous impurities present in the solid interstices. After an hour of pumping, the absolute pressure is below 1 μ. The reverse procedure is then employed to release the CO_2—namely, the temperature is raised to about 900°C, and the regenerated CO_2 is collected in a trap cooled by liquid nitrogen. Clean-up of the calcium oxide is made at 1000°C. Under such temperature and vacuum conditions, it is necessary to use quartz tubes to hold the calcium oxide. Fig. 3 shows the purification system diagrammatically.

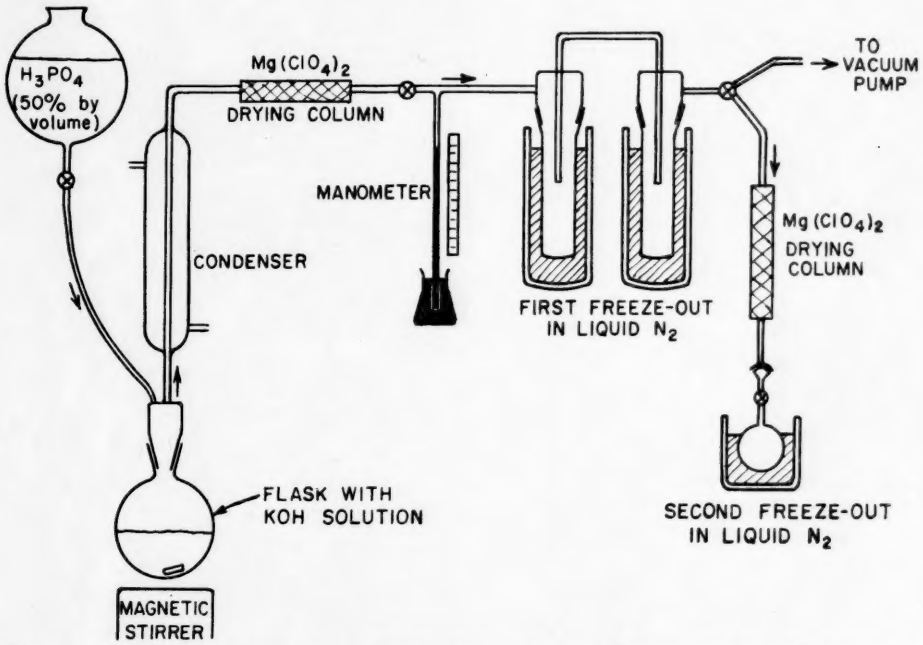

FIG. 2. Schematic diagram of the system used to release and dry the CO_2 absorbed in a KOH solution.

4. *Handling of related organic samples*

Living marine samples are often useful as independent checks of the radio-carbon activity of dissolved oceanic bicarbonate. So far, only plankton and mollusks have been analyzed, but there is no reason why kelp, starfish and other underwater organisms will not prove useful in the future.

From the standpoint of laboratory handling, living samples fall into two categories—calcium carbonate hard parts and soft organic tissue. Since the first is converted to CO_2 in the same acidification procedure used with KOH solutions, nothing more need be said. However, CO_2 from organic tissue is produced by a combustion process which is described below. In many ways it is similar to the methods of DEVRIES and BARENDSEN[10] and of RAFTER.[11]

In brief, the oven-dried organic material is burned in a stream of tank oxygen and the combustion products are sent through several solid and liquid purifying reagents before the semi-pure CO_2 is frozen out in liquid nitrogen. Final purification is then made on the calcium oxide furnace—as described above.

Fig. 4 shows the combustion–purification train in diagrammatic fashion. For maximum yield of CO_2, the burning is in two stages: the first stage involves thermally volatilizing certain combustible sample components within a nitrogen atmosphere, moving these products out the $\frac{1}{8}$ in. diameter hole in the end of the Vycor sample tube, and igniting the combustibles in the oxygen atmosphere outside the tip of

* By trial and error, it is possible to find a commercial brand of reagent-grade $CaCO_3$ which will be sufficiently radium-free to introduce insignificant radon contamination into the purified CO_2 gas. If storage facilities are available, however, CO_2 samples with radon contamination can be stored for several weeks prior to counting so that the radon-222 (3·8 day half-life) can decay away. $CaCO_3$ is decomposed to CaO before it is placed in the quartz tubes.

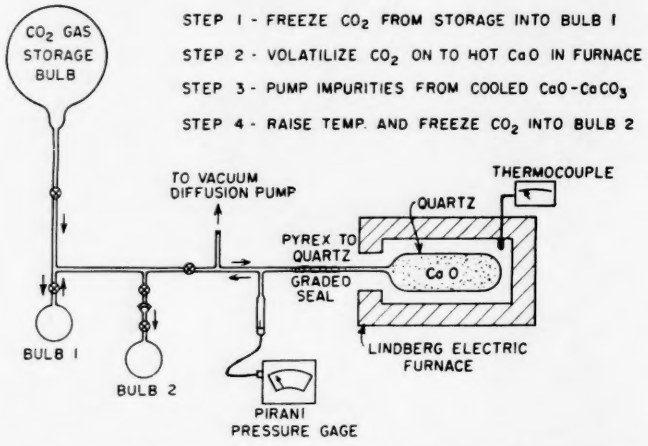
CO_2 GAS STORAGE BULB
STEP 1 - FREEZE CO_2 FROM STORAGE INTO BULB 1
STEP 2 - VOLATILIZE CO_2 ON TO HOT CaO IN FURNACE
STEP 3 - PUMP IMPURITIES FROM COOLED $CaO-CaCO_3$
STEP 4 - RAISE TEMP. AND FREEZE CO_2 INTO BULB 2
TO VACUUM DIFFUSION PUMP
THERMOCOUPLE
QUARTZ
PYREX TO QUARTZ
GRADED SEAL
CaO
BULB 1
BULB 2
LINDBERG ELECTRIC FURNACE
PIRANI PRESSURE GAGE

FIG. 3. Schematic diagram of the system used to ultrapurify CO_2 gas. The CO_2 is absorbed on CaO as $CaCO_3$, and then after pumping away gas phase impurities the $CaCO_3$ is thermally decomposed, releasing the purified CO_2.

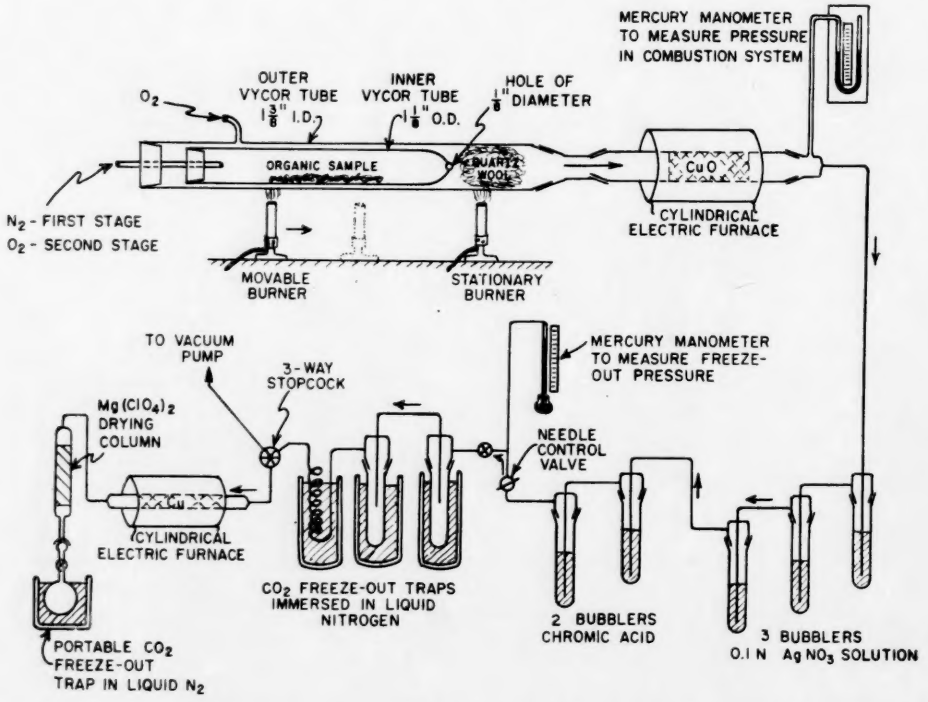

FIG. 4. Schematic diagram of the system used to convert the carbon of organic materials into CO_2 gas. The two-stage combustion process involves (1) burning over the quartz wool of volatile organic materials which are driven off the nitrogen-blanketed sample and (2) burning of the charred sample in place. Impurities such as CO, HCl, SO_2, O_2, N_2, NO, NO_2 and H_2O are removed by the purification train.

VOL. 7 1959/6

the tube; the second stage occurs when all the volatiles have been driven off and simply involves direct burning of the charred sample remains in the inner sample tube. If burning were carried out inside the sample tube from the very beginning, tarry products would be carried beyond the burning tube and their carbon lost to combustion. The consequent yield loss and clean-up would be undesirable.

After several tries, a physical arrangement providing immediate ignition of the stage-one volatiles has been obtained. The size of the outer Vycor tube (now $1\frac{3}{8}$ in. i.d.) has been decreased so as to approach that of the inner sample tube ($1\frac{1}{8}$ in. o.d.); this has permitted the bunsen burner to maintain all parts of the quartz wool igniter at high temperature, thereby igniting the first combustibles that come through. From then on until the first stage is finished, burning occurs in a flame outside the tip of the inner tube.

The combustion gas consists primarily of CO_2 and water vapor along with an excess of oxygen. During the first burning stage a little nitrogen is also present; it is added slowly to maintain the inert atmosphere within the sample tube. In addition to these major constituents, there are small amounts of gaseous products of the minor organic elements—namely, SO_2, NO_2 and halogen compounds. If any carbon monoxide is present, it is oxidized to CO_2 in the hot (about 500°C) cupric oxide which follows the combustion tube. Further on in the train are three bubblers filled with 0·1N $AgNO_3$ solution for removal of halogen compounds. Then come two bubblers with standard laboratory cleaning solution (concentrated H_2SO_4 plus $K_2Cr_2O_7$), the purpose of which is two-fold:

(1) oxidation of SO_2 to SO_3 and subsequent absorption and
(2) removal of water vapor.

Thus, when the gas stream leaves the last bubbler it consists of CO_2, excess oxygen, nitrogen during stage 1, and a small amount of NO_2. If the partial pressure of oxygen is kept below 12 cm absolute, it is possible to freeze the CO_2 out at liquid nitrogen temperature without also condensing the oxygen. Thus the excess oxygen, together with any nitrogen, is continuously pumped out through the vacuum pump during the burning process. By proper adjustment of the needle valve just before the freeze-out traps, the low freeze-out pressure is maintained while the system before the needle valve is held close to atmospheric pressure.

Since NO_2 freezes out with CO_2, its removal must be carried out at the end of the burning. After the freeze-out traps are isolated by shutting off the needle valve, the solid CO_2 is evaporated and sent through a tube of hot copper filings, the NO_2 being reduced to nitrogen gas. Any excess oxygen that was occluded within the dry ice is also picked up by the hot copper. After passing through a drying column of magnesium perchlorate which follows the hot copper, the CO_2 is ready for ultra-purification on calcium oxide and then for measurement of C^{14} activity.

RADIO-CARBON ASSAY OF CO_2 GAS

1. *Equipment design*

Radio-carbon analyses are made in one of two identical 5 l. proportional counters mounted permanently in an iron shield 8 in. thick. As shown in Fig. 5 the counters are closely surrounded by 1 in. of mercury housed in a figure-eight shaped iron container. This, in turn, is surrounded by a ring of twenty-three 2 in. diameter commercial Geiger counters (with internal quench) operated in anticoincidence with the sample counters.[12]

The counters are constructed of copper. The tungsten center wire (1 mil diameter) is electrically insulated from the ends of the counter by double glass-to-kovar seals of the type originally used by HAGEMANN of the Argonne National Laboratories. Since the major portion of the voltage is applied to the counter shell, each counter is housed in a polystyrene tube which electrically isolates it from the mercury shield. Fig. 6 is a diagram of one of the counters.

From a vacuum system mounted on the side of the shield the counters are filled with CO_2 gas to a pressure of either one or two atmospheres. Pressure is measured with a mercury manometer readable to the nearest millimeter; at the time of filling the shield temperature is recorded to the nearest 0·2°C. With these two measurements, the relative amount of carbon dioxide in the counter is precisely known. Twenty-four pairs of 5 l. bulbs connected to the filling system provide convenient storage of purified samples.

The electronic equipment used in conjunction with the counters was designed and constructed at the Lamont Laboratory under the direction of R. JANES. A block diagram of the system is shown in Fig. 7. The power for all the units is supplied by one master

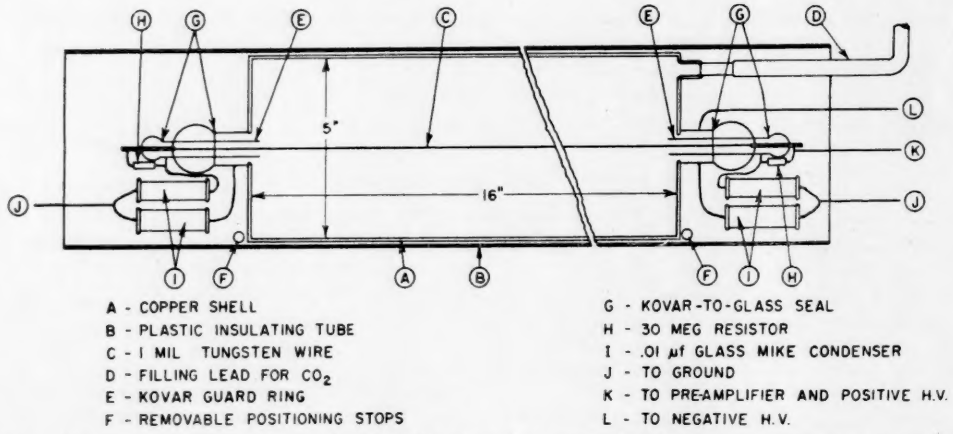
5"
16"
A - COPPER SHELL
B - PLASTIC INSULATING TUBE
C - 1 MIL TUNGSTEN WIRE
D - FILLING LEAD FOR CO_2
E - KOVAR GUARD RING
F - REMOVABLE POSITIONING STOPS
G - KOVAR-TO-GLASS SEAL
H - 30 MEG RESISTOR
I - .01 μf GLASS MIKE CONDENSER
J - TO GROUND
K - TO PRE-AMPLIFIER AND POSITIVE H.V.
L - TO NEGATIVE H.V.

FIG. 6. Diagram showing the constructional details of the 5 l. proportional counters used for the C^{14} assay.

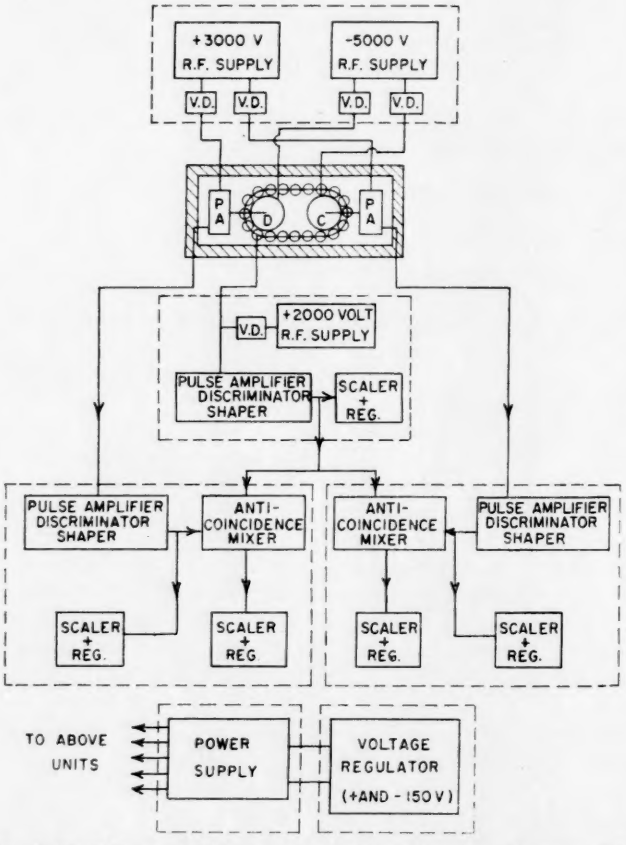

FIG. 7. Block diagram of the electronics used in conjunction with the two 5 l. proportional counters (labelled and C D). V.D. stands for voltage divider, P.A. for preamplifier, and REG. for counting register.

VOL. 7 1959/6

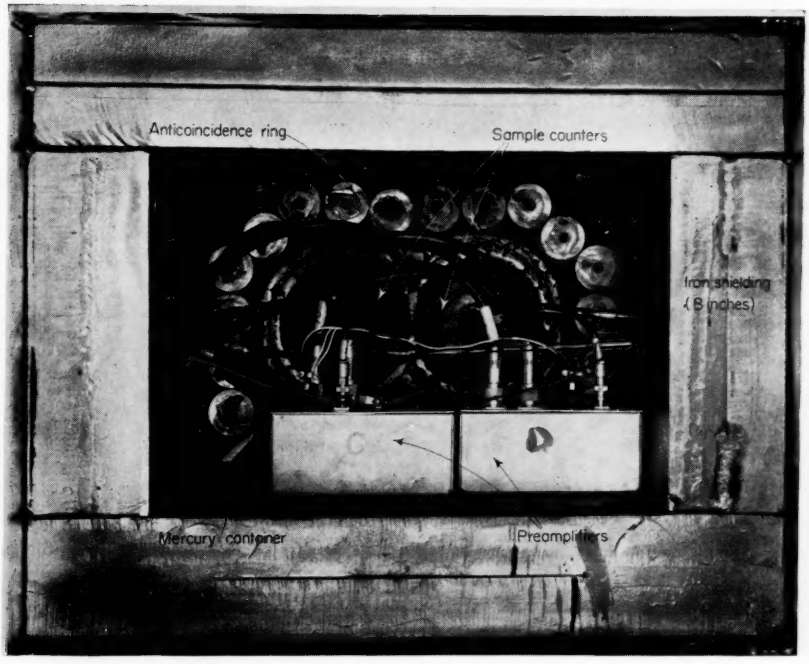

FIG. 5. Photograph of the interior of the shield which contains the two 5 l. proportional counters. The iron and mercury shielding minimize γ-ray background, while the ring of permanent Geiger counters essentially eliminates meson background.

OL.
7
9/60

VOL.
7
1959/

unit which provides the filament voltages as well as the regulated plus and minus 150 V plate voltages. The two R.F. high voltage supplies can feed as much as 8000 V independently to each counter; minus 5000 to the shell and plus 3000 to the center wire. With the amplification system now in use, pulses as small as 1 mV are recorded. Registers total up the counts both before and after mixing with the pulses from the permanent ring and also the total counts from the permanent ring itself. The electronic system has proven workable and reliable over 3 yr of operation.

2. *Counter characteristics*

The characteristics of the counters are summarized in Table 1. Energy spectrum analyses suggest a detection efficiency of greater than 95 per cent for the active portion* of the counter. Using this rather crude calibration a specific activity of 13·4 ± 0·5 counts/min is obtained for age-corrected 1890 wood grown on the Lamont grounds. In Table 2 this result is compared to those published by other workers.

Approximately half of the residual background in the counters results from the nucleonic component of cosmic rays. As pointed out by DeVries[16] and by Fergusson and McCallum[15] this component of the background varies significantly with time, largely as a result of the variation in the thickness of the atmospheric absorber. Since the meson flux also varies with atmospheric pressure, it can be used as an approximate index of the total change in the background. Fig. 8 is a plot of background measurements versus average meson flux during the time of measurement. Covering a 1 yr period, the data are from one counter (D) operated at one atmosphere pressure; each point represents about 1000 min of counting. The slope of the best line through the points indicates a background rise of about 0·06 count/min per unit increase in the meson

Table 1

Counter	Pressure (atm.)	Moles CO_2	Half sensitivity voltage	Operating voltage	Length of plateau (V)	Background unshielded	Background shielded	Meson count rate	1890 Wood net count rate	Background variation counts/min bgd. / counts/min meson	Plateau slope at operating voltage (for C^{14})
C	1	0·20	3200	4000	300	1000	15	430	31	0·06	1%/100 V
C	2	0·40	4300	5300	400	1000	17	430	62	0·06	1%/100 V
D	1	0·20	3200	4000	300	1000	11	430	31	0·06	1%/100 V
D	2	0·40	4300	5300	400	1000	13	430	62	0·06	1%/100 V

Table 2

	Material	Method of standard calibration	dpm / g	dpm† / g
Libby[12]	recent woods	absolute counting	15·3 ± 0·1	15·6
Hayes *et al.*[14]	*p*-cymene	mass spectrometer and half life‡	13·6 ± 0·2	13·9
Suess[13]	pre-1900 woods	mass spectrometer* and half life‡	14·7 ± 0·4	14·7
Fergusson[9]	recent woods	absolute counting	12·5 ± 0·2	12·8
This paper	1890 wood	absolute counting	13·4 ± 0·5	13·4

* Using standard of known C^{14} content (by weight) supplied by the U.S. National Bureau of Standards.

† Corrected for the Suess effect (i.e. dilution of the atmosphere due to industrial CO_2); the corrections were arbitrarily applied by the present authors assuming a 2·5 per cent reduction in C^{14} activity for the three cases where recently grown organics were used.

‡ 5568 yr.

* That portion defined by the cylindrical wall of the counter and planes perpendicular to the center wire at its ends

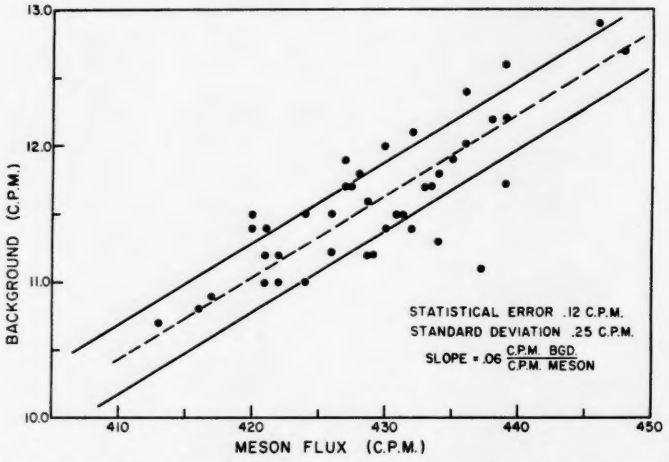

FIG. 8. Plot of background versus meson count rate for individual overnight runs in counter D. All backgrounds within a 1 yr period are included. Much of the variation in both the meson and background count rates results from variation in the thickness of the atmospheric absorber, as reflected by barometric pressure.

flux. If each background measurement plotted in Fig. 8 is corrected to a fixed meson flux on the basis of the 0·06 slope, the standard deviation of the corrected backgrounds is only twice what would be expected on the basis of counting statistics alone. Table 3 illustrates how useful such correction can be during periods when atmospheric pressure fluctuates widely.

3. *Counting procedure*

The normal counting procedure is as follows. The counters are filled each morning. Check counts at voltages corresponding to one-third and two-thirds full sensitivity are made using a Co^{60} γ-ray source inserted into the iron shield. These check counts will deviate from their normal value if the sample gas is slightly impure or if the electronic

VOL. 7 1959/

TABLE 3. Correction for background variation: 1890 oak sample

Counter C 2 atm. CO_2

Date (1956)	Sample + background (counts/min)	Meson flux (counts/min)	Co^{60} rate (counts/min)	Corrected* sample + background (counts/min)
3/16	77·7 ± 0·3	453	4488	75·6
3/17	76·8 ± 0·3	446	—	75·4
3/21	74·2 ± 0·3	421	4430	75·0
3/26	75·3 ± 0·3	433	4400	75·0
4/2	75·3 ± 0·3	426	4433	75·6
4/7	76·2 ± 0·3	443	4445	75·0
			average	75·3
			standard deviation	0·3

* 1 per cent meson change = 1·6 per cent change in background (background = 17 counts/min).

sensitivity or voltage output has changed. If the checkpoint count rates deviate by more than 10 per cent from their normal values, an investigation is made to determine the cause of the shift. If it is caused by gas impurity, the sample is repurified on the CaO furnace. The variation in counter detection sufficiently pure and the electronics are operating properly, the slope of the plateau is checked by making 60 min counts 100 V above and below the normal operating voltage. A check is then made with the counter voltage off in order to determine that no spurious noise is present.

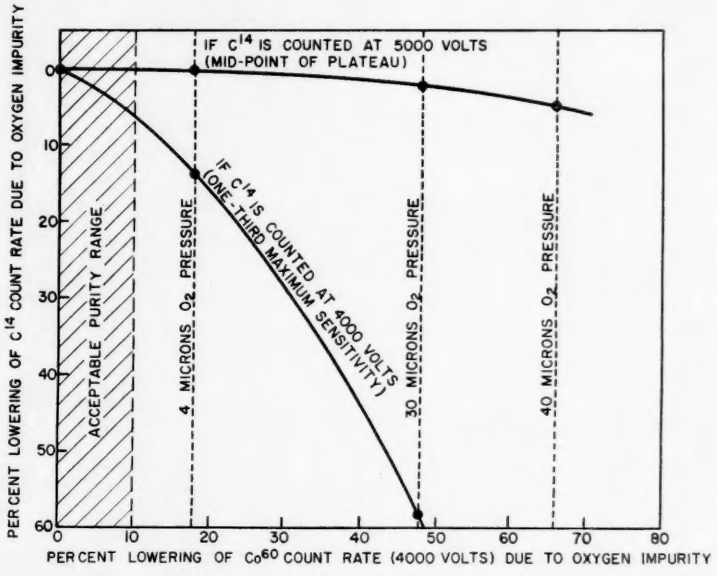

FIG. 9. Graph showing the effect of electronegative impurities (specifically oxygen) on the sensitivity of a 0·5 l. proportional counter filled to 2 atmospheres with CO_2 gas. As would be expected, small amounts of O_2 produce large decreases in the efficiency of C^{14} detection at a point on the rise to the plateau, whereas only small changes in efficiency occur at the mid-point of the plateau. By monitoring the count rate from a Co^{60} source at a voltage on the rise to the plateau, a sensitive check on the purity of a sample can rapidly be made.

efficiency caused by electro-negative gas impurities is illustrated in Fig. 9. If oxygen to a pressure of 30 μ is deliberately added to a pure CO_2 sample and the counter voltage is set at 4000 V (i.e. the lower curve representing the rise before the counting plateau), the sensitivity will be lowered by 53 per cent in the case of sample C^{14} β-particles and by 47 per cent in the case of γ-rays from the Co^{60} source. When the voltage is raised to the plateau mid-point value of 5000 V, the sensitivity to C^{14} β-particles will be only 2 per cent lower than for a pure CO_2 sample (see upper curve).

Once it is established that a sample is sufficiently pure and the electronics are operating properly, the slope of the plateau is checked by making 60 min counts 100 V above and below the normal operating voltage. A check is then made with the counter voltage off in order to determine that no spurious noise is present.

After the checks have been completed, the sample is counted until the following morning, a period of about 1000 min. Each sample is counted for at least two overnight periods spaced at least 4 days apart. When the measurements have been completed, a small portion of the CO_2 gas is put aside for measurement of the C^{13}/C^{12} ratio; the remainder is absorbed in NH_4OH and precipitated as $CaCO_3$ for storage.

Since the range of C^{14}/C^{12} ratios in samples of dissolved bicarbonate from the Atlantic Ocean and adjacent seas is only 15 per cent, the highest accuracy can be obtained by a direct comparison of the sample activity

with that of a standard of similar activity. The latter is counted once every 4–7 days. During the first year of operation 1938 Oak wood (L-313) was used as a standard, during the next two years 1890 Oak wood (L-314) was used and since early in 1958 the National Bureau of Standards oxalic acid standard (L-456) has been used. These three standards have been carefully intercalibrated.

4. *Form of results*

The results are ultimately expressed as per mil differences from a standard; the exact expression is as follows:

$$\delta C^{14} = \left[\frac{A^*_{\text{sample}} - 0{\cdot}950A^0_{\text{standard}}}{0{\cdot}950A^0_{\text{standard}}}\right] \times 1000$$

where A^*_{sample} is the net C^{14} activity of the sample corrected for radioactive decay between the time of collection (or formation) and measurement and A^0_{standard} is the net C^{14} activity of the National Bureau of Standards oxalic acid standard corrected for radioactive decay between 1 January, 1958 and the time of measurement. The factor of 0·950 is a defined constant introduced to place the zero on the δC^{14} scale close to the value of 19th century wood samples.[17]

5. *Sources of errors*

The major potential sources of error in δC^{14} results are:

(1) statistical error in counting,
(2) non-statistical variations in background,
(3) counting efficiency variations,
(4) the presence of radon in the CO_2 gas and
(5) isotopic fractionation during the processing of the sample.

Statistics. The statistical error is the dominant one. For a single 1000 min run the error in δC^{14} is 7·5 per mil (0·75 per cent) for runs at one atmosphere pressure, and 5·2 per mil for runs at two atmospheres. In the calculation of these errors, the count rate error for the standard is obtained by averaging four 1000 min counts. The statistical uncertainty in the background average turns out to be negligible even if only a single background count is made.

Background. Although the non-statistical variations in background count rate exceed the statistical deviations in some cases, the meson correction described previously reduces the deviations to the point where they are not significant.

Efficiency. Errors related to variation in counter efficiency are also small compared to the statistical error. The Co^{60} check allows close duplication of conditions from run to run, assuring reproducibility of the plateau position to within 20 V. Since the plateau slope in the region of the counting voltage is about 10 per mil per 100 V, changes in efficiency introduce errors of no more than 2 per mil.

Radon. Although radon has been observed in some samples prepared from marine shell, in dissolved ocean bicarbonate samples it has been below detectability in every case but one. Currently the presence of radon α-activity is checked for daily by a 50 min count at a voltage low enough that C^{14} β-particles are not recorded.

Fractionation. Whenever recovery is below 100 per cent in physical processes such as extraction and absorption, there exists the possibility of isotopic fractionation. Here, specifically, the problem arises in releasing and absorbing oceanic CO_2. Although the actual per cent recovery of CO_2 from ocean water is not measured directly, it is certainly not 100 per cent and may often be less than 50 per cent. In addition, the radio-carbon assay is almost always made on CO_2 from the first KOH bubbler, the second being used only if the first provides insufficient CO_2. Small amounts of isotopic fractionation are thus to be expected, and indeed occur—as shown in Fig. 10. Fortunately, it is possible to correct for isotopic fractionation through a mass spectrometric measurement of the sample C^{13}/C^{12} ratio. The details of this correction—called normalization—are discussed later. Even without normalization, however, fractionation of C^{14} introduces an average δC^{14} error of only 4 per mil.

Although the standard deviation of the several counts on the same sample is unaffected by fractionation effects and non-radioactive gas impurities, radon contamination, background variation, and electronic

VOL. 7 1959/

shifts can introduce non-statistical variations in count rate, causing the standard deviation to exceed that predicted from counting statistics. That such non-statistical effects are almost insignificant is indicated by the following two facts of experience:

(1) the average of the standard deviations* of 90 samples run at one atmosphere pressure is 7·1 per mil compared to the statistical error of 7·5 per mil and

(2) the similar average for 30 two atmosphere samples is 5·6 per mil compared to the statistical error of 5·2 per mil.

Therefore, if there exist errors of a magnitude comparable to or greater than the statistical error, they are of a type which do not produce a spread in repeated counting analyses. Further evidence that such errors are small is presented below in the section dealing with the consistency of results on samples from the same ocean water mass.

Since replicate measurements reduce uncertainty, the error quoted on a given analysis is computed as follows. If the standard deviation of the several measurements *exceeds* 10 per mil, it is divided by the square root of the number of measurements. If the standard deviation is *less than* 10 per mil, 10 per mil is divided by the square root of the number of measurements. Thus, the errors are computed in a conservative manner. In no case has an error of less than 5 per mil been quoted.

6. C^{13} *Analysis*

As pointed out in the previous section, the stable isotope ratio in the sample carbon is needed to correct for isotopic fractionation. Using a portion of the CO_2 gas previously assayed for radio-carbon, the C^{13}/C^{12} measurement is made in a double-collecting mass spectrometer made by the Consolidated Engineering Corporation (Model 401). Although the details of the measurement procedure have been described by AULT[18], a brief description is given here.

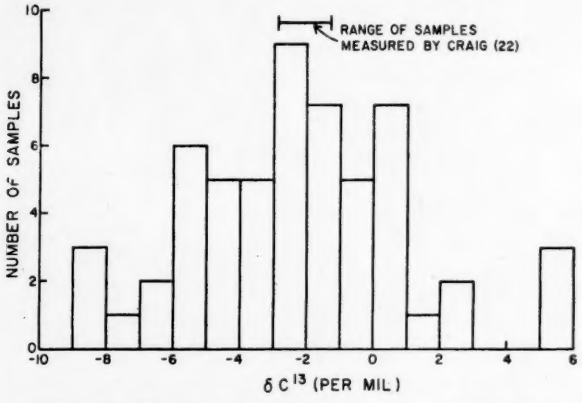

FIG. 10. Histogram of the δC^{13} results on samples of CO_2 gas prepared from oceanic bicarbonate. Since the results show a larger spread than the 5 samples measured by CRAIG[21], it appears that isotope fractionation occurs during the shipboard processing of the samples. The resultant changes in the sample C^{14}/C^{12} ratios are corrected for by normalizing the results to a common C^{13}/C^{12} ratio.

Since CO_2 is analyzed rather than carbon, the mass ratio 45/44 is measured. Instead of a direct absolute measurement, the sample is compared to a standard (tank CO_2) of known C^{13}/C^{12} ratio. For each sample 5 standard and 4 sample measurements are made in an alternate sequence, the entire procedure requiring about 1 hr. The tank

* Each standard deviation is based on two or more individual 1000 min counts on the same sample.

CO_2 standard has been carefully calibrated against the U.S. National Bureau of Standards Solenhofen limestone standard. Since CRAIG's work[19] has shown that there is a 1·1 per mil difference between the N.B.S. standard and his Belemnite standard, the Lamont results can be expressed on CRAIG's δC^{18} scale. This is defined as follows:

$$\delta C^{13} = \left[\frac{R_{\text{sample}} - R_{\text{belemnite}}}{R_{\text{belemnite}}}\right] \times 1000$$

where R stands for C^{13}/C^{12} ratio. The precision of the C^{13}/C^{12} measurements is about 0·5 per mil. Since an uncertainty exists in the isotope composition of the oxygen in the CO_2 analyzed, the results are probably good to only about 1 per mil.[20]

The δC^{13} values for ocean water bicarbonate analyzed to date are summarized in the histogram of Fig. 10, showing that both enrichment and depletion of C^{13} do occur. Comparison of the δC^{13} results with the bubbler distribution ratio (the ratio of CO_2 absorbed in the first bubbler to that in the second) on the same sample indicates that when this ratio is greater than 10 δC^{13} lies close to the range found by CRAIG[21], who made precise δC^{13} measurements on 5 Atlantic Ocean water samples. For distribution ratios between 1 and 2, however, CO_2 from the first bubbler is significantly fractionated, having a more negative δC^{13} value. This is consistent with the fractionation observed by CRAIG[20] in samples of CO_2 absorbed from the atmosphere by open trays of basic solution. C^{12} is preferentially absorbed in both cases.

In order to eliminate differences introduced by fractionation, the results are normalized to a common C^{13}/C^{12} ratio. The normalization equation is as follows:

$$\Delta C^{14} = \delta C^{14} - 2\delta C^{13}\left[1 + \frac{\delta C^{14}}{1000}\right] - 50{\cdot}0$$

where δC^{14} and δC^{13} are defined as above and the constant factor (−50·0) is introduced in order to place the zero on the scale at a convenient point. Details of the above equation are given elsewhere.[17]

TABLE 4. Reproducibility of results from same ocean water mass

Lamont no.	Collection date	Measurement date	δC^{14}
North Atlantic surface water			
326A	10/55	8/56	−9 ± 7
326B	11/55	5/56	−5 ± 6
326C	11/55	3/56	+4 ± 6
326D	11/55	5/56	+5 ± 6
326E	11/55	5/56	+6 ± 5
326F	11/55	3/56	+14 ± 7
326G	11/55	3/56	+10 ± 10
326H	11/55	3/56	+8 ± 5
		average = +4·2	
		standard deviation = ±7·6	
North Atlantic deep water mass			
334X	4/56	6/56	−62 ± 6
334S	4/56	7/56	−56 ± 7
282R	6/55	8/56	−50 ± 7
334N	4/56	7/56	−74 ± 7
334F	2/56	6/56	−49 ± 6
287A	7/55	8/56	−43 ± 10
287C	7/55	8/56	−58 ± 7
287H	7/55	9/56	−40 ± 13
287L	7/55	9/56	−73 ± 13
287N	7/55	8/55	−43 ± 10
287M	7/55	8/56	−53 ± 7
287K	7/55	2/57	−68 ± 5
287I	7/55	9/56	−76 ± 13
282Y	6/55	8/55	−60 ± 13
282Z	6/55	9/56	−56 ± 7
282X	6/55	9/56	−52 ± 9
282W	6/55	9/56	−33 ± 13
282U	6/55	9/55	−40 ± 13
282L	6/55	10/55	−53 ± 20
282P	6/55	10/56	−58 ± 8
282N	6/55	9/55	−45 ± 13
334J	4/56	9/56	−53 ± 7
		average = −54·3	
		standard deviation = ±11·5	
Caribbean surface water			
326K	11/55	4/56	+11 ± 7
326L	11/55	4/56	+9 ± 7
326J	11/55	4/56	+4 ± 7
326I	11/55	6/56	−1 ± 6
326O	12/55	5/56	+9 ± 6
326R	12/55	4/56	−1 ± 7
326Q	12/55	4/56	−5 ± 7
		average = +3·7	
		standard deviation = ±6·0	

VOL. 7 1959/6

7. *Reproducibility of results*

The most critical test of precision is to compare the results on samples obtained from the same water mass. The standard deviation of such results will provide an upper limit on the analytical error because it will include any real differences among samples from the same water mass (as well as any produced by variable isotope fractionation). Table 4 is a summary of results from the North Atlantic surface water system, the Caribbean surface water system, and the North Atlantic deep water mass.* For each of the three water masses the standard deviation of individual samples from the mean is given; the values, respectively, are 7·6, 6·0 and 11·5 per mil. Since these are essentially equal to the average measurement error quoted for an individual analysis, there is no indication of any large systematic error.

SUMMARY AND CONCLUSIONS

(1) A workable and highly reliable method has been developed for the shipboard extraction of the dissolved bicarbonate from 100 gal sea water samples. The CO_2 is released by acidification, swept out by CO_2-free air, and reabsorbed in two 1 l. bubblers each half filled with KOH solution.

(2) A system for the assay of the C^{14}/C^{12} ratio in such samples has been developed, allowing a precision of between 0·5 and 1·0 per cent to be obtained routinely. The C^{14}/C^{12} ratio is determined by measuring the C^{14} activity of CO_2 gas. Procedures of DeVries and Barendsen[10] and of Rafter[11] have been followed in several parts of the system.

(3) In order to correct for small amounts of isotopic fractionation during processing, a C^{13}/C^{12} assay of the counting gas is made so that the radio-carbon results can be normalized to a common C^{13}/C^{12} ratio.

(4) The close agreement among samples from the same water mass demonstrates that the results are reliable within the limits set by the measurement error. Oceanographic implications of the data will be discussed in future publications.

Acknowledgements—The authors received original encouragement and much help from Maurice Ewing and J. Lawrence Kulp who first conceived the idea of applying the radio-carbon method to problems of deep ocean circulation. In addition, French T. Hagemann, James Gray, Hans Suess, and G. J. Fergusson have given the authors valuable advice concerning the many problems involved in low-level gas counting of CO_2. Bruce C. Heezen, John Ewing, Charles Drake, Robert Gerard, Walter Beckman, William Taminga, and Taro Takahashi all contributed to the development of the shipboard sampling and processing techniques. In the laboratory the authors were aided by James Hubbard and Marylou Zickl in making the C^{14} assays and by Wayne Ault, Glen Ericson, and Roland Kologrivov in making the C^{13}/C^{12} measurements. Financial support was provided by the U.S. Atomic Energy Commission (Contract No. AT(30-1)-1808) and by funds for the International Geophysical Year.

REFERENCES

1. Kulp J. L., Tryon L. E., Eckelmann W. R., and Snell W. A. *Science* **116,** 409 (1952).
2. Craig H. *Tellus* **9,** 1 (1957).
3. Arnold J. R. and Anderson E. C. *Tellus* **9,** 28 (1957).
4. Revelle R. and Suess H. E. *Tellus* **9,** 18 (1957).
5. Rafter T. A. and Fergusson G. J. *N.Z. J. Sci. Tech.* **B38,** 871 (1957).
6. Sverdrup H. V., Johnson M. W., and Fleming R. H. *The Oceans*, Prentice-Hall, Englewood Cliffs, N.J. (1942).
7. Perry J. H. *Chemical Engineers' Handbook*, McGraw-Hill (1950).
8. DeVries Hl. *Appl. Sci. Res., Hague* **B5,** 387 (1956).
9. Fergusson G. J. *Nucleonics* **13,** 18 (1955).
10. DeVries Hl. and Barendsen G. W. *Physica's Grav.* **19,** 987 (1953).
11. Rafter T. A. *N.Z. J. Sci. Tech.* **B36,** 363 (1955).
12. Libby W. F. *Radio-carbon Dating.* University of Chicago Press (1952).
13. Suess H. E. *Science* **120,** 467 (1954).

* Since not all the C^{13}/C^{12} analyses have been completed, δC^{14} results are compared. Variable fractionation will then contribute to the differences among the results.

14. Hayes F. N., Anderson E. C. and Arnold J. R. Liquid scintillation counting of natural radiocarbon. *Proceedings of the First International Conference on the Peaceful Uses of Atomic Energy, Geneva* 1955. Vol. 14, p. 188. United Nations.
15. DeVries Hl. *Nuclear Phys.* **3,** 65 (1957).
16. Fergusson G. J. and McCallum G. J. *N.Z. J. Sci. Tech.* **B38,** 577 (1957).
17. Broecker W. S. and Olson E. A. *Amer. J. Sci.*, Radio-carbon Supplement. 1, 111 (1959).
18. Ault W. U. Ph.D. Thesis, Columbia University (1957).
19. Craig H. *Geochim. et Cosmoch. Acta* **3,** 53 (1953).
20. Craig H. *Geochim. et Cosmoch. Acta* **12,** 133 (1957).
21. Craig H. *J. Geol.* **62,** 115 (1954).

VOL.
7
1959/

International Journal of Applied Radiation and Isotopes, 1959, Vol. 7, pp. 19–22. Pergamon Press Ltd. Printed in Northern Ireland

Automatic Contour Scanner for Myelography*

ROBERT L. BELL† and GEORGE J. HERTSCH‡

(*Received* 9 *March* 1959)

An automatic constant geometry tracking device for irregular contours is described which facilitates radioactive myelography. The main advantage of the method is the use of a completely absorbable material in the subarachnoidal space. This technique provides high resolution pictures in examples of complete subarachnoidal block but fails to demonstrate minimal subarachnoidal block.

LE TRACEMENT AUTOMATIQUE DES CONTOURS POUR LA MYELOGRAPHIE

Un moyen automatique à géométrie constante pour faire le tracé des contours irreguliers est décrit, qui se destine á faciliter la myelographie par substances radioactives. Le principal avantage de la méthode réside dans l' emploi d'un matériel totalement résorbable dans l'espace sous-arachnoïdien. Par cette technique il est possible d'obtenir des images à contrastes marqués dans des cas de blocs sous-arachnoïdiens complets, par contre les cas d'obstructions minimes passent inaperçus.

АВТОМАТИЧЕСКИЙ ПРИБОР ДЛЯ МИЭЛОГРАФИЧЕСКИХ ИССЛЕДОВАНИЙ

Дано описание автоматического прибора с неизменной геометрией для исследования неправильных контуров, который облегчает миэлографию радиоактивными веществами. Главная особенность этого метода заключается в применении вещества, целиком поглощаемого в субарахноидальном пространстве. Эта методика дает возможность получать очень четкие изображения в случаях полного блокирования субарахноидального пространства, но недостаточна для обнаружения случаев частичного блокирования.

EIN AUTOMATISCHER KONTUREN-SCANNER FÜR MYELOGRAPHIE

Ein konstantes automatisches geometrisches Messungsgeraet fuer unregelmaessige Konturen wird beschrieben, welches die radioaktive Myelography erleichten. Der Vorteil dieser Methode besteht in der Verwendungsmoeglichkeit eines vollkommen absorbierbaren Materials im subarachnoiden Raum. Faelle mit vollstaendigem subarachnoiden Verschluss ermoeglichen mit dieser Methode hohe Resolutionsablesungen, waehrend geringgradige Verschluesse nicht dargestellt werden koennen.

ALTHOUGH DANDY[1] first described the use of air as a roentgenographic contrast medium, it remained for WINDERÖE[2] to specifically use this material to demonstrate evidence of encroachments upon the spinal subarachnoidal space. Unfortunately air afforded poor contrast and therefore led SICARD and FORESTIER[3] to use iodized oil, lipiodol. Although considered innocuous, there appeared in the literature reports indicating that this

* Supported in part by the E. Jefferson Browder Neurosurgical Foundation.

† Department of Neurosurgery, State University of New York, Downstate Medical Center, and the Neurosurgical Service of Kings County Hospital, Brooklyn, New York.

‡ Physics Department of the City of New York, Department of Hospitals, Delafield Hospital, New York, N.Y.

material produced undesirable complications. Chemical meningitis, arachnoiditis, and even degenerative lesions of the spinal cord were observed. Later RADOVICI[4] used Thorotrast as a contrast medium to demonstrate roentgenographically lesions of the vertebral canal, but this substance was not an improvement in contrast over lipiodol and in addition was radioactive. ARNELL and LINDSTRÖM[5] preferred Skiodan (Abrodil) a water soluble iodine preparation; however, the material was generally unavailable during World War II and has since been replaced by a more usable product, pantopaque. The first comprehensive report on the use of pantopaque was published by STEINHAUSEN.[6] It has the advantage of inducing fewer side reactions and has satisfactory radiographic contrast. The principal disadvantage was the lack of absorption of the compound from the subarachnoidal space. Because of the undesirable features attending the introduction of opaque media into the subarachnoidal space, other methods have been sought. BAUER and YUHL[7] proposed radio-iodinated human serum albumin for myelography. Their original observations were confirmed and supported by the work of PERRYMAN.[8] The level of almost complete to complete spinal subarachnoidal block was readily demonstrated by this technique; however, small lesions of the vertebral canal producing minimal encroachment on the subarachnoidal space were frequently unidentified. Furthermore, isotope myelography is not as precise as pantopaque myelography because of excessive tissue scatter and the limitation of the efficiency of the collimator. The favorable aspects of the radioactive material are the absence of secondary arachnoiditis, myelitis, meningitis, and the complete absorption of the substance.

INSTRUMENT

There are three major limitations in available scanning equipment:

(1) Inability to tilt the patient in order to produce gravitational flow of the radioactive material in the subarachnoidal space;

(2) relatively constant geometry to a highly irregular surface could not be maintained with the probe; and

(3) inability to conduct an automatic scan without danger of injuring the patient.

The scanner herein described has corrected these basic deficiencies and in addition is an instrument with which a speedy and accurate examination can be carried out with minimum discomfort to the patient.

The first defect has been resolved by the use of a radiographic tilt table (Fig. 1). The patient is able to lie prone in a comfortable position. The entire table and attached scanner is able to tilt 90° to the horizontal. A servo system permits the detector to ride a fixed distance above the skin level despite the irregular contours of the back. This allows the single hole detector to have a constant geometry to the tissue under observation and the detector scans the irregular surface without possible injury to the patient. The roller (Fig. 2) which rests on the skin, is mechanically connected by the curved arm to the shaft of a small selsyn attached to the detector. Vertical movements of the roller due to the variations in the contour will result in an angular displacement of the autosyn shaft. For a specific distance between detector and skin, in this case $\frac{1}{2}$ in., this shaft can be oriented with respect to the curved arm such that the autosyn rotor is at a null point; i.e., the useful electrical output is zero. There is always some residual output at the null, but this is a quadrature component which does not result in motor torque. Rotation of the shaft in either direction about this point results in an output voltage the phase of which changes 180 electrical degrees in passing through the null. For small angular displacements the magnitude of the voltage is roughly proportional to the angle. This voltage is fed into a power amplifier (Fig. 3), the output of which drives one phase of a two-phase motor. Power for the second phase of the motor is derived from the 60 cycles/sec line. An upward motion of the roller results in a signal which drives the motor in such a direction as to raise the detector until the

VOL. 7 1959/

OL.
7
9/60

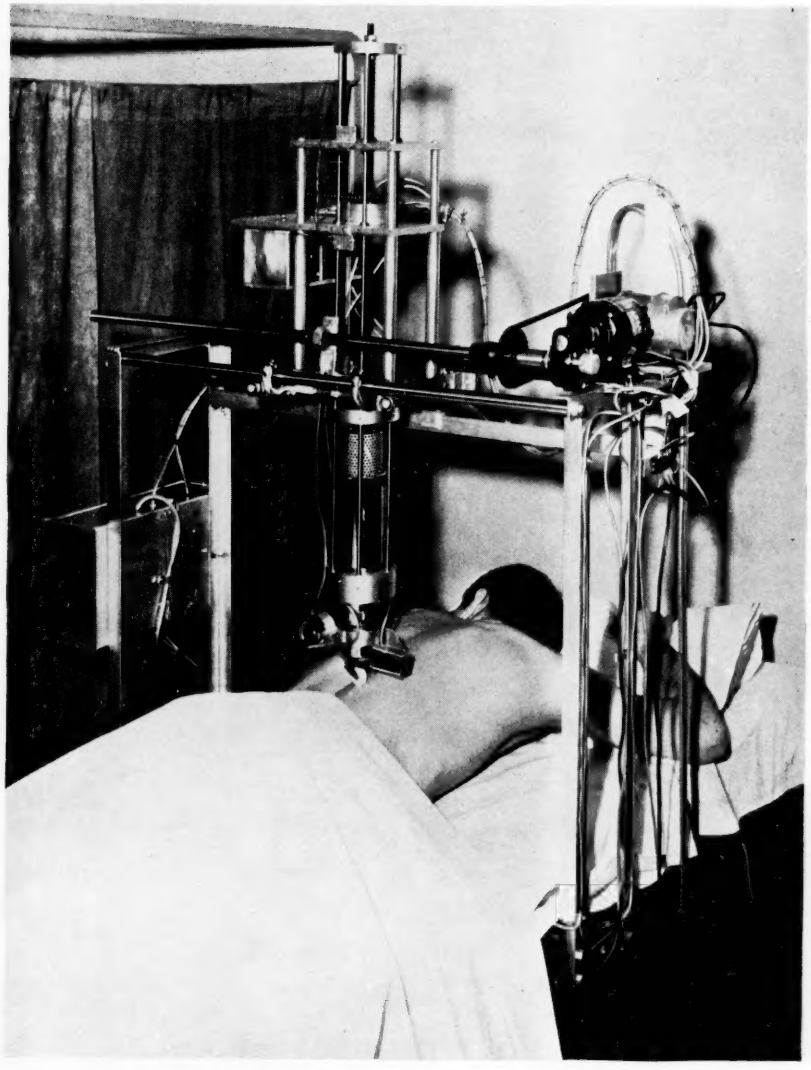

FIG. 1. The patient lies prone on the tilt table. Note the special probe mount which permits vertical motion as it scans in the other two planes.

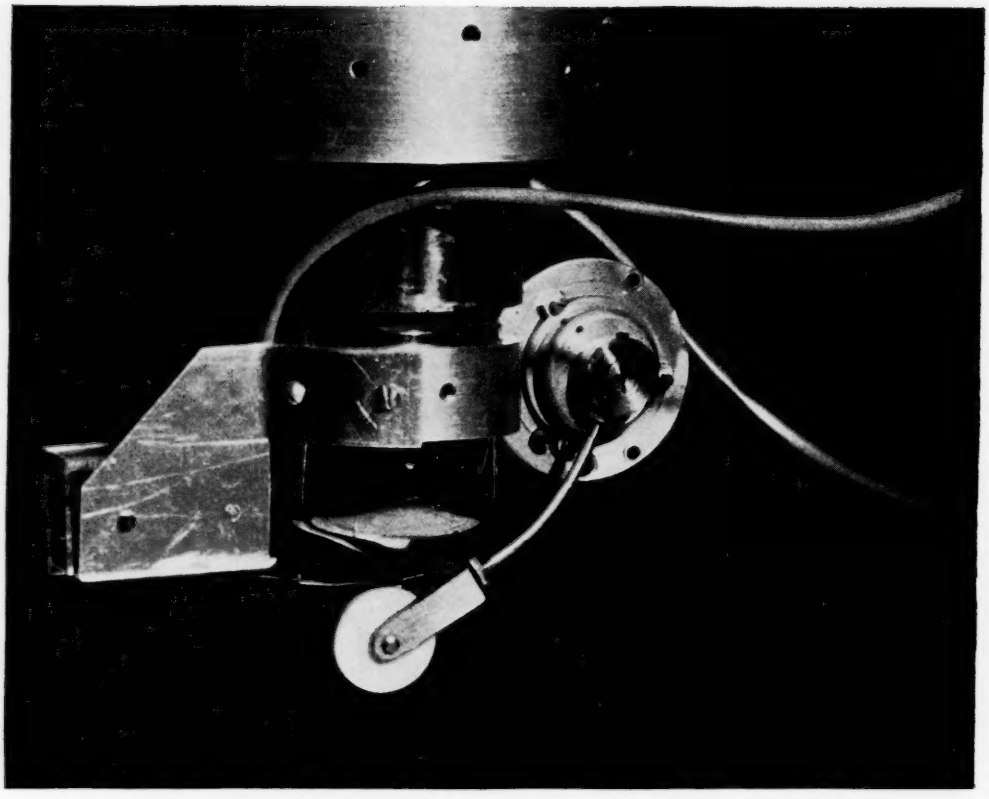

FIG. 2. Close-up of the autosyn and the sensing wheeled-arm. The microswitch is part of a fail-safe mechanism.

VOL.
7
1959/6

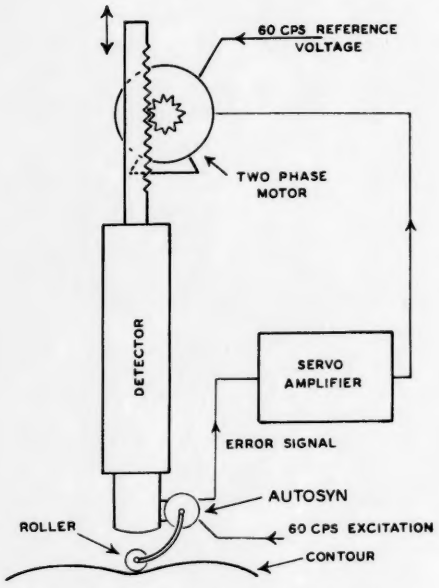

FIG. 3. Schematic of the servo system employed in the automatic vertical positioning system.

autosyn output is again zero which corresponds to the selected distance between detector and skin. Since a two-phase motor will reverse if the phase of the voltage applied to the control winding is shifted 180°, it follows that the detector will be driven downwards if the rotor is lowered from the position corresponding to the null. With this simple servo the distance between detector and skin is held to $\frac{1}{2}$ in. plus or minus $\frac{1}{32}$ in. This latter factor will depend on the speed of traverse and the rate of contour change.

The recorder is a servo X–Y plotting board mounted at another location (Fig. 4). This board is equipped with split nut clutches for quick adjustment. This arrangement allows pictures to be recorded in a constant horizontal plane completely free of variations in angle of the scanning table. The photographic head, also used for cranial scanning, has been described in a previous communication.[9]

PROCEDURE

The patient is placed beneath the scanner in a prone position (Fig. 1). A distal lumbar spinal puncture is carried out and a Queckenstedt test performed. One hundred microcuries (100 μc) of radio-iodinated human serum albumin are injected into the subarachnoidal space. This material should be about 2 cm^3 in volume which can be easily obtained when the activity of the original shipment has decayed to a suitable level. The spinal needle is withdrawn. The tilt table is elevated or depressed with a manual control until the material shows arrest against the block or is in the region of the suspected lesion as is indicated by the examination with a survey meter. The detector is then centered above or below the area to be scanned and the scanner activated. A scan is usually completed in 20 min. The restlessness of infants and small children cannot be completely controlled physically. Therefore, the scan is limited to the spinal axis.

RESULTS

Since completion of construction of the apparatus herein described, radioactive myelography has been carried out on a series of twelve patients. Three of these had normal spinal subarachnoidal spaces as demonstrated by conventional pantopaque and additional radioactive myelograms. Two patients showed minimal lateral protrusions of lumbar discs with pantopaque myelography, but these lesions were not demonstrated by radioactive myelography. One combination examination was performed on a patient with a suspected space taking lesion at the level of the fourth thoracic vertebra. Nine cm^3 of pantopaque and 100 μc of RISA were introduced. The pantopaque descended to the level of the lesion since it was heavier than spinal fluid and also heavier than the RISA. The maximum activity was recorded at the caudal end of the column of pantopaque. The remaining six patients had complete subarachnoidal block. All were

shown to have sharp cut-off as demonstrated (Fig. 5). The width of the column as seen by the radioactive detector is almost identical in width to the pantopaque column as is noted on regular roentgenographic spot films.

CONCLUSIONS

An automatic constant geometry tracking device for irregular contours is described to facilitate radioactive myelography. The technique described permits rapid non-toxic myelography to be performed even in children.

REFERENCES

1. Dandy W. *Ann. Surg.* **68,** 5 (1918).
2. Winderöe S. *Norsk. Mag. Laegevidensk.* **82,** 491 (1921).
3. Sicard J. A. and Forestier J. *Bull. Soc. Méd. Paris* **46,** 463 (1922).
4. Radovici A. and Meller O. *Pr. Méd.* **40,** 1933 (1932).
5. Arnell S. and Lindström F. *Acta Radiol. Stockh.* **12,** 287 (1931).
6. Steinhausen T. B., Dungan C. E., Furst J. B., Plati J. T., Smith S. W., Darling A. P., Wolcott E. C., Warren S. L. and Strain W. H. *Radiology* **43,** 230 (1944).
7. Bauer F. K. and Yuhl E. T. *Int. J. Appl. Rad. Isotopes* **2,** 52 (1957).
8. Perryman C. R., Noble P. R. and Bragdon F. H., *Amer. J. Roentgenol.* **80,** 104 (1958).
9. Bell R. L. *J. Neurosurg.* **14,** 674 (1957).

VOL.
7
1959/6

OL.
7
9/60

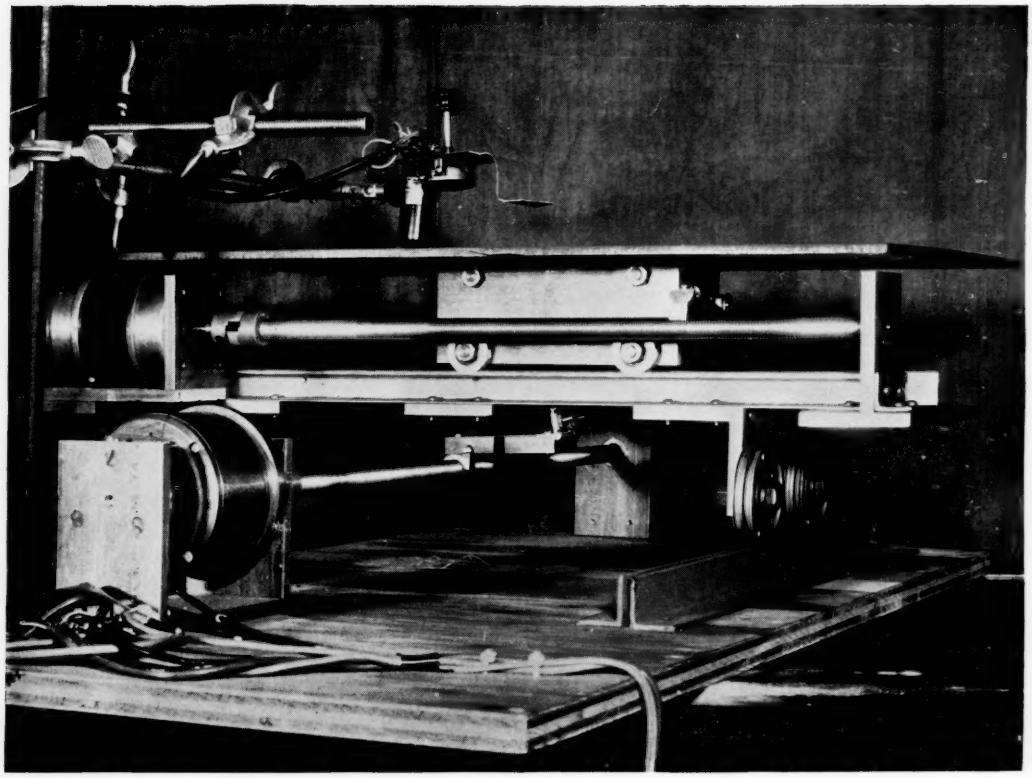

FIG. 4. The scanner is connected electrically to a servo X–Y plotter.

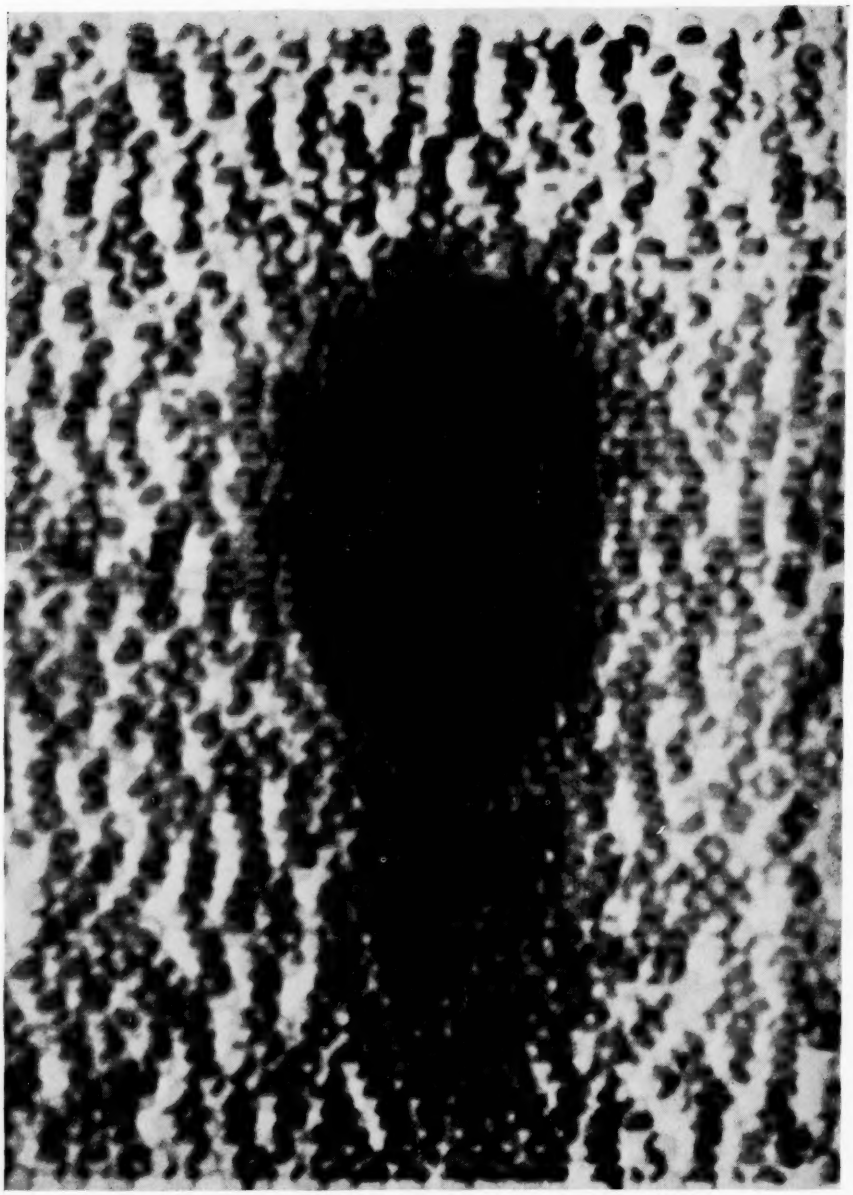

FIG. 5. Typical example of subarachnoidal block. The level of cut-off is at the D12-L1 vertebral level.

VOL.
7
1959/6

International Journal of Applied Radiation and Isotopes, 1959, Vol. 7, pp. 23–32. Pergamon Press Ltd. Printed in Northern Ireland

The Relative Flow Rates of Red Cells and Plasma—Peripheral and Central Circulation Studies in the Dog*

MILTON G. CRANE, JOHN E. HOLLOWAY,
RALPH ADAMS and IVOR C. WOODWARD

With the technical help of G. REYNOLDS

Departments of Internal Medicine and Radiology, College of Medical Evangelists, Los Angeles, California and The Respiratory and Rehabilitation Center for Poliomyelitis, Ranch Los Amigos Hospital, Dowey, California

(*Received* 31 *October* 1958; *in revised form* 24 *March* 1959)

The relative flow rates of I^{131}-labeled plasma and Cr^{51}-labeled red cells injected as a mixture were studied in the pulmonary and peripheral (leg and head) circulations of the dog. The red cells traversed the pulmonary circulation an average of 3·7 per cent (S.D. ± 2·2) faster than the plasma. The red cells traversed the peripheral capillaries of the leg circulation 10·7 per cent (S.D. ± 5·9) faster than the plasma. In the head circulation the red cells flowed 12·8 per cent (S.D. ± 5·5) faster than the associated plasma. The differences between the flow rates of the two phases were significant ($P < 0·01$) in all three vascular beds. Also, the difference between the mean transit times of the two phases was significantly shorter ($P < 0·01$) in the lung circulation than it was in either of the peripheral beds tested.

The calculated hematocrit of all three vascular beds tested was significantly lower ($P < 0·01$) than the simultaneously obtained large vessel hematocrit.

These findings can be partially explained by the hydrodynamic laws of Poisseuille and Bernoulli, but the vascular beds are too complex considering the perfusing liquid to allow full quantitation by the existing formulas.

LES TAUX RÉLATIFS D'ÉCOULEMENT DES CELLULES ROUGES ET DU PLASMA—ÉTUDES DE LA CIRCULATION PÉRIPHÉRALE ET CENTRALE CHEZ LE CHIEN

Les flux rélatifs du plasme marqué par I^{131} et des globules rouges marqués par Cr^{51} injectés comme mélange ont été observés dans la circulation pulmonaire (la jambe) et la circulation périphérique (la tête) chez le chien.

Les globules rouges ont transversé la circulation pulmonaire 3·7 pour cent (S.D. ± 2·2) plus vite que le plasme, et les vaisseaux capillaires périphériques de la jambe 10·7 pour cent (S.D. ± 5·9) plus vite que le plasme.

Dans la circulation de la tête, les globules rouges se sont écoulés 12·8 pour cent (S.D. ± 5·5) plus vite que le plasme.

La différence des deux flux est signifique en tous les trois *vascular beds*. Aussi, la différence des temps de transit était plus courte dans la circulation pulmonaire que dans les deux autres *peripheral beds*.

* This research was supported in part by research grant No. H-2195 from the National Heart Institute of the National Institutes of Health, Public Health Service and by the Los Angeles County Heart Association.

L'hématocrite calculé pour les trois *vascular beds* était moins que celui obtenu au mème temps pour le grand vaisseau.

Les observations s'expliquent en partie salon les lois hydrodynamiques de Poisseuille et de Bernoulli, mais les *vascular beds* sont trop complexes, en considérant la perfusion, pour permettre l'emploi libre des formules existantes.

СРАВНИТЕЛЬНЫЕ СКОРОСТИ ТОКА ЭРИТРОЦИТОВ И ИССЛЕДОВАНИЕ ПЕРИФЕРИЧЕСКОГО И ЦЕНТРАЛЬНОГО КРОВООБРАЩЕНИЯ У СОБАКИ

Сравнительные скорости тока плазмы, меченой I^{131}, и эритроцитов, меченых Cr^{51}, изучались на легочном и периферическом (нога и голова) кровообращениях собаки. Эритроциты циркулировали в легочном кровообращении в среднем на 3,7% (S.D. $\pm$ 2,2) быстрее, чем плазма, и в кровообращении в периферических капиллярах ноги на 10,7% (S.D. $\pm$ 5,9) быстрее, чем плазма. В кровотоке головы эритроциты двигались на 12,8% (S.D. $\pm$ 5,5) быстрее, чем плазма. Различия между скоростями тока этих двух фаз были значительны ($P < 0{,}01$) во всех трех сосудистых руслах. Различие между средними временнами прохождения двух фаз было значительно меньшим ($P < 0{,}01$) в легочном кровообращении, чем в любом из исследованных периферических русел.

Вычисленное значение гематокрита всех трех исследованных сосудистых русел было значительно ниже ($P < 0{,}01$) значений, полученных одновременно для крупных кровеносных сосудов.

Эти Данные могут быть частично объяснены гидродинамическими законами Пуазейля и Бернулли, но благодаря проникновению жидкости через стенки сосудов сосудистые русла являются слишком сложными для получения количественных данных на основе существующих формул.

DIE RELATIVEN DURCHFLUSSGESCHWINDIGKEITEN VON ROTEN BLUTKÖRPERCHEN UND PLASMA: PERIPHERE UND ZENTRALE BLUTKREISLAUFSTUDIEN BEIM HUND

Die relative Durchflussgeschwindigkeit des I^{131}-markierten Plasmas und der Cr^{51}-markierten roten Blutkörperchen, als Mischung in die Blutbahn injiziert, wurden im pulmonalen und peripheren (Bein und Kopf) Kreislauf des Hundes untersucht. Die roten Blutkörperchen durchflossen den pulmonalen Kreislauf im Durchschnitt 3,7 Prozent (S.D. $\pm$2,2) schneller als das Plasma, und die Geschwindigkeit der roten Blutkörperchen im Kopf war ebenfalls 12,8 Prozent (S.D. $\pm$5,5) schneller als die des begleitenden Plasmas. Ein Unterschied der Durchflussgeschwindigkeit der beiden Phasen ($P < 0{,}01$) war deutlich. Auch die mittleren Durchgangszeiten für beide Phasen waren im Lungenkreislauf bedeutend kleiner ($P < 0{,}01$) als in den beiden untersuchten peripheren Bahnen.

Der errechnete Hematocrit aller drei untersuchter Kreisläufe war ebenfalls bedeutend niedriger ($P < 0{,}01$) als der gleichzeitig bestimmte Hematocrit der grossen Blutgefässe.

Diese Ergebnisse können zum Teil durch die hydrodynamischen Gesetze von Poiseuille und Bernoulli erklärt werden. Doch ist der Gefässplexus und die ihn durchstroemende Flüssigkeit zu komplex, um zur Zeit eine Verallgemeinerung zu erlauben.

INTRODUCTION

THE hematocrit as determined upon samples from the larger vessels in the body does not give a correct representation of the percentage of red cells in the smaller vessels and capillaries. This has been demonstrated indirectly by two groups,[1,2] and has been reported following simultaneous measurement of the plasma volume and red cell volume by several investigators.[3–9] The ratio of the total body hematocrit to large vessel hematocrit is about 0·91. A portion of the vascular bed has a lower hematocrit than the veins and arteries from which blood samples are usually obtained.

In 1929, FAHRAEUS[10] reported that in glass tubes from 0·05 to 0·1 mm diameter

VOL. 7 1959/6

red cells flowed in the central stream and at a faster rate than the plasma.

There have been three reports of the simultaneous flow rates of plasma and red cells in the central circulation of the dog,[9,11,12] and two reports of a similar study in the human.[13,14] To our knowledge only two reports have appeared in the literature of the simultaneous flow rates of plasma and red cells in the peripheral circulation. Both of these studies[15,16] were on the forearm of the human. No values were given for the difference in the mean transit times of red cells and plasma in the peripheral circulation in either of these studies.

This report is of the relative flow rates of red cells and plasma in the nembutalized dog measuring as precisely as possible the flow rates, volume of distribution, and hematocrit ratios in the pulmonary, leg and cerebral blood vessels. The method affords a simultaneous measurement of both red cells and plasma in a continuously flowing sample.

METHOD AND APPARATUS

The instrumentation has been previously discussed.[17] Fig. 1 is the block diagram of the apparatus. Dogs weighing 8–18 kg were sedated with nembutal. To test the central circulation and the circulation to the leg, polyethylene catheters were placed from 3 to 4 cm centrad into the femoral artery, and about 20 cm centrad into the analogous femoral vein. To test the cerebral circulation, a thin-walled T-tube was inserted in the common carotid artery, and the external carotid branch was ligated. The test sample was drawn from the (unobstructed) analogous jugular vein.

Preparation of test material

A sample of the dog's red cells was tagged with high specific activity of Cr^{51}, and sufficient RISA* was added to give counting rates approximately equal on the respective recording channels. This injection mixture contained about 75 μc of Cr^{51} and 8 μc of I^{131} as RISA per ml with a hematocrit of about 75 per cent. The standard consisted of a 1:100 dilution of the injection mixture. The peripheral and central circulation studies were then carried out.

Method of test

In a typical run the sampling pump and the recorder were started and were allowed to run for 10 sec or more to obtain the background counting rates.† The mixed tracer material was then injected into the appropriate catheter and the time of injection recorded on the timing channel by a pressure mechanism. It was found that if the plastic tubing used for injection and sampling was "primed" with carrier albumin there was negligible sticking of RISA to the tubing. Sampling and recording were continued until recirculation peaks were recognized. A portion of sampled blood obtained near the primary circulation peak was reserved for duplicate hematocrits. A correction of 2·5 per cent was made in the hematocrit for trapped plasma. (This value was obtained by direct measurement in our laboratory.) The cross-channel contribution of each isotope was determined just before and after each run. The standard was counted in the same geometry as the blood samples initially and at about 30 min intervals. To measure peripheral circulation 2 ml of injection mixture with a 5 ml saline rinse was injected rapidly by a precision injection pipette into the femoral artery or the cerebral artery. Similarly, 3 ml of the mixture with 10 ml rinse was injected into the femoral vein to measure the central circulation.

The constant sampling rate (0·95 ml/sec) to counting geometry volume (0·2 ml) ratio was kept about 4·8. We found that when

* Abbot Laboratories, North Chicago, Illinois.

† Instrumentation background counting rate plus counting rate of previously injected isotopes is the total background.

square wave changes in indicator concentration were introduced into this system with the tubing length used that it required 1·3 sec for the counting rate to go from 2 per cent to 90 per cent of the peak or static counting rate of the indicator.

The decrease of statistical accuracy due to the rising background precluded the advisability of having more than six or seven runs in a given dog. Fig. 2 shows typical plotted curves of peripheral and central circulation.

Calculation of data

The time of injection was corrected for the number of seconds required for the sampled blood to traverse the tubing from the catheter tip to the well crystal. From this point of reference, net pip intervals per sec were found by subtracting background from the number of pip intervals actually counted at each second.[18]

At a scale of 64 counts per pip, the peak values ranged from 8 to 15 pip intervals per sec. As background increased with successive runs, the scale was raised to 128 counts per pip. (With a recording paper speed of 50 mm per sec, up to 40 pips per sec are readily identifiable.)

Correction was then made for cross-channel activity, and the resulting values were plotted on semilogarithmic paper to obtain the extrapolated portion of the downslope. Mean transit times (MTT), flow rate, and volumes were calculated from these using the following formulas.

$$\text{Whole blood flow rates} = \frac{C_s \times I \times \text{dilution of standard}}{C_{av} \times T}$$

C_s is the counting rate of the respective standard, I equals the volume injected, C_{av} equals the average concentration, and T is the time base of the curve.

$$\text{MTT} = \frac{\Sigma(C \times T)}{\Sigma C}$$

C is concentration and T is elapsed time of each concentration from zero time (corrected injection time).

The mean transit time and the whole blood flow rate for each of the two curves were calculated. The red cell flow rate was determined from the whole blood flow rate of the red cell curve and from the hematocrit. Plasma flow rates were obtained similarly using the plasmacrit and whole flow rate of the RISA curve. The central (or peripheral) volume of both plasma and red cells was calculated from the product of the respective mean transit times and flow rates. The calculated hematocrit of the central or peripheral blood was then determined using the plasma and red cell volumes. The respective peripheral volumes were also calculated using the washout slope and flow rate method as described by NEWMAN.[19]

Statistical analysis

The over-all statistical accuracy was related to

(1) the accuracy of the volume injected,
(2) the homogeneity of the injection mixture,
(3) the preparation of the standard dilutions,
(4) the number of counts made on the standards,
(5) the number of counts recorded on the sample before recirculation,
(6) the error in the slope on the extrapolated portion of the curve, and
(7) the deviation of the constants of cross-channel contribution (which influence items 4, 5, and 6.)

The standard deviation of No. 1 above, measured gravimetrically, was $\pm 1{\cdot}0$ per cent. Any error in volume of injection, however, will influence both the red blood cells and plasma in the same direction.

Homogeneity of the injection mixture was obtained by gentle agitation of its container each time before a dose was withdrawn into the injection pipette (No. 2 above). Since counting rates made on duplicate standard dilutions were nearly always within the limits of counting error, it is assumed that the error in preparation of a standard solution is not greater than the statistical counting error of the standard

VOL 7 1959

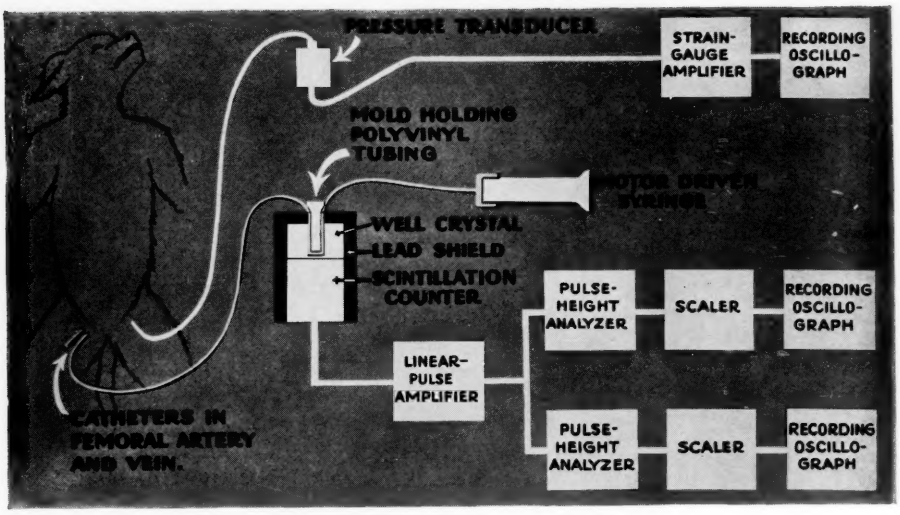

FIG. 1. Arrangement of equipment for the study.

VOL.
7
59/60

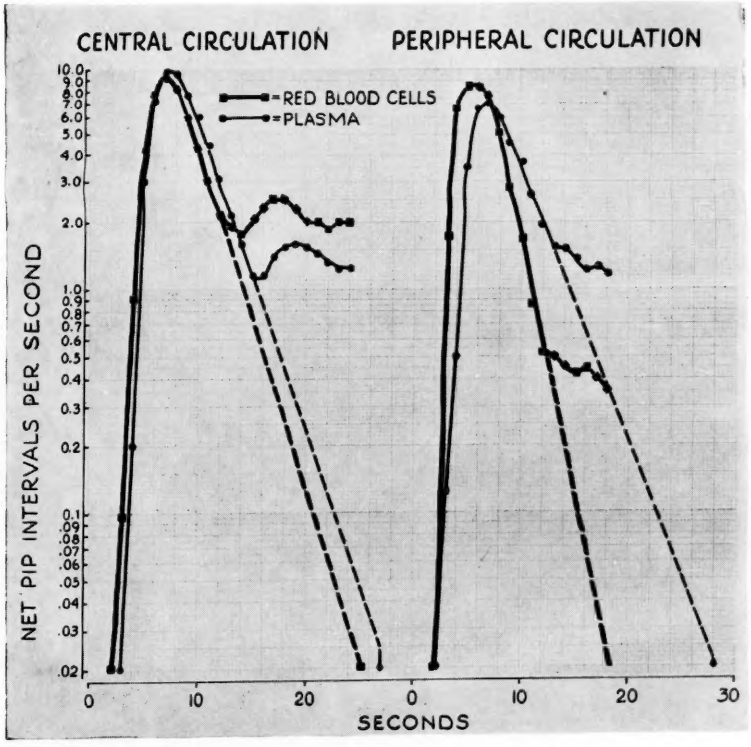

FIG. 2. Typical graphs of the simultaneous measurement of labeled red cells and labeled plasma in the pulmonary and peripheral circulation of the dog. Net counts per sec can be obtained by multiplying net pip intervals per sec by the scale setting (64).

VOL
7
1959

(No. 3 p. 26). The standard deviation of the counting of the standard solution was $\pm 0{\cdot}4$ per cent since a total of 50,000 counts was made on the standard solutions (No. 4 p. 26). This was increased to $\pm 1{\cdot}0$ when the influence of cross-channel contributions was considered. The total number of counts of the part of the curves before recirculation had occurred was usually greater than 4000 (and the standard deviation was $\pm 1{\cdot}6$ per cent (No. 5 p. 26). The standard deviation of the curves to recirculation point becomes $\pm 1{\cdot}9$ per cent with consideration of error introduced by cross-channel contribution.

The standard deviation in the slope of the extrapolated portion of the curve varied from animal to animal, but was approximately 4·0 per cent (No. 6 above). This becomes $\pm 5{\cdot}7$ per cent when the influence of cross-channel contribution is considered. The standard deviation of the slope is also the standard deviation of the area under the extrapolated portion of the curve and comprises approximately 10 per cent of the area under the entire curve. The error in the location of the slope introduces approximately $\pm 0{\cdot}6$ per cent standard deviation in the calculated output.

In the peripheral circulation as tested, flow from some accessory channels distorted the downslope which resulted in a shorter portion for use in extrapolation. The standard deviation for the area under the extrapolated portion would obviously be greater in such instances. Accordingly we omitted those curves in which the portion for extrapolation demonstrated less than a 50 per cent decrease in concentration before obvious recirculation.

VOL.
7
959/60

RESULTS

Fig. 2 is a graph of an actual test of the pulmonary and leg capillaries showing the counting rates of Cr^{51}-labeled red blood cells and RISA-labeled plasma plotted against time in seconds. There is a noticeable slight delay in the formation of the plasma curve as compared to the red cell curve in the central circulation. The difference is even more noticeable in the peripheral circulation curves. The curves of the head circulation resemble those of the leg peripheral circulation.

Central (pulmonary) circulation

Table 1 presents the results of the central circulation tests in 20 dogs. The average mean transit time (MTT) for plasma was $8{\cdot}77 \pm 1{\cdot}65$ sec. The average MTT for red blood cells was $8{\cdot}44 \pm 1{\cdot}38$ sec. The average MTT for red blood cells was shorter in all instances and averaged $0{\cdot}33 \pm 0{\cdot}23$ sec less than the MTT for plasma. The per cent difference between the two mean transit times ranged from 1·0 to 9·1 and averaged $3{\cdot}7 \pm 2{\cdot}2$. Repeat runs were made on 12 of the dogs. It was found that the variation of per cent difference in red blood cell and plasma MTT was no greater from animal to animal than between the two tests on the same animal.

The average total cardiac output was $156{\cdot}8 \pm 38{\cdot}6$ ml/min/10 per kg. There was no significant variation between the whole blood flow as determined by the two tracers. The central volumes of plasma and red blood cells were determined by the mean transit time method and by the slope method. Hematocrits calculated from these volumes were compared with the conventionally determined large vessel hematocrits. The ratio of the hematocrits obtained by the MTT method with the large vessel hematocrit ranged from 0·90 to 1·03 and averaged $0{\cdot}97 \pm 0{\cdot}04$. The corresponding ratio using the central volumes by the slope method ranged from 0·85 to 1·03 and averaged $0{\cdot}96 \pm 0{\cdot}06$.

Peripheral (leg) circulation

Table 2 presents the results of the leg circulation studies of 20 dogs. The average MTT for plasma was $15{\cdot}51 \pm 9{\cdot}61$ sec. The

TABLE 1. Normal values of central circulation

Dog No.	Mean transit time (sec)				Mean arterial pressure (mm Hg)	Total cardiac output (ml/min/10 kg)	Central volume by MTT (ml)			Central volume by slope method (ml)		
	Plasma	RBC	Diff.	Percent diff.			Plasma	RBC	PCV ratio	Plasma	RBC	PCV ratio
1	8·54	8·30	0·24	2·8	123	153	134	81	0·99	37	23	1·03
2	8·62	8·40	0·22	2·6	123	131	140	84	0·98	36	22	1·00
3	8·14	7·81	0·33	4·1	64	135	85	58	0·98	18	12	0·99
4	11·14	10·89	0·25	2·2	132	150	309	186	0·98	80	45	0·96
5	10·71	10·59	0·12	1·1	101	137	170	122	0·97	61	42	0·95
6	6·67	6·58	0·09	1·3	143	188	205	129	1·01	56	35	1·02
7	10·39	9·86	0·53	5·1	112	146	221	127	0·99	59	29	0·89
8	7·56	7·23	0·33	4·4	79	231	215	157	1·03	73	50	1·00
9	9·20	8·85	0·35	3·8	78	146	176	88	0·90	54	33	1·02
10	7·62	7·19	0·43	5·6	113	234	208	113	1·01	49	28	1·03
11	7·98	7·81	0·17	2·1	112	203	154	87	0·91	44	24	0·90
12	8·20	7·68	0·52	6·3	134	139	145	78	0·96	44	20	0·87
13	10·85	10·33	0·52	4·8	126	135	266	141	0·92	25	14	0·92
14	8·00	7·83	0·17	2·1	126	153	165	98	0·96	47	26	0·92
15	7·58	7·47	0·11	1·5	121	132	157	93	0·96	44	26	0·96
16	7·10	6·89	0·21	3·0	151	173	180	104	0·97	54	30	0·96
17	8·26	8·18	0·08	1·0	120	167	241	131	1·00	75	44	0·98
18	9·66	9·43	0·23	2·4	109	74	109	56	0·98	39	19	0·94
19	7·30	6·70	0·60	8·2	108	202	212	121	0·99	98	49	0·91
20	11·92	10·84	1·08	9·1	102	106	142	101	0·90	43	27	0·85
Ave.	8·77	8·44	0·33	3·7	113·8	156·8	176·7	107·8	0·97	51·8	29·9	0·96
S.D.	±1·65	±1·38	±0·23	±2·2	±21·1	±38·6			±0·04			±0·06

average MTT for red blood cells was 13·91 ± 8·76 sec. The MTT for red blood cells was shorter in all animals and averaged 1·61 ± 1·35 sec less than the MTT for plasma. The per cent difference between the two mean transit times ranged from 0 to 19 and averaged 12·1 ± 5·7. The ratio of the hematocrits obtained from the peripheral volume measurements by the MTT method to the hematocrit of the large vessel ranged from 0·71 to 1·03 and averaged 0·89 ± 0·07. The corresponding ratio using the peripheral volumes obtained by the slope method ranged from 0·63 to 1·02 and averaged 0·87 ± 0·09. Repeat tests were made on 5 dogs. Analysis of the results showed that the variation of per cent difference in MTT was no greater from animal to animal than between two consecutive tests on the same animal.

Peripheral (head) circulation

Table 3 presents the results of 10 head circulation studies on 6 dogs. The average MTT for plasma was 16·50 ± 7·00 sec. The average MTT for red blood cells was 14·30 ± 5·94 sec. The MTT for red blood cells was shorter in all the tests and averaged 2·20 ± 1·30 sec less than the MTT of plasma. The per cent difference between the two mean transit times ranged from 5 to 21 and averaged 12·8 ± 5·5. The ratio of hematocrits obtained from the peripheral volumes by the MTT method to the hematocrits of the large vessels ranged from 0·86 to 0·93 and averaged 0·90 ± 0·02. The corresponding ratio using the peripheral volumes obtained by the slope method ranged from 0·74 to 0·87 and averaged 0·82 ± 0·04.

TABLE 2. Normal values of peripheral circulation (leg)

Dog No.	Mean transit time (sec)				Mean arterial pressure (mm Hg)	Peripheral flow rate (ml/min/ 10 kg)	Peripheral volume by MTT (ml)			Peripheral volume by slope method (ml)		
	Plasma	RBC	Diff.	Per cent diff.			Plasma	RBC	PVC ratio	Plasma	RBC	PVC ratio
1	15·09	12·23	2·86	19	75	82	90	48	0·92	73	23	0·63
2	25·33	20·51	4·82	19	108	34	96	71	0·86	68	43	0·78
3	14·67	12·86	1·81	12	115	70	163	68	0·90	102	41	0·88
4	12·34	12·06	0·28	2	90	117	218	94	0·94	97	38	0·88
5	6·84	6·04	0·80	12	88	231	145	82	0·93	70	40	0·92
6	5·61	4·84	0·77	14	122	178	104	54	0·87	47	25	0·89
7	8·49	7·13	1·36	16	129	114	121	61	0·87	60	29	0·75
8	5·87	5·32	0·55	9	84	61	28	20	0·98	14	10	0·98
9	21·04	17·31	3·73	18	133	44	165	90	0·90	117	57	0·83
10	7·09	6·50	0·59	8	104	103	85	57	0·95	28	20	1·02
11	4·52	3·80	0·72	16	96	107	64	34	0·85	28	17	0·92
12	13·01	12·78	0·23	2	106	109	162	96	1·03	121	68	1·00
13	20·23	17·27	2·96	15	117	79	148	78	0·87	103	51	0·83
14	5·80	5·01	0·79	14	133	107	83	35	0·83	42	18	0·85
15	5·46	4·74	0·74	14	133	55	50	31	0·96	81	38	0·84
16	31·88	30·31	1·57	5	120	22	109	60	0·71	101	48	0·84
17	23·76	23·75	0·01	0	150	52	193	97	0·81	161	79	0·89
18	16·36	13·61	2·75	17	116	28	85	44	0·89	49	21	0·76
19	32·73	31·67	1·06	3	136	8	35	22	0·91	26	16	0·90
20	34·10	30·40	3·70	11	108	12	68	42	0·90	36	25	0·95
Ave.	15·51	13·91	1·61	10·7	113·2	80·7	110·6	59.2	0·89	71·2	35·4	0·87
S.D.	±9·61	±8·76	±1·35	±5·9	±19·3	±54·3			±0·07			±0·09

TABLE 3. Normal values of head circulation

Dog No.	Mean transit time (sec)				Mean arterial pressure (mm Hg)	Peripheral flow rate (ml/min/ 10 kg)	Peripheral volume by MTT (ml)			Peripheral volume by slope method (ml)		
	Plasma	RBC	Diff.	Per cent diff.			Plasma	RBC	PCV ratio	Plasma	RBC	PCV ratio
1	11·42	9·16	2·26	20	119	33	59	23	0·90	39	13	0·74
1	9·07	8·63	0·44	5	113	37	51	24	0·91	21	9	0·87
2	21·10	16·01	4·09	19	90	21	62	30	0·89	45	19	0·79
3	31·88	27·38	4·50	14	82	100	275	229	0·90	218	112	0·81
3	23·06	20·62	2·44	11	82	118	341	182	0·86	203	99	0·81
4	10·51	9·24	1·27	12	93	35	40	29	0·92	26	17	0·87
4	16·05	14·62	1·43	9	93	39	71	50	0·87	44	30	0·84
5	12·98	10·19	2·97	21	117	30	69	37	0·93	45	20	0·82
5	9·35	8·91	0·44	5	113	117	319	173	0·91	78	35	0·80
6	19·60	17·20	2·40	12	108	30	96	63	0·91	70	40	0·83
Ave.	16·50	14·30	2·20	12·8	101	56	138	84	0·90	78·9	39·4	0·82
S.D.	±7·00	±5·94	±1·30	±5·5	±10·1	±8·22			±0·02			±0·04

VOL. 7 959/60

DISCUSSION

In 1920, HOOPER *et al.*[1] noted that the red cell volume was always overestimated when calculated from the plasma volume and hematocrit. Subsequently, studies in which both the red cell mass and plasma volume were measured by several investigators showed that the ratio of total body hematocrit to large vessel hematocrit ranged from 0·89 to 0·91 in the dog[4,6,8,9] and from 0·91 to 0·94 in the human subject.[3,5,6,7] REEVES *et al.*[8] observed a drop in this hematocrit ratio from an average of 0·98 to 0·90 in the dog after splenectomy. The total body hematocrit is considerably lower than the large vessel hematocrit in such conditions as acute burns,[20] shock states,[21] and to a minor degree in congestive heart failure.[22] This phenomenon is important in that the whole blood volume as calculated by plasma volume and the large vessel hematocrit is slightly greater than the actual value. Conversely, whole blood volume calculated from a red cell mass measurement and the large vessel hematocrit will be underestimated.

SMITH *et al.*[3] recognized a possible explanation of this difference in the two hematocrits from microscopic observation by others[23] that the red cells flowed in the central portion of the stream in smaller blood vessels. This increased red cell flow rate would be accompanied by a decreased concentration of red cells in the capillaries. FAHRAEUS[10] found such a decreased red cell concentration in blood flowing through glass tubes from 1·1 to 0·05 mm i.d.

DOW *et al.*[11] found that Fe^{59}-tagged red cells flowed somewhat faster than T-1824-labeled plasma in the central circulation of 2 dogs. (Samples of blood were obtained by exsanguination.) LAWSON *et al.*[12] reported the average plasma MTT to be 11·09 sec and 1·18 sec longer than the corresponding red cell MTT in the central circulation of the dog. The sampling for the red cells was different than for the plasma in their study. Recently, LILIENFIELD *et al.*[13] reported a difference of 0·46 sec between the Cr^{51}-labeled red cell MCT and the MCT of RISA-labeled plasma in the lung circulation of some patients with cardiovascular and/or pulmonary disease. RAPAPORT *et al.* found that in the pulmonary circulation of dogs[9] the average plasma MTT was 10·71 sec and the average difference between the plasma and red cell mean transit times was 0·51 sec. In 16 patients[14] with mitral stenosis they found the average plasma MTT to be 23·93 sec, or 1·18 sec longer than the red cell MTT.

Two studies have been reported on the peripheral (human forearm) circulation. FREIS *et al.*[15] found the red cell mean velocity to be greater than that for plasma. In a summary article, LILIENFIELD *et al.*[24] reported no significant difference between the forearm capillary hematocrit and the large vessel hematocrit. No values for mean transit times were given in these two studies.

Our method permits simultaneous and continuous measurement of tagged red cell and tagged plasma concentrations following a single injection of the doubly-labeled blood. We have also collected samples in a device similar to ROTHE's.[25] The determination of the concentration curves by this sampling method is tedious, but gives comparable results.

In the central circulation we found a significant difference ($P < 0{\cdot}01$) between the MTT of plasma and red cells. In this respect our findings differ from the report of LILIENFIELD.[13] We found no significant difference between the whole blood flow rates as measured by the two tracers. The hematocrits obtained from the central volumes differed significantly from the large vessel hematocrits. P was $<0{\cdot}01$ for the values obtained by both the MTT and the slope methods.

An important unknown is the ratio of blood volume within the smallest vessels of the lung to the total volume tested. The volume within the pulmonary capillaries can be measured, but even with that measurement one cannot estimate the volume of adjoining or contiguous pulmonary vessels of nearly the same diameter. From the data of FAHRAEUS[10] it appears that tubes with an i.d. less than 0·25 mm affect the relative

VOL 7 1959/

flow rates quite markedly; whereas larger vessels alter relative flow rates but little. The critical diameter in the living subject is not known, but presumably it would be close to that value. The average central volume tested in our studies was 1·7 times the average leg peripheral volume and 1·3 times the average head peripheral volume. This relatively greater proportion of blood in large vessels in the central circulation tested as compared with the peripheral circulation selected cannot account for all of the difference between pulmonary and peripheral hematocrit ratios. In a small series of tests in which the tracers were injected into the pulmonary artery and the blood sample was withdrawn from the aortic arch with a central volume comparable to the peripheral volumes in this study, we were unable to obtain a lower hematocrit ratio. It may be that that portion of the pulmonary vascular bed which is less than the critical diameter is comparatively small, volumewise, in the living subject.

In both the head and leg capillary beds the MTT for plasma was significantly ($P < 0{\cdot}01$) greater than that for red cells. The peripheral capillary hematocrit was found to be significantly ($P < 0{\cdot}01$) lower than the large vessel hematocrit in both the head and leg capillary beds. This was true for both the slope volumes and the MTT volumes.

There was no significant difference between the corresponding entities of the leg and head peripheral beds with the exception of the slope volume hematocrit ratios. The reason for this slope volume hematocrit ratio exception is not readily apparent. Curves obtained on the head circulation were more consistent and had a longer exponentially descending limb before recirculation when compared with leg circulation curves.

The average difference and the per cent difference between the plasma and red cell MTT of the central circulation were significantly ($P < 0{\cdot}01$) less than the corresponding values for both the cerebral and leg circulations. From this it would seem justifiable to conclude that the pulmonary capillary bed has a larger over-all average diameter than do the head and leg peripheral capillary beds.

Poisseuille's equation for the flow of Newtonian fluids, applied to blood flow in cylindrical tubes, has been used to describe the flow of blood in the vessels of the body. However, FAHRAEUS[10] felt that blood did not follow this law *in vivo*. JEFFORD and KNISELY[26] have presented an excellent discussion of this topic. They point out that arteries and veins are not cylinders but truncated cones with only the capillaries being cylindrical. Further, the vessel walls have a parameter of elasticity. An equation to describe the pulsatile flow of Newtonian fluid in such tubes would be quite complex. This would be especially true in a group of parallel-connected elastic tubes which are first reducing cones, then cylindrical tubes, and then enlarging cones. Since blood is a two-phase system with solid particles in a liquid phase, a further difficulty is introduced to complicate mathematical representation of the flow of blood through the vascular beds of the body.

Bernoulli's law states that the lateral pressure of a fluid in a tube is inversely proportional to the velocity of flow. A red blood cell flowing between the stream center and the vessel wall would be exposed to a greater pressure on the side facing the wall than on the axial stream side. This would force the cellular structures into the axial portion of the stream. The smaller the blood vessels, the greater would be the velocity gradient between the axial and lateral portions. As a result the cellular structures in a smaller vessel would be forced relatively further into the axial stream and thus there would be a greater difference between the mean transit times of the two phases than would be found in a larger vessel. Further, it is known[26] that in some of the peripheral capillaries the size (i.e. diameter) of the red cells is such that they must either be folded (or otherwise deformed) or must distend the vessel wall in order to traverse the given capillary. This also requires energy and would be difficult to include in a comprehensive equation.

VOL.
7
59/60

In a two-phase system, most of the energy required to maintain flow is dissipated in the peripheral sleeve of the flow cross-section in contradistinction to the axial stream. As the percentage of red cells decreases in the peripheral sleeve, the effective viscosity decreases. COULTER and PAPPENHEIMER[27] have presented evidence suggesting that under certain conditions the Reynold's number may be exceeded for the peripheral zone, resulting in turbulence in this zone. Under such circumstances the peripheral zone of flow could be turbulent while the axial stream remained laminar. Turbulence would increase the resistance to blood flow. Absence of peripheral zone turbulence would decrease mixing of the tracers. This effect would be most noticeable in the plasma phase. Our results suggest, but do not prove, that tracer mixing was fairly complete hence that some turbulence existed in the peripheral sleeve during the test.

The application of Bernoulli's and Poisseuille's laws explains the greater average velocity of red cells as compared with plasma, but these laws fall short of quantitatively expressing the flow of blood in the arterioles, capillaries, and venules.

Acknowledgements—The authors acknowledge the technical assistance of DOROTHY TEEPLE in this project, and the assistance of ROBERT WOOD in the statistical analysis of the method.

REFERENCES

1. HOOPER C. W., SMITH H. P., BELT A. E. and WHIPPLE G. H. *Amer. J. Physiol.* **51,** 205 (1920).
2. STEAD E. A. JR. and EBERT R. V. *Amer. J. Physiol.* **132,** 411 (1941).
3. SMITH H. P., ARNOLD H. P. and WHIPPLE G. H. *Amer. J. Physiol.* **56,** 336 (1921).
4. HAHN P. F., BALFOUR W. M., ROSS J. F., BALE W. F. and WHIPPLE G. H. *Science* **93,** 87 (1940).
5. HEVESY G., KOSTER K. H., SORENSON G., WARBURG E. and ZERAHN K. *Acta Med. Scand.* **116,** 561 (1944).
6. GIBSON J. G., PEACOCK W. C., SELIGMAN A. M. and SACK T. *J. Clin. Invest.* **25,** 838 (1946).
7. BARNES D. W. H., LOUTIT J. F. and REEVE E. B. *Clin. Science* **7,** 135 (1948).
8. REEVES E. B., GREGERSON M. I., ALLEN T. H. and SEARS H. *Amer. J. Physiol.* **175,** 195 (1953).
9. RAPAPORT E., KUIDA H., HAYNES F. W. and DEXTER L. *Amer. J. Physiol.* **185,** 127 (1956).
10. FAHRAEUS R. *Physiol. Rev.* **9,** 241 (1929).
11. DOW P., HAHN P. F. and HAMILTON W. F. *Amer. J. Physiol.* **147,** 493 (1946).
12. LAWSON H. C., COUTRELL W. F., SHOW J. E., BLACKBURN D. L. and ADAMS S. *Amer. J. Physiol.* **170,** 277 (1952).
13. LILIENFIELD L. S., KOVACH R. D., MARKS P. A., HERSCHENSON L. M., RODNAN G. P., EBAUCH F. G. JR. and FREIS E. D. *J. Clin. Invest.* **35,** 1385 (1956).
14. RAPAPORT E., KUIDA H., HAYNES F. W. and DEXTER L. *J. Clin. Invest.* **35,** 1393 (1956).
15. FREIS E. D., STANTON J. R. and EMERSON C. P. *Amer. J. Physiol* **157,** 153 (1949).
16. LILIENFIELD L. S., KOVACH R. D. and FREIS E. D. (Abst.) *Circulation* **12,** 741 (1955).
17. ADAMS R., WOODWARD I. C., CRANE M. G. and HOLLOWAY J. E. *Int. J. Appl. Rad. Isotopes* **3,** 156 (1958)
18. CRANE M. G., ADAMS R. and WOODWARD I. C. *J. Lab. Clin. Med.* **47,** 802 (1956).
19. NEWMAN E. V., MERRELL M., GENECIN A., MONGE C., MILNOR W. R. and MCKEEVER W. P. *Circulation* **4,** 735 (1951).
20. SALZBERG A. M. and EVANS E. I. *Ann. Surg.* **132,** 746 (1950).
21. GIBSON J. G., II, SELIGMAN A. M., PEACOCK W. C., FINE J., AUB J. C. and EVANS R. D. *J. Clin. Invest.* **26,** 26 (1947).
22. SCHREIBER S. S., BAUMAN A., YALOW R. S. and BERSON S. A. *J. Clin. Invest.* **33,** 578 (1954).
23. KROGH S. A. S. *Yale University Press* **28,** (1922).
24. LILIENFIELD L. S., KOVACK R. D., HERSHENSON L. M., RODMAN G. P., MARKS P. A., EBAUGH F. G. JR. and FREIS E. D. *Clin. Research Proc.* **3,** 110 (1955).
25. ROTHE C. F. and SAPERSTEIN L. A. *Amer. Heart J.* **48,** 141 (1954).
26. JEFFORD J. V. and KNISELY M. H. *Angiology* **7,** 105 (1956).
27. COULTER N. A. JR. and PAPPENHEIMER J. R. *Amer. J. Physiol.* **159,** 401 (1949).

VOL
7
1959/

International Journal of Applied Radiation and Isotopes, 1959, Vol. 7, pp. 33–37. Pergamon Press Ltd. Printed in Northern Ireland

Resolution and Image Spread in Autoradiographs of Tritium-labeled Cells*

J. S. ROBERTSON, V. P. BOND and E. P. CRONKITE
Medical Research Center, Brookhaven National Laboratory,
Upton, L.I., New York

(*Received* 29 *March* 1959)

Calculations of the radiation dose rate about point sources of tritium have been extended to explain the variations in image spread seen in autoradiographs of cells labeled with tritiated thymidine. The resolution attainable with tritium sources in contact with the sensitive emulsion is much sharper (0·2 μ) than that attainable with C^{14} (2 μ). With sources at a micron or more depth, however, the effect of the very low energy tritium β^- particles on improving the resolution is lost and the resolution deteriorates. As the depth of a tritium-labeled cell nucleus in the tissue section increases, the grain density decreases, the resolution becomes poorer, and the image spread increases.

RÉSOLUTION ET DISPERSION D'IMAGE DANS LES AUTORADIOGRAPHIES DES CELLULES MARQUÉES AVEC LE TRITIUM

On a étendu les calculs du taux de la dose de radiation autour des sources sans dimension afin d'expliquer les variations dans la dispersion d'image qui se font voir dans les autoradiographies des cellules marquées avec de la thymidine tritiée. La résolution qu'on peut atteindre avec des sources de tritium en contacte avec la pellicule sensible est bien plus précise (0,2 μ) que celle obtenable avec le C^{14} (2 μ). Cependant, avec des sources à une profondeur d'un micron ou plus, l'amélioration de la résolution qu'effectue les particules β de très petite énergie sortant du tritium se perd, et la résolution se détériore. À mesure qu'augmente la profondeur du noyau de la cellule marquée au tritium dans la section de tissu, l'intensité de grain diminue, la résolution s'affaibli et la dispersion d'image augmente.

РАЗРЕШЕНИЕ И РАЗМЫВАНИЕ ИЗОБРАЖЕНИЙ В РАДИОАВТОГРАФАХ КЛЕТОК, МЕЧЕНЫХ ТРИТИЕМ

Расчеты мощности дозы точечных источников трития были использованы для объяснения изменений четкости изображения, наблюдающихся в радиоавтографах клеток, меченых тимидином, содержащим тритий. Тритиевые источники, находящиеся в контакте с чувствительной эмульсией, дают значительно более высокое разрешение (0,2 μ), чем источники с C^{14} (2 μ). Однако, если источники находятся на глубине в микрон и больше, действие 0-частиц трития с их очень малой энергией перестает сказываться и разрешение ухудшается. С увеличением глубины расположения меченых тритием клеточных ядер в ткани плотность зерен становится меньше, разрешение понижается и размывание изображения увеличивается.

AUFLÖSUNG UND BILDVERGRÖSSERUNG BEI AUTORADIOGRAPHIEN VON TRITIUM-MARKIERTEN ZELLEN

Es wurden Berechnungen der Dosis der Strahlung von punktförmigen Tritiumquellen durchgeführt, um Veränderungen der Bildvergrösserung bei Autoradiographien von Zellen, die mit Tritium-hältigen Thymidin markiert sind, zu erklären.

Die Auflösung, die mit Tritiumquellen in Kontakt mit der empfindlichen Emulsion erreicht werden kann, ist bedeutend schärfer (0·2 μ), als bei C^{14} (2 μ). Für Quellen von 1μ

* Research supported by the U.S. Atomic Energy Commission.

VOL. 7 59/60

Dicke und darüber, geht jedoch dieser Effekt der verbesserten Auflösung, welche durch die sehr geringe Energie der β-Teilchen des Tritiums bewirkt wird, wieder verloren, und die Auflösung verschlechtert sich. Im gleichen Masse wie der Abstand des Tritium-markierten Zellkernes von der Oberfläche des Gewebeschnittes zunimmt, vermindert sich die Dichte der geschwärzten Körner, verschlechtert sich die Auflösung, und die Unschärfe des Bildes nimmt zu.

THE autoradiographic method[1] has been particularly useful in studies of the distribution of radioactivity at the microscopic level in histological and cytological preparations, and the availability of tritiated thymidine[2] has appreciably extended this method's usefulness by providing a label which is essentially confined to the cell nucleus both by selective incorporation of the material and by the short range of the β^- particle emitted. In autoradiographs of blood smears labeled with tritiated thymidine, the image is confined almost exactly to the area occupied by the cell nucleus,[3,4] but in studies of sections of tissues it has been noted that in some cells there is a greater spread of the autoradiographic image, with an appreciable number of darkened grains appearing outside of the borders of the cell nucleus.[5] As an illustration, in Figs. 1 and 2 two tritiated thymidine-labeled cells are compared, with the autograph in Fig. 2 showing the greater degree of image spread.

Because in the literature on autoradiography there is no completely satisfactory explanation of this variation in image spread, the physical factors involved in the use of tritium in autoradiography were examined in finer detail and the calculations presented here were made in order to provide an explanation of the observed phenomena.

VOL. 7 1959/6

IMAGE SPREAD IN AUTORADIOGRAPHS (GENERAL)

DONIACH and PELC[6] first considered the problem of autoradiographic image spread by calculating the radius of the image to be expected about a point source and about a line source of radioactivity placed normal to the emulsion, using the inverse square law to describe the reduction of radiation intensity with distance from the source. This problem is further considered by LAMERTON and HARRISS[7] and by HARRISS[8] for extended sources in the form of uniformly labeled right cylinders of 1 to 10 μ radius. As will be shown below, although the use of the square of the distance and the assumption of uniform labeling suffice in considerations of energetic β-particles, they are inadequate when tritium is involved.

RANGE OF TRITIUM β^- PARTICLES

The tritium β^-particle has a maximum energy of only 18 keV and a consequent maximum range in water of 6 to 7 μ.[9] It must be borne in mind that relatively very few of the tritium β^-particles have the maximum energy and that those of average energy (5·7 keV)[10,11] have a range of only about 1 μ.[9] Since tissue sections are several microns thick, the precise depth of the radioactivity in the section therefore strongly affects the percentage of the β^-particles which get through to the sensitive emulsion. As experimental evidence of the importance of the short range of tritium β^-particles, Fig. 3 presents two photomicrographs of autoradiographs of a section of the small intestine of a mouse labeled with tritiated thymidine.[12] In part A the emulsion was in contact with the section, but in part B a 1 μ layer of celloidin was interposed. These two pictures are from the same section and, except for the celloidin layer in B, the exposure and development conditions were identical, so the relative sparsity of grains in B is attributable to absorption in the 1 μ celloidin layer. When tritium is used, therefore, the depth of the cell nucleus within the section must be considered in calculations of the expected image density.

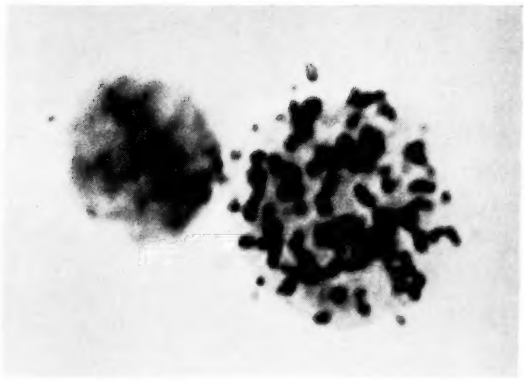

FIG. 1. Autoradiograph of tritium-labeled cell in a blood smear. The boundaries of the cell nucleus and the darkened grains coincide.

OL.
7
9/60

FIG. 2. Autoradiograph of tritium-labeled cell from a mouse embryo section. Many grains are well outside the borders of the cell nucleus.

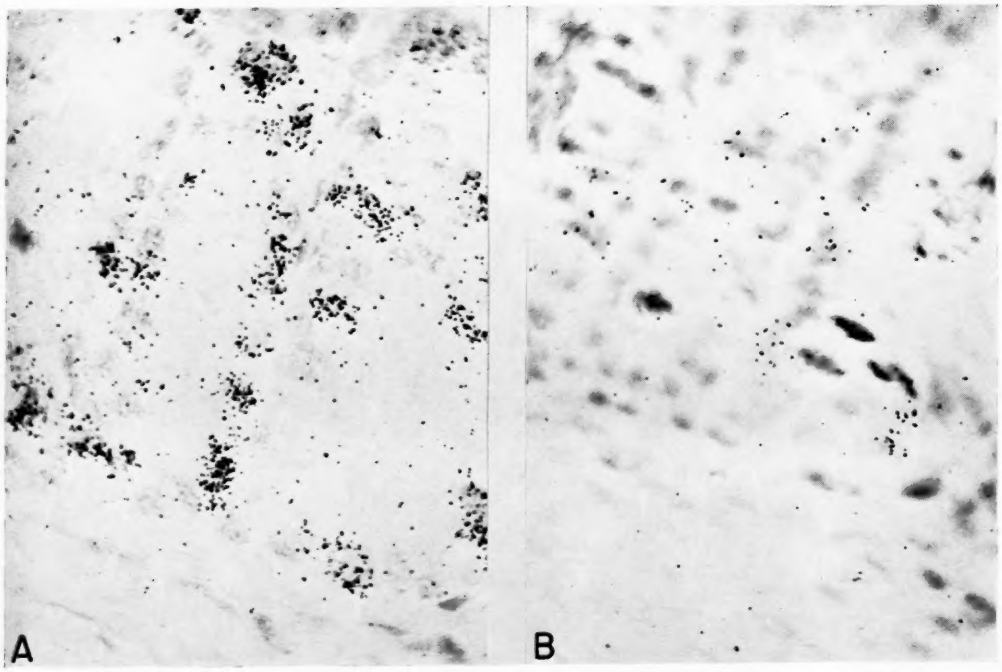

FIG. 3. Effect of a 1 μ celloidin layer on grain count. Section A was in contact with the film. Section B was coated with celloidin.

VOL.
7
1959/6

RESOLUTION AS A FUNCTION OF DEPTH OF TRITIUM-LABELED CELL NUCLEI

As the starting point for the present analysis, a previous calculation[13] of the radiation dose rates about a point source of tritium as a function of the distance from the point source may be taken. This previous calculation is based on the shape of the

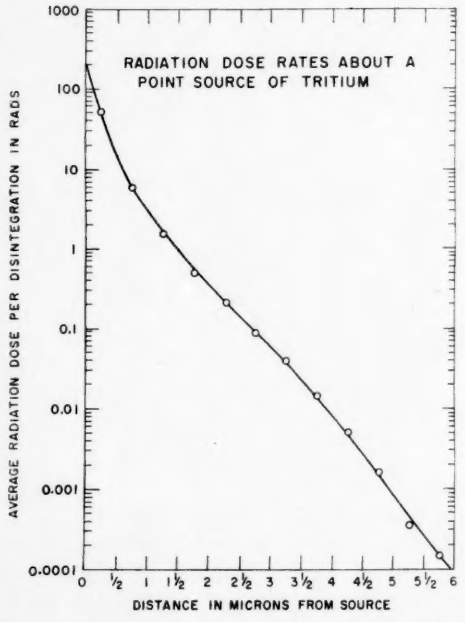

FIG. 4. Radiation dose per tritium disintegration as a function of distance from a point source. Reproduced by courtesy of Yale University Press.[13]

tritium β^-spectrum and does take the diminution of intensity resulting from absorption, as well as that due to geometry (inverse square of the distance) into account. The calculated curve is shown in Fig. 4. This curve is closely represented by the equation $d = 185 \exp(-5{\cdot}55\rho) + 15 \exp(-1{\cdot}92\rho)$ where d is the average dose per disintegration in rads and ρ is the distance in microns from a point source. The shape of this curve is different from those for more energetic β^- particles in that the latter curves can usually be fitted by an expression of the type $d = d_0 \exp(-\mu\rho)/\rho^2$, whereas the curve for tritium cannot be so fitted. In the range of β^- energies from P^{32} ($E_{max} = 1{\cdot}71$ MeV) down to S^{35} ($E_{max} = 0{\cdot}167$ MeV) and C^{14} ($E_{max} = 0{\cdot}158$ MeV), the fall-off of radiation intensity due to the effect of the square of the distance from a point source (the $1/\rho^2$ component) is a much stronger function than the decrease of intensity due to absorption (the $\exp(-\mu\rho)$ component). Therefore, the resolution attained is largely due to the effect of geometry and does not improve greatly between P^{32} and C^{14} despite the vast decrease in energy. In the case of tritium, however, the rate of decrease due to energy loss by collision is a sufficiently strong function to give an appreciable sharpening of the resolution attainable. (For the definition of resolution in autoradiographs, see LAMERTON and HARRISS.[7])

Fig. 5 shows a quadrant of the dose rate contours about a point source of tritium located at the origin of the graph. These contours were constructed from the data depicted in Fig. 4. The stippling indicates very roughly the kind of fall-off of intensity to be expected, if it is assumed that the grain density depends directly upon the radiation dose. It is difficult to demonstrate with

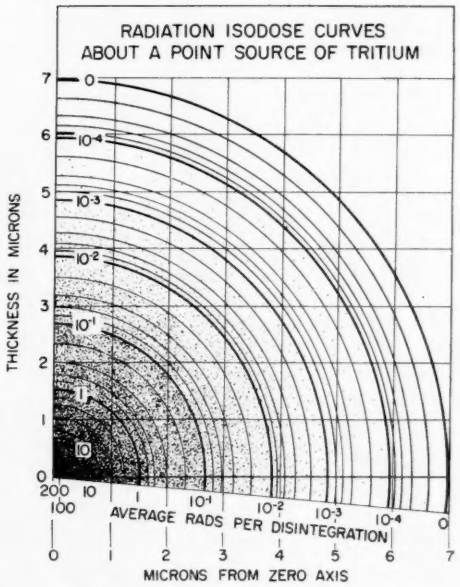

FIG. 5. Radiation isodose curves about a point source of tritium. Dose–distance relationships obtained from Fig. 4.

tritium that the intensity does fall off in the manner calculated, but as an analogy Fig. 6 shows the result of exposure of autoradiographic stripping film to a 1 mm diameter source of P^{32}. Since the P^{32} β^-particles have a range of about 8 mm, the result is comparable to a magnification of the intensity pattern to be expected from a 1 μ wide source of tritium, although differences in the shapes of the two β^-spectra[11] and the fact that the absorption curve is not linear[13] make a precise simulation impossible to achieve with a single isotope.

Returning to consideration of the tritium case, the sensitive emulsion may be considered to be located at various heights along the ordinate in Fig. 5 for corresponding variations in the depth of the source. In addition to the variation in intensity there will be a variation in the shape of the intensity curves at different depths. This kind of variation is shown in Fig. 7. The curves shown in Fig. 7 were constructed by numerically integrating within each 1 μ tier the dose along ordinates spaced at intervals of 0·2 μ from the zero axis. These calculations were achieved with the use of an IBM-610 electronic digital computer.* The curves presented in Fig. 7 are normalized relative to their center ($r = 0$) intensity. It is to be noted that the rate of fall-off of intensity with distance from the center is by far the steepest in the 0–1 μ level section, and, of course, this section will yield by far the sharpest resolution, the (calculated) width at half maximum being only 0·2 μ. In the other tiers the resolution deteriorates to 2 μ, a value attainable in practice with P^{32}.[7] According to this kind of calculation, some improvement in resolution should occur as the depth approaches the end of the range (6 to 7 μ), but this is an unrealistic conclusion because

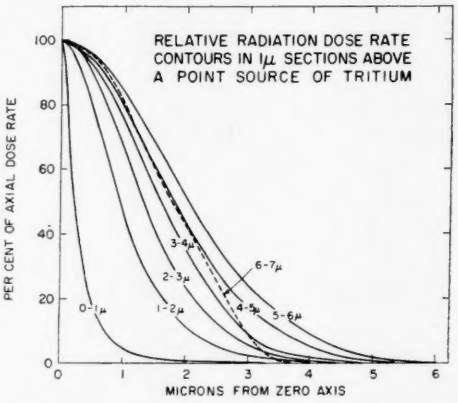

FIG. 7. Radiation dose contours in 1 μ thick tiers above a point source of tritium. Position of each tier indicated in Fig. 6.

at this distance the relative dose rate has fallen to such a low value that prohibitive amounts of activity would have to be present to produce autoradiographs in reasonable exposure times, and because the effects of straggling and scatter have not been fully considered. It should also be noted that the 0·2 μ resolution calculated is only theoretically attainable (in the sense of distinguishing two adjacent sites) because the grain size in the stripping film used has about the same dimensions.

IMAGE SPREAD ABOUT TRITIUM SOURCES

Applying the above results to the problem of an extended source the size of a cell nucleus, it is apparent that the question of whether appreciable image spread will be seen or not depends upon the relative effect of the radioactivity located at the periphery of a given cell nucleus. In the nuclei located at a depth of, say, 3 μ from the photographic emulsion, it is true that the higher energy β^- particles cannot get as far from the axis as in the case of those in contact with the emulsion, but on the other hand such a large number of the lower energy particles do not even get to the emulsion in the former case

* The assistance of L. K. Potter in programming and running this problem on the IBM-610 is gratefully acknowledged.

VOL. 7 1959/6

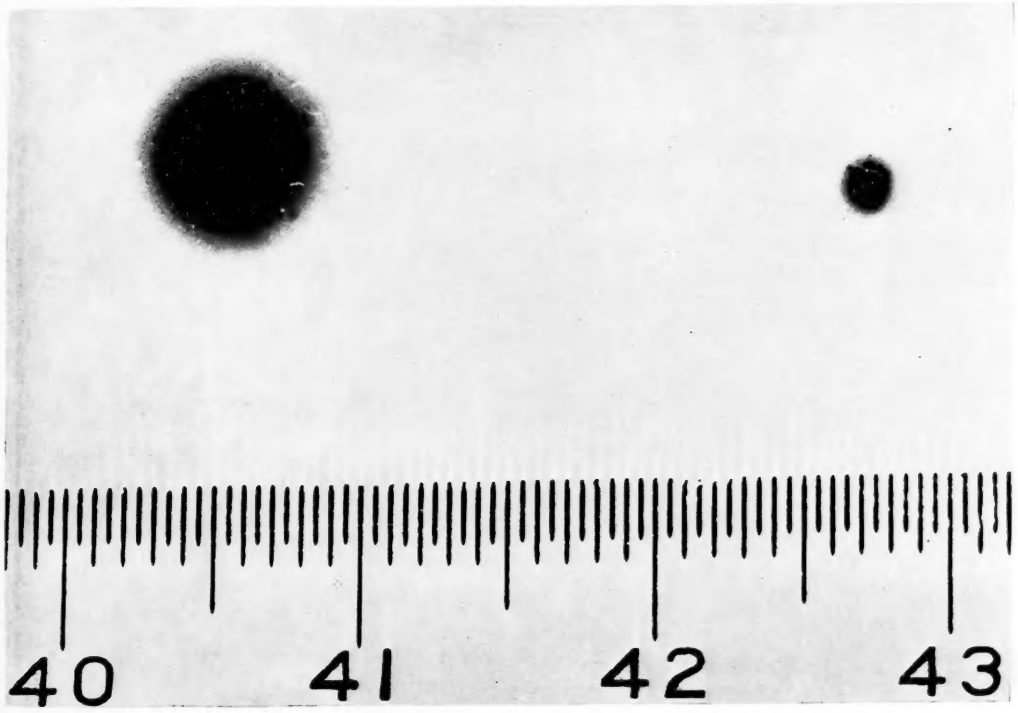

FIG. 6. Autoradiographic image density about a 1 mm diameter P^{32} source. Fine divisions on the scale are 1/2 mm. Film was clamped between Lucite blocks during exposure. The exposure for the left-hand image was 90 times that for the right-hand image. The subtle gradation in density within the dark area does not reproduce well, but densitometer readings* on the original film show that there is a continuous decrease in density, with an absorption coefficient (see text) of about $\mu = 11{\cdot}4\ cm^{-1}$. No darkening is seen at a radius of 8 mm, corresponding to the maximum range of P^{32} β^-particles. This figure is presented as a scaled-up ($\times 1000$) depiction of relative radiation doses about a 1 μ diameter source of tritium.

* Densitometer measurements taken by M. SLAVIN.

VOL.
7
1959/6

that the relative effect of the more energetic particles is enhanced. Thus it is to be expected that the nuclei located close to the emulsion will show not only the greatest grain density, but also the highest resolution and the least image spread, whereas those at intermediate depths will show the maximum image spread.

REFERENCES

1. Fitzgerald P. J., Simmel E., Weinstein J. and Martin C. *Lab. Investigation* **2,** 181 (1953).
2. Taylor J. H., Woods P. S. and Hughes W. L. *Proc. Nat. Acad. Sci., Wash.* **43,** (1), 122 (1957).
3. Bond V. P., Fliedner T. M., Cronkite E. P., Rubini J. R., Brecher G. and Schork P. K. *Acta Haemat.* **21,** 2 (1959).
4. Cronkite E. P., Bond V. P., Fliedner T. M. and Rubini J. R. *Lab. Investigation* **8,** 263 (1959).
5. Atlas M., Bond V. P. and Cronkite E. P. Incorporation of tritiated thymidine in uterine and embryonic tissues of the mouse. *J. Histochem. Cytochem.* In press (1959).
6. Doniach I. and Pelc S. R. *Brit. J. Radiol. N.S.* **23,** 184 (1950).
7. Lamerton L. F. and Harriss E. B. *J. Photogr. Sci.* **2,** 135 (1954).
8. Harriss E. B. *Medicamundi* **2,** 1–8 (1956).
9. Nelms A. T. Energy loss and range of electrons and positrons. *NBS Circular* **577** (1956).
10. Jenks G. H., Ghormley J. H. and Sweeton F. H. *Phys. Rev.* **75,** 701 (1949).
11. Loevinger R. *Physics in Medicine and Biology* **1,** 330 (1957).
12. Tonna E. A. and Cronkite E. P. *Stain Tech.* **33,** 255 (1958).
13. Robertson J. S. and Hughes W. L. *Proceedings of the National Biophysics Conference*, p. 278. Yale University Press (1959).

OL.
7
9/60

International Journal of Applied Radiation and Isotopes, 1959, Vol. 7, pp. 38–42. Pergamon Press Ltd. Printed in Northern Ireland

Use of Tertiary Alkyl Primary C_{12}–C_{14} Amines for the Assay of $C^{14}O_2$ by Liquid Scintillation Counting

R. A. OPPERMANN,* R. F. NYSTROM,† W. O. NELSON* and R. E. BROWN*
University of Illinois, Urbana

(*Received* 25 *March* 1959)

The use of Primene 81-R (Rohm and Haas Co., Philadelphia, Pa., U.S.A.), a mixture of tertiary alkyl primary long chain (C_{12}–C_{14}) amines, as a reagent for the quantitative trapping and scintillation counting of $C^{14}O_2$ is described. The 160°C *in vacuo* distillation of Primene 81-R yields a colorless distillate which when diluted with methanol to a molarity of from 0·25 to 2·0 rapidly and quantitatively traps CO_2. The Primene–$C^{14}O_2$ complex is stable at 25°C and compatible with scintillation fluid composed of 3 g 2,5-diphenyloxazole per liter of toluene. Primene 81-R causes little or no quenching when used in the concentrations recommended.

VOL.
7
1959/

L'USAGE D'AMINES PRIMAIRES À CHAÎNE ALKYL TERTIAIRE (C_{12}–C_{14}) POUR LE DOSAGE DE $C^{14}O_2$ PAR COMPTAGE À L'AIDE D'UN SCINTILLATEUR LIQUIDE

On décrit l'usage du Primène 81-R (Rohm et Haas Co., Philadelphie, Pa., U.S.A.), un mélange d'amines primaires à longue chaîne alkyl tertiaire (C_{12}–C_{14}), comme réactif pour l'absorption quantitative et le comptage par scintillation du $C^{14}O_2$. La distillation sous vide à 160°C donne un distillat incolore qui, dilué dans du méthanol, à une molarité de 0,25 a 2, absorbe rapidement et quantitativement le CO_2. Le complexe Primène–$C^{14}O_2$ est stable à 25°C et compatible avec le liquide scintillateur composé de 3 g de 2,5-diphénylazole par litre de toluène. Le Primène 81-R provoque un affaiblissement nul ou très réduit de la lumière quand il est employé aux concentrations recommandées.

ПРИМЕНЕНИЕ ТРЕТИЧНОГО АЛКИЛА ПЕРВИЧНЫХ C_{12}–C_{14} АМИНОВ ДЛЯ АНАЛИЗА $C^{14}O_2$ ПРИ ПОМОЩИ ЖИДКОГО СЦИНТИЛЛЯТОРА

Описывается применение Примена (Primene 81-R; Rohm and Haas Co. Philadelphia, Pa., U.S.A.), который состоит из смеси третичных алкилов первичных длинноцепных (C_{12}–C_{14}) аминов, в качестве реактива для количественного улавливания и измерения $C^{14}O_2$ при помощи сцинтиллятора. Дистилляция Примена в вакууме и при температуре 160°C дает бесцветный дистиллат, который после разбавки метанолом (молярность 0,25–2,0) быстро и количественно улавливает CO_2. Комплекс Примен–$C^{14}O_2$ устойчив при 25°C и применим с сцинтиллирующей жидкостью, состоящей из Э г 2,5-дифенилоксазола в одном литре толуола. Когда Примен 81-R применяется в рекомендованной концентрации, гашение не происходит совсем или очень слабо.

* Department of Dairy Science, College of Agriculture.
† Radiocarbon Laboratory, Graduate College.

ANWENDUNG VON TERTIAEREN ALKYL-PRIMAEREN(C_{12}–C_{14})-AMINEN ZUR UNTERSUCHUNG VON $C^{14}O_2$ DURCH FLUESSIGE FUNKENZAEHLUNG

Die Benutzung von Primene 81-R (Rohm and Haas, Philadelphia, Pa.)—eine Mischung von tertiaeren langkettigen (C_{12}–C_{14})-Aminen—als Reagens fuer quantitative Absorbierung und Funkenzaehlung von $C^{14}O_2$ wird beschrieben. *In vacuo*-Destillierung von Primene bei 160°C liefert ein farbloses Destillat, das nach Verduennung mit Methanol zu einer molaren Konzentration von 0,25 bis 2,0 schnell und quantitativ absorbiert. Der Primene–$C^{14}O_2$-Komplex ist stabil bei 25°C und vertraeglich mit einer Funkenfluessigkeit bestehend aus 3 g 2,5-Diphenyloxazol pro Liter Toluene. In der empfohlenen Konzentration verursacht Primene keine oder nur geringe Loeschung.

DURING investigations using C^{14}-labelled substrates *in vivo* to determine metabolic pathways in animal systems it often becomes necessary to assay for $C^{14}O_2$. Techniques employing flow-gas counting of barium carbonate-C^{14} are cumbersome and time-consuming and therefore are not the method of choice when numerous $C^{14}O_2$ samples are to be processed.

Improved techniques for the assay of $C^{14}O_2$ by liquid scintillation counting[1,2] using an amine-base prepared from Hyamine 10-X (methylbenzethonium chloride) (Rohm and Haas Co., Philadelphia, Pennsylvania) have permitted the relatively rapid assay of $C^{14}O_2$ at low levels of activity. Preparation of the $C^{14}O_2$ trapping agent used in these techniques involves repeated recrystallization of the amine-chloride from toluene prior to the conversion to the amine-base.[2] The hydroxide of Hyamine usually is highly colored which causes "quenching".

The chemistry of primary amines suggests that such compounds might be useful as trapping agents for $C^{14}O_2$, as follows:

$$RNH_2 + \overset{*}{C}O_2 \rightarrow RNH\overset{*}{C}OOH \quad (a)$$

$$RNH_2 + RNH\overset{*}{C}OOH \rightarrow RNH\overset{*}{C}OOH_3NR \quad (b)$$

Recently a mixture of tertiary alkyl primary long chain amines (C_{12}–C_{14}), Primene 81-R (Rohm and Haas Co., Philadelphia, Pennsylvania), has become available commercially. This tertiary amine was selected for study not only for its potential affinity for CO_2 but also because its structure should add to the stability and solubility of the amine–CO_2 product in organic solvents. The following report describes the use of Primene 81-R for the trapping and counting of $C^{14}O_2$.

METHODS AND MATERIALS

A Tri-Carb automatic liquid scintillation spectrometer (Model No. 314X, Packard Instrument Company, LaGrange, Illinois) was used throughout this study. Samples were counted at −8°C in 5 dram screw neck vials having cork lined aluminum faced caps.

Primene 81-R, a red-brown liquid mixture of *t*-amines with an average mol. wt. of 191, was distilled at 160°C *in vacuo* to yield a colorless distillate necessary to minimize quenching. A working solution of 0·25 M Primene in methanol was prepared from the distillate and was used as the $C^{14}O_2$ trapping reagent.

The gas samples were passed through an analytical train and the $C^{14}O_2$ was trapped in methanolic Primene contained in a gas washing bottle equipped with a fine sintered glass sparger. Total CO_2 was quantitated by adding 1 ml of the Primene–CO_2 reaction product to 10 ml of methanol and titrating with aqueous 0·1 N NaOH to a thymolphthalein endpoint. The meq. of CO_2 was calculated from these data corrected by a blank titration.

A second 1 ml aliquot of the Primene–CO_2 complex was added to 13 ml of scintillation fluid and counted at high-voltage tap 3 (810 V) or tap 4 (890 V) using discriminator setting of 10–50 V and 50–100 V. The scintillation fluid was prepared by dissolving 3 g of 2,5-diphenyloxazole (PPO) in 1 l. of high purity toluene. The specific activity of the $C^{14}O_2$ (dis/min/mM) was calculated from the titration and spectrometer data.

RESULTS AND DISCUSSION

The CO_2 trapping capacity of Primene was tested by volumetric analysis of known gas mixtures and by recovery of CO_2 released from known quantities of Na_2CO_3 acidified in a closed system. An average of 95 per cent of the CO_2 was trapped in 10 ml of 0·25 M methanolic Primene contained in the first collection vessel when a gas mixture of 52 per cent of $C^{14}O_2$, 24 per cent CH_4 and 24 per cent air was passed through the analytical train at a rate of 100 ml/min. Only minor quantities of $C^{14}O_2$ were encountered in the second and third collection vessels of the gas train. The CO_2 titration values averaged 2 to 3 per cent higher than the values obtained when CO_2 was released in a high vacuum line and measured manometrically. The data indicate that 1 mole of Primene will trap at least 1 mole of CO_2.

The Primene–$C^{14}O_2$ complex is stable and no loss of activity occurred when the complex was stored at 25°C for periods up to 14 days. Similarly, no loss in activity occurred when 1 ml of Primene–$C^{14}O_2$ complex was added to scintillation fluid and the resultant solution stored at −8°C for 14 days. It should be noted that an apparent loss of activity which was encountered in the sample of 0·10 mM $C^{14}O_2$ sample on the sixth and fourteenth day of storage at −8°C could not be verified by three additional trials. Therefore, the apparent decrease in activity at −8°C is considered as an artifact associated with this one preparation. The loss in activity of 0·22 mM concentrations of $C^{14}O_2$ held in scintillation fluid at 25°C was not appreciable until after 2 days of storage. Thereafter the activity of the sample decreased rapidly with time. Approximately 90 per cent of the activity of smaller concentrations of $C^{14}O_2$ trapped by Primene and added to scintillation fluid was lost when such samples were stored at 25°C for 1 day. These data are shown in Table 1.

TABLE 1. Stability of Primene–$C^{14}O_2$ complex in scintillation fluid held at −8° and 25°C

$C^{14}O_2$	Specific activity*	Storage temp.	Disintegrations/min after storage for:						
			0 Days	1 Day	2 Days	3 Days	4 Days	6 Days	14 Days
(mM)	(dis/min/ mM)	(C°)							
0·2295	234,874	−8	44,921	53,652	53,593	53,710	52,988	53,228	53,467
0·2295	234,714	+25	48,673	47,033	47,367	34,794	24,795	10,035	1,441
0·1001	203,412	−8	16,887	19,190	19,715	19,533	19,729	12,480	184
0·1001	203,412	+25	16,835	1,265	78	44	46	31	32
0·0353	13,054	−8	465	461	485	466	482	517	500
0·0353	13,054	+25	426	53	44	23	22	36	29
0·1011†	203,412†	+25	19,595	19,420	19,319	19,440	not tested	19,590	19,668

* Separate determination.

† 1 ml Primene–$C^{14}O_2$ complex added to 13 ml scintillation fluid each day and counted.

Conditions: 1 ml of 0·25 M methanolic Primene–CO_2 complex was made up to 14 ml with PPO scintillation fluid. Duplicate samples were stored at −8 and +25°C. The radioactivity of each sample was measured on the day shown.

The loss of activity which occurred when Primene–$C^{14}O_2$ complex was diluted with scintillation fluid and held for several days at 25°C was eliminated by flame-sealing the samples in glass ampoules. The activity could also be stabilized in scintillation fluid by using larger aliquots of the Primene–$C^{14}O_2$ complex or by the addition of unreacted 0·25 M methanolic Primene. The activity of $C^{14}O_2$ trapped in 1 M Primene remained constant when the complex was diluted with scintillation fluid and stored in capped counting vials at 25°C. These data are

VOL. 7 1959/

shown in Table 2. As shown, an increase in disintegrations/minute occurred in the samples to which unreacted Primene solution had been added. This increase was due to the quenching effect of the Primene solution which has displaced the spectral curve for Primene in methanol were examined is attributed to the quenching effect of the methanol. These data are presented in Table 3.

During the course of this investigation a report detailing the use of Primene 81-R as

TABLE 2. Effect of concentration Primene on stability of Primene–$C^{14}O_2$ complex at 25°C

Additions		$C^{14}O_2$	Specific activity‡	Disintegrations/min after storage for:				
Primene–$C^{14}O_2$* (ml)	Unreacted Primene (ml)	(m/M)	(dis/min/mM)	0 Days	2 Days	4 Days	5 Days	6 Days
2	0	0·2002	203,412	32,851	31,745	30,461	27,801	27,886
4	0	0·4004	203,412	74,452	75,264	73,837	68,353	68,833
6	0	0·6006	203,412	100,358	102,770	101,075	94,269	94,491
1	1	0·1001	203,412	13,202	13,110	13,069	12,319	12,619
1	3	0·1001	203,412	14,396	14,759	14,635	14,146	14,000
1	5	0·1001	203,412	18,412	18,434	17,346	15,840	16,071
1†	0	0·0287	169,665	4,816	4,936	—	4,885	4,832
1†	0	0·2197	106,541	23,003	23,424	—	22,989	23,358

* 0·25 M Primene–$C^{14}O_2$ complex diluted as indicated with unreacted 0·25 M Primene and made to a total volume of 14 ml with scintillation fluid.

† $C^{14}O_2$ trapped in 1 M methanolic Primene and diluted with scintillation fluid as above.

‡ Separate determinations.

C^{14} to include more pulses in the 10–50 V window.

The use of undiluted Primene as a trapping agent would cause a moderate quenching. The slight quenching observed when from 0·25 M to 2·0 M concentrations of a reagent for the liquid scintillation counting of sulfuric acid was published.[3] The data presented in the present report detail the use of Primene 81-R as an analytical trapping reagent for the liquid scintillation counting of $C^{14}O_2$.

TABLE 3. The quenching effect of Primene 81-R and methanol

Sample no.	Standard* (ml)	Methanol (ml)	Primene (Molarity)	Primene (g)	Activity (dis/min)
1	1	—	—	—	5,250
2	1	—	—	0·048	5,115
3	1	—	—	0·8084	4,829
4	1	—	—	1·6168	4,292
5	1	1	0·25	0·048	4,990
6	1	1	0·50	0·096	4,982
7	1	1	1·00	0·192	4,934
8	1	1	2·00	0·348	4,875
9	1	3	0·25	0·144	3,648
10	1	6	0·25	0·288	2,297

* 5,230 disintegrations/min.

Conditions: All samples were made up to 14 ml by the addition of PPO scintillation fluid (3 g/l. toluene). Each sample was counted under the same conditions in the Tri-Carb scintillation counter.

SUMMARY

In vacuo distillation of Primene 81-R at 160°C yields a colorless mixture of primary amines which is suitable for the trapping and subsequent counting of $C^{14}O_2$ in liquid scintillation counters.

The mixture of amines has a great affinity for $C^{14}O_2$ thus allowing fast absorption and good recovery. The Primene–$C^{14}O_2$ complex is stable at 25°C for at least 14 days. However, appreciable loss of $C^{14}O_2$ occurred when the Primene–CO_2 compound was added to scintillation fluid and stored at 25°C for 24 hr. When similar samples were stored at −8°C the loss was negligible. Stability at 25°C was greatly increased by use of a higher concentration of the amine.

REFERENCES

1. Fredrickson D. S. and Ono K. *J. Lab. Clin. Med.* **51,** 147 (1958).
2. Passman J. M., Radin N. S. and Cooper J. A. D. *Analyt. Chem.* **28,** 484 (1956).
3. Radin N. S. and Fried R. *Analyt. Chem.* **30,** 1926 (1958).

VOL.
7
1959/6

technical notes

Precision Blood Volume Procedure using RIHSA

(*Received* 16 *April* 1959)

THIS laboratory has been concerned with increasing the accuracy, reducing the work time, decreasing the radiation exposure, and making more economical the blood volume test utilizing radioactive human serum albumin (RIHSA). By employing a spacer in a scintillation well counter for geometrical attenuation instead of a volumetric standard, many of the concomitant errors of the latter are eliminated.[1-6] Present sensitivities of the system allow the usage of as small as 3 μc of I^{131} in the test if 1 min counts are desired with ± 2 per cent P.E. statistics. All disposable items such as syringes, needles, and plastic test tubes are used, considerably reducing the cleaning and assembly time. Kits or packs are assembled awaiting immediate usage.

Experimental

Materials (Fig. 1, opposite p. 44):

3 μc RIHSA*

1 ml isotonic sodium chloride† solution (sterile)

One 2 ml plastic disposable syringe‡ with 20 gauge needle, $1\frac{1}{2}$ in. long

One 5 ml plastic disposable syringe* with 20 gauge needle, $1\frac{1}{2}$ in. long

One plastic test tube, 3/8 in. O.D., 4 in. long with metallic screw-caps calibrated for 5 ml†

One Wintrobe tube

One sterile plastic test tube‡, 3/8 in. O.D., $1\frac{1}{2}$ in.

Apparatus:

One Scintillation Well Counter 2 in. $\times$ 2 in. NaI (Tl)

One Scaler

One Aluminum Tube Spacer, 5/8 in. O.D., $\frac{1}{2}$ in. I.D., 8 in. long.

* Volk Radiochemical Company, Chicago, Illinois.
† Abbott Laboratories, Oak Ridge, Tennessee.
‡ Tomac Disposable, Type 41741.
* Tomac Disposable, Type 41767.
† Atomic Accessories, Inc.
‡ Lusteroid Corporation, Maplewood, New Jersey.

Procedure:

(1) Withdraw approximately 3 μc RIHSA from dose bottle with 2 ml syringe and Q.S. to 1 ml with isotonic sodium chloride if necessary.

(2) Inject contents into sterile plastic tube and count in aluminum spacer, 7 in. above bottom of well for 1 min.

(3) Withdraw contents of test tube into 2 ml syringe and inject contents into antecubital vein. Flush syringe with patient's blood at least once.

(4) Count used empty plastic test tube in spacer for 1 min.

(5) Count empty 2 ml syringe with needle in spacer for 1 min.

(6) Withdraw, without stasis, 6 ml of blood in 5 ml syringe from antecubital vein in exactly 15 min. Inject 5 ml into calibrated plastic test tube and count directly in scintillation well counter for 1 min being careful to shake before counting. Inject sixth ml into Wintrobe tube and centrifuge at 3000 rev/min for 15 min.

(7) Calculate the blood volume from the following:

$$\text{B.V.} = \frac{(C_{1\text{ ml}} - C_{SY} - C_{PT}) \times G}{C_{5\text{ ml}}}$$

where $C_{1\text{ ml}}$ = Net counts/1 min from 1 ml dose in spacer.
C_{SY} = Net counts/1 min from empty syringe and needle.
C_{PT} = Net counts/1 min from empty test tube in spacer.
$C_{5\text{ ml}}$ = Net counts/1 min from 5 ml blood in well.
G = Attenuation factor of 1 ml in spacer to 5 ml in well*.

* The attenuation factor for a scintillation well counter may be derived in the following manner:

(a) Count 1 ml (3 μc) of RIHSA in saline in spacer. Spacer should have shelf 1 in. from top for test tube support.

(b) Remove 5λ (0·005 ml) with pipette and deposit into new plastic test tube with 5 ml saline. Wash pipette twice.

(c) Count 5 ml of new solution in bottom of well

$$G = \frac{C_{\text{well}}}{C_{\text{spacer}}} \times 5 \times 200.$$

(8) Read the hematocrit. Calculate the plasma volume from the following:

Blood volume − [(blood volume) hematocrit] = plasma volume.

(9) The discrepancy between venous and total body hematocrit and the trapping of plasma in hematocrit determination can be compensated for by multiplying the hematocrit by a factor of 0·915. The procedure may be varied to suit the needs of the user. If serial determinations are made, a zero sample must be counted and later subtracted from the 15 min blood sample.

Results

The results of the tests performed on known volumes *in vitro* of blood demonstrated accuracies of ±2 per cent of the measured quantities. Duplicate tests made on patients in short time intervals were reproducible to ±2 per cent.

Normal values used were the following:

Whole blood volume	= 73 ml/kg (± 5 ml)
Plasma volume	= 43 ml/kg (± 5 ml)
Red cell volume	= 30 ml/kg (± 5 ml)

Radioisotope Service T. Fields
Veterans Administration Hospital E. Kaplan
Hines, Illinois, U.S.A. A. A. Imperato

References

1. Crispell K. R., Porter B. and Nieset R. T. *J. Clin. Invest.* **29,** 512 (1950).
2. Berlin N. I., Hyde G. M., Parsons R. J. and Lawrence J. H. *New Engl. J. Med.* **247,** 675 (1952).
3. Kruger S., Baker L. and Mosiman W. D. *Gastroenterology* **21,** 516 (1952).
4. Ross J. F., Chodos R. B., Baker W. H. and Freis E. D. *Trans. Ass. Amer. Physcns.* **65,** 75 (1952).
5. Sherr R. and Gerhart J. B. *Rev. Sci. Instrum.* **23,** 770 (1952).
6. Fields T. and Seed L. *Clinical Use of Radioisotopes*, pp. 47–60. Yearbook, Chicago, Ill. (1957).

Nomogram for Estimating Tissue Dose from Internally Deposited β-Emitting Radioisotopes

(*Received* 23 *October* 1958; *in revised form* 26 *January* 1959)

In biological work involving the administration of radioisotopes to humans it is always necessary to have some knowledge of the estimated radiation dose to the subject.

The accompanying nomogram (Fig. 1, p. 45) makes this estimation possible for any β-emitting radioisotope whose half-life and average energy is known. The average energy is assumed to be one-third the maximum energy. Maximum energy is the value usually given in tables.

The dose is given in rads and is based on the equation

$$D = 74\bar{E}T_{\frac{1}{2}}C$$

where

D = dose in rads absorbed by tissue after complete decay

$\bar{E}$ = average β-ray energy in MeV

$T_{\frac{1}{2}}$ = effective half-life in days

C = concentration of isotope in μc/g.

The nomogram gives dose at infinite time, that is, the worst possible case.

Conversion to dose in roentgens may be easily accomplished by dividing the dose in rads by 0·96.

Use of this nomogram can also be made in the case of very weak gamma or X-ray emitters having energies below 10 keV.

Henry Lanz
Radioisotope Service, Mary Sue McCall
Veterans Administration Hospital,
Dallas, Texas

VOL. 7 1959/6

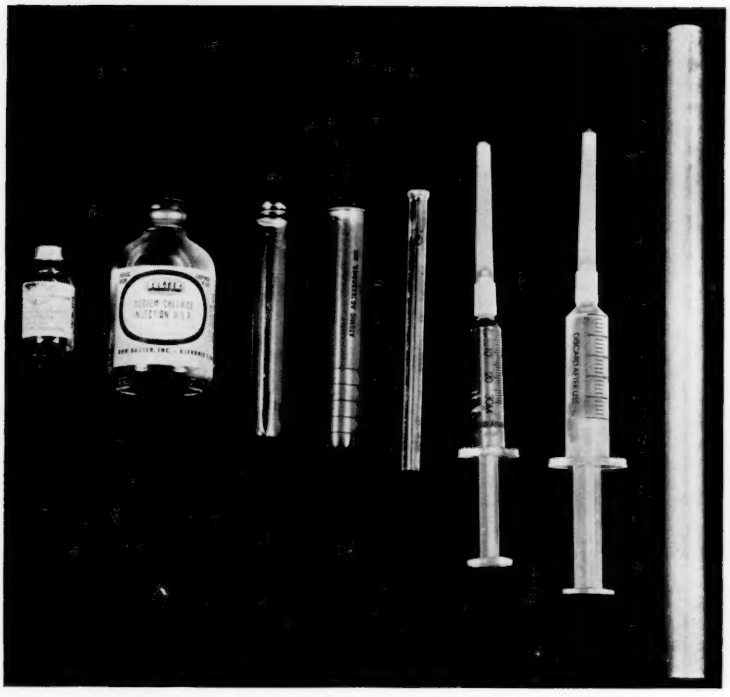

FIG. 1. Materials for precision blood volume procedure.

VOL.
7
1959/

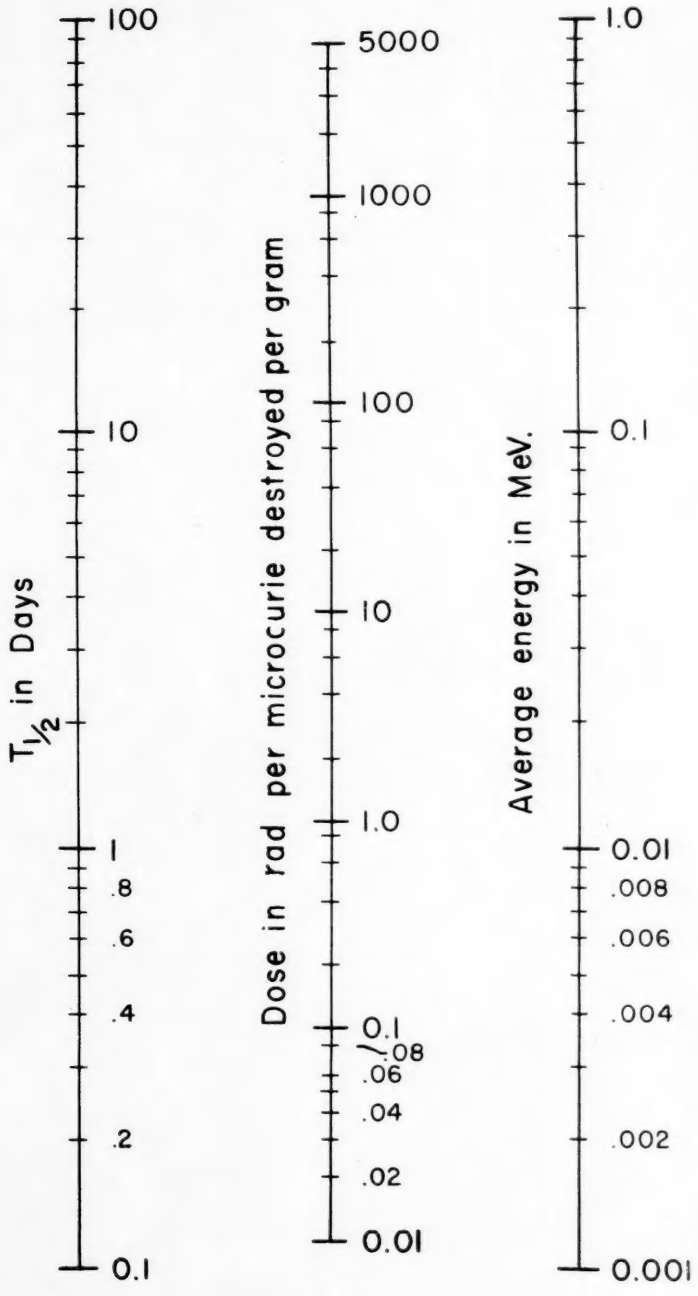

FIG. 1.

OL.
7
69/60

book reviews

D. E. Barnes and Denis Taylor: **Radiation Hazards and Protection.** George Newnes, London, 1958. x + 178 pp. 30s.

This modestly written and pleasantly produced work of twenty-three short chapters, neither too simple nor too recondite, is addressed to all who work with or are interested in radioactive materials or radiation generators. The authors write with clarity and conciseness. Mr. Barnes is Superintendent Health Physics, Aldermaston, and Dr. Taylor a pioneer at Harwell and elsewhere in radiation measurement and dosimetry and in electronics since the early days of radar.

No book of this length can deal with all aspects of radiation hazards and protection and it says nothing, for example, about practical methods of decontamination and of dealing with radioactive spillages, about fire risks, or about the interesting recent developments in medical and chemical methods of treating severely over-exposed radiation workers. Most surprising however in a book with this title is the heavy bias towards protection requirements in radiochemical laboratories to the virtual exclusion of X-ray hazards and protection which receive little more than passing reference. Medical and industrial users of X-rays account for approximately half the number of premises using ionizing radiations and they and many industrial users of radioactive thickness gauges, static eliminators, radiographic equipment, irradiation caves, etc. will need to refer also for detailed practical guidance to the Hospital Code of Practice (HMSO), to the publications of H.M. Factory Inspectorate and the ILO, and to the invaluable series of U.S. National Bureau of Standards Handbooks.

However, as Dr. Johnson said, "When it shall be found that much is omitted let it not be forgotten that much is likewise performed.". Early chapters on the nature and properties of radiation, radioactivity, units, (the "rep" surely is now obsolete), lead up to a particularly well balanced treatment of biological effects and permissible doses. It is a pity that the imminent publication of revised ICRP recommendations will slightly alter the latter and their control periods.

Effective radiation protection turns largely on accurate measurement and dosimetry and efficient instrumentation and monitoring. The middle chapters deal with these aspects in a most competent manner. Apart from a misprint of "100" for "1000" volts as the Geiger counter plateau (p. 54) the only criticism here is that the authors skate far too lightly over the admittedly difficult subject of beta dosage estimation. There follow valuable chapters on laboratory and shielding design, personal protection, contamination, sampling and radioassay, waste disposal, transport of active material and radiation from nuclear weapons.

This book appears most opportunely when at long last national authorities in the United Kingdom and elsewhere are promulgating a whole series of regulations or codes of practice covering the safe use, transport and disposal of radioactive materials in factories, hospitals, universities, technical colleges and schools, and when the ILO, the IAEA, and many other international bodies are publishing their Model Codes on various aspects of radiological protection. It should prove particularly useful to the "competent persons" so beloved of our legislators.

Kenneth L. Goodall

Symposium on Information Theory in Biology (Edited by Yockey H. P.). Pergamon Press, London, 1958. 418 pp. 80s.

Information theory is now well established in the field of communication engineering and has also received considerable recognition in psychology. The idea of thinking explicitly in terms of some suitably defined (and preferably quantitative) concept of "information" arises quite naturally in the context of transmitting ordinary written messages. In communication problems we want to know how much information there is to start with, how much will arrive, what the effect of "noise" will be, how large the channel should be, what information may be lost in using cipher, and so on. Again, in psychology there is a very similar state of affairs in studying the problems of perception and learning. The real difficulties arise when attempts are made to extend the application of information theory to a much wider domain.

There is a rapidly increasing literature on the comparatively new subject of cybernetics, of which information theory is an important part. Reactions vary from undiluted enthusiasm to angry disapproval! A strong emotional element is involved because a different way of looking at things is entailed. And this calls in question long-established patterns of thought. Statistics has in the past met with a similar response (and to some extent still does). There is a certain similarity here, in that both statistics and information theory attempt to deal explicitly with the diversity of their subject matter. But a vital distinction is that while statistics tries to establish various patterns and laws *in spite of* the diversity, information theory deals directly with the diversity as an essential

VOL.
7
1959/

ingredient, without which communication (in the broadest sense) would be impossible.

Considered in detail, the application of information theory to new fields seems highly promising. In the opinion of the reviewer, it is well worth taking seriously, especially in subjects like biology and medicine where the basic material is essentially multifarious. What may finally emerge is still a matter for speculation.

The *Symposium on Information Theory in Biology* presents a fascinating collection of over thirty papers, starting off with an elementary introduction to the subject in Part I. In Part II, dealing with "Storage and Transfer of Information", there are discussions of a cryptographic approach to the problems of protein synthesis, negative feedback in liver regeneration, and fluctuations in neural thresholds. Part III contains a number of biochemical applications, including the discrimination of states and reactivities at low temperatures, the pathways of co-factors, and antigenic specificity. Parts IV and V cover several aspects of radiation phenomena, such as the inactivation of proteins, ageing, thermal killing, mutation and cancer. Part VI investigates a probability model for morphogenesis and the determination of pattern in mosaic receptors. This is then followed by a short general discussion.

It will be seen that a very wide range of topics is subjected to the information theoretic approach. The total effect, on the reviewer at any rate, is extremely stimulating and encouraging. It must be admitted, however, (as indeed explicitly indicated in the discussion) that information theory has not so far produced any new facts or results in the biological field, although there are many cases in which the new approach will produce known results more easily. At the same time one feels intuitively that the new way of looking at things does provide fresh insights that may easily prove extremely fruitful.

The main obstacle to handling biological investigations quantitatively is the inescapable variety and complexity of the material. Some difficulties have been overcome by a judicious use of statistical theory. A great many others seem likely to yield in due course to the methods of information theory. For this reason the application of information theory to biological problems is well worth serious consideration. And the *Symposium* under review goes a long way towards encouraging the understanding and development of this new approach.

NORMAN T. J. BAILEY

E. H. QUIMBY, S. FEITELBERG and S. SILVER: **Radioactive Isotopes in Clinical Practice.** Lea and Febiger, Philadelphia, 1958. 451 pp. $10.00.

THE authors have had a wide and varied experience in the use of radioactive materials in medicine. This background has resulted in an authoritative and well conceived book. Many of the procedures which involve the use of radioactive materials in diagnosis and therapy have been original contributions by the authors.

Approximately one-half of the book is devoted to the basic physics related to radioactivity, its measurement, interaction with matter and radiobiology. The text is written clearly and permits the reader with the ordinary scientific background to achieve a good understanding of radiation physics.

Part two is concerned more directly with specific instrumentation for making measurements *in vitro* and *in vivo*.

The final section is devoted to clinical applications and has been written for the physician who has had little or no previous training or experience in the use of radioactive isotopes and whose background in mathematics is limited. The techniques for estimating thyroid function make up by far the greatest part of the discussion. However other diagnostic and therapeutic uses are described and an adequate bibliography given to permit consultation of original published material.

This book should find an important place in the libraries of physicians interested in entering the field and will serve as a reference book for those already using radioisotopes in clinical medicine.

JOHN A. D. COOPER

WILLIAM H. BLAHD, FRANZ K. BAUER and BENEDICT CASSEN: **The Practice of Nuclear Medicine.** Charles C. Thomas, Springfield, Ill.; Blackwell, Oxford; Ryerson Press, Toronto, 1958. xix + 407 pp. 95s.

IN an introduction to this book Paul C. Aebersold of the United States Atomic Energy Commission remarks "In the field of medicine over a million patients per year are being diagnosed or treated with radioisotopes". The authors of the book, who have evidently had wide first-hand experience, survey critically a large number of the diagnostic and therapeutic procedures, involving radioactive isotopes, to which these patients are being submitted. About 200 pages are devoted to discussions of some 35 types of diagnostic procedure, 100 pages to therapeutic methods and 100 pages to basic physical principles, instrumentation, handling and laboratory design. As the title indicates, emphasis throughout is on medical practice, but the authors endeavour to give the historical background for the various isotope techniques and to emphasize their limitations as well as their advantages.

A reader's chief impression from the diagnostic

section must be that so much ingenuity has had, as yet, a disappointing reward. For example, in a chapter of 27 pages on "Tumour localizing procedures" diagnostic tests for 10 different sites in the body are described in careful detail. Yet of these it is evident that the authors can at present recommend, without considerable qualification, only two as clinically practical, namely the localization of brain tumours using in particular radio-iodinated human serum albumin and the localization of cerebrospinal fluid fistulae also by means of RIHSA. The authors' comments on tests for the diagnosis of abnormal gastrointestinal function range from "indications for this test are somewhat limited", applied to the determination of gall bladder function using I^{131} di-iodofluorescein or I^{131} labelled rosebengal, to quite enthusiastic support for the use of the latter compound in a test of liver function. Similar critical appraisal is given to isotope methods that have been tested in the diagnosis of haematological disease, abnormal cardiovascular and renal function, thyroid function and to isotope dilution techniques. Since about nine of the tests described involve RIHSA it is surprising to find no reference to the possibility of self-radiation effects in this compound. It is also surprising that no mention is made of Co^{58} as a practicable, shorter lived substitute for Co^{60} in labelled vitamin B-12.

In the shorter therapeutic section of the book, the treatment of hyperthyroidism, of euthyroid cardiac disease and the management of thyroid cancer with radioactive iodine are quite fully discussed from the clinical point of view. The useful account of the therapeutic uses of colloids rightly draws attention to the possible advantages of chromic phosphate P^{32} over colloidal gold Au^{198} and to the technical difficulties met in the attempts to produce satisfactory yttrium Y^{90} colloids. The authors point out that for the proper therapeutic use of discrete radioactive sources, by implantation, applicators or teletherapy, the resources of a large medical centre are necessary, and for this reason they give only a summary of recent advances in this field. They suggest that "source therapy is still in its infancy; the boundaries of this vast field have yet to be explored."

Laboratories and counting equipment are systematically, if superficially, described, but the chapter devoted to units, dosimetry and radiation biology is very brief (9 pages) and only one reference is given. The authors refer from time to time to the possible radiation hazards of radioactive isotope diagnostic tests, but remark "clearly, present methods of determining maximum allowable doses of isotopes in medicine rest on a shaky foundation". They feel that "perhaps a sounder approach" (p. 40) is to administer the least quantity, in a specific diagnostic procedure that will give a useful answer. In discussing the treatment of haemolytic and malignant disease with radioactive phosphorus, the curious statement (p. 281) is made "1 μc of radiophosphorus is equal, in terms of ionisation, to 37 r of X-ray". There is an alchemical air about their remark that P^{32} "may be produced by the exposure of stable sulfur to the emanations of a uranium pile". The emphasis is undoubtedly on medicine rather than the nucleus and readers will need to go elsewhere, particularly to the original literature, for many technical details and virtually the whole of dosimetry.

However, the book, which is beautifully produced and has more than 100 illustrations and 400 references, should prove useful to many physicians and other medical men as a guide to the role of radioactive isotopes in medicine at the present time.

N. G. Trott

Notes for Authors (Revised edition). Institute of Physics, London, 1959. 36 pp. 3s. 6d.

The Institute of Physics has just published a 36-page revised edition of its booklet to assist less experienced authors and to serve as a reference booklet for all those who wish to contribute to the Institute's publications. Under its new title "Notes for authors", it gives hints on the preparation of scripts and diagrams, on the layout of mathematics, the correction of proofs and so on. In addition to a bibliography of reference books and works on technical writing, the pamphlet also contains lists of the spellings, symbols and abbreviations used by the Institute.

Copies of this booklet are obtainable from The Institute of Physics, 47 Belgrave Square, London, S.W.1, price 3s. 6d, including postage.

Source Material for Radiochemistry. Nuclear Science Series Report No. 27 (March 1959). 23 pp. *Available free from:* Division of Physical Sciences, National Research Council, 2101 Constitution Ave., Washington 25, D.C., U.S.A.

This is a compilation of references by a subcommittee of the U.S. National Academy of Sciences in "an attempt to list current source material of interest to the radiochemist". It consists mainly of references to review articles, conference reports and symposia with very brief abstracts and details of availability of each publication.

The present list contains almost exclusively American references (all but four), but future revision is anticipated and the compilers invite suggestions of other references to be added to the list.

J. L. Putman

VOL. 7 1959/6

International Journal of Applied Radiation and Isotopes, 1959, Vol. 7, pp. 49–75. Pergamon Press Ltd. Printed in Northern Ireland

Report of Meeting*

International Atomic Energy Agency Conference on the Application of Large Radiation Sources in Industry and Especially to Chemical Processes

Warsaw, Poland, September 1959

THE Conference on the Application of Large Radiation Sources in Industry and Especially to Chemical Processes took place in Warsaw, Poland during 8–12 September, 1959. It was the first world-wide conference sponsored by the International Atomic Energy Agency and it drew the participation of some 160 nuclear scientists and engineers from twenty-four countries and six international agencies.

Despite numerous pre-conference problems that beset the organizing group in its maiden effort, the conference was a success from almost every point of view. The language barrier was largely overcome by simultaneous translations of the proceedings into French, English, Russian and Spanish. Abstracts and preprints of most papers were available in advance of their presentation; there was usually adequate time for questions and comments from the floor; there was a great deal of informal discussion between the delegates; also the host country and the Agency provided physical circumstances for the conference that were always comfortable and frequently elegant.

There was one major shortcoming, a shortcoming that is common to all scientific meetings other than the justly famed Gordon Conferences. There was a detectable tone of almost diplomatic formality during the meeting. Thus, floor discussions were somewhat less vigorous than they could have been and there was very little open disagreement between members of a delegation. The result is that several "promising applications" in the chemical and food field that were treated quite severely in private discussions will emerge almost unscathed in the official transcript of the proceedings.

The papers covered the fields of source technology, chemonuclear reactions, radiation effects of polymers, radiation-induced polymerization and grafting, radiation chemistry, radiation cost studies, and biological, medical and food applications. The papers were not limited to nuclear radiation; two United States contributions (CW/IVB/63) and (CW/IIIp/71) were devoted to successful electron machine applications and another (CW/IIA/72) recommended the use of ultraviolet light and chemical sensitizers for many grafting and cross-linking applications that are usually performed with hard radiation.

Source technology

Several papers were presented describing large γ-source installations for research and processing. Major interest was focused on a joint industry–government facility in France (CW/Ipl/40). Designed for 100,000 c of Co^{60}, it is to be completed in 1959 and used mainly for food processes that the industrial group believes to be of real commercial value. Also to be completed shortly (1959–1960) is the Westminster Carpet Co^{60} facility in Australia and a similar installation at the Wantage

* Report prepared by JOSEPH SILVERMAN.

Laboratory in England. Both will house 150,000 c sources. The Australian source is to be used for the irradiation of goat's hair to eliminate anthrax; the Wantage source is an experimental demonstration device.

Among the papers presented on the properties of large radiation sources, there are a few contributions that merit special mention. The potential value of extended β-sources in low dose applications as well as the dose and efficiency equations for such sources were presented in a U.S. paper (CW/I/69). Because of initially favorable developments in this field, Dr. PAUL AEBERSOLD, Head of the U.S. delegation, announced that the USAEC currently plans to build a large demonstration β-irradiator in 1962.

Comprehensive parametric studies of the properties of slab irradiators of various γ-emitters were described in another U.S. paper (CW/I/70). The calculations were within 5 per cent of dosimetric measurements on low level mockups of several source–target arrangements. This work represents a laudable program to develop detailed handbook information for source designers. An independent treatment of the same problem by more approximate methods was presented in a U.S.S.R. paper (CW/Ipl/79).

Chemonuclear reactions

A lively discussion followed three fine papers on chemonuclear reactions (CW/Ip2/13, CW/Ip2/23, CW/Ip2/24). It was the conclusion of the panelists that of the reactions considered thus far, only nitrogen fixation offered any industrial promise. United Kingdom and Belgian representatives felt that economic production of nitric acid could only be accomplished as a byproduct in a multipurpose nuclear reactor. The U.S. panelist held the view that the possibility of a practical single purpose reactor for nitric acid production could not be ruled out.

Plastics and elastomers

The session opened with an excellent survey paper by CHARLESBY (U.K.), outlining the accomplishments, opportunities and problems in the plastics field.

Another interesting paper of the British (CW/IIA/8) described a low dose method for cross-linking of PVC with diallyl and triallyl esters.

A Japanese study (CW/IIA/31) of the free radical concentration in irradiated high polymers using electron spin resonance techniques is also noteworthy. According to the authors, the trend of the measured free radical yield for the series of polymers investigated is opposite to that of the published *G*-values for cross-linking. These results conflict with U.S. data which show an opposite trend and also U.K. work that shows no correlation between the two variables.

A U.S.S.R. paper on the radiation-induced vulcanization of silicone rubber with 10–25 Mrad aroused industrial interest. The product is superior to the conventional material and easier to manufacture.

Polymerization and grafting

Almost all the papers in this session are recommended for reading. They range from a Japanese paper (CW/IIB/33d) on energy transfer and ionic polymerization to a detailed U.S.S.R. study (CW/IIB/82) of the radiation-induced polymerization of ethylene with obvious industrial overtones. Other noteworthy contributions include a Hungarian paper (CW/IIB/3) on low dose grafting by the intermittent irradiation technique and a Japanese paper (CW/IIB/36) on grafting to the inner layer of cellulosic fibers using an irradiation pretreatment to accelerate swelling of the fibers by monomer.

Two major impressions were derived from this session. First, it is apparent that the Soviet program to develop a large-scale plant for radiation-induced ethylene polymerization is advancing rapidly. The U.S.S.R. work report was done at higher temperature and pressure conditions than that reported elsewhere. However, despite the good yield and premium quality of the radiation product, there is serious doubt that it can be produced profitably in Western countries. Secondly, there is a strong and effective Japanese effort in radiation applications to plastics and textile manufacturers. Surprisingly, there were no U.S. papers on radiation grafting or polymerization.

VOL. 7 1959/6

Chemical reactions

Perhaps the most stimulating paper in this series was the U.S.S.R. paper (CW/IIB/83) on the irradiation of benzene–water–oxygen mixtures to produce phenol. The work described in the previous literature has been extended considerably and here again it points to what appears to be a determined Soviet effort to realize the process on an industrial scale. A program to carry it one step beyond the bench scale is now in effect. Nevertheless, private conversations and discussions from the floor developed two important points:

(1) Laboratories in England, France, and the United States have thus far failed to obtain with consistency the high *G*-values for phenol production and the pronounced post-irradiation effect reported in the Soviet work.

(2) Even with $G = 70$, (the highest value reported), the requisite plant size according to Western standards leads to source requirements of a few hundred kilowatts, which is impractically large at present.

Another paper of note is the U.S. paper (CW/IIC/14) on the radiolysis of pentane adsorbed on silica gel and zeolites. The product spectrum differs sharply from that of pure pentane for reasons that are still not clear. This work has opened up a new area of radiation chemistry, one that could have broad applications.

A German paper (CW/IIC/50) proposed the use of radiation as a means of synthesizing small quantities of organic chemicals for laboratory rather than commercial purposes. For example exposure of PCl_3 and *cyclo*hexane to large doses (~50 Mrad) converts 25 per cent of the reagents to a product 50 per cent of which is $C_6H_{11}PCl_2$. This is a simpler and neater synthesis than can be achieved by standard methods.

Two papers with possible industrial significance dealt with cracking of normal hydrocarbons (CW/IIC/84-USSR) and the methanation of coal (CW/IIC/1d-USA). Substantial radiation enhancement of both reactions was reported. Similar work on radiation cracking at somewhat lower temperatures and pressures has been described in earlier publications, but whereas the U.S. attitude on the commercial application is negative, the Soviet scientists appear to be pressing for a radiation cracking plant.

Radiation economics

In the brief session on radiation costs, the most comprehensive comparison is to be found in a U.S. paper (CW/IIIp/71). There was also a French analysis (CW/IIIp/41) of the relative merits of Co^{60} and spent fuel elements on a cost basis, an analysis that generally favored Co^{60}. Many will find interest in the U.S. paper (CW/IIIp/54) that details the cost picture on the only irradiated product sold in multimillion pound per year quantities: irradiated polyethylene.

Food

The only paper on food (CW/S/7-USA) brought on an extended discussion. Despite obvious problems, the tone of the speech was optimistic. The optimism seems to be shared by the Russian and French delegations, but not by representatives of the United Kingdom and the Food and Agriculture Organization. The FAO representative briefly summarized the viewpoint of his organization with a statement to the effect that radiation preservation, while it may be a significant factor in advanced food technology, had no obvious role in the food problems of undeveloped countries.

Biomedical applications

From the applied point of view, the U.S. paper (CW/IVB/63) on sterilization of hospital supplies and pharmaceuticals is perhaps the most interesting. The analysis is based on the eminently successful radiation sterilization of sutures by electron beam radiation on a production scale by the Ethicon Company, Somerville, N.J.

Also described were the U.S. program on insect eradication by radiation sterilization of males (CW/IVC/2), U.K. studies of the susceptibility of grain and rice insects to gammas (CW/IVC/76), and γ-induced inactivation of viruses (CW/IVB/65-UK).

ABSTRACTS OF PAPERS PRESENTED AT THE MEETING

A Mobile Irradiator Design Study. F. G. RICE, Commercial Products Division, Atomic Energy of Canada Ltd., Ottawa, Canada.

The need for data on the technical and economic feasibility of commercial potato irradiation using cobalt-60 γ-rays, led to a design and cost study of a mobile irradiator. Investigation of handling and storage of potatoes in major growing areas in Canada and the United States showed that the irradiator should process at least 6000 lb (2700 kg) per hour in bulk or in 100 lb (45 kg) bags. Tests on irradiated potatoes indicated that a dose of 8000 rads would effectively inhibit sprouting at a storage temperature of 68°F (20°C).

Based on source configurations of other AECL irradiation facilities, calculations and measurements of dosage uniformity were made showing that ± 33 per cent variation occurred when using two passes on each side of the line source. The source was designed to have increased activity near the ends. The calculated radiation utilization efficiency was 48 per cent.

A truck-mounted irradiator was studied in some detail and was found to be too heavy for easy transportation. An irradiator using a railroad flatcar and weighing 60 tons (54,000 kg) was then considered. Although its movement is restricted, most potato warehouses are located near railroad sidings and are easily reached by a railroad car.

The processing cost, including depreciation, source replacement and operating costs, was estimated to be 0·9 per cent per lb (2·0 cents per kg) for 1200 hr operation per year. A longer operation time per year results in a decrease in this processing cost. The above figure is based on estimated costs for a prototype unit. Somewhat lower costs are indicated for production irradiators.

Experimental Parametric Study of Large-scale Co^{60}, Na^{24} and Cs^{137} Slab Irradiators. B. MANOWITZ, O. A. KUHL, L. GALANTE, R. H. BRETTON and S. ZWICKLER, Brookhaven National Laboratory, Upton, New York.

There are several important parameters in the design of slab irradiators. Target parameters include capacity (energy input per unit mass per unit time), residence time, minimum dose required, maximum dose variation permitted, target dimensions and target density and composition. Source parameters include source composition (photon energy, source density and atomic number), total activity (curies), average specific activity, activity distribution, source dimensions and source-to-target geometry.

Large-scale slab sources of low-activity level of Co^{60}, Na^{24} and Cs^{137} were assembled. The Co^{60} was in the form of cobalt metal, sp. gr. 8·9, the Na^{24} was in the form of a dilute aqueous solution of $Na_2{}^{24}Co_3$, sp. gr. 1, and the Cs^{137} was in the form of a compressed solid composed of a homogeneous mixture of Cs^{137}, Cl and $BaSO_4$, sp. gr. 2·7. Several static finite slab targets of paraffin wax were used in all experiments. Measurements were made with calibrated instruments of the exposure dose at many points in the target delivered over known periods of time. The specific activity and total activity of the source materials were determined by radiochemical analysis.

Source and target parameters, including source dimensions, source activity distribution and source-to-target geometry, were varied in such a way as to obtain information on specific dose rate and dose distribution in the target. Various absorbers between source and target were also studied.

For calculation purposes, the finite source was divided into a number of line elements. Using the uncollided flux equation with the NDA-NBS build-up factor modified for finite media, the contribution of each element to various points in the target was calculated. The conformity of the experimental data to the theoretical is discussed.

The data were applied to a set of specifications and for a particular design a comparison is made between available Co^{60}, Na^{24} and Cs^{137} sources.

VOL. 7 1959/6

The Technology and Applications of Large Fission Product Beta Sources. JOSEPH SILVERMAN,* Radiation Applications Inc.

Beta emitters have not received consideration as large sources of radiation power because in the past, the radiation processes of interest have been based on particles with high penetration power; hence the great emphasis on gammas and artificially accelerated electrons. About 4 years ago, it became apparent that a broad field of potential applications involving surface radiation treatment was developing, e.g. surface modification of formed plastics by graft copolymerization and surface pasteurization of food. For these applications, penetration in depth is wasteful and potentially harmful. Also there are two other areas for which machine electrons were not well suited: radiation-induced chemical syntheses in pressure vessels, and certain types of free radical chain reactions for which the production rate per kilowatt decreases with the square root of the dose rate. Broad area β-sources showed obvious potential advantages in all these categories and, since they are available in good yield from the fission process, merited a careful re-appraisal.

On the basis of these considerations an AEC sponsored study of the applications and technology of fission product β-sources was performed. The results indicate the following:

(1) There are promising areas for commercial application of fission product β-emitters in the radiation processing field, particularly in the graft copolymerization modification of formed plastic surfaces and textiles.

(2) Massive, rugged, inert, safe, inexpensive β-sources may be fabricated by suitable extensions of existing techniques. Source-bearing glass formulations show particular promise.

(3) β-Absorption calculations indicate that extended sources can be designed with power utilization efficiencies as high as 20 per cent. Equations and curves describing dosage and β-utilization efficiency as a function of the geometry and composition of various source–target systems were developed. An experimental program is in progress to test the validity of the calculations.

(4) An engineering cost analysis indicates that fission product β-power can be competitive with alternative sources of radiation.

* Current address: State University of New York, Oyster Bay, New York.

Effect of Gamma Radiation on Polyethylacrylate. H. HEYNS and V. DESREUX, Laboratory of Physical Chemistry, University of Liége, Belgium.

The effect of γ-radiation (cobalt source) on samples of polyethylacrylate of different molecular weights in the solid state and also in benzene and carbon tetrachloride solutions has been studied. The results are discussed in function of the direct and indirect effects and also in function of the degree of cross-linking. This last effect is detected in concentrated solutions and in the solid state by combined measurements of viscosity and sedimentation.

Chemical Changes of Methacrylamide Under the Influence of Gamma Radiation. A. ORSZAGH, T. ACHMATOWICZ and J. ZURAKOWSKA-ORSZAGH, Polish Academy of Science, Institute of Nuclear Research, Laboratory of Radiochemistry.

Methacrylic acid amide has been submitted to γ-ray irradiation. Physicochemical properties of the product obtained and its infra-red spectrum have been studied. On the basis of these investigations the character of chemical changes in methacrylamide has been determined.

Physical Properties of PVC Attenuated Network Copolymers Produced by Ionizing Radiation. S. H. PINNER, Tube Investments Research Laboratories, Hinxton Hall, Cambridge, U.K.

The cross-linking of polyvinyl chloride with ionizing radiation poses special problems. Due to rather unfavourable cross-linking and dislinking parameters for this polymer, the radiation doses necessary for high cross-link densities are uneconomically large and discoloration and dehydrohalogenation are simultaneously produced.

These difficulties have been overcome by the incorporation into the PVC, prior to irradiation, of diallyl and triallyl esters. Heavily cross-linked products are thereby obtained with relatively low doses of ionizing radiation. Examination of the physical properties of the products suggests that these are not simply graft copolymers, which term normally implies the presence of long branch chains, but are polymer attenuated allyl networks. In these materials, the desirable properties of the parent polymer and of the allyl network are combined.

The tensile strength, modulus and elongation of the attenuated network copolymers are presented and discussed as a function of temperature and of the concentration and functionality of the allyl ester. Reference is also made to the swelling and chemical resistance of the products.

Electron Spin Resonance Study of Radiation Chemistry of High Polymers. SHUNICHI OHNISHI, MICHIE KASHIWAGI, YUICHI IKEDA and ISAMU MITTA, Osaka Laboratories, Japanese Association for Radiation Research on Polymers, 508 Mii, Neyagawa-Shi, Osaka-Fu, Japan.

The electron spin resonance (ESR) spectra of a number of γ-irradiated polymers have been measured to investigate their radiation chemical processes.

(1) *ESR spectra and the identification of the trapped radicals.* The identification has been found to be difficult in many cases because the spectra may be complicated and broaden by several reasons:

(a) Spectra may be the superposition of that of several kinds of radicals. In the case of polyvinyl alcohol (PVA) when the spectra was observed immediately after irradiation had stopped: it was triplet and the intensity ratio was about 1 : 3 : 1. But, gradually, the ratio changed and after 50 days peaks on both sides almost entirely disappeared. This change might mean the existence of two kinds of radicals in the irradiated PVA, one of which has a longer life than the other.

(b) In some cases the spectra of the radicals trapped in the different states of aggregation of polymers have been found to be different.

(c) Spectra were affected by the dose rate at which polymers were irradiated and also by the total dose. Considering these facts, we need first to separate the spectra into components and to assign the radicals and we have tentatively done so in the case of polyvinyl alcohol.

(2) *ESR spectra and the state of aggregation of polymers.* For some irradiated polymers such as nylon, polyethylene and polyvinyl alcohol, spectra of the stretched sample, the unstretched one and the heat treated one seem to be all different from each other; while, in the case of tetoron (polyethylene terephthalate), the stretching, the double orientation and the heat treatment did not make the spectra different. When the two kinds of irradiated tetoron samples, sample A (untreated, crystallinity 5 per cent) and sample B (heat treated, crystallinity 39 per cent), were heated for 40 min at 88°C after irradiation at room temperature, radicals were not found in sample A, while in sample B about 40 per cent of them were still remaining and the shape of the spectra was the same before and after heating. We might think that (a) on warming above the glass transition temperature ($T_g = 70$°C), the radicals trapped in the amorphous region have disappeared, while the radicals in the crystalline region are still alive, (b) the radicals trapped in the different states of aggregation are of the same kind and (c) they show the same spectra. Also we might conclude that the primary processes are the same in both regions.

(3) *Kinetic study of radical formation and radical decay.* We have measured the concentrations of the radicals formed by irradiation against the doses by means of ESR absorption measurements and also calculated the G_R-values (G-values for radical formation) from the initial slope of these curves. For polymethyl methacrylate irradiated at constant

VOL. 7 1959/

dose rate (7×10^5 r/hr), the following equation has been obtained:

$$R = 5{\cdot}8 \times 10^{-7} \tanh (6{\cdot}4 \times 10^{-5}t)$$

where R is the radical concentration in moles/cm^3 and t is the irradiation time in seconds. The rate of decay of the trapped radicals has also been measured at several temperatures. We have estimated the activation energy for the decaying process of the radicals in polymethyl methacrylate to be 28 kcal/mole and it might be concluded that the motions of the chain segments are the rate-determining step of the decaying reaction.

(4) *Conditions of the radicals to be trapped in irradiated polymers.* Higher G_R-values and longer life of trapped radicals might be the conditions for more efficient radical trapping. G_R-values and lives of the trapped radicals for a number of polymers obtained by ESR absorption method were tabulated. Near the glass transition temperature, radicals trapped in amorphous polymers will disappear in the order of magnitude of minutes and above T_g they will disappear so quickly as to be observed. The lifetime τ of the radicals at temperature T might be expressed as

$$\tau = \tau_g(T_g/T) \exp [\{\Delta H^*(1/T - 1/T_g)\}/R]$$

where τ_g means the lifetime at T_g and ΔH^* is the activation energy for the decaying reaction.

(5) *To follow reactions of the radicals with some reagents such as oxygen.* A sudden remarkable change of the spectra has been observed on introducing air to some powdered polymers irradiated in vacuum. Polypropylene, polyethylene, polyvinyl chloride and polymethyl methacrylate are the examples. The change might be interpreted as corresponding to the reaction of such kind as $R \rightarrow RO_2$ or RO. The rate of decay of the oxygenated radicals has been measured and compared with the rate of growth of the carbonyl band in their infra-red spectra.

Role of Electronic Excitation in the Chemical Effects of Radiation on Plastics. GERALD OSTER, Institute for Polymer Research, Polytechnic Institute of Brooklyn, Brooklyn 1, New York.

The chemical effects of ionizing radiation on high polymers are generally regarded to be due both to ionization and to electronic excitation. By employing ultraviolet light as the radiation source one can study the purely electronic excitation factors.

We have examined the chemical effects of far ultraviolet light on the same high polymers which have been studied previously using ionizing radiation. For polyethylene and many other high polymers crosslinking occurs upon ultraviolet light irradiation. The photochemical reactions require the presence of a sensitizer which on photolysis abstracts hydrogen atoms from the polymer substrate.

There are a number of chemical effects of photochemical action which resemble those of ionizing radiation. The differences lie mainly in the special distribution (e.g. amorphous versus crystalline regions, etc.) of the chemical action.

Radiation Effects of Polyvinyl Alcohol. MASAKAZU MATSUMOTO, Kurasiki Rayon Co., Kurasiki, Japan and AKIBUMI DANNO, Japan Atomic Energy Research Institute.

Polyvinyl alcohol (PVA) has been classified by Charlesby as a kind of polymer that became crosslinked by irradiation, but no detailed experimental results about PVA seem to have been reported except for the case of aqueous solution. Many studies of PVA irradiated in dry solid state in Japan show that PVA does not crosslink but degrades even if in vacuum, with the exception of the work by Danno *et al.* Recently the authors in collaboration with I. Sakurada found independently that PVA in dry solid state may crosslink by irradiation under appropriate conditions.

When PVA was exposed to cobalt-60 γ-radiation in air, the degradation process was observed in low radiation dose range (107 r) independently of dose rate. But in high dose range radiation effects were remarkably dependent on dose rate, and crosslinking of PVA occurred more easily the higher the dose rate. On the other hand, irradiation in vacuum caused gelation at a lower dose rate and a lower total dose as

compared with irradiation in air. These results suggest that oxygen plays an important role both in solid state and in aqueous solution. We have, therefore, to consider the influence of oxygen dissolved in aqueous solution and diffused into solid state from the surface of the sample.

It is well known that PVA crosslinks by radiation in the aqueous solution if the concentration is high enough (C 0·3 per cent). However PVA does not crosslink in the dimethyl sulfoxide solution even if exposed to 10^7 r. In the mixtures of dimethyl sulfoxide and water, minimum dose necessary to the gelation of PVA increases with dimethyl sulfoxide content and in 5% dimethyl sulfoxide aqueous solution PVA no longer forms a gel.

Chemical changes of both the irradiated PVA in solid and aqueous solution were studied. The contents of the total carbonyl groups including the ones at the end and in the main chain of PVA, and the carbonyl group only in the main chain were determined by a hydrazone method and an alkali treatment method respectively. The content of carboxyl group was determined by an electric conductivity titration method. The content of the total carbonyl groups in irradiated PVA in air was larger than that in vacuum as expected. The content increased approximately linearly with the total dose in low dose range (10^7 r) independently of the dose rate. The initial rate of increase of the carbonyl groups in aqueous solution was several times larger than in solid state. The proportion of the carbonyl groups in the main chain to the total was about half in the solid state and about 90 per cent in the aqueous solution. The content of the carboxyl groups was much less than that of the carbonyl groups.

Studies on the Gamma-initiated Polymerization of Vinyl Acetate in Aqueous Medium. Seizo Okamura,*† Takuhiko Motoyama,* Tomonobu Manabe* and Hiroshi Inagaki.*

* Department of Textile Chemistry, Kyoto University, Kyoto, Japan.

† Osaka Laboratory, Japanese Association of Radiation Research on Polymers, Neyagawa, Osaka, Japan.

(1) *Gamma-initiated polymerization of vinyl acetate in aqueous solution of uranyl acetate.* From the consideration of the rate and the degree of polymerization of γ-initiated polymerization of vinyl acetate in three systems (vinyl acetate–acetic acid, vinyl acetate–acetic acid–water, and vinyl acetate–acetic acid–water–uranyl acetate), the G-values of each component for the initiation of γ-ray initiated polymerization are estimated as following:

$$G^{\text{initiation}}_{\text{vinyl acetate}} = 10{,}6$$

$$G^{\text{initiation}}_{\text{acetic acid}} = 52$$

$$G^{\text{initiation}}_{\text{water}} = 480$$

$$G^{\text{initiation}}_{\text{uranyl acetate}} = 23{,}000.$$

(2) *Gamma-initiated polymerization of vinyl acetate in aqueous solution of cationic detergent.* Commercial cationic emulsion of polyvinyl acetate has been hitherto obtained by the emulsion polymerization in the aqueous solution of suitable anionic detergent with coexistence of excess cationic surfactant.

Pure cationic emulsion of polyvinyl acetate is here found to be obtained very stably by γ-initiated polymerization of vinyl acetate with the presence of aqueous solution of cationic detergent.

The rates of the cationic and also anionic emulsion polymerization of vinyl acetate are measured in γ-ray polymerization, and the anionic one is found faster than the cationic one.

The Synthesis of Non-random Copolymers in Emulsion System by Gamma Radiation. P. Hayden and R. Roberts, AERE, Wantage Radiation Laboratory, Grove, Wantage, Berks, U.K.

Gamma irradiation of vinyl monomers emulsified in polymer lattices has been shown to be a useful method for the synthesis of non-random copolymers. A number of different systems are considered. The reactions are complete after a relatively small dose and no provision need be made to exclude air. Fractional precipitation techniques have been used to separate the reaction products. The graft copolymers

VOL. 7 1959/

obtained using this technique may have important applications in the polymer industry.

Production of Polymers by Irradiation of Heptane–$TiCl_4$–Monomer Mixtures. J. A. Hearne and R. W. Hummel, AERE, Wantage Radiation Laboratory, Grove, Wantage, Berks, U.K.

Results are given of work in progress on the systems heptane–$TiCl_4$–ethylene and heptane–$TiCl_4$–propylene irradiated with ionizing radiations. Their behaviour with respect to variations in component concentrations, temperature and dose rate, in so far as they affect the yield and properties of the polymer produced, are described.

Synthesis of Graft Copolymers by Small Doses of Irradiation. Dobó János, Somogyi Miklósné and Kiss László, Institute for the Organic, Chemical and Plastic Industries, Budapest, Hungary.

Parallel with radiation grafting there is often an undesirable alteration in the properties of the original polymer. The great degrees of grafting obtained in our laboratories at small doses may therefore be of interest.

In consequence of irradiation there occurs a grafting reaction not only on the original polymeric backbone, but also on the grafted side-chains. The result is an acceleration of grafting. The effect is especially pronounced in the case of preformed polymers, if irradiation is caused out intermittently.

The grafting of styrene can be accelerated by the addition of some solvents suppressing the protecting effect of styrene on the polymer. Grafting can also be accelerated by other additives.

In the grafting of methylmethacrylate into polyethylene we succeeded in achieving a graft of 6400 per cent by a dose of 31,400 r. We examined the structure of the copolymers obtained.

The Preparation of Graft Polymers of Acrylonitrile and Dimethyl Siloxane by Means of Co^{60} Gamma Rays. F. Dalton and R. Roberts, AERE, Wantage Radiation Laboratory, Grove, Wantage, Berks, U.K.

A study has been made of the effect of Co^{60} γ-rays on evacuated solutions of acrylonitrile in dimethyl siloxane fluids. The dependence of the reaction rate on monomer concentration, radiation intensity and temperature has been determined and a kinetic explanation is offered. Some data on the solvent resistance of the graft polymers formed are presented.

Studies on the Gamma-initiated Graft Copolymerization on the Surface and in the Inner Layer of Fibers. Seizo Okamura,*† Tatsue Iwasaki* and Naruo Kobayashi.†

(1) *Gamma-initiated graft copolymerization on the surface of nylon fibers.* Irradiation of nylon fiber in an atmosphere of nitrogen by Co^{60} γ-rays is found to cause gel formation, while irradiation in air causes degradation. After irradiation in a nitrogen stream, the nylon fiber is dipped into an aqueous solution of acrylamide and then reirradiated with γ-rays.

By these procedures, the surface graft polymerization is recognized to occur completely only on the surface of the fiber.

Photographs of the cross section of treated nylon show the surface grafting obtained by the preirradiation in nitrogen atmosphere, and show the inner layer grafting processed by the preirradiation in air.

(2) *Gamma-initiated graft copolymerization into the inner layer of cellulosic fibers.* After treatment for swelling the cellulosic fibers in 5–10% formamide–methanol solution the fibers are irradiated by γ-rays in the presence of the methanol solution of styrene. The amount of polymerization in the fiber is reached above several hundred percentages to original weight of fiber, holding almost the same tensile strength. The polymer formed in the inner layer of cellulosic fiber cannot be extracted by the usual solvent extraction method.

* Department of Textile Chemistry, Kyoto University, Kyoto, Japan.

† Osaka Laboratory, Japanese Association of Radiation Research on Polymers, Neyagawa, Osaka, Japan.

The effect of formamide concentration in methanol as the swelling solution on the weight increase of the fiber (viscose rayon) is measured and maximum amount of grafting is found at 5% formamide–methanol as pretreating solution.

The effect of styrene concentration in methanol as the solution for the radiation-induced polymerization, on the weight increase of the fiber (viscose rayon) is also studied and maximum grafting is found at 70% styrene concentration.

Radiation-induced Graft Copolymerization to Poly(Vinyl Alcohol). Ichiro Sakurada, Toshio Okada and Eiko Kugo, Department of Textile Chemistry of Kyoto University, Kyoto and Osaka Laboratories of Japanese Association for Radiation Research on Polymers, Neyagawa-shi, Osaka-fu.

In order to improve the properties of poly(vinyl alcohol) films and fibers, studies were carried out on the graft copolymerization of various vinyl monomers to poly(vinyl alcohol) films by γ-ray irradiation.

When thin dry films of poly(vinyl alcohol) were suspended in test tubes in a large excess of styrene and then irradiated, no graft copolymerization but only homopolymerization of styrene was observed. But with films which contained more than 5 per cent water the grafting proceeded smoothly. The highest value of styrene grafted was about 1000 per cent. The presence of water in the monomer solution was also effective for the grafting.

Methyl methacrylate behaved similarly to styrene in the grafting to poly(vinyl alcohol) films. The presence of a certain amount of water was essential. It was further found that the efficiency of the grafting of methyl methacrylate for any given dose was generally larger than that of the grafting of styrene. The highest value of the grafted methyl methacrylate was 4000 per cent and obtained by the γ-ray irradiation of 5×10^5 r.

Some experiments were carried out with acrylonitrile and vinyl acetate but the efficiencies of the grafting of these monomers were not so high, in comparison with styrene and methyl methacrylate.

The degrees of swelling of the graft copolymers of poly(vinyl alcohol)–styrene (or methyl methacrylate) in organic solvents were measured at 30°C. The relationship between the degree of swelling and the percentage of monomer grafted may be given by

$$(\text{degree of swelling } \%) = k(\text{monomer grafted } \%)^n.$$

For the polymers grafted with styrene n was equal to unity but for those grafted with methyl methacrylate it was generally smaller than unity. n and k have characteristic values which depend on the organic solvents.

Radiolysis in the Adsorbed State.* J. W. Sutherland and A. O. Allen, Brookhaven National Laboratory, Upton, New York.

The radiolysis of pentane adsorbed on mineral solids, studied by Caffrey and Allen (*J. Phys. Chem.* **62,** 33 (1958) and *Proceedings of the All-Union Conference, Isotopes and Radiations in Chemistry*, p. 135, Moscow (1957)) has been further investigated. Extensive blanks have been run to show that the observed decompositions result only when the pentane and solid are irradiated together. High product yields do not arise from an activation of the solid by the radiation, followed by catalytic decomposition of the pentane. Rather, a transfer of energy occurs during irradiation.

The radiolysis of pentane occluded within the crystal lattice of dehydrated synthetic zeolites (Lindo Molecular Sieves 13X and 5A) has been studied. For the sodium zeolite 13X, the hydrogen yield (the quantity of hydrogen produced per unit energy input to the entire system of solid plus pentane) varies but little with the amount of pentane present, as though the radiation energy were pooled and resulted in decomposition with efficiency independent of the amount of pentane present. The yield is small, $G = 0{\cdot}32$–$0{\cdot}4$, over the range 2–17 per cent

* Research performed under the auspices of the U.S. Atomic Energy Commission.

VOL. 7 1959/6

pentane in the zeolite. Partial replacement of the sodium ions in the zeolite with manganous ions lowered the hydrogen yield, but with cobaltous ions the yield increased many-fold.

Caffrey's high values for hydrogen yield from radiolysis of pentane on silica gel have been confirmed and also his finding that at low percentages of pentane a large yield of branched hydrocarbon, notably *iso*pentane and *iso*butane, results. At higher percentages of pentane (5–13 per cent) these branched products no longer appear, but the higher hydrocarbons from hexane to decane occur, and the course of the radiolysis seems to resemble that of liquid pentane, with energy from the silica gel contributing. The isomerization reactions occur only at low coverages, when the pentane molecules are more nearly isolated from one another.

Gamma-radiation-induced Peroxidation of Certain Hydrocarbons. M. Durup, J. Durup and M. Magat, Laboratoire de Chimie Physique de la Faculté Sciences, Paris, France.

Chain oxidation of hydrocarbons becomes possible at various fairly high temperatures, depending on their structure. If the process is initiated by ionizing radiation, which is independent of temperature, it is frequently possible to select a temperature at which peroxidation takes place at an adequate speed but secondary reactions, such as decomposition of the peroxides formed, remain negligible. The reaction can be further accelerated by adding certain substances. This aspect of peroxidation is discussed taking cumene as an example. The prospects for industrial application are also reviewed.

Where chain oxidation does not take place, mainly diperoxides are formed, which are difficult to obtain by purely chemical processes. As an illustration, the peroxidation of *iso*-octane is considered.

The employment of polymer peroxidation under various conditions for the preparation of grafted polymers of various structures is discussed.

Radiochemical Oxidation of Hydrocarbons. Roger Montarnal and Monique Brun, Laboratoire Radiochimique, Institut Français du Pétrole, Centre d'Études Nucléaires de Grenoble.

The use of radiation presents a method of initiating radical chain reactions and, in particular, the oxidation of liquid-phase hydrocarbons by molecular oxygen.

The paper describes an apparatus for carrying out this work using 200 kV X-rays. It then gives results obtained for oxidation of olefines and paraffins and from study of the stability under irradiation of the peroxides obtained.

In the case of olefinic hydrocarbons, kinetic study made it possible to determine the fundamental characteristics of the *cyclo*hexene and di-*iso*butylene oxidation chain reaction: $\sqrt{I}$-law, total G-count, radical G-count, length of chain and energy of activation. The effect of homogeneous (CCl_4), or heterogeneous (ZnO) sensitizers was also studied.

In the case of saturated hydrocarbons, the obstacles in the way of a thorough study are more serious in that the propagation constant of the oxidation chain is weaker than with certain olefines; the researcher may have to operate at a temperature at which the oxidation products decompose and contribute to initiation. In the case of cetane and *cyclo*hexane, it was possible to define the most favourable temperature ranges and to identify a number of characteristics of the oxidation reactions.

Finally, a study was made of the stability of certain hydroperoxides under irradiation.

A Comparison of the Production of the Insecticide "Gammexane" (1:2:3:4:5:6-Hexachloro*cyclo*hexane) by Ultra-violet and Cobalt-60 Gamma Radiation. P. R. Hills, R. Robert and M. W. Spindler, AERE, Wantage Radiation Laboratory, Grove, Wantage, Berks, U.K.

A comparative study has been made of the synthesis of the γ-isomer of 1:2:3:4:5:6-hexachloro*cyclo*hexane "Gammexane", both by ultra-violet and cobalt-60 γ-radiation.

Experiments with light of wavelength 3650 Å, employing a variety of experimental conditions, have established an optimum quantum yield of $8{\cdot}67 \times 10^3$ for the production of the hexachloro-compound which contains $13{\cdot}2 \pm 1{\cdot}3$ per cent of the γ-isomer. The introduction of additives did not improve either the γ- or γ-isomer yield.

For radiation-initiated experiments the Gammexane content is $15{\cdot}3 \pm 1{\cdot}6$ per cent and is independent of dose rate, benzene concentration and duration of the chlorination process. Reaction at low temperatures effects small improvements in the γ-isomer yield.

A comparison of both methods of initiation shows that the absorbed energy is utilized with equal efficiency in each case.

Radiochemical Chlorination of a Carbon Chain Linked to a COO- Group: Propionic Acid and Some Derivatives. PH. TRAYNARD and P. VERRIER, Institut Français du Pétrole.

Under the effect of ionizing radiations, chlorine dissolved to saturation point in one of these liquid compounds is substituted for a hydrogen atom in the carbon chain. As in the case of photolysis, it is a radical reaction and subject to a chain process.

The radicals derive from the radiolytic decomposition of the liquid medium and the chlorine is the chain propagating agent.

This chain, which is particularly long, produces a very high real *G*-value, which varies with the radiation intensity and may exceed 10^5. Thus the reaction is economically profitable and might be put to industrial use, as the monochloro- or dichloropropylic acids or esters yield corresponding acrylic derivatives.

Under low intensity radiation, the initial speed of the reaction is proportional to the square root of this parameter, but as the intensity increases the initial speed tends to become independent of this factor.

Chlorination may be taken to the final stage of substitution of the five H atoms in the carbon chain and even to the pentachloropropionic acid chloride stage, yielding a range of perfectly reproducible and often crystallizable substances.

Some Industrial Aspects of Radiation-induced Chlorination Reactions. IRVING ROSEN, Diamond Alkali Company, Painesville, Ohio.

This paper presents the experience and thinking of a major industrial producer of chlorinated products in the United States on the potential industrial use of large radiation sources to initiate halogenations.

Considerations of basic economics and of process conditions show that the costs of chlorination products from long chain free radical reactions will not be reduced by substitution of fission product energies for conventional initiator energies. Therefore, for large radiation sources to be commercially attractive, they should offer a means to good yields of chlorination products which cannot be obtained with conventional photo-initiators.

In 1954, the first reports appeared which described products obtained from the γ-radiation-induced chlorination of toluene as being markedly different from those obtained by conventional free-radical chlorination initiators. To clarify those reports, a comparison was made in our laboratories of the γ- and ultraviolet radiation-induced chlorinations of toluene and butyric acid. Toluene was chlorinated in the presence of ultraviolet light at 15°C to give a hexachlore addition product similar to that reported in the literature from γ-initiation. Butyric acid was chlorinated in the presence of γ-radiation to give chlorobutyric acid isomer mixtures which were about the same as those reported in the literature from ultraviolet initiation. These results suggest that γ-radiation has about the same effect as photo-initiation on the course of aliphatic substitution and additional chain chlorination reactions, and acts merely as a free radical initiator.

The recently reported results of other workers on free radical radiation-induced halogenations and sulfochlorinations also support this conclusion.

In our opinion, the future use of large radiation sources for chlorination reactions

VOL. 7 1959/6

depends upon, and still awaits, the development of unique applications and products.

Radiation Damage to Solids and Catalysts.* JOHN TURKEVICH, Princeton University, Princeton, New Jersey.

A review will be given of the numerous attempts to alter the catalytic activity of solids by exposure to nuclear radiation. The results obtained will be interpreted in terms of the studies made at the Princeton Chemical Laboratories on the catalytic activity of and the radiation damage to charcoal and zinc sulfide. A graded set of charcoals produced by varying thermal treatment was characterized for catalytic activity by the study of the ortho–para hydrogen conversion and the hydrogen–deuterium exchange. This set was also studied by electron spin resonance techniques. The results obtained will be shown to have important implications in the question of how radiation damage affects the catalytic activity of solids. The other system studied was that of the zinc sulfide phosphor. The change in the many luminescent properties of this material on neutron damage also gives evidence as to the nature of the damage centers produced in the solid. These results will also be used to interpret the effects of radiation damage on the catalytic properties of solids.

The Use of Ionizing Radiation in Heterogeneous Catalysts. ELLISON H. TAYLOR, HEROLD W. KOHN and GEORGE E. MOORE, Oak Ridge National Laboratory,† Oak Ridge, Tennessee.

Two recent developments have aroused interest in irradiating heterogeneous catalysts. The first is the gradual incorporation of ideas from solid-state physics into catalytic theory, and the realization that some of the point-defects produced by ionizing radiation are likely to influence catalytic properties. The second is the availability of large radiation sources, offering the possibility of rapid production of defects, and, more remotely, of making practical improvement in catalysts.

There is evidence that major alterations in catalytic activity can be produced by ionizing radiation, and the changes that have been observed are varied enough to suggest further exploration. Thus, the activity of zinc oxide for hydrogenation of ethylene is reduced by irradiation with γ-rays, while its activity for hydrogen deuterium exchange is increased. The activity of γ-alumina for the latter reaction is increased by γ-irradiation, but the increase depends upon previous poisoning of the catalyst. Remarkably large increases for the same reaction occur upon irradiation of silica gel, but here prior poisoning is unnecessary.

It is hoped that such observations may help to define those features of solids which are responsible for the activity of ordinary catalysts. It is known, for instance, that lattice vacancies, interstitial atoms and trapped electrons are produced by radiation, and it should be useful to be able to define the role of these defects in catalysis.

Prospects for application of radiation for the improvement of catalysts are rather remote, principally because most of the effects disappear on heating into the temperature range of most commercial processes. A related possibility for practical application, the irradiation of a substrate in the presence of a solid surface, has been suggested by others and may depend upon related phenomena.

Preparative Radiation Chemistry: New Synthesis of Dichloro-phosphines and Nitroso-compounds. ARNIM HENGLEIN, Radiation Research Laboratories, Mellon Institute, Pittsburgh, Pennsylvania.

Intense high-energy electron beams have been used to synthesize new compounds in preparations which are considerably more convenient than conventional methods. The reactions studied may be classified in either of two principal categories: those in which the product is formed by combination of

* This work has been supported by the United States Atomic Energy Commission.

† Operated by Union Carbide Corporation for the U.S. Atomic Energy Commission.

free radicals from the radiolysis of different components of a mixture ("combination reactions") and those in which radicals react with a scavenger present at low concentration and which has to be continuously delivered to the system during irradiation ("scavenging reactions").

Dichlorophosphines can be directly synthesized from phosphorus trichloride and aliphatic, olefinic and aromatic hydrocarbons. The reaction proceeds via a combination mechanism. The yields amount to about 50 per cent of the reacted material at a conversion of 25 per cent. The by-products are mainly hydrogen chloride and undistillable residues and only small amounts of organic chlorides, phosphorus tetrachloride and higher hydrocarbons. In the case of olefins radiation yields of up to 12 molecules per 100 eV of absorbed energy have been observed for the total consumption of phosphorus trichloride and hydrocarbon. The double bond is not affected and the PCl_2-group is directed mainly into α-position. Values for G of 5–7 have been observed in mixtures with aliphatic hydrocarbons and somewhat smaller yields in the case of aromatic compounds. Some other chlorides react with hydrocarbons in a similar way. For instance, in mixtures of phosphorus oxychloride and hydrocarbons phosphine oxides are formed.

Nitric oxide acts as a radical scavenger in organic liquids. New nitroso compounds may be synthesized by the addition of free radicals to nitric oxide. In CCl_4–NO mixtures trichloro-nitroso-methane is formed. Dichloro-nitroso-methane, which had not been previously synthesized, is formed in $CHCl_3$–NO mixtures. A polymer is produced in PCl_3–NO mixtures, probably by polymerization of the intermediate dichloro-nitroso-phosphine.

Radiochemical Synthesis of Colorants. F. Balestic and M. Magat.

Some syntheses of colorants by radiation were attempted. A more complete study of the synthesis of Lanth purple made it possible to determine the influence of various factors on the efficiency of the reaction.

The Current Concept and Status of the Uses of Radiation in Food Preservation. U.S. Army Quartermaster Corps, Washington, D.C.

Much progress has been made during the last decade on the treatment of goods with ionizing radiations. It is now possible to evaluate its various potentialities with a reasonable degree of accuracy. This is covered in the paper, following a description of the nature of the process itself.

The current state of the art is also discussed. This includes the available and planned sources of ionizing radiations, the effects on organisms, the effects on foods and the economics of the process.

Cobalt-60 Irradiator and Its Use for Plant Genetics. Seiji Matsumura, Taro Fujii and Sohei Kondo, National Institute of Genetics, Misima, Japan.

A facility for Co^{60} γ-ray irradiation was first built in Japan in the National Institute of Genetics, Misima, in 1956. The γ-irradiation room and the emitter were specially designed to give a fairly wide range irradiation over a horizontal plane for the investigation of induced mutations and other radiobiological effects upon plants and animals. The emitter consists mainly of an irradiator head and a remote controller. The former has the maximum capacity to contain Co^{60} of 100 curies and the latter serves for remote control of the vertical position of the irradiator head. The lead filters were designed to produce three regions of roughly constant but different dose rates. For simplicity's sake in the design only primary radiation was taken into account. Our best estimate of the effective source strength, determined with Fricke's ferrous sulphate chemical dosimeter and Victoreen ion chamber, was 31·3 c as of 1 November 1957.

Determination of radiosensitivity in plants such as LD 50, is fundamental for radiobiological studies and plant breeding by

VOL. 7 1959/6

radiation. Radiosensitivity has been found to be quite different between different plant species. Comparative studies of radiosensitivity in various kinds of plants, especially related plants of various polyploid series, were carried out from 1956 through 1958.

Dry dormant seeds were exposed to Co^{60} γ-rays. The dose range was from 10 to 100 kr, and radiosensitivity was examined from decrease in germination and/or survival rates. Germination rate in most of the plants gradually decreased with increasing doses, but that of *Cryptotaenia*, *Lilium* or *Oryza* abruptly decreased to 0 at a certain dosage. As for several species, e.g. *Glycine* or *Raphanus*, the germination ability up to appearance of cotyledons did not much decrease even at 100 kr but most of the seedlings died immediately after the germination, and only a few plants could survive. Radiosensitivity must therefore be determined by the percentage of seedlings which had developed two or three leaves. The genera *Cryptotaenia* and *Lilium* were found most sensitive to radiation, while *Cosmos* and *Brassica* were most resistant.

Differences of sensitivity between di-, tetra- and hexaploid plants were compared in several species and varieties of *Triticum* and *Aegilops*. Dry dormant seeds were irradiated from 20 to 70 kr by γ-rays. Radiosensitivity was determined by the decrease of germination rate and the average length of the seedlings. Genus *Aegilops* showed more tolerance to radiation than genus *Triticum*. The germination rate of tetraploid species of *Aegilops* remained the same as of the control even at 30 kr, while that of the tetraploid *Triticum dicoccum* showed a marked decrease at 30 kr. Diploid species of *Triticum* and *Aegilops* were the most sensitive to radiation, and the hexaploid *Triticum* species were not more resistant than the tetraploid ones. These facts show that radiosensitivity depends not only on polyploidy but also on the kind and number of genomes.

In vegetatively propagating plants use of radiations to obtain induced bud or somatic mutations is one of the most promising methods for plant breeding. Cuttings or young seedlings of camphor tree, citrus fruits, carnation and chrysanthemum, runners of strawberry, bulbs of tulip and gladioli and tubers of sweet potato were exposed to X- or γ-rays at the dosage 0·5–15 kr. For any case, the number of successfully planted ones and that of their sprouts, per plant, decreased with increasing radiation dosage. X-rays were more effective in this respect than γ-rays. Also, the number of plants with radiation-induced abnormal leaves or flowers increased roughly with increasing dosage and so did the rate of somatic mutation and chimera for chrysanthemum, carnation, tulip, gladioli and sweet potato. Some of them are promising for plant breeding.

Uses of Large Radiation Sources in Botanical Research.* ARNOLD H. SPARROW, Brookhaven National Laboratory, Upton, L.I., New York.

Cobalt-60 γ-sources have been extensively used over a 10-year period at Brookhaven National Laboratory to study various aspects of plant radiobiology. In the outdoor field irradiation the strength of the source was increased each year from 16 curies in 1949 to 200 in 1953 and to about 1800 c in 1954. During the 10-year period a number of smaller sources have been used in a special greenhouse.

Cytological, genetic, physiological and morphological effects of chronic and acute exposures have been studied in a large number of plant species and varieties. A summary of this work will be presented with particular emphasis on the significance of dose, dose rate, dose fractionation, duration of exposure and of temperature in modifying genetic or cytogenetic effects.

Studies on the comparative radiosensitivity of different plant taxa have shown that a range of about 1000-fold exists in the higher plants. Chemical composition, chromosome

* Research carried out at Brookhaven National Laboratory under the auspices of the U.S. Atomic Energy Commission.

size and number, and other factors contribute to this variation.

Developmental and physiological disturbances in many species have been observed. These vary from severe growth inhibition to growth stimulation and from minor morphological abnormalities to gross abnormalities classified as tumours. So far our results do not suggest that growth stimulation will be of much (if any) practical value, but the exact cause of the stimulation may be of considerable scientific interest. On the other hand, growth inhibition, e.g. of sprouting in vegetables, promises to be a useful application in certain instances.

Large γ-sources represent an extremely useful and versatile facility for plant, radiobiological research. Such research is providing valuable fundamental information in various botanical disciplines as well as mutations of practical or potentially practical value.

The Use of Gamma-ray Sources for the Inactivation of Viruses. E. C. POLLARD and W. R. GUILD, Yale University, New Haven, Connecticut.

The inactivation of viruses serves two main purposes. The first is the removal of the infectivity from foodstuffs or drugs in which it would be considered harmful. The second is in the formation of killed vaccines which retain their antigenicity while having lost their infective property.

The problem of the removal of virus activity by ionizing radiation is one which can be rather straightforwardly described. Ionizing radiation, in general, produces exponential inactivation of viruses with occasionally a second component which is usually not very greatly different in slope from the first. One can therefore rather confidently predict the degree of inactivation of plant, animal or bacterial virus after irradiation by a source such as, for example, a cobalt γ-ray source. The inactivation curves for a whole series of plant, animal and bacterial viruses will be given and the intensities of sources necessary for producing varying degrees of inactivation will be proposed. The effect of combined thermal and ionizing radiation is also of interest and a description of experiments showing the effect of these two will be included.

The problem of making vaccines is of great interest inasmuch as existing methods of inactivating polio virus, for example, by formalin seem to have run into a great many troubles in the actual processing. It is quite likely that a technique which used moderate thermal elevations together with γ-ray inactivation would yield virus which was antigenically quite potent while at the same time not infectious. The rationale behind this approach will be discussed and one or two preliminary experiments described.

Sterilization of Pharmaceuticals and Hospital Supplies by Ionizing Radiation. CHARLES ARTANDI and WALTON VAN WINKLE, JR., Ethicon, Inc. Somerville, New Jersey.

The pharmaceutical industry has been in need of a method of sterilization of proteins, enzymes, steroids and other sensitive materials which does not involve heat or very reactive chemicals.

Ionizing radiation can successfully be used to destroy micro-organisms at doses which are harmless to most of these compounds.

This new method of sterilization has three important advantages:

(1) The final sealed package can be sterilized.
(2) New, less expensive and more convenient packaging materials may be used (plastics).
(3) Easy adaptability for continuous process.

Electron accelerators (Van de Graaff electrostatic or linear accelerators) should be the preferred sources of radiation, whenever penetration of the product is no problem. Gamma emitters and X-ray machines provide great penetrating power, but their dose rate is low and good utilization of energy requires complex engineering designs due to the problems of geometry.

Electron accelerators have high power output; the beam can be scanned to cover the conveyorized product. A sterilizing dose is delivered in a second or less. The accelerators can be turned off when not in use;

VOL. 7 1959/

repairs and maintenance can be done safely.

If the penetration is not adequate, several approaches can be tried, like:

(1) Redesigning the package
(2) Accelerator of higher energy
(3) Irradiation from two sides if the product permits.

The performance of the machines can be routinely checked by meters, monitors and recorders. Various dosimetry systems are available for the calibration of machine performance and spot check of production.

Irradiation is not economical for products which can be sterilized by heat. Its higher cost, however, is only of secondary importance when a quick and efficient method is needed for sterilizing sensitive materials.

Sutures of all kinds, dressings, ointments, enzymes, injectibles and other items are being sterilized on production scale by irradiation, and the field is open for many more products.

Insect Eradication by Release of Sterilized Males. R. C. BUSHLAND, Entomology Research Division, Agricultural Research Service, U.S. D.A., Kerrville, Texas.

Doses of γ-radiation in the range of 5000 to 10,000 r, given to insects either as adults or well-developed pupae, are tolerated by somatic tissues but produce dominant lethal mutations in the germ cells, thus sterilizing the insects.

Male screw-worm flies, irradiated as pupae, compete for mates when released in nature. Female screw-worms mate only once, so those mated to sterile males cannot reproduce. In nature screw-worm flies number at most only a few hundred per square mile because they breed only in wounds in living animals. Hence, they can be outnumbered by sterilized flies reared in the laboratory on ground meat and blood. When the native population is outnumbered by sterile insects, the majority of the native females make sterile matings. This reduction in biotic potential causes a decline in numbers of each new generation. By maintaining a constant high population of released sterile insects, the native population is overwhelmed in a few generations.

Following these principles, screw-worms were eradicated from the Island of Curacao by 4 months of release in 1954.

An eradication programme is now under way in the southeastern United States. Releases were started early in 1958 at the rate of 100 sterile males per square mile per week, and this prevented a build-up of the native population that survived the winter. By fall, more than 25 million sterilized males were being released each week from airplanes over 80,000 square miles in Florida, Georgia and Alabama.

These releases were so effective that no native screw-worms were found after 19 February 1959. Releases are being continued until 6 months after the last case of myiasis. Subsequent observations will show whether eradication has been achieved.

The success with screw-worms has stimulated research to apply the sterilized male technique to the eradication of other insects. Research is being done with various species of fruit flies which do not now occur in the continental United States, but which may be accidentally introduced to menace our fruit and vegetable industries. The method may also have application to the control of other insects which are subject to having their populations so reduced by insecticidal or cultural procedures that they can be outnumbered by sterilized males.

Susceptibility of the Grain and Rice Weevils, *Calandra granaria* **L. and** *C. oryzae* **L. to Gamma Radiation.** P. B. CORNWELL and J. A. MORRIS.

This paper forms a contribution to present knowledge of the entomology of radiation treatment of grain. A review of the literature in this field suggests that the present study is the most extensive of its kind. An examination is made of the effects of γ-radiation on the two principal grain pests, when these are reared and retained under near-optimum conditions for the species. Doses are evaluated for the commercial application of radiation treatment against various sized populations.

The effects of radiation on the complete life-history of a laboratory strain (ex Pest

Infestation Laboratory, D.S.I.R.), of the grain weevil *C. granaria* were examined at 24-hourly intervals during the life-history. Each stage of development was subjected to seventeen doses ranging from 250–20,000 rep. Three criteria were used to determine radiation susceptibility: (1) emergence of immature stages as adults from grain, (2) survival after emergence and (3) the production of adult progeny. Similar observations on all stages of the rice weevil *C. oryzae* allow a comparison of susceptibility in the two species.

Additional studies with *C. granaria* include: (1) radiation susceptibility of the sexes, (2) periodicity in fertility at sub-sterilizing doses and (3) an examination for radiation induced resistance in offspring of irradiated parents.

Experiments are described in which doses evaluated for commercial disinfestation are tested against massive populations and under a limited range of commercial storage conditions.

Gamma Radiation Facilities at the Australian Atomic Energy Commission Research Establishment. D. W. George and J. N. Gregory, The Australian AECRE, Lucas Heights, New South Wales, Australia.

The used fuel elements from the AAEC experimental reactor HIFAR are to be stored on removal from the reactor for a period of about 40 days in a water-cooled storage cell. During this period, the γ-activity and thermal heating will fall by a factor of about ten. The average γ-activity of each fuel element during storage is about 10^5 curies. The fuel elements will be stacked vertically during storage in a regular square pattern with a total of forty-eight positions at 7 in. pitch. The centre position has been substituted by an irradiation thimble 9 in. in diameter. This thimble is closely surrounded by eight symmetrically placed fuel element positions. The storage capacity is somewhat larger than the normal requirement so that there will usually be considerable choice in the arrangement and selection of fuel elements in the position close to the thimble.

The experimental irradiation space is a volume about 7 in. in diameter and 2 ft 6 in. long. Material for irradiation is to be attached to a shielding plug and will be introduced into and moved from the thimble by the reactor vertical handling flask. The shielding plug has a number of access tubes which will permit heating or cooling of the irradiated material, temperature measurement, control of atmosphere and withdrawal of liquid or gaseous reaction products.

The extra expense of adding this unit to the storage cell was very small and since it uses the radiation from the fuel elements during compulsory storage, radiation costs are virtually zero. It should also give valuable information on the feasibility of using fuel elements during such storage periods as radiation sources for large-scale operations.

The paper will also describe the radiation facilities available directly from HIFAR and plans for using fuel elements after cropping as a further radiation source. In this it is hoped to install a fuel element irradiation "box" in the cropping pond.

Cobalt Radiation Sources for Research on the Radiation Treatment of Rubber and Plastics. Ing. Šimorda, VUGPT, Gottwaldov.

The paper includes a description of the following:

A 250-curie source, its construction and production experience gained.

Design for a 2000-c cobalt source for the vulcanization by radiation of experimental rubber tyres or other products.

General layout of a source, disposition of emitters, and protective shielding for workers.

Spatial arrangement of emitters for achieving maximum uniformity of dose intensity in the working chamber.

Means of inserting and removing emitters.

Economic results of employing radiation treatment processes in the production and processing of rubber and plastics.

The Cobalt-60 Irradiation Facility at Risoe. A. Brynjolfsson and W. Holm, Risoe, Denmark.

A description is given of the facility and some of its applications, as well as the

VOL. 7 1959/

techniques of the dosimetry carried out there.

Cobalt-60 Irradiation Unit for Laboratory Purposes. J. VÁLYI-NAGY, Central Research Institute for Physics, Department of Chemistry, Budapest.

Design of the irradiation spaces. The difference between irradiation spaces in industrial and laboratory devices is analysed, and the design suitable for irradiation spaces for laboratory use is discussed.

Design considerations in the choice of the type of irradiation units. Economy and design of some irradiation units developed abroad are surveyed. The apparatus designed by the author is discussed with a view to possible further development.

Design and Use of 10-kc Source of Cobalt-60. AKIBUMI DANNO, Japan Atomic Energy Research Institute, Tokai, Ibaraki, Japan.

A high intensity γ-radiation source of Co^{60} with 10 kilocuries has been in operation for a year at the Gamma Radiation Facility of the Japan Atomic Energy Research Institute. A source with dose rate greater than 10^6 r/hr is required for studying radiation chemistry of organic compounds, radiation effects on high polymers and radiation damage of non-metallic materials. It was designed primarily for the irradiation of relatively large samples at high intensity and with uniform γ-flux. A cylindrical cage type of source seems to be suitable to satisfy these requirements.

The source consists of a bundle of 110 Co^{60} rods. The specific activity of each rod is about 10 c/g. Each rod is 3 mm in diameter and 125 mm in length. The 110 Co^{60} rods were obtained from the MTR at USAEC National Reactor Testing Station, Idaho, and were given a certified rating of 11,230 curies on 19 December 1957. After receiving the source, the total activity of 110 Co^{60} rods was measured by several methods during August 1958 at our laboratory. From the calorimetric measurement, a value of $(10{\cdot}7 \pm 1{\cdot}1) \times 10^3$ c was obtained as the total activity of the source.

Two rods are inserted end to end in a pencil made of stainless steel of 0·3 mm thickness. These pencils are mounted coaxially in two circular holders whose diameters are 10·0 cm and 11·8 cm respectively. The dimensions of the source cylinder are 40·5 cm in height 13·4 cm in outer diameter and 8·6 cm in inner diameter. It can be separated into two cylinders; the inner one contains 30 pencils arranged at the same interval and the outer one includes 25 pencils. Thus three different field strengths can be utilized when the inner and the outer cylinder are used together or separately.

Samples to be irradiated with dose rate from 2×10^6 r/hr to 5×10^4 r/hr are placed inside or around the source cylinder. These are the effective regions for the irradiation of high dose rate with this source. Dose rates were measured chemically by ceric–cerous dosimeter or physically by vectorial roentgen rate meter. The dose rate at the centre of the axis of the source cylinder is $(2{\cdot}2 \pm 0{\cdot}1) \times 10^6$ r/hr. When the inner and the outer cylinders are separately used, the dose rates at the centres are about $1{\cdot}4 \times 10^6$ r/hr and $0{\cdot}8 \times 10^6$ r/hr, respectively. The distribution of the field strengths which was measured by chemical method was in good agreement with the dose rate calculation based on an assumed activity of 10 kc.

Irradiation experiments are carried out in the irradiation cave which was designed to satisfy the following conditions:

(1) The irradiation cave and the source must be suitable for irradiation of materials under a variety of conditions.

(2) The experimental condition must be controlled with the same accuracy as is obtained in unshielded laboratory work.

(3) The radiation intensity in the outside of the cave must be less than 30 mr/48 hr week.

(4) In the design of the cave and its facilities, automatic protection device has been incorporated wherever possible.

The irradiation cave consists of three cells in line; the centre one for storing the source and two others for irradiation experiments. Each cell is shielded with a wall of 100 cm in thickness made of high-density concrete

having a density of 3·8. The adjacent cells are separated from each other by a steel door. A shielding window and a pair of manipulators are mounted on the front wall of each cell. At the rear side of each cell, a step-door made of high-density concrete is installed. A chain conveyer running through a labyrinth for carrying samples into the cell is mounted on the side wall of the irradiation cell.

Design Experience on a Multi-megacurie Radiation Facility. D. C. BRUNTON, J. DONOVAN and L. VOYVODIC, Curtiss-Wright Corporation, Princeton, New Jersey and Armour Research Foundation, 10 W. 35th Street, Chicago 10, Illinois.

This paper describes the research and development work on radiator design and engineering which has been carried out with respect to the design of the "High Intensity Food Irradiator". The problems discussed are those common to all large, package irradiators. The first phase of the research and development work was devoted to achieving a clear understanding of plaque-type radiators and the effect of changes in the design parameters on the performance of such a unit. Initially, the performance of a single plaque radiator was studied theoretically, experimentally and by computer analysis. The parameters studied were source size and specific activity, source thickness and cladding, target density and geometrical factors including source and target heights, lengths and widths, and size of air gap between source and target. The performance was examined with respect to capacity, dwell time in the unit, dose uniformity, unit efficiency and overall cost.

Simplified expressions for radiator performance have been developed and verified by experiment. A three-dimensional code for applying a Monte Carlo type analysis to radiator performance has been developed and applied to this problem with good agreement with experimental measurements.

The radiator design programme was expanded to include an investigation of multi-plaque, multi-pass systems and hence includes essentially the three-dimensional matrix of sources as well as plaque-type radiators.

Engineering requirements with respect to conveyors for product handling are examined in conjunction with source design and effect on performance specifications. Source handling methods, safety systems and facility controls are likewise reviewed. Finally the preparation of the source material itself, including measurement, encapsulation and leak testing is described.

Use of Microporous Nuclear Fuels as a Means of Utilizing the Kinetic Energy of Fission Products in Chemical Synthesis. R. COEKELBERGS,* P. GOSSELAIN,† J. JULIENS,‡ L. SCHOTSMANS† and M. VAN DER VENNE,§ Ecole Royale Militaire, Centre des Sciences Nucléaires, Brussels.

The paper begins by briefly outlining possible uses of the kinetic energy of fission products in the case of gaseous phase weak *G*-reactions. The problem is mainly one of the amount of energy available; industrial production would require ionizing radiation energies of several tens of megawatts.

At the second Geneva Conference (September 1958), some of the present authors proposed, for the first time, the use of microporous nuclear fuels as a solution. A body of supplementary data obtained with these fuels is given; they refer to decomposition of N_2O and to nitrogen fixation in the form of oxides. The results of the experiments are described with reference to the following parameters: pressure, duration of irradiation, type of rays, type and dimensions of the microporous support surface.

This work confirms the existence of a phenomenon which we term "heterogeneous radiocatalysis" and enables its nature to be better defined.

* Professor at the Ecole Royale Militaire, Scientific Adviser to the Société Belge de l'Azote et des Produits Chimiques du Marly.

† Doctors of Science, attached to the Research Laboratories of the Société Belge de l'Azote et des Produits Chimiques du Marly.

‡ Civil Engineer, Head of Department at the Centre d'Etudes de l'Energie Nucléaire.

§ Doctor of Science, in charge of research at the Institut Interuniversitaire des Sciences Nucléaires.

VOL. 7 1959/6

The nitrogen fixation reaction carried out with these fuels possesses a number of interesting features. During irradiation of the air, the speed of formation of the nitrogen oxides varies little for rates of oxygen consumption exceeding 90 per cent. The apparent G, calculated with reference to the total fission energy dispersed in the "solid/reactive gas" system varies, according to circumstances, between 0·1 and 0·3. The temperature is 80°C and the pressure approximately 25 atmospheres.

A thorough study of the microstructure of the solids utilized has been begun, and the spectrum of the pores has been measured. The progressive changes in physical characteristics under the effect of irradiation have been observed and from them, in certain cases, the nature of radiation damage caused by the passage of fission products in a microporous structure can be more precisely ascertained. A rough theoretical sketch of the phenomenon of heterogeneous radiocatalysis is tentatively proposed.

The paper ends with a discussion of the possibilities of utilization of such microporous fuels, indicating the difficulties still to be overcome.

Chemical Production Using Fission Fragments. J. K. Dawson and F. Moseley, AERE, Harwell, U.K.

Some reactor design considerations of the use of fission recoil fragment energy for the production of chemicals of industrial importance have been discussed previously in a paper given at the Second United Nations International Conference on the Peaceful Uses of Atomic Energy (A/Conf. 15/P.76). The present paper summarizes more recent progress made on this topic at AERE, Harwell.

The range–energy relationship for fission fragments is discussed in the context of the choice of fuel system for a chemical production reactor, and the experimental observation of a variation of chemical effect along the length of a fission fragment track is described for the irradiation of nitrogen–oxygen mixtures.

Recent results are given on the effect of fission fragments on carbon monoxide–hydrogen gas mixtures and on water vapour. No system investigated to date shows any outstanding promise for large-scale chemical production.

Present Status of Nitrogen Fixation by Reactor Radiation. P. Harteck, S. Dondes and D. E. Neil, Rensselaer Polytechnic Institute, Troy, New York.

Investigations in nitrogen fixation by reactor radiation which have been carried out at Rensselaer and Brookhaven National Laboratory for a number of years, have used the fission recoil energy directly as ionizing radiation by means of the dispersion of uranium-235 in glass fibers about 5 microns in diameter. The effects of temperature, pressure and nitrogen–oxygen ratio on the G-value for nitrogen fixation have been determined and reported in the literature. A brief summary of this work is given.

The above work has been done in static systems; more recent work has involved both static and flow systems. In static systems, major emphasis has been placed on the effect of radiation intensity especially at the kinetic radiation equilibrium. It has been found that the production of NO_2 and N_2O in 4 : 1 and 2 : 1 nitrogen–oxygen mixtures proceeds to the point of total oxygen consumption.

A flow (cycling) system is now operating in a loop in the Brookhaven reactor. Data are presented on the effects of temperature, pressure, mixture ratio and radiation intensity which may be applied to the design of a future chemonuclear reactor. The present system is operating at 10 atmospheres and 150°C. The temperature is a function of the fission energy released in the glass fibers and the heat resistance of the loop. Another loop to operate at 50–75 atmospheres and 600°C is under construction. These loops make possible the evaluation of the characteristics of a continuous system, including the behaviour of the fission products released in the gas stream.

The complicated kinetics of nitrogen oxidation are outlined in three stages: initial reactions in the systems, reactions after

some fixed nitrogen has been produced, and finally the kinetics at radiation equilibrium. The conditions for the formation of N_2O_3, N_2O_4 and O_3 are considered, together with their effects on the overall process.

The Comparative Economic Advantages of using Cobalt Sources and Spent Bars from a Reactor as High-energy Radiation Sources. J. M. PUIG.

Plans for an industrial plant for the production of chemical products by radiation were drawn up, using (1) cobalt sources and (2) spent bars from a reactor. The matter is studied in detail from the economic point of view, thus making it possible to indicate the conditions in which these two sources of energy can be used.

The Cost-evaluation of the Radiation-induced Chlorination of Polymers. S. OKAMURA and K. HAYASHI, Osaka Laboratory, Japanese Association of Radiation Research on Polymers.

Radiation-induced halogenation is performed here by the γ-rays of cobalt-60 for polyvinyl alcohol, polymethyl methacrylate, polymethyl acrylate, polyacrylonitrile, polyvinyl acetate, polystyrene and polyethylene. The chlorination is recognized to occur very easily to high chlorine contents and also by low dosage in the solution of carbon tetrachloride.

Also the costs-evaluation of radiation-induced chlorination of polystyrene and of polyvinyl chloride is done here in the scale of the present industrial conditions in Japan. Costs evaluated are recognized relatively cheaper than that hitherto estimated.

Technology and Economics of Large Radiation Sources. MICHAEL MICHAELIS, Arthur D. Little, Inc. Cambridge, Massachusetts.

A major study was recently undertaken for the U.S. Atomic Energy Commission to summarize and analyze world technology relevant to industrial applications of high-level penetrating radiation. This paper, derived in part from that study, presents a comprehensive and quantitative account of the present status and foreseeable trends in the technology and economics of radiation sources now in use and under development in the United States.

Principal attention is focused on radioisotope sources such as cobalt-60 and cesium-137, and on electron accelerators such as Van de Graaff, resonant transformer, dynamitron and linear accelerator. Technological features of these sources are discussed in relation to existing and potential industrial process applications. Cost factors are analyzed and quantitative data are presented on capital, installation, operating and maintenance costs of various sources. Estimates are presented for the total cost per kilowatt-hour of radiation output as a function of type and size of the source.

It is recognized that these "radiation-production cost factors" are only some of the variables in the economic equation of radiation technology. Attention is therefore drawn to some of the following "application factors" which must be taken into account in arriving at sound economic judgements:

Unique product properties, and/or process savings.

Improvements in processing or product handling made possible by the introduction of the irradiation step.

Efficiency of radiation utilization in the particular application.

Cost of absorbed radiation relative to other process costs and to the market value of the product.

Intangible considerations, if any, associated with the use of radiation in the particular application, which may be expected to increase or decrease the marketability of the product.

As far as radiation-production costs are concerned, it is concluded that there are good prospects for achieving costs as low as 10 cents/kWh of radiation output, whereas present-day costs are in the range of one to ten.

VOL. 7 1959/6

Irradiated Polyethylene: A Case Study in the Economics of Production Use of Electron Beam Radiation. J. W. RANFTL, General Electric Company, Milwaukee, Wisconsin.

Machines which produce radiation in the form of electron beams are now in use in production irradiation processes and are attractive to the investigators of new production processes because of the great amounts of radiation available, the large product output and resultant low processing costs.

A very significant case in point is the irradiation of polyethylene. The cross-linking effect of the radiation produces a superior product, opening new applications for the use of polyethylene because of improved mechanical, electrical and chemical properties. Irradiated polyethylene film has been sold for several years. More recently and since 1955, electrical wire has been made with irradiated polyethylene as the insulating jacket.

At this time the radiation power of electron machines operating or being installed for production processing by irradiation exceeds 100 kW. This does not include the many others installed for research work.

As an example to study the cost of radiation processing we will consider a production process for the cross-linking of polyethylene by radiation, operating 4000 hours per year corresponding to two 8-hr shifts on a 5-day week basis. Many individual factors enter into the economics of electron beam irradiation. The investment costs include:

(1) The capital cost of the apparatus
(2) Building and shielding costs
(3) Conveyor and auxiliary equipment.

Operating costs account for other costs and include:

(4) Maintenance cost for equipment
(5) Labour costs of process attendants
(6) Power costs.

Before material throughput and processing costs can be calculated the efficiency of the process must be considered and will include:

(7) Time efficiency of machine utilization
(8) Absorption efficiency of the product and process.

The output is best thought of in terms of megarad pounds from which the pounds of material output are easily calculated after the megarad dose is established.

The development of high-powered electron-beam generators has made the cost of irradiation processing very realistic today. It is expected that machine improvements will result in even lower costs in the coming years.

Cross-linking of Polyvinyl Alcohol by Gamma Radiation. H. DIEU and V. DESREUX, Laboratory of Physical Chemistry, University of Liége, Belgium.

The action of γ-radiation on aqueous solutions of polyvinyl alcohol has been followed by viscosity, sedimentation and reacetylation. There is a sharp critical concentration for the gel formation; above this concentration the important phenomenon seems to be intermolecular cross-linking; below this concentration, the results are interpreted in function of partially internal cross-linking.

Polymerization of Olefines by Radiation. G. DE GAUDEMARIS and CHARLES WALTHER, Laboratoire Radiochimique, Institut Français du Pétrole, Centre d'Études Nucléaires de Grenoble.

The results obtained at the radiochemical laboratory of the Institut Français du Pétrole with the polymerization of olefines by accelerated electrons have been reproduced on a larger scale by means of irradiation in a nuclear reactor. In this way significant quantities of polymers can be produced for research purposes.

The reactor used in this project was the "Mélusine" reactor of the Centre d'Études Nucléaires at Grenoble. This is an ordinary water-moderated and cooled, swimming-pool-type reactor, operating on MTR type 20 per cent enriched uranium fuel.

The total flux of the reactor operating at 1000 kW was used without any filtration. At the point of irradiation the thermal flux was 10^{13} n/cm^2 per sec, and the fast flux 10^{12} n/cm^2 per sec, the energy diffused by the

ionizing radiations totalling approximately 0·2 W/cm³.

A continuously operating loop was formed to permit the separation of the polymer formed. This installation, which enables any liquid hydrocarbon to be treated at environmental temperature, has numerous safety devices. It is described below in detail.

The polymers obtained were purified and their physical constants are quoted in the paper.

Studies on the Excitation Energy Transfer and the Cationic Polymerization as one of the Primary Processes of the Interaction of High-energy Radiation with Matter. Siezo Okamura,*† Tomonobu Manab,* Shigeru Futami* and Toshinobu Higashimura.*

(1) *Excitation energy transfer observed by the quenching of γ-ray luminescence in benzene solution by the presence of monomers, polymers and copolymers.* In the radiation effects of organic systems, sensitization and protection have already been observed. These phenomena may be illustrated as the excitation energy transfer from one component to another. On the other hand, it has also been known that the luminescence of a liquid scintillator could be quenched by the addition of a quenching agent and the quenching might be due in part to the excitation energy transfer from the excited state of the solvent to quenchers.

Here the quenching experiments of γ-induced luminescence are performed in benzene solution especially by using vinyl monomers, polymers and copolymers. Experiments are done first on the quenching of *p*-terphenyl fluorescence in benzene solution by several vinyl monomers. The ease of energy transfer from benzene to quenchers (monomers) is found to be as follows:

Conjugated monomers (acrylonitrile, methylacrylate, styrene, ethylacrylate and methyl methacrylate) > unconjugated monomer (vinyl acetate) > corresponding saturated compounds (ethyl acetate, methyl propionate, ethyl propionate, ethyl benzene and propionitrile).

The quenching experiments of *p*-terphenyl fluorescence in benzene solution are performed in cases of several polymers. The efficiencies of quenching are found in the following order: crepe rubber > polystyrene > polyvinylacetate > acrylic polymers (polymethylacrylate, polymethylmethacrylate, polyethylacrylate).

The quenching of *p*-terphenyl fluorescence in benzene solution is also measured in the case of poly(styrene comethyl methacrylate). The quenching efficiencies are found to be smaller than that of homopolystyrene even in the concentration scales of pure styrene units. This means that the quenching is more effective in the repeated phenyl units as in homopolymer molecules than in the isolated one as in copolymer molecules.

(2) *Gamma-initiated cationic polymerization of styrene in methylene dichloride solution at low temperature.* As hitherto reported, a complete explanation has been given by the radical mechanism on the γ-initiated polymerization of vinyl monomers especially at temperatures above room temperature. But recently the negative temperature dependence and also the independence of the dose rate on the rate of polymerization are considered as one of the characteristics of the ionic polymerization mechanism in the case of the polymerization of *iso*butene especially in the presence of zinc oxide powder at minus 80°C.

Here methylene dichloride is chosen as one of the special solvents for showing the ionic polymerization of styrene and also the ionic copolymerization of styrene and methyl methacrylate in the completely homogeneous system at minus 80°C by γ-radiation with a dose rate of $2{\cdot}3 \times 10^4$ r/hr. The linear dependence of the polymerization rates on the radiation intensities is found here as one of the characteristics of ionic polymerization mechanism.

The composition of copolymer obtained here in the γ-initiated polymerization at minus 80°C in methylene dichloride solution

* Department of Textile Chemistry, Kyoto University, Kyoto, Japan.

† Osaka Laboratory, Japanese Association of Radiation Research on Polymers, Neyagawa, Osaka, Japan.

VOL. 7 1959/6

shows the characteristics of ionic polymerization mechanism.

Use of Fission Products in a Pilot Set-up to Initiate the Oxidation of Paraffin. G. Icanid,* A. Dragut,* J. Drimus,* V. Dumitresco† and I. Stoian.†

Previous publications have laid down the optimum laboratory conditions for initiating the oxidation of paraffin by using a Co^{60} source of 50 g Ra equivalent.

The research described in this paper concerned the use of large radiation sources (fission products from the nuclear reactor) in a pilot set-up.

The paper includes:

(1) A description of the set-up for the irradiation of paraffin without air-bubbling;

(2) The results relating to the oxidation of pre-irradiated paraffin; and

(3) The optimum working conditions for the source used and data on the doses absorbed in the course of the experiments.

The Effects of Nuclear Radiation on Coal and Methanation Reactions. Ernest J. Henley, Stevens Institute of Technology, Hoboken, New Jersey.

A model compound, anthracene, was selected for initial study. Attempts to lower the threshold temperature for cracking or methanation by use of radiation were unsuccessful. Methanation runs at hydrogen pressures between 1000 and 1800 psig and temperatures of 850–860°F showed a marked susceptibility to radiation catalysis. *G*-values of about 700 to 900 were obtained. Of forty runs made, seventeen were made in a 43,000 r/hr γ-radiation field.

A number of experiments with high-temperature coke and anthracite were undertaken. These were generally unfruitful; it was found that radiation would not lower the threshold methanation temperature.

Hydrogenation of a retorted, high-volatile, Illinois B-bituminous coal was accomplished in and out of radiation fields. Radiation had no effect on the rate of methane formation for the seventeen runs conducted at 950–960°F and pressures between 800–1800 psig. Unless specifically stated, retorted, Illinois B-bituminous coal was used for all runs.

A number of catalysts were investigated. Ammonium molybdate, ferrous sulfate, fluorescent powder, zinc sulfide and lead were without effect on the rate of methane production at 950–960°F and hydrogen pressures of 800–1400 psig. Stannous chloride, calcium hydridge, sodium borohydridge and sodium increased the rate of methane formation from 1·5- to 3-fold. Radiation did not enhance these catalytic effects.

Fifty-four runs were made on the char–water systems at temperatures of 1180–1200°F, and pressures of 1900–2500 psig. Twenty-five of these runs were carried out under irradiation fields of 52,200 r/hr. Atomic radiation greatly increased the rate of methane formation, *G*-values of 1500 to 3340 being obtained.

These runs were repeated in the Brookhaven National Laboratory's γ-pool. At a dose rate of 174,000 r/hr, ten runs gave an average *G*-value of 1500.

The kinetics and mechanisms of the reactions are discussed.

The Effect of Acute, Chronic and Fractionated Doses of Gamma Radiation on the Induction of Somatic Mutations in *Trifolium repens*. D. R. Davies, Wantage Radiation Laboratory, Wantage, Berks., U.K.

Clonal lines of *Trifolium repens* heterozygous for the V^{by} leaf marking allele have been exposed to acute and chronic γ-irradiation from a Co^{60} source. Mutations resulting both in the loss of all or part of the leaf mark, and in the production of other forms of mark have been observed. The dose–response curve for the induction of these mutations appeared linear. However, fractionation of the dose, or exposure to chronic irradiation, resulted in a considerable reduction in the induced mutation frequency. Mutant tillers ultimately appeared on several plants and progeny tests of these are planned, to test the nature of the genetic changes.

* Institute of Chemical Research, Bucharest.

† Institute of Atomic Physics, Magurele, Rumania.

Sterilization of Medicaments by Gamma Radiation. Note I. Ampoules of Distilled Water. PAUL ADRIAN,* DAN ARIZAN,* ALEXANDRE CONSTANTINIDE,* STEPHANIE BALIU,† MARIE OANCEA,† MATHILDE ROSETTI,* FLORICA STANESCO‡ and VIRGINIE COSMA.‡

The work described here related to the industrial application of cold sterilization by means of radiations and consisted of the following stages:

(1) The ampoules containing distilled water were subjected to varying doses of γ-radiation from a Co^{60} source;

(2) The radiation dose sufficient to sterilize industrially produced ampoules of distilled water was determined;

(3) The work was rounded off with a study of the doses necessary for sterilizing ampoules artificially contaminated with various aerobic and anaerobic microorganisms in different concentrations;

(4) With a view to applying the process in industry, the effect of γ-radiation emitted by uranium fission products was studied; and

(5) Lay-outs and equipment were designed for two alternative γ-sources: Co^{60} and fission products.

(6) The conclusion was drawn that cold sterilization by means of γ-radiation could be applied with great economic advantage to the industrial production of ampoules of distilled water.

(7) This work constitutes the first stage of a general programme of research now under way.

The United States Industrial Radiation Programme. PAUL C. AEBERSOLD, Office of Isotopes Development, U.S. Atomic Energy Commission.

Adequate sources of ionizing radiation for commercial scale processing are now available from radioisotopes, nuclear reactors and several types of machines. Costs of radiation power are beginning to come within ranges attractive to industry. Increased research efforts, however, are necessary to develop processes which merit large-scale economic demonstration.

A brief review is presented of U.S. efforts to discover major industrial radiation applications. Included is a summary description of more than 200 U.S. radiation facilities, exclusive of nuclear reactors. A broad programme of basic radiation chemistry research is being performed at government laboratories, universities and a limited number of private companies. Radiation studies by most U.S. companies, however, are highly applied. The level of effort on industrial radiation process research in the United States is estimated at $10,000,000 annually.

In view of the great potentials for radiation processing, the USAEC has established an Industrial Radiation Programme to help deal with the major problems involved. Five phases of this programme are discussed. First, radiation chemistry efforts are being increased and are now more concerned with ion–molecule reactions. Also, more basic research efforts will be directed toward chemical systems of industrial significance. Emphasis is placed on obtaining greater knowledge about atomic and molecular species formed by radiation. This should permit development of techniques for controlling yields and reactions of primary radiation products.

Second, applied research is being conducted to examine major parameters, including temperature, pressure and catalysis, which affect broad classes of radiation-induced reactions. Specific examples of applied research on particular systems are presented.

Third, a new field of "radiation engineering" is developing. This includes the design and production of sources and irradiators for performing specific radiation processes. Current work on large-scale radioisotope source production and fabrication is briefly described. Also discussed is construction of a versatile engineering research irradiation facility of megacurie capacity for studies on

* Radiomedicine and Radiochemistry Laboratory, Institute of Chemical Research, Bucharest.

† Laboratory of Microbiology, Institute for Pharmaceutical Research and Drugs Control, Bucharest.

‡ "Fiole" Medical Supplies Factory, Bucharest.

VOL. 7 1959/

irradiator design using a variety of sources.

Fourth, the development of nuclear reactors as sources of radiation is described. Studies of reactor irradiation schemes and industrial process requirements commensurate with the use of reactors are presently under way. Several U.S. companies have designs for reactors using fission fragment energy for nitrogen fixation.

Finally, the Atomic Energy Commission, through its Oak Ridge Fission Product Pilot Plant and several Commission-owned reactors, is presently the only U.S. producer of large radioisotope sources. A discussion is presented of the problems of predicting industrial requirements for radioisotopes, assuring their continued availability and, most important, encouraging private production.

Elementary Processes Characteristic of Radiation Chemistry and Possible Industrial Implications. MILTON BURTON, University of Notre Dame, Notre Dame, Indiana.

Elementary physical and chemical processes particularly characteristic of radiation chemistry not only explain some of the observed differences between such chemistry and the older and more conventional branches but also give promise of possible new industrial developments. Of course, some of the more obvious differences (e.g. in possible intensity of energy input at low temperature) may have special technological significance for gases as well as for condensed systems. However, this paper is concerned essentially only with elementary processes unique to radiation chemistry and their special implications.

Most outstanding of these processes are ionization and the decomposition and reactions of ions. In gases particularly, reactions of molecules with positive or negative ions may play a new and important industrial role. The effect of pressure in pure gases and gaseous mixtures is yet to be explored from this viewpoint.

In liquids and other condensed systems (and sometimes in gases at high pressure), the special differences between radiation chemistry and other branches of kinetics are emphasized and exaggerated by the local microscopic distribution of primary effects in ionization columns and in spurs. In addition to the possibilities of reactions involving ions and neutralization of ions, we must consider ionization and excitation transfer, rapid internal conversion processes, the role of metastable (e.g. triplet) excited states, sternvolmer reactions of excited molecules, reactions of excited molecules with each other, and diffusion controlled processes involving four or more radicals. Industrial applications of radiation chemistry are an obvious result of the exploitation of such unique elementary processes not only at high temperatures but perhaps particularly at very low ones.

Description of Radiation Sources Installed at the French Atomic Energy Commissariat. P. LÉVÊQUE.

Cobalt sources and a casemate which utilizes spent rods from the EC3 reactor are placed at the disposal of all research workers. These facilities are described and discussed in detail.

Note

At the time of going to press the text of abstracts of certain of the Conference papers was not available. These abstracts will be published in Volume 7 No. 2 of the *International Journal of Applied Radiations and Isotopes.*

forthcoming papers

JOEL R. GUTMANN: Use of the isotope effect in the study of heterogeneous catalytic reactions.

JOSHUA JORTNER and GABRIEL STEIN: Hydrogen isotope effects in the photo- and radiation chemistry of aqueous solutions.

E. A. HALEVI: The secondary hydrogen isotope effect.

J. C. N. WAKELEY, BRENDA MOFFATT, ANN CROOK and J. R. MALLARD: The distribution and radiation dosimetry of zinc-65 in the rat.

P. R. HILLS, R. ROBERTS and M. W. SPINDLER: The radiation-induced synthesis of the insecticide "Gammexane"—I. Synthesis by ultra-violet light.—II. Synthesis by high-energy radiation.

A. R. G. LANG and S. G. MASON: A counter for solid samples containing labile tritium.

D. J. CHLECK, F. J. BROUSAIDES, W. SULLIVAN and C. A. ZIEGLER: Lithium aluminum tritide in active hydrogen analysis.

J. F. CAMERON and J. R. RHODES: Beta-excited characteristic X-rays as energy reference sources.

M. L. SAZONOV and L. A. SCHWARZMAN: Use of radioactive isotopes of arsenic and niobium for investigations on metallurgical reactions.

GEORGE V. LEROY, GEORGE T. OKITA, EDWARD C. TOCUS and DONALD CHARLESTON: Continuous measurement of specific activity of $C^{14}O_2$ in expired air.

VOL.
7
1959/

International Journal of Applied Radiation and Isotopes, 1959, Vol. 7, pp. 77–86. Pergamon Press Ltd. Printed in Northern Ireland

An Instrument and Technique for the Continuous Measurement of Respiratory CO_2 Patterns in Metabolic Tracer Studies

F. J. DOMINGUES, K. J. GILDNER, R. R. BALDWIN and J. R. LOWRY
General Foods Research Center, Tarrytown, New York

(*Received* 9 *March* 1959; *in revised form* 7 *April* 1959)

To facilitate metabolic tracer studies with white rats, an instrument has been developed for the continuous analysis and recording of respiratory CO_2. This instrument measures radioactive CO_2 by means of a vibrating reed electrometer, and total CO_2 by means of infra-red absorption. Specific activity is recorded separately. A linear integrator makes it possible to read total respired radioactive CO_2 at any point in a metabolic experiment.

With this instrument, metabolic data may be obtained by feeding to white rats test materials with C^{14} tags at appropriate positions in the molecule, and measuring radioactive and total CO_2 respired.

By an indirect approach, metabolic information has been obtained on toxic agents by measuring the effect of these agents on metabolism of a normal nutrient, such as C^{14} tagged glucose. The very preliminary results herein reported indicate that ingestion of toxic agents constitutes a biochemical stress with resulting changes in the metabolic pattern of glucose. Parathion and carbon tetrachloride produce significant differences in the metabolic behavior of radio-glucose in white rats subjected to single administrations of sublethal levels of the above agents.

UN INSTRUMENT ET UNE TECHNIQUE POUR LA MESURE CONTINUELLE DES MOTIFS DU CO_2 RESPIRATOIRE DANS LES ÉTUDES MÉTABOLIQUES À INDICATEUR

Pour faciliter les études métaboliques à indicateur chez les rats blancs on a mis en point un instrument pour l'analyse continuel et l'enregistrement du CO_2 respiratoire. Cet instrument mesure le CO_2 radioactif au moyen d'un électromètre à lame vibrante et le total du CO_2 par l'absorption infra-rouge. L'activité spécifique est enregistrée séparément. Un intégrateur linéaire rend possible de lire le total du CO_2 respiré à aucun instant au cours d'une expérience métabolique.

Avec cet instrument on peut obtenir les données métaboliques en nourissant des rats blancs avec des matières d'essai marquées de C^{14} aux positions convenables dans la molécule, et en mesurant la quantité radioactive et la quantité totale du CO_2 respiré.

Par un accès indirecte, on a obtenu de l'information métabolique sur des agents toxiques en mesurant l'effet de ces agents sur le métabolisme d'un aliment normal, tel que le glucose marqué de C^{14}. Les résultats fort préliminaires rapportés ci-dessous indiquent que l'ingestion des agents toxiques constitue une tension biochimique produisant des altérations dans le motif métabolique du glucose. Le parathion et le tetrachlorure de carbone produisent des différences significatives dans le comportement métabolique du radioglucose dans les rats blancs soumis à des doses uniques sous-léthales des agents nommés ci-dessus.

OL.
7
9/60

1

ПРИБОР И МЕТОДИКА ДЛЯ НЕПРЕРЫВНОГО ИЗМЕРЕНИЯ РАСПРЕДЕЛЕНИЯ ДЫХАТЕЛЬНОГО CO_2 ПРИ ИССЛЕДОВАНИИ ОБМЕНА ВЕЩЕСТВ С ПОМОЩЬЮ ИЗОТОПОВ

Чтобы облегчить изучение обмена веществ у белых мышей бал сконструирован прибор для непрерывного анализа и регистрации дыхательного CO_2. Этот прибор измеряет радиоактивную фракцию CO_2 посредством вибрационного электрометра, а общее количество CO_2 определяется по инфра-красному поглощению. Удельная активность регистрируется отдельно. Линейный интегратор позволяет производить отсчеты общего количества радиоактивного CO_2 в любой момент эксперимента.

При применении этого прибора данные по обмену веществ можно получать путем скармливания белым мышам соответствующих соединений, меченых C^{14} по определенным положениям молекулы, с последующим измерением выдыхаемого радиоактивного и общего CO_2.

Данные по обмену веществ для токсических агентов были получены косвенным путем, определяя действие этих агентов на обмен какого-нибудь обычного питательного вещества, например глюкозы, меченой C^{14}. Сообщенные здесь сугубо предварительные данные показывают, что введение токсических веществ приводит к биохимическому напряжению, вызывающему соответствующие изменения в картине обмена глюкозы. Паратион и четыреххлористый углерод вызывают значительные изменения в обменном поведении радиоглюкозы у белых мышей при однократном введении суб-летальных доз указанных агентов.

MESSGERÄTE UND TECHNIK ZUR KONTINUIERLICHEN BESTIMMUNG DES ATMUNGS-CO_2 BEI STOFFWECHSEL-SPURENUNTERSUCHUNGEN

Zur Erleichterung von Stoffwechsel-Spurenuntersuchungen an weissen Ratten wurde ein Gerät zur kontinuierlichen Analyse und Registrierung des Atmungs-CO_2 entwickelt. Dieses Gerät misst radioaktive Kohlensäure mit Hilfe eines vibrierenden Rohrelektrometers und den totalen CO_2-Gehalt durch Infrarotabsorption. Die spezifische Aktivität wird gesondert registriert. Ein linearer Integrator ermöglicht die Ablesung der gesamten Menge des ausgeatmeten CO_2 zu jedem Zeitpunkt des Stoffwechselexperimentes.

Mit Hilfe dieses Instrumentes erhält man Stoffwechselwerte, indem man weisse Ratten mit Testsubstanzen füttert, die mit C^{14} an entsprechender Stelle im Molekül markiert sind, und anschliessend die Aktivität und die gesamte Menge des ausgeatmeten CO_2 bestimmt.

Auf indirektem Wege wurden auch Auskünfte über den Stoffwechsel bei Anwendung von Giften gewonnen, dadurch dass die Wirkung dieser Stoffe auf den Metabolismus gewöhnlicher Nahrungsmittel, z.B. C^{14}-markierte Glukose, untersucht wurde. Die ersten Versuchsergebnisse, die hier vorgelegt werden, deuten darauf hin, dass die Verdauung des giftigen Agens eine biochemische Belastung hervorruft, welche sich in einer Veränderung des Ablaufs des Glukosestoffwechsels äussert. Parathion und Tetrachlorkohlenstoff ergeben deutliche Unterschiede des stoffwechselmässigen Verhaltens von Radioglukose bei weissen Ratten nach einmaliger Verabreichung einer sublethalen Menge dieser Substanzen.

VOL. 7 1959/

Considerable new knowledge has been obtained in the fields of nutrition and toxicology by using radiotracers in feeding studies with test animals to study distribution and metabolic fate of various food additives. The availability of C^{14} along with advances in synthetic and biosynthetic procedures for labeling complex food materials has made this new knowledge possible. If a food component or a food additive follows a normal metabolic pathway and if a turnover and a material balance can be established, the likelihood is good that the material will be safe for food use. In many cases metabolic pathways can be determined in a relatively short period of time by the use of C^{14} labeled compounds.

The conversion of a carbon-containing food component or additive to energy and CO_2 can be followed readily with C^{14} tagged material in test animals. Since the conventional procedures for measuring respiratory CO_2 and $C^{14}O_2$ by collection in alkali and subsequent precipitation, weighing, and counting, are time consuming and tedious, an instrument was developed for the

accurate and continuous analyses and recording of respiratory carbon dioxide. This instrument measures radioactive CO_2 by means of a vibrating reed electrometer, and total CO_2 by means of infra-red absorption. It is so designed that specific activity is recorded separately. The instrument also contains a linear integrator such that total radioactivity may be read at any point in the experiment.

With this continuous radioactive gas analyzer a number of C^{14} tagged food additives have been tested and evaluated in a preliminary way. The direct approach to the problem is to prepare test material, with C^{14} tags at appropriate positions in the molecule, feed or intubate the test material to white rats, place the test animal in a metabolism chamber and follow respiratory CO_2 by means of the continuous radioactive gas analyzer.[1] If the test material is metabolized a respiratory plot is obtained. A background count is generally achieved in about 24 hr. The metabolism chambers used in these experiments are designed such that urine and feces samples are collected separately for analysis. This information, along with the autopsy data—analysis of carcass and particularly of vital organs—will generally give considerable information on absorption, excretion, storage, detoxification mechanism, and utilization. Careful analysis of the data is of great help not only with respect to the preliminary evaluation of food additives, but also with respect to defining the type and extent of additional feeding and toxicology studies which may be required.

Unfortunately, perhaps, it is sometimes difficult, impractical or impossible to label certain complex food components or food additives with C^{14}. In such cases an indirect approach to the problem of screening these additives has been undertaken and is currently under investigation. Results are quite preliminary but sufficiently promising to suggest that considerable new information may be obtained on nutrition and metabolism pertinent to the problem of safety of food additives.

The dynamic nature of metabolism and the interaction of the endogenous metabolic stores with the exogenous sources of energy are well known and in many instances well defined. The interference with these reactions by a foreign toxic material should be expected and might be of significant and measurable magnitude. If the interference is widespread instead of localized at a cellular level, investigation of changes in a common end-product of metabolism, such as CO_2, should yield useful information. For example, when C^{14} labeled glucose is intubated or fed to a white rat, under a standard set of conditions, a uniform and reproducible respiratory pattern of specific activity is obtained. It has been demonstrated that this respiratory pattern may be altered when a toxic agent is administered to the rat. To date, only a limited amount of experimental work has been carried out, but the procedure seems to have potential not only for rapid screening of food additives but also for the early detection of metabolic changes brought about by a variety of stresses placed on the animal organism.

In this initial study only uniformly labeled glucose-C^{14} has been used as a test substrate. Other specifically labeled carbohydrates, proteins, fats or other test substrates would provide additional information, and may prove to be specific for certain types of stress.

In this study the indirect approach of measuring changes in the oxidative rate of uniformly labeled glucose C^{14}, in the presence of small amounts of two widely different toxic agents, carbon tetrachloride and parathion, has been investigated by the continuous radioactive gas analyzer.

DESCRIPTION OF APPARATUS

The vibrating reed electrometer is considered to be the most sensitive, stable, and accurate current measuring device that can be used with ionization chambers.[2] There are two basic methods of using an electrometer–recorder combination to measure this current from an ionization chamber. They are called the "rate-of-charge" method and

the "high-resistance-leak" method. In the "high-resistance-leak" method a high resistance (10^{12}–10^{13} ohms) is connected between the center electrode of the ionization chamber and the feedback circuit. This resistance draws off the current being produced in the ionization chamber by the radioactivity present. This is the method that is most generally used for continuous monitoring of a radioactive gas stream.

The "rate-of-charge" method has been previously used for measurement of individual samples of radioactive gas, where greater sensitivity and precision of measurement is required. In the "rate-of-charge" method, the ionization chamber probe is connected to the input terminal of the vibrating reed electrometer. This probe is directly connected to the rest of the circuit through a condenser. The electrons, formed by the ionization of the air within the chamber by radioactivity, collect on the probe, and the potential of this center electrode increases in direct proportion to the number of electrons collected. The increase of this potential, in respect to time, is directly related to the amount of radioactivity within the chamber. Since the capacity of the electrometer head is very small ($\sim$10 $\mu\mu$F), production of a very small number of electrons produces a significant charge in the system, making the "rate-of-charge" method a more sensitive procedure for measuring small currents.

For the "rate-of-charge" method the theoretical calibration factor for C^{14} in air is $2{\cdot}47 \times 10^{-5}$ μc/MV per min charge rate. For the high-resistance-leak method the theoretical calibration factor for C^{14} in air is $1{\cdot}24 \times 10^{-4}$ μc/MV potential with a 10^{12} ohm leak resistor.[2] Observed values,[2] using from 1 to 20 l. ionization chambers, only approached this value, while in chambers less than 1 l. in volume, were considerably less sensitive.

The "high-resistance-leak" method has certain disadvantages. Since this method depends upon resistors, the limit of accuracy is dependent upon the choice of excellent quality resistors. For maximum sensitivity, very large resistors must be used (10^{12}, 10^{13} ohms) and, therefore, large time constants are introduced into the measurement. These large time constants can be troublesome when integration with other measurements along with the radioactive determination is desired.

The "rate-of-charge" method is more precise, sensitive and accurate than the "high-resistance-leak" method. Furthermore, the measurement does not involve a time constant. The time, however, required to establish a measurement slope can be significantly large.

The "rate-of-charge" method has been adopted to permit its use in the continuous monitoring of radioactive carbon dioxide. This has been accomplished by a differential timer which discharges the ionization chamber at preset desired intervals.

The time interval selected for discharge of the ion chamber is determined by the amount of radioactivity present. With high amounts of radioactivity, the rate of charge is high and the ion chamber requires frequent discharging. With low amounts of radioactivity a larger time interval between discharging is desirable to permit sufficient accumulation of charge to differentiate between background and low levels of radioactivity. The $C^{14}O_2$ pattern from a rat which has been fed radioactive glucose is shown in Fig. 1.

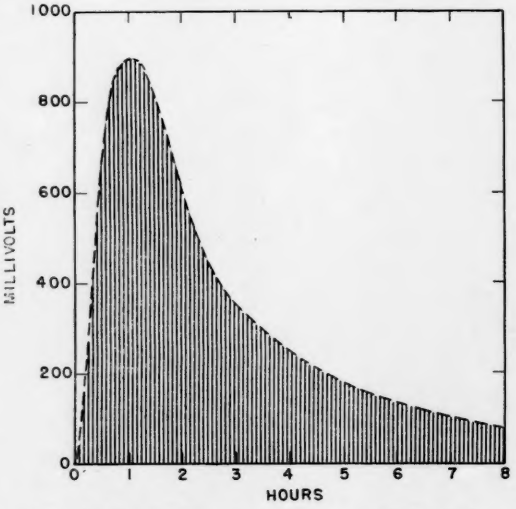

FIG. 1. The $C^{14}O_2$ pattern of a rat administered radioactive glucose.

VOL. 7 1959/6

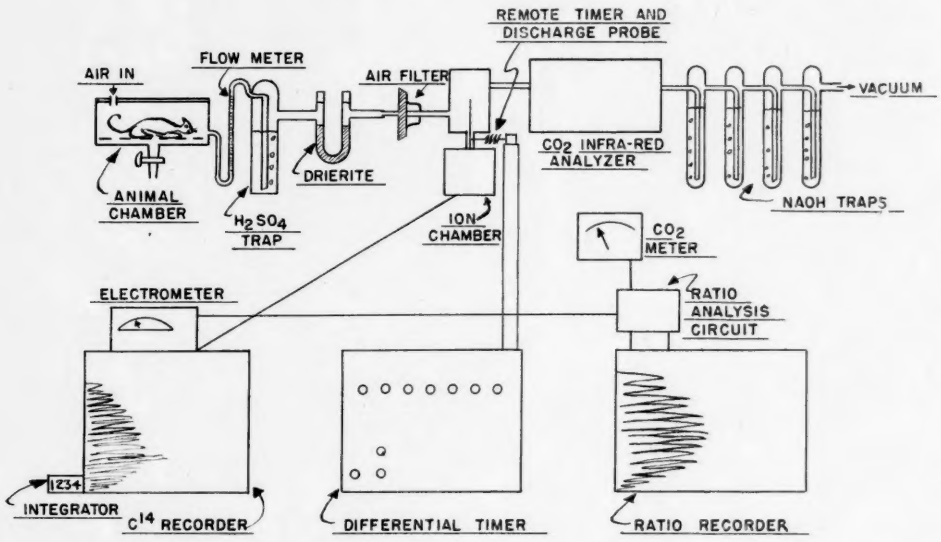

Fig. 2. Schematic diagram of the continuous carbon dioxide analyzer.

The envelope of the above figure describes the rate at which $C^{14}O_2$ appears in the breath of the animal.

The height of the individual spike is a measurement of millivolts per time interval which is a slope measurement. By continuously measuring this slope, which is a differential measurement, the rate of the reaction is established. Integration of this differential yields total millivolts, which is directly proportional to the amount of $C^{14}O_2$ excreted.

Since the area under this curve is a direct measurement of the total radioactivity expired, a linear integrator* was installed on a recorder. A remote switch feeds the pulses to an externally mounted Veeder-Root Counter and the area under the curve, total radioactivity, is read out continuously on the external face of the analyzer.

It was considered necessary to augment the total radioactive measurement with a specific activity measurement, i.e. the ratio of $C^{14}O_2$ to total CO_2. The specific activity provides the true index of metabolism rate of a given radioactive compound. If only the radioactive measurements were made, variations in the respiration rate of the animal could cause artifactual peaks in the recorded activity pattern. Total CO_2 excretion is measured by infra-red absorption. The percentage change in specific activity is directly proportional to changes in either the infra-red or ionization chamber outputs. The ratio circuit is supplied with attenuation so that either the C^{14} or CO_2 signal can be dampened and the specific activity changes remain proportional. Attenuation allows the full scale deflection of the specific activity recorder under conditions where either the C^{14} or CO_2 signal may be too small in respect to one another (Fig. 2).

Over a wide range of flow rates (100–1000 ml/min) the infra-red measurement of total CO_2 was not affected. The ion chamber measurement of radioactivity is affected by flow rate. The following figure is the result of pulling through a 250 ml ion chamber a gas of constant specific activity at various flow rates (Fig. 3).

At the higher flow rates the response is less flow dependent than at the lower flow rates. However, the sensitivity is lowered as a result of the shorter ion chamber "dwell-time."

* Manufactured by Libroscope, Inc.

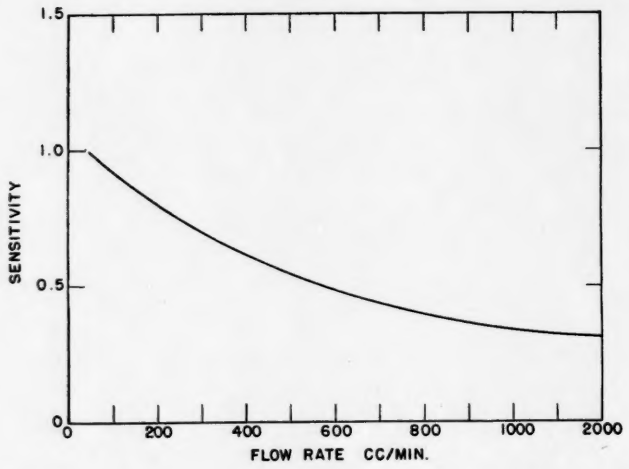

FIG. 3. The effect of flow rate on the sensitivity of the C^{14} ion chamber measurement.

In any system of significant volume, it is necessary to have relatively high flow rates in order that the emptying time and the response time be as short as possible. It is evident from Fig. 3 that one limiting factor of resolution would be flow rate. It is necessary to maintain a constant flow rate. It is equally important to maintain a constant volume in the system so that emptying and response time do not change from day to day operation.

Since experimental animals vary in weight and therefore volume, a "variable-volume control" was introduced into the system (see Fig. 2). This syringe has a capacity of 100 ml and therefore allows use of animals of weight ± 50 g around an optimum mean. For animals outside this weight range a different size syringe can be substituted. Thus, a "constant head space" and constant flow rate can be maintained regardless of animal size.

The particular system described in this paper has a total volume of 2500 ml and a response time of 35 sec. One-half emptying time is 84 sec at a flow rate of 1000 ml/min and 99 per cent emptying time is 10 min.

The infra-red CO_2 measuring device has a 99 per cent full electrical response time of 0·7 sec. The ionization chamber response time is for practical purposes instantaneous. A problem of phasing rests with the different sizes of the ion chamber and infra-red cell. The CO_2 analyzer employs a 10 ml cell while the ionization chamber can be any value from 100 ml to 20 l. As previously mentioned, one gains sensitivity with the larger ion chamber but the problem of phasing becomes proportionately more difficult. By using a 250 ml ion chamber, which is less sensitive than a 1 l. chamber, there is the advantage of rapid emptying of the ion chamber so that the lag time between the ion chamber and infra-red cell is reduced. The lag time between the two instruments is less than 15 sec.

EXPERIMENTAL PROCEDURE

The animal to be studied is intubated with a C^{14} labeled compound and placed in a metabolism chamber. A vacuum line provides air flow through the chamber at a flow rate of 1 l/min (Fig. 2). A Hoke valve provides control of flow rate, which is measured by a Brooks Roto-meter. The air is pulled from the chamber through a sulfuric acid trap to eliminate water. The variable volume control syringe is placed in the line

immediately following the H_2SO_4 acid trap and before a "Seitz" filter which removes particulate matter from the air stream. The clean dry air then goes into the infra-red carbon dioxide analyzer and the ionization chamber. The air is finally pulled through a continuous gas analyzer at a constant rate of 1 l/min. Each experimental period was of 24 hr duration. Each rat used in the experiment was initially intubated with a dose of radioactive glucose, proportional to its starved weight. The excreted CO_2 was

TABLE 1. Effect of toxic agents on glucose metabolic coefficients

Treatment of animals	Dose glucose (mg) per 100 g body weight	Dose toxicant (mg) per 100 g body weight	Peak time (min)	Peak height (corr.)*	% of CO_2 excreted
Glucose	71·9	—	70	29·5	47·9
Glucose + CCl_4	75·6	386	115	18·8	68·9
Glucose	81·6	—	65	20·3	—
Glucose + CCl_4	68·0	185	100	29·7	—
Glucose	73·6	—	70	22·0	56·5
Glucose + CCl_4	74·8	79	70	23·5	73·3
Glucose	75·9	—	65	34·3	45·1
Glucose + parathion	74·6	$4{\cdot}79 \times 10^{-3}$	55	32·0	56·2
Glucose	80·0	—	82	21·9	44·6
Glucose + parathion	81·9	$3{\cdot}31 \times 10^{-3}$	40	28·8	70·6
Glucose	70·0	—	65	24·9	40·1
Glucose	64·5	—	65	30·7	49·1
Glucose	96·4	—	60	21·2	56·0
Glucose	86·8	—	65	21·0	64·4

series of NaOH traps to trap the radioactive CO_2.

Male, albino, Charles River–Wistar strain litter mate rats were used in the experiment. The weights ranged from 100 to 250 g. The animals were fasted overnight but were allowed free access to water. The radioactive glucose (0·1 g glucose containing 0·0015 g radioactive glucose (1–2 μc/kg) in 1 ml of water) and the test compound were intubated by stomach tube and the rats immediately placed in the metabolism chamber. Air was pulled through the chamber into the analyzed and recorded for the 24 hr. Following this procedure, the animal was removed from the chamber and allowed free access to food and water for 2 days. This animal was fasted the evening of the third day (post intubation) and intubated the following day with radioglucose first and then the toxicant in two separate intubations; one immediately following the other. By this procedure each animal served as its own control. Three different levels of carbon tetrachloride and two levels of parathion, low and intermediate, were run (Table 1).

RESULTS AND DISCUSSIONS

TABLE 2. Standard error of standard deviations of control vs. toxicant

	Peak height	Peak time	% of CO_2
Control–CCl_4	0·5	7·32	5·11
Control–Parathion	not significant 2·44	3·25	3·63

When S.E.$_\sigma$ = 2·00 is equal to 95% confidence level.

Normal $C^{14}O_2$ excretion patterns for glucose were established and the effects of parathion and carbon tetrachloride on these patterns were determined. The radio active variables studied were:

(1) percentage of intubated glucose excreted as $C^{14}O_2$ in 24 hr,
(2) peak time, i.e. the time from intubation to maximum specific activity,
(3) peak height corrected for dose and body weight, i.e. maximum specific activity at peak time per dose of radioactive glucose intubated.

These results, along with their significances, are listed in Tables 1 and 2.

In all cases, with either parathion or carbon tetrachloride, there was a significant increase in $C^{14}O_2$ excretion during the 24 hr test period compared to the control. In addition, parathion induced an increase in the oxidative rate of glucose with a resulting decrease in peak time and increase in peak height. Conversely, carbon tetrachloride induced an inhibition of the initial oxidative rate, with a resulting increase in peak time (see Fig. 4).

It should be noted that parathion at very low levels ($3–5 \times 10^{-3}$ mg/100g body weight) affected all three variables, percentage of $C^{14}O_2$ excreted, peak time and peak height. It took relatively large amounts of CCl_4 (100 mg/100 g) to affect peak time and percentage of $C^{14}O_2$ excreted.

Both agents, at the levels used, caused a significant shift in the metabolism of glucose. Based on the levels required to cause these shifts, parathion had a greater effect on glucose metabolism than did carbon tetrachloride.

The effect of parathion appears to fall in the "general alarm" type of reaction. The overall acceleration of glucose oxidation might be

VOL. 7 1959/

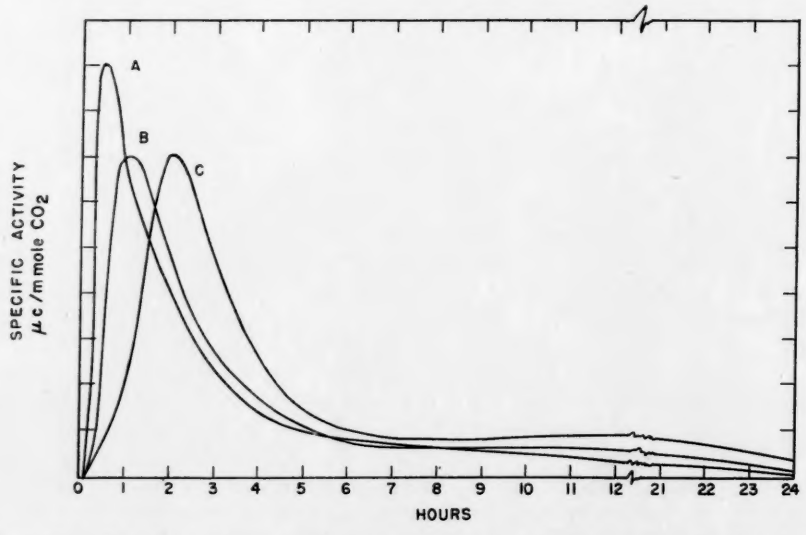

FIG. 4. The effect of parathion and carbon tetrachloride on the CO_2 excretion of radioactive glucose.
A = Glucose + parathion B = Glucose C = Glucose + CCl_4

expected if adrenalin were released as it would be in an "alarm reaction."

The effect of parathion in accelerating the oxidation of glucose is well supported by work reported in the literature. LOCKER and SIEDER[3] have reported increases in respiration of liver slices by the addition of 10^{-3} M parathion. Work on a closely related pharmacological compound, prostigmine, showed that compounds of this general nature caused liberation of epinephrine[4] by the adrenal gland. The absorption, action, and excretion of these compounds occur rapidly, less than 2 hr being required for the complete cycle. Intravenous injection of esterase blocking agents such as parathion,[5] cause an increase in respiratory frequency and volume. These data are consistent with the present reported results. Extremely small doses are effective in changing the rate of glucose metabolism (Table 1). GAGE[6] has reported that the inhibiting action of parathion is due to the breakdown of parathion to a derivative of *p*-nitrophenol. The amount of inhibitor is in the order of 0·1 per cent of the injected parathion and its concentration in the tissues is a balance between the rate of formation from parathion and its destruction by enzymes. The increased rate of glucose oxidation has been observed in a compound which is a well-known inhibitor of acetylcholinesterase.

Carbon tetrachloride is known to be a liver poison and glucose is known to be well metabolized by the liver. The retarded rate of oxidation and delayed peak time is consistent with the fact that CCl_4 affects the liver adversely. The increased excretion of $C^{14}O_2$ may be accounted for by the fact that CCl_4 has inhibited phosphorylase and as a result, glucose to glycogen conversion is impaired. Since these rats had been fasted prior to intubation, it is reasonable to assume that the glycogen stores have been reduced. The control rats would shunt part of the intubated glucose into glycogen storage. If the CCl_4 truly inhibits phosphorylase, reducing glycogen deposition, then more glucose is available for subsequent oxidation. It has recently been reported by GIUSTI[7] that CCl_4 inhibits succinic dehydrogenase. Apparently, the liver cannot deal with glucose efficiently when poisoned by CCl_4. The glucose is then utilized by other tissues in the rat which oxidizes glucose at a slower rate than the liver. This may explain why the oxidative rate of glucose has been retarded when the animal is subjected to CCl_4.

CONCLUSIONS

An instrument for the continuous analysis and recording of CO_2 respired from test animals is described. This instrument measures radioactive CO_2 by means of a vibrating reed electrometer, and total CO_2 by means of infra-red absorption. A "rate-of-charge" ionization chamber has been modified for sensitive and continuous measurement of $C^{14}O_2$. Specific activity is recorded separately. A linear integrator makes it possible to read total respired $C^{14}O_2$ at any time during an experimental run.

Metabolic and toxicity information may be obtained with this instrument by feeding to test animals appropriately C^{14} tagged test materials and analyzing the CO_2 respiratory patterns obtained.

The instrument has been used to measure the effect of known toxic agents on the metabolism of a normal nutrient such as C^{14} tagged glucose. Changes have been observed in the respiratory patterns. For example, parathion caused an increase in the $C^{14}O_2$ excretion of glucose, an increase in maximum specific activity, and a decrease in the time required for reaching maximum specific activity. A second test material, carbon tetrachloride, also caused an increase in total $C^{14}O_2$ excretion of glucose, but in this case the time required for reaching maximum specific activity was increased. In each of the aforementioned cases, the white rats served as their own control. Radioglucose was given alone and then in the presence of sublethal levels of the test agents.

The careful measurement and analysis of CO_2 respiration patterns may well provide a basis for preliminary but rapid screening of

test agents which might be under consideration as potential food additives.

Acknowledgements—The authors are indebted to Anthony Nacci for technical assistance and to R. Thiessen, Jr., without whom this work could not have been accomplished, for continued support and co-operation.

REFERENCES

1. Long C. L., Domingues F. J., Studer V., Lowry J. R., Zeitlin B. R., Baldwin R. R. and Thiessen R. Jr. *Arch. Biochem. Biophys.* **77,** 428 (1958).
2. Tolbert B. B. Ionization chamber assay of radioactive gases. *Unclassified Report* UCRL-3499, University of California, Radiation Laboratory, Berkeley, California (1956).
3. Locker A. and Sieder H. *Z. Ges. Exp. Med.* **119,** 314 (1952).
4. Goodwin L. and Gilman A. *The Pharmacological Basis of Therapeutics*. Macmillan, New York (1955).
5. Kempe H. D. and Lukning W. *Arch. Exp. Path. Pharmak.* **225,** 359 (1955).
6. Gage J. C. *Biochem. J.* **54,** 426 (1953).
7. Giusti G. and Coltorte M. *Biochim. Appl.* **4** (4) (1957).

VOL. 7 1959/

International Journal of Applied Radiation and Isotopes, 1959, Vol. 7, pp. 87–96. Pergamon Press Ltd. Printed in Northern Ireland

The Mode of Action of Perchlorate Ions on the Iodine Uptake of the Thyroid Gland

M. ANBAR, S. GUTTMANN and Z. LEWITUS
Isotope Dept., The Weizmann Institute of Science, Rehovoth, Israel and the Isotope Dept., The Beilinson Hospital, Petach Tikva, Israel

(*Received* 16 *May* 1959)

In the course of investigating the physiological iodine uptake mechanism in the thyroid gland, it was found that perchlorate ions concentrate in the thyroid tissue and compete with iodide ions for the limited uptake capacity of the thyroid gland. Using $KClO_4$ labelled with Cl^{36} and O^{18}, it was shown that ClO_4^- does not undergo metabolization in the human body and it is excreted at a fast rate; these results exclude the participation of ClO_4^- in a redox reaction. It was suggested that the competition of the perchlorate ion is due to its similarity in size to that of the iodide ion. Other ions of a size similar to ClO_4^-, including monofluorosulphonates, difluorophosphates and fluoroborates were shown to exhibit a similar action on the iodine uptake like perchlorate ions. These findings on the behaviour of perchlorate and related ions may be relevant to the elucidation of the iodide trapping mechanism of the thyroid gland.

LE MODE D'ACTION DES IONS DE PERCHLORATE SUR L'ABSORPTION DE L'IODE DANS LA GLANDE THYROIDE

Au cours de la recherche dans le mécanisme physiologique de l'absorption de l'iode dans la glande thyroide, on trouva que les ions de perchlorate sont concentrés dans le tissu thyroide et qu'ils sont en concurrence avec les ions d'iodure pour la capacité absorptive limitée de la glande thyroide. L'emploi du $KClO_4$ marqué au Cl^{36} et à l'O^{18} montra que le ClO_4^- ne subit pas la métabolisation dans le corps humain et qu'il est excrété rapidement; ces résultats défendent au ClO_4^- la participation dans une réaction rédox. On proposa que la concurrence de l'ion de perchlorate serait dûe à sa similarité de grandeur à celle de l'ion de chlorure. D'autres ions comparables en grandeur au ClO_4, y compris les monofluorosulphonates, les difluorophosphates et les fluoroborates, montrèrent une action pareille à celle des ions de perchlorate sur l'absorption de l'iode. Les résultats ainsi trouvés sur le comportement des ions de perchlorate et des ions apparentés pourraient être pertinents à l'élucidation du mécanisme par lequel la glande thyroide attrape l'iode.

ХАРАКТЕР ВЛИНИЯ ПЕРХЛОРАТНЫХ ИОНОВ НА УСВОЕНИЕ ИОДА ЩИТОВИДНОЙ ЖЕЛЕЗОЙ

При исследовании механизма физиологического усвоения иода щитовидной железой было найдено, что перхлоратные ионы концентрируются в ткани щитовидной железы и конкурируют с ионами иодида в отношении усвоения их щитовидной железой. Способность последней к усвоению ограничена. При помощи $KClO_4$, меченого Cl^{36} и O^{18} было показано, что ClO_4^- не подвергается обмену в человеческом организме, а экскретируется с большой скоростью. Эти результаты исключают участие ClO_4^- в окислительно-восстановительной реакции. Было высказано предположение, что перхлоратный ион может конкурировать с ионами иодида благодаря сходным размерам этих ионов. Было показано, что усвоение других ионов, близких к по размеру, включая монофторсульфонаты, дифторфосфаты и фторбораты, подобно усвоению ионов перхлората. Эти данные по поведению перхлоратных и родственных им ионов могут способствовать выяснению механизма усвоения иодидов щитовидной железой.

DER EINFLUSS VON PERCHLORATIONEN AUF DIE JODAUFNAHME DER SCHILDDRÜSE

Im Zuge der Untersuchungen über den physiologischen Mechanismus der Jodaufnahme der Schilddrüse wurde gefunden, dass Perchlorationen im Schilddrüsengebiet konzentriert werden und zusammen mit den Jodionen für die begrenzte Aufnahmefähigkeit der Schilddrüse verantwortlich sind. Mit Hilfe von $KClO_4$, welches von Cl^{36} und O^{18} markiert ist, wurde gezeigt, dass ClO_4^- im Stoffwechsel des menschlichen Körpers nicht teilnimmt, sondern sehr schnell ausgeschieden wird. Diese Ergebnisse schliessen die Teilnahme von ClO_4^- am Redoxprozess aus. Es wurde vorgeschlagen, dass die Konkurrenz der Perchlorationen zufolge ihrer den Jodionen ähnlichen Grösse zustande kommt. Andere Ionen mit ClO_4^- vergleichbarer Grösse, einschliesslich Monofluorsulphonat, Difluorphosphaten und Fluorbonaten, zeigten eine ähnliche Wirkung auf die Jodaufnahme wie die Perchlorationen. Diese Ergebnisse über das Verhalten von Perchloratund verwandten Ionen mag für die Klärung des Jodauffangmechanismus der Schilddrüse von Wichtigkeit sein.

INTRODUCTION

THE effect of inorganic reagents on the thyroid physiology created a wide interest in the last two decades. First as a useful tool to investigate different states of normal and deranged thyroid function[1–5] as well as for diagnostic and therapeutic purposes.[6,7] Some monovalent anions like ClO_4^-, CNS^- and NO_3^- were found to have a remarkable effect on the iodine uptake of the gland.[4,5] Other anions such as F^-, Cl^-, Br^-, NO_2^-, BrO_3^-, $SO_4^=$ and $HPO_4^=$ were found to exert only a slight effect. A similarity between the modes of action of ClO_4^- and CNS^- was suggested since both of them block the iodine uptake of the thyroid and eject the trapped inorganic iodine from the gland. This similarity between the effects of ClO_4^- and CNS^- suggested a common mechanism of action, although it was pointed out that this resemblance may be only superficial.[6] The mode of action of thiocyanate ions has been thoroughly investigated. By tracer experiments it was shown that CNS^- undergoes metabolization in the thyroid, resulting in protein bound sulphur, but does not accumulate in the gland.[8,9,10] It was therefore suggested that CNS^- undergoes a chemical change, interfering with the iodine uptake of the gland.[8] Perchlorate ions on the other hand, are known as inert chemical species and it appeared rather unlikely that they participate in a redox reaction analogous to that of thiocyanate.

The purpose of this study was first to find out whether perchlorate ions accumulate in the thyroid gland, and secondly, whether they undergo metabolization similar to thiocyanate ions. In order to elucidate these problems, the behaviour of perchlorate ions was studied using Cl^{36} and O^{18}.

EXPERIMENTAL

Materials

Synthesis of $KCl^{36}O_4$. To HCl^{36} (specific activity 103 μc/g) obtained from Amersham Radiochemical Center, metallic lithium was added until the solution became slightly alkaline. The $LiCl^{36}$ solution was boiled down to a 4 M concentration and was subsequently electrolysed[11] in a semimicro electrolysing cell (4 ml capacity) with stationary platinum electrodes (electrode area 1 cm^2). The cell was cooled by a water jacket, the temperature maintained between 20°C and the solution was stirred constantly by a magnetic stirrer. The electrolysis was carried out at a current density of 1 A/cm^2. Sixteen ml of $LiCl^{36}$ were electrolysed for 30–36 hr; this long period of electrolysis was required because water is decomposed simultaneously. The formation of certain amounts of ozone was noticed during this electrolysis. After electrolysis the solution was diluted to a five-fold volume and concentrated potassium nitrate was added to precipitate $KClO_4$. The precipitate was separated by centrifugation

VOL. 7 1959/6

and was then subjected to digestion with concentrated hydrochloric acid, in order to eliminate any $KClO_3$ present. Next the HCl was boiled off and then $KClO_4$ was recrystallized from boiling water. The total yield was 92–94 per cent.

Synthesis of $KCl^{36}O^{18}$. Anhydrous $LiCl^{36}$ was prepared by evaporating some of the $LiCl^{36}$ solution under vacuum. $LiCl^{36}$ was dissolved in H_2O^{18} (45 atom per cent O^{18}) to form a 4 M solution. This solution was treated as described above. It was shown that ClO_4^- does not exchange its oxygen with water during the digestion with hydrochloric acid.[12]

Determination of the distribution of perchlorate and iodide in various tissue of rats

Either $KCl^{36}O_4$ or NaI^{131} (or both together) dissolved in saline, were injected intraperitoneally to white rats and rabbits. To a number of them 1 mg propylthiouracil dissolved in saline was injected 1 hr prior to the $KClO_4$ or NaI administration,[10] in order to block the formation of organic bound iodine. One group of rats was made goiterous by feeding them 10 mg of propylthiouracil daily for 4 weeks.

After predetermined intervals the animals were sacrificed—the rats by ether and the rabbits by intracardial injection of air. Organs were removed, 100–1000 mg were weighted (accuracy $\pm 0{\cdot}2$ mg) and iodine-131 was radioassayed in a sodium iodide well-type scintillation counter. In order to determine $KCl^{36}O_4$ the organs were ashed in a fuming HNO_3–HCl mixture to which some H_2O_2 was added and the inorganic residue was dried in a counting dish. This procedure was shown to remove any radio-iodine or radio-chlorine present in the sample in any other form than ClO_4^-. The samples were now assayed for radiochlorine in flow-type proportional counters. These counters having a fairly constant background of 8–9 counts/min, were suitable for the low level radioassay required in this study. In all radioassays at least 1000 counts were counted limiting the statistical error to ± 3 per cent. The samples of least activity gave still twice the activity of the background. The specific activities of the organs were calculated as counts per minute per gram of tissue. The relative specific activity was defined as the ratio of the specific activity of the organ to that of the blood. Relative specific activities above unity are a measure of the capacity of the organ to accumulate ClO_4^- or I^- over the level in the blood.

Determination of the metabolization of ClO_4^- *in man*

Two hundred milligrams of potassium perchlorate were administered orally to each of four patients in the course of their thyroid function examination. The perchlorate ions were double labelled both with Cl^{36} (26 μc/g $KClO_4$) and with O^{18} (44·3 atom per cent O^{18} *vide infra*). Each patient received by this means a dose of 5 μc of Cl^{36} which is 2 per cent of the maximum permissible dose of Cl^{36} for continuous consumption. Their urine was collected 3 hr after administration and the following tests were performed:

1. *Determination of chloride and chlorate ions originating from* $Cl^{36}O_4^-$. Each urine sample was concentrated to 1/6 of the initial volume after adding a little nitric acid. The following tests were performed with 4 aliquots of the concentrated urine.

(a) 1 ml of the urine was transferred to a counting dish, dried and counted. The sample contained *chloride*, *perchlorate* and *chlorate* ions if present.

(b) 1 ml of the urine was diluted with 2 ml 1 N HNO_3 and 1 ml 1 N silver perchlorate was added. The precipitated silver chloride was centrifuged, washed with water and separated from the supernatant liquid. Then it was dissolved in concentrated ammonia, and was transferred to a counting dish, dried and counted. This sample contained only the *chloride* ions present.

(c) 1 ml urine was digested with 6 ml of concentrated hydrochloric acid, dried and counted. This sample contained only the *perchlorate* present. The chloride was expelled in the form of volatile HCl and the chlorate ions were reduced by hydrochloric acid[13] and converted to chlorine, which was subsequently volatilized.

(d) 1 ml urine was diluted with 2 ml 1 N

HNO_3 and 1 ml 1 N sodium nitrite was added. After heating for a while, until all the nitrite decomposed, 1 ml 1N silver perchlorate was added and the silver chloride treated as described above for sample (b). Sample (d) contained the *chloride* and the *chlorate* present. The chlorate ions were reduced by nitrous acid to chloride[14] and their joint activity determined.

2. *Determination of isotopic exchange* in vivo *of* O^{18} *labelled perchlorate ions.* The isotopic composition of oxygen in perchlorate was determined by precipitation of $KClO_4$, and decomposing 25–50 mg of the dry salt in a sealed evacuated glass ampoule at 400°C. The glass ampoule having a break-off seal, was opened on the vacuum line of the mass spectrometer and the isotopic composition determined. The mass spectrometer used for this study was a CEC type 21-401.

The minimum amount of potassium perchlorate required for a single oxygen isotopic assay exceeded the amount of perchlorate that could be isolated from the urine samples of the above mentioned patients. The rate of excretion of perchlorate ions by normal patients was found to be about 200 μg/min.[15] Considering the solubility of $KClO_4$ in aqueous solution this would mean collection of urine for an extended period before a sufficient amount of $KClO_4$ could be separated. In order to avoid this limitation, unlabelled $KClO_4$ as "carrier" was added to facilitate the isolation of the $KClO_4{}^{18}$ and the specific activity of Cl^{36} of the isolated $KCl^{36}O^{18}$ were determined simultaneously. The determination of the Cl^{36} specific activity by dilution analysis[16] enabled the determination of the isotopic composition of the oxygen of the $KClO_4$ present originally in the urine. It has been shown[17] that if $KClO_4$ of two different isotopic compositions is mixed and decomposed, the oxygen evolved is totally equilibrated.

The following experimental details of procedure for the determination of the isotopic exchange *in vivo* of perchlorate are presented:

(a) *Determination of the absolute efficiency of the counting system.* 171·7 mg $KCl^{36}O_4{}^{16}$ were diluted in 100 ml water. One ml of the solution was diluted again in 25 ml water. Samples of 1 ml were taken from both solutions, dried and counted. The concentrated solution had an activity of 18,310 counts/min per ml; the dilute solution gave 761 counts/min per ml = 19,050 counts/min per 25 ml. Comparing both values, a correction of 3·7 per cent for self absorption in the concentrated sample is derived. Since specific activity was 26 μc/g $KClO_4$, the efficiency of our counting system was 19·3 per cent.

(b) *The determination of the total amount of perchlorate in the urine solution.* One ml of the urine solution was diluted to 25 ml and 1 ml of the dilute solution was dried and counted, giving 362 counts/min; this meant $9{\cdot}4 \times 10^3$ counts/min per ml of solution X or 0·788 mg $KClO_4$ ml of solution.

(c) *Dilution of the* $KClO_4{}^{18}$. To 35 ml of the above solution were added 10 ml of 0·122 N $NaClO_4$ of normal isotopic composition and $KCl^{36}O_4{}^{18}$ was precipitated by adding KNO_3 in excess. The precipitate was centrifuged and the supernatant was separated. The precipitate was dried and 65·2 mg were weighed and diluted in 50 ml water. One ml was taken, dried and counted; it had an activity of 2015 counts/min. From this we calculate a specific activity for the precipitate of 3·6 μc/g. This gives us a dilution factor of 7·22.

(d) *Oxygen isotopic analysis A.* Samples of 30 mg of the separated and dried $KCl^{36}O^{18}$ of paragraph (c) were sealed in evacuated ampoules and were decomposed in an oven at 400°C. The oxygen formed was analysed by CEC Type 21–401 isotope ratio mass spectrometer. The isotopic concentration of the samples gave an average value of 6·21 $\pm$ 0·35 atom per cent O^{18}. Taking the dilution factor 7·22 derived in paragraph (c), we obtain for the isotopic composition of the original $KClO_4{}^{18}$ in solution the value of 43·6 atom per cent O^{18}.

(e) *Oxygen isotopic analysis B.* Taking the specific activity obtained in paragraph (b), namely 0·788 mg $KClO_4$/ml, we obtain for 35 ml an amount of 27·6 mg $KCl^{36}O_4{}^{18}$; to this an equivalent of 170 mg $KClO_4{}^{16}$ was

VOL. 7 1959/6

added, giving a dilution factor of 7·16—leading to a value of 43·3 atom per cent O^{18} for the original $KClO_4{}^{18}$. Comparing our results with the value of 44·3 atom per cent of the $KCl^{36}O_4{}^{18}$ ingested by the patients, we may conclude that the oxygen in the perchlorate does not undergo appreciable isotopic exchange *in vivo* if at all.

RESULTS

The distribution of perchlorate ions in various organs of rats and rabbits is presented in Table 1. Each value in Table 1 is an average of determinations in at least two animals.

TABLE 1. The distribution of $Cl^{36}O_4^-$ in various organs (counts/min per g tissue)

Time after injection	Rat	Rabbit	Rat	Rat	Rabbit
	30 min	2 hr	4 hr	9·5 hr	12 hr
Blood	202	557	832	31	149
Thyroid	436	644	1213	137	652
Muscle	38	122	228	14	18
Liver	145	186	641	38	57
Spleen	80	217	377	44	49
Ovaries	—	—	881	—	81
Testes	53	291	—	119	—
Salivary gland	273	—	—	73	88
Adrenal gland	159	287	446	36	48
Mammary gland	—	—	551	—	—
Hypophysis	—	—	225	—	—

It can be seen that in all cases the perchlorate concentration in the thyroid gland is higher, whereas in all other tissues it is lower than that in blood. Still there are indications for retention of ClO_4^- in the salivary gland and in the testes, which are manifested only when the ClO_4^- level in blood falls to a very low value.

The ratio of the specific activity of perchlorate in thyroids vs. the specific activity in blood determined in twelve rats gave an average value of 3·1 with a standard deviation of $\pm 1{\cdot}0$; in nine rabbits this ratio was $3{\cdot}0 \pm 1{\cdot}8$. Although these values fluctuate over a rather wide range they significantly demonstrate the fact that the thyroid concentrates perchlorate ions. Following the specific activity ratio with time, a trend is observed demonstrating a gradual rise; it seems that a limiting value of $4{\cdot}3 \pm 0{\cdot}3$ is reached in rats and in rabbits, at about 5–6 hr after the injection. This result indicates that an equilibrium between blood and thyroid perchlorate concentration is reached only after that interval. In the group of eight goiterous rats which had thyroid glands averaging five times the weight of normal glands, we found the same value of relative specific activity, although the absolute activity was much higher than in normal rats. Comparing these results with the specific activity ratio for other tissues e.g. muscle, we find a constant ratio of $0{\cdot}27 \pm 0{\cdot}08$ both for rabbits and for rats (see Fig. 1).

The only study on distribution of perchlorate ions in body tissues was published in 1938 by DURAND[18], who used a rather elaborate analytical method. DURAND, however, did not determine the ClO_4^- in the thyroid, thus we cannot compare the results. We could not confirm his claim for very large concentrations of perchlorate in the adrenals,

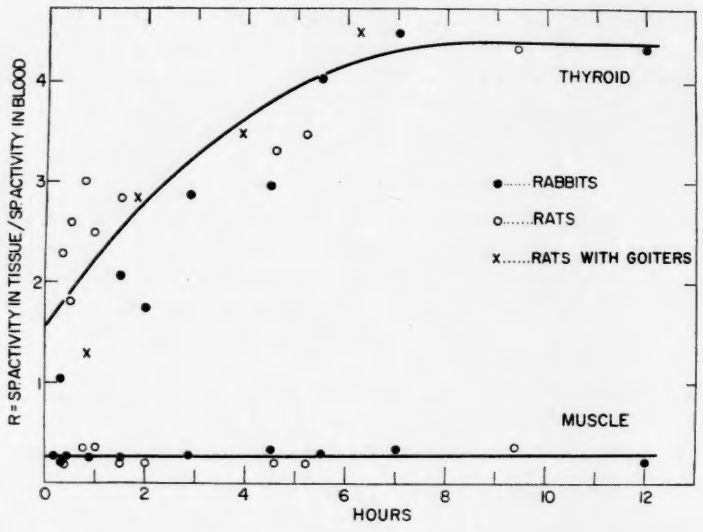

FIG. 1. Accumulation of perchlorate in thyroids of rats and rabbits.

spleen and ovaries as compared with the concentration in blood.

It may be interesting to compare our results with the iodine distribution determined by PERLMAN *et al*[19]. In their work they determined the iodine distribution both at tracer level (10^{-8} molar) and at a dose of 0·5 mg I^- per rat. They found that the only tissue that concentrates iodine is the thyroid gland, whilst the kidney showed a slightly higher iodine concentration than that in blood—all other tissues showed a lower iodine concentration than blood. They also found that at the 0·5 mg I^- level, a 150-fold concentration in the thyroid compared with the liver; at tracer level this ratio rose to 2600-fold 5 hr after administration and to about 30,000 one hundred hours later. In another study[2] it has been shown that if the iodide dose per rat is increased up to 10 mg (the range of concentration used in this study), the thyroid manifests only a *three-fold* concentration over that in blood; this value is well within the range obtained by us. We may conclude therefore, that there is a similarity between the behaviour of perchlorate and iodide ions in the mammal organism.

It has been pointed out that the thyroid capacity for iodide ions is limited and that its unique affinity toward iodide ions may be manifested at tracer level only. Tracer level iodide has an activity of 74 mc/μg as compared to 13 mc/g for carrier free $Cl^{36}O_4^-$; unfortunately, carrier free Cl^{36} is not available, and the highest specific activity commercially available and used by us is 26·1 μc/g ClO_4^-. This leaves us with a factor of 10^9 between the dilution that can be attained using I^{131} on one hand and Cl^{36} on the other. This low specific activity of Cl^{36} limits the approach to the range of concentrations comparable to iodine tracer studies. A possibility of checking the competitive nature of the actions of I^- and ClO_4^- in the thyroid gland is to increase the iodide concentrations. Therefore competition of ClO_4^- and I^- in the *same* range of concentrations was investigated.

One ml of saline solution 0·14 N in I^- and 0·14 in ClO_4^-, having a specific activity of 7·0 and 3·64 μc/mole respectively, was injected intraperitoneally to rats and the distribution of I^- and ClO_4^- determined independently (see experimental section).

Table 2 presents the relative distribution of iodine and perchlorate ions in various tissues 70 min after injection; the data average duplicates.

TABLE 2. The distribution of ClO_4^- and I^- at equimolar concentration in various organs of rats. (Relative specific activity organ/blood)

Organ	I^{131}	$Cl^{36}O_4^-$
Thyroid	1·80	1·69
Muscle	0·22	0·16
Liver	0·41	0·33
Spleen	0·38	0·30
Ovaries	0·43	0·32
Testes	0·29	0·23
Salivary gland	0·47	0·014
Adrenal gland	0·32	0·17
Mammary gland	0·44	—

From Table 2 it may be seen that the thyroid is the only organ that accumulates large concentrations of both iodide and perchlorate. In all other tissues examined, the relative concentrations of iodide and perchlorate ions at equimolar concentrations are comparable. In the salivary glands and in the adrenals iodide concentrates to a higher extent than ClO_4^-.

In order to follow the accumulation of perchlorate and iodide ions in the thyroid at comparable concentrations, thirty-six young rats (average weight 100 g) were injected simultaneously with labelled perchlorate and iodide ions in saline. Half of this group was injected with propylthiouracil 1 hr before the $I^- + ClO_4^-$ injection; no appreciable difference between these and the untreated rats was found, except after a long time following the injection. In this series only thyroid and blood were examined. The blood samples were weighed, whereas the specific activity of the thyroid glands was calculated assuming an average weight of 12 mg per thyroid[1]. An additional group of sixteen rats with induced goiters (see experimental section) was also used in this experiment and their thyroid glands were weighed individually (average weight 60 mg). Each sample was assayed for radio-iodine, ashed as described above and counted again to determine the radio-chlorine; the results are summarized in Table 3 (each value is an average of two animals at least).

Table 4 presents the ratio between the concentration of the two ions in the gland.

TABLE 3. The relative concentration of perchlorate and iodide ions in thyroid glands of rats after simultaneous administration $\left(\frac{\text{sp. activity in thyroid}}{\text{sp. activity in blood}}\right)$*

	Dose (mmols)		Perchlorate			Iodide		
	ClO_4^-	I^-	60 min	120 min	360 min	60 min	120 min	360 min
3·1	0·028	—	—	2·4 2·8†	—	—	—	—
3·2	0·14	—	2·2* 1·8†	3·2 2·7†	4·3 5·1†	—	—	—
3·3	0·14	0·028	2·3	4·5	4·3	2·3	4·0	6·3 13·1*
3·4	0·14	0·14	1·7 1·3†	4·7*	4·4	1·0 0·7†	4·0* 2·4†	6·9
3·5	0·028	0·14	1·9	2·3	3·7	2·7*	3·5	4·7
3·6	—	0·14	—	—	—	2·5	4·5* 4·2†	7·6 28·0*
3·7	—	0·07	—	—	—	2·4	—	—
3·8	—	0·028	—	—	—	—	22·0	—

* All rats but those (*) received 1 mg propylthiouracil 1 hr before injection.
† Goiterous rats by feeding propylthiouracil for 4 weeks.

TABLE 4. The ratio between concentrations of iodide and perchlorate ions in the thyroid

$$\left(\text{ratio} = \frac{\text{concentration of iodide in thyroid}}{\text{concentration of perchlorate in thyroid}}\right)$$

	Time (min)		60	120	360
	Dose (mmols)		Ratio I^-/ClO_4^-		
	I^-	ClO_4^-			
4·1	0·14	0·028	4·7	6·9	3·3
4·2	0·14	0·14	2·1	2·7	2·2
4·3	0·028	0·14	0·53	0·58	0·67

In Table 5 the concentration of iodide and perchlorate ions in different rats 2 hr after injection of an equimolar dose is presented.

TABLE 5. Concentration of iodine and perchlorate ions in thyroid 2 hr after injection (per cent of injected dose)

	Rat	I^-	ClO_4^-	Ratio I^-/ClO_4^-
5·1	A	2·1	0·87	2·4
5·2	B	2·5	0·82	3·0
5·3	C	3·2	1·08	3·0
5·4	D	4·4	1·66	2·7

From the experimental results of Table 3 it may be seen that perchlorate reduces the accumulation of iodide in the gland even at equimolar concentration of the two ions (cf. 3·6–3·4; 3·8–3·4); the same is true, but to a smaller extent, of the effect of iodide on the perchlorate concentration (cf. 3·2–3·4; 3·1–3·5). The competition of both ions is demonstrated again when the actual concentration of iodide and perchlorate in the gland are compared (cf. 4·1, 4·2, 4·3). The values of the thyroid/blood concentration ratio for both ions, at doses of 0·14 mmols, average about 3–4 both for normal and for goiterous glands. In the latter case the total concentration of perchlorate or iodide in the gland becomes five-fold the normal level. The comparable behaviour of both ions becomes more apparent when the concentration of both ions in individual animals is compared. In Table 5 four rats with a rather different capacity to accumulate both iodide and perchlorate are compared; still the ratio of the accumulation capacity for both ions remains remarkably constant. It may be concluded therefore that there is little difference between the behaviour of perchlorate and iodide ions at high concentrations.

In order to examine whether perchlorate ions undergo metabolization in mammalian organisms a series of experiments was carried out in man, to determine if radioactive chloride or chlorate could be detected as metabolites of radioactive perchlorate ions. These experiments were described in detail in the experimental part of this study. Table 6 gives a summary of these tests.

Comparing the first and third samples in

TABLE 6. Summary of determination of radioactive chloride and chlorate ions in urine (Activity counts/min per ml urine)

	1st sample ($ClO_4^- + ClO_3^- + Cl^-$)	2nd sample (Cl^-)	3rd sample (ClO_4^-)	4th sample ($ClO_3^- + Cl^-$)
Urine A	2287	0·2	2215	0·9
Urine B	8039	1·1	7987	1·5
Urine C	4146	2·9	4160	3·0
Urine D	5436	3·2	5423	2·5

Table 6 it is seen that the differences between them are well within experimental error. Samples 2 and 4 give an upper limit for the metabolization of perchlorate ions, namely less than 1/1000 of the excreted perchlorate. This value may be well overestimated because there was always the possibility that the $KCl^{36}O_4$ contained 0·1 per cent or less of KCl^{36}; it is also probable that some perchlorate is absorbed on the precipitated silver chloride and is not entirely washed out. In view of these considerations it may be assumed that there is practically no reduction of perchlorate ions *in vivo*. In another series of experiments described in the experimental section, it has been shown that perchlorate ions do not undergo any isotopic oxygen exchange *in vivo* either.

DISCUSSION

It has been shown that perchlorate ions interfere with the iodine uptake of the thyroid gland.[4,5,6] In this study we have shown that unlike thiocyanate ions[8,9] perchlorate ions without undergoing any chemical change *in vivo*, accumulate selectively in the thyroid. The extent of perchlorate accumulation in the thyroid is comparable to that of iodide at high concentrations.[2,18] The competitive nature of the behaviour of both ions has been demonstrated using simultaneously labelled ClO_4^- and I^-.

These findings point to a common factor in the uptake mechanism of both ions which does not involve the chemical properties of these ions. Chemically, iodide and perchlorate ions are quite different; moreover, it has been shown that perchlorate does not undergo any chemical change under the conditions involved. We suggest therefore, that the similarity in behaviour of perchlorate and iodide ions is due to the similarity in size of both ions.[20] This hypothesis led to other ions having a similar size to perchlorate which have been found to exert a similar action on the iodine uptake like perchlorate ions. Outstanding among these ions is BF_4^- which is a chemically inert species like ClO_4^-. Experiments with BF_4^- labelled with F^{18} have shown that fluoroborate ions accumulate in the thyroid.[21]

The mechanism of iodide trapping by the thyroid gland has been hitherto unknown. The findings of this study, continued by the comparative investigation[20] of the action of SO_3F^-, PO_2F_2 and BF_4^- strongly suggest a simple mechanism for the iodide trapping.

The fact that the thyroid proteins selectively absorb anions fulfilling certain requirements of space and charge, may be of interest to biochemists concerned with protein structure. Moreover, it is interesting to note the evolutional adaptation of a certain protein to accumulate iodide ions required for the hormone synthesis by some spatial arrangement of the protein. The effect of TSH (thyroid stimulating hormone) on the capacity of the thyroid to accumulate these monovalent anions is now under study.

SUMMARY

(1) It has been shown that perchlorate ions accumulate selectively in the thyroid gland.

(2) Perchlorate ions have been shown to undergo no metabolization and are not involved therefore in any chemical change in the gland.

(3) Perchlorate and iodide ions were shown to compete with each other for the limited capacity of the gland. The capacity of the gland to trap perchlorate ions is parallel to the iodide trapping capacity.

(4) It is suggested that the trapping mechanism of the gland involves a factor which is selective to inorganic ions, fulfilling certain requirements of charge and size. This hypothesis was confirmed by showing that other monovalent anions having a comparable size to ClO_4^- have a similar effect on the iodine uptake of the gland.

REFERENCES

1. Taurog A., Chaikoff I. L. and Feller D. P. *J. Biol. Chem.* **171,** 189 (1947).
2. VanderLaan J. E. and VanderLaan W. P. *Endocrinology* **40,** 403 (1947).
3. Baumann E. J. and Metzger A. L. *Proc. Soc. Exp. Biol. N.Y.* **70,** 563 (1949).
4. Wyngaarden J. B., Wright B. M. and Ways P. *Endocrinology* **50,** 534 (1952).
5. Wyngaarden J. B., Stanbury G. B. and Rapp B. *Endocrinology* **52,** 568 (1953).
6. Stanbury G. B. and Wyngaarden J. B. *Metabolism* **1,** 533 (1952).
7. Godley A. F. and Stanbury G. B. *J. Clin. Endocrin.* **14,** 70 (1954).
8. Wood J. L. and William E. F. *J. Biol. Chem.* **177,** 59 (1949).
9. Wood J. L. and Kingsland N. *J. Biol. Chem.* **185,** 833 (1950).
10. Wollman S. H. *Amer. J. Physiol.* **186,** 453 (1956).
11. Izgaryshev N. A. *Izv. Akad. Nauk SSSR* 15 (1950).
12. Hoering T. C., Ishimori F. T. and McDonald H. O. *J. Amer. Chem. Soc.* **80,** 3876 (1958).
13. Treadwell F. P. and Hall W. T. *Analytical Chemistry* Vol. II, p.391. John Wiley, N.Y. (1942).
14. Kurtenacker A. *Mh. Chem.* **41,** 91 (1920).
15. Lewitus Z., Anbar M. and Guttmann S. To be published.
16. Rosenblum C. *Analyt. Chem.* **29,** 1740 (1957).
17. Anbar M. To be published.
18. Durand J. *Bull. Soc. Chim. Biol. Paris* **20,** 423 (1938).
19. Perlman I., Chaikoff I. L. and Morton M. E. *J. Biol. Chem.* **139,** 433 (1941).
20. Anbar M., Guttmann S. and Lewitus Z. *Nature* **183,** 1517 (1959).
21. Anbar M., Lewitus Z. and Guttmann S. To be published.

VOL.
7
1959/

International Journal of Applied Radiation and Isotopes, 1959, Vol. 7, pp. 97–110. Pergamon Press Ltd. Printed in Northern Ireland

The Effect of Recirculation on the Shape of the Arterial Concentration Curve after an Instantaneous Injection of Indicator*

MILTON G. CRANE, JOHN E. HOLLOWAY, CHARLES SEARS, JAMES McEACHEN and RALPH ADAMS

The Department of Internal Medicine, College of Medical Evangelists, Los Angeles, California and the Respiratory Center for Poliomyelitis, Hondo, California

(*Received* 11 *April* 1959)

We present our observations on 15 patients at cardiac catheterization showing by two-site sampling that recirculating indicator begins to influence the downslope on the cardiac output curve from 1 to 9 sec before the point of obvious recirculation. The concentration points of the last 38 per cent of the exponential portion of the downslope were slightly increased resulting in a decreased slope. The result is a false low value for the cardiac output estimated at 1·2 ± 1·5 per cent. This is well within the limits of tolerance for the method and less than that proposed on theoretical basis by other investigators. The total error is probably greater when the injection is made into a vein rather than into the heart because of the slower rate of decline of the downslope, but insufficient data are available in this study for statistical evaluation.

A comparison was made of the various portions of the arterial concentration curves. The vein–right ventricle, right ventricle–brachial artery, and vein–brachial artery arterial concentration curves are compared as to appearance time, peak concentration time, mean transit time, cardiac output, and central volume as measured by both the mean transit time and slope method. This comparison shows that the cardiac output measurement as calculated from the vein–right ventricle curve and right ventricle–brachial artery curve are larger than that calculated from an arterial concentration curve of the circulation from vein–brachial artery. The values of the central volumes by the MTT method of these two portions of the circulation when summed average slightly larger than that measured by the vein–brachial artery curve.

LES EFFETS DE LA RECIRCULATION SUR LA CONFIGURATION DE LA COURBE DE LA CONCENTRATION ARTÉRIEL APRÈS L'INJECTION INSTANTANÉE D'INDICATEUR

Nous présentons nos observations sur 15 patients à cathéterization cardiaque en échantillonage à deux locations. Les résultats montrent que l'indicateur recirculatoir commence à influencer la pente de la courbe du débit sanguin d'une à neuf secondes avant le point évident de recirculation. Les points de concentration des derniers 38 pour cent de la partie exponentielle de la pente ont été légèrement augmentées et par consequent la pente a été diminuée. Le résultat est une valeur basse fausse du débit sanguin cardiaque à 1·2 ± 1·5 pour cent. Cette erreur est bien dans les limites de tolérance de la méthode et c'est moins que proposé par d'autres investigateurs sur des bases théoriques. L'erreur totale est probablement plus grande quand on fait l'injection dans la veine plutôt que dans le coeur à cause du ralentissement de la vitesse de la déclination de la pente, mais des données insuffisante sont sous la main dans cette recherche pour être d'une valeur statistique.

* This investigation was supported in part by research grant No. H-2195 from the National Heart Institute of the National Institutes of Health, Public Health Service, and by the Los Angeles County Heart Association.

Une comparaison a été faite de portions variées des courbes de concentrations artérielles. La veine–ventricule droit, ventricule droit–artère brachiale et veine–artère brachiale courbes de concentration artérielles ont été comparées au point de vue de temps d'apparence, de temps moyen de transit, de temps de concentration maximum, de débit sanguin cardiac et du volume central en employant les deux méthodes; le temps moyen de transit et la méthode de pente. Cette comparaison montre que les mesures du débit sanguin cardiaque comme calculées de vein–ventricule droit courbes et ventricule droit–artère brachiale courbes sont plus grandes que celles calculées des courbes de concentrations artérielles de la circulation de la veine–artère brachiale. Les valeurs des volumes centraux par la méthode MTT de ces deux portions de la circulation sont légèrement plus grandes quand additionnées que celles mesurées par la courbe veine–artère brachiale.

ВЛИЯНИЕ РЕЦИРКУЛЯЦИИ НА ФОРМУ КРИВОЙ КОНЦЕНТРАЦИИ АРТЕРИАЛЬНОЙ КРОВИ ПОСЛЕ ВСПРЫСКИВАНИЯ ИНДИКАТОРА

Приводятся наблюдения над 15 больными, которых исследовали с помощью катетеризации сердца. Двухсторонний отбор проб показал, что эффект индикатора сердечной деятельности начинает сказываться за время от одной до девяти секунд до начала истинной рециркуляции, о чем можно судить по нисходящей ветви кривой. В последних 38 процентах экспоненциальной части этой ветви число точек, выражающих концентрацию, несколько увеличилось, что привело к уменьшению наклона кривой. В результате было получено заниженное значение измеряемой величины, равное примерно $1{,}2 \pm 1{,}5\%$. Эта величина находится в пределах допустимой применимости метода и она ниже тех, которые приводятся другими авторами на основании теоретических исследований. При введении индикатора в вену, а не в сердце, погрешность будет вероятно больше благодаря более медленному спаданию кривой, но настоящее исследование не дает достаточно данных для статистической оценки.

Дается сравнение различных отрезков кривых концентрации артериальной крови. Кривые вена–правый желудочек, правый желудочек–плечевая артерия и артерия–плечевая вена сравниваются по появлению индикатора, моменту максимальной концентрации, среднему времени передвижения, показателям сердечной деятельности и центрального объема, определяемым как методом среднего времени передвижения, так и методом измерения наклона кривой. Сравнение показывает что показатели сердечной деятельности, измеренные по кривым вена–правый желудочек и вена–плечевая артерия превышают значения, расчитанные по кривой вена–правый желудочек. При суммировании значений центрального объема, расчитанным по времени среднего передвижения, было найдено, что значения для первых двух кривых несколько превышают значения, полученные по кривой вена–плечевая артерия.

DIE WIRKUNG DES RÜCKFLUSSES AUF DIE FORM DER ARTERIELLEN KONZENTRATIONSKURVE UNMITTELBAT NACH INJEKTION DES INDIKATORS

Die vorliegenden Beobachtungen an 15 Patienten durch doppelte Blutprobenentnahme an zwei verschiedenen Stellen während Herzkatheterisierung zeigen, dass der Rückfluss des Indikators den absteigenden Teil der cardialen Ausströmungskurve eine bis 9 Sekunden vor dem tatsächlichen Rückfluss zu beeinflussen beginnt. Die Konzentrationspunkte der letzten 38 prozent des experimentellen Teiles der absteigenden Abklingkurve werden etwas erhöht zufolge des verminderten Abfalles. Dies gibt schätzungsweise einen um den Faktor $1{,}2 \pm 1{,}5$ zu niedrigen Wert für die cardiale Herz-Ausströmung.

Dieser Wert liegt innerhalb der Genauigkeitsgrenze der Methode und ist kleiner als von anderen Autoren von theoretischer Basis vorgeschlagen wurde. Der Gesamtfehler, ist wahrscheinlich grösser bei intravenöser Injektion, als bei Herzinjektion zufolge der geringeren Neigung des Kurvenabfalles. Es liegen jedoch noch zuwenig Ergebnisse für eine statistische Auswertung vor.

Ein Vergleich zwischen den verschiedenen Teilen der arteriellen Konzentrationskurven wurde unternommen.

Die arterielle Konzentrationskurven für Vene–rechter Ventrikel, rechter Ventrikel–Bronchialarterie und Vene–Bronchialarterie wurden verglichen auf Grund der Zeit des

VOL. 7 1959/6

Aufscheinens, Zeit der Maximalkonzentration, mittlere Durchflusszeit, cardialer Ausfluss und des Zentralvolumens, sowohl mit Hilfe der mittleren Durchflusszeit, als auch auf Grund der Abklingmethode. Diese Vergleiche zeigen, dass die cardiale Ausströmung, welche sich aus der arteriellen Kurve für Vene–rechte Ventrikel und aus der rechter Ventrikel und Bronchialarterie errechnen lässt, grösser ist als der, aus der arteriellen Konzentrationskurve für Zirkulation in Vene und Bronchialarterie berechnete. Die Werte für das Zentralvolumen, bestimmt nach der MTT-Methode, für diese beiden Zirkulationsabschnitte, ist im Mittel etwas höher als die, welche mittels der Vene–Bronchialarterie gemessen werden.

SINCE HAMILTON[1] introduced a means of separating initially circulating indicator from recirculating indicator by plotting the arterial concentration curve on semilogarithmic paper, several articles[2–5] have appeared discussing the possibility that early recirculation may change the configuration of the arterial concentration curve of indicator before the point of obvious recirculation. In general, it has been considered that the recirculating indicator could influence the downslope in such a way as to cause an increased average concentration of the indicator, resulting in a falsely low cardiac output measurement. In addition to this, we feel that if the configuration of the downslope is to be used in evaluating left-to-right shunts, then the time of obvious appearance of recirculating indicator becomes quite important in the analysis of cases with minimal shunts.

HENRIQUES[6] showed, by injecting into the left ventricle and sampling from a peripheral artery, that the indicator did not completely traverse the circulation initially before recirculation appeared from a short pathway. MOORE[7] estimated the rapidity with which dye injections traversed the short pathway of the systemic circulation in dogs and in man. HAMILTON *et al.*[8] using the dye injection method reported that the total circulation time in man in the resting state ranged from 10 to 15 sec. STARR and COLLINS[9] have reported experiments in dogs in which the infusion was made into the left auricle and samples were drawn every 5 sec from the aorta and pulmonary artery. They found that over 35 per cent of the blood leaving the left side of the heart of the dog returned to the right side of the heart within 15 sec.

SUTTON[3] reported observations in three patients in which samples were taken every 15 sec from the right ventricle during a steady infusion of tagged red cells in the pulmonary artery. By this method the fastest complete circulation was 7 to 9 sec. These results have been criticized[10] because of the backward extrapolation through concentrations of samples drawn at 15 sec intervals.

This is a report of an attempt to quantitate the effect of recirculating indicator on the initial circulation values of the arterial concentration curve. By measuring the concentrations of the recirculating indicator at each second as it begins its second trip through the heart and lungs and then superimposing this curve of recirculating indicator over the recirculation curve obtained in the brachial artery, it is possible to approximate the values of the recirculating indicator and separate them from the values of the initial circulation. We have studied the shape of the arterial concentration curve at cardiac catheterization by sampling continuously from both the right ventricle and the brachial artery following an injection into the main pulmonary artery and an injection in an antecubital vein.

METHOD

Fig. 1 is an overall diagram of the apparatus used. At cardiac catheterization a double-lumen catheter was positioned so that the distal orifice was in the main pulmonary artery and the proximal orifice was in the right ventricle or main pulmonary artery. During the test a blood sample from a brachial artery was drawn continuously through a polyvinyl tube (inside diameter 2·1 mm) at a regulated flow rate of 40 ml/min. The blood sample from the catheter in the right ventricle was drawn similarly

through a tube of smaller diameter which contained approximately half as much volume within the counting geometry as the first well crystal. The sampling rate was held constant at 18 ml/min, air being excluded from the system. The tubes were held in rigid geometry in well crystals.

The constant-sampling-rate to counting-geometry-volume ratio was kept at 4·8 for both systems. We found on testing the two systems that when square wave changes in indicator concentration were introduced into the tubing system used for the arterial sample, that it required 1·3 sec for the counting rate to go from 2 per cent to 90 per cent of the peak (static) counting rate of the indicator. When a similar study was done on the catheter sampling system (including the catheter) with the same sampling-rate to geometry-volume ratio, we found that it required 5·3 sec for the counting rate to go from 2 per cent to 90 per cent of the peak counting of the indicator.

The counting rate was detected and recorded on separate channels of a Polyviso* recorder by the pip interval method which we have previously described.[11]

When the test was run, 2 ml of RISA† solution at a concentration to give about 1·1 μc/kg body weight was injected through the distal orifice of the catheter by an injection pipette with a 10 ml saline flush. The exact time of injection was recorded on the tracing. Fifteen minutes later an injection was made into an antecubital vein in a similar manner, and sampling was done from the same two sites as for the catheter injection.

Immediately after the last patient determination a 1 : 1000 dilution of the injection material was counted in the respective tubing of the two well crystals. Carrier albumin was used in the standard preparation.[12,13] The carrier albumin in the standard and the plasma albumin of the patient prevented RISA from sticking to the glassware and plastic tubing. The time required for the sample to pass from the tip of the needle in the brachial artery and from the proximal orifice of the double lumen catheter to the respective well crystals was subtracted from the time of injection so that, when graphed, the plot of the two curves using every second of time would represent the concentrations at the point of sampling in the right ventricle and brachial artery respectively. One further adjustment was made on the right ventricle tracing to compensate for the difference in the counting volume and efficiencies of the two assemblies. The concentration at each second was multiplied by a factor derived from the counting rates of the standards in the respective well crystals so that the counting rates of the right ventricle and brachial artery samples would be directly comparable. The values were then graphed, and the calculations performed according to accepted formulas.[11] The central volume was calculated from the mean transit time. The slope volume was calculated as described by NEWMAN.[14]

Table 1 lists the subjects studied and their diagnoses. In the first six patients the injection was made into both an antecubital vein and the pulmonary artery. In the last nine patients the injection was made into the pulmonary artery only.

VOL. 7 1959/6

RESULTS

Fig. 2 shows the concentration of indicator at each second appearing at the right ventricle (RV) and brachial artery (BA) following an injection into an antecubital vein. Fig. 3 shows similar data when the injection was made through the distal lumen of the catheter into the main pulmonary artery.

1. *Comparison of* T_{ap}, T_{pc} *and* T_{mtt} *of the curves*

The appearance time (T_{ap}), the peak concentration time (T_{pc}), and mean transit

* Sanborn Company, Cambridge, Massachusetts.
† Abbott Laboratories, North Chicago, Illinois.

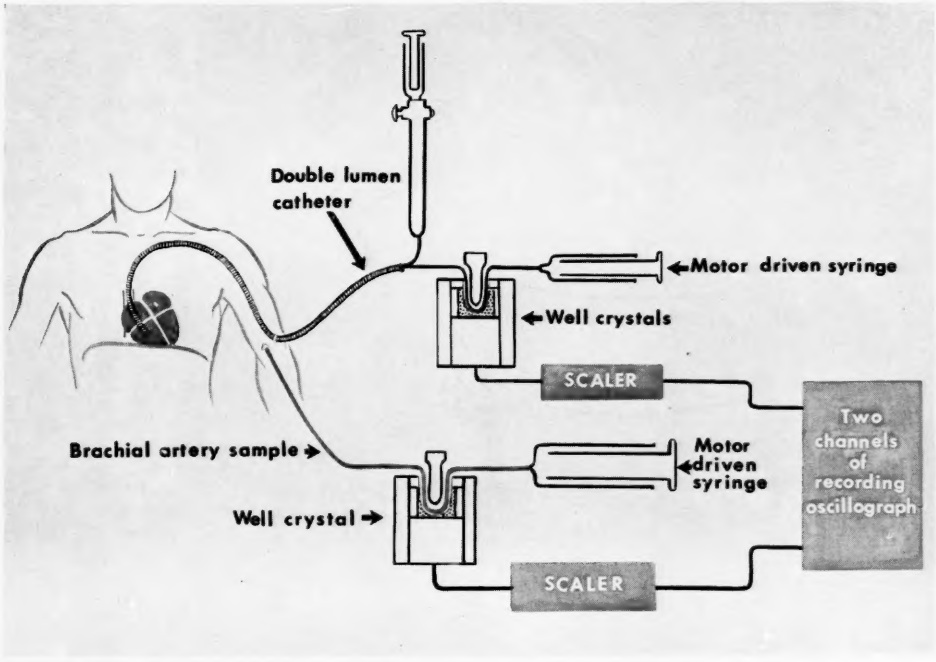

FIG. 1. Diagram of the equipment used for this study. All injections in the catheter made through the tip orifice of the double lumen catheter.

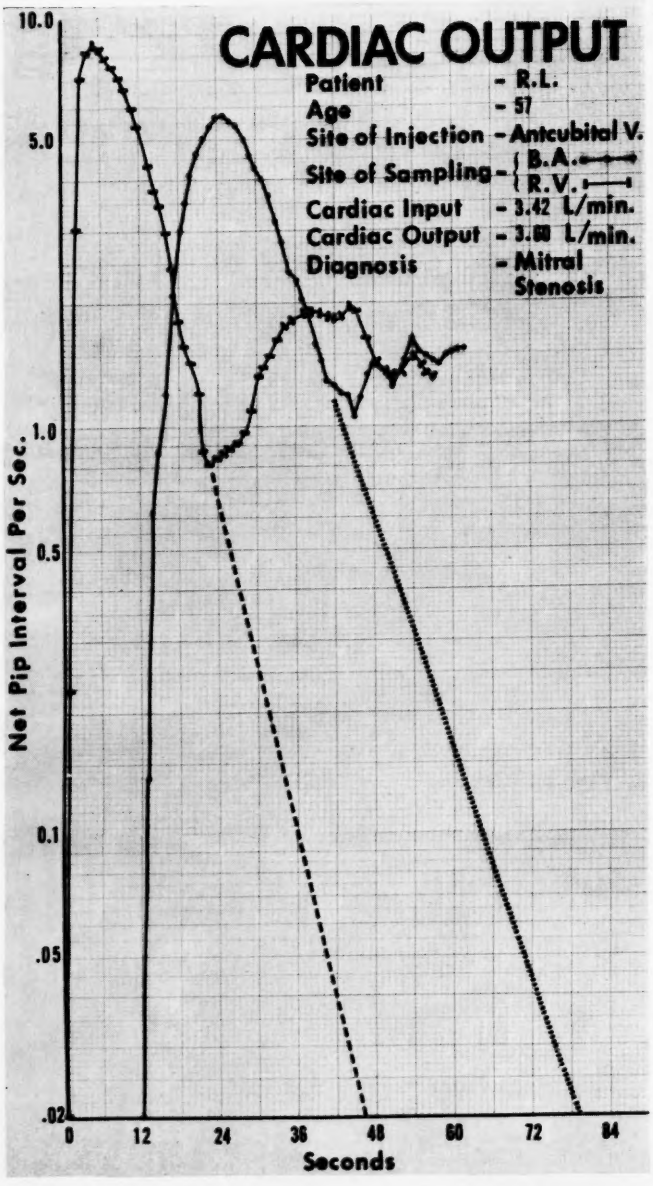

FIG. 2. Right ventricle sample curve (on the left) and brachial artery sample curve (on the right) obtained following an injection into an antecubital vein.

VOL.
7
1959/

TABLE 1. Patients in this study

Patient	Sex	Age (yr)	Height (cm)	Weight (kg)	Diagnosis
B. H.	F	44	162	70	Mitral stenosis
F. F.	F	39	152	55	Atrial fibrillation in failure, cause undetermined
R. P.	M	66	146	62	Mitral stenosis
R. L.	F	57	162	63	Mitral stenosis
C. D.	M	42	174	192	Obesity–hypoventilation syndrome
C. K.	F	41	160	52	No heart disease
C. H.	M	44	157	53	Pulmonary stenosis
D. D.	M	60	174	46	Pulmonary emphysema
D. M.	F	32	161	50	Mitral stenosis
V. M.	F	35	156	62	Mitral stenosis, moderate
J. W.	M	37	169	79	Pulmonary cysts without heart disease
S. C.	F	10	122	25	Paroxysmal tachycardia, cause undetermined
L. M.	F	46	150	51	Mitral stenosis
M. M.	F	33	154	51	Mitral stenosis
J. P.	F	51	156	79	Constrictive pericarditis

TABLE 2. Appearance time* (T_{ap})

Patient	A From vein to RV (sec)	B From RV to BA (sec)	C From vein to BA (A + B) (sec)	D From vein to BA (sec)	% Difference between D and C
B. H.	1	6	7	11	−36
F. F.	2	4	6	11	−45
B. P.	6	14	20	32	−38
R. L.	1	8	9	12	−25
C. K.	0·5	4	4·5	8·5	−47
C. D.	3	5	8	11	−27
Average					−36·5
S. D.					±9·0

* Values from vein to RV and vein to BA determined from the same injection. Value from RV to BA determined from a separate injection 15 min before A and D. Value C calculated from A and B.

time (T_{mtt}) were all shortest in the vein–RV curves and longest in the vein–BA curves as one would expect. Table 2 presents the data on the appearance times. If the vein–RV appearance times are added to the RV–BA appearance times as shown in column C, these sums average 36·5 ± 9·0 per cent less than the appearance time from vein–BA as measured by the antecubital vein injection. Table 3 shows the data on the peak concentration times. If the vein–RV peak concentration times are added to the RV–BA values as shown in column C, these sums average 3·8 ± 15·2 per cent less than ($p > 0·5$) the

TABLE 3. Peak concentration time* (T_{pk})

Patient	A From vein to RV (sec)	B From RV to BA (sec)	C From vein to BA (A + B) (sec)	D From vein to BA (sec)	% Difference between D and C
B. H.	5	12	17	17	0
F. F.	9	12	21	21	0
B. P.	17	28	45	53	−15
R. L.	5	15	20	25	−20
C. K.	5	8	13	14·5	−10
C. D.	11	12	23	18	+22
Average					−3·8
S.D.					±15·2

* Refer to footnote Table 2.

TABLE 4. Mean transit time* (MTT)

Patient	A From vein to RV (sec)	B From RV to BA (sec)	C From vein to BA (A + B) (sec)	D From vein to BA (sec)	% Difference between D and C
B. H.	8·7	14·1	22·8	21·0	+8·5
F. F.	15·2	16·2	31·4	28·5	+10·2
B. P.	21·7	43·5	65·2	71·7	−9·1
R. L.	10·6	18·6	29·2	29·5	−1·0
C. K.	9·6	8·8	18·4	17·9	+2·8
C. D.	13·2	12·8	26·0	21·7	+19·8
Average					+5·2
S.D.					±10·0

* Refer to footnote Table 2.

directly measured vein–BA peak concentration time. Table 4 lists the data on the mean transit times. If the vein–RV mean transit times are added to those of the RV–BA curves, these sums average 5·2 per cent greater ($p < 0{\cdot}2$) than the vein–BA mean transit times measured from the antecubital vein injection.

2. *Comparison of cardiac output values*

Table 5 lists the whole blood flow rates as calculated from these three curves. Comparison of whole blood flow rates shows that the values obtained from the vein–RV curve (which might be termed cardiac input) average 3·1 ± 5·2 per cent greater than those derived from the vein–BA curve ($p > 0{\cdot}1$). Similarly, the RV–BA values were 5·4 ± 3·3 per cent greater than the vein–BA values ($p < 0{\cdot}01$).

3. *Comparison of central volumes by MTT*

Table 6 presents the central volume measurements as determined by the mean transit time method which theoretically measures the volume from the site of injection

TABLE 5. Whole blood flow rate

Patient	A From vein to BA (l/min)	B From vein to RV (l/min)	% Difference between A and B	C* From RV to BA (l/min)	% Difference between A and C
B. H.	5·42	5·58	+3·0	5·80	+7·0
F. F.	3·61	3·68	+1·9	3·64	+0·8
R. P.	2·65	2·95	+11·3	2·77	+4·5
R. L.	3·60	3·42	−5·0	3·70	+2·8
C. K.	5·38	5·59	+3·9	5·87	+9·1
C. D.	10·86	11·24	+3·5	11·75	+8·2
Average			+3·1		+5·4
S.D.			±5·2		±3·3

* Run made 15 min before the AB test.

TABLE 6. "Central" volumes by MTT method

Patient	A From vein to RV (ml)	B* From RV to BA (ml)	C From vein to BA (A + B) (ml)	D From vein to BA (ml)	% Difference between D and C
B. H.	808	1363	2171	1892	+14·7
F. F.	934	983	1917	1716	+11·7
R. P.	1065	2006	3071	3167	−3·0
R. L.	605	1133	1738	1770	−1·8
C. K.	840	861	1701	1606	+5·6
C. D.	2465	2512	4977	3960	+25·7
Average					+8·8
S.D.					±10·9

* Run made 15 min before the AD test.

to the site of sampling. The vein–RV volume when added to the RV–BA volume should equal the vein–BA volume. However, these summed values as shown in column C averaged 8·8 ± 10·9 per cent greater ($p > 0{\cdot}05$) than the vein–BA volume as measured by the antecubital vein injection. The major part of this difference is due to the much larger volume of patient C.D. who weighed over 400 lb. By omission of this patient's data the percentage difference becomes 5·3 ± 7·9 ($p > 0{\cdot}1$). His values also affected the average of the mean transit times but not the average cardiac outputs for the entire group.

4. *Comparison of volume by slope method*

When the slopes of the vein–RV, vein–BA, and RV–BA curves were compared, it was found that the downslopes of the RV–BA curves are consistently the steepest and the downslopes of the vein–BA curves show the most gradual decline of the three. The ratio

TABLE 7. Slope method volume

Patient	A From vein to RV (ml)	B* From RV to BA (ml)	C From vein to BA (A + B) (ml)	D From vein to BA (ml)	% Difference between D and C
B. H.	500	404	904	507	+78·3
F. F.	613	410	1023	734	+39·4
R. P.	362	1004	1366	1210	+12·9
R. L.	322	351	673	571	+17·9
C. K.	446	211	657	342	+92·1
C. D.	991	567	1558	1042	+49·5
Average					+48·4
S.D.					±29·1

* Run made 15 min before the AD test.

of the average downslope values of the three groups of curves was as follows:

Vein–BA . . . . . 1·0
Vein–RV . . . . . 1·2
RV–BA . . . . . 1·6

Table 7 lists the volume measurements as calculated using the slope method. The average volumes of distribution from vein–RV and RV–BA are nearly the same, but the ratio between these two compartments varies considerably from patient to patient. The sums of vein–RV and RV–BA volumes averaged 48·4 per cent higher than the vein–BA volume as determined by the antecubital vein injection. The volume of the pool measured by the vein–BA curve averaged 55·0 per cent greater than that pool measured by the RV–BA curve.

5. *Determination of recirculation indicator on RV–BA curve*

Fig. 3 shows a graph of the indicator as it appeared in the right ventricle and brachial artery following injection into the main pulmonary artery. The left-hand graph is a plot of the concentrations as they appeared at the right ventricle and brachial artery. The right ventricular sample records only recirculating indicator which has a configuration virtually identical with the main recirculation peak of the brachial artery curve. This suggests that the RV catheter sample data could be shifted so as to be superimposed over the main recirculation portion of the brachial artery curve. Using this maneuver, we should have a method for separating the recirculating indicator from the initially circulating indicator. In other words, with the recirculation curve shifted in this manner we have a measure at each second of the contribution of the recirculating indicator to the arterial curve. The recirculating indicator is diluted somewhat in its transit from the right ventricle to the brachial artery. However, a comparison of the relative heights of the recirculation peaks as measured at the right ventricle and brachial artery showed that the recirculation peak at the right ventricle measured from 0 to 20 per cent higher than the recirculation peak at the brachial artery. This means that the RV sample values used to estimate the amount of recirculating indicator hidden in the exponential portion of the downslope are slightly higher at the RV than when they arrived at the brachial artery. When the recirculating indicator as obtained from the shifted RV curve was subtracted from the BA curve, it was found that there was an unaltered exponential drop in concentration followed later by a pronounced sagging of

VOL. 7 1959/6

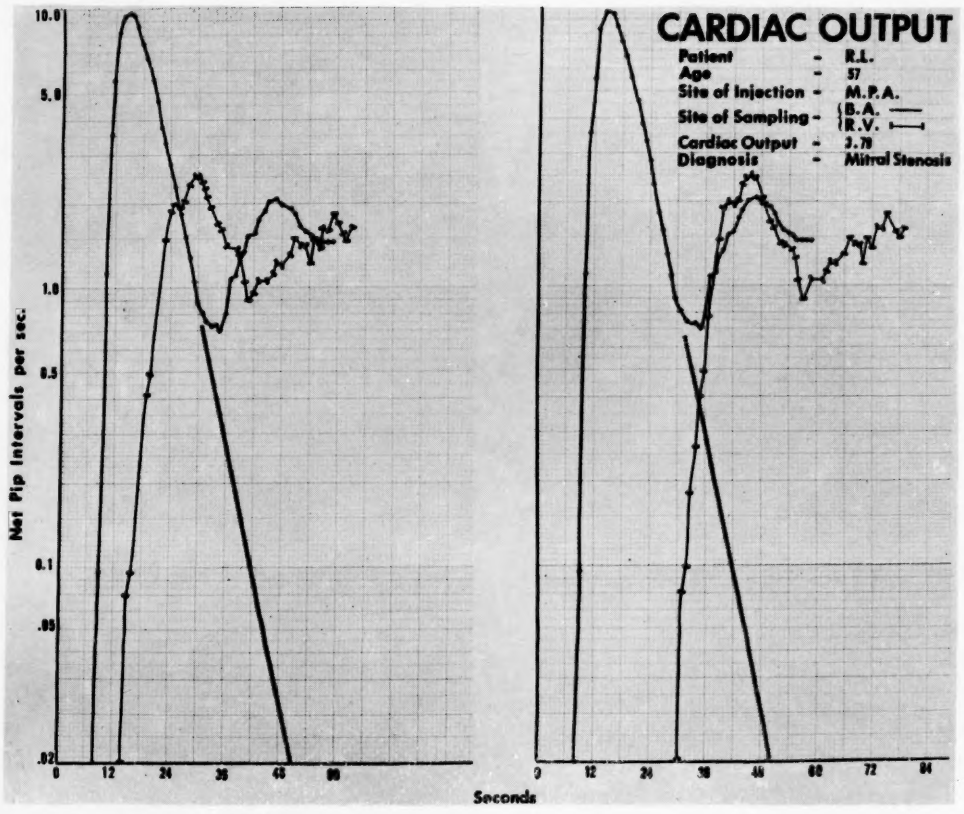

FIG. 3. The right ventricle sample curve and the brachial artery sample curve (higher peak) obtained following an injection into the main pulmonary artery. The left hand portion is plotted with time relationships as they actually existed, and the right hand portion with the right ventricle curve shifted so as to cause its initial peak to coincide with the brachial artery recirculation peak.

OL.
7
9/60

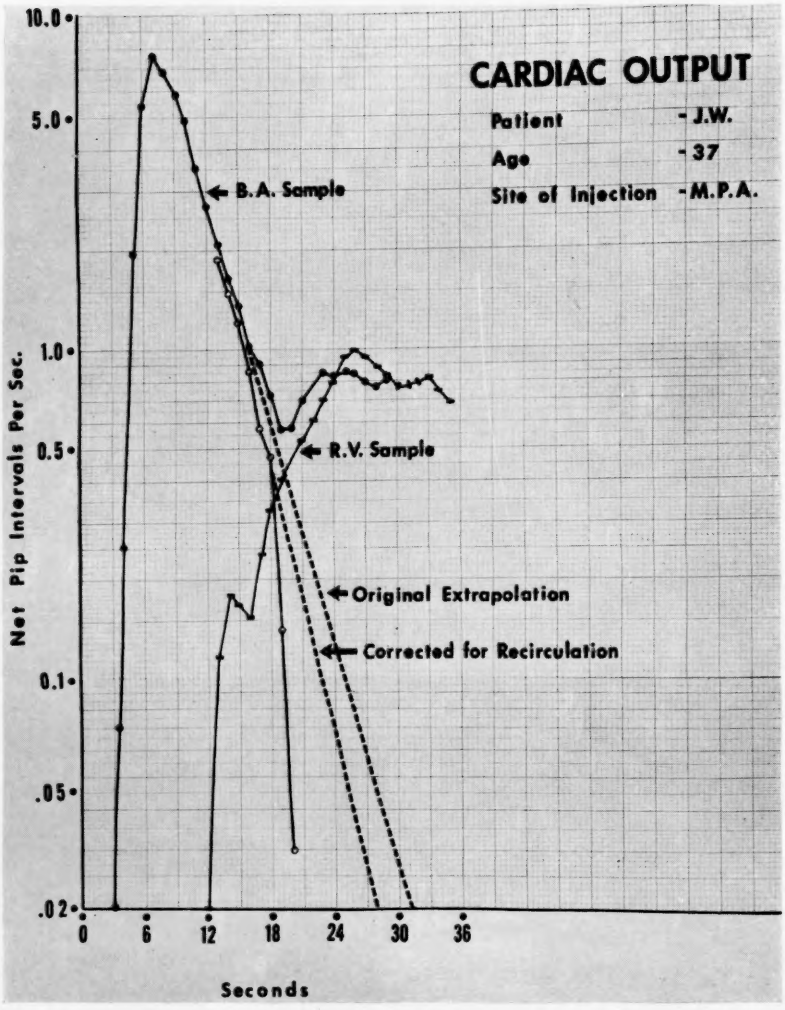

FIG. 4. Brachial artery sample curve showing the original extrapolation and the extrapolation after the downslope concentrations were corrected for recirculating indicator. The amount of correction for each second is obtained from the shifted right ventricle sample concentrations.

VOL.
7
1959/6

TABLE 8. Increase in computed cardiac output due to recirculation

Patient	Exponential portion of downslope: % of downslope affected	Exponential portion of downslope: A % increase in ΣC of expon. portion	Extrapolated portion: B % of total curve area	Extrapolated portion: C % change in slopes	Extrapolated portion: D % increase in total curve area (B × C)	Total % error due to recirc. (A + D)
B. H.	69	2·5	2·3	22·8	0·5	3·0
F. F.	41	0·3	11·7	8·1	0·9	1·2
R. P.	14	0·05	16·6	0·0	0·0	0·0
R. L.	21	1·0	5·4	0·0	0·0	1·0
C. H.	11	0·03	6·9	0·0	0·0	0·0
D. D.	33	0·5	9·6	4·1	0·4	1·3
V. M.	43	0·6	3·8	2·6	0·1	0·7
D. M.	36	0·6	4·0	0·0	0·0	0·6
J. W.	67	4·1	5·0	23·4	1·2	5·3
J. W.	50	1·9	2·5	20·6	0·5	2·4
S. C.	50	1·4	4·3	11·6	0·5	1·9
L. M.	17	0·2	3·5	0·0	0·0	0·2
C. K.	25	0·04	1·7	0·0	0·0	0·0
M. M.	82	1·7	1·2	10·0	0·1	1·8
J. P.	13	0·1	1·5	0·0	0·0	0·0
Average	38·1	1·0			0·28	1·3
S.D.	21·4	±1·1			±0·37	±1·4

(A) Calculated on the segment of the exponential portion affected by recirculation

$$\frac{\Sigma \text{ concentrations of RV sample affecting exponential portion of downslope}}{\Sigma \text{ Concentrations of BA sample from } T_{ap} \text{ to point of recirculation}} \times 100.$$

(B) $$\frac{\Sigma \text{ area under extrapolated portion of curve}}{\text{area under entire curve}} \times 100.$$

(C) Slopes calculated before and after correction for recirculating indicator: $\frac{\ln C_2 - \ln C_1}{t_2 - t_1}$

(D) Percentage change in slope (C) multiplied by the percentage area under the extrapolated portion (B).

the downslope. This is graphically demonstrated in Fig. 4. This sagging of the downslope is further evidence that the amount of recirculating indicator that was subtracted from the initial circulation was slightly greater than actually existed.

6. *Amount of error due to recirculating indicator on RV–BA curve*

Table 8 presents the results of calculations made on the RV–BA curves using the concentrations of the right ventricle sample when superimposed, to measure the amount of contribution of recirculation to the exponential portion of the downslope. The concentration on the brachial artery curve at which recirculation was first detected by the shifted right ventricle curve was at a point 23 ± 15 per cent below the highest concentration (not the peak) on the exponential portion of the downslope (see Fig. 5). In other words, there was an average drop in concentration of 77 per cent in the exponential portion before it was affected by recirculating indicator. The recirculating indicator was demonstrated by the RV

sample to affect the conventional brachial artery curve from 1 to 9 sec before obvious recirculation. An average of 38·1 ± 21·4 per cent of the seconds in the exponential portion of the downslope was increased by recirculating indicator. Although such a high proportion of seconds were affected, the percentage increase in the sum of the concentrations due to recirculating indicator was small and ranged from 0·03 to 4·1 per cent (averaged 1·0 ± 1·1) of the total sum of the curve to the point of recirculation.

Recirculating indicator not only caused an increase in the sum of the concentrations in the exponential portion, but it also affected the extrapolated portion of the downslope. The difference in the slopes ranges from zero to 23·4 per cent. Since the area under the extrapolated portion of the curve was such a small percentage of the total curve area, the error introduced by just the extrapolation ranged from 0 to +1·2 per cent and averaged only 0·28 ± 0·56 per cent. The combined error in cardiac output estimation introduced by both the increase in the sum of the concentrations and the change in the slope averaged 1·3 ± 1·4 per cent.

Fig. 4 is a graph of the brachial artery tracing on patient B.H. who had the greatest percentage error due to recirculating indicator. This graph shows the maximum amount of displacement of the slope due to recirculating indicator that we encountered.

Table 9 compares the data of the brachial artery and right ventricular tracings of the fifteen patients. The indicator should appear later at the right ventricle than at the brachial artery following injection into the main pulmonary artery. The indicator appeared at the brachial artery before it appeared in the right ventricle in all but one of the patients. The average difference in appearance times between the two sites was 4·4 ± 3·4 sec. The peak of indicator was present at the brachial artery from 5 to 20 sec before the peak of recirculating indicator arrived at the right ventricle.

The number of seconds that the right ventricular tracing had to be shifted so as to have its peak concentration superimposed on the recirculation peak of the brachial artery was from 4·5 to 32 sec and averaged 11·7 ± 6·3 sec. This time should be a measure of the transit time from right ventricle to brachial artery. It is noticed that this time so determined corresponds quite closely with the peak concentration time of the brachial artery curve. A comparison of the transit times for each patient with the data of columns C and D of Tables 3 and 4 supports the assumption that this transit time is slightly longer than the peak concentration time and somewhat shorter than the mean transit time.

All of the brachial artery tracings in this study were calculated before and after correction for recirculation by subtracting the recirculating indicator concentrations obtained by the right ventricular sample. The values of the mean transit time, flow rate, and central volumes as calculated from the original curves are compared with the respective values obtained from the brachial artery curve corrected for the recirculating indicator. The mean transit time averaged 0·9 ± 1·4 per cent lower after the downslope was corrected for recirculation ($p > 0{\cdot}05$).

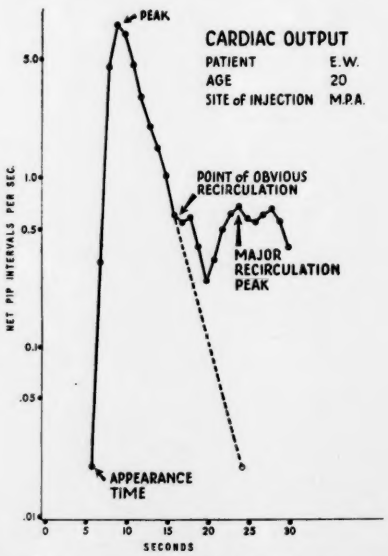

FIG. 5. This is an actual brachial artery curve representing the various portions of the curve and depicting a small peak of recirculating indicator affecting the downslope of the main curve. For explanation see text.

VOL 7 1959/

CIRCULATION RESEARCH, VOL. 7 MAY 1959

TABLE 9. Cardiac output before and after correction for recirculation contribution
(Injection into main pulmonary artery)

Patient	Appearance time (sec)			Peak time (sec)			Transit time (a) from RV to BA (sec)	MTT (sec)			Flow rate (l/min)			Central volume (ml)		
	at BA	at RV	Difference (sec)	at BA	at RV	Difference (sec)		by original curve	by corrected curve*	% Difference	by original curve	by corrected curve*	% Difference	by original curve	by corrected curve*	% Difference
B. H.	6	6	0	12	21	9	12	14·1	13·7	−2·8	5·80	5·98	3·1	1363	1365	0·1
F. F.	4	9	5	12	28	16	12	16·2	15·9	−1·9	3·64	3·72	2·2	983	985	0·2
R. P.	14	25	11	28	48	20	32	43·5	43·5	0	2·77	2·77	0	2006	2006	0
R. L.	8	14	6	15	29	14	16	18·4	18·4	0	3·70	3·70	0	1133	1133	0
C. H.	2	9	7	6	19	13	6	7·9	8·0	1·3	3·54	3·55	0·3	467	471	0·9
D. D.	3	8	5	9	19	10	9	12·3	12·2	−0·8	4·45	4·49	0·9	907	914	0·8
V. M.	5	8	3	12	26	14	14	14·5	14·5	0	3·18	3·21	0·9	769	773	0·5
D. M.	8	13	5	15	29	14	11	17·3	17·4	0·6	3·87	3·85	−0·5	1117	1115	−0·2
J. W.	3	5	2	7	17	10	7	10·0	9·6	−4·0	5·68	5·90	3·9	947	945	−0·2
J. W.	2	6	4	6	20	14	6	8·1	7·9	−2·5	5·88	6·03	2·6	798	795	−0·4
S. C.	1	1	0	4	9	5	4·5	4·4	4·3	−2·3	4·94	5·03	1·8	363	362	−0·3
L. M.	4	12	8	11	21	10	11	13·1	13·1	0	3·03	3·03	0	662	662	0
C. K.	4	5·5	1·5	8	14·5	6·5	9·5	8·8	8·8	0	5·92	5·92	0	868	868	0
M. M.	5	4	−1	13	26	13	13	14·8	14·6	−1·4	4·17	4·27	2·4	1029	1040	1·1
J. P.*	8	17	9	13	29	16	13	15·7	15·7	0	3·94	3·94	0	1032	1032	0
Average			4·4			12·3	11·7			−0·9			1·2			0·2
S.D.			±3·4			±3·8	±6·3			±1·4			±1·3			±0·4

(a) The number of seconds that the RV curve must be shifted in order to superimpose its buildup and peak on that of the recirculation portion of the brachial artery curve.

* Downslope corrected for contribution made by recirculating indicator.

The cardiac output was 1·2 ± 1·3 per cent higher after correction for recirculation ($p > 0{\cdot}05$), and the central volume was 0·2 ± 0·4 per cent higher by the corrected curve ($p > 0{\cdot}4$). The error of 1·2 per cent in the cardiac output as determined from the regraphed corrected curve is quite close to the total error of 1·3 per cent that was predicted from the percentage increase in sum of concentration and percentage change in downslope.

7. *Further evidence of effect of recirculating indicator*

In seven of twenty-three additional patients without shunts in which the injection was made into the right heart or pulmonary artery, we found evidence of a small discrete quantity of recirculating indicator which preceded the major recirculating peak. This is graphically demonstrated in Fig. 5. The terminal portion of the downslope is disturbed by a small peak of recirculating indicator which can be shown to have a shape quite similar to the main curve. This indicator we believe to be from the coronary circulation because of the time of occurrence and the calculated area involved is about 4 per cent of the area under the major curve. We have not recognized these small extra peaks on the terminal portions of the downslopes when the injections were made in the antecubital vein or when a sampling-rate to counting-geometry system was used with a longer response time.

DISCUSSION

The accuracy of the injection method for determining cardiac output has been compared in circulation models[11,15] and with the Fick method.[7,16–20] Other general comparisons have appeared in the literature. To our knowledge no systematic error in the injection method has been reported. In general, it has been noted that the average cardiac output values by the injection method are slightly greater than by the Fick method. We[20] have found the average percentage difference to be less between two injection method outputs than between a Fick and an injection method output. The Fick method has certain unavoidable errors which limit its accuracy.

Several reports have appeared comparing the estimated cardiac outputs obtained from multiple sites of injection. Coe *et al.*[21] found that when the injections were made centrally the cardiac output values were larger than when the injections were made peripherally. Later Lawson[4] analyzed the difference in the shape of the curves of two indicators injected intracardiac and into a peripheral vein simultaneously and notes the higher cardiac value of the intracardiac injection. He further stated that since injection into a peripheral vessel would result in a broader time concentration curve tending to mask recirculating indicator the possibility still remains open that undetected recirculation was the cause for this difference. We have observed[20] in two groups compared with the Fick method that there is a tendency for the cardiac output values to be slightly higher when the injections were made in the pulmonary artery than when the injections were made in an antecubital vein. However, there is not universal agreement that the estimated cardiac output varies with the injection site.[22] Dow[5] has analyzed the injection curves of T-1824 from both human and dog experiments in an effort to evaluate troublesome curves showing a departure from semilogarithmic decay in the descending limb of the curve before obvious recirculation. He[10] recognized that recirculating indicator could be included twice resulting in a falsely low cardiac output. The present study shows that the "cardiac input" values as obtained from the vein–RV curve are slightly higher than the values obtained from the vein–BA curve although not a statistically significant difference. There was, however, a significantly higher cardiac output value found when the injection was made in the main pulmonary artery than when the injection was made in the antecubital vein. Since it takes a longer period of time to form the curve when the injection is made into a peripheral vein, more recirculating indicator

VOL 7 1959/

would be hidden in the downslope. Even so the percentage error in cardiac output introduced by recirculating indicator is quite low and is certainly less than other unavoidable errors in the method. Certainly the percentage error introduced into the cardiac output by recirculating indicator can be ignored, when the injection is made centrally.

In some instances recirculating indicator can be detected before the obvious point of recirculation with our response time sampling. Some detecting and recording systems[23] have a relatively long response time. As the response time of the system is increased, more and more of the recirculating indicator would be included in the downslope without recognition of its presence. Using the recording and sampling system as in this study we have been able to consistently recognize in patients without shunts small quantities of recirculating indicator affecting the last 10 to 20 per cent of the downslope. When this occurs, the extrapolated portion should be drawn to omit the recirculating indicator.

Early recirculation from a left-to-right shunt can be detected on the downslope of the BA tracing. Significant left-to-right shunts produce definite clearcut evidence on the brachial artery curve. Care should be used in sampling, so that the configuration of the curve can be used for the detection of left-to-right shunts. The method here introduced can be used for the localization of left-to-right shunts by selecting the site of sampling and injection within the heart.[24]

The results of the cardiac outputs by the injection method have been thought to be falsely low in patients in congestive failure who have a prolonged circulation time. This is because of the long time period for the formation of the curve allowing more time for recirculation to affect the downslope. In our experience, however, the shape of the arterial concentration curve in congestive failure is essentially the same except for the prolonged time required for its formation due to the sluggish circulation. When the curve of a patient in heart failure is plotted with a compressed time scale, the curve appears to be essentially normal in shape. In other words, both the central circulation and the peripheral circulation are slowed in congestive heart failure so that the same percentage of the total curve can be formed without being affected by recirculating indicator when the circulation rate is slow. One patient in this series (R. P.) was in grade III congestive failure, and two patients (F. F. and R. L.) were in grade II congestive failure. In those patients in failure it was difficult to assess any more influence on the cardiac output by recirculating indicator than in the other individuals included in this study who had no evidence of slowed circulation.

We have found that the recirculating indicator may start to appear in the right ventricle as early as 1 or as late as 25 sec after injection, and it may be as short as 3 or as long as 23 sec from appearance time to peak concentration time. In view of this, it would seem that attempts to estimate the fastest complete circulation would be rather fruitless because of the marked variation in flow rate from subject to subject and because of the varying length of pathways for systemic circulation.

The major recirculation peak, which is demonstrable in most individuals,would most likely be that from a pathway of major peripheral flow. Freely diffusible substances such as NaI^{131}, $NaBr^{82}$, and I^{131} tagged diodrast differ very little from RISA in flow rate and central volume measurements and in the ratio of the major peak concentration and their respective recirculation peaks. This suggests that the peripheral pathway of circulation which channels that portion of recirculating indicator which forms the major recirculation peak does not permit significant transcapillary exchange of readily diffusible electrolytes.

The central volumes as determined by the mean transit time method are slightly larger when the two portions of the circulation are compared with the total circulation. This we believe to be due to the less than instantaneous injection and to the response times of the two systems. Both of these tend to affect the shape of the curve in such a way as to prolong the MTT and increase the calculated cardiac output. In addition, the cardiac output and the mean transit time

OL.
7
59/60

are both affected by recirculating indicator but the inclusion in the curve data of recirculating indicator tends to prolong the MTT and decrease the cardiac output value with little effect in the central volume values.

In 1951 NEWMAN[14] presented his observations on circulation model experiments from which he proposed formulas for the estimation of the main mixing volume in the central circulation. These were based upon trials to measure the major volume of dilution in central circulation. Our measurements of the volumes from antecubital vein to right ventricle by the slope method are in the same order of magnitude as those from the right ventricle to the brachial artery without an organ comparable to the lungs in the circuit from vein to right ventricle. With the catheter positioned as it was, the volume measurements by the mean transit time from the vein to right ventricle averaged 24 per cent less than the volume from right ventricle to brachial artery. The downslopes of the right ventricle to brachial artery curves were consistently steeper than the slopes of the vein to brachial curve. Also, the pool volume measured by the vein–BA curve averaged 55·0 per cent greater than the pool measured by the RV–BA curve. These data would appear to support the concept that the slope cannot be used as a measurement of the heart and lung mixing chamber.

Acknowledgement—The authors wish to acknowledge the assistance of Drs. LISELOTTE WEINERT, RONALD SELVESTER, CLIFFORD ANDERSON, JACK HACKNEY, CLARENCE COLLIER, and of DOROTHY TEEPLE, R.N.

REFERENCES

1. HAMILTON W. F., MOORE J. W., KINSMAN J. M. and SPURLING R. G., *Amer. J. Physiol.* **85,** 377 (1928).
2. FRIEDLICH A., HEIMBECKER R. and BING R. J., *J. Appl. Physiol.* **3,** 12 (1950).
3. SUTTON G. C., KARNELL J. and NYLIN G., *Amer. Heart J.* **39,** 741 (1950).
4. LAWSON H. C., SHADLE O. W., COLEMAN E. S. and HOLTGRAVE D. E., *Circulation Res.* **2,** 251 (1954).
5. DOW P., *J. Appl. Physiol.* **7,** 399 (1955).
6. HENRIQUES V., *Physiol. u. Pathol.* **56,** 230 (1913).
7. MOORE J. W., KINSMAN J. M., HAMILTON W. F. and SPURLING R. G., *Amer. J. Physiol.* **89,** 331 (1929).
8. HAMILTON W. F., SPRADLIN M. C. and SAAM H. G., *Amer. J. Physiol.* **100,** 587 (1932).
9. STARR I. Jr. and COLLINS L. H., *Amer. J. Physiol.* **93,** 690 (1930).
10. DOW P., *Physiologist* **36,** 77 (1956).
11. CRANE M. G., ADAMS R. and WOODWARD I. *J. Lab. Clin. Med.* **47,** 802 (1956).
12. REEVE E. B. and FRANKS J. J., *Proc. Soc. Exp. Biol.* **93,** 299 (1956).
13. CRANE M. G., Unpublished data.
14. NEWMAN E. V., MERRELL M., GENECIN A., MONGE C., MILNOR W. R. and MCKEEVER W. P. *Circulation* **4,** 735 (1951).
15. KINSMAN J. M., MOORE J. W. and HAMILTON W. F., *Amer. J. Physiol.* **89,** 322 (1929).
16. HAMILTON W. F., RILEY R. L., ATTYAH A. M., COURNAND A., FOWELL D. C., HIMMELSTEIN A., NOBLE R. P., REMINGTON J. W., RICHARDS D. W. Jr., WHEELER N. C. and WITHAM A. C., *Amer. J. Physiol.* **153,** 309 (1948).
17. WERKE L., LAGERLOF H., BUCHT H., WEHLE B. and HOLMGREN A., *Scand. J. Clin. Lab. Invest.* **1,** 109 (1949).
18. DOYLE J. T., WILSON J. S., LEPINE C. and WARREN J. V., *J. Lab. Clin. Med.* **41,** 29 (1953).
19. NEELY W. A., WILSON F. C. Jr., MILNOR J. P., HARDY J. D. and WILSON H., *Surgery* **35,** 22 (1954).
20. CRANE M. G., SEARS C., HACKNEY J., HOLLOWAY J., COLLIER C., *J. Lab. Clin. Med.* **51,** 248 (1958).
21. COE W. S., BEST M. M. and LAWSON H. C., *Amer. J. Physiol.* **163,** 704 (1950).
22. HETZEL P. S., SWAN H. J. C. and WOOD E. H., *J. Appl. Physiol.* **7,** 66 (1954).
23. FOX I. J., SUTTERER W. F. and WOOD E. H., *J. Appl. Physiol.* **11,** 390 (1957).
24. CRANE M. G., HOLLOWAY J. E., MCEACHEN J., SEARS C. and SELVESTER R., *Int. J. Appl. Rad. Isotopes* **5,** 218 (1959).

VOL. 7 1959/

International Journal of Applied Radiation and Isotopes, 1959, Vol. 7, pp. 111–117. Pergamon Press Ltd. Printed in Northern Ireland

Use of the Kinetic Tracer Method for Investigations on the Mechanism of *n*-Decane Liquid-phase Oxidation

N. M. EMANUEL, Z. K. MAIZUS and L. G. PRIVALOVA
Institute of Chemical Physics of the Academy of Sciences of the U.S.S.R.

True rates of the formation and consumption of *n*-decyl hydroperoxide in the oxidation of *n*-decane were determined by means of the kinetic tracer method. The complicated changes in these values in the course of the oxidation process were shown to be accounted for by changes in the reaction mechanism with increase in the degree of conversion. The effective constant of the chain propagation reaction rate was established from evidence on the hydroperoxide formation rate and the rate of branching. Changes in the mechanism of the oxidation process were shown to be related to changes in the nature of the chain propagation reaction. The inference of the variation in the activity of chain carrying radicals with accumulation of oxygenated products is suggested as one of the possible explanations of the phenomena observed.

OL.
7
59/60

EMPLOI DE LA MÉTHODE KINÉTIQUE À INDICATEUR POUR L'EXAMEN DU MÉCANISME DE L'OXYDATION EN PHASE LIQUIDE DU *n*-DÉCANE

Les taux actuels de la formation et de la consommation du hydroperoxyde *n*-décylique au cours de l'oxydation du *n*-décane furent dosés par la méthode kinétique à indicateur. On montra que les variations compliquées de ces valeurs durant le procédé l'oxydation s'expliquaient par les changements du mécanisme de la réaction avec augmentation du degré de conversion. La constante effective du taux de la réaction de propagation en chaîne fut établie selon les indications sur le taux de formation de l'hydroperoxyde et sur le taux d'embranchement. Les changements du mécanisme du procédé d'oxydation montrèrent un rapport aux variations dans la nature de la réaction de propagation en chaîne. On propose l'inférence de la variation dans l'activité des radicaux portant des chaînes avec l'amas des produits oxygénés comme une des explications possibles des phénomènes observés.

ПРИМЕНЕНИЕ КИНЕТИЧЕСКОГО ИЗОТОПНОГО МЕТОДА ДЛЯ ИССЛЕДОВАНИЯ МЕХАНИЗМА ОКИСЛЕНИЯ Н-ДЕКАНА В ЖИДКОЙ ФАЗЕ

С помощью изотопного кинетического метода определены истинные скорости образования и расходования гидроперекисей н-децила в процессе окисления н-декана и показано, что сложный характер изменения этих величин в ходе процесса окисления обусловлен изменением механизма процесса по мере увеличения глубины реакции. На основании данных о скорости образования гидроперекисей и скорости разветвления, измеренной методом ингибиторов, оценена величина эффективной константы скорости реакции продолжения цепи и показано, что изменение механизма процесса окисления связано с изменением характера реакции продолжения цепи. В качестве одного из возможных объяснений наблюдаемых явлений рассмотрено предположение об изменении активности радикалов, ведущих цепную реакцию, по мере накопления в реагирующей смеси кислородсодержащих продуктов окисления.

DIE KINETISCHE SPURENMETHODE FÜR UNTERSUCHUNGEN DES MECHANISMUS DER *n*-DEKAN-OXYDIERUNG IN FLÜSSIGER PHASE

Die tatsächlichen Werte für Bildung und Verbrauch von *n*-Decyl-Wasserstoffsuperoxyd bei der Oxydierung von *n*-Dekan wurde mit Hilfe der kinetischen Spurenmethode untersucht. Die komplizierten Veränderungen dieser Werte während des Oxydierungsprozesses konnten auf Veränderung des Reaktionsverlaufes mit wachsendem Grad der Konversion zurückgeführt werden. Die tatsächliche Konstante der Kettenbildungsgeschwindigkeiten wurde an Hand von Ergebnissen der H_2O_2-Bildung und des Ausmasses der Verzweigungen ermittelt.

Es wurde gezeigt, dass Veränderungen des Mechanismus des Oxydierungsprozesses mit einer Veränderung der Kettenbildungsreaktion zusammenhängen. Der Einfluss der Änderung der Aktivität der kettentragenden Radikale mit der Anhäufung von oxydierten Produkten, wird als mögliche Erklärung für das beobachtete Phänomen vorgeschlagen.

As established in a series of experiments[1] the liquid phase oxidation of hydrocarbons should be considered as pertaining to the class of degenerate branching reactions first postulated by SEMENOV[2].

However a variety of recently established experimental facts does not fit into classic concepts of the theory and the latter should be further elaborated in accordance with the new findings.

The latter are: the discrepancy between the experimental value for the rate of *n*-decane oxidation and that calculated from the conventional oxidation scheme; decrease in the effective constant for the hydroperoxide decomposition rate with increase in the degree of conversion[3]; self-retardation of the reaction at a high degree of conversion[4] and so on.

The theory of liquid phase oxidation would imply that at a quadratic chain termination the reaction rate be

$$w = \frac{k_2[\mathrm{RH}]}{\sqrt{k_5}}\sqrt{(w_{\mathrm{branch}} + w_0)}$$

$$= \frac{k_2[\mathrm{RH}]}{\sqrt{k_5}}\sqrt{w_{\mathrm{branch}}}$$

where k_2 is the rate constant for the chain propagation reaction $RO_2\cdot + RH \rightarrow RO_2H + R$

k_5 is the rate constant for the recombination of $RO_2\cdot$ radicals;

w_{branch} is the chain branching rate;

w_0 is the chain initiation rate.

The *n*-decane oxidation rate obtained experimentally cannot be described by this equation purporting the unchangeability of k_2, k_5 and w_{branch} constants throughout the reaction course.

The particularities of *n*-decane oxidation can, in principle, be explained on the assumption that the oxidation mechanism, and consequently the chain propagation, branching, and termination constants, change in the course of the reaction as a result of variations in the mixture composition. Thus exact knowledge of these changes with the degree of conversion would be necessary for a clear understanding of the *n*-decane oxidation process.

We have recently measured the branching rate constant in *n*-decane oxidation by means of inhibitors[5] and it appeared to remain unchanged throughout the oxidation process.

The present work was concerned with investigations on variations in the chain propagation rate.

On the assumption that the peroxide radical recombination constant (k_5) does not change considerably in the course of the oxidation process, and this is quite possible since the radical recombination proceeds without activation energy and the steric factors for various radicals do not differ essentially, the ratio $w/\sqrt{w_{\mathrm{branch}}}$ can be taken as the effective chain propagation rate (see equation 1).

The w_{branch} values can be readily computed by means of the branching rate constant evaluated in one of our works.[5] Consequently only one value should be measured

VOL. 7 1959/6

to obtain the effective propagation rate constant, namely the reaction rate w, or the true rate of hydroperoxide formation in *n*-decane oxidation.

Since from the start of the *n*-decane oxidation process hydroperoxides are not only formed, but also consumed, the true rate of their formation can be determined only by means of the kinetic tracer method.[6]

EXPERIMENTAL

The conventional kinetic tracer method involves the addition of a small amount of the species to be measured containing a radioactive isotope, for instance C^{14}.

However, this technique is not adequate for the purpose of this work, as *n*-decane oxidation yields not a single peroxide, but a mixture of isomer peroxides and consequently the addition of only one isomer would not be sufficient to obtain the complete reaction pattern, whilst synthesis of a hydroperoxide mixture similar to that produced in oxidation appears to be impossible.

Thus a modification of the kinetic tracer method was chosen. A small amount of labelled initial hydrocarbon was introduced into the reacting mixture after a certain lapse of time from the beginning of the reaction. Inactive reaction products (for instance hydroperoxides in *n*-decane oxidation) were diluted by radioactive reaction products, and the activity of various species formed increased in the course of the reaction tending at the limit to the specific activity of the initial hydrocarbon (α_0).

The rates of formation and consumption of separate reaction products can be obtained from kinetic curves for the accumulation of products and increase in their specific activity, by means of equations of the kinetic tracer method.

n-Decane containing two atoms of C^{14} in positions 5 and 6 was chosen as an additive. Synthesis of the labelled *n*-decane can be represented by a series of consecutive reactions.

$$C_4H_9J \xrightarrow{Mg} C_4H_9MgJ \xrightarrow{C^{14}O_2}$$
$$C_4H_9C^{14}OOH \xrightarrow{CH_2N_2}$$
$$C_4H_9C^{14}OOCH_3 \xrightarrow{LiAlH_4}$$
$$C_4H_9C^{14}H_2OH \xrightarrow{HBr}$$
$$C_4H_9C^{14}H_2Br \xrightarrow{Na} (C_4H_9C^{14}H_2)_2$$

Magnesium iodide butyl carbonization was carried out by means of $C^{14}O_2$ in an ether mixture at 50°C and with vigorous mixing.[7] A white precipitate of $C_4H_9C^{14}OO$ MgJ was formed. It was then decomposed by 20% sulphuric acid; the iodine evolved was reduced by solid sodium thiosulphate. Valeric acid was salted out of the ether layer by a 20% solution of NaOH which was added until it gave an alkali reaction for phenolphthalein. The alkali layer was then separated and neutralized by 20% H_2SO_4. Retransfer of the sodium acid into free acid was carried out by means of introducing $KHSO_4$ until full saturation was obtained. The valeric acid was then isolated from the aqueous layer by fourfold extraction with ether. The ether solution was dried, the ether distilled off and the remaining valeric acid distilled in vacuum. The activity yield at this stage of the synthesis was 81 per cent of the theoretical value. At the next stage valeric acid was reduced to amyl alcohol, being previously converted into its methyl ester, since ester reduction is considerably easier than that of the free acid.

Methylation was conducted by means of gaseous diasomethane flowed through an ether solution of valeric acid until the appearance of a yellow coloration that remained stable for some time. The coloration was accounted for by excess of diasomethane.[8] The reaction yield was practically 100 per cent.

The valeric acid methyl ester was reduced with an ether solution of lithium aluminium hydride in nitrogen with vigorous mixing for 5–6 hr.[9] The white precipitate formed consisting of complex compounds $(C_4H_9CH_2O)_4LiAl$ and $(CH_3O)_4LiAl$ was decomposed by a 10% H_2SO_4 solution, and the methyl and amyl alcohols evolved were extracted with ether. Then the ether and

methyl alcohol were distilled off in a water bath with subsequent distillation of the amyl alcohol in vacuum.

The amyl alcohol yield was 90 per cent of the theoretical value.

The amyl alcohol was then brominated with a mixture of 48% HBr and concentrated H_2SO_4 whilst boiled during 10–12 hr. The amyl bromide formed was distilled off and washed with concentrated H_2SO_4, water and a 10% Na_2CO_3 solution. Final bromide purification was attained by distilling it in vacuum. Purified amyl bromide was then subjected to the action of metal sodium in absolute ether for 10–12 hr. After the reaction was completed sodium was separated from the *n*-decane-containing ether solution, the ether was distilled off, and the *n*-decane purified by concentrated H_2SO_4 and distilled in vacuum. The overall activity yield was 27 per cent of the whole amount of $C^{14}O_2$.

After a certain lapse of time from the beginning of oxidation the *n*-decane formed was added to inactive decane. The experiments were carried out in a special oxidation cell,[1] oxygen being fed continuously. Samples were withdrawn at regular intervals after the addition of labelled *n*-decane, and the concentration of hydroperoxides and their specific activity were determined.

A special technique was developed for the isolation of hydroperoxides from the variety of oxidation products. It was based on the method for isolation of *n*-heptyl hydroperoxides described in an article on *n*-heptane oxidation.[11] Oxidized decane withdrawn directly from the reaction vessel was gleaned from acids by treating it with a 5% K_2CO_3 solution. In order to change hydroperoxides into their sodium salts the decane, containing neutral compounds and hydroperoxides, was treated with a 10% aqueous solution of NaOH, in the cold, whilst vigorously shaken. The neutral compounds carried away were then carefully washed off the alkali layer by petroleum ether. The alkali layer was then acidified with concentrated sulphuric acid (1·5–2·0 ml) in the presence of chloroform (3 ml), whilst vigorously shaken. The hydroperoxide salts were again transformed into free hydroperoxides that passed from the aqueous into the chloroform layer. The latter was then dried and transferred into a quartz ampoule. The chloroform was distilled off in vacuum. Only pure *n*-decyl hydroperoxides remained then in the ampoule and they were burned in a quartz tube in an oxygen atmosphere. The CO_2 formed was absorbed by barite water and used for the determination of hydroperoxide specific activities.

It appeared possible to isolate in this way 25–30 per cent of the whole amount of *n*-decane hydroperoxides present in the sample.

This amount is amply sufficient for the determination of hydroperoxide specific activities. As has been shown in investigations on *n*-heptane[11] and *n*-decane[12] in the case of oxidation of saturated hydrocarbons with a long chain all secondary carbon atoms are evenly attacked by oxygen, that is isomeric hydroperoxides are formed in about equal amounts under these conditions. Consequently the activities of all hydroperoxides formed will be similar. Thus even on the assumption that not all hydroperoxide salts are isolated under alkali treatment, but only one or several isomers, the specific activity of the isolated species may still serve as a quantitative characteristic of the hydroperoxide formation process.

The initial *n*-decane specific activity was determined by burning a sample withdrawn from the reaction vessel and thoroughly cleaned from oxidation products by manifold treatment with concentrated sulphuric acid.

The purity of isolated hydroperoxides was tested by adding decanone-2, decanol-2, and *n*-decane labelled with C^{14} to inactive oxidized decane containing hydroperoxides. After all the manipulations on the isolation and burning of the hydroperoxides were made, the $BaCO_3$ precipitates appeared to be completely inactive. This confirms the possibility of isolating them in a pure state without admixtures of any decane oxidation products.

VOL. 7 1959/

EXPERIMENTAL RESULTS

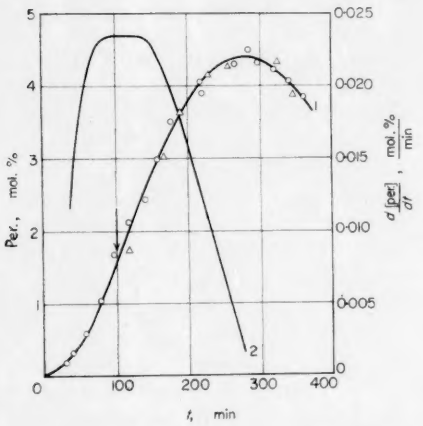

FIG. 1. Kinetic curve for hydroperoxide accumulation (1) and its differential curve (2). Time of introducing the labelled additive shown by arrow.

n-Decane oxidation was carried out at 140°C at a rate of oxygen flow of 1·6 l./hr. *n*-Decane labelled with C^{14} was introduced into the reacting mixture 100 min after the start of the reaction. As can be seen from the kinetic curve for hydroperoxide accumulation (Fig. 1, curve 1), a considerable amount of hydroperoxides will be formed in this time in the reacting mixture.

Variations in specific activities of hydroperoxides formed under these conditions after the addition of C^{14} are shown in Fig. 2

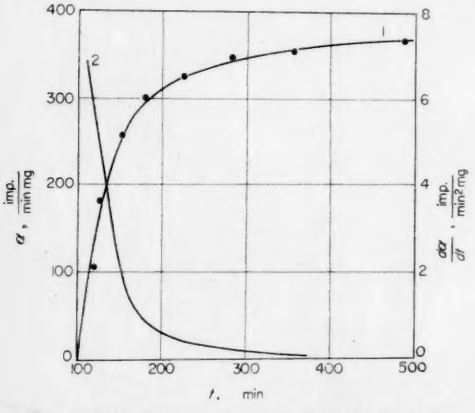

FIG. 2. Kinetic curve for variations in the hydroperoxide specific activity (1) and its differential curve (2). $T = 140°C$.

(curve 1). The hydroperoxide specific activity can be seen to continuously increase and already after 150 min it reaches its limiting value, that is the *n*-decane specific activity.

The rapid activity rise shows that the rates of hydroperoxide formation and consumption are very high. The results obtained permit determination of the hydroperoxide formation rate in *n*-decane oxidation from equations of the kinetic tracer method.

$$w_{\text{form}} = \frac{C}{\alpha_0 - \alpha_t} \times \frac{d\alpha}{dt}. \qquad (2)$$

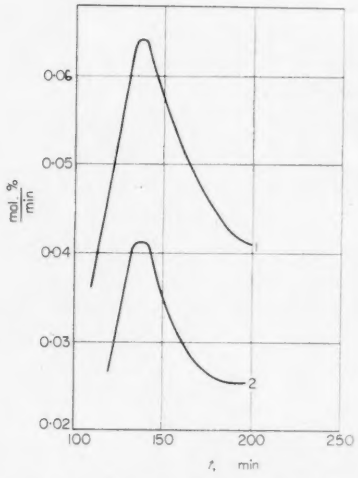

FIG. 3. Kinetic curves for the rates of formation (1), and consumption (2) of hydroperoxides in *n*-decane oxidation at 140°C. Labelled *n*-decane is introduced 100 min after the start of the oxidation reaction.

The hydroperoxide consumption rate will be

$$w_{\text{cons}} = w_{\text{form}} - \frac{dC}{dt}. \qquad (3)$$

Fig. 3 shows variations in the values of w_{form} and w_{cons} in the course of the reaction. The hydroperoxide formation and consumption rates begin with increasing, then reach a certain maximum, after which they fall off again.

The nature of these variations can also be established from calculations based on general

concepts of the degenerate branching mechanism in the oxidation of hydrocarbons.

Indeed, if the hydroperoxide formation rate is expressed as the difference between the formation and consumption rates

$$\frac{d[\mathrm{ROOH}]}{dt} = \frac{k_2[\mathrm{RH}]}{\sqrt{k_5}}\sqrt{w_{\mathrm{branch}}} - k_4[\mathrm{ROOH}]$$

or

$$\frac{d[\mathrm{ROOH}]}{dt} = k\sqrt{(\mathrm{ROOH})} - k_4[\mathrm{ROOH}]$$

and passing over to dimensionless values

$$\mathrm{ROOH} = a\eta \quad \text{and} \quad t = b\tau$$

the hydroperoxide accumulation rate will be expressed by

$$\frac{d\eta}{d\tau} = \sqrt{\eta} - \eta. \tag{4}$$

By integrating this equation we obtain an expression for the hydroperoxide formation rate in dimensionless coordinates

$$\eta = 1 - e^{-\tau/2} \tag{5}$$

and for the hydroperoxide consumption rate

$$\eta = (1 - e^{-\tau/2})^2. \tag{6}$$

Theoretical kinetic curves obtained from equations (5) and (6) (Fig. 4) show the nature of variations that would take place in the rates of hydroperoxide formation (curve 1), consumption (curve 2), and accumulation (curve 3), if *n*-decane oxidation were to proceed by the classic degenerate branching scheme. In this case the hydroperoxide formation and consumption rates would continuously increase tending to a stationary value, and only at a sufficiently high degree of conversion the reaction rate would fall off due to initial hydrocarbon consumption.

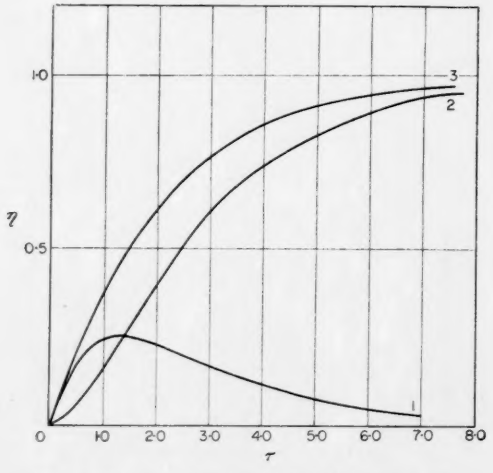

FIG. 4. Theoretical curves for the rates of accumulation (1), consumption (2), and formation (3) of hydroperoxides calculated from the scheme for degenerate branching oxidation of hydrocarbons.

However, comparison of theoretical and experimental curves (Fig. 3) distinctly shows a disparity between the two curve sets. Contrary to theoretical kinetic plots the maximum in hydroperoxide formation and consumption rates is observed at a relatively early stage, when the absolute amount of hydroperoxides responsible for degenerate branching keeps on increasing.

The incompatibility of experiment with the general chain theory concepts can be considered as a direct proof of the change in the reaction mechanism in the course of *n*-decane oxidation.

As has already been pointed out one of the reasons for this change in the overall mechanism of *n*-decane oxidation can be the change in the chain propagation reaction which has an effective rate constant characterized by the $w/\sqrt{w_{\mathrm{branch}}}$ ratio.

The true hydroperoxide formation rates obtained by the kinetic tracer method make it possible to follow variations in the value of $w/\sqrt{w_{\mathrm{branch}}}$ throughout the course of the process.

Fig. 5 shows the dependence of $w/\sqrt{w_{\mathrm{branch}}}$ on the duration of the *n*-decane oxidation process. As can be seen, the effective chain propagation constant value does not remain unchanged throughout the process. $w/\sqrt{w_{\mathrm{branch}}}$ begins with increasing, passes through a maximum, and then falls off again.

This is consistent with the suggestion that the change of the overall oxidation mechanism with increase of the degree of conversion is related to the change of the effective chain propagation constant.

One of the possible explanations of the reaction mechanism change would be the radical activity variations postulated by DENISOV and ENIKOLOPYAN.[13,14]

Oxygenated products are formed in the

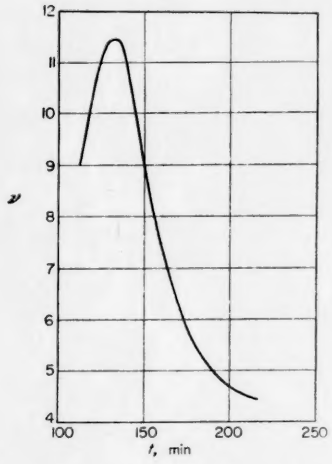

FIG. 5. Variations in the effective propagation rate constant in the course of *n*-decane oxidation. $T = 140°C$.

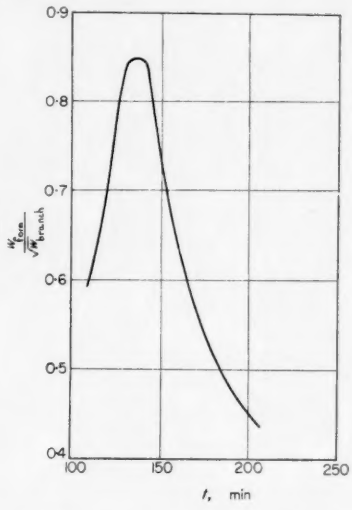

FIG. 6. Kinetic curve for variations in the length of chain in *n*-decane oxidation. $T = 140°C$.

oxidation of *n*-decane, namely: alcohols, carbonyl compounds, acids and esters. The interaction of $RO_2\cdot$ with these species may well compete with the basic chain propagation reaction $RO_2\cdot + RH$ since these substances are more reactive (have a weaker C–H bond) than the initial decane.

Consequently the process may be considerably accelerated even at relatively low product concentrations.

This viewpoint would help towards an understanding of the increased effective rate constant of the chain propagation reaction at relatively early reaction stages.

Further diminishing of the effective constant can be accounted for by the fact that new radicals formed in the interaction of $RO_2\cdot$ with oxidation products are less active than $RO_2\cdot$ and consequently the overall degenerate branching rate falls off.

Thus the results obtained lead to a conclusion that the change in *n*-decane oxidation kinetics can be explained by a change in the nature of the chain propagation reaction.

The chain length in the *n*-decane oxidation reaction can be calculated from the *n*-decyl hydroperoxide formation rates (Fig. 6).

REFERENCES

1. KNORRE D. G., MAIZUS Z. K., OBOUKHOVA L. K. and EMANUEL N. M. *Usp. Khim.* **26,** 417 (1957).
2. SEMENOV N. N. *Chemical Kinetics and Chain Reaction.* Oxford University Press (1935).
3. VARTANYAN L. S., MAIZUS Z. K. and EMANUEL N. M. *Zh. Fiz. Khim.* **30,** 856 (1956).
4. EMANUEL N. M. *Voprosy Khimicheskoy Kinetiki, Katalyza i Reakzionnoy Sposobnosty* (Edited by Acad. Sci. USSR) (1955).
5. KNORRE D. G., MAIZUS Z. K. and EMANUEL N. M *Dokl. Akad. Nauk SSSR* **123,** 123 (1958).
6. NEIMAN M. B. *Zh. Fiz. Khim.* **28,** 1235 (1954).
7. LOUKOVNIKOV A. F., NEIMAN M. B., BAG A. A., RODIONOVA L. M., SAMOUKINA I. S. and BLIZNUYAK I. V. *Dokl. Akad. Nauk SSSR* **88,** 297 (1953).
8. OBOUKHOVA L. K. *Zh. Anal. Khim.* **2,** 193 (1956).
9. ROGINSKAYA E. V. *Usp. Khim.* **21,** 3 (1952).
10. KNORRE D. G., MAIZUS Z. K. and EMANUEL N. M *Zh. Fiz. Khim.* **29,** 710 (1955).
11. PRITZKOW W. *Angew Chem.* **67,** 399 (1955).
12. BENTON J. Z. and WIRTH M. M. *Nature, Lond.* **173,** 269 (1953).
13. DENISOV E. T. *Zh. Fiz. Khim.* **31,** 1481 (1957).
14. ENIKOLOPYAN N. S. *Dokl. Akad. Nauk SSSR* **112,** 93 (1957).

International Journal of Applied Radiation and Isotopes, 1959, Vol. 7, pp. 118–122. Pergamon Press Ltd. Printed in Northern Ireland

On the Kinetic Isotope Effect in Cracking

A. M. BRODSKY, R. A. KALINENKO and K. P. LAVROVSKY
Institute of Petrochemical Synthesis of the Academy of Sciences of the U.S.S.R.

Investigations on the kinetic isotope effect in cracking of $C^{14}H_3$–$C^{12}H_3$ and $C^{14}H_3$–$C^{14}H_3$ are described. The results obtained are consistent with the suggested hypothesis on the effect of symmetry on decomposition rates.

SUR L'EFFET KINÉTIQUE DES ISOTOPES DANS LA DÉGRADATION

On décrit des recherches sur l'effet kinétique des isotopes dans la dégradation du $C^{14}H_3$–$C^{12}H_3$ et du $C^{14}H_3$–$C^{14}H_3$. Les résultats obtenus sont d'accord avec l'hypothèse proposé sur l'effet que prète la symétrie aux taux de décomposition.

О КИНЕТИЧЕСКОМ ИЗОТОПНОМ ЭФФЕКТЕ КРЕКИНГА

Описывается исследование кинетического изотопного эффекта при высокотемпературном крекинге этанов $C^{14}H_3$–$C^{12}H_3$ и $C^{14}H_3$–$C^{14}H_3$. Результаты опытов согласуются с выдвинутой гипотезой о влиянии эффектов симметрии на скорость распада.

ÜBER DEN KINETISCHEN EFFEKT VON ISOTOPEN BEI HOCHTEMPERIERTER SPALTUNG

Untersuchungen über die kinetische Wirkung von Isotopen bei der Spaltung von $C^{14}H_3$–$C^{12}H_3$ und $C^{14}H_3$–$C^{14}H_3$ werden beschrieben. Die Ergebnisse sind in Übereinstimmung mit der vorgeschlagenen Hypothese über den Symmetrie-Effekt auf die Dekompositionsrate.

VOL. 7 1959/

The present paper is concerned with investigations on the kinetic isotope effect in high-temperature cracking of $C^{14}H_3$–$C^{12}H_3$ and $C^{14}H_3$–$C^{14}H_3$.

The kinetic isotope effect is the effect of variations in the rate of chemical transformations due to changes in isotopic composition. Studies of this phenomenon are known to have led to important conclusions both on principles governing elementary chemical acts, and on mechanisms of overall reactions. Investigation of the kinetic isotope effect in the decomposition of C_2H_5Br, for instance, made it possible to establish that the reaction proceeded by a molecular, and not by a chain mechanism.[1]

The kinetic isotope effect in high-temperature cracking has been studied so far only for propanes $C_2{}^{12}H_5C^{13}H_3$[2] and $C_2{}^{12}H_5C^{14}H_3$.[3] By measurements of the isotopic composition of methane† formed in the cracking of a mixture of these propanes with $C_2{}^{12}H_5C^{12}H_3$ it was possible to determine that at high temperatures the C^{12}–C^{12} bond is broken with an 8 per cent greater frequency than that observed for the C^{14}–C^{12} and C^{13}–C^{12} bonds.

According to current theoretical notions,[4,5] at high temperatures when the rôle of isotopic variations in the activation energy is relatively unimportant, the main contribution to the kinetic isotope effect in the case of a unimolecular dissociation reaction would be the "kinematic" action of the mass change. This action is dependent upon the magnitude of the reduced mass corresponding to the vibrational frequency of reacting bonds, the ratio of rate constants K

† The isotopic composition of other cracking products is not mentioned in reference 3, whilst that of methane is given only for two very high degrees of conversion.

and K' for the rupture of R_1–R_2 and R_1'–R_2' bonds on excitation of one ith vibration being approximately†

$$\frac{K}{K'} = \frac{K_0}{K_0'} \exp\left[\frac{-(E-E')}{RT}\right]$$

$$= \sqrt{\frac{m'}{m}} \exp\left\{\frac{1}{RT}\left[\frac{h}{2}(\nu_i^0 - \nu_i'^0) - \Delta E_i^*\right]\right\}$$

$$\cong 1 + \alpha\left(1 + \frac{C}{T}\right) \leq 1 + \alpha \qquad (1)$$

where $$\alpha = \sqrt{\frac{m'}{m}} - 1 \ll 1$$

$$\Delta E_i^* = E_i^* - E_i^{*\prime},$$

$$C = \frac{1}{R}\left(\frac{h\nu_i^0}{2} - \frac{1+\alpha}{\alpha}\Delta E_i^*\right) \leq \frac{1}{R}\frac{h\nu_i^0}{2} \qquad (2)$$

ν_i^0 and $\nu_i^{0\prime}$ are the normal frequencies in an unexcited state, E^* and $E^{*\prime}$ are energies of the excited (activated) state prior to decomposition, m and m' are reduced masses for normal vibrations corresponding to a bond being broken. Primes denote values for isotopically substituted molecules.

Let us consider the range of possible C values. In the case of a model with weakly interacting vibrations and if anharmonicity is neglected, C will be equal by order of magnitude to $-n\frac{h\nu_i^0}{R} < 0$.

In case $\Delta E^* \ll h(\nu_i^0 - \nu_i^{0\prime})/2$ (considerations in favour of the validity of this inequality can be found in reference 5), C will be maximum and its value would be readily calculated from spectral data. For C–C bonds in hydrocarbons, at cracking temperatures of 700–900°, the upper value of C/T appears to be about 0·5, i.e. at high temperatures the main part of the effect determined by the difference $(K/K') - 1$ will be exerted by α alone.

It will be noted that interpretation of the isotope effect dependence upon temperature variations will permit experimental determination of the frequency values for an excited (activated) state, as can be seen from the above equations.

According to equation 1 analogous to a similar equation used in references 4–6, the relative change in the frequency of a C–C bond rupture in propane will be proportional to α and will be, not 8 per cent, as in the case of references 2 and 3, but merely about 2 and 3·7 per cent for the rupture of C^{12}–C^{13} and C^{12}–C^{14} bonds respectively (extrapolating to $T = \infty$).

Thus the abnormally high value of the isotope effect and its similarity in the rupture of C^{12}–C^{13} and C^{12}–C^{14} bonds cannot be explained within the limits of the given theoretical treatment.

A possible explanation of this discrepancy would be that in the case of hydrocarbon molecules having a symmetry plane normal to the chain direction, or a corresponding rotational axis of symmetry followed by a reflection in a plane, the introducing of labelled carbon into the carbon skeleton causes disturbance in symmetry. This would essentially affect the decomposition rate, as the existence of an additional symmetry plane, or of a rotational axis of symmetry followed by a reflection in a plane, imposes certain restrictions with respect to transitions from the initial to the final or activated state. At the same time wave functions of the $C^{12}H_3$–$C^{14}H_3$ molecule exhibit no parity (symmetry properties) that would be definite in this sense and consequently there will be no restrictions for a molecule of this kind.‡

Thus, generally speaking, on replacing "symmetrical" molecules by "asymmetrical" ones variations in the isotopic composition of hydrocarbons will result in an important kinetic effect.

The mechanism of the kinetic isotope effect was verified experimentally by comparative investigations on high-temperature cracking of $C^{12}H_3$–$C^{12}H_3$, $C^{12}H_3$–$C^{14}H_3$ and $C^{14}H_3$–$C^{14}H_3$. If these suggestions are true, the kinetic isotope effect may appear to be more important for $C^{14}H_3$–$C^{12}H_3$ than for $C^{14}H_3$–$C^{14}H_3$, the equal zero spin of C^{14} and C^{12} nuclei being essential. Inversely, according to simplified equation 1 the isotope effect

† Equation 1 can readily be generalized for the case of a reaction involving several bonds (normal vibrations).

‡ It will be noted that quantitative evaluation of the above symmetry effect must be treated separately.

in the rupture of a C^{12}–C^{14} bond would be about two times less marked than in C^{14}–C^{14}.

Ethane cracking was selected for study since the mechansim of this reaction is exceedingly simple. This is essential for interpretation of experimental results. In particular, the following ambiguity is encountered in determination of the isotope effect for methane in the cracking of propane. According to reference 3 the isotope effect will be accounted for in this case by rupture of the C–C bond in a CH_3–C_2H_5 molecule, or in a propyl radical. Another explanation is given in reference 2, where the isotope effect is supposed to be related to the rupture of a C–H bond in a metathetic reaction

$$C^{13}H_3\text{–}C_2H_5 + R \rightarrow C^{13}H_2\text{–}C_2H_5 + RH$$

with subsequent decomposition of $C^{13}H_2$–C_2H_5 into $C^{13}H_2$–CH_2 and CH_3, the decomposition rate being similar for all cases. It will be noted that this reasoning does not account for the predominant formation of *iso*propyl radicals with their subsequent isomerization, as accepted currently for metathetic reactions.[9] Besides in the case of ethane the effective mass selection in equation 1 becomes practically unambiguous, as this equation corresponds to vibrations at the C–C bond in an excited state and does not change essentially, whether the CH_3 radical vibrates as a whole, or there is displacement of C with respect to H.

The latter simplifies interpretation of experimental results by means of equation 1. Experiments were carried out in a reacting vessel with practically complete intermixing, at 850° and a pressure of 50–80 mm Hg, using the technique described in reference 10. In a reactor of this kind the concentration of any product in the reacted mixture is directly proportional to its formation rate constant. Thus the specific activity of a given end-product will be directly proportional to the ratio of formation rates of an active and an unlabelled compound.

Separation and analysis of the reaction products were carried out chromatographically.[11] Microadmixtures were carefully removed from the original gases, also by means of chromatography. Careful purification is essential in view of the weak effect and small amounts of methane formed. In the first series of runs the original ethane consisted of a mixture of $C_2{}^{12}H_6$ and $C^{12}H_3C^{14}H_3$ and its activity was 213 imp/min per mm Hg, as measured by an internal counter of the Russian mark SBM-8. This corresponds to $A^{I} = 1520$ imp/min per cm^3.

A mixture of $C_2{}^{12}H_6$ and $C^{14}H_3$–$C^{14}H_3$ with an activity of $A^{II} = 11000$ imp/min per cm^3, and containing practically no $C^{14}H_3$–$C^{12}H_3$ was used in the second series of runs.

Experimental results have shown that the methane activity was not $\frac{1}{2}A^i$ (i = I, II) as would be expected in the absence of the isotope effect, but had a lower value.

Methane activities in per cent of $\frac{1}{2}A^{I}$ obtained in the first series of runs, relative to the ethylene content of cracked gas characterizing the degree of conversion,† are summarized in Table 1.

The difference in activity of original ethane and ethylene was within experimental error and did not exceed 1–1·5 per cent.

Methane activities obtained in the second series of runs, as well as the activities of ethylene formed in cracking are summarized in Table 2.

TABLE 1. Methane activities obtained in experiments with $C^{14}H_3C^{12}H_3$ at $T = 850°C$

No. of run	Pressure (mm Hg)	Ethylene content of cracking gas (per cent by volume)	CH_4 activity (per cent of $\frac{1}{2}A^{I}$)
1	50	7·7	91 ± 3
2	50	10·7	85 ± 3
3	30	11	86 ± 2
4	88	12·3	86 ± 2
5	90	16·2	87 ± 2
6	89	23·5	90 ± 2
7	84	23·7	88 ± 1

† Detailed information on the composition of ethane cracking products under these conditions can be found in reference 10.

VOL. 7 1959/6

TABLE 2. Methane and ethylene activities in experiments with $C^{14}H_3$–$C^{14}H_3$ at $T = 850°C$

No. of run	Pressure (mm Hg)	Ethylene content of cracking gas (per cent by volume)	Activity	
			CH_4 (per cent of $\frac{1}{2}A^{II}$)	C_2H_4 (per cent of A^{II})
1	96	9·3	—	97 ± 1
2	95	12·7	94 ± 2·5	—
3	94	15·3	95 ± 1	97·9 ± 0·5
4	92	24·9	95 ± 1·5	97·8 ± 1

In both series of runs the relative molar concentrations of radioactive ethanes in the original gas was very low (10^{-4}–10^{-5}). Thus the kinetic isotope effect value on rupture of the C–C bond in ethane can always be obtained directly from deviation of the methane activity from $\frac{1}{2}A^i (i = I, II)$.

Indeed, in a vessel with complete intermixing and at moderate degrees of conversion

$$\frac{[CH_4^{14}]}{[CH^4]} = \frac{K'[CH_3C^{14}H_3]}{2K[C_2H_6] + K'[CH_3C^{14}H_3]} \simeq \frac{\beta}{2}\frac{K'}{K}A^I$$
$$\frac{[C^{14}H_4]}{[CH_4]} = \alpha\frac{2K'[C^{14}H_3C^{14}H_3]}{2K[C_2H_6]} = \beta\frac{K'}{K}\tfrac{1}{2}A^{II} \qquad (3)$$

where α and β are certain proportionality coefficients. It follows from equation 3 that in any case

$$\frac{K'}{K} = \frac{\beta^{-1}[C^{14}H_4]}{\frac{1}{2}A^i[CH_4]} = \frac{A^{CH_4}}{\frac{1}{2}A^i} \quad (i = I, II) \qquad (4)$$

where A^{CH_4} is the activity of methane formed in cracking.

These results show that when methane is produced in cracking of $C^{14}H_3$–$C^{12}H_3$ the kinetic isotope effect will be 12 ± 2 per cent, greatly exceeding the value of 5 ± 1 per cent obtained in cracking of $C^{14}H_3$–$C^{14}H_3$. Allowing for the admixture of about 15 per cent of C^{12}–C^{13} contained in natural C^{12}–C^{12},[12] the value of 5 ± 1 will be in good agreement with that (~6·5 per cent) derived from equation 1, where only the kinematic changes of the mass at C = 0 are taken into account. The experimental results obtained, showing the absence of direct proportionality between the kinetic isotope effect and the reduced mass, can be considered as a qualitative confirmation of the suggestion that an effect of symmetry disturbance is taking place in this case.†

It follows from experimental evaluation for $C^{14}H_3$–$C^{14}H_3$

$$\frac{C}{T} \leqslant 0{\cdot}01$$

and from equation 2 that

$$\frac{\nu^0_{C-C} - \dfrac{\Delta E^*(1+\alpha)}{\alpha}}{\nu^0_{C-C}} < \frac{2 \times 10^{-2}RT}{h} \simeq 0{\cdot}05 \qquad (5)$$

It can be seen from the above that by order of magnitude the isotopic displacement value of vibrational energies in an excited state is close to displacement in the initial state. Indirect dependence of the rates of unimolecular reactions involved in cracking on various nuclei states can be seen from the results obtained. This leads to a variety of important kinetic consequences. A relatively marked effect for ethylene (~2 per cent) exceeding the value obtained from equation 1 for the C–H bond rupture (~0·3 per cent) will also be noted. This and also the ratio of isotope effects for C^{12}–C^{14} and C^{14}–C^{14} bonds can be interpreted as a consequence of the formation of C_2H_4 by a molecular, rather than by a chain mechanism (as in the case of reference 1). This statement is consistent with the conclusions drawn in reference 10 and based on different considerations.

However it will be noted that the measurements obtained are not sufficiently reliable for deriving unambiguous conclusions.

† It will be noted that the abnormally marked effect observed on degradation should be taken into account in considering the C^{12}/C^{13} ratio in oil and gases.[12]

REFERENCES

1. Friedman H. L., Bernstein R. B. and Gunning H. E. *J. Chem. Phys.* **23,** 109 (1955).
2. Stevenson D. P., Wagner C. D., Beeck O. and Otvos J. W. *J. Chem. Phys.* **16,** 993 (1948).
3. Frey H. M., Danby C. J. and Hinshelwood C. *Proc. Roy. Soc.* A**234,** 301 (1956).
4. Bigeleisen J. and Mayer M. G. *J. Chem. Phys.* **15,** 261 (1947).
5. Kondratiev V. N. *Kinetika Khimitcheskykh Gazovykh Reaktzy* (*Kinetics of Chemical Gas Reactions*). Edited by the Academy of Sciences of the U.S.S.R., Moscow (1958).
6. Roginsky S. Z. *Teoretichesky Osnovy Isotopnykh Metodov Izoutchenya Khimitcheskykh Reaktzy* (*Theoretical Basis of Tracer Methods for Studying Chemical Reactions*). Edited by the Academy of Sciences of the U.S.S.R., Moscow (1956).
7. Bigeleisen J. *J. Chem. Phys.* **17,** 344 (1949).
8. Landau L. and Lifshitz E. *Kvantovaya Mekhanika* (*Quantum Mechanics*). Gostekhizdat, Moscow (1948).
9. Semenov N. N. *Some Problems of Chemical Kinetics and Reactivity*. Pergamon Press, London (1958–9).
10. Brodsky A. M., Kalinenko R. A., Lavrovsky K. P. and Titov V. B. *Dokl. Akad. Nauk SSSR* **116,** 789 (1957); **117,** 1013 (1957).
11. Brodsky A. M., Kalinenko R. A. and Lavrovsky K. P. *Khim. i Technol. Topliva* No. 8, 18 (1956).
12. Rankama K. *Isotope Geology*. London (1954).

VOL.
7
1959/6

International Journal of Applied Radiation and Isotopes, 1959, Vol. 7, pp. 123–125. Pergamon Press Ltd. Printed in Northern Ireland

An Autoradiographic Method for Determining the Distribution of Iron on Recording Tape

S. M. MAKIN and A. E. NUNLEY
Isotope Division, Atomic Energy Research Establishment, Harwell

(*Received* 6 *January* 1959; *in revised form* 27 *April* 1959)

Autoradiography has been found to be a suitable method of measuring the distribution of iron in the magnetic coating on recording tape. Non-uniformity has been found on a macroscopic and microscopic scale. Autoradiographs taken with Fe^{55} and Fe^{59} have revealed irregularities over distances of 1 to 3 mm and further non-uniformity has been found on 5 μ scale.

UNE MÉTHODE AUTORADIOGRAPHIQUE POUR DOSER LA DISTRIBUTION DU FER SUR LES RUBANS ENREGISTREURS

L'autoradiographie s'est démontrée une méthode convenable à la mesure de la distribution du fer dans la couche magnétique sur le ruban enregistreur. On a trouvé un manque d'uniformité à l'échelle macroscopique et à la microscopique. Des autoradiogrammes achevés avec le Fe^{55} et le Fe^{59} ont découvert des variations par des distances de 1 à 3 mm et de plus on a trouvé un manque d'uniformité à l'échelle de 5 μ.

МЕТОД РАДИОАВТОГРАФИИ ДЛЯ ОПРЕДЕЛЕНИЯ РАСПРЕДЕЛЕНИЯ ЖЕЛЕЗА В ЛЕНТЕ САМОПИСЦА

Радиоавтография оказалась пригодным методом для определения распределения железа в магнитном покрытии ленты самописца. Неравномерное распределение было обнаружено в макроскопическом и микроскопическом масштабах. Радиоавтографы, снятые с помощью Fe^{55} и Fe^{59}, показали неравномерное распределение на участках от 1 до 3 мм и то же было обнаружено в масштабе 5 μ.

EINE AUTORADIOGRAPHISCHE METHODE ZUR BESTIMMUNG DER EISENVERTEILUNG AUF MAGNETOPHONBÄNDERN

Die Autoradiographie erwies sich als brauchbare Methode zur Messung des magnetischen Überzuges auf Magnetophonbändern. Makroskopische und mikroskopische Inhomogenität wurde vorgefunden. Autoradiographien mit Fe^{55} und Fe^{59} ergaben Unregelmässigkeiten in Abständen von 1 bis 3 mm, ausserdem zeigte sich Inhomogenität im Bereich von 5 μ.

INTRODUCTION

The quality of reproduction from recording tape is affected by the uniformity of the magnetic coating which is deposited upon the polyester and polythene backing. Five samples of tape were examined; 1a, 1b, 1c on polyester backing and 2a and 2b on polythene. The thicknesses of the deposits were 0·45, 0·2, 0·1, 0·45, 0·20 $\times$ 10^{-4} in. respectively. A part of each of these samples was irradiated and autoradiographs taken on Kodaline film.

METHOD

A preliminary test was made on a part of each sample using a 2 hr irradiation in BEPO in a neutron flux of 10^{12} neutrons/cm^2 per sec. This short irradiation time was chosen because cross-linking changes the physical properties of the backing material during irradiation[1]; this limits the irradiation time to about 5 days. Two autoradiographs were taken of each sample and the γ-ray spectrum was determined in order to identify the isotope. During the first 2 days following irradiation by far the largest part of the activity was found to arise from an impurity which had a half-life of about 12 hr. There was a conspicuous γ-energy peak at about 0·51 MeV, which was possibly due to copper. It cannot be assumed that the distribution of the impurity necessarily follows the distribution of the iron. Consequently all subsequent tests were made at least 4 days after irradiation.

The next set of samples were irradiated in BEPO for 5 days in the same neutron flux and the gamma ray spectrum measured 4 days later. The spectrum from the samples with the polythene backing corresponded to that of iron only. The samples coated on polyester backing however showed not only the iron spectrum but also a 0·58 MeV γ-energy of unknown origin. Autoradiographs were set up on Kodaline film 4·5 days after irradiation and exposed for a day. A second set of exposures was started 12 days after irradiation; these exposures were adjusted to allow for the relative thickness of the magnetic coating and confirmed the results obtained earlier.

Exposures were also tried on a finer grain film* of lower sensitivity which was capable of higher resolution. These were not successful however, as exposures of at least a month were necessary at the level of activity obtained. The irradiation time could not be increased however without distorting the polythene and polyester backing.

VOL. 7 1959/

RESULTS AND DISCUSSION

The autoradiographs showed a non-uniform distribution of photographic density which was easily visible with the naked eye. Fig. 1 shows this distribution on sample 2b and $\times 12$ magnification. The autoradiographs of specimens 1a, 1b and 1c viewed at the same magnification showed parallel bands at different photographic densities.

These three films also showed a uniform fogging due to the 0·58 MeV γ-radiation from the polyester backing. This was plainly shown at the edge of these samples where the $\frac{1}{8}$ in. $\times \frac{1}{2}$ in. strip of backing was not covered with magnetic coating and registered alone on the autoradiograph. However the details of the iron distribution in the coating were clearly visible above this background.

The autoradiographs were also examined at $\times 1200$ magnification in order to search for non-uniformities with a separation of a few microns. A Vickers projection microscope was used with a 1·3 NA oil immersion objective and a 1·3 NA oil immersion condensing system. This equipment should be capable of resolution to 0·2 μ. Fig. 2 shows a photograph of specimen 2b taken under these conditions and should be compared with Fig. 3, which is a similar enlargement of the same film fogged with a 15W electric lamp and developed under identical conditions. The dark regions on the photographs correspond to developed silver grains. Fig. 2 shows the distribution of these grains due to a diffuse light when the overall photographic density is approximately the same as that produced by the radioactivity in Fig. 3. Comparing the photographs, the non-uniformity in the autoradiographs in Fig. 3 can be seen to exceed that due to the uniform exposure shown in Fig. 2. A control exposure was also made with an unirradiated sample; no blackening was obtained, showing that the distribution of blackening was not due to pressure marking. The examination of the other specimens showed similar non-uniformity in the distribution of Fe^{55} and Fe^{59}.

* Kodak V6028.

FIG. 1. Macroscopic distribution of iron. Kodaline autoradiograph of sample 2b. (× 12.)

OL.
7
59/60

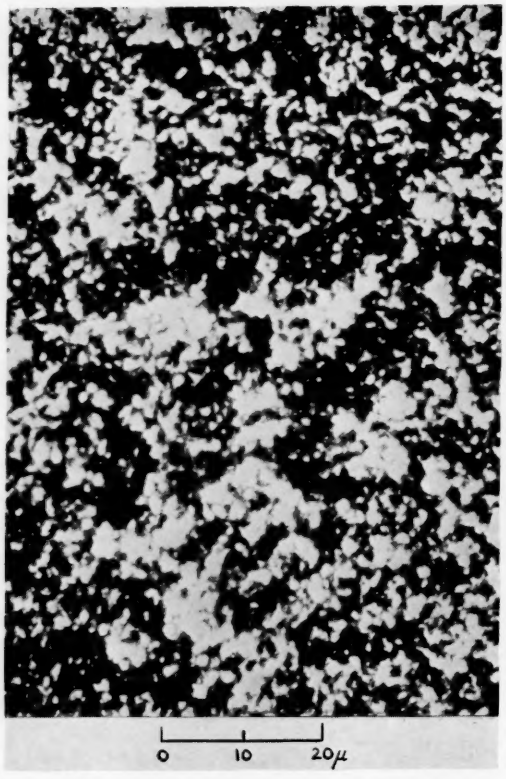

FIG. 2. Microscopic distribution of iron. Kodaline autoradiograph of sample 2b. (× 1200.)

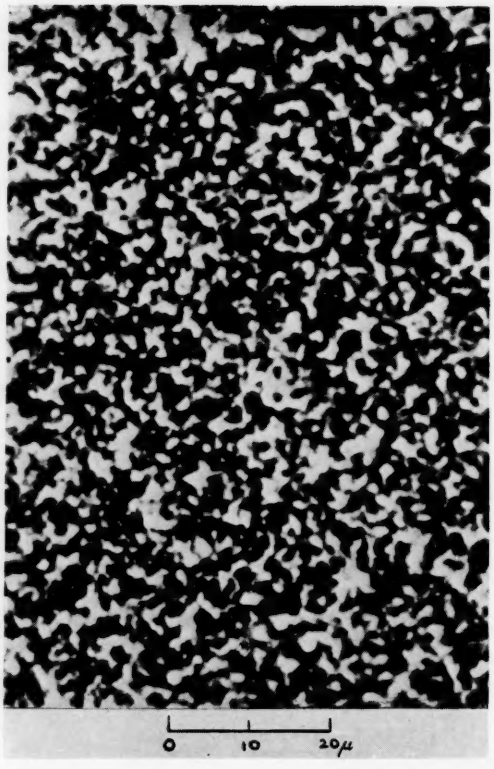

FIG. 3. Control sample of Kodaline developed under same conditions. (× 1200.)

VOL.
7
1959/

CONCLUSIONS

It has been shown that autoradiography is a suitable method of searching for non-uniformity in the distribution of iron in the magnetic coatings used on recording tapes. Autoradiographs taken with Fe^{55} and Fe^{59} can be obtained when the samples are irradiated in BEPO for 5 days at pile factor 10 and allowed to decay for 4 days. An exposure of a day on Kodaline film produces sufficient blackening for examination at magnifications up to $\times 1200$ and will show irregularities in distribution down to 5 μ.

Acknowledgements—We would like to express our gratitude for the co-operation of E.M.I. Sales and Service Ltd., Blyth Road, Hayes, Middlesex, who suggested the work. This firm has also kindly supplied the tape and financed the work. Our thanks are also due to Dr. D. Gibbons of A.E.R.E., Harwell, who carried out the γ-spectrometry on the samples.

REFERENCE

1. Charlesby A. *Proc. Roy. Soc.* A**215,** 187 (1952).

OL.
7
59/60

International Journal of Applied Radiation and Isotopes, 1959, Vol. 7, pp. 126–133. Pergamon Press Ltd. Printed in Northern Ireland

The Oxidation of Irradiated Polyethylene—I Radio-oxidation

R. M. BLACK* and A. CHARLESBY†

(*Received* 9 *October* 1958; *in revised form* 28 *May* 1959)

When polyethylene is subjected to high energy ionizing radiation—either electrons, γ- or X-rays, protons or α-particles—a number of chemical changes are produced which result in profound changes in the physical properties. These changes include the formation of crosslinks, main chain fracture, and unsaturation. If irradiation is carried out in the presence of oxygen, further changes take place due to the interaction between the oxygen and the free radicals formed during the irradiation process.

This radio-oxidation has been studied by infra-red and ultra-violet absorption measurements, by chemical analysis and by the measurement of the dielectric loss angle.

The oxidation process is discussed and some tentative mechanisms are proposed for the type of reaction involved. The effect of the addition of various types of conventional antioxidants to the system prior to irradiation has been investigated.

VOL. 7 1959/6

L'OXYDATION DU POLYÉTHYLÈNE IRRADIÉ—I. LA RADIO-OXYDATION

Lorsque le polyéthylène est soumis au rayonnement ionisant de haute énergie, soit des électrons, des rayons γ ou X, des protons ou des particules α, il se produit un nombre de changements chimiques qui aboutissent en des changements profonds dans les propriétés physiques. Ces changements comprennent la formation de liaisons transversales, la fracture de la chaîne principale et la désaturation. Si l'irradiation s'achève en la présence de l'oxygène, des changements supplémentaires ont lieu à cause de la réaction entre l'oxygène et les radicaux libres produits pendant le procédé de l'irradiation.

Cette radio-oxydation a été étudiée au moyen des mesures de l'absorption infra-rouge et ultra-violette, de l'analyse chimique et de la mesure de l'angle de perte diélectrique.

On discute le procédé d'oxydation et on propose quelques mécanismes vraisemblables pour le genre de réaction impliqué. On a recherché l'effet d'ajouter au système, avant l'irradiation, des espèces différentes d'antioxydants conventionnels.

ОКИСЛЕНИЕ ОБЛУЧЕННОГО ПОЛИЭТИЛЕНА—I. РАДИАЦИОННОЕ ОКИСЛЕНИЕ

Облучение полиэтилена частицами высокой энергии-электронами, γ или рентгеновскими лучами, протонами или α-частицами вызывает ряд химических изменений, приводящих к глубоким изменениям физических свойств. Эти изменения заключаются в сшивании, нарушении основной цепи и появлении непредельности. Если облучение производится в присутствии кислорода, то происходят дальнейшие изменения, вызываемые взаимодействием кислорода и свободных радикалов, образующихся во время облучения.

Такое радиационное окисление было исследовано при помощи измерения инфракрасных и ультрафиолетовых спектров, химического анализа и измерения угла диэлектрических потерь.

Рассматривается процесс окисления и предлагается ориентировочный механизм реакций этого типа. Исследовано влияние введения в систему перед началом облучения различных типов обычных анти-окислителей.

* British Insulated Callender's Cables Ltd, Research Organisation.
† Royal Military College of Science, Shrivenham.

DIE OXYDIERUNG VON BESTRAHLTEM POLYÄTHYLEN—I. RADIOOXYDIERUNG

Wird Polyäthylen einer hoch energetischen ionisierenden Strahlung ausgesetzt—seien es Elektronen, γ-oder Röntgenstrahlen, Protonen oder α-Teilchen—dann wird eine Reihe von chemischen Veränderungen hervorgerufen, welche grundlegende Veränderungen der physikalischen Eigenschaften bewirken. Diese Veränderungen bestehen aus der Bildung von Querverbindungen, Unterbrechungen der Hauptkette und Bildung von ungesättigten Zuständen. Wird die Bestrahlung in Gegenwart von Sauerstoff durchgeführt, dann treten weitere Veränderungen auf, infolge der Wechselwirkung von Sauerstoff mit den während der Bestrahlung gebildeten freien Radikale.

Diese Radiooxydierung wurde mit Hilfe von Infrarot- und Ultraviolettabsorption, durch chemische Analyse und durch Messung des dielektrischen Verlustwinkels untersucht.

Dieser Oxydierungsprozess wird diskutiert und es werden versuchsweise Mechanismen für die einzelnen Reaktionsarten vorgeschlagen. Die Wirkung von Zusätzen verschiedener Arten der üblichen oxydationsverhindernden Mittel vor der Bestrahlung wurde untersucht.

INTRODUCTION

When polyethylene is subjected to high energy radiation in a nuclear reactor, or in a beam of X-rays, γ-rays or electrons, profound changes are induced in its physical properties.[1] These result from changes in the chemical constitution and it has been established that in the absence of oxygen the following are the main modifications produced:

(1) Crosslinking takes place with the formation of carbon–carbon bonds between the molecules of the polymer and with the evolution of hydrogen. This crosslinking gives rise to an infusible three dimensional network structure which is insoluble in the customary hydrocarbon solvents.[1]

(2) A small number of breaks are produced in the main polymer chain and in the side chains, which results in the production of low molecular weight hydrocarbons and an increased sol fraction of the polymer.[2,3,4]

(3) Changes are brought about in the amount of the unsaturation present in the polymer. The unsaturation is of three main types—*trans*-vinylene (—CH=CH—), vinyl (—CH=CH_2) and vinylidene ($\rangle$C=CH_2) and on irradiation the principal change is the formation of *trans*-vinylene groups. The initial low concentration of vinylidene unsaturation is reduced, while there is a small increase in the concentration of vinyl groups.[5,6]

If the irradiation is carried out in the presence of air, the above primary changes are accompanied by an oxidation process, radio-oxidation, resulting in further changes in the physical and electrical properties and the formation of characteristic oxidation products. These further changes are undesirable as they result in a polymer with poor electrical properties and an increased ease of oxidation at elevated temperatures. This is a serious disadvantage in that one of the principal applications of irradiated polyethylene is in the insulation of wires and cables intended for high temperature operation in the region 85°C–150°C where a good service life is essential.

The present paper describes some of the chemical changes which occur when irradiation takes place in the presence of oxygen. A subsequent paper will consider the effect of irradiation of polyethylene on its subsequent oxidative properties (thermal oxidation).

EXPERIMENTAL

Units

The unit of γ- or electron radiation dose used here is the rad (radiation absorbed dose) which corresponds to an energy absorption of 100 ergs/g. For BEPO pile irradiations, unit dose is defined as an integral thermal

neutron flux of 10^{17} neutrons/cm^2 plus the associated fast neutrons and gammas. In polyethylene this corresponds to a γ- or electron dose of $4{\cdot}6 \times 10^7$ rad at room temperature.

Irradiation data

Most of the specimens of polyethylene studied (Alkathene grade 7) were exposed in a fixed position in the BEPO nuclear reactor at Harwell operating at constant power. The radiation dose was proportional to the exposure time.

The thermal neutron flux in the position used was of the order of 10^{12} neutrons/cm^2 per sec and the temperature 70°C; thus unit radiation dose corresponded to an exposure of some 16 hr at this temperature.

Specimens to be irradiated in vacuum were sealed in silica glass tubes; other specimens were irradiated in air enclosed in the customary 3 in. aluminium cans. For higher doses the restriction of circulation of the air thus obtained may have decreased slightly the amount of oxidation taking place in the samples.

A number of specimens were irradiated in a beam of 4 MeV electrons from a travelling wave linear accelerator, and in the γ-flux from a 400 c Co^{60} source. Under these conditions irradiations were in air at room temperature.

Infra-red and ultra-violet absorption

The infra-red absorption spectra of thin films of the polymer were recorded over the range 660 to 5500 cm^{-1} on a Perkin Elmer model 12C infra-red spectrophotometer equipped with a rock salt optical system.

Ultra-violet absorption measurements were made upon a Hilger Uvispek spectrophotometer.

Estimation of hydroperoxides

The hydroperoxides produced during the oxidation were estimated by the method described by SULLEY[7], the polyethylene film being introduced into the refluxing chloroform–acetic acid mixture in the form of a neat bundle which was weighted with a small piece of glass tubing.

Power factor measurements

Measurement of the dielectric loss angle (tan δ) was made upon the irradiated polyethylene in the form of thin sheet (0·1 cm), by means of a Marconi Circuit Magnification meter operating at a frequency of 1000 kc/s. The specimens were formed into capacitors by sticking tin foil electrodes on to the polyethylene with petroleum jelly.

VOL. 7 1959/6

RESULTS AND DISCUSSION

Chemical changes produced on irradiation in air

Fig. 1 shows a typical series of absorption spectra of films of polyethylene irradiated in the presence of air. In addition to increases of the intensity of the absorption bands characteristic of the various types of unsaturation, a number of new bands appears. The band at 3420 cm^{-1} is usually ascribed to the O—H stretching frequency of an alcohol, but it is possible that the production of hydroperoxides in the oxidation process could also give rise to absorption in this region. A new band also appears at 1714 cm^{-1} due to the C=O stretching frequency in the carbonyl group. This is associated generally with the presence of aldehydes and ketones.

The principal changes in the infra-red spectrum of polyethylene on irradiation are summarized in Table 1.

Fig. 2 shows a typical series of ultra-violet absorption curves obtained for the polyethylene films. These show a maximum in the region 220–230 mμ and a submerged maximum at 260–270 mμ. These absorption bands can be ascribed to conjugation effects between carbonyl groups and *trans*-vinylene unsaturation which could arise from the attack of oxygen upon the α-carbon atom adjacent to the double bond. In the absence of air the absorption spectrum would suggest that a small percentage of the vinylene groups are themselves conjugated.

Inhibition of crosslinking and double bond formation

The presence of oxygen is usually held to

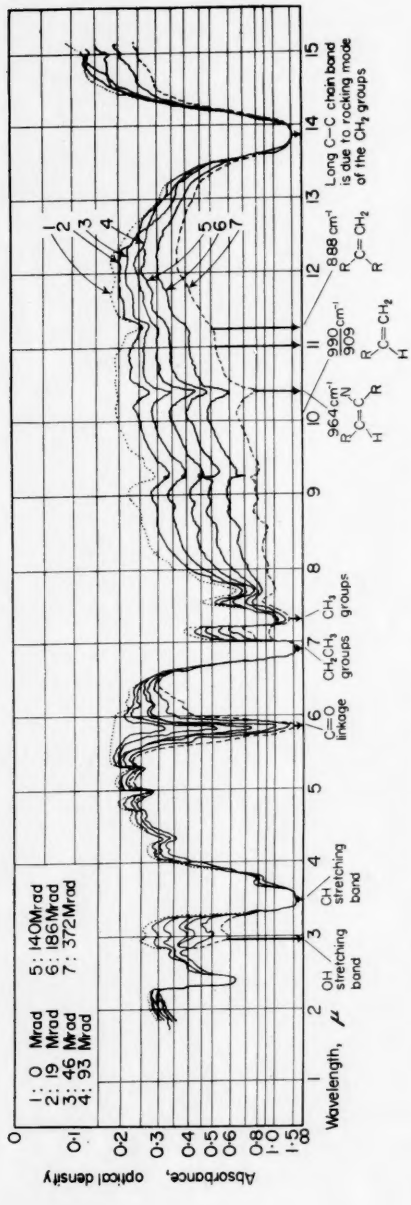

FIG. 1. Infra-red spectrum of electron-irradiated polyethylene (0–372 Mrad).

Table 1. Changes in the infra-red spectrum of polyethylene irradiated in air

Absorption band max. cm^{-1}	Assignment	Oxidation product
3420	—O—H stretching	alcohol
1714	C═O stretching	aldehyde and ketone
1645	C═C stretching	
1434	$—CH_2$ modified by C═C	
1410	—CHO, C═O	aldehyde
1170	C═O	carboxylic acids
1167	C—O—C	esters
1181	C—O	alcohol or ester
964	—CH═CH— (*trans*)	
909	$—CH═CH_2$	
888	$>C═CH_2$	

interfere with the reactions induced by ionizing radiation and, particularly where thin films are involved, the efficiency of processing is found to be very low. Calculation of the degree of crosslinking of polyethylene by measurement of the elastic modulus at 150°C has shown that with samples irradiated in vacuum the crosslinking is proportional to the radiation dose and results in 0·004 per cent of the carbon atoms in the main polymer chain being crosslinked for a radiation dose of 10^6 rad. In the presence of air and with thin film specimens the crosslinking corresponds to 0·001 per cent carbons crosslinked for a dose of 10^6 rad. This value applies to BEPO pile radiation, but varies according to irradiation conditions.

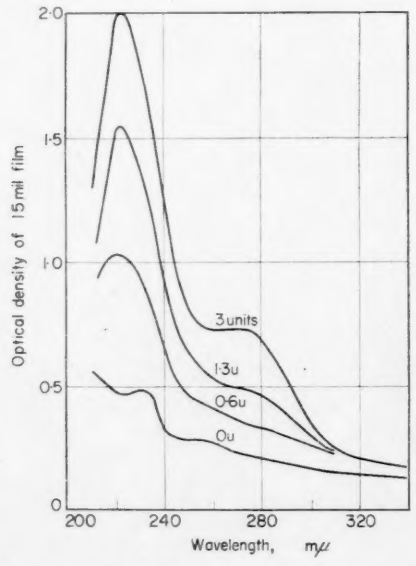

FIG. 2. The ultra-violet absorption of irradiated polyethylene irradiated in air (radiation close in pile units).

ALEXANDER and TOMS[8] in their experiments on very thin films (50–175 μ) have concluded that the number of crosslinks formed is not reduced in the presence of air, but that the ratio of main chain fractures to crosslinks is increased. This would not appear to be borne out by elastic modulus measurements which are a reasonably reliable method of estimating the number of crosslinks produced. PIERRE and DEWHURST[10] have also concluded that oxygen acts by inhibiting the crosslinking reactions.

Estimation of the amount of unsaturation produced in polyethylene films, irradiated in vacuum and in air, by infra-red absorption spectrophotometry has shown that there is a significant difference in the amounts of *trans*-vinylene double bonds formed when air is present. Figures obtained for vinyl and vinylidene unsaturation are not of sufficient accuracy to permit the drawing of any conclusions, but there would appear to be very little change. Increase in the number of chain breaks might be confirmed by the increase in the concentration of vinyl double bonds as these could arise by a disproportionation process. Unsaturation values obtained for thin film specimens irradiated in vacuum and in air are shown in Table 2.

The rate of formation of oxidation products

Information upon the rate of formation of the oxidation products: hydroperoxides, aldehydes, ketones, etc., is of necessity rather difficult to obtain, but a certain indication of the build up of these products can be obtained from the infra-red and ultra-violet spectra.

Fig. 3 shows a plot of the number of crosslinks per 100 carbon atoms in the main chain and double bonds (*trans*-vinylene) formed against the radiation dose. A

VOL. 7 1959/6

Table 2. Unsaturation changes in polyethylene on irradiation in air

Radiation dose (Mrad)	Unsaturation found %w/w		
	>C=CH$_2$	—CH=CH$_2$	—CH=CH—
0	0·092	0·005	0·022
Vacuum			
70	0·037	0·012	0·186
93	0·031	0·017	0·367
465	0·037	0·022	0·847
Air			
19	0·004	0·037	0·046
46	0·008	0·036	0·093
93	0·015	0·026	0·149
140	0·017	0·029	0·179
190	0·016	0·032	0·250
372	0·017	0·035	0·276

1% w/w is equivalent to 0·58 double bonds per 100 C atoms.

sigmoid curve for the formation of hydroperoxide is also shown, as is the total number of sites attacked by oxygen (calculated from the difference between the unsaturation and crosslinking figures obtained from samples irradiated in vacuum and in air).

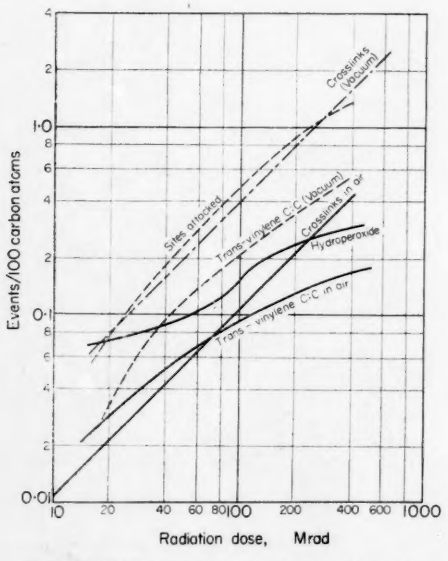

FIG. 3. Crosslinking and unsaturation in polyethylene film irradiated in air and vacuum.

While there is no infra-red evidence for the formation of *cis*-vinylene unsaturation, it has been suggested[5,6] that this is present to the same extent as the *trans*-form. If this is so, the hydroperoxide figures, which may be on the low side because of the presence of aldehydes and ketones, would indicate the formation of about one hydroperoxide group per double bond. The situation is, however, complicated by the surface effect.

The surface effect

The radio-oxidation of polyethylene is very largely a surface effect, as the rate of oxidation is dependent upon the rate of diffusion of air into the polymer. It would therefore be expected that the thinner the film, the greater would be the observed effect. This is, in fact, observed to be the case. The following values were obtained for the optical density of the carbonyl band in the infra-red at a frequency of 1714 cm^{-1} on a series of films of various thicknesses (Table 3).

CHARLESBY[1] has shown that the oxidation effect which occurred during irradiation was related to the surface area exposed. BALLANTINE and his co-workers[11] carried out infra-red measurements on the same carbonyl band and found that the optical density A could be expressed as the sum of a surface A_s and volume effect A_v:

$$A = 2A_s + dA_v$$

Table 3. Increase in carbonyl absorption with electron irradiation in air

Radiation dose (Mrad)	Optical density of 1714 cm^{-1} for film thickness (cm)		
	0·0058	0·0116	0·0178
4·6	0·031	0·055	0·077
18·6	0·116	0·159	0·199
93·0	0·485 (0·55)	0·616 (0·60)	0·671 (0·67)
186·0	1·200 (1·20)	1·420 (1·40)	1·68 (1·70)

(Values in brackets are calculated with values of A_s, A_v given below.)

where d is the specimen thickness. The results obtained were, however, insufficient for quantitative analysis.

Our own results for 4 MeV electron irradiation can be more readily separated into surface and volume effects. The values of A_s obtained by extrapolation to zero thickness are approximately proportional to the radiation dose r expressed in megarads:

$$A_s = 2{\cdot}69 \times 10^{-3}\, r \qquad (2)$$

This confirms that the surface effect is not limited by the diffusion rate of the oxygen.

On the other hand, the volume coefficient A_v, which would depend upon the diffusion rate and hence upon the exposure time, is not proportional to the radiation dose. For the higher doses studied the following relationship holds approximately:

$$A_v = 1{\cdot}059 \times 10^{-3}\, r^2 \qquad (3)$$

when d is expressed in cm. For low radiation doses this relationship fails to represent the effect adequately and the addition of a squared term would probably be necessary to represent the data more fully:

$$A_v = \alpha r + \beta r^2 \qquad (4)$$

The results available are, however, insufficient to enable the parameters α and β to be determined exactly.

The optical densities in Table 3 differ very considerably from those given by BALLANTINE for films of similar thickness which had been subjected to electron irradiation at approximately the same temperature. Moreover, these investigators found considerable differences between γ- and electron radiation at the same temperature, and, in addition, a marked temperature effect. The differences found lie well outside experimental error, and it is suggested that they are largely due to varying times of exposure to oxygen under differing irradiation conditions. Such an effect has been reported by CHAPIRO[12] for tensile measurements on polyethylene at various dose rates in the presence of oxygen. In these circumstances no significance can be attached to the coefficients A_s and A_v unless the irradiation conditions are specified.

The effect of antioxidants

In view of the observation that the subsequent thermal oxidation of irradiated polyethylene is influenced by the presence of radio-oxidation products, attempts were made to study the effect of antioxidant addition to the polymer before irradiation, with a view to reducing the extent of the radio-oxidation under given processing conditions. In view of the apparent analogy between photo- and radio-oxidation, and the possibility of the inhibition of radiation

Table 4. The effect of antioxidants and other additives on the power factor of polyethylene irradiated in air (pile)

Addition	Power factor at 1 Mcycle 20°C		
	Initially	After 0·50 units	After 3·00 units
Control sample			
Alkathene 7	0·0004	0·0016	0·0046
Protective agents			
Allyl thiourea*	0·0022	0·0072	0·0074
Allyl thiourea†	0·0022	0·0047	0·0050
Pyrene*	0·0008	0·0010	0·0045
8-Hydroxy quinoline†	0·0005	0·0022	0·0085
8-Hydroxy quinoline*	0·0006	0·0013	0·0035
Phenol*	0·0005	0·0011	0·0066
Amine antioxidants			
Di-β-naphthyl-*p*-phenylene diamine‡	0·0007	0·0006	0·0044
Diphenylamine	0·0004	0·0005	0·0053
Phenyl-β-naphthylamine	0·0002	0·0007	0·0036
Diphenyl guanidine	0·0005	0·0011	0·0022
Diphenyl phenylene diamine	0·0002	0·0004	0·0083
Di*cyclo*hexylamine	0·0006	0·0010	0·0055
2 : 2 : 4 Trimethyl decahydroquinoline	0·0004	0·0032	0·0059
Phenol antioxidants			
Octylated xylenols	0·0004	0·0005	0·0046
Tert.-butyl hydroquinone	0·0004	0·0005	0·0035
2-*Tert.*-butyl-4-methoxy phenol	0·0011	0·0011	0·0098
Benzyl cresylic acid	0·0006	0·0007	0·0056
2 : 6-Di-*tert.*-butyl-*p*-cresol	0·0007	0·0214	0·0123

* 10% w/w † 5% w/w ‡ 0·5% w/w

All other antioxidants added 0·2% w/w

VOL. 7 1959/

effect such as crosslinking by radical acceptors, such additions did not seem to hold much promise.[13]

A range of antioxidants and protective agents were, however, incorporated in batches of polyethylene sheet samples, and their effectiveness assessed by power factor measurements before and after irradiation. The power factor or dielectric loss angle has proved to be a very sensitive indication of the presence of polar oxidation products. Two doses were given—of $2{\cdot}5 \times 10^7$ and $15{\cdot}0 \times 10^7$ rad—and the results are shown in Table 4. It was concluded that with both phenolic and amine type antioxidants only marginal protection could be obtained for the lower dose samples. Since these substances may also act as radiation protective agents, and thereby decrease the degree of crosslinking produced by the radiation for a given dose, it is not clear that any worth-while reduction in the radio-oxidation can be achieved while maintaining the same degree of crosslinking.

The mechanism of oxidation

It is difficult from the data so far available to postulate a mechanism by which radio-oxidation takes place. The oxidation process results in the formation of carbonyl compounds and hydroperoxides at the expense of carbon–carbon crosslinks and *trans*-vinylene unsaturation. For the surface effect, in which the rate of oxygen diffusion is not significant, the build up of carbonyl compounds is proportional to the radiation dose.

It might appear that the initial step involves either the attack of molecular oxygen upon a radical site produced as a result of the irradiation, or the attack of O_2^- radicals as suggested by ALEXANDER and TOMS due to the high affinity of oxygen for electrons.

Certain theories of crosslinking assume an ionic mechanism, and the effect of oxygen may then arise from its ability to capture electrons ejected during ionization, thus interfering with subsequent reactions.

Acknowledgements—The authors wish to thank their colleagues at Harwell and Wood Lane for their assistance with the experimental work, and are also indebted to Dr. H. M. FINNISTON, recently Chief Metallurgist, A.E.R.E., and to Dr. L. G. BRAZIER, Director of Research and Education, British Insulated Callender's Cables Ltd., for their interest in the investigation and for permission to publish this paper.

REFERENCES

1. CHARLESBY A. *Proc. Roy. Soc.* A**215,** 187 (1952).
2. CHARLESBY A. *Proc. Roy. Soc.* A**224,** 120 (1954).
3. BASKETT A. C. and MILLER C. W. *Nature, Lond.* **174,** 364 (1954).
4. BASKETT A. C. Simposia Internazionale di Chim. Macromoleculare, Milan (1955).
5. DOLE M., KEELING C. D. and ROSE D. G. *J. Amer. Chem. Soc.* **76,** 4304 (1954).
6. BLACK R. M. *J. Appl. Chem.* **8,** 159 (1958).
7. SULLEY B. D. *Analyst* **79,** 86 (1954).
8. ALEXANDER P. and TOMS D. *J. Polym. Sci.* **22,** 343 (1956).
9. BLACK R. M. *Nature, Lond.* **178,** 305 (1956).
10. ST. PIERRE L. E. and DEWHURST H. A. *J. Chem. Phys.* **29,** 241 (1958).
11. BALLANTINE D. S. *et al., J. Polym. Sci.* **13,** 410 (1954).
12. CHAPIRO A. *J. Chim. Phys.* **52,** 246 (1955).
13. PROSS A. W. and BLACK R. M. *J. Soc. Chem. Ind.* **69,** 113 (1950).

International Journal of Applied Radiation and Isotopes, 1959, Vol. 7, pp. 134–140. Pergamon Press Ltd. Printed in Northern Ireland

The Oxidation of Irradiated Polyethylene—II Thermal Oxidation

R. M. BLACK* and A. CHARLESBY†

The oxidative changes which take place in irradiated polyethylene on exposure to air or oxygen at elevated temperatures have been followed by infra-red and ultra-violet spectrophotometry, by weight loss and oxygen absorption measurements and by estimation of the hydroperoxides produced.

While the data presented are insufficient to enable a mechanism for the oxidation process to be proposed it is found that the radiation induced changes in the constitution of the polymer exert a significant effect on the subsequent rate of thermal oxidation.

L'OXYDATION DU POLYÉTHYLÈNE IRRADIÉ—II.
L'OXYDATION THERMIQUE

Les changements oxydatifs qui prennent lieu dans le polyéthylène irradié lors de son exposition à l'air ou à l'oxygène aux températures élevées ont été poursuivis aux moyens de la spectrophotométrie infra-rouge et ultra-violette, des mesures de perte de poids et d'absorption d'oxygène et du dosage des hydroperoxydes engendrés.

Bien que les données offertes soient insuffisantes à permettre la proposition d'un mécanisme pour le procédé d'oxydation, on trouve que les changements dans la constitution de la polymère induits par le rayonnement exercent un effet significatif sur le taux subséquent de l'oxydation thermique.

ОКИСЛЕНИЕ ОБЛУЧЕННОГО ПОЛИЭТИЛЕНА—II.
ТЕРМИЧЕСКОЕ ОКИСЛЕНИЕ

Изменения, вызываемые в облученном полиэтилене, при окислении воздухом или кислородом при высоких температурах, определялись с помощью инфракрасной и ультрафиолетовой спектрофотометрии по потерям в весе и поглощению кислорода, а также по количеству полученных гидроперекисей.

Хотя полученные данные недостаточны для установления механизма процесса окисления, однако выяснено, что изменения в строении полимера, вызванные облучением, оказывают значительное влияние на последующую скорость окисления.

DIE OXYDIERUNG VON BESTRAHLTEM POLYÄTHYLEN—II.
THERMISCHE OXYDIERUNG

Oxydative Veränderungen an bestrahltem Polyäthylen unter Einwirkung von Luft oder Sauerstoff bei erhöhten Temperaturen wurden untersucht mit Hilfe von Infrarot-Ultraviolett-Spektrophotometrie, Gewichtsverlust und Sauerstoff-Absorptionsmessungen und durch die Bestimmung des erzeugten Wasserstoffsuperoxydes.

Die vorliegenden Ergebnisse reichen zwar nicht aus, um einen Mechanismus für den Oxydierungsprozess angeben zu können, es wurde jedoch gefunden, dass die strahlungsbedingten Veränderungen der Konstitution des Polymers, eine deutliche Wirkung auf das Ausmass der darauf folgenden thermischen Oxydierung ausüben.

INTRODUCTION

In the previous paper in this series[1] an account was given of the oxidation which takes place when the irradiation of polyethylene is carried out in the presence of air or oxygen. The oxygen interacts with the free radicals and double bonds formed

* British Insulated Callender's Cables Ltd., Research Organisation.
† Royal Military College of Science, Shrivenham.

VOL. 7 1959/

during the irradiation process to form oxidation products such as alcohols, acids aldehydes or ketones, hydroperoxides, ethers and vinylene compounds which have been identified by infra-red spectroscopy.

The present paper is concerned with the oxidation changes which take place when irradiated polyethylene is subsequently heated in the presence of air.

Apart from its scientific interest, this oxidation is of considerable technical importance, since irradiated polyethylene is being increasingly used because of its improved mechanical properties at higher temperatures, which cannot be sustained by ordinary polyethylene. Oxidation at these higher temperatures is known to modify both mechanical and electrical properties, and to cause further chemical changes.

EXPERIMENTAL

The irradiated polyethylene used in the experiments was produced by exposing sheets and films of Alkathene grade 7 supplied by I.C.I. in a fixed position in the BEPO atomic pile at Harwell. The radiation dose is proportional to the exposure time, unit radiation dose being defined as an integral flux of 10^{17} thermal neutrons/cm^2 plus the associated fast neutrons and gammas. Polyethylene film was irradiated *in vacuo* or under an atmosphere of nitrogen as described in Part I,[1] so that no oxidation occurred during irradiation.

The various changes produced during irradiation and on subsequent heating in air at 110°C in a thermostatically controlled air oven were followed and examined by a number of physical and chemical methods:

(a) *Infra-red and ultra-violet absorption*

The infra-red absorption spectrum of the polymer in the form of thin film was recorded over a range 2·5 to 15 μ with a Perkin Elmer model 12C infra-red spectrophotometer equipped with a rock salt optical system.

Ultra-violet absorption measurements using a Hilger Uvispek spectrophotometer were also made on this film. In these measurements polyethylene specimens of various thicknesses were examined.

(b) *Hydroperoxide formation*

The hydroperoxides were estimated by the method substantially as described by SULLEY.[2]

(c) *Power factor measurements*

Measurements of the dielectric loss angle (tan δ) were made upon the treated polyethylene in the form of thin sheet (0·025 to 0·050 in.) by means of a Marconi Circuit Magnification meter operating at a frequency of 10^6 cycles/sec. The technique used was similar to that described in Part I.

(d) *Weight changes*

Weighed rectangular specimens of the irradiated polyethylene sheet, approximately 0·076 cm in thickness were supported on a frame in an air oven operating at a temperature of 110°C. Changes in weight were followed by periodically removing, cooling in a desiccator, and weighing.

(e) *Oxygen absorption measurements*

The rate of oxygen absorption of the irradiated polyethylene was measured in the following manner: about 0·1 to 0·5g of the polymer was cut into slivers and placed in a thin glass bulb connected by way of a B14 cone and socket joint and a capillary tube to a thermostatted gas burette containing oxygen over mercury. A small test tube containing barium oxide was included in the bulb to absorb any carbon dioxide and water that might be produced.

The glass bulb was immersed in an oil bath, thermostatically controlled to a temperature of 120°C and readings were taken of the volume of gas in the burette and of the barometric pressure at regular intervals. The reservoir of the gas burette was adjusted from time to time so that absorption took place at approximately constant pressure. The volume of the absorbed gas was corrected to n.t.p.

RESULTS AND DISCUSSION

TABLE 1. Changes in optical density during thermal oxidation of irradiated polyethylene (30×10^6 rad of pile radiation)

Time of heating at 100°C (hr) after radiation	Optical density of 1·5 mil film		
	3402 cm^{-1} (–OH)	1720 cm^{-1} (C=O)	966 cm^{-1} (C=C)
0	0·085	0·116	0·024
48	0·079	0·573	0·008
144	0·003	0·703	0·004

Infra-red absorption

The formation of vinylene unsaturation is known to occur on irradiation in vacuum, and to be independent of film thickness. The changes in optical density on subsequent heating show that the mechanisms of radiation and thermal oxidation are different in several respects. Some approximate figures for the changes in optical density of the absorption bands for alcohols, ketonic carbonyl and *trans*-vinylene unsaturation are given in Table 1.

It is noticeable that the *trans*-vinylene unsaturation and alcohol (bonded hydroxyl) groups are reduced in concentration while the ketonic carbonyl is increased. It may be concluded from this that at the temperature of the experiment the attack of oxygen on the polymer is across the double bonds rather than at the α-carbon atom.

The general background absorption between 800 and 1700 cm^{-1} is intensified and the absorption bands occurring in the region (1110 cm^{-1}, 1172 cm^{-1}) can be ascribed to ethers and carboxylic compounds. There appears also to be some displacement towards the low frequency end of the spectrum, and a band which appears at 1180 cm^{-1} after radio-oxidation is transposed to the region of 1170 cm^{-1} by thermal oxidation. A similar increase in intensity was noted by THOMPSON and TORKINGTON[3] in their examination of the thermal oxidation of natural rubber. This effect is thought to be partially due to optical scattering by the solid film since RICHARDS[4] finds that the transmission of an oxidized film of polyethylene increases considerably on melting.

Changes in ultra-violet absorption

On heating a thin film of irradiated polyethylene in air there is a general increase in the absorption in the ultra-violet region of the spectrum. This can be seen in Fig. 1, where after 120 hr at 91°C the optical density increases in both the 220–230 mμ and 250–270 mμ regions. Increase in the latter region must be due to the increase in the ketonic carbonyl, also shown in the infra-red region.

At lower temperatures the oxidation increases as a power of the heating time, as would be expected from a chain reaction for auto-oxidation. At higher temperatures however the rate of increase of oxidation, as measured by the optical density is reduced. This reduction may be due to the diffusion rate of oxygen, which now becomes the limiting factor, or to a change in the nature of the reaction. Instead of oxygen attacking the α-carbon atom, as at temperatures below 100°C, it may react with the double bonds formed by radiation.

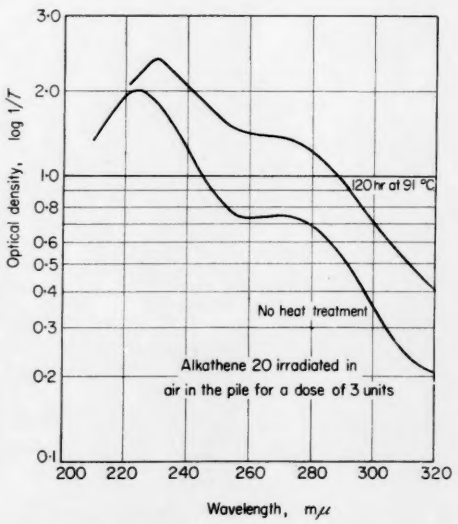

FIG. 1. Changes in the u.v. absorption spectrum on heating in air.

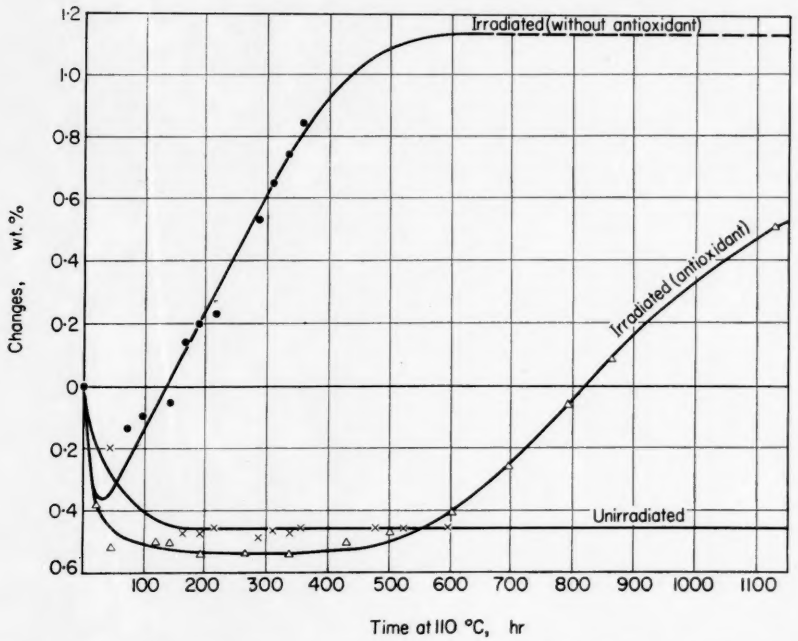

FIG. 2. Weight changes on thermal oxidation of unirradiated and irradiated (3 units) polyethylene.

Weight changes and absorption of oxygen

The progress of oxidation of irradiated polyethylene has also been followed by the change in weight of specimen which is of a sufficient magnitude to be observed with the aid of an ordinary analytical balance. Curves typical of those obtained are shown in Fig. 2. The complex shape of these curves is thought to be due to the conditions of the experiment under which increase in weight due to oxidation and loss of weight due to volatilization of the oxidation products can take place simultaneously.

The following are the successive stages during the weight changes:

(a) initial loss of volatiles from the irradiation process,

(b) induction period (depending upon the presence of antioxidants),

(c) a period of steady increase (proportional to the time),

(d) saturation of the polymer.

All the specimens examined tended to lose up to 0·5 per cent of their initial weight over the first 2 days of the heat treatment (stage (a)) and this can be ascribed to the slow volatilization of the lower molecular compounds and of any radio-oxidation products formed during the irradiation process. After this initial period the unirradiated polymer shows little further change for at least 1000 hr at 92°C. On the other hand, after the initial weight loss irradiated polyethylene (3 units of pile radiation) passes straight over to stage (c) without any induction period whatever. The weight then increases until saturation is reached after approximately 550 hr, corresponding to a total weight increase of 1·1 per cent.

In the presence of an antioxidant (0·3 per cent *sym*-di-β-naphthyl-*p*-phenylene diamine) an induction period (b) of some 400 hr elapses before stage (c) is reached; once this induction period has been passed the rate of weight increase for the polyethylene containing antioxidant is similar to that for pure irradiated polyethylene, differences in the rate being partly due to differences in surface area.

Measurements of the rates of absorption of oxygen at constant pressure have shown

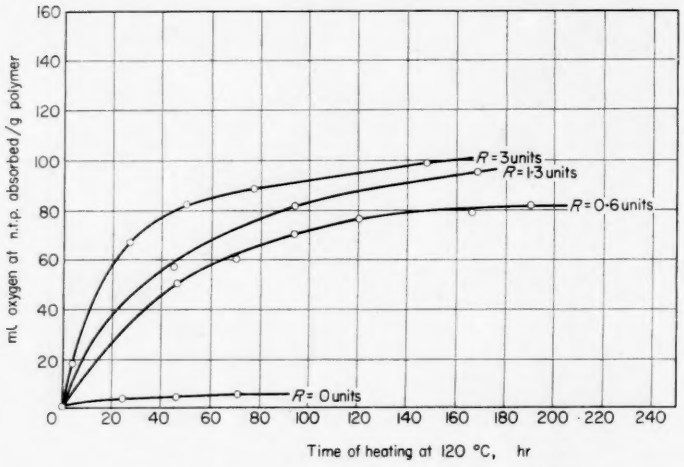

FIG. 3. Oxygen absorption during thermal oxidation.

that the initial rate of absorption appears to be directly proportional to the amount of unsaturation present in the specimen providing that thin film specimens are used in the experiment so that oxygen diffusion is not a limiting factor. For such specimens it has been found that the rate of absorption is proportional to the mass of the specimen rather than to its surface area.[5] Discrepancies observed with lightly irradiated specimens arise from their tendency to fuse together due to the large sol fractions present.

Fig. 3 shows some typical curves for oxygen absorption. The unirradiated polymer shows a very low oxygen absorption in comparison with the irradiated specimens. Table 2 compares the rate of oxygen absorption at 100°C with the initial unsaturation present in the polymer prior to heating. It is seen that the rate of oxygen absorption is proportional to the unsaturation.

No direct relationship between the observed weight increase and the oxygen absorption has been obtained owing to the different conditions under which the experiments were carried out. The differences in film thickness alone would tend to invalidate any quantitative comparison.

Changes in power factor

In the absence of an antioxidant the power factor at 10^6 cycles/sec of irradiated polyethylene increases rapidly and attains a maximum value after about 200 hr heating at 110°C. The rate of increase of power factor can be reduced considerably by the addition of an antioxidant but if this is incorporated prior to irradiation its chemical constitution should be chosen so that the antioxidant is not decomposed by radiolysis to give innocuous products which are incapable of preventing oxidation. A selection of the curves obtained in the presence of various antioxidants is shown in Fig. 4.

TABLE 2. Unsaturation and initial rate of oxygen absorption of irradiated polyethylene at 100°C (thin specimens–1·5 mils)

Radiation dose 10^6 rad	Initial rate O_2 absorbed (ml/hr/g)	Unsaturation found (% w/w)	Absorption rate (C = C)
30	1·75	0·34	5·15
65	2·60	0·51	5·10
150	3·65	0·67	5·43

1% w/w corresponds to 0·58 double bonds per 100 C atoms.

Formation of hydroperoxides

Estimation of the hydroperoxides showed that these increase to a maximum during the first 100 hr of heating at 110°C in air. After this time the rate of thermal decomposition of the hydroperoxides is greater than their rate of formation and after about

VOL. 7 1959/6

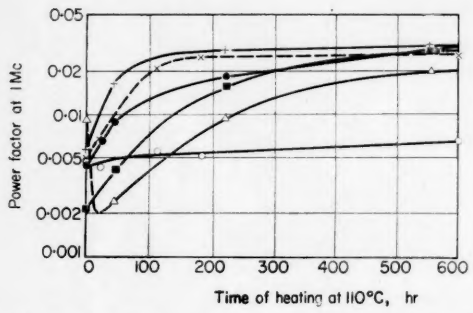

FIG. 4. Changes in dielectric loss on thermal oxidation. Radiation dose 3 units.

× Control
+ Di*cyclo*hexylamine 0·2%
○ *Sym*-di-β-naphthyl-*p*-phenylene diamine 0·3%
● Octylated xylenols 0·2%
△ Di-β-naphthyl-*p*-phenylene diamine 0·2%
■ Diphenyl guanidine 0·2%

500 hr, no hydroperoxides can be detected in the specimens (Table 3). From the oxygen absorption curves for the same polymer it would seem that the slowing up of the rate of formation of the peroxide can be ascribed to the exhaustion of the supply of suitable sites for oxygen attack. Such suitable sites are the α-carbon atoms adjacent to the irradiation-produced double bonds, and possibly the tertiary bonded hydrogen atoms where branching or cross-linking occurs in the polymer chain.

The mechanism of the thermal oxidation

The early work of FRANCIS[6,7,8] on the oxidation of long chain hydrocarbons such as paraffin wax, showed that at temperatures in the neighbourhood of 100°C water, formic acid, ketones, hydroxyl compounds and long chain fatty acids are produced. It might be expected that in the case of polyethylene a somewhat similar series of reactions takes place and absorption bands typical of products of this nature can be observed in the infra-red absorption spectrum of the oxidized product. In addition there is a marked increase in the dielectric loss angle and a decrease in the melt viscosity (corresponding to a reduced average molecular weight) of the unirradiated polymer.

TABLE 3. The effect of heating at 110°C on the hydroperoxide content
(Polyethylene irradiated in vacuum for a dose of 3 pile units)

Time of heating (hr)	Hydroperoxide content found (% O–O w/w)		
0	0·1	0·015	0·01
50	0·055		
100	0·155	0·205	
200	0·04		
400	0·015		

1% O–O w/w is equivalent to 0·45 hydroperoxide groups per 100 carbon atoms.

Due to the presence of side chains and the associated tertiary carbon atoms, polyethylene oxidizes more readily than would a purely straight chain hydrocarbon and on irradiation the case of oxidation is further increased by the larger number of tertiary carbon atoms resulting from crosslinking and by the presence of vinylene unsaturation. A further complicating factor is the possible presence of the products of radio-oxidation (hydroperoxides) unless precautions are taken during the radiation processing to exclude oxygen. The thermal decomposition of the hydroperoxides will initiate oxidation reactions.

From the evidence available it is not possible to put forward a mechanism by which the oxidation proceeds. The decrease in the amount of vinylene unsaturation would suggest an attack by the oxygen across the double bonds, whereas the intense coloration, which is shown by an increase in the ultra-violet absorption would indicate that conjugated systems (oxygen containing chromophores) are formed. In thicker specimens propagation of the oxidation reaction by a chain mechanism is restricted by the solid state of the polymer and the dependence of the reaction upon the rate of oxygen diffusion.

Acknowledgements—The authors' thanks are due to their colleagues at Harwell and Wood Lane for their assistance with the experimental work. They are also indebted to DR. H. M. FINNISTON, recently Chief Metallurgist, A.E.R.E. and to DR. L. G. BRAZIER, Director of Research and Education, British Insulated Callender Cables Limited, for their interest in the investigation and for permission to publish this paper.

REFERENCES

1. Black R. M. and Charlesby A. *Int. J. Appl. Rad. Isotopes* **7,** 126 (1959).
2. Sulley B. D. *Analyst* **79,** 86 (1954).
3. Thompson H. W. and Torkington P. *Trans. Faraday Soc.* **41,** 246 (1945).
4. Cross L. H., Richards R. B. and Willis H. A. *Disc. Faraday Soc.* **9,** 235 (1950).
5. Biggs B. S. and Hawkins W. L. *Mod. Plast.* **31,** 121 (1953).
6. Francis F. *J. Chem. Soc.* **121,** 496 (1922).
7. Francis F. *et al. J. Chem. Soc.* **125,** 381 (1924).
8. Francis F. and Gauntlett H. F. *J. Chem. Soc.*, 2377 (1926).

VOL.
7
1959/

International Journal of Applied Radiation and Isotopes, 1959, Vol. 7, pp. 141–144. Pergamon Press Ltd. Printed in Northern Ireland

The Preparation and Some Properties of Radioactive Quinol–Krypton Clathrate Compounds

D. J. CHLECK and C. A. ZIEGLER
Tracerlab, Inc., Waltham 54, Mass.

(*Received* 20 *March* 1959)

A new technique has been developed for the preparation of quinol–krypton-85 clathrate compounds. Samples of different specific activities have been prepared and studied. A maximum specific activity of 3·0 c of Kr^{85}/g of quinol was obtained. The radioactive compound displayed exceptional stability, gave little or no evidence of internal radiation damage and closely paralleled the reported behavior of its non-radioactive homologue.

LA PRÉPARATION ET QUELQUES PROPRIÉTÉS DES COMPOSÉS CLATHRATES RADIOACTIFS QUINOL–KRYPTON

On a mis en point une nouvelle technique pour la préparation des composés clathrates quinol–krypton-85. On a préparé des échantillons ayant une variété d'activités spécifiques. On a obtenu une activité spécifique maximum de 3,0 c de Kr^{85} par gramme de quinol. Le composé radioactif montra une stabilité exceptionnelle, donna peu ou point d'indication de détérioration interne dûe à la radiation et approcha fortement au comportement rapporté au préalable de son homologue non-radioactif.

ПОЛУЧЕНИЕ И НЕКОТОРЫЕ СВОЙСТВА РАДИОАКТИВНЫХ ХИНОЛ-КРИПТОНОВЫХ КЛАТРАТНЫХ СОЕДИНЕНИЙ

Была разработана новая методика получения клатратных соединений хинол-криптон^{85}. Были получены и изучены образцы с различной удельной активностью. Максимальная удельная активность была 3.0 кюри Kr^{85} на грамм хинола. Полученное радиоактивное соединение обладало исключительной устойчивостью, было совершенно или почти совершенно нечувствительно к облучению и его поведение было очень близко к поведению его нерадиоактивного гомолога.

DARSTELLUNG UND EIGENSCHAFTEN VON RADIOAKTIVEN QUINOL-KRYPTON-CLATHRAT-VERBINDUNGEN

Eine neue Technik zur Darstellung von Quinol-Krypton-Clathrat-Verbindungen wurde entwickelt. Dabei wurden Proben verschiedener spezifischer Aktivität hergestellt und untersucht. Eine maximale spezifische Aktivität von 3,0 Curie Kr^{85} pro Gramm Quinol wurde erhalten. Die radioaktive Verbindung erwies sich als ausserordentlich stabil, zeigte keine, oder nur geringe Anzeichen von interner Zerstörung durch die Strahlung und verhält sich weitgehend gleichartig wie seine, bereits früher bekannten nicht radioaktiven Homologen.

INTRODUCTION

The formation of clathrate compounds from solution with hydroquinone and inert gases has been described.[1] These compounds are characterized by the general formula: 3-quinol·X. The general requirements under which clathrate compounds can form are

limited and specific. The most important are as follows:[2]

(1) An open crystal structure in the enclosing component. This requires directed linkages holding the molecule and crystal together with a sufficient extension of these groups to provide a rigid structure and a cavity of sufficient size.

(2) Small access holes to the enclosed cavity. This may result from the disposition of groups during crystal formation.

(3) Ready availability of the trapped component when the cavity is closed.

The first two requirements outline properties that are characteristic of quinol which ordinarily exist in the α-crystal form. When grown in the presence of sufficient concentration of inert gas a β-form, different from the α, is produced whose molecules are of suitable size to stabilize the cage structure.

The last requirement is of importance in the actual yield of the cage complex, and is controlled by two factors, i.e. pressure of inert gas and crystal growth period.

While the technique outlined by POWELL is satisfactory for production of non-radioactive clathrates in high percentage yields, the practical difficulties involved in the preparation of radioactive homologues indicate the desirability of preparation by some other procedure.

The problems to be overcome are filtration of radioactive material, the handling of radioactive aqueous solutions and cross contamination of the expensive radioactive inert gas with water vapor.

A procedure has been developed which minimizes or eliminates these difficulties. The technique employed is that of growth from the melt.

EXPERIMENTAL

A. Clathrate preparation

A sample of normal quinol is incorporated in a pressure bomb, atmospheric gases are eliminated and the bomb pressurized with radioactive Kr^{85}. The pressure bomb is heated to 185°C to melt the quinol. The temperature of the bomb is held at this temperature for about 2 hr so that a melt equilibrium can be established. The system is cooled slowly to room temperature over a long time period. The bomb is then opened, the sample removed and measured. The entire purpose of the pressure is to provide a sufficient quantity of dissolved gas in the melt so that the atoms of gas will be available at the point of crystal formation and be trapped in the clathrate. The pressure is not required to prevent dissociation, since once the rare gas atom is enclosed it is retained by the strength of its cage. The rate of cooling is important in that the slower rates will allow equilibrium to be re-established after local depletion of the rare gas atom at the crystal formation site. Thus high pressures and slow cooling rates give greater yields of clathrated crystals.

B. Measuring apparatus

Two procedures were employed to determine the extent of the clathrating process. The first was a standard chemical technique for measuring total evolved gas. The other was a radioactive technique for counting evolved gases over long time periods.

A glass bulb of known volume was connected to a manometer in the first technique. Samples of clathrated quinol of known weight were placed within the bulb which was then evacuated. The compound was heated slowly until evolution of gas ceased, and the decrease in vacuum noted. No changes in pressure were observed on cooling. This measurement provided a means of determining overall clathrating efficiency.

The second technique consisted of a glass bulb connected to a steel cylinder containing a Geiger tube. The free volume of the cylinder was about 2 l., which was large in comparison with the glass bulb. The radioactive clathrate was placed within the bulb and the entire apparatus sealed. The gases evolving from the compound diffused over into the counting chamber and were recorded. This apparatus provided a method of determination of leakage characteristics. The Geiger tube–cylinder arrangement provided 11·2 per cent counting efficiency with

VOL 7 1959/

Kr^{85}. Equilibrium diffusion conditions were complete within 16 hr and the recording of leakage could be started at that point. For those conditions where the clathrate contained large amounts of Kr^{85}, counting efficiency was reduced to 0·3 per cent by shielding the Geiger counter. This was accomplished by wrapping the tube with appropriate thicknesses of aluminum foil.

C. Radioactivity measurements

The specific activity of the various radioactive clathrate samples was checked by means of a thin window air ionization chamber. An estimation of activity was obtained from the current readings after such factors as geometry and self absorption were taken into account. The amounts of activity observed were correlated with the chemical technique outlined above.

RESULTS AND DISCUSSION

A number of hydroquinone–krypton-85 clathrates have been prepared. Samples containing three different ranges of activity (30 μc, 15 mc and 1·5 c) each in about 0·5 g of quinol were examined for leakage characteristics.

The clathrate compound prepared from the melt results in a hard fused mass. This composition proved advantageous over that of a powder of fine crystal form which would be obtained from solution growth. It provides easier handling and minimizes the danger of radioactive dust.

A series of different pressures and growing periods were tried. The clathrating efficiencies which resulted were considerably below that reported by POWELL for solution growth. However, no attempts could be made to sort individual crystals since the clathrated material was in the form of a hard fused mass. The results obtained indicate that the combination of high pressure and long growth periods provide the greatest yields. The maximum process temperature should be held to the minimum required for melting quinol. Considerable decomposition of quinol will occur if higher temperatures are used, resulting in lower overall yields. Pressures of up to 60 atmospheres were employed with growth periods as long as 72 hr. The greatest clathrating efficiency obtained under these conditions was 28·3 per cent which would provide 25·8 equivalent atmospheres at 15°C.

Relatively good yields were obtained with lower pressures and shorter growing periods. A pressure of 20 atmospheres and a growth period of 17 hr gave a clathrating efficiency of 17 per cent. The minimum combination employed was a pressure of 10 atmospheres and a growth of 4 hr. The results of this run were poor but the fact that some clathrate did form is interesting. POWELL reported that at 120°C complete decomposition of the clathrate was obtained, with no tendency to reform on cooling. This was found to be correct in the measurements made with the glass bulb–manometer apparatus. The melting point of quinol is 173°C. It appears that if sufficient pressure of gas is present, on solidification, some β-crystal form will remain.

Figs. 1 and 2 show the leakage characteristics for a 30 μc and a 15 mc clathrate compound. For measurements of the 1·5 c clathrate, the efficiency of the diffusion apparatus was lowered to 0·3 per cent. Measurements of periods of more than 1 day could not be made due to the high counting rates obtained even with the lowered efficiency. The total diffusion per day for

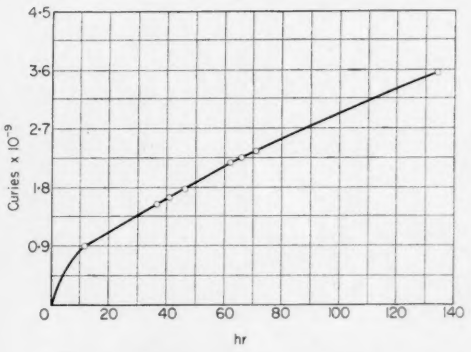

FIG. 1. Diffusion of 30 μc clathrate source.

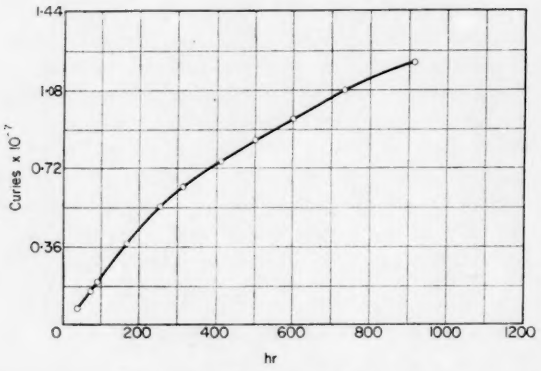

FIG. 2. Diffusion of 15 mc clathrate source.

this sample was about 3 μc. This leakage rate was ten times that of the 15 mc sample (on a per unit activity basis) but considerably below the rate shown by the 30 μc sample. All of the leakage rates, however, appeared extremely low, in the region of parts per million per day. This observation correlates well with the data reported by POWELL. Apparently the clathrates are stable at room temperatures and resistant to radiation breakdown. This effect was anticipated in view of the aromatic structure of quinol.

CONCLUSIONS

(1) A new technique for the preparation of quinol-rare gas clathrates was developed which is particularly useful for radioactive work.

(2) Clathrate compounds containing various specific activities of Kr^{85} were prepared.

(3) The specific activities of radioactive rare gas employed ranged up to 100 mc/ml (5% Kr^{85}) resulting in compounds containing as much as 1·5 c in 0·5 g of quinol.

(4) These compounds are stable and provide a convenient solid source of Kr^{85}.

Acknowledgements—This work was conducted under a contract from the Office of Isotopes Development, U.S. Atomic Energy Commission. The authors wish to express their thanks for the assistance and advice rendered by the members of this office during the course of the work.

The authors also wish to thank Messrs. T. SCAVITTO and J. DROBINSKI for their help and DR. W. PEACOCK, Technical Director, Tracerlab Inc., for his guidance in various phases of this work.

REFERENCES

1. POWELL H. M. *J. Chem. Soc.* 298, 300, 468 (1950).
2. MOELLER T. *Inorganic Chemistry*. John Wiley and Sons, New York, N.Y. (1952).

VOL.
7
1959/

International Journal of Applied Radiation and Isotopes, 1959, Vol. 7. pp. 145–147. Pergamon Press Ltd. Printed in Northern Ireland

The Preparation of S^{35}- and/or Cl^{36}-labelled SO_2Cl_2

A Simple Technique for the Quantitative Preparation of Micro- as well as Macro-quantities

G. A. OVEZALL-KLAASEN and J. HALBERSTADT
Isotope Laboratory Philips-Duphar, Weesp, Netherlands

(*Received* 16 *May* 1959)

Radioactive sulphuryl chloride labelled with S^{35} and/or Cl^{36} can be prepared in every quantity and with every possible specific activity by mixing calculated quantities of radioactive $S^{35}O_2$ with a small excess of Cl_2 gas, or $Cl_2{}^{36}$ gas with a small excess of SO_2. Mixing is done in a reaction vessel in which a small quantity of charcoal acts as a catalyst. The yields are practically 100 per cent.

LA PRÉPARATION DU SO_2Cl_2 MARQUÉ AU S^{35} ET/OU AU Cl^{36}

Le chlorure sulphurylique radioactif marqué au S^{35} et/ou au Cl^{36} peut se produire en toutes quantités et ayant toutes activités spécifiques possibles en mêlant la quantité calculée de $S^{35}O_2$ radioactif avec un surplus léger de Cl_2 gazeux, ou de $Cl_2{}^{36}$ gazeux avec un surplus léger de SO_2. Le mélange se fait dans une bouteille à réaction où une petite quantité de charbon sert de catalyseur. Les rendements sont près de 100 pour cent.

ПОЛУЧЕНИЕ SO_2Cl_2, МЕЧЕНОГО S^{35} И/ИЛИ Cl^{36}. ПРОСТАЯ МЕТОДИКА ПОЛУЧЕНИЯ МИКРО, А ТАКЖЕ МАКРОКОЛИЧЕСТВ

Радиоактивный сульфурилхлорид, меченый S^{35} и/или Cl^{36} можно получать в любом количестве и с любой удельной активностью путем смешивания расчитанных количеств радиоактивного $S^{35}O_2$ с небольшим избытком газообразного Cl_2 или газообразного $Cl_2{}^{36}$ с небольшим избытком SO_2. Синтез производится в реакционном сосуде с применением небольшого количества древесного угля в качестве катализатора. Выходы практически стопроцентные.

DIE DARSTELLUNG VON S^{35}-UND/ODER Cl^{36}-MARKIERTEM SO_2Cl_2. EINE EINFACH TECHNIK ZUR QUANTITATIVEN DARSTELLUNG VON MIKRO- UND MAKROMENGEN

Radioaktives Sulfurylchlorid, markiert mit S^{35} oder Cl^{36}, oder mit beidem, kann in jeder Menge und jeder spezifischen Aktivität hergestellt werden, wenn aliquote Mengen mit radioaktivem $S^{35}O_2$ mit geringem Überschuss an gasförmigem Cl_2 oder Cl^{36} mit geringem Überschuss von SO_2 gemischt werden. Die Mischung erfolgt in einem Reaktionsgefäss in welchem kleine Mengen von Kohle als Katalysator wirksam sind. Die Ausbeute beträgt praktisch 100 Prozent.

INTRODUCTION

The usual technique for the preparation of SO_2Cl_2 by conducting a gas mixture of SO_2 and Cl_2 through a column packed with charcoal cannot be used for the preparation of small quantities, as a considerable percentage of Cl_2 and SO_2 is lost before the reaction starts. Furthermore a rather high percentage of SO_2Cl_2 is lost by absorption on the

5A—(4 pp.)

charcoal column and by evaporation, even at low temperatures.

A quantitative preparation proved to be possible by working in a closed system.

The preparation of radioactive SO_2Cl_2 with high specific activities by exchange between inactive SO_2Cl_2 and Cl_2^{36} or $S^{35}O_2$ was also attempted. Although some exchange was found, it was too slow at normal temperatures (0–100°C).

MATERIALS AND METHODS (see Fig. 1)

$SO_2Cl_2^{36}$

Cl_2^{36} gas is prepared by the slightly modified method of BROWN *et al.*[1] in which radioactive hydrochloric acid is oxidized with potassium persulphate under controlled conditions (vessel *A*). The radioactive chlorine is directed, with the aid of an N_2 stream, through a drying tube packed with anhydric $MgSO_4$ and then condensed in vessel *B* by cooling *B* with a dry-ice–acetone mixture.

Other gases, mainly oxygen, are conducted through stopcock K_3 and two washing bottles with alkaline-sulphite solution.

In this way even last traces of Cl_2^{36} are collected in *B*.

Then stopcocks K_1 and K_2 are closed.

A slight excess of SO_2 from a cylinder is collected in liquid form in a calibrated vessel *E*, by cooling *E* with dry-ice–acetone. The stopcocks K_8 and K_9 are closed.

Now K_3 is turned to connect *B* with reaction vessel *C*. K_4 and K_6 are opened, K_5 is closed. *C* and D are evacuated through K_7.

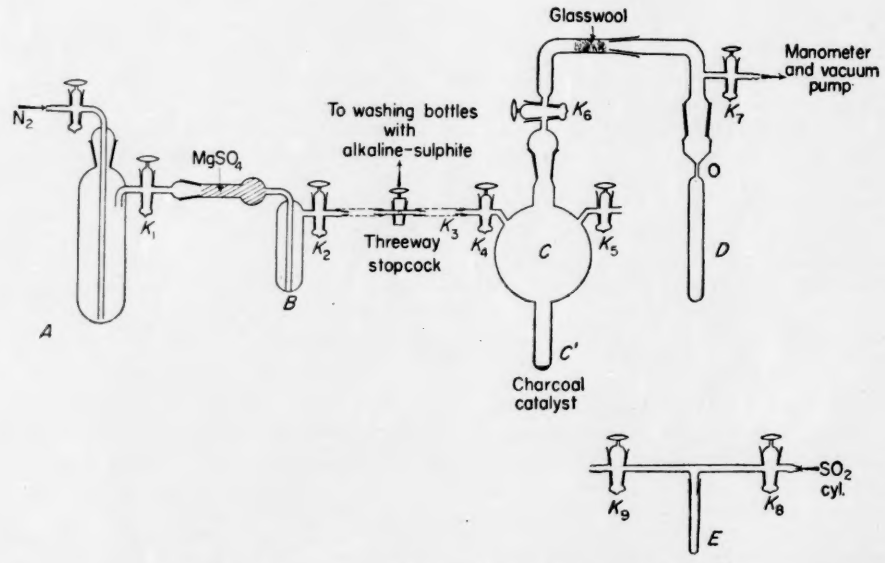

FIG. 1. Apparatus for the synthesis of radioactive SO_2Cl_2.

Vessel *C* contains some milligrams of charcoal in extension *C'*.

Then K_2 is opened carefully. The cooling mixture around *B* is removed slowly and *C'* is cooled with liquid air (or nitrogen). After all chlorine has been distilled into *C'*, K_4 is closed.

E is connected with *C* through K_5 and K_9. The cooling mixture around *E* is removed and SO_2 distilled into *C'*. K_5 is closed.

Now the liquid air around *C'* is removed very slowly and the reaction is started.

VOL. 7 1959/6

When *C* and *C′* have reached room temperature the reaction and the formation of SO_2Cl_2 have already finished.

C′ is cooled again with liquid air to solidify the SO_2Cl_2 formed. K_6 is opened. The liquid air is removed from *C′* to *D* and the SO_2Cl_2 is distilled into *D*.

Then *D* is warmed to 0°C and N_2 gas is introduced through K_7 till normal pressure is reached.

D is disconnected and a sample for radioassay is taken quickly. *D* is stoppered and placed in a cooling vessel. When the results of the radioactivity measurements are satisfying, *D* is closed at 0 with glass blowing torch.

After cleaning vessel *A* and connecting a new ampoule *D*, the apparatus is ready for another preparation. The charcoal in *C′* can be used many times.

$S^{35}O_2Cl_2$

A desired quantity of $S^{35}O_2$ is prepared from a known quantity of concentrated $H_2S^{35}O_4$, with known specific activity, by heating it, after mixing with a slight excess of charcoal, in a tube connected with vessel *E* through K_8. *E* is cooled with a dry-ice–acetone mixture.

Chlorine is taken from a cylinder and collected in *B*.

After that the preparation of $S^{35}O_2Cl_2$ is exactly the same as for SO_2Cl_2[36].

STANDARDIZATION OF RADIOACTIVE SO_2Cl_2

A known sample (0·1–0·5 ml) of the total quantity prepared is brought into 1 ml of 0·1 M NaOH solution and mixed thoroughly. Decomposition to sulphate and chloride takes place almost immediately.

The solution is diluted to a desired volume and mixed again. Then 0·1 ml is brought on a planchette and dried *in vacuo*.

A standard solution is made from a known quantity of a neutralized HCl^{36} solution or $H_2S^{35}O_4$ solution. From this solution too a 0·1 ml sample is dried on a planchette.

The activities of both samples are compared after measurement under identical conditions with an end-window type G.M. counter or a windowless flow counter.

REFERENCE

1. Brown F., Gillies A. and Stevens W. H. *Canad. J. Chem.* **31** (8), 768 (1953).

technical notes

The Preparation and Use of Br^{82}-Labelled Triolein and Oleic Acid

(*Received* 5 *May* 1959)

I^{131} HAS been used for some years as a label for fats and fatty acids in the study of fat absorption in the human. In some investigations involving the study of fats and fatty acids given simultaneously it was necessary to find another label for fats and fatty acids which could readily be determined in the presence of I^{131}. It was found that Br^{82}-labelled triolein and oleic acid could be readily prepared and the activity of I^{131} and Br^{82} in a mixture determined by a simple method.

Br^{82} was prepared by irradiation of 0·1 g NH_4Br in BEPO for 7 days, with pile factor 10–12, giving an activity of about 30 mc. The active ammonium bromide was dissolved in 10 ml water and 1 ml of this solution used as described below. As some free bromine is produced during irradiation, it is essential to carry out all chemical procedures in a well-ventilated fume cupboard.

Preparation of brominated triolein or oleic acid

Reagents

M/20 potassium bromide (0·595 g KBr in 100 ml)
M/20 potassium bromate (0·835 g $KBrO_3$ in 100 ml)
Wash solution containing 5 g KBr and 5 g $Na_2S_2O_3$ in 100 ml water.

Pyridine solution: dissolve 0·2 ml pyridine and 0·15 ml conc. H_2SO_4 in 50 ml glacial acetic acid. Prepare just before use.

Preparation

To 1 ml NH_4Br^{82} solution, containing about 2 mc Br^{82}, in a 10 ml glass-stoppered tube, add 1 ml M/20 KBr, 0·3 ml M/20 $KBrO_3$, 0·6 ml N H_2SO_4 and 3 ml CCl_4. Shake well to extract the free bromine into the lower CCl_4 layer and remove and discard the upper, aqueous, layer using a Pasteur pipette. Dissolve 1 g triolein or oleic acid in 5 ml CCl_4 in a 50 ml glass-stoppered centrifuge tube. Add 10 ml glacial acetic acid, 1 ml freshly prepared pyridine solution and all of the CCl_4 solution of bromine. Mix well and leave in the dark at room temperature for 30 min. Wash twice with an equal volume of bromide-thiosulphate wash solution, removing the upper, aqueous, layer by aspiration and then wash three times with an equal volume of distilled water. The CCl_4 and aqueous phases should separate rapidly but, if necessary, separation can be achieved by centrifugation. Filter the CCl_4 solution through a 9 cm No. 43 Whatman paper into a 150 ml glass-stoppered flask and evaporate on a boiling water-bath until there is no odour of carbon tetrachloride. This takes about 30 min. Cool the flask, add 50 ml distilled water and 0·5 ml Tween 80 and shake well. The resulting stable emulsion has an activity of 7–10 μc/ml.

The emulsion may be kept at room temperature without deterioration for at least a week. As, however, the activity of the Br^{82} decreases to about a quarter of its initial value after 3 days, in practice the emulsion should be prepared not more than 6 days before it is to be used. A suitable dose for studying blood levels after oral administration of Br^{82}-labelled fats was found to be 6–10 μc. Using an ion-exchange column with the resin Deacidite J (Permutit Co. Ltd.), less than 1 per cent of the activity was found to be due to inorganic bromide.

Determination of Br^{82} and I^{131} in mixtures

This may be carried out in a scintillation counter by making use of the fact that the counting rate (counts/min) of I^{131} falls much more rapidly as the discriminator bias is increased than the counts per minute of Br^{82}. Determine the counts per minute of each isotope and the mixture of isotopes at bias settings of 5 and 45 V:

Let r be the ratio of the counts/min at bias 5 and 45 V for I^{131}

s this ratio for Br^{82}

C_5 the counts/min for the mixture at bias 5 V

C_{45} the counts/min for the mixture at bias 45 V;

then

$$Br_{45} = \frac{rC_{45} - C_5}{r - s}$$

$$I_{45} = C_{45} - Br_{45}$$

where Br_{45} and I_{45} are the counts per minute of these substances at bias 45 V.

The formula is derived on the assumption that radioactive decay can be ignored. This is true if the readings at the two bias settings are made within 15–20 min of each other.

VOL. 7 1959/6

Discussion

The ease of preparation of Br^{82}-labelled triolein and oleic acid of high specific activity makes possible the use of double tracer studies in the investigation of fat absorption in the human, utilizing apparatus readily available in a radioisotope laboratory. Result of such studies will be reported elsewhere. It is of interest to find that brominated triolein is absorbed more rapidly from the human intestine than iodinated triolein. By studying the simultaneous absorption of brominated oleic acid and iodinated triolein, it has been possible to devise a test of pancreatic function which appears to be specific for this organ.

Br^{82}-labelled triolein has several advantages over I^{131}-labelled triolein when blood studies are to be carried out. Bromine is not selectively concentrated in the thyroid but is distributed through the extracellular body fluid. This, together with its shorter half-life and smaller necessary dose, makes Br^{82} less of a radioactive hazard than I^{131}. Further, investigations can be carried out more frequently. The short half-life of Br^{82} is a disadvantage for faecal studies, but it is possible to use it where collections of faeces up to 4 days are made after administration of the dose.

Summary

Triolein and oleic acid can be labelled with Br^{82} using pyridine bromide in glacial acetic acid. A simple method is described for measuring the activities of Br^{82} and I^{131} in a mixture. The use of double tracer methods in the study of fat absorption in the human is discussed briefly.

West Middlesex Hospital M. Lubran
Isleworth, Middlesex
Clinica Medica dell'Universita di Pisa G. Corsini*

* Present address: Guy's Hospital, London.

Holds fellowship of Consiglio Nazionale delle Ricerche Italiano.

Abtrennung von Sb^{125} aus Sn^{113} durch galvanische Abscheidung des Antimons

(*Received* 7 *July* 1959)

Als radioaktiver Indikator für Zinn wird im allgemeinen Sn^{113} verwendet, ein langlebiges ($T_{1/2}$ 119*d*), durch Elektroneneinfang zerfallendes Isotop, das durch die energiereiche γ-Strahlung seines Folgeprodukts 104 min In^{113m} bequem nachzuweisen ist. Sn^{113} wird meist durch Beschuss von metallischem Zinn mit langsamen Neutronen gewonnen. Dabei entsteht durch Sn^{124} (n, $\gamma\beta^-$) als radioaktive Verunreinigung 2,0*a* Sb^{125}, das vor allem in älteren Sn^{113}-Präparaten einen beträchtlichen Anteil der γ-Aktivität stellen kann. Sein Folgeprodukt, 58*d* Te^{125m}, stört dagegen kaum, wenn Sn^{113} durch γ-Messung bestimmt wird, da die weiche γ-Strahlung des Te^{125m} stark konvertiert ist.

Zur Entfernung von Sb^{125} aus Sn^{113}-Lösungen verwenden wir die bekannte galvanische Abscheidung des Antimons an metallischem Eisen. Dazu werden 2–3 ml der salzsauren Sn-Lösung mit einer Spirale aus weichem Eisendraht gerührt. Die Abscheidungsgeschwindigkeit hängt stark von der HCl-Konzentration ab (Abb. 1). In 7n HCl werden in 15 min über 99 Prozent des Sb^{125} abgeschieden, gleichgültig ob trägerfrei oder mit Trägerzusatz gearbeitet wird. Die Zinnmenge ist ohne Einfluss auf die Abscheidung; selbst bei 200 mg Sn/ml Lösung war keine Abnahme der Sb-Abscheidung festzustellen. Die Lösung enthält nach der Abscheidung grössere Mengen Eisen, das nach Oxydation zu Fe^{III} durch Extraktion mit Diisopropyläther entfernt werden kann, ohne dass Verluste an Sn zu befürchten sind.[1] Wenn man diese Extraktion vermeiden will, kann man die Sb-Abscheidung auch an metallischem Zinn vornehmen. Allerdings muss man dabei mit einer nicht unbeträchtlichen Verminderung der spezifischen Aktivität des Sn^{113} rechnen.

Zur Gewinnung von Sb^{125} behandelt man den Eisendraht etwa 1 min mit 7n HNO_3-Weinsäure, um Antimon praktisch vollständig abzulösen. Dabei gehen 50–100 mg Eisen mit in Lösung. Durch Eindampfen wird die Weinsäure zerstört; der Rückstand wird mit 2n HCl aufgenommen, mit Natriumdithionit reduziert und auf eine Dowex 1 × 10 Säule (2 cm lang, 4 mm Durchmesser, Cl-Form) gegeben. Fe^{II} wird nicht adsorbiert[2] und kann durch Nachwaschen mit einigen ml 2n HCl vollständig entfernt werden. Das adsorbierte[2] Sb^{III} wird mit etwa 7ml 2n HCl—0,5m HF eluiert,[3] etwa 5–6 Prozent des Sb^{125} verbleiben dabei auf der Säule. Das Verfahren kann ohne Schwierigkeiten mit trägerfreiem Sb^{125} durchgeführt werden.

Zur Herstellung trägerfreier Sb^{125}-Präparate auf dünner Unterlage, etwa für kernphysikalische Untersuchungen, kann das Sb^{125} von der Eisenspirale bei 1200°C im Stickstoffstrom auf die wassergekühlte Unterlage aufgedampft werden. Nach einer Stunde sind etwa 50 Prozent des Sb^{125} übergegangen. Wir verwenden dazu das gleiche Verdampfungsrohr wie bei der Herstellung trägerfreier Ra*E*(Bi^{210})-Präparate,[4] d.h. eine nur wenig abgewandelte Form der

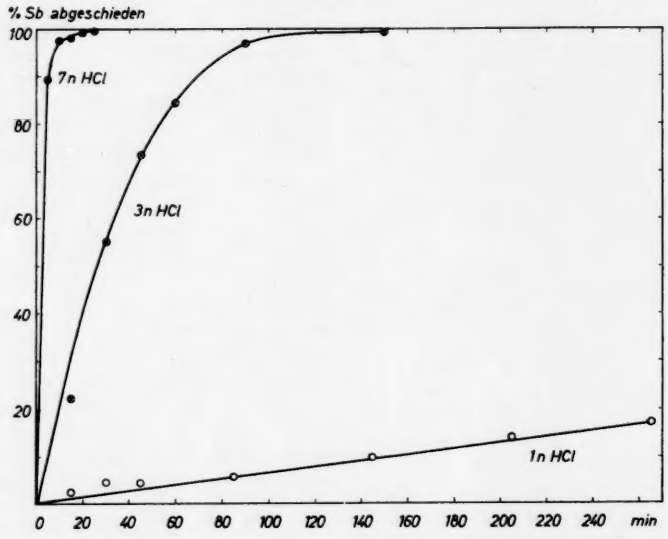

ABB. 1. Galvanische Abscheidung von Antimon an Eisendraht in Abhängigkeit von der Versuchsdauer und der Salzsäurekonzentration.

von W. GEILMANN und Mitarbeitern[5] für die Spurenanalyse entwickelten Anordnung.

Te^{125m} wird bei der Abscheidung des Antimons auf dem Eisendraht ebenfalls reduziert. In Gegenwart von etwa 100 μg Tellurträger findet jedoch keine Abscheidung auf dem Draht statt, sondern es bildet sich ein feiner schwarzer Tellurniederschlag, der abzentrifugiert werden kann. Über das Verhalten von trägerfreiem Tellur haben wir keine Erfahrungen.

Herrn Prof. Dr. F. STRASSMANN danken wir für sein freundliches Interesse, Herrn E. RÖDER für die Durchführung der Verdampfungsversuche. Die finanzielle Unterstützung durch das Bundesministerium für Atomkernenergie und Wasserwirtschaft sei ebenfalls dankbar vermerkt.

EMIL KLEEMANN
GÜNTER HERRMANN

Anorganisch-chemisches Institut
Universität Mainz

Literatur

1. POHL F. *Z. Anal. Chem.* **161,** 108 (1958).
2. KRAUS K. A. und NELSON F. *Proceedings 1st International Conference on the Peaceful Uses of Atomic Energy, Geneva* 1955 Bd.7, S.113 ff. United Nations, Geneva (1955).
3. KRAUS K. A. und NELSON F. *Symposium on Ion Exchange and Chromatography in Analytical Chemistry* S.27 ff. American Society for Testing Materials, Philadelphia (1958).
4. RÖDER E. und HERRMANN G. erscheint demnächst.
5. GEILMANN W. *Z. Anal. Chem.* **160,** 410 (1958).

The Preparation of Potassium-43 Using an Interrupted Cyclotron Beam

(*Received* 15 *May* 1959)

POTASSIUM-43 may be prepared in a cyclotron by the (α,p) reaction on A^{40}, by allowing the α-particle beam to enter a vessel containing argon at atmospheric pressure or at a pressure of 2–3 atmospheres.[1,2] The activity collects on the walls of the vessel from which it may be removed by washing with distilled water. This procedure is somewhat awkward especially when it is desired to collect the activity in a small volume (2–5 ml) of solvent, and an alternative was sought. The method to be described was devised for use with the 30 MeV external α-particle beam of the Medical Research Council's cyclotron at Hammersmith Hospital, and is now employed semi-routinely for the production of K^{43} with high specific activity for medical purposes.

The active deposit from radon and thoron may be collected on a wire or disc exposed to these gases, and it has long been known that the strength of sources prepared in this way may be increased by charging the wire with respect to the container.[3] It was suggested to us that this principle could be applied to the present problem, by introducing a collecting rod into the argon-filled bombardment vessel and applying a negative potential in the region of 1 kV. The potassium is expected to be formed as positive ions which would then be attracted to the rod. It was found however that the potential cannot be maintained when the cyclotron beam is on, because

VOL. 7 1959/

of the large ionization current; the great majority of the activity appeared on the inner wall of the bombardment vessel, as before.

The problem has been solved by periodically interrupting the α-particle beam by means of a rotating shutter so that bombardment and collection phases alternate. The potential rises to its full value during the "off" phase, and collection of potassium ions can take place. It is convenient to use a stainless steel collecting rod, $\frac{1}{4}$ in. in diameter, supported at the remote end only, and extending almost the whole length of the vessel which is approximately 3 ft in length and 6 in. in diameter. The argon is normally at a pressure of 2 atmospheres, and an escape valve is provided to prevent a rise of pressure when the gas becomes hot during the bombardment.

Migration time

The drift velocity v of a positive or negative ion is proportional to the electric field strength E and is characterized by the mobility μ (inversely proportional to pressure) such that $v = \mu E$. The time taken for an ion to drift, along a radius, from a point distant R from the axis to the collecting rod can be calculated by evaluating the integral $1/\mu \int dr/E(r)$ between the limits $r = R$ and $r = r_1$, where r_1 is the radius of the rod, and $E(r) = V_0/r \log_e (r_1/r_2)$ where V_0 is the potential difference between rod and vessel, and r_2 is the radius of the vessel.

The mobility of ions in gases is influenced markedly by the presence of traces of impurity. This is especially true of ions which are more than about 10^{-3} sec old, and the mobility in a given set of conditions cannot be predicted with any accuracy. Rossi and Staub[4] quote a value for μ (at atmospheric pressure) of 1·3 cm/sec per V/cm for A^+ ions in argon; but Loeb[5] gives a value of 2·78 for ("new") K^+ ions (natural potassium) in argon, and theoretical values very close to this for A^+ ions in argon.

In the present circumstances only an approximate calculation is needed, and for μ a value of 2 cm/sec per V/cm (at atmospheric pressure) has been used. At a pressure of 2 atmospheres, and for an accelerating voltage of 1 kV, the time taken to drift from the full radius of the vessel to the rod is calculated to be 0·1 sec.

The shutter is butterfly-shaped, providing two "on" and two "off" phases per revolution. A speed of approximately 100 rev/min is used giving a collection time of 0·15 sec. The shutter was designed to give equal bombardment and collection times and can be seen, attached to the vessel, in the photograph (Fig. 1, opposite p. 152).

Yields

The yield of potassium-43 is approximately 15 μc/μA hr; a bombardment of 5 hr at a *mean* current of 20 μA in the vessel (i.e. an incident current of 40 μA) gives a yield of approximately 1·5 mc. The energy of the α-particle is reduced by the aluminium windows of the cyclotron and the vessel, and by the air space between the two, to 16–18 MeV. The yields are determined by γ-ray measurements in a re-entrant ionization chamber, using radium as a standard. They are calculated on the basis of a specific γ-emission for K^{43} of 5·7 r/hr per mc at 1 cm calculated in turn from the decay scheme data quoted by Strominger *et al.*[6] There is a slight uncertainty in the decay scheme, and so the yields cannot be measured accurately.

With a negative potential of 1 kV on the rod, and with the shutter rotating, approximately three-quarters of the total removable activity appears on the rod. After the bombardment the rod is removed from the vessel and drawn through cotton wool soaked in warm distilled water, to which 2–10 μg of potassium chloride per ml is added unless particularly high specific activities are called for. If the washing is repeated, very little further activity can be removed, so it is unlikely that any appreciable potassium activity remains on the rod after the first washing.

The K^{43} is identified by its half-life of 22·4 hr, and by its γ-ray spectrum. It is contaminated to the extent of about 10 per cent by K^{42} (half-life 12 hr) presumably formed by the (α,np) reaction on the A^{40}. There is also a contaminant with a half-life in the region of 60 days, present to the extent of about 1 part in 10^4 of K^{43} activity at the end of bombardment. The amounts of this contaminant have been insufficient to enable it to be identified.

This interrupted beam technique is therefore a great advantage in the preparation of this radioisotope, and it could presumably be used in other situations where a solid product is formed during the bombardment of a gaseous target.

Acknowledgements—We should like to acknowledge the part played by Mr. D. D. Vonberg and his staff in operating the cyclotron during the bombardments, and especially Mr. J. Sharp for attending to the mechanical design and construction of the vessel and shutter. We are particularly indebted to Mr. G. R. Newbery (senior physicist of this Unit) for his enthusiasm and interest.

N. A. Dyson*
P. E. Francois†

Medical Research Council
Radiotherapeutic Research Unit
Hammersmith Hospital
London

* Now in the Department of Physics, Birmingham University.

† Now with the Central Electricity Generating Board.

References

1. Lindqvist T. and Mitchell A. C. G. *Phys. Rev.* **95,** 444 (1954).
2. Reasbeck P. Private communication.
3. Rutherford E., Chadwick J. and Ellis C. D. *Radiations from Radioactive Substances.* Section 128. Cambridge University Press (1930).
4. Rossi B. B. and Staub H. H. *Ionization Chambers and Counters*, Section 1.5. McGraw Hill, New York (1949).
5. Loeb L. B. *Fundamental Processes of Electrical Discharges in Gases*, Chapter 1. John Wiley, New York (1939).
6. Strominger D., Hollander J. M. and Seaborg G. T. *Rev. Mod. Phys.* **30,** 585 (1958).

An Easy Way of Calculating the Composition of a Two-component System from Two-channel Spectrometry

(*Received* 8 *June* 1959)

The determination of the concentration of a substance which yields a characteristic spectrum (e.g. light absorption or γ-emission) is usually simple. If two substances with overlapping spectral curves are mixed the analytical procedure immediately becomes more complicated, but can be performed by analyses of the resulting complex spectrum at two wavelengths (two spectral bands or channels).[1,2] This may be seen in Figs. 1 and 2 where in addition to γ-spectra light absorption curves are shown. The concentrations must, however, be kept sufficiently low, so as to retain a linear relationship between the concentration or activity of the mixture and the extinction or counting rate (Bouget–Lambert–Beer's law or coincidence loss). A simple dilution can serve as a check that linearity exists.

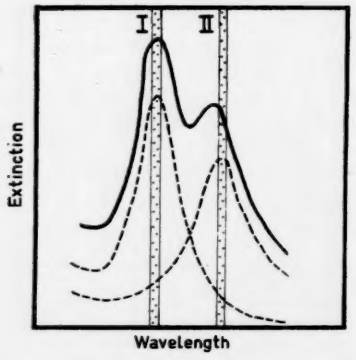

Fig. 1. Light absorption curve (——) resulting from a mixture of two absorbing components (– – –). These two components can be estimated from extinction readings in two spectral bands I and II.

Readings (e.g. extinction or counting rate) are taken in these two channels. They will be denoted as $N^{\mathrm{I}}_{\mathrm{tot}}$ and $N^{\mathrm{II}}_{\mathrm{tot}}$ meaning the total intensity in channel I and II respectively. It is obvious that these two entities equal the sum of the effect of the participating components. If these intensities are denoted by C we obtain:

$$N^{\mathrm{I}}_{\mathrm{tot}} = C_A{}^{\mathrm{I}} + C_B{}^{\mathrm{I}} \tag{1}$$

$$N^{\mathrm{II}}_{\mathrm{tot}} = C_A{}^{\mathrm{II}} + C_B{}^{\mathrm{II}} \tag{2}$$

The reason for the two different notations N and C was given by Öbrink and Ulfendahl[3]. The relation between $C_A{}^{\mathrm{I}}/C_A{}^{\mathrm{II}}$ is always a constant as is also $C_B{}^{\mathrm{I}}/C_B{}^{\mathrm{II}}$ and these quotients are determined by standard solutions of each substance separately.

Thus

$$C_A{}^{\mathrm{I}}/C_A{}^{\mathrm{II}} = q_A \tag{3}$$

$$C_B{}^{\mathrm{I}}/C_B{}^{\mathrm{II}} = q_B \tag{4}$$

A combination of these four equations gives

$$C_A{}^{\mathrm{I}} = \frac{q_A N^{\mathrm{I}}_{\mathrm{tot}} - q_A q_B N^{\mathrm{II}}_{\mathrm{tot}}}{q_A - q_B} \tag{5}$$

$$C_A{}^{\mathrm{II}} = \frac{N^{\mathrm{I}}_{\mathrm{tot}} - q_B N^{\mathrm{II}}_{\mathrm{tot}}}{q_A - q_B} \tag{6}$$

$$C_B{}^{\mathrm{I}} = \frac{-q_B N^{\mathrm{I}}_{\mathrm{tot}} + q_A q_B N^{\mathrm{II}}_{\mathrm{tot}}}{q_A - q_B} \tag{7}$$

$$C_B{}^{\mathrm{II}} = \frac{-N^{\mathrm{I}}_{\mathrm{tot}} + q_A N^{\mathrm{II}}_{\mathrm{tot}}}{q_A - q_B} \tag{8}$$

These equations are by no means original but have been used by many authors before.[3] A simpler procedure than algebraic method has been adopted for the solution of the equations.

If the fraction of the value (e.g. counting rate) observed due to one component compared to the total is calculated we have

$$C_A{}^{\mathrm{I}}/N^{\mathrm{I}}_{\mathrm{tot}} = f_A{}^{\mathrm{I}} = \frac{1/q_X - 1/q_B}{1/q_A - 1/q_B} \tag{9}$$

$$C_A{}^{\mathrm{II}}/N^{\mathrm{II}}_{\mathrm{tot}} = f_A{}^{\mathrm{II}} = \frac{q_X - q_B}{q_A - q_B} \tag{10}$$

$$C_B{}^{\mathrm{I}}/N^{\mathrm{I}}_{\mathrm{tot}} = f_B{}^{\mathrm{I}} = \frac{1/q_X - 1/q_A}{1/q_B - 1/q_A} \tag{11}$$

or

$$C_B{}^{\mathrm{II}}/N^{\mathrm{II}}_{\mathrm{tot}} = f_B{}^{\mathrm{II}} = \frac{q_X - q_A}{q_B - q_A} \tag{12}$$

Here

$$q_X = N^{\mathrm{I}}_{\mathrm{tot}}/N^{\mathrm{II}}_{\mathrm{tot}} \tag{13}$$

VOL 7 1959/

VOL.
7
59/60

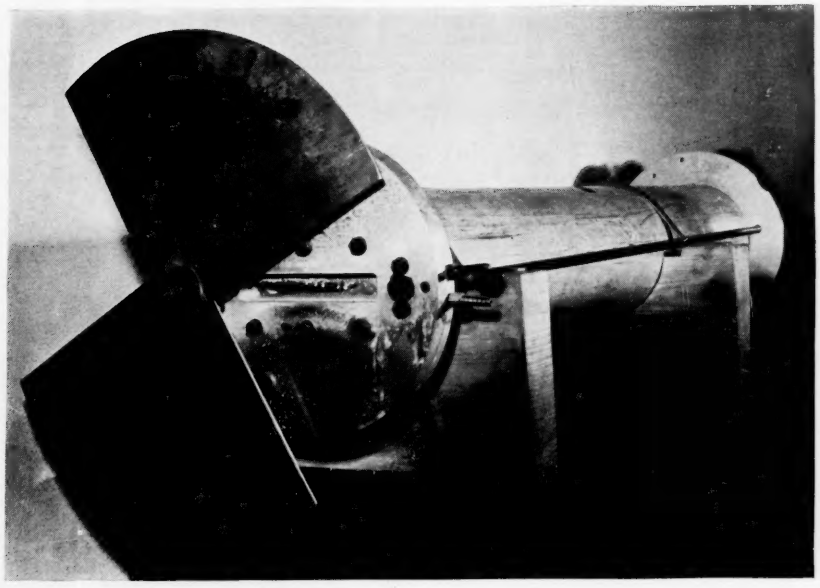

FIG. 1.

VOL.
7
1959/

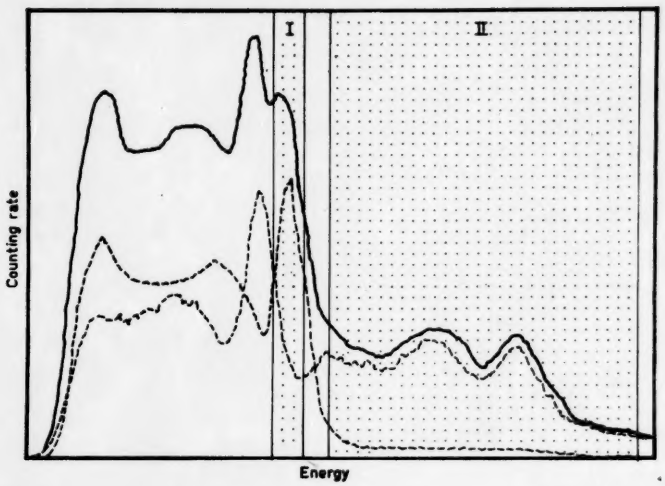

FIG. 2. Gamma energy spectrum (——) from a mixture of two different radioisotopes (– – –). In this case they are Na^{24} and K^{42}. The two components can be estimated from counting rate determinations in two energy channels I and II.

From these four equations C or f can be calculated. In the case of f it is irrelevant which one is determined. One is sufficient as $f_A^{\,I} + f_B^{\,I} = f_A^{\,II} + f_B^{\,II} = 1$. Obviously C can be determined from f if desired.

To visualize the meaning of f let us choose equation (10). Fig. 3 shows the two functions (3) and (4) as the lines A and B and equation (13) as the line X. It is obvious that a sample containing very much of B and very little of A will give a q_X rather close to q_B, whereas samples with increasing amounts of A will yield values of q_X progressively approaching q_A. The line X is thus always between A and B. Equations (9), (11) and (12) can be visualized in similar ways.

In order to make the calculations easier let us

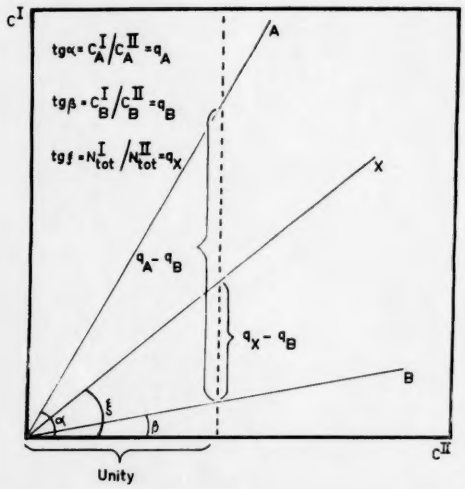

FIG. 3. Graphic representation of equation (3) (line A) and equation (4) (line B). The line X represents the unknown sample, the q_X of which is the slope of that line. If the counting rates in channel II are the same in all q-determinations the distances on the broken line represent the parameters in equation (10).

consider equations (9), (10), (11) and (12) as having the general form

$$f = \frac{x - b}{a - b} \qquad (14)$$

This can be solved by a simple electric analog. Fig. 4 shows the circuit. Across the three 10-turn Helipot potentiometers a variable voltage is applied.

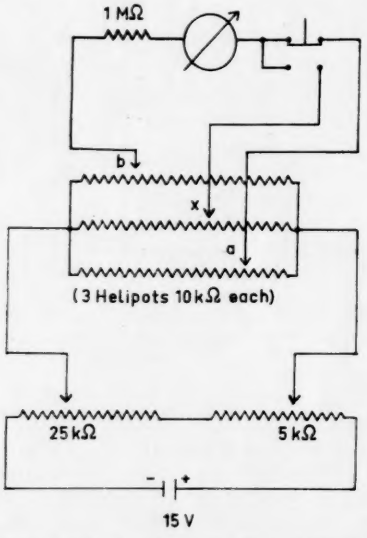

FIG. 4. A simple electric analog for calculating the fraction of an isotope in a mixture of two according to equation (14).

The voltage is directly proportional to the reading of the potentiometer scale. The values a and b are set on the dials and the galvanometer having a linear scale from 0 to 100 is adjusted by the voltage supply divider to read either exactly 100 or a number equal to the pertinent N_{tot}. The voltage difference between x (set on the third potentiometer) and b will then give either the fractional reading in per cent on the galvanometer or the value of the corresponding C, depending on the setting $(a - b)$.

The procedure has the advantage of being simple and fast. The q-values must, however, be calculated first. Direct usage of the primary data N^{I}_{tot} and N^{II}_{tot} in equations (5) to (8) is possible in more complicated analog computers.

Summary

When determining the individual activities or concentrations of two substances in a mixture from their spectral curves analysed by two spectral bands the calculations can be much simplified if the quotients of the values observed in the two channels are first calculated.

A way of using a simple electric analog for computing the constituents in the two component system from the spectrometric data is presented.

Institute of Physiology
University of Uppsala
Sweden

A. BILL
K. J. ÖBRINK
H. R. ULFENDAHL

VOL. 7 1959/6

References

1. VIERORDT K. *Die quantitaive Spektralanalyse in ihrer Anwendung auf Physiologie, Chemie und Technologie.* Tübingen (1876).
2. DRABKIN D. L. Spectroscopy: photometry and spectrophotometry. *Medical Physics* Vol. II, p. 1039. Otto Glasser (1950).
3. ÖBRINK K. J. and ULFENDAHL H. R. *Int. J. Appl. Rad. Isotopes* **5,** 99 (1959).

letters to the editors

Total-count Technique for Flow Measurement

(*Received* 25 *May* 1959)

In a recent issue of the *Journal*, D. E. Hull published a paper entitled: "The total-count technique: a new principle in flow measurement".[1] The basic idea, believed by Hull to be new, was the fact that a flow rate Q could be determined by registering a total number of N counts from a known amount of radiotracer, A μc, placed in the stream. The relationship is given as:

$$Q = F\frac{A}{N} \tag{1}$$

where F is a calibration factor with typical units such as $\frac{\text{counts/minute}}{\mu\text{c/gallon}}$; i.e. it translates count rate into specific activity. He makes the point that N will be the same at any downstream point, even though the time distribution of the count rate varies from place to place.

Apparently Hull seems to be unaware of the fact that the same basic method has been described and used for a long time in the medical literature to determine the so-called cardiac output; i.e. the volume of blood passing through the heart per unit time and quoted as liters/minute. A fairly recent and comprehensive description of both theory and practice for external recording, including references, is in the *Proceedings of the Second Radioisotope Conference* held at Oxford in July, 1954 and published by Academic Press, Inc., London.[2] The paper is by Veall *et al.* and is entitled "A method for the determination of cardiac output." On page 185 there appears the same equation as the one quoted by Hull:

$$F = \frac{Q}{a\int_0^\infty N\,dt} \tag{2}$$

with the notation:

F = flow rate
Q = quantity of injected isotope
N = count rate
$\int_0^\infty N\,dt$ = total count recorded
$\frac{1}{a}$ = the calibrating factor with the units of count rate/specific activity.

Hull's method of calibration (obtaining the steady count rate when a known specific activity is placed in a pipe *similar* to the one used in the field) has also been anticipated, except that the medical scientist need not be concerned about the similarities of the "calibrating pipe" since they are one and the same in the case of calibrating for cardiac output. One simply waits for equilibrium, which occurs a few minutes after injection, and measures N_{equil} counts/min. A sample of blood is then withdrawn and a determination is made of C_{equil} μc/ml by an assay in a well counter under conditions of known counting efficiency, with

$$\frac{1}{a} = \frac{N_{equil}}{C_{equil}}.$$

Equation (2) (or (1)) is just an application of conservation of "material" and is simply a reformulation of a measuring technique long known in medical literature as the dilution method for determining flow rate.

It does not matter whether the marker substance is a radioactive isotope, a dye or any material capable of being assayed. The dilution equation is just equation (2) and simply expresses the fact of conservation of the marker material, a principle well known and understood for a long time.

The idea of using the basic dilution conservation method was first proposed by Stewart,[3] to determine the rate of cardiac flow, using a known amount of indicator along with a measurement of specific dilution of the material. Indeed Dr. Stewart's work is rather heroic considering the type of equipment then available as well as the signal fact that he indeed had invented a new technique for determining flow rate.

The concepts were reviewed by Stewart,[4] by Bock and Buchholtz[5] and by Kinsman,[6] who formulated the following equation:

$$F = \frac{60I}{CT} \tag{3}$$

where F is flow rate in l./min
C is average concentration of dye in mg/l.
T is duration of flow in seconds
I is mg of dye injected.

The authors describe how to obtain CT by integrating the concentration versus time curve of dye dilution.

Again the position of the downstream sampling point is one of convenience. This principle was widely used and finally reviewed by HAMILTON,[7] and the concentration measured continuously from arterial sampling, with the formula of flow becoming:

$$F = \frac{0{\cdot}06\ Q}{\int_0^\infty C\ dt} \qquad (4)$$

where F is flow rate in l./min
C is concentration of the dye in mg/cm^3
Q is quantity of injected dye in mg
t is time in seconds

The credit for the qualitative idea of using a γ-emitting radioisotope via the measurement of counts with a G.M. detector to study flow dynamics in humans goes to PRINZMETAL *et al.*[8] Another effort in external detection of cardiac output was reported by NYLIN and CELANDER[9] using the standard equation with a marker consisting of red cells tagged by P^{32}.

In this same period of time others who reported on the same subject were NEWMAN *et al.*[10] and NICHOLSON and WOOD.[11] POWERS *et al.*[12] used Na^{24} and β-counting for the same purpose. In 1953 GILFORD *et al.*[13] described a continuous and external recording of the time–concentration function of dye in blood using the standard equation (4).

In 1951 MACINTYRE *et al.*[14] had incorporated the use of radioactive labeled markers (RISA) to the dilution technique, as detected by continuous arterial sampling.

The same group of investigators fully incorporated the external detection procedure, for determination of cardiac output in the report by PRICHARD *et al.*[15] They published information regarding the simultaneous measurement of cardiac output by external recording and continuous arterial sampling technique. There was an average agreement within ± 8 per cent, thus encouraging the wider use of this procedure in medicine.

Perhaps the moral of this tale is the need for the various disciplines to communicate and thus minimize unplanned duplications. This is particularly true for those who wish to use radioisotopes since this material is truly ubiquitous in the world of today.

M. A. GREENFIELD
ISMAEL MENA

Department of Radiology
School of Medicine
University of California
Medical Center, Los Angeles 24, California

References

1. HULL D. E. *Int. J. Appl. Rad. Isotopes* **4,** 1 (1958).
2. VEALL N., PEARSON J. D., HANLEY T. and LOWE A. E. *Proceedings of the Second Radioisotope Conference*, p. 183. Academic Press, London (1955).
3. STEWART G. N. *J. Physiol.* **22,** 159 (1897).
4. STEWART G. N. *Amer. J. Physiol.* **57,** 27 (1921).
5. BOCK J. and BUCHHOLTZ J. *Arch. Exp. Path. Pharmacy* **88,** 192 (1920).
6. KINSMAN J. M., MOORE J. W. and HAMILTON W. F. *Amer. J. Physiol.* **89,** 322 (1929).
7. HAMILTON W. F. *Circulation* **8,** 527 (1953).
8. PRINZMETAL M., CORDAY ELIOT, BERGMAN H. C. SCHWARTZ L. and SPRITZLER R. *Science* **108,** 340 (1948).
9. NYLIN G. and CELANDER H. *Circulation* **1,** 76 (1950).
10. NEWMAN E. V., MERRELL M., GENECIN A., MONGE C., MILNOR W. and MCKEENER W. *Circulation* **4,** 735 (1951).
11. NICHOLSON J. W. III, and WOOD E. H. *J. Lab. Clin. Med.* **38,** 588 (1951).
12. POWERS S. R., ROSSI H. H. and PAPPER E. M. *Rev. Sci. Instrum.* **23,** 178 (1952).
13. GILFORD S. R., GREGG D. E., SHADLE O. W., FERGUSON T. B. and MARZETTA L. A. *Rev. Sci. Instrum.* **24,** 696 (1953).
14. MACINTYRE W. J., PRITCHARD W., ECKSTEIN R. and FREIDELL H. *Circulation* **4,** 552 (1951).
15. PRITCHARD W., MACINTYRE W. and MOIR T. W. *Circulation* **18,** 1147 (1958).

VOL. 7 1959/6

Reply to letter of 20 May from M. A. Greenfield and I. Mena

(*Received* 3 *July* 1959)

ALL of us who use radioisotopes in engineering are indebted to Drs. GREENFIELD and MENA for their well documented account of the development of the dilution method used in medical research to measure the flow of blood through the heart. Since 1950, when radioactivity was first substituted for dye in this method, the technique has developed to a point where it could almost be used in the total-count method, developed by an entirely different route. Indeed, the most recent papers in the medical field use an equation which is clearly analogous to the equation $Q = AF/N$ in my paper.

Nevertheless, there is an important difference in principle between the total-count method and the concentration-integral technique. The difference is most clearly brought out in the transmutation of the dimensions of the counting factor, F. This is determined as a ratio of count rate to specific activity, $\frac{\text{counts/minute}}{\mu\text{c/gallon}}$; but in the total-count method, it is used in the dimensionally equivalent form $\frac{\text{counts}}{\mu\text{c}}$. $\frac{\text{gallon}}{\text{minute}}$ to translate counts directly into flow rate. GREENFIELD and MENA are confused on this point. They say F is used to translate count rate into specific activity. This is true in the older method. It is not true of the total-count method, and it is just in this that its novelty lies.

Obvious differences in technique further distinguish the two methods. First, because of the short recirculation time in the cardiac system, a total count is never observed. After the counting rate passes its peak, it does not return to background but levels off at 20 per cent to 40 per cent of the peak value. It is necessary, then, to plot the concentration, either of samples withdrawn at intervals or of a stream exposed to a counting ratemeter. In this plot, there generally appears a short exponential portion. Its slope must be determined so that it can be extrapolated along the time axis in order to get an integral of the concentration. The slope of this curve really represents a rate equal to the cardiac output divided by the cardiac volume. To get a curve suitable for extrapolation, it is necessary to make a practically instantaneous injection; otherwise the exponential part of the curve does not appear or it has a misleading slope. An accumulated total count on a scaler would be meaningless in these circumstances.

These limitations do not apply to the total-count method. The injection may be made at any arbitrary rate, either constant, varying, or interrupted, without changing the final result. No attention is given to the counting rate during the test; neither counting rate nor concentration need be calculated at all. The final count is simply read off the scaler, corrected for background, and put into the equation $Q = AF/N$ to calculate the flow rate. After the tracer has passed the counter and the final background is observed, it takes only a minute's work with a slide rule to calculate the result.

In contrast to the medical technique, in which accurate timing is essential in principle and in execution, the total-count equation does not even contain time as a factor. (The only reason a watch is needed is to determine the background correction. In many tests, this could be ignored if an accuracy of 10–20 per cent were sufficient.) The dimension of time enters the flow rate equation through a calibration constant determined, independently of the flow measurement, in a static experiment; but time is not involved in the measurement made on the flowing stream. All these distinctions make it clear that the method used for cardiac output measurements is not the same as the total count method, even though the equations can be written with analogous terms.

STEWART in 1897 first used the dilution method to measure blood flow from the heart. He injected salt solution at a constant rate for, say, 10 sec. He inferred from the loudness of an audible signal from a conductivity cell on an artery that the salt concentration was steady over an approximately equal interval and withdrew a sample during that interval. He determined the dilution ratio of the salt solution in the sample and multiplied the injection rate by this ratio to get the blood flow rate.

However, STEWART was not the first, as GREENFIELD and MENA believe, to use the dilution method to measure flow rates. This method was invented in 1863 by SCHLOESING, a chemist in France.[1] He wrote the equation $F/f = \psi/\phi$, where the right-hand term is the dilution ratio of salt from a small stream with measured flow f to a large stream with flow F to be determined. This method has been used extensively since then, especially by civil engineers to measure flow rates in turbines and open streams.[2] It is exactly the method STEWART used. Later medical researchers modified the dilution method used by STEWART. When dye was substituted for salt and more quantitative measurements were made, the tracer concentration was found not to be constant; so, from 1929 on, the average concentration was measured in a series of samples during the passage of the tracer and used in the equation $F = 60\ I/CT$. This is still the dilution method, and its history cannot properly be cited to prove that "the same basic method has been described and used for a long time in the medical literature."

In 1950, NYLIN *et al.* substituted radiophosphorus for dye. They did not use the old standard equation but wrote $\int C\,dt$ instead of CT. In taking this step, they broke away from the dilution method of STEWART and replaced it with the concentration-integral method. This is the method that GREENFIELD and MENA are really talking about as being analogous to the total-count method. The analogy between the total-count method and the more general integral-measurement principle, of which concentration integration is a particular example, was pointed out in my paper. It was not claimed that the general principle is new. In fact, this method, used in medical research since 1950 was also anticipated by SCHLOESING. In his 1863 paper, he clearly expounded

the concentration-integral method in these words: "Au lieu de prendre pour l'analyse un énchantillon unique du mélange des fluides, it conviendra d'échantilloner continûment pendant toute la durée de l'expérience, et d'analyser la somme des échantillons successifs. On s'affranchira ainsi de la condition de constance de l'écoulement de f, et il suffira de connaître la quantité que s'en est débitée du commencement à la fin de l'expérience."

The 1954 paper by VEALL *et al.* is the first to use the expression $\int N\,dt$; but it is not, as GREENFIELD and MENA state, the total count *recorded*, because a total count cannot be recorded in this system. It is, rather, an integral of a *calculated* curve of counting rate versus time. Their factor a is used, as stated above, to translate count rate to concentration. Nowhere in their paper do VEALL *et al.* refer to this as the total count. Such a description is made first in the present interpretation by GREENFIELD and MENA in the terms introduced in my paper.

Perhaps, if the human cardiac system did not have such a short recirculation time and if the nature of medical work had not dictated the general use of counting ratemeters rather than scalers, the total-count principle might have emerged in the medical field by now. But the published record shows that the total-count concept was first explicitly enunciated in my patent application of 29 October, 1954,[3] and publicly expounded in my paper at the Berkeley meeting of the American Association for the Advancement of Science in December 1954.[4]

Reasoning by analogy from our experience in measuring flow through refinery tanks and pipes, I would suggest that it may be possible to modify the medical technique so as to avoid the recirculation problem. If this succeeds, the total-count method can be used and accuracy of 2 per cent may be possible in cardiac output measurements. A catheter should be inserted through an artery, not clear into the heart, but so that its end is in the aorta just above the aortic valves. A sample should be drawn out of another artery at a steady rate through a tube that passes through a scintillation counter connected to a *scaler*, in an arrangement like that used by CRANE *et al.*[5] If the sampling tube is built to hold a liquid volume of 5 cm^3 within the crystal, sodium-24 will have a counting factor of about $4000\ \frac{\text{counts}}{\mu c} \cdot \frac{\text{liters}}{\text{minute}}$; and injection of 7 μc (the total body tolerance) would give 5600 counts, enough for 2 per cent accuracy. The calibration factor is measured in an aqueous solution beforehand, so the loss of sodium to the extracellular space before coming to equilibrium would not interfere with the accuracy. Having eliminated the holdup in the heart by injecting the tracer directly into the aorta, one might expect that the counting rate would return nearly to background before the recirculation wave appears. Then the scaler reading will give the total count. Precise results by this technique may be found critically dependent upon good mixing in the aorta before its first branch; but STEWART's 1897 experiments seem to have established the turbulent nature of flow in the blood vessels, and hence the mixing should be adequate. This point could be tested experimentally by taking samples simultaneously (or in successive tests) from different arteries. For example, the same total count being found from the right brachial artery, coming out of the aorta's first branch, and from a femoral artery would show complete mixing.

As for the moral of the story, the implication that because I did not know of the cardiac flow technique my invention and development of the total-count technique was an "unplanned duplication" of earlier work seems unwarranted. STEWART presumably did not know of SCHLOESING's paper and, therefore, invented the dilution method independently. But even in the case of STEWART's work, which actually was anticipated in a paper a generation earlier, should such an epithet be applied? Would it be fair to say that his work and that reported in dozens of medical papers since then were an "unplanned duplication" of SCHLOESING's work? I think not. Independent developments of related techniques in fields so diverse as medicine and chemical engineering are to be expected and are not necessarily undesirable. When, on occasions such as this, cross-fertilization occurs, it should contribute something to the vigor of both fields.

Certainly, had I planned a research program on a better way to measure flow rates in pipelines, I would not have looked in the medical literature for clues. Even if I had, it is hardly likely that I would have conceived the total-count principle from studying the medical technique as it stood in 1953. Once the total-count principle has been set forth in its basic simplicity, it is easy to see the analogy to other flow measurements. But it might have taken years of planned research to extract this simple idea from the specialized medical procedure and to recognize its wide range of applications in engineering. It does not detract from the total-count method that it was built on another foundation.

D. E. HULL

California Research Corporation
Richmond Laboratory
576 *Standard Avenue*
Richmond 1, *California*

VOL. 7 1959/

References

1. SCHLOESING M. T. *C.R. Acad. Sci., Paris* **57,** 164 (1863).
2. GROAT B. F. *Trans. Amer. Soc. Civ. Engrs.* **80,** 951 (1916).
3. *U.S. Pat.* 2, 826, 699.
4. HULL D. E. *Nucleonics* **13** (4), 18 (1955).
5. CRANE M. G., ADAMS R. and WOODWARD I. *J. Lab. Clin. Med.* **47,** 803 (1956).

Reply to D. E. Hull's letter of 3 July

(*Received* 4 *September* 1959)

AFTER reading Mr. HULL's response to our letter commenting on his paper we believe that our different points of view may be settled after defining the terms "new principle" and "new application of an old principle." A new principle is a new basic law, while a new application of an old principle is a new use for an old basic law, possibly by the introduction of a new method of visualizing a phenomenon. In the present case the law of conservation of the marker was enunciated by STEWART in 1897, or possibly as early as 1863 by SCHLOESING as Mr. HULL states. We believe that Mr. HULL's contribution is essentially a new method of measuring flow by the automatic integration of the dilution curve. The total counting technique is, for this reason, another application of the law of conservation of the marker. Whether or not the shape of the dilution curve can offer additional information, such as ruling out artifacts, is something to be decided by each investigator with regard to his particular problem. These points become evident after analyzing the basic flow equation:

$$f = aQ/\int R\,dt$$

with f gal/min, Q μc, R c/min, a $\dfrac{\text{c/min}}{\mu\text{c/gal}}$.

This equation is the same for all flow applications. Whether one writes a as above or as c—gal/min—μc makes no difference; it is quite the same thing.

We are pleased to have the opportunity to introduce to workers in the engineering fields the existing medical literature on the subject of flow measurements.

M. A. GREENFIELD
ISMAEL MENA
Dept. of Radiology
School of Medicine
University of California Medical Center
Los Angeles, California

OL.
7
9/60

book reviews

C. G. Bell Jr. and F. N. Hayes: **Liquid Scintillation Counting.** Pergamon Press, London, 1958. 292 pp. 70s.

This book is a compilation of lectures given by some of the foremost authorities in this field, at the Northwest University Conference on Liquid Scintillation Counting, held at Evanston, Illinois in August 1957 and organized by the editors. It is the first volume ever published on this method of radiation measurement, and while little of the material is completely new, such a comprehensive and up to date survey of the theory, techniques and applications of the method is of immense value to its many users.

The first part of the book is on fundamental principles and the authors deal thoroughly with the basic processes of energy transfer and quenching in the scintillator itself and then with such technical aspects as photomultiplier spectral sensitivity, fluorescence spectra, wavelength shifters, efficiency of reflection and light collection, light guides and photomultiplier noise. This section of the book should be of great interest to practical users.

Instrumentation is the subject of the second part and the relative complexity of coincidence apparatus and some of the relative advantages of single phototube apparatus are described with special emphasis on the counting of the low energy beta emitters, tritium and C^{14}. For estimating these isotopes, counting efficiencies are only significant when corresponding backgrounds are given, and it is to be regretted that the latter are sometimes omitted in this and subsequent sections. Some contributions from individuals identified with commercial firms tend to be biased in favour of particular designs and overemphasize their advantages without mentioning their disadvantages.

Part 3 is entitled "Chemistry of the counting sample" but is more comprehensive than the title would suggest. It includes discussions on solvents, solutes and suspension counting. It covers effects of particle size on light absorption and the stability of gels, methods of counting $C^{14}O_2$, acids and other substances in liquid scintillators, phosphorescence in glass sample containers, oxygen quenching and the use of balance point operation to minimize the effect of quenching and gain variations.

The remaining three chapters, which occupy slightly more than half of the book are concerned with general and specific applications and contributions from laboratories outside the United States. While some of the subject matter is somewhat specialized, most authors have endeavoured to emphasize aspects of their work which are of general interest. This section contains a wealth of useful information on all aspects of the subject which is unfortunately difficult to locate without reading each chapter in detail. An index would have enabled the reader to make much fuller use of the contents. The segregation of "developments in foreign laboratories" in a separate chapter shows a rather insular attitude on the part of the organizers.

In general the presentation is good and there is no serious repetition as sometimes happens in conferences of this type. The diagrams are clear, concise and uniform and in only one paper is the information incomplete; in Figs. 1 and 3 on pages 284 and 286, no keys are given to the numbered details.

John F. Cameron

O. Hart and O. Karstens: **Radioaktive Isotope in der Dickenmessung.** V.E.B. Verlag Technik. Berlin, 1959. DM 24, 304S.

Die Technik der Dickenmessung mit radioaktiven Isotopen ist in vielen Industrien gebraucht die mit der Produktion oder Verarbeitung von Materialen in der Form von Streifen, Blechen, Folien oder Filmen zu tun haben. Verbesserung in Produktqualität, oder das Sparen von Rohstoff- und Lohnkosten, sind die Ergebnisse. Ein Bericht des gegenwärtigen Zustandes dieser verhältnissmässig neuen Technik ist daher begrüsst.

Die Verfasser haben sich keine Anstrengungen in der Literaturforschung und Veröffentlichung der Dickenmessgerätbenutzer und auch der Fabrikanten erspart. Vollkommenheit und Genauigkeit sind Ihre Ziele, obgleich die Klarheit leided, und man gelegentliche Abschweifungen in Bereiche kaum relevant zur Verständigkeit des Hauptthemas findet.

Das Buch ist für Personen bestimmt, die mit dem Gebrauch der Dickenmessgeräte in verschiedenen Niveaus der Industrie, beschäftigt sind. Sie werden hauptsächlich die zweite Hälfte des Buches für einleitende Studien oder als Nachschlagwerk anspornend und brauchbar finden. Die erste Hälfte ist für Jene brauchbar, die nur wenig oder keine vorige Erfahrungen von Strahlen Physik aber gute Kentniss

VOL. 7 1959/

in Allgemeiner Physik und Elementarer Mathematik besitzen.

Das Buch öffnet mit einer kurzen Beschreibung von verschiedenen bekannten Dickenmessgeräten mit und ohne Berührung des Messgutes (12 Seiten).

Kapitel 2 und 3 (100 Seiten) führen den Leser in die Gebiete der "Kern Physik" und "Radioaktivität". Die Eigenschaften von Alpha, Beta und Gamma Strahlen, und auch deren Wechselwirkung mit der gemessenen Substanz (Absorption, Streuung, Sekundärstrahlung) sind erklärt. Der Leser bekommt auch einen Blick in die Werkstatt der modernen Alchemiker, die mit Reaktoren, Bleiziegeln, Periskopen und riesen Manipulatoren künstliche radioaktive Isotopen produzieren und trennen.

Kapitel 4 (28 Seiten) handelt sich um die Physik der Strahlen Nachweisgeräte: Scintillations Zähler, Ionisationskammern und Geiger–Müller-Zählrohren. Wir finden nur wenige, kurze Hinweise auf elektronischen Schaltungen und zum statistischen Verhalten der Strahlenquellen.

Hier verlassen wir die Physik und betreten das Gebiet der Techniker. Kapitel 5 (14 Seiten) ist ein tapferer Versuch die Zwangsjacke der logischen Einteilung über die grosse Auswahl von Isotop-Dickenmessgeräte anzuziehen. (Kapitel 6 = 24 Seiten). Es folgt eine gut illustrierte kritische Übersicht der meisten Europäischen und Nordamerikanischen Instrumenten in gegenwärtiger Produktion.

Nun beginnen wir die Runde der Hauptbenutzerindustrien: (Kapitel 7 = 46 Seiten). Papier, Gummi, Kunststoff und Metall. Die relevanten Herstellungsprozesse und Betriebsanlagen sind beschrieben. Die Stufen wo Dickenmessgeräte eingesetzt werden können, sind vorgestellt und deren Zweck erklärt. Sie mögen als Hilfe für Handbedienung dienen, durch das Geben von sichtlichen oder hörbaren Signalen, wenn Dicke oder Flächengewicht des Produkts von einem vorgeschriebenen Sollwert übermässig abweicht. Logischer Weise folgt bei vielen Anwendungen die automatische Kontrolle der Anlage, wo das Abweichungssignal des Dickenmessgerätes zweckenmässige Kontrollpulse an die Betriebsanlage anwendet. Die Folgerung von Entfernung oder Zeitabstand zwischen Kontroll- und Messpunkt sind betont.

Kapitel 8 (15 Seiten) beschreibt einige Fehlerquellen welche die Messgenauigkeit beeinflussen können. Obgleich der Einfluss von Veränderungen der Lufttemperatur im Luftraum zwischen Strahler und Empfänger sehr sachlich beschrieben und berechnet ist, fehlt eine Erklärung oder grössenmässige Auskunft über den Fehler der durch elektrostatische Aufladungen des Messgutes ersteht.

Auf Seite 251 sagen die Verfasser, dass die Geschwindigkeit auf dem Laufband einer Papiermaschine Messfehler verursachen kann, aber Sie geben keine Erklärungen oder Literaturnachweise um diesen überraschenden Anspruch zu unterstützen.

Kapitel 9 (15 Seiten) berührt die biologischen Wirkungen der radioaktiven Strahlung, Messung der Dosis, Schutzmassnahmen und Gesetzliche Bestimmungen.

Das Buch schliesst mit einer umfassenden und geschickt zusammengesetzten Bibliographie (288 Referenzen).

Im Allgemeinem ist es ein nützliches Werk welches für die Einleitung zum Verstehen und Gebrauch von radioaktiven Dickenmessgeräten in der Industrie empfehlt werden kann.

G. Syke

Techniques of thickness measurement with radioactive isotopes are now used in many industries concerned with the manufacture or processing of materials in the form of strip, sheet, foil or film. Improvement in product quality or saving in raw material and labour cost are the results. A survey of the present state of this relatively new art is thus very welcome.

The authors have spared no effort in compiling publications and information from thickness gauge users and makers alike. Completeness and accuracy are their aims, though clarity suffers and there are some digressions into fields hardly relevant to the understanding of the main subject.

The book is intended for people at various levels in industry, who are concerned with the use of thickness gauges. They will find—particularly the second half—stimulating and useful for introductory studies or subsequent reference. The first half is useful to those having little or no previous knowledge of radiation physics, but are versed in general physics and elementary mathematics.

The book opens with a brief description of known alternative contact and non-contact thickness gauges (12 pages).

Chapters 2 and 3 (100 pages) take the reader into the realms of nuclear physics and radioactivity. The properties of alpha, beta and gamma radiations as well as their interaction with the substance to be measured (absorption, scatter, secondary radiation) are explained. The reader also gets a glimpse into the workshop of the modern alchemists, who—among reactors, lead castles, periscopes and giant manipulators—produce and separate man-made radioactive isotopes.

Chapter 4 (28 pages) deals with the physics of radiation detectors: scintillation counters, ion chambers and Geiger–Müller tubes. There are—all

too brief—references to the associated electronic circuits and source statistics.

Here we leave physics and enter the domain of engineering. Chapter 5 (14 pages) is a valiant attempt to pull the straightjacket of logical classification over the great variety of isotope thickness gauges. This is followed (chapter 6—24 pages) by a well illustrated critical survey of most European and North American manufacturer's current products.

We then (chapter 7—46 pages) make the round of the main user industries: paper, rubber, plastics and metal. The relevant manufacturing processes and plants are described. The stages at which thickness gauges can be installed are pinpointed and their purpose explained. They may serve as an aid to manual control by giving visual or audible signals when the thickness or "weight per unit area" of the product excessively deviates from a preset nominal value. This logically leads in many applications to automatic control schemes, where the error signal of a thickness gauge applies appropriate corrective pulses to the plant. The implications of distance or time lag between control point and gauging point are emphasized

Chapter 8 (15 pages) lists some of the factors which may affect gauging accuracy. Whilst the error due to air temperature changes in the measuring gap is very fully described and calculated, there is no explanation or quantitative information about the error due to electrostatic charge on the measured web. On page 251 it is said that the speed of the web on a paper machine can cause some measuring error, without any explanation or literature reference to substantiate this surprising claim.

Chapter 9 (15 pages) touches on the biological effects of ionizing radiations, measurement of dose, safety measures and regulations.

The book concludes with a comprehensive and skilfully classified bibliography (288 references).

On the whole it is a useful work to be recommended as an introduction to the understanding and use of radioactive thickness gauging in industry.

G. SYKE

K. H. HÖCKER und K. WEIMER: **Lexikon der Kern- und Reaktortechnik,** 2 Bände. Franckh'sche Verlagshandlung, Stuttgart, 1959. DM 125.

DIE ausserordentlich schnelle Entwicklung der Kern- und Reaktortechnik stellt eine beachtliche Leistung einer vernünftig gelenkten Organisation dar. Eine ungewöhnlich grosse Zahl einzelner Spezialgebiete musste für das endgültige Gelingen entscheidend wichtige Beiträge liefern. Neue Forschungsgebiete und neue Erkenntnisse erzwingen oft die Einführung neuer Begriffe. Das gemeinsame Ziel macht es erforderlich, dass die in jedem Fachgebiet sich neu entwickelnden Spezialbegriffe allgemein verständlich sind und irrtümliche Deutungen ausschliessen. Das unter Mitwirkung einer ganzen Reihe namhafter Fachleute entstandene Lexikon versucht, diese Forderung zu erfüllen. Man kann Herausgeber und Verfasser zum Ergebnis ihrer Bemühungen gleichermassen beglückwünschen. Eine reichhaltige Sammlung alter und neuer Begriffe, die heute in der Reaktor- und Kerntechnik eine Rolle spielen, sind alphabetisch aufgeführt und in einer Weise ausführlich erläutert, die ihre mühelose Eingliederung in die Fachsprache des Spezialisten ermöglicht, vor allem den unvermeidlichen Verkehr mit Behörden und allen Teilnehmern am öffentlichen Leben erleichtert, von denen Spezialkenntnisse auf diesem wichtigen Gebiet nicht erwartet werden dürfen. Die Anschaffung kann daher vorbehaltlos allen interessierten Stellen empfohlen werden. Einige harmlose Druckfehler beeinträchtigen den Wert in keiner Weise.

F. STRASSMANN

VOL. 7 1959/

International Journal of Applied Radiation and Isotopes, 1959, Vol. 7, pp. 163–167. Pergamon Press Ltd. Printed in Northern Ireland

Further Abstracts of Papers Presented at the International Atomic Energy Agency Conference on the Application of Large Radiation Sources in Industry and Especially to Chemical Processes

Warsaw, Poland, September 1959

Survey of Recent Trends in Polymer Radiation Work. A. CHARLESBY, U.K.

A brief summary is given of the lines of development in the polymer field. The criteria for the economic production of various materials by radiation are discussed and it is concluded that in the polymer field, the cost of radiation processing should not be excessive. Radiation initiated polymerization is considered and it is pointed out that the new techniques of low temperature polymerization and also the addition of finely divided surfaces to the polymerization media offers considerable possibilities.

The curing of polyester resins and the vulcanization of rubbers are briefly discussed. It is felt that the main emphasis on research should be on systems which are reactive only to radiation. The importance of the investigation of oriented materials is also stressed.

In conclusion it is felt that much more fundamental research is needed and that a closer understanding of the fundamentals of the subject will lead to new lines of development.

Chemonuclear Reactors for In-pile Process Irradiation. L. S. MIMS, U.S.A.

The potential economic incentive for the utilization of nuclear reactors for in-pile irradiation of process streams is discussed. It is assumed that a dual fluid reactor for in-pile irradiation can be constructed and operated for approximately the same cost per thermal kilowatt, as a single fluid reactor for production of steam for industrial heating.

According to a recent study, the cost of thermal energy from nuclear reactors of the pressurized water, boiling water, and organic cooled types is approximately U.S. $1 per million B.T.U. for units of the order of 40 thermal MW. On this basis it is estimated that 80,000 lb of material may be irradiated with 10 Mrad for about U.S. $100.

A dual flow organic cooled reactor is selected for this study. The paper only attempts to establish the economic possibility and typical features of this type of chemonuclear reactor.

Gamma Radiation Sources of the Technological Irradiation Group, U.K.A.E.A. S. JEFFERSON, G. S. MURRAY and F. ROGERS.

The paper describes both the construction and operation of two large radiation units, which are capable of handling quantities sufficient for pilot scale trials. These units are additional to the twenty-three experimental cobalt units ranging in activity from 100 to 10,000 curies each.

The first unit described uses the spent fuel elements from the materials testing reactors DIDO and PLUTO. The second unit uses a Co^{60} γ-radiation source of approximately

150,000 c providing doses in the range of 10,000 rad to 5 Mrad. It is indicated that this unit will be able to give a $2\frac{1}{2}$ Mrad dose to 200 ft^3 of processed material per day.

The Radiation Induced Graft Copolymerization of Methacrylic Acid to Nylon. R. ROBERTS and J. K. THOMAS.

The grafting of methacrylic acid to nylon by the preirradiation technique has been studied. The rate of grafting is appreciably larger than that of homopolymerization. No simple relation exists between reaction rate and total dose. The temperature dependence of the rate of grafting to the fibre, preirradiated in air, indicates that initiation of grafting is likely to take place by decomposition of peroxide groups formed on irradiation.

Electrical resistance measurements on the irradiated fibre indicate that this has been reduced by a factor of 10.

The Use of Ionizing Radiation in the Vulcanization of Silicon Rubber. A. S. KUZMINSKY, T. S. NIKITINA and L. A. OKSENTEVICH, The Rubber Research Institute, Moscow.

The main purpose of the work is a detailed study of the properties of materials obtained by irradiating mixtures of polydimethylsiloxane rubber and various fillers (special silicic acid, titanium dioxide, flue dust, chimney soot and lamp black).

The irradiation was done with a powerful X-ray unit and a Co^{60} γ-ray source of 20,000 g radium equivalent.

The relative speed of formation of the space lattice of the vulcanized material was evaluated (by the size of the equilibrium constant and the maximum degree of swelling in benzene). Changes in tensile strength and specific elongation during the irradiation process were studied. The optimum vulcanization regime was chosen and the basic physico–mechanical characteristics of the vulcanized materials were defined. Changes in the properties of the irradiated vulcanized material during hot ageing at temperatures of 150°, 200° and 250° were studied.

Irradiation in vulcanization removes the necessity for carrying out the process at high temperatures and for keeping the product under controlled temperature conditions for long periods after vulcanization. This new method of vulcanizing allows the use of carbon black as a filler. The use of ionizing radiation makes it possible to simplify the technique of vulcanizing silicon rubber and to improve the properties of the vulcanized material.

Possibility of Commercial Application of Radiation–Thermal Cracking of Normal Hydrocarbons. A. V. TOPCHIEV, L. S. POLLAK, N. YA. CHERNYAK, V. E. GLUSHNEV, I. V. VERESHCHINSLY and P. YA. GLAZUNOV, Institute of Petroleum Chemistry Synthesis of the Academy of Sciences of the U.S.S.R. and Institute of Physical Chemistry of the Academy of Sciences of the U.S.S.R.

At present the commercial application of radiation cracking is determined by the following factors:

(a) possibility of radiation initiating of a chain reaction with an acceptable chain length,

(b) possibility of obtaining high yield of products (particularly, unsaturated products) in readily separable mixture,

(c) possibility of utilizing irradiated fuel elements or other reactor and atomic power station wastes.

As our experimental studies have shown, a chain reaction can be effected by way of radiation–thermal cracking (RTC) in which radiation creates centres which initiate the reaction, while the temperature (200 to 300°C below the temperature of standard thermal cracking) eliminates the activation barriers blocking chain development. By proper choice of dose rate, integral dose and the temperature it has been found possible to ensure a considerable increase in the yield of unsaturated compounds, and in the production of considerable amounts of molecular hydrogen. However, RTC is accompanied by the formation of a perceptible fraction of methane and other low-molecular alkanes.

It has been shown that under proper

VOL. 7 1959/

conditions yields of the order of 10^3 molecules per 100 eV can be obtained after a 2 to 4 min irradiation of an alkane in the gaseous (vaporous) phase.

In prolonged exposures the composition of the RTC products is affected not only by secondary processes caused by the reactions of the RTC products present in the irradiation zone, but also by their protective radiation–chemical action. At such exposures in the linear region some 10–20 per cent of the initial product is transformed. Moreover as the temperature rises the composition of the RTC products approaches that of conventional thermal cracking products.

Preliminary calculations are carried out and the efficiencies of commercial RTC are discussed.

Radio-initiation of Chain-branched Reactions and its Sensitization. E. V. Barelko, L. I. Kartashova, P. N. Komarov and M. A. Proskurnin, Karpov Physico-Chemical Institute, Moscow, U.S.S.R.

This paper describes the results of experiments by the writers with radio-initiation of chain-branched reactions of the oxidation of organic compounds. The function of radiation as an initiating agent is described with reference to the oxidation of several unsaturated hydrocarbons and butanol. The reaction is self-accelerating and proceeds spontaneously after radiation has ceased.

A detailed investigation was made of a process from oxidizing benzene, which has a high radiation resistance.

The writers devised a method of sensitizing the radio-initiation of the oxidation of radiation-resistant substances by chemically inert but non-radiation-resistant substances.

The main quantitative features of the process for the radio-oxidation of benzene are stated to be the accumulation of various reaction products, and the effect of temperature, pressure, power and radiation dosage on the process of such accumulation. Information was obtained about the mechanism of the process. The design of circulating equipment is described. (Translated from Russian.)

Ethylene Polymerization by Gamma Irradiation. S. S. Medvedev, A. D. Abkin and P. M. Khomikovsky.

Radiation polymerization of ethylene has some advantages over other methods of polyethylene production for it yields high purity product and requires comparatively low pressure (100 to 300 atmospheres) and room temperature. For these reasons the investigation of the process is of great interest.

The main obstacle for the commercial production of radiation polyethylene is the low initiation rate (according to preliminary data, it equals 1 to 2 radicals per 100 eV). To increase the rate initiation polymerization was carried out in solutions of organic substances (alcohols, acetone, aliphatic hydrocarbons). It was shown that at a constant pressure of 50 atm and room temperature the rate of the process in solution is ten to fifteen times higher than in the gaseous medium. This is due to an increase in the rate initiation, and to a higher concentration of ethylene in the solution (at a constant concentration of 0·17 g/cm^3 and 25°C the rate of the process in a 60 per cent heptane solution is three to four times higher than in gas). However, the resulting polymers have low molecular weight and poor mechanical properties.

A detailed study was made of ethylene polymerization when irradiated with a cobalt-60 source in gas, pressure (50 to 300 atm), dose rate (20 to 160 r/sec) and temperature (0 to 50°C) being the variables. The rate of the process, the radiation–chemical yield and mean molecular weight of the polymers exhibit a sharp increase with pressure (from 50 to 200 atm the rate of polymerization is proportional to the fourth power of ethylene concentration). The polymerization rate depends but little on the dose rate (it being proportional to the 0·3 power of the dose rate), while the radiation–chemical yield and mean molecular weight of the polymers increase as the dose rate drops. The rate of the process and the

molecular weight show some increase as the temperature rises.

The possible explanation of the kinetic regularities observed is discussed in the report.

Radiation polyethylene is distinguished from high pressure one by increased density and crystallization. The polymer with a characteristic viscosity of over 1 (obtained at a pressure of 100–200 atm) is similar by its chemical properties to high-pressure polyethylene.

The Main Technological Characteristics of Apparatus for Industrial Radiochemical Processes, in Particular Ethylene Polymerization. N. P. Syrkus, A. K. Breger and B. I. Weinstein, Karpov Physico-Chemical Institute, Moscow, U.S.S.R.

The paper gives a general review of some of the main technological features of apparatus, for instance spherical apparatus, for industrial radiochemical processes.

A method is proposed for estimating the effectiveness of apparatus of any given construction by comparing it with the output of an infinitely large apparatus having the same radiation source.

An account is given of the technological features of an apparatus for radiopolymerizing ethylene at 200 atmospheres and 25°C* with a rod-shaped γ-radiation source (Co^{60}) of variable activity. This apparatus can be designed to suit the mean dose rate which the power efficiency of the apparatus allows.

It is shown that the yield Q of the apparatus is, other things being equal, a constant ratio of the power W_0 of the γ-radiation of the apparatus. In the apparatus reviewed, $Q \sim W_0^{0.5}$. (Translated from Russian.)

Indium–Gallium Radiation Circuit of IRT Nuclear Reactor. A. K. Breger, Y. S. Ryabukhin, S. G. Tulkes and E. N. Volkov.

(1) On the basis of an earlier published theoretical paper† an indium–gallium radiation circuit—a new type of high activity γ-source (without neutrons)—has been developed for the IRT nuclear reactor.

The first indium–gallium radiation circuit (model PK-I) is now under construction for the IRT reactor of the Institute of Physics of the Georgian Academy of Sciences.

(2) The operating principle of the radiation circuit is as follows: a eutectic liquid indium–gallium alloy (melting point 16·5°C) circulating in a closed circuit, is activated by stray neutrons in the reflector and releases its γ-energy in an irradiator placed in a chamber shielded from the neutron radiation of the reactor.

(3) Calculation of the activation of indium–gallium alloy. Calculation of the radiation circuit. Provision for the highest possible specific radiation power of the circuit (i.e. the power in the irradiator divided by the total amount of the alloy in the circuit) under the condition of maximum utilization of stray neutrons with allowance made for technical feasibility of the design.

(4) Structural elements of radiation circuit: activity generator, irradiator, electromagnetic pump, compensator, auxiliary systems (for forcing the alloy in and out by pumping argon, for rinsing the circuit with oxalic acid solution and distillate) and control and indication devices. Selection of structural materials. Assembly of radiation circuit elements in reactor tank and in "hot" chamber.

(5) Feed system for liquid and gaseous substances in irradiation zone. Transportation of solid irradiation objects.

(6) Estimation of indium–gallium radiation circuit. At IRT reactor power of 2000 kW the radiation power of the circuit is equivalent to a γ-radiation source of approximately 20,000 g of radium.

(7) The possibility of using the IRT indium–gallium radiation circuit for experimental and pilot units. The possibility of using radiation circuits in general, their

VOL. 7 1959/

* See "The polymerization of ethylene by gamma-radiation", S. S. Medvedev, A. D. Abkin and P. M. Khomikovski (CW/IIB/82).

† Ryabukhin Yu. S. and Breger A. K. *Atomnaya Energiya* **5** (5), 533 (1958).

advantages and disadvantages compared to sources with solid long-lived isotopes.

(8) Transition to a radiation reactor, i.e. to a reactor with a γ-ray carrier introduced into the core.

Some Problems of Calculation and Design of High Activity Gamma Units. A. V. BIBERGAL, N. I. LESHCHINSKY, U. Y. MARGULIS and V. G. KHRUSHEV, U.S.S.R.

The report describes the principal requirements for γ-units intended for various purposes.

Several methods of calculating the dose fields for various forms of irradiators are given, as well as graphs, nomograms and formulae to estimate the amount of γ-ray dose absorbed by the irradiated object from cobalt-60 and caesium-137. Some of the calculated data have been confirmed by experiment.

The advantages of irradiators of various geometry employed in experimental and commercial units are discussed.

The irradiation technique for various objects is analysed and the optimum irradiation conditions (radiation utilization factor, dose field homogeneity, etc.) are discussed.

Several rational shielding systems are suggested to simplify the irradiation process and recharging, and to reduce the cost of design and operation.

Cobalt-60 and Caesium-137 Gamma Sources. E. E. KULISH and G. M. FRADKIN, U.S.S.R.

The paper gives the main technical characteristics of γ-sources produced in the U.S.S.R. using cobalt-60 and caesium-137 and discusses some of the problems of their production technology.

The paper contains information on the radiation spectra of Co^{60} and Cs^{137} and of the source material from which they are prepared. Data are given on the dependence of the activity of cobalt sources upon the intensity of the neutron beam and the geometrical size of the sample. The yield of caesium by uranium fission is also analysed. The problem of hermetic sealing of the sources is discussed and a complete nomenclature is listed of all the sources manufactured in the U.S.S.R., their size and activity also being indicated. In conclusion a comparison of Co^{60} and Cs^{137} sources is made.

NOTE

After Volume 7 No. 1 of *International Journal of Applied Radiation and Isotopes* had been sent to press, it was learnt that certain papers (abstracts of which were included in Volume 7 No. 1) had been withdrawn from the Conference. The papers were:

P. HAYDEN and R. ROBERTS: The synthesis of non-random copolymers in emulsion systems by gamma radiation.

J. A. HEARNE and R. W. HUMMEL: Production of polymers by irradiation of heptane–$TiCl_4$–monomer mixtures.

AKIBUMI DANNO: Design and use of 10-kc source of cobalt-60.

G. DE GAUDEMARIS and CHARLES WALTHER. Polymerization of olefines by radiation.

forthcoming papers

TIEN-CHENG KAO, KUANG-CHU WANG, SHEH-FANG YANG and JUI-SAN CHEN: Iodine-131 thyroid uptake study of endemic goiter patients.

JEANNE C. BATEMAN, HARRY N. CARLTON, RALPH C. CALVERT and GORDON E. LINDENBLAD: Investigation of distribution and excretion of C^{14} tagged triethylene thiophosphoramide following injection by various routes.

P. HAYDEN and R. ROBERTS: The synthesis of non-random copolymers by the gamma irradiation of emulsion systems—II.

M. LEFORT et X. TARRAGO: Dosimétrie des rayonnements au moyen de matières plastiques—I. Détermination de la dose point par point dans une enceinte irradiée aux rayons gamma du radiocobalt.

SEIZO OKAMURA and SHIGERU FUTAMI: Ionic polymerization of styrene in methylene dichloride by ionizing radiation.

P. A. OSINSKI: Detection and determination of tritium labelled compounds on paper chromatograms.

H. J. M. BOWEN: Biological fractionation of isotopes.

VOL
7
1959/

International Journal of Applied Radiation and Isotopes, 1960, Vol. 7, pp. 169–181. Pergamon Press Ltd. Printed in Northern Ireland

The Isotope Dilution Method and Its Application to Analysis of Inorganic Substances

I. P. ALIMARIN and G. N. BILIMOVITCH
Institute of Geochemistry and Analytical Chemistry of the Academy of Sciences of the U.S.S.R.

General principles of isotope dilution with radioactive and stable tracers are considered.

The importance of the purity of recovered substances and the dependence of accuracy on various factors are discussed.

Practical application of the isotope dilution method to analysis of inorganic substances is briefly discussed. Determinations of antimony, yttrium, tantalum and niobium are given as illustrations.

LA MÉTHODE À DILUTION D'ISOTOPES ET SON APPLICATION AU DOSAGE DES MATIÈRES INORGANIQUES

Une déliberation est faite sur les principes généraux de la dilution d'isotopes avec des indicateurs radioactifs et stables.

On discute l'importance de la pureté des matières retrouvées ainsi que la dépendance de la précision sur différents facteurs.

On parle brièvement de l'application pratique de la méthode à dilution d'isotopes au dosage des matières inorganiques. On montre comme exemples des dosages d'antimoine, d'yttrium, de tantale et de niobium (columbium).

МЕТОД ИЗОТОПНОГО РАЗБАВЛЕНИЯ И ЕГО ПРИМЕНЕНИЕ ДЛЯ АНАЛИЗА НЕОРГАНИЧЕСКИХ ВЕЩЕСТВ

В работе рассматриваются общие принципы метода изотопного разбавления с применением радиоактивных и стабильных изотопов.

Обсуждается значение чистоты выделяемых соединений, точность метода в зависимости от различных факторов.

Кратко рассмотрено практическое применение метода изотопного разбавления для анализа неорганических веществ и приведены примеры определения сурьмы, иттрия, тантала и ниобия.

ISOTOPEN-VERDÜNNUNGS-METHODE UND IHRE ANWENDUNG BEI DER ANALYSE VON ANORGANISCHEN SUBSTANZEN

Allgemeine Gesetze der Isotopenverdünnung mit radioaktiven und stabilen Indikatoren werden betrachtet. Der wichtige Einfluss der Reinheit der wiedergewonnen Substanz und die Abhängigkeit der Genauigkeit von verschiedenen Faktoren wird besprochen.

Die praktische Anwendung der Isotopenverdünnungsmethode für die Analyse anorganischer Stoffe wird diskutiert. Als Illustration wird die Bestimmung von Sb, Y, Ta, und Nb angegeben.

VOL. 7 59/60

CONVENTIONAL methods of inorganic analysis are known to involve complete recovery of the substance investigated.

However this is a matter of some difficulty. Often very small amounts of impurities cannot be recovered from the bulk of the main substance without considerable losses in the course of analysis. The isotope dilution method making use of stable and radioactive tracers would be of great

help in the solution of complicated analytical problems of this kind.

The isotope dilution method is widely applied in:

(1) biochemistry, for analysis of complicated mixtures of substances, including those of great importance from the biological standpoint, such as vitamins, antibiotics, insecticides;
(2) organic chemistry, for analysis of complex mixtures, for example of amino and fatty acids, and for polymers;
(3) inorganic chemistry, as a check on conventional analytical methods, especially for quantitative determination of difficultly separable elements exhibiting similar properties, and also for determination of elements that are not yet quantitatively detectable by available methods, first of all of rare elements.

The isotope dilution method now comes into use not only in chemical analysis, but also in emission-spectral, and mass-spectral analysis.[1,2]

In a variety of cases the method can be used for determining various constants of use in analytical chemistry, for example the instability constant for complex compounds.[3,4]

A mass-spectrometer is used for stable tracer measurements and a Geiger–Müller counter for radioactive tracers. The latter is not so expensive and less time consuming.

The fact that radioactive tracers can be detected at much higher dilutions than corresponding compounds labelled with stable isotopes is also in the favour of the former. The recovered amounts of the elements can be determined by weight methods (electrolysis, spectrophotometry, polarography) or by some other appropriate chemical or physico–chemical technique.

Proper purification is obtained by means of precipitation, extraction, electrolysis, ion exchange chromatography, ionophoresis, distillation, crystallization, etc.

Various modifications of the isotope dilution method and their application to analysis of inorganic substances will be considered here, leaving aside its possible use in organic chemistry, medicine, biology and biochemistry, since this has already been extensively described in reviews.[5–8]

VOL. 7 1959/

1. DILUTION WITH RADIOACTIVE ISOTOPES (DIRECT ISOTOPE DILUTION)

This variant found widest application in quantitative organic and inorganic analysis. The method is based on variations in the initial specific activity of the tracer, as a result of dilution with the inactive compound under investigation.

(1) The most simple case would be that when the amount of the active compound added is so small compared with the unknown inactive substance, that it can be disregarded, the amount of the recovered active compound being directly proportional to that of the recovered inactive compound.

Calculation would then be made by the equation

$$W_2 = W_3 \frac{A_1}{A_3} \qquad (1)$$

where W_2 is the amount of the element to be determined; W_3 is the amount of the recovered element; A_1 is the activity introduced with the tracer; A_3 is the activity of the recovered compound.

(2) If the diluting substance amount is not to be disregarded, a certain amount (W_1) of the radioactive isotope will be added to an unknown amount (W_2) of the elements to be determined, the specific activity of W_1 having a value of $S_1 = A_1/W_1$ being determined previously.

The equation for calculating the amount of the element to be determined will be

$$W_2 = W_1 \left(\frac{S_1}{S_2} - 1 \right) \qquad (2)$$

W_1 and S_1 being known and after determining S_2, it will be possible to calculate W_2 by (2).

Calculation of $S_2 = S_3 = A_3/W_3$ can be readily made by precipitating, for instance, a certain part of the mixture of $(W_1 + W_2) = W_3$, weighing the precipitate and measuring its activity.

The difference between the straightforward radiometric correction and the isotope dilution method lies in the need for the latter to subtract the amount of the labelled substance added. In practice choice of the calculation mode would depend upon the specific activity of the tracer.

Radioactive atom concentrations are usually so small (not exceeding 1 per cent) that they have no effect on the molecular weight of the sample, whereas in the case of stable isotopes changes in molecular weight cannot be neglected and appropriate corrections would be necessary. GEST *et al.* have developed mathematical computation methods for investigations making use of stable isotopes.[9]

The formula for computation is somewhat different:

$$W_2 = W_1 \left(\frac{E_0}{E} - 1\right) \frac{M_1}{M_2} \qquad (3)$$

where M_1 is the molecular weight of the inactive compound and M_2 is the molecular weight of the active compound. The atomic percentages of the given stable isotopes in the labelled (E_0) and unlabelled (E) compounds are introduced in place of specific activities.

The M_1/M_2 ratio will be of practical importance if there is a marked difference between the molecular weights of the two isotopic compounds and the atomic percentage of the excess in the carrier is high. At low isotope concentrations the M_1/M_2 factor can be disregarded.

2. DILUTION WITH INACTIVE ISOTOPES (REVERSE ISOTOPE DILUTION)

A modification of the isotope dilution method will be used for determining small amounts of substances that cannot be recovered from the complicated multicomponent mixture in their pure form.

Dilution with inactive isotopes is usually applied for determining radioactive isotope yields in radiochemical investigations on nuclear transformations. Inactive carriers are also widely used for recovery and determination of radioactive isotopes in radioactivation analysis.

(1) For determining the radioactivity of a compound in a mixture with other active substances, an inactive isotope carrier is added to the solution investigated, in an amount greatly exceeding that of the active compound, and the element to be determined is then recovered. In this case the amount of the recovered carrier will be a direct measure of the recovered active compound.

Calculations can be made by the following equation:

$$A_1 = A_2 \frac{W_{\text{add}}}{W_{\text{rec}}} \qquad (4)$$

where A_1 is the total activity of the element to be determined; A_2 is the activity of the precipitate recovered; W_{add} is the amount of the carrier added; W_{rec} is the amount of the carrier recovered.

(2) For the determination of a separate radioactive compound with a known specific activity in a mixture with other radioactive compounds, analysis is carried out as follows. A certain amount of the inactive carrier is added to the mixture, a part of the mixture sufficient for isotopic analysis is withdrawn and the specific activity is determined.

The amount of the initial substance can be calculated from (2) making use of the following notations:

W_2 for the amount of the element to be determined; $S_1 = A_1/W_2$ for its specific activity; W_{add} for the weight of the added carrier; S_2 for the specific activity upon dilution

$$W_2 = \frac{S_2}{S_1}(W_{\text{add}} + W_2). \qquad (5)$$

Then

$$W_2 = W_{\text{add}} \left(\frac{S_2}{S_1 - S_2}\right). \qquad (6)$$

If the amount of the carrier added greatly exceeds that contained in the sample, i.e. $W_{\text{add}} \gg W_2$, then W_{add} can be introduced

into equation (5) in place of the sum of $(W_{add} + W_2)$, and the desired equation will become

$$W_2 = \frac{S_2}{S_1} \cdot W_{add} \cdot \qquad (7)$$

This variant would require knowledge of the initial specific activity and for that reason it is often used in metabolic investigations, where direct quantitative recovery is very difficult due to the very small amount of the substance to be determined. This method is also of great help as a check on the purity of radioactive tracers and of the stability of compounds labelled with radioisotopes.[10,11]

3. MULTIPLE DILUTION WITH INACTIVE ISOTOPES (DOUBLE ISOTOPE DILUTION)

The initial specific activity is often unknown. In this case the amount of the element to be determined can be established by multiple isotope dilution of the investigated mixture aliquots.

Analysis is carried out as follows: different but known quantities of inactive isotopes are added to two equal investigated mixture aliquots (a ten or twenty-fold excess compared with the amount of the element to be determined is recommended). Parts of the mixture $(W_2 + W_{add_1})$ and $(W_2 + W_{add_2})$ are withdrawn and their specific activities S_1 and S_2 are measured. The following formula is used for calculations:

$$W_2 = \frac{S_2 W_{add_2} - S_1 W_{add_1}}{S_1 - S_2} \cdot \qquad (8)$$

Analogous equations are obtained for the case when equal amounts of carrier are added to different amounts of radioactive substances. The main advantage of this method as compared to the one described above is the possibility of working with microconcentrations (<1 mg).

VOL. 7 1959/

4. A DERIVATIVE DILUTION METHOD

A labelled reagent of a known specific activity is added to the mixture. The role of the radioactive reagent is to determine the specific activity of the unknown constituent by forming a radioactive derivative. Double labelling is applied as a check on the complete formation of this derivative and its identification.

A carrier is introduced if the labelled derivative cannot be recovered in its pure form. Mathematically this variant is identical to dilution with inactive isotopes (reverse isotope dilution) when the initial activity is known. The derivative dilution method is very sensitive and permits determination of the smallest amounts of substances. The method is very spectacular but for the present not widely applied, being used mainly in biological investigations.[12]

5. MULTIPLE DILUTION METHOD FOR DETERMINING SMALL AMOUNTS OF IMPURITIES

The method is based on different changes in the tracer specific activity arising from dilution of its different amounts with equal aliquots of the substance under investigation. If m_1 mg of the appropriate radioactive isotope with a specific activity of S_0 are added to a solution containing X mg of the substance investigated, the specific activity of the mixture will become

$$S_1 = \frac{S_0 m_1}{m_1 + X}.$$

If the amount added is m_2 mg the specific activity will be

$$S_1 = \frac{S_0 m_2}{m_2 + X}.$$

By recovering from both solutions equal amounts (Ymg) of the substance investigated, it would be possible to determine the amount of the initial substance directly from the activities of these amounts.

The activity of the substance recovered from the first solution will be

$$A_1 = S_1 Y = \frac{S_0 m_1}{m_1 + X} Y$$

and of that from the second

$$A_2 = S_2 Y = \frac{S_0 m_2}{m_2 + X} Y.$$

Solving a system with two equations for two unknown quantities, we obtain

$$X = \frac{m_1 m_2 (A_1 - A_2)}{A_1 m_2 - A_2 m_1} = \frac{m_2 (A_2 - A_1)}{B A_1 - A_2}.$$

Since under definite conditions the sample activity will be proportional to the counting rate

$$X = \frac{m_2 (I_2 - I_1)}{B I_1 - I_2} \qquad (9)$$

where I_1 and I_2 are counting rates of the samples recovered from solutions 1 and 2 respectively. Thus to determine unknown quantities of the substance investigated it would only be necessary to know the amount of m_1 and m_2 and to measure the counting rate of I_1 and I_2.

Optimal conditions for use of the given equations would be $m_1 = X$ and $m_2 \gg X$.

This technique eliminates the main disadvantage of isotope dilution, i.e. necessary measurements of the specific activity, whilst permitting at the same time determination of small quantities of the order of 10^{-5}–10^{-7} per cent.[13] Its own drawback is the necessity of devising in each case some methods for the recovery of equal amounts of the substance investigated.

SELECTION OF THE ISOTOPE

First of all the tracer used should be of a very high chemical and radiochemical purity.

The half-life periods of radioactive isotopes should be sufficiently long, of the order of several days and up to a year, and their energy of radiation should be readily measurable. In the case of short-lived radioisotopes a correction for decay should be made by the well-known formula for the general law of radioactive decay

$$A = A_0 \exp(-\lambda t). \qquad (10)$$

Simultaneous measurements of the recovered samples and of a standard prepared beforehand proved to be more adequate in practice than calculations of the corrections by the above formula.

Knowledge of the tracer oxidation degree is very important. If there are several valency states, as in the case of iron, cerium, etc., analysis should be carried out under conditions assuring identical valency both of the tracer and of the element investigated. In order to ensure rapid and reliable exchange of the stable and active atoms, the tracer should be introduced as a compound identical to the one investigated, and should correspond to an appropriate formula composition. For example $HP^{32}O_3$ impurities in $H_3P^{32}O_4$ are inadmissible.

In biological and biochemical investigations the labelled compound should not be subject to oxidation and decomposition under conventional conditions.

The accuracy of the method is in a high degree dependent upon the tracer specific activity. Thus it would be feasible to use carrier-free radioactive isotopes, or else their specific activity must be sufficiently high.[14–16]

Another question arises as to the stability of radioactive tracers under given storage conditions. This problem is of special importance for aqueous solutions due to possible occurrence of radiation-induced processes. In order to avoid this difficulty solutions should be diluted to 1 Mc/ml, and high activity preparations kept in the cold.

PURITY OF RECOVERED COMPOUNDS

The purity of recovered compounds and its effect on the accuracy of the isotope dilution method are of great importance. The principal requirement of this method is to obtain recovery of sufficiently pure substances. If the one active isotope added is an inactive compound, inactive admixtures of other substances can have no marked effect on the accuracy of analysis (after multiple purification of the recovered compound). Only usual errors connected with quantitative analysis, such as inaccurate weighing, unreliable colorimetric determinations, etc. will then have to be considered.

Combination of various methods such as precipitation, extraction, electrolysis, crystallization, distillation, chromatography, etc. enables the attainment of constant specific activity. This can serve as a measure of the purity of the recovered compound. These considerations do not pertain to multiple dilution with radioactive isotopes, when the only requisite would be the recovery of equal quantities, and chemical purity is of no special importance.

ACCURACY OF THE METHOD

Dependence of the accuracy of the radioactive isotope dilution method on various factors, such as the amount of the recovered element, its content in the initial samples, the ratio of the element to tracer amounts in the solution under investigation, etc. was determined by means of precipitating bismuth and lead with organic and inorganic reagents.[17] Bi^{210}(Ra*E*) with $E_\beta = 1{\cdot}17$ MeV, and Pb^{212}(Th*B*) with $E_\beta = 0{\cdot}355$ MeV and $0{\cdot}589$ MeV were used as active tracers. The geometry of measurements, and also the sample weight were shown to become of great importance in measurements of β-active preparations. Repeated preparation of a standard yielding a precipitate similar to that from the sample was avoided by drawing a standard plot for the dependence of self-scattering and self-absorption on the sample weight. A correction factor permitting determination of the true activity, was found from this plot and the known weight of the sample. Another technique would be the drawing of a standard plot for the dependence of the precipitate weights on specific activity. This is also very convenient, since when the specific activity of the recovered compound is found, the initial amount of the element can readily be obtained directly from the plot. To establish the effect of the element amounts to be determined on the accuracy of the method, different quantities, from 1 to 20 mg, were precipitated and measured. The recovery of bismuth in experiments 1, 2, 4, 5 and 8 was carried out by the pyrogallic method. In all other experiments cited in Table 1 bismuth was separated as benzene sulphinate $Bi(C_6H_5SO_2)_3$. Best results can be seen to be obtained with amounts of 8–10 mg.

For amounts less than 0·5 mg the error is from 5 to 10 per cent. Amounts exceeding 20 mg are inconvenient on account of the considerable weight of the precipitate. Moreover the accuracy would be affected by decrease in specific activity.

In studying the dependence of accuracy on the recovered compound specific activity determination of the amounts sought was made graphically. The range of element concentrations was chosen depending upon the amounts to be determined. Lead was precipitated as benzene sulphinate by a specially devised technique.

The same amount of tracer was added to solutions containing different amounts of lead.

After the specific activity of recovered precipitates was determined, the amount of the element investigated was found from the plot. The results obtained are summarized in Table 2.

The accuracy of the method can be seen to decrease with decreasing specific activity. Sufficient accuracy is obtained with a specific activity of 400 imp./min per mg. To find out its dependence on the ratio of

VOL. 7 1959/6

TABLE 1. Dependence of the accuracy of the method on the element content of the sample

No. of experiment	Bismuth taken W_2	Bismuth recovered W_3	Activity introduced with the tracer (A_1) (imp./min)	Activity of the recovered compound (A_3) (imp./min)	The amount of Bi found W_2 (mg)	Error (%)
1	17·35	17·15	6913	6870	17·23	−0·7
2	17·35	16·95	6913	6925	17·09	−1·5
3	16·92	11·09	7274	4690	17·17	+1·5
4	8·57	8·57	6987	6984	8·57	0
5	8·57	8·72	6987	7070	8·85	+3·3
6	8·46	5·54	3625	2322	8·65	+2·2
7	4·23	2·37	1778	914	4·62	+9·2
8	4·23	1·80	1778	703	4·56	+7·8
9	1·74	1·36	6913	5007	1·85	+6·6

TABLE 2. Dependence of the accuracy of the method on the specific activity of compound recovered

No. of experiment	Lead taken (mg)	Specific activity of the compound recovered S_2 $\left(\frac{\text{imp./min}}{\text{mg}}\right)$	$\frac{1}{S_2}$ $\left(\frac{\text{mg}}{\text{imp./min}}\right)$	W_2 found	Error (%)
1	7·30	981	$10{\cdot}4 \times 10^{-4}$	7·2	−1·2
2	8·04	819	$12{\cdot}2 \times 10^{-4}$	8·0	−0·4
3	11·28	521	$19{\cdot}4 \times 10^{-4}$	11·6	−2·8
4	14·69	388	$25{\cdot}8 \times 10^{-4}$	14·9	+1·4
5	18·74	302	$31{\cdot}8 \times 10^{-4}$	17·9	−4·7
6	17·68	299	$33{\cdot}4 \times 10^{-4}$	18·7	+6·3
7	19·10	270	$37{\cdot}1 \times 10^{-4}$	20·5	+6·9

element to tracer amounts various quantities of inactive carrier were added to a carrier-free bismuth isotope. The tracer was then added to the investigated solution in such amounts as to obtain ratios of element amounts introduced with the tracer to that contained in the initial solution of 1 : 5, 1 : 2, 1 : 1. Bismuth was precipitated as pyrogallate.

The results are summarized in Table 3.

The optimal ratio would obviously be $W_1 : W_2 = 1 : 5$.

In determining small amounts of elements by dilution with inactive isotopes the accuracy of the method is dependent on the degree of dilution, since excessive dilution would lead to algebraic identity (see equation (8)). Best results are obtained at maximum twenty-fold dilution, on condition that $W_{\text{add}_1} = 2W_{\text{add}_2}$ and that the radiometric measurements are accurate to ~1 per cent. The method will then be accurate within 20 per cent.

On multiple dilution with radioactive tracers maximum variations in specific activity at small variations in the amounts of the substance under investigation would ensure the greatest accuracy. Considerable

TABLE 3. Dependence of the accuracy of the method on the ratio of the investigated element to tracer amounts

No. of experiment	$W_1 : W_2$	Bismuth taken W_1 (mg)	Bi + Bi * recovered (mg)	Initial specific activity S_1 $\left(\frac{\text{imp./min}}{\text{mg}}\right)$	Final specific activity S_2 $\left(\frac{\text{imp./min}}{\text{mg}}\right)$	Bismuth found W_2 (mg)	Error (%)	Bismuth taken W_2 (mg)
1	1 : 5	1·69	8·97	3190	535	8·37	−1·1	8·46
2		1·69	8·98	3190	532	8·44	−1·2	8·46
3	1 : 2	3·38	8·62	1735	589	6·61	−2·4	6·77
4		3·38	8·63	1735	584	6·66	−1·6	6·77
5	1 : 1	5·08	8·89	1670	887	4·48	−11·8	5·08
6		5·08	8·65	1670	797	5·58	+9·2	5·08

difficulties arise in developing a method for the recovery of identical amounts of the substance from solutions having various concentrations. However, in this case the amounts of recovered substances are not essential and the presence of other impurities would not interfere; of importance are only the equality of these amounts and incomplete separation. This technique is accurate to about 20 per cent.

In the two methods, both for multiple dilution with inactive isotopes and for dilution with active isotopes a very important part is played by statistics of the radiometric measurements.

VOL. 7 1959/

APPLICATION OF THE ISOTOPE DILUTION METHOD TO ANALYSIS OF INORGANIC SUBSTANCES

Let us consider works on inorganic analysis carried out recently in various countries and in the U.S.S.R.

A fair amount of these works is concerned with application of the isotope dilution method in conjunction with mass-spectral determination of small quantities of elements.[18]

For instance the determination of microquantities of lead by the isotope dilution method was described in 1955.[19] Ra*D* (Pb^{210}) was added to the solution under investigation and lead was recovered chemically. The precipitate was then subjected to isotopic analysis by means of a mass-spectrometer.

The amount of lead was calculated from the isotope ratio found and the quantity of Ra*D* added. This technique permitted determination of 10^{-7} g of lead with an error within 10–20 per cent. Rubidium[20] in sea water was determined by the isotope dilution method. The samples analysed mass-spectrometrically contained about 0·01 μmg of Rb_2SO_4. A stable rubidium isotope contained 15·05 per cent of Rb^{85} and 84·9 per cent of Rb^{87}. Lithium[21] and rubidium[22] in sea water and graphite were determined by dilution with stable isotopes. The results obtained are in good agreement with those yielded by radioactivation analysis. The accuracy was $\pm$1–2 per cent. In the case of lithium the sensibility was 3×10^{-10} g.

The isotope dilution method using U^{233} with subsequent application of the mass-spectrometric technique for simultaneous determination of the total amount and ratios of U^{234}, U^{236} and U^{238} in solutions formed in the reprocessing of fuel rods enriched with U^{235}, were described recently. Prior to determination uranium was separated from other fission products and foreign elements by extraction in a 3 per cent solution of tributylphosphate in *n*-hexane. The method can be used at uranium

concentrations in the range of 0·001–350 mg/ml. The duration of one assay is 2 hr.[23] Strontium in sea water[24] was determined by the isotope dilution method making use both of active and of stable isotopes. A number of works was concerned with the determination of gases. For example small amounts of oxygen in copper,[25] radiogenic helium in zircon,[26] etc. were determined by the isotope dilution method with an accuracy within ±2–3 per cent.

In chemical analysis the method of dilution with radioactive isotopes was applied for determining cobalt[27] after electrolytic recovery and separation from interfering elements. The initial amount of cobalt was found by the calibration curve. The samples analysed contained from 0·14 to 0·47 per cent of Co. The absolute error was 0·02 per cent.

Mo^{99} was used for determining molybdenum in steel.[28] The amounts determined were from 1 to 20 mg. The activity was measured from β- and γ-radiations. Molybdenum was determined after precipitation with hydrogen sulphide.

Ruthenium[29] in diluted solutions was determined upon distillation and also after electrolytic recovery of ruthenium on the cathode. The error was ±5 per cent. Isotope dilution was also used in assaying mixtures of Ca–Sr upon repeated precipitation of strontium as nitrate. Fair results were also obtained for semi-microquantities of Ca–Sr.[30]

KHALIZOVA and SENYAVIN determined yttrium in mineral raw material[31] by the isotope dilution method after chromatographic separation from other elements. Yttrium was determined simply by finding out the maximum activity fraction representing pure yttrium on the yield curve. Table 4 shows comparative data on the determination of yttrium content in a mixture of rare-earth elements. The two sets of results were obtained by means of X-ray analysis and by the isotope dilution method, upon chromatographic separation.

ZIMAKOV and ROZHAVSKY[13] devised a method of multiple dilution with radioactive isotopes and determined small quantities of antimony impurities in lead (10^{-5} per cent). Antimony was extracted with toluene as a complex with methyl-violet from a solution of HCl 1 : 9. A special technique was previously devised for recovering equal amounts of antimony from solutions of various concentrations. The results obtained are summarized in Table 5. The method is accurate within 10 per cent.

TABLE 4. Determination of yttrium by the X-ray and chromatographic methods

	Yttrium content		
X-ray method	80	50	30
Chromatographic method (isotope dilution)	88	48	33

Most expedient is the isotope dilution method in investigations on difficultly separable elements exhibiting similar properties, when purity and quantitative recovery exclude each other. The authors of this paper have applied the isotope dilution method to determination of Nb–Ta, Nb–Zr, Ta–Zr pairs. Nb^{95}, Ta^{182} and Zr^{95} were used as tracers. The latter was previously purified from daughter niobium by multiple co-precipitation of Nb^{95} with MnO_2. Radioactive isotopes were introduced as complex compounds of the same form as the stable isotope in question. Tantalum and niobium were precipitated with an ammonium salt of the benzene seleninic acid 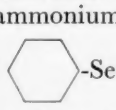 -SeO_2NH_4 first applied in 1956 by ALIMARIN and SOTNIKOV to determination of titanium, iron, zirconium and a number of other elements.[33–36] The authors of this paper have studied in detail the precipitation of niobium and tantalum from various complex-forming media such as tartaric, oxalic, trioxyglutaric acids, with addition, or in the absence of mineral acids. Tantalum is precipitated more readily and completely than niobium.

On recovery from solutions of oxyacids without addition of a mineral acid the

TABLE 5. Determination of antimony impurities in lead

Weighed portions of lead (g)	Amount of active antimony introduced γ		Activity of the aliquot recovered (imp./min)		Sb found in the weighed portion (%)	Mean content of Sb impurities (%)	Results of spectral analysis (%)	Results of colorimetric analysis (%)
	m_1	m_2	I_1	I_2				
10	6	12	380	450	0·000027			
10	6	24	380	510	0·000031	$2·9 \times 10^{-5}$	—	—
10	12	24	450	510	0·000029			
10	30	60	52	81	0·00070			
10	30	60	42	64	0·00066	$6·6 \times 10^{-4}$	$6·5 \times 10^{-4}$	$8·0 \times 10^{-4}$
5	30	60	99	131	0·00057			
10	60	90	72	101	0·0038			
5	30	60	57	97	0·0028	$3·4 \times 10^{-3}$	$3·0 \times 10^{-3}$	$3·0 \times 10^{-3}$
2	30	60	93	142	0·0034			

precipitation of tantalum and niobium is very slight. Best recovery of tantalum is obtained from a solution containing 2 per cent of citric acid and 15 per cent of hydrochloric acid.

Zirconium does not precipitate under these conditions. Optimum conditions for niobium recovery would be the use of a 0·5 per cent citric acid and 15 per cent hydrochloric acid.

VOL. 7 1959/

DETERMINATION OF TANTALUM IN THE PRESENCE OF NIOBIUM

Determination of tantalum in alloys can be given as an example. Analytical data obtained by the method of β-back-scattering[37] and by a conventional chemical method using tannin as a precipitating agent are given in Table 6, as compared with results obtained by the isotope dilution method. Results obtained by β-back-scattering and the isotope dilution method can be seen to be in good agreement. Chemical analysis yields erroneous values.

Thus the isotope dilution method may be successfully applied to determination of tantalum in alloys, upon previous separation with ammonium salt of the benzene seleninic acid.

TABLE 6. Analysis of niobium and tantalum electrolytic alloys

Sample	Weighed portion (mg)	Activity introduced with Ta^{182} (imp./min)	Activity of recovered Ta^{182} (imp./min)	Tantalum recovered (mg)	Tantalum content (%)		
					Isotope dilution method	β-Back scattering method	Chemical method
41	102·38	21595	8160	30·3	78·3	79·5	76·6
	102·38	—	8200	30·5	79·9		
91	99·60	3111	908	15·2	51·9	55·0	40·3
	100·20	—	877	14·9	52·9		
	100·41	—	902	15·0	51·6		
101	102·10	24470	5420	8·7	38·5	40·0	25·4
	97·21	—	6150	9·0	36·9		

TABLE 7. Determination of niobium in solutions containing zirconium (15·0 mg of niobium taken)

No. of experiment	Nb : Zr	Activity introduced with Nb^{95} (imp./min)	Activity of Nb^{95} recovered (imp./min)	Niobium recovered (mg)	Specific activity of the compound recovered $\left(\frac{\text{imp./min}}{\text{mg}}\right)$	Niobium found (mg)	Error (%)	Number of repeated precipitations
1	1 : 1	4800	1920	5·92	324	14·82	−1·2	1
2			2060	6·52	316	15·22	+1·5	1
3	1 : 25	4800	1780	5·54	321	14·99	−0·3	2
4			1820	5·78	316	15·18	+1·2	2
5	1 : 50	4800	1500	4·79	313	15·37	+2·5	3
6			1360	4·39	310	15·54	+3·6	3

DETERMINATION OF NIOBIUM IN THE PRESENCE OF ZIRCONIUM

Of no smaller interest is the application of the isotope dilution method to determination of niobium in the presence of zirconium. The former was also precipitated with benzene seleninic acid from a solution containing 0·5 per cent of citric and 15 per cent of hydrochloric acid. As can be seen from Table 7 good results are obtained at a ratio of Nb : Zr = 1 : 25.

DETERMINATION OF TANTALUM IN THE PRESENCE OF ZIRCONIUM

TABLE 8. Determination of tantalum in solutions containing zirconium (15·0 mg of tantalum were taken)

No. of experiment	Ta : Zr	Activity introduced with Ta^{182} (imp./min)	Activity recovered with Ta^{182} (imp./min)	Tantalum recovered (mg)	Specific activity of the compound recovered $\left(\frac{\text{imp./min}}{\text{mg}}\right)$	Tantalum found (%)	Error (%)	Number of repeated precipitations
1	1 : 1	6730	4700	9·73	483	15·15	+1·0	0
2			4580	10·10	454	14·85	−0·8	0
3	1 : 10	6730	4450	9·98	446	15·08	+0·5	0
4			4600	10·36	445	15·19	+1·3	0
5	1 : 50	6730	3360	7·66	440	15·27	+1·8	1
6			3280	7·38	446	15·16	−1·1	1
7	1 : 100	6730	543	1·31	415	16·26	+8·4	2
8			665	1·58	442	15·80	+5·3	2

Separation of tantalum from zirconium was carried out in a solution of 2·5 per cent citric acid and 15 per cent hydrochloric acid at different element ratios. The final concentration of the precipitating reagent was 1·5 per cent. The results are summarized in Table 8. Good results can be seen to be obtained at a ratio of Ta : Zr = 1 : 50. The purity of recovered samples was checked by the constancy of specific activities of the

TABLE 9. Determination of small amounts of tantalum in the presence of large amounts of zirconium

No. of experiment	Ta : Zr	Tantalum taken W_2 (mg)	Amount of carrier added to sample I W_{add_1} (mg)	Amount of carrier added to sample II W_{add_2} (mg)	Specific activity of sample I $\left(\frac{\text{imp./min}}{\text{mg}}\right)$	Specific activity of sample II $\left(\frac{\text{imp./min}}{\text{mg}}\right)$	Tantalum found (mg)
1	1 : 10	1·7	26·0	13·0	493	950	2·0
2		0·5	10·8	5·4	588	1152	0·4
3	1 : 50	1·7	26·0	13·0	307	730	1·4
4		0·5	10·8	5·4	425	777	0·6

substances recovered. Qualitative determination of zirconium contamination in tantalum precipitates was obtained in previous experiments with Zr^{95}.

Thus a new organic reagent, the benzene seleninic acid, was first used for the determination of niobium and tantalum and their separation from zirconium. It was shown that it was possible to separate niobium and tantalum from a citric acid medium by means of the benzene seleninic acid, on addition of HCl, and also to determine small quantities of these elements in the presence of relatively large amounts of zirconium.

By using the double isotope dilution method it is possible to determine relatively small amounts of tantalum, in the presence of relatively large amounts of zirconium, from the Ta : Zr ratio shift observed on dilution of the initial solution with inactive tantalum. The results obtained are given in Table 9.

The disadvantage of the method is the relatively small difference in two similar values of the numerator in equation (8). Accuracy of the analysis will then be determined by the reliability of specific activity values of S_1 and S_2.

All the above leads to the conclusion that the isotope dilution method permits fairly reliable and accurate solution of a number of analytically complicated problems connected with the determination of elements exhibiting similar properties.

VOL. 7 1959/

REFERENCES

1. VINOGRADOV A. P. Physico-chemical methods for control of uranium production. Reports of the Soviet Delegation at the International Conference on Peaceful Uses of Atomic Energy. Volume: *Investigations in the Field of Geology, Chemistry and Metallurgy*, p. 72. [Edited by the Academy of Sciences of U.S.S.R.] Moscow (1955). (In Russian.)
2. VAINSTEIN E. E. Use of labelled atoms in spectral analysis. All-Union Conference on the application of isotopes and nuclear radiations. Volume: *Isotopes and Radiations in Chemistry* p. 171. [Edited by the Academy of Sciences of U.S.S.R.]. Moscow (1955). (In Russian.)
3. BRODSKY A. I. *Chemistry of Isotopes* p. 445 (1957). (In Russian.)
4. COOK C. M. and LONG F. A. *J. Amer. Chem. Soc.* **73,** 4119 (1951).
5. EFREMOV V. YA., NEIMAN M. B. and PANFILOV V. N. Determination of alcohols by the isotope dilution method. Reports of the Committee on Analytical Chemistry, Vol. IX (XII), p. 361. [Edited by the Academy of Sciences of the U.S.S.R.] Moscow (1958). (In Russian.).
6. PINAJAN I. I., CHRISTIAN I. E. and WRIGHT W. E *J. Amer. Pharm. Assoc.* **42,** 301 (1953).
7. ALIMARIN I. P. and BILIMOVITCH G. N. *Khim. Nauk i Prom.* **1,** 74 (1956).
8. BRODA E. and SCHÖNFELD T. *Handbuch der mikrochemischen Methoden.* Bd II, *Verwendung der Radioaktivität in der Mikrochemie.* Isotopenverdunnungsmethode, p. 142. Wien (1955).
9. GEST H., KAMEN M. D. and REINER I. R. *Arch. Biochem.* **12,** 273 (1947).
10. ROSENBLUM C. and GRAIG I. *Nucleonics* **14,** 58 (1956).

11. Rosenblum C. *Analyt. Chem.* **29,** 1740 (1957).
12. Keston A. S., Udenfriend S. and Cannan R. K. *J. Amer. Chem. Soc.* **68,** 1390 (1946).
13. Zimakov I. E. and Rozhavsky G. S. *Zavodskaya Lab.* **24,** 922 (1958).
14. Rudenko N. P. *Zh. Neorgan. Khim.* **3,** 167 (1958).
15. Rudenko N. P. On the obtaining of carrier-free radioactive isotopes. All-Union Conference on the application of isotopes and nuclear radiations. Volume: *Isotopes and Radiations in Chemistry* p. 158. [Edited by the Academy of Sciences of U.S.S.R.] Moscow (1958). (In Russian.)
16. Korenman I. M. and Sheyanova F. R. *Usp. Khim.* **26,** 936 (1957).
17. Bilimovitch G. N. and Alimarin I. P. *Zh. Analyt. Khim.* **12,** 685 (1957).
18. Inghram M. G. *Ann. Rev. Nuclear Sci.* **4,** 81 (1954).
19. Buttlar H. V. *Naturwissenschaften* **42,** 90 (1955).
20. Smales A. A. and Webster R. K. *Geochim. et Cosmoch. Acta* **11,** 139 (1957).
21. Smales A. A. and Webster R. K. *Analyt. Chim. Acta* **18,** 587 (1958).
22. Smales A. A. and Webster R. K. *Analyt. Chim. Acta* **18,** 582 (1958).
23. Goris P., Duffy W. E. and Tingey F. H. *Analyt. Chem.* **29,** 1590 (1957).
24. Hummel R. W. and Smales A. A. *Analyst* **81,** 110 (1956).
25. Kirschenbaum A. D. and Grosse A. V. *Z. Anal. Chem.* **148,** 377 (1955).
26. Damon P. E. and Kulp J. L. *Trans. Amer. Geophys. Un.* **38,** 945 (1957).
27. Salyer D. and Sweet T. R. *Analyt Chem.* **29,** 2 (1957).
28. Geldhof M., Eeckhaut J. and Cornand P. *Bull. Soc. Chim. Belg.* **65,** 706 (1956).
29. El Guebely M. A. *Analyt. Chim. Acta* **15,** 580 (1956).
30. Leliaert G. and Eeckhaut J. *Analyt. Chim. Acta* **16,** 311 (1957).
31. Senyavin M. M. Application of radioactive isotopes to chromatographic separation of mixtures of alkali metals and rare-earth elements. All-Union Conference on the application of isotopes and nuclear radiations. Volume: *Isotopes and Radiations in Chemistry* p. 186. [Edited by the Academy of Sciences of U.S.S.R.] Moscow (1958). (In Russian.)
32. Alimarin I. P. and Bilimovitch G. N. Application of the isotope dilution method to determination of some rare elements. Reports of the Committee on Analytical Chemistry, Vol. IX(XII), p. 219. [Edited by the Academy of Sciences of U.S.S.R.] Moscow (1958). (In Russian.)
33. Alimarin I. P. and Sotnikov V. S. Weight and radiometric volumetric methods for determination of iron, making use of benzene- and naphthalene seleninate ammonium. Reports of the Committee on Analytical Chemistry, Vol. IX(XII), p. 213. [Edited by the Academy of Sciences of U.S.S.R.] Moscow (1958). (In Russian.)
34. Alimarin I. P. and Sotnikov V. S. *Zh. Analyt. Khim.* **13,** 332 (1958).
35. Alimarin I. P. and Sotnikov V. S. *Vestnik Moskov Gos. Univ.* No. 6, 137 (1957).
36. Alimarin I. P. and Sotnikov W. S. *Chemia Analityczna* **2,** 222 (1957).
37. Gaidadymov V. B. and Ilyina L. I. Analysis of binary tantalum–niobium alloys by means of β-rays reflection technique (back scattering). Reports of the Committee on Analytical Chemistry, Vol. IX (XII), p. 240. [Edited by the Academy of Sciences of the U.S.S.R.] Moscow (1958). (In Russian.)

International Journal of Applied Radiation and Isotopes, 1960, Vol. 7, pp. 182–185. Pergamon Press Ltd. Printed in Northern Ireland

Lithium Aluminum Tritide in Active Hydrogen Analysis

D. J. CHLECK, F. J. BROUSAIDES, W. SULLIVAN and C. A. ZEIGLER
Tracerlab Inc., Waltham 54, Mass.

(*Received* 27 *July* 1959)

The feasibility of radiochemical assaying for active hydrogen using lithium aluminum tritide (LAT) has been demonstrated. The sensitivity of the method allows very small quantities of material to be analyzed. The procedure is readily adaptable for the routine quantitative analysis of compounds containing active hydrogen.

LE TRITURE DE LITHIUM–ALUMINIUM DANS LE DOSAGE DE L'HYDROGÈNE ACTIF

On a démontré qu'il est faisable d'employer le triture de lithium–aluminium (LAT) pour le dosage radiochimique de l'hydrogène actif. La sensibilité de la méthode permet l'emploi de très petites quantités de matériel pour l'analyse. Le procédé s'adapte facilement au dosage répétitif des composés qui contiennent de l'hydrogène actif.

ПРИМЕНЕНИЕ ЛИТИЙ-АЛЮМИНИЙ-ТРИТИДА ($LiAlT_4$) ДЛЯ АНАЛИЗА АКТИВНОГО ВОДОРОДА

Показана возможность определения активного водорода путем радиационно-химического анализа с применением литий-алюминий-тритида (LAT). Чувствительность метода позволяет анализировать очень малые количества вещества. Этот способ может быть легко приспособлен к обычным методам количественного анализа веществ, содержащих активный водород.

LITHIUM-ALUMINIUM-TRITID IN DER ANALYSE VON AKTIVEM WASSERSTOFF

D ie Anwendbarkeit radiochemischer Bestimmung von aktivem Wasserstoff unterVerwendung von Lithium-Aluminium-Tritid (LAT) wurde gezeigt. Die Empfindlichkeit der Methode ermöglicht die Analyse sehr kleiner Mengen. Das Verfahren ist einfach anwendbar für routinemässige Quantitatierungsanalysen von Verbindungen, welche aktiven Wasserstoff enthalten.

LITHIUM aluminum hydride (LAH) reacts with a variety of organic compounds containing active hydrogen to liberate hydrogen gas. This reaction has been the basis of a gasometric method by KRYNITSKY *et al.*[1] for using LAH as a reagent for active hydrogen determination. Radioassay of tritium labeled organic compounds[2] using LAH has been performed. In this study active hydrogen compounds were reacted with LAT.

The technique used was to introduce the sample to be analyzed for active hydrogen into a solution of LAT (specific activity 5–20 $\times$ 10^{-4} mc/mM) in diethyl carbitol and count the evolved tritium using an internal flow proportional counter.[3] The counts above background and solvent correction are proportional to the amount of active hydrogen.

EXPERIMENTAL

Chemicals

The LAH was obtained from Metal Hydrides, Inc. LAT was supplied by New England Nuclear Corporation and had a specific activity of 2·5 mc/mg. The diethyl carbitol was dried by refluxing with sodium

VOL. 7 1959/6

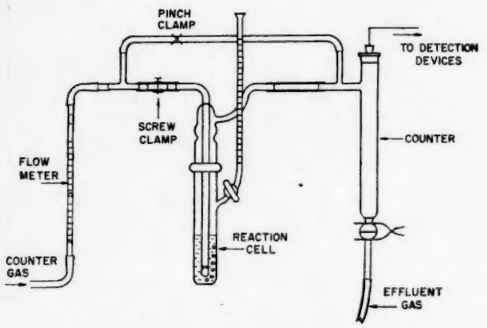

FIG. 1. Apparatus for active hydrogen analysis.

and distilling three times under reduced pressure. The tetrahydrofuran was dried by distilling from a LAH mixture, the fraction boiling at 64–65°C being taken. All other chemicals used were of reagent grade and were used without further purification.

Apparatus

The apparatus used is shown in Fig. 1. The reaction cell was 6½ in. long and 20 mm in diameter and fitted with a 24/40 T/S joint. The cell had a usable volume of about 25 ml and was fitted with a graduated pipette for sample addition. The cell was closed with a socket fitted with two tubes. One is an immersion tube to introduce counter gas into the reaction mixture, the other conducts counter gas and hydrogen into the counter. Effluent gases were conducted by tygon tubing into the flue of a laboratory hood. Fine adjustment of counter gas pressure was made with a screw clamp on a tygon tube connection between the reaction cell and the flow meter (Fischer and Porter Co.). A by-pass connection of tygon tubing was also made between the reaction cell and the counter and was shut off during a run by a pinch clamp. The detection equipment consisted of a Tracerlab pulse pre-amplifier, amplifier, and "1000" scaler. The counter gas was Tracerlab Proportional Counting Gas (90% argon, 10% methane).

Procedure

Approximately 0·2 M LAT in diethyl carbitol was used as the reaction mixture, 15 ml of which were transferred to the reaction cell. The pinch clamp was closed and counter gas was bubbled through the cell at a flow rate of 40 cm³/min. After the background had settled, the sample diluted in tetrahydrofuran was introduced and counts taken over a 10-min period. A correction curve for the tetrahydrofuran was also prepared.

In the preparation of LAT in diethyl carbitol no attempt was made to prepare a solution of a given specific activity, or even known activity. To do so is unnecessary and troublesome. This increases the value of the method as an analytical tool since standardized radioactive starting material does not have to be used. The only factor to be considered is that the specific activity must be of sufficient magnitude to yield adequate counting rates.

RESULTS AND DISCUSSION

Four typical compounds containing active hydrogen were analyzed. These included *n*-butanol, benzoic acid, aniline and water. Plots of the data obtained are given in Figs. 2–5. With each compound LAT of a different specific activity was used. Since the stoichrometry of the reaction of LAH and active hydrogen compounds has been studied by KRYNITSKY *et al.*, no attempt here was made to correlate data between compounds. What was desired in this study was to determine the linearity of response of the method and its applicability as an analytical tool.

Linearity was obtained in all four plots. Practically all points fell well within a counting error of one sigma,* which corresponds to a confidence level of 68 per cent. The statistical counting rate error may be reduced to a minimum with the use of high counting rates, accomplished by using higher specific activities or more sample.

Any of the four calibration curves, using the same specific activity of LAT, could be used to determine the active hydrogen

* Sigma (σ) is the root mean square deviation of a measurement n and is equal to $\sqrt{n}$.

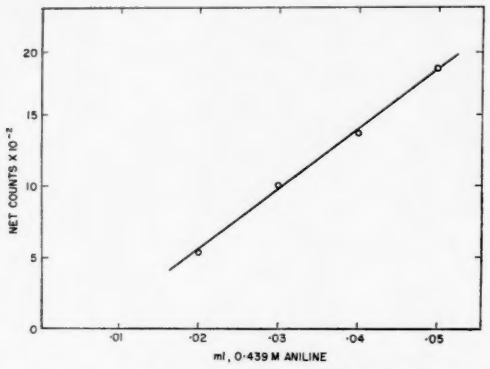

FIG. 2. Analysis of aniline in tetrahydrofuran.

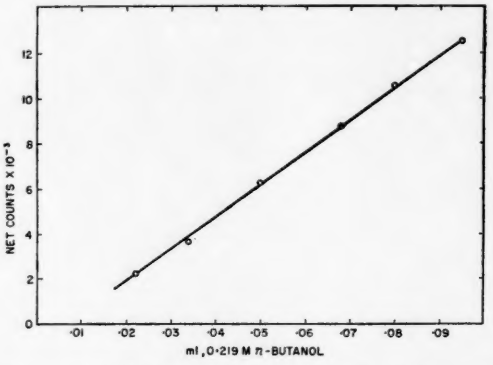

FIG. 4. Analysis of *n*-butanol in tetrahydrofuran.

content of an unknown. If the number of active hydrogens is known, or a calibration curve has been taken, the compound could be analyzed quantitatively in inert media.

It may be noted that the plots all fall below the origin. This appears to be due to fixed losses of hydrogen in sample "hold-up", sample volatilization before reaction, or possibly gas not fully swept out of the cell in the allotted reaction period. This error could be reduced with better cell design.

The sensitivity of the method is very high. With LAT of greater specific activity than used in this study, the sensitivity could be easily brought into the sub-microgram range. For small sample volumes a better system of injection could be devised and means for sample protection from air moisture could be incorporated into the assembly. It may be noted that the LAT used in this study had a specific activity of 2·5 mc/mg which was diluted with LAH by a factor of 10^5. Thus, the ultimate theoretical sensitivity would be of the order of 10^{-8} mM of active hydrogen compound. For practical purposes the sensitivity attainable is limited only by the ingenuity of the analyst in devising more efficient techniques.

Fifty or more samples may be analyzed on one filling of the reaction cell. In practice the cell should be refilled after half of the available hydride has been consumed.

A more efficient method than that used in this study could be the utilization of a gas–solid reaction. Essentially, the procedure would be to volatilize the active hydrogen compound and pass it over solid LAT. The liberated tritium would be counted and related to the amount of active hydrogen compound. This technique could be modified to detect any hydrocarbon by including a

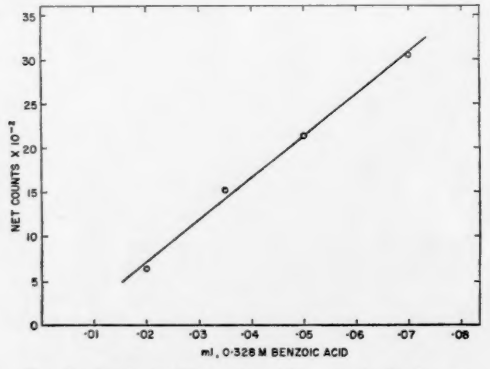

FIG. 3. Analysis of benzoic acid in tetrahydrofuran.

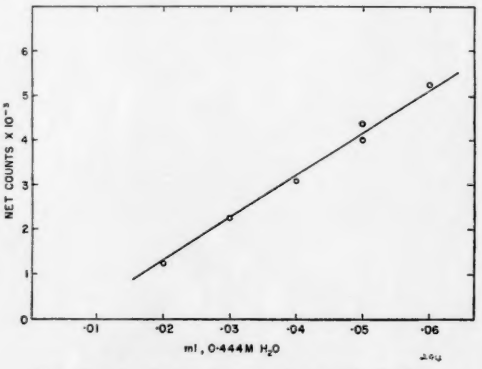

FIG. 5. Analysis of water in tetrahydrofuran.

VOL. 7 1959/6

CuO combustor. This would also tend to magnify the effective sensitivity as indicated by the following reaction:

$$C_n H_m \xrightarrow{CuO} {}_nCO_2 + \frac{m}{2} H_2O. \quad (1)$$

Such a method would parallel gas chromatographic techniques.

Acknowledgement—This work was supported under contract with the U.S. Atomic Energy Commission under the Isotopes Development Program.

REFERENCES

1. Krynitsky J. A., Johnson J. E. and Carhart A. W. *J. Amer. Chem. Soc.* **70,** 486 (1948).
2. Biggs M. W., Kritchivsky D. and Kirk M. R. *Analyt. Chem.* **24,** 223 (1952).
3. Wolfgang R. and Mackay C. F. *Nucleonics* **16** (10), 69 (1958).

OL.
7
9/60

International Journal of Applied Radiation and Isotopes, 1960, Vol. 7, pp. 186–191. Pergamon Press Ltd. Printed in Northern Ireland

Use of the Isotope Effect in the Study of Heterogeneous Catalytic Reactions*

JOEL R. GUTMANN
Israel Atomic Energy Commission, Rehovoth, Israel

(*Received* 26 *May* 1959)

The applicability of the isotope effect on heterogeneous reaction rates as a kinetic tool is discussed. The isotope effect on the exchange reaction rate of ammonia and hydrogen on iron catalyst has been measured using deuterium and tritium as labelling isotope. A general rate equation is derived for this exchange reaction, and it is shown that under certain conditions information on the reaction mechanism can be obtained from the measured isotope effect.

L'EMPLOI DE L'EFFET ISOTOPIQUE POUR ÉTUDIER LES RÉACTIONS CATALYTIQUES HÉTÉROGÈNES

On discute l'applicabilité de l'effet isotopique comme instrument kinétique sur la vitesse des réactions hétérogènes. On a mesuré l'effet isotopique sur le taux de la réaction d'échange du gaz ammoniac et de l'hydrogène sur un catalyseur de fer, en utilisant le deutérium et le tritium comme marques isotopiques. On a obtenu une équation générale de vitesse pour cette réaction d'échange, et on démontre que, sous des conditions particulières, on peut s'informer sur le mécanisme de la réaction par la mesure de l'effet isotopique.

ИСПОЛЬЗОВАНИЕ ИЗОТОПНОГО ЭФФЕКТА В ИССЛЕДОВАНИЯХ ГЕТЕРОГЕННЫХ КАТАЛИТИЧЕСКИХ РЕАКЦИЙ

Обсуждается возможность использования изотопного эффекта в кинетических исследованиях гетерогенных реакций. Изотопный эффект в реакциях обмена между аммонием и водородом при применении железного катализатора был определен с помощью метки дейтерием и тритием. Для этой реакции обмена выведено общее кинетическое уравнение и показано, что в определенных условиях измерение изотопного эффекта позволяет получить данные о механизме реакции.

DIE VERWENDUNG DES ISOTOPIE-EFFEKTES FÜR UNTERSUCHUNGEN VON HETEROGENEN KATALYTISCHEN REAKTIONEN

Die Verwendbarkeit des Isotopie-Effektes auf heterogene Reaktionsraten als kinetisches Hilfsmittel wird besprochen. Der Isotopie-Effekt bei der Austauschreaktionsrate von Ammonium und Wasserstoff an Eisen-Katalysatoren wurde mittels Markierung mit Deuterium und Tritium gemessen. Für diese Austauschreaktion wurde eine allgemeine Geschwindigkeitsgleichung abgeleitet und es wird gezeigt, dass unter bestimmten Bedingungen Aussagen über den Austauschmechanismus aus dem gemessenen Isotopeneffekt gewonnen werden können.

ISOTOPES have been widely used as tracers in the study of heterogeneous catalytic reactions. However, little use has been made of the isotope effect on the rate of such reactions, mainly because of the difficulty in interpreting results unequivocally. The understanding of the kinetic implications of the isotope effect has increased considerably lately so that wider application of this useful research tool is now possible in catalysis.

Catalytic reactions on metals proceed through a sequence of elementary steps. Preceding the reaction proper at least one of

* Lecture delivered at the Tenth Farkas Memorial Symposium held on 29 December 1958 at Jerusalem

VOL. 7 1959/

the reactants is adsorbed on the surface, in most cases by dissociative chemisorption. This step is followed by one or several surface reactions, such as migration dissociation, isomerization or combination. Finally a desorption step occurs. Substituting one isotope for another in the reactants can affect every one of these steps, the effect being most pronounced in the case of the hydrogen isotopes. The isotopic method will be of use in elucidating the reaction mechanism only in so far as the measured overall effect can be correlated with a definite elementary reaction step.

The isotope effect on the adsorption and desorption of molecules, especially of hydrogen, has been measured on a number of catalysts. The rate of adsorption is generally determined by the gas kinetic properties of the isotopic molecules because of the usually small activation energy of the process. The isotope effect therefore is not very large. One case where even this small effect on the adsorption rate of hydrogen and deuterium seemed to be absent, has led to the introduction of the much debated surface site activation theory.[1]

The isotope effect on the desorption step can be quite large in those cases where a hydrogen to metal bond is broken. This effect is well known. The difference in the desorption rate between light and heavy hydrogen has been utilized to separate the two isotopes.

Where the system involves a surface reaction, a change in the isotopic composition of the reactants can affect the concentration of adsorbed reacting species on the surface of the catalyst, as well as the velocity constant of the rate determining step. Since in addition many catalytic reactions are accompanied by fast isotopic exchange reactions between reactants and products, it is no easy task to give a kinetic interpretation of the overall velocity change resulting from the isotopic substitution.

The hydrogenation of ethylene, the oxidation of hydrogen and the decomposition of ammonia are three of the very few examples[2] in which the isotope effect on a heterogeneous reaction rate has been measured. In the latter case JUNGERS and TAYLOR[2] compared the decomposition rate of NH_3 and of ND_3 on tungsten wire at 1000°C and found the heavy ammonia reaction slower by a factor of 1·6. The experiment was carried out under conditions where no appreciable change in the surface concentration of the reacting species (C_a) was to be expected (zero order kinetics). In this case the reaction rate can be expressed[4] as

$$\left[v = C_a \frac{kT}{h} \exp\,(-E/RT),\right]$$

and the measured change in rate can be related to a change of $\Delta E = 900$ cal/mole in the stability of the dissociating species. This corresponds to the difference between the N–H and N–D bonds and rules out the possibility of such a step as $N(a) \rightarrow \frac{1}{2}N_2(g)$ being rate determining in the decomposition, as it is in the decomposition of ammonia on iron. This result is in agreement with the data on nitrogen adsorption on tungsten[5] and emphasizes the difference between the catalytic properties of tungsten and metals of the iron group in reactions of ammonia. There are no comparable experiments on other catalysts. It would be of interest to repeat such measurements on iron, where one would predict the absence of a hydrogen isotope effect on the ammonia decomposition reaction. The success of JUNGERS and TAYLOR in interpreting the experimental results in terms of a reaction mechanism can be related to their use of pure isotopic species (so that no exchange between reactants and products can obscure the results), and to a choice of experimental conditions where the surface concentration of reactants was not markedly perturbed by the change in isotopic composition. Given these conditions, the measured isotope effect is the effect on the surface reaction proper.

The study of exchange reactions has an important place in catalytic research. The isotope effect on the rate of these reactions has not been much used for kinetic studies because it was not well understood. In principle the effect of isotopic substitution on the rate of such reactions can be observed in two ways. One is by a method of double

labelling e.g. by D and T, by comparing the exchange rates of two related reactions such as $AH + BD = AD + BH$ and $AH + BT = AT + BH$. The other is by comparing the transfer rates of one labelling isotope in the two directions of one exchange reaction. This can be achieved in a reaction such as $AH + BD = AD + BH$ by approaching the equilibrium from both sides, namely by comparing the rate of the D transfer from AD to BH (initial condition so that there is an excess of D in the form of AD) to the rate of transfer from BD to AH (initial conditions of an excess of BD). From general thermodynamic considerations it would appear that one could expect quite large changes in the rate constants, especially when one of the reactants is elementary hydrogen, because the equilibrium constants of these reactions deviate strongly from the classical equipartition value. It was thought that this effect is independent of the actual reaction path. Recently the kinetic aspects of the isotope effect in exchange reactions have been treated theoretically by BUNTON *et al.*[6] after they had first been discussed by HARRIS[7]. It was shown by these authors that the reaction rate depends on the actual reaction path in cases where the exchange proceeds through a dissociative stage. Heterogeneous catalytic processes generally are characterized by dissociated (adsorbed) intermediates. It seemed probable therefore that the isotope effect on the rate of catalytic exchange reactions could be used to obtain information on the mechanism of these reactions. An attempt of this kind has been performed for the exchange of hydrogen and ammonia on iron catalyst and is reported below.

The exchange of both deuterium and tritium between ammonia and hydrogen was measured. At the start of each experiment the labelling isotope was alternately either in the ammonia or the hydrogen gas only. The exchange rates of D and T in the forward and backward steps of the exchange are therefore compared in these experiments. The runs using tritium differ however from the runs where D is the labelling isotope, in that trace amounts only of tritium were used, whereas the D labelled exchange started from pure isotopic species.

TABLE 1. The exchange rate of deuterium and tritium between labelled ammonia and hydrogen on 65 mg of iron catalyst

	Reactants (initial state)	Temperature (°C)	Isotope transfer rate (min^{-1})*
(1)	$NH_3 + D_2$	243	$4{\cdot}7 \times 10^{-3}$
(2)	$ND_3 + H_2$	243	$4{\cdot}4 \times 10^{-3}$
(3)	$NH_3 + D_2$	298	0·014
(4)	$ND_3 + H_2$	299	0·014
(5)	$NH_3 + D_2$	301	0·017
(6)	$NH_3 + D_2$	331	0·043
(7)	$ND_3 + H_2$	331	0·041
(8)	$NH_3 + D_2$	267	0·015†
(9)	$NH_3 + HT$	265	0·015‡
(10)	$NH_2T + H_2$	265	$4{\cdot}4 \times 10^{-3}$
(11)	$NH_3 + HT$	244	$6{\cdot}5 \times 10^{-3}$
(12)	$NH_2T + H_2$	243	$1{\cdot}8 \times 10^{-3}$
(13)	$NH_3 + D_2$	243	$6{\cdot}0 \times 10^{-3}$
(14)	$ND_3 + H_2$	244	$7{\cdot}6 \times 10^{-3}$

* Rates are normalized to exchange rate of pure isotopic species.

† Mean value of three experiments; agreement better than 5 per cent.

‡ Mean value of four experiments; agreement better than 10 per cent.

The experimental results are summarized in Table 1 which gives the initial state of the reactants and the extrapolated initial exchange rate corresponding to this state. Results grouped together may be compared with each other, but activity changes of the catalyst occurred in between groups of experiments. Experimental details are given in the appendix. The results of Table 1 seem paradoxical at first sight. While no isotope effect on the transfer rate of D in the two directions of the exchange reaction is observed at all (the equilibrium constant of the reaction $NH_2D + H_2 = HD + NH_3$ at these temperatures is 2·4), one finds that the ratio of tritium rates in the two directions is 3·4 (which is close to the measured equilibrium constant of the $NH_3 + HT = NH_2T + H_2$ reaction). Starting from labelled hydrogen no difference is found in the rates

of transfer of D and T. If the experiment is repeated however starting from labelled ammonia, the rates of transfer of D and T are found to differ by more than a factor of three.

The exchange reaction was investigated under conditions where previous work[8,9] has established that the exchange occurred stepwise, so that one hydrogen atom is exchanged at a time by interaction of singly dissociated ammonia residues with hydrogen which is in rapid isotopic equilibrium with hydrogen gas. The surface is almost completely covered by the ammonia residues, the order of reaction being zero for ammonia and one for hydrogen, (the order for hydrogen drops to $\frac{1}{2}$ at lower gas pressures). Assuming absence of secondary isotope effects (this being the only assumption in the treatment to follow) the exchange can be represented by the following reaction scheme for the deuterium labelled exchange:

$$NH_3 \underset{k'_H}{\overset{3k_H}{\rightleftharpoons}} NH_2(a) + H$$

$$D + NH_2(a) \underset{k'_D}{\overset{k_D}{\rightleftharpoons}} NH_2D \underset{k'_H}{\overset{2k_H}{\rightleftharpoons}} NHD(a) + H$$

$$D + NHD(a) \underset{k'_D}{\overset{2k_D}{\rightleftharpoons}} NHD_2 \underset{k'_H}{\overset{k_H}{\rightleftharpoons}} ND_2(a) + H$$

$$D + ND_2(a) \underset{k'_D}{\overset{3k_D}{\rightleftharpoons}} ND_3$$

For the case of tritium labelled exchange, where only trace amounts of the labelling isotope are used, one has to take into account only the singly labelled molecules. The reaction scheme is accordingly simpler:

$$NH_3 \underset{k'_H}{\overset{3k_H}{\rightleftharpoons}} NH_2(a) + H$$

$$T + NH_2(a) \underset{k'_T}{\overset{k_T}{\rightleftharpoons}} NH_2T \underset{k'_H}{\overset{2k_H}{\rightleftharpoons}} NHT(a) + H$$

The contribution to the exchange of each elementary reaction in the scheme can now be evaluated. For example the surface interaction rate due to the reaction $NHD(a) + D$ is $k'_D C'_{NHD} C'_D$ where C'_{NHD} is the surface concentration of $NHD(a)$ and C'_D is a surface concentration term of the interacting heavy hydrogen. (The treatment does not specify the molecular form of the interacting hydrogen; from general considerations it seems probable however that the hydrogen is in the form of adatoms.) As the product of the surface reaction NHD_2 leaves the surface, another ammonia molecule will, on the average, dissociate and take its place in the adsorption layer. Only if this dissociation results in the splitting off of an H atom from the ammonia will a net change in the D content of the reactants result. The contribution of the reaction $NHD(a) + D$ to the D transfer rate from hydrogen to ammonia can therefore be written as:

$$\frac{dD}{dt} = k'_D C'_{NHD} C'_D \times \frac{3k_H C_{NH_3} + 2k_H C_{NH_2D} + k_H C_{NHD_2}}{3k_H C_{NH_3} + (2k_N + k_D) C_{NH_2D} + (k_H + 2k_D) \times C_{NHD_2} + 3k_D C_{ND_3}}$$

By properly summing up all possible such exchange reactions one obtains from these equations the following expression for the change with time of the isotope fraction in the hydrogen gas:

$$\frac{dD}{dt} = \frac{k'_D C'_A C'_B}{\varepsilon\{1 - \alpha(k_H - k_D)/k_H\}} \times [\varepsilon(1 - \alpha)\beta - (1 - \beta)\alpha].$$

α, β are the D mole fraction in the hydrogen and ammonia respectively; C'_A and C'_B are the surface concentration terms of the two reactants irrespective of the isotopic composition ($C'_A = C'_{NH_3} + C'_{NHD} + C'_{ND_3}$), and are to a first approximation invariants during the course of the exchange; $\varepsilon = k_H k'_D / k_D k'_H$ is a pure thermodynamic factor and is related to the equilibrium constants of the system. A similar set of equations can be derived for the case of the tritium labelled exchange with appropriate change of the reaction constants.

The formal similarity of these equations to the ones derived by BUNTON *et al.*[6] for the homogeneous dissociative exchange should be noted. In the homogeneous case very small steady state concentrations of the

intermediates could be assumed. In the heterogeneous reaction however $k_H, k_D, k_T > k'_H, k'_D, k'_T$; the similarity to the homogeneous reaction formula is due to the finite and constant number of sites that are available on the catalyst's surface, so that only a small and constant part of the total molecules are in the form of intermediates. This, of course, has been implied in the derivation of the rate equation.

The rate equation reduces to a simple form at the start of the exchange ($t = 0$) when only one of the reactants is labelled initially (α_0 or $\beta_0 = 0$). These are the conditions chosen for experimental verification and reported in Table 1. For deuterium exchange of pure isotopic species one obtains, when $\alpha_0 = 0$, $\beta_0 = 1$ ($NH_3 + D_2$),

$$\left[\left(\frac{dD}{dt}\right)_{0;\alpha_0=0;\beta_0=1} = k'_D C'_A C'_B.\right]$$

This is the surface reaction rate of either NH_2, NHD or ND_2 with D atoms. When $\alpha_0 = 1$, $\beta_0 = 0$ ($ND_3 + H_2$) one obtains

$$\left[\left(\frac{dD}{dt}\right)_{0;\alpha_0=1;\beta_0=0} = -k'_H C'_A C'_B\right]$$

which is the rate of combination of ammonia adradicals with H atoms. The ratio of these rates of exchange (which refer to exchange of NH_3 with D_2 and of ND_3 with H_2) must therefore be k'_D/k'_H which is a ratio of constants of elementary steps of the exchange. The experimental results (experiments 1 and 2, 3 and 4, 6 and 7, and 13 and 14) show this ratio to be unity. This result points to some step involving the breakage of a N to metal bond as the rate determining step in the exchange of ammonia and hydrogen on iron.

The same equation reduces to quite different initial rates for the case of trace concentrations. Applying the formula to tritium exchange one obtains

$$\left[\left(\frac{dT}{dt}\right)_{0;\alpha_0=0;\beta_0\ll 1} = k'_T C'_A C'_B \beta_0;\right]$$

$$\left[\left(\frac{dT}{dt}\right)_{0,\alpha_0\ll 1,\beta_0=0} = \frac{-k'_T}{\varepsilon_T} C'_A C'_B \alpha_0.\right]$$

The ratio of these rates, normalized for comparison with pure isotopic species by dividing the rate by β_0 and α_0 respectively, equals ε_T — the equilibrium constant of the exchange reaction. This ratio has no kinetic significance as it is a purely thermodynamic factor. MELANDER[10] has shown that this is generally true for trace concentration exchanges; however it follows quite naturally from the present reaction scheme. Experiments 9 and 10, and 11 and 12 are therefore a measure of the equilibrium constant $C_{NH_2T}C_{H_2}/C_{NH_3}C_{HT}$. This has been shown to be the case by direct independent measurement of this constant.[11]

It is of interest to compare the rates of exchange of deuterium and of tritium with (light) hydrogen in this system. If the exchange rates of pure isotopic species are compared, no isotope effect is anticipated when $\beta_0 = 0$, $\alpha_0 = 1$, as in both the deuterium and the tritium reaction the same reaction constant k'_H is measured. For the initial state of $\alpha_0 = 0$, $\beta_0 = 1$ however, a ratio of true kinetic significance, namely k'_D/k'_T would be found.

The results reported in Table 1 refer to tritium in trace concentrations. For these conditions the ratio of rates is k'_D/k'_T when the hydrogen is labelled at the beginning of the exchange (experiments 8 and 9, 11 and 13). When the ammonia contains the heavy hydrogen initially (experiments 12 and 14) the ratio found equals $\varepsilon_T k'_H/k'_T = k_H/k_T$, and is a measure of the ease of detachment on the surface of an H or T respectively from the ammonia. This bears no direct relationship to the rate determining step of the reaction. In the system under investigation (where all k' have been shown to be equal) this ratio equals ε_T. This is confirmed by the experimental results.

When both labelling isotopes are in trace concentration another result is obtained. For the $\alpha_0 = 0$ case the ratio of rate of the D and T labelled exchange reactions is again k'_D/k'_T. For the $\beta_0 = 0$ case however a ratio of $k'_T\varepsilon_D/k'_D\varepsilon_T$ will result.

This exposition shows that conditions of exchange have to be judiciously selected to give the desired kinetic information, and special attention paid to which one of the reactants is to be labelled at the start.

VOL. 7 1959/

HANNERZ[12] recently used the technique of double labelling for investigating the hydrogen–water exchange on platinum. Specifically, the rates of exchange of D_2, HD and of HT with water were measured. The mechanism claimed by HANNERZ for the exchange resembles the scheme described above for the ammonia reaction. Using the same approach for interpretation of results, the rates measured by HANNERZ can be expected to yield data on the surface interaction step of OH and hydrogen radicals. As these rates were found by HANNERZ to be equal to a first approximation, an oxygen–metal detachment step must be assumed in the exchange reaction of hydrogen with water.

In the treatment previously described the reaction rate is calculated in terms of the total isotope content of the gas. Whenever mass spectrometric analysis of the isotopic molecules is available, as in HANNERZ' case, one can investigate secondary isotope effects and enlarge the scope of the research accordingly. In the case of the work of HANNERZ where the detailed isotopic composition of the hydrogen gas was measured, this enabled some deduction to be made on the chemical form of the interacting hydrogen. A detailed theoretical treatment of the secondary isotope effect on the kinetics of exchange reactions is still not available however.

EXPERIMENTAL*

The results presented in Table 1 were obtained by interacting the properly labelled ammonia and hydrogen gas on 65 mg of pure reduced iron powder. The apparatus used has been described previously.[8,9,11] The isotopic composition of the reactants was measured as a function of time. The measured rates of exchange were extrapolated to $t = 0$ and corrected to the rate of exchange at some arbitrary partial pressures of the reactants taking into account the known pressure dependence of the exchange rate. The rates are expressed in terms of change of mole fraction (or activity) of the labelling isotope in minutes, normalized by dividing with the initial mole fraction (or activity) of the reactant.

The preparation and purification of NH_3, H_2 and D_2 gas has also already been described.[8] ND_3 was prepared from magnesium nitride and D_2O; its isotopic purity was checked by an isotope dilution technique using D_2 of known composition. The tritium labelled hydrogen and ammonia were obtained by respectively reducing tritiated water (supplied by Harwell, 0·003 mc/cm^3) on zinc, and exchanging NH_4Cl with the tritiated water.

The D content of the hydrogen was measured in a thermal conductivity gauge. The tritium activity of the hydrogen and ammonia gas separately was determined by gas counting in the Geiger region.[11]

REFERENCES

1. PAGE J. and TAYLOR H. S. *J. Chem. Phys.* **2,** 578 (1934).
2. ROGINSKY S. Z. *Theoretical Principles of Isotope Methods for Investigating Chemical Reactions*, p. 255. AEC-tr-2873 (1956).
3. JUNGERS J. and TAYLOR H. S. *J. Amer. Chem. Soc.* **57,** 679 (1935).
4. LAIDLER K. J. *Catalysis* [Edited by EMMETT P.] p. 213 (1954).
5. VAN CLEAVE *Trans. Faraday Soc.* **34,** 1174 (1938).
6. BUNTON C. A., CRAIG D. P. and HALEVI E. A. *Trans. Faraday Soc.* **51,** 196 (1955).
7. HARRIS G. M. *Trans. Faraday Soc.* **47,** 716 (1951).
8. GUTMANN J. R. *J. Phys. Chem.* **57,** 309 (1953).
9. GUTMANN J. R. *J. Phys. Chem.* **59,** 478 (1955).
10. MELANDER L. *Ark. Kemi* **7,** 287 (1955).
11. GUTMANN J. R. In press.
12. HANNERZ K. *Acta Chem. Scand.* **10,** 655 (1956).

* The experimental part was performed as part of a study submitted in 1955 to the Senate of the Hebrew University in Jerusalem in fulfillment of the requirements for a Ph.D. degree.

International Journal of Applied Radiation and Isotopes, 1960, Vol. 7, pp. 192–197. Pergamon Press Ltd. Printed in Northern Ireland

The Secondary Hydrogen Isotope Effect*

E. A. HALEVI
Department of Chemistry, Israel Institute of Technology

(*Received* 26 *May* 1959)

Secondary isotope effects are reviewed with particular regard to their interpretation within a consistent scheme. It appears that adherence to formal considerations of vibrational frequency shifts is inadequate for the interpretation of many experimental results, and that these may be more fruitfully discussed in terms of "electronic" substituent effects, which differ for isotopic molecules by virtue of their slightly different mean configurations.

L'EFFET SECONDAIRE ISOTOPIQUE DE L'HYDROGÈNE

On regarde les effets secondaires isotopiques avec une considération particulière envers leur interprétation dans un système conséquent. Il paraît que les considérations formelles des déplacements de la fréquence de vibration ne suffisent pas à l'interprétation de beaucoup des résultats donnés par l'expérience, et que l'on pourrait discuter ceux-ci avec plus grand avantage en termes des effets de substitution "électroniques", lesquels varient entre les molécules isotopiques vu la différence légère de leurs configurations moyennes.

ВТОРИЧНЫЙ ИЗОТОПНЫЙ ЭФФЕКТ ВОДОРОДА

Дан обзор вторичных изотопных эффектов, причем особое внимание обращено на точное согласование данных со схемой. Оказывается, что формальные соображения о сдвиге колебательных частот неприменимы при истолковании многих экспериментальных результатов, которые удается объяснить в рамках ''электронных'' эффектов заместителей, приводящих к несколько иной усредненной конфигурации.

VOL. 7 1959/6

A QUARTER of a century ago, the late Professor Farkas was one of the central figures in a period of concerted interest in isotopes in general, and isotope effects in particular. Naturally enough, this activity centred for the most part on heavy hydrogen, the only isotope readily available in practical concentrations in the early 1930s. Moreover, since the principal property in which isotopic atoms differ from each other is their mass, it was reasonable to begin the study of isotope effects with the isotopes of hydrogen, where the relative mass difference is greatest.

The other lectures in this symposium bear witness to the fact that isotope effects have come a long way since then, and the theoretical framework for dealing with both thermodynamic[1 2] and kinetic[3] isotope effects has been formulated. Recently, however, a series of observations were made—again not surprisingly with isotopes of hydrogen—of isotope effects that did not fit easily into the general framework, and it is these "secondary isotope effects" that I shall discuss in this paper.

In order to judge in what way and to

* Lecture delivered at the Tenth Farkas Memorial Symposium held on 29 December 1958 at Jerusalem.

what extent secondary isotope effects require modification of the standard approach, let us first review the general treatment briefly in its most elementary form.[4]

The potential energy of a diatomic hydride molecule (HX) is given conventionally by a

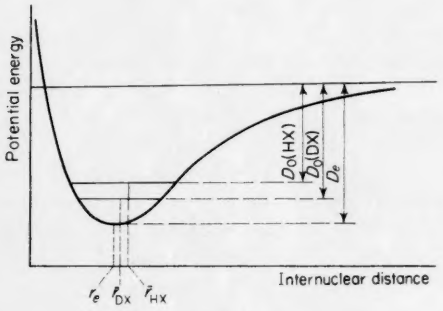

FIG. 1.

Morse curve, as shown in Fig. 1. Since the potential energy is to a very high approximation independent of isotopic mass, the same curve represents both HX and DX. Their vibration frequencies will differ, however, being for the classical harmonic oscillator:

$$\nu = \frac{1}{2\pi}\sqrt{\frac{k}{\mu}} \qquad (1)$$

in which k, the force constant, is common to both molecules, and the reduced mass μ, for sufficiently heavy X, may be taken as equal to the mass of the hydrogen or deuterium atom.

If, as we may reasonably assume for diatomic hydrides, the molecules of each species are virtually all in its lowest vibrational level, the difference in zero-point vibrational energy:

$$\tfrac{1}{2}h(\nu_H - \nu_D) = \frac{h}{4\pi}\sqrt{k}\left(\frac{1}{\sqrt{\mu_H}} - \frac{1}{\sqrt{\mu_D}}\right)$$
$$\cong \frac{h}{4\pi}\sqrt{k}\left(1 - \frac{1}{\sqrt{2}}\right) \qquad (2)$$

will show up as the difference in the dissociation energies (D_0) of the two isotopic species.

The dissociation of, say, a CH bond in a polyatomic molecule could also be discussed in terms of a Morse curve, i.e. the variation of potential energy with CH bond extension while keeping all the other bond lengths and angles unchanged. Actually, however, as a bond is extended the other atoms do not stand still, but arrange themselves so as to minimize the increase in potential energy. The net displacement, which is here no longer simply a change in the CH bond length, but also comprises lesser changes in other bond lengths and angles, is commonly called the "reaction co-ordinate" ξ. Plotting the potential energy as a function of the reaction co-ordinate, we get the familiar curve shown in Fig. 2.

In the activated complex, at the curve's maximum the CH bond is not yet completely broken, a further increase in ξ, i.e. further bond extension, along with the associated stabilizing configurational changes, leading to a decrease in potential energy.

It should be remembered, however, that CH bond extension, *without* the stabilizing configurational changes included in ξ, would be opposed by a restoring force. Therefore, we may legitimately speak of a CH force

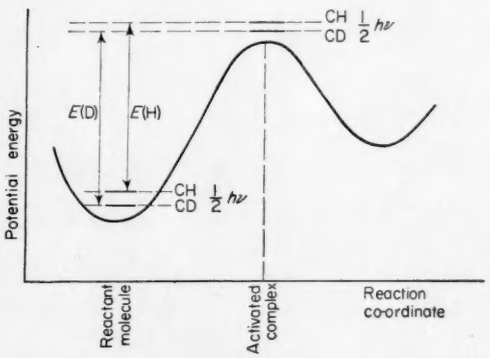

FIG. 2.

constant in the activated complex and of vibrational energy still present in the CH bond undergoing rupture.

Kinetically, the significant quantity is the activation energy: the difference in energy between the lowest vibrational level of the reactant molecule and the activated complex. The more completely broken the CH bond

in the activated complex, the lower its restoring force constant k, and by equation (2), the closer together the levels of the two isotopic species. It is obvious from Fig. 2, that the closer these levels lie, the more closely will the activation energy difference $(E_{(D)} - E_{(H)})$ approach the zero-point energy difference in the reactant molecule. This, for a CH bond, is about 1·2 kcal, so that rupture of a CD bond should be, in the limit, about seven times as slow as rupture of a CH bond. If the bond is still relatively strong in the activated complex, the rates would be more similar, differing perhaps by a factor of two or three.

The conclusions of this oversimplified qualitative argument are borne out by experiment, and also by BIGELEISEN's more rigorous quantitative treatment.[3]

So much for the primary isotope effect.

About 5 years ago, LEWIS[5] and SHINER[6] and their co-workers observed that solvolytic reactions of the S_N1 type, e.g.:

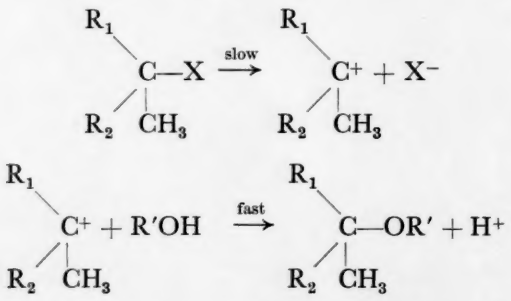

are slowed down by up to several tens of per cent by deuterium substitution in a β-methyl or methylene group. This effect was called "secondary", because rupture or formation of a carbon–hydrogen bond is not involved in the reaction, but an attempt was made to include it in the general framework of isotope effects as follows:

Although the CH bonds remain intact, they are weakened in the activated complex, presumably as a result of hyperconjugative electron release in the incipient carbonium ion:

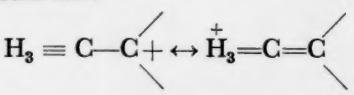

Such a weakening implies a decrease in the force constant, and consequently, a slight crowding of the lowest vibrational levels of CH and CD. The result would be an isotope effect in the observed direction, completely analogous to, but on a much smaller scale than, the primary isotope effect.

Attractive as this hypothesis is in the case of solvolysis, the rate of which is known to be strongly dependent on hyperconjugative effects, it ran into difficulties when it became necessary to accommodate the marked influence of solvent variation on the isotope effect.[7] More serious deficiencies appeared as non-solvolytic reactions were investigated. The presence of an effect in base catalysed enolization[8] could be reconciled with the "vibrational level crowding" hypothesis only by abandoning the particularly well-authenticated mechanism of this reaction.[9] The complete absence of a secondary isotope effect in aromatic nitration, and its weakness in aromatic substitution in general,[10] was equally difficult to understand. Clearly an essential element was lacking.

A year or so ago, workers in several laboratories[11–14] demonstrated the retarding effect in solvolysis of deuteration in the α-position. In a wide variety of molecules reacting according to:

$$RCH_2X \xrightarrow{slow} RCH^{2+} + X^-$$

$$RCH_2^+ + R'OH \xrightarrow{fast} RCH_2OR' + H^+$$

deuteration on the *alpha* carbon atom led to a decrease in rate of about 15 per cent per deuterium atom. STREITWIESER's interpretation of these results was as follows:

In the plane-trigonal carbonium ion the out-of-plane CH bending frequency is considerably lower than that of the corresponding mode in the initial state, where hybridization is tetrahedral. Consequently, there will here too be a decrease in the zero-point energy—though here of the bending modes—and an attendant crowding of the levels in the activated complex. Moreover, in the consideration of *any* isotope effect, bending as well as stretching frequencies should be taken into account. On this basis, STREITWIESER went beyond the crude treatment

VOL. 7 1959/

outlined above, and included secondary isotope effects in BIGELEISEN's treatment, which takes into account not only zero-point energy differences, but also the population of the higher vibrational levels as a function of temperature.

One thing, however, should be clear. As long as we remain in the purely kinetic domain, it is impossible to substantiate the "level crowding" hypothesis experimentally, since we can scarcely hope to isolate the activated complex and measure its infra-red spectrum. STEWART[15] has recently found an example of the α-effect in a *thermodynamic* system, the dissociation of benzhydrol to a carbonium ion:

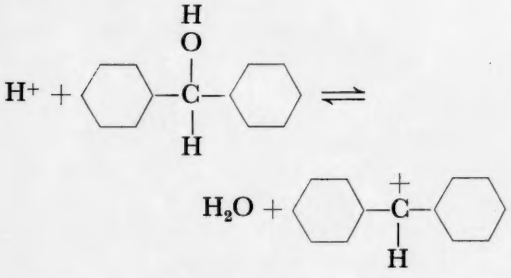

A demonstration of a shift of the CH bending mode to lower frequencies would go a long way toward substantiating STREITWIESER's hypothesis of the α-effect.

The approach of our group at Haifa to the general problem was a somewhat different one. We felt that in addition to the gross effect of a change in mass on vibrational frequencies, there might be more subtle influences that would lead to appreciable differences in ground state properties, such as electron distribution or resonance energy, and as a result of which a CD_3 group, for example, could be regarded as a different—perhaps an only slightly different—substituent from an ordinary methyl group.

The basic idea is by no means original. As far back as the 1930s the dipole moment of ND_3 was shown to be 0·02–0·03*D* larger than that of ammonia.[16] BELL and COOP[17] not only found a small difference between the moments of HCl and DCl, but produced a quantitative interpretation along the following lines:

The Morse curve (Fig. 1) is anharmonic, being tilted towards the right even very near the minimum. In the lowest vibrational level, both HCl and DCl are slightly longer in the mean than the distance r_e corresponding to minimum potential energy. The mean length of DCl (r_{DCl}) is smaller than that of HCl, since the lowest vibrational level of the former lies closer to the minimum. If the dipole moment changes with bond length, as indeed it must since the molecule absorbs in the infra-red, it follows that:

$$\mu_{DCl} - \mu_{HCl} = (\bar{r}_{DCl} - \bar{r}_{HCl}) \frac{d\mu}{dr}. \qquad (3)$$

It was possible to extend this treatment to polyatomic molecules, in which several vibrations, bending and stretching, must be taken into account, to estimate the differences in bond lengths and angles between two isotopic species of the same molecule.[18] The dipole moment difference calculated for ND_3 vs. NH_3 was in good agreement with that previously measured.

Assuming that this phenomenon is general, there is every reason to suppose that differences in the mean bond lengths and angles of a CD_3 relative to CH_3 group would affect the polar properties of organic molecules, perhaps sufficiently to have chemical consequences.

With this in mind, the dissociation constants of several deuterated organic acids and bases were measured.[19–21] In systems as different as acetic acid-d_3 vs. acetic acid on the one hand and 2:4:6-trinitro-N-methyl-d_3-aniline vs. 2:4:6 trinitro-N-methylaniline on the other, the acid dissociation constant was 10–12 per cent lower, or the basic dissociation constant was correspondingly higher in the deuterated compound. Moreover, the constancy of the effect per α-deuterium atom and its strong damping through a saturated carbon atom forcibly suggest that inductive electron release from CD_3 or CD_2 is stronger than from CH_3 or CH_2 respectively.

It has been argued[12] that an effect of this sort would also arise if the "methyl" vibrational frequencies of acetate ion, say, were sufficiently lower than those of acetic

acid. However, complete vibrational analyses of these two molecules exist,[22,23] and it is evident that the relevant frequencies do not shift as required by this interpretation.

In the examples given above, there is no opportunity for conjugation, which is presumably so important in the solvolytic secondary isotope effects. The obvious next step was to go on to a conjugated system, but one that would still show a difference in equilibrium rather than kinetic properties.

Aromatic hydrocarbons are well known to act as electron donors, forming complexes with electron acceptors such as chloranil, trinitrobenzene and many others:[24]

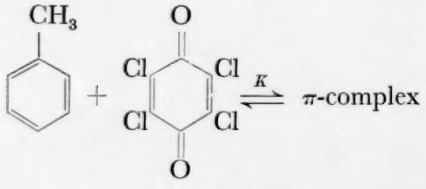

In such a system, the greater the electron accession to the ring, the larger the association constant K. Hexamethylbenzene, for example, forms a stable complex with chloranil, that was characterized many years ago.[25]

Trideuteration in the methyl group of toluene (or in one such group of *m*-xylene) *decreases* the dissociation constant by about 7 per cent.[26] Clearly, in spite of the more effective inductive electron release by CD_3, the net electron accession to the ring has been reduced. This is consistent with the conclusion that *hyperconjugative* electron release is less effective from CD_3 than from CH_3, in agreement with the secondary isotope effects observed in solvolysis.

Whereas the "vibrational level crowding" hypothesis does not admit experimental verification in a purely kinetic system, such an experimental test can be carried out in the case of π-complex equilibria: To be consistent with the observed isotope effect, the methyl bending and stretching frequencies in the complex should shift to the red by a total of about 100 cm^{-1}. In the solid complex between hexamethylbenzene and chloranil, there is a considerably smaller shift of the methyl frequencies *in the wrong direction.*[27] Thus, in this instance at least, the "vibrational level crowding" hypothesis is as powerless to explain the decreased efficiency of CD_3 for hyperconjugative electron release as it is to explain the enhanced inductive effect of CD_3.

The question which now arises is whether a sound theoretical basis can be found for both effects in terms of differences in mean bond lengths and angles between normal and deuterated molecules. In principle, differences the effective electronegativity of hydrogen bonded to carbon could arise from are:

(a) the change with bond extension of the intrinsic polarity of the CH bond;
(b) the change of hybridization with changing bond angle;
(c) the change with both bond length and bond angle of the non-bonding H . . . H interactions.

Hyperconjugative electron release would be affected, in addition to the above, by

(d) the change in overlap between the orbitals of the methyl carbon atom on that of the H_3 pseudoatom.

Calculations on toluene and toluene α-d_3[28] have to date yielded the conclusion that *in the ground state* electron release to the ring is greater in the deuterated molecule. However, there are indications, now being pursued further, that the situation may be different in the case of electron deficient molecules, such as carbonium ions.

In conclusion, it must be admitted that much of the evidence pertaining to secondary isotope effects is fragmentary and inconclusive. Some sort of picture does however seem to be emerging, and there is every reason to hope that these effects will eventually become a useful tool in the study of mechanism.

Note added October 1959

In view of their vibrational origin, secondary isotope effects can, in principle, be treated in terms of BIGELEISEN's partition function ratio-treatment.[2,3] The "vibrational level crowding" hypothesis is an approximation to this treatment.[12] It is now recognized (M. WOLFSBERG, R. PAUNCZ

VOL. 7 1959/

and E. A. HALEVI, to be published) that the "electronic substituent effect" treatment may also be obtained from it as an approximation of a rather different kind.

For the experimental results described in this lecture, and for an increasing number of newly discovered secondary isotope effects, the author believes the second approximation to be less restrictive and the corresponding treatment more fruitful.

REFERENCES

1. UREY H. C. *J. Chem. Soc.* 562 (1947).
2. BIGELEISEN J. and MAYER M. G. *J. Chem. Phys.* **15,** 261 (1947).
3. BIGELEISEN J. *J. Chem. Phys.* **17,** 675 (1949).
4. WIBERG K. B. *Chem. Rev.* **55,** 713 (1955).
5. LEWIS E. S. and BOOZER C. E. *J. Amer. Chem. Soc.* **74,** 6306 (1952) and later papers.
6. SHINER V. J. JR. *J. Amer. Chem. Soc.* **75,** 2925 (1953) and later papers.
7. SHINER V. J. JR. and VERBANIC C. J. *J. Amer. Chem. Soc.* **79,** 373 (1957).
8. EMMONS W. D. and HAWTHORNE M. F. *J. Amer. Chem. Soc.* **78,** 5593 (1956).
9. INGOLD C. K. *Structure and Mechanism in Organic Chemistry,* Chapter 10. Cornell University Press (1953).
10. SWAIN C. G., KNEE T. E. C. and KRESGE A. J. *J. Amer. Chem. Soc.* **79,** 505 (1957).
11. STREITWIESER A., JR. and FAHEY R. C. *Chem. & Ind. (Rev.),* 1417 (1957)
12. STREITWIESER A., JR., JAGOW R. H., FAHEY R. C. and SUZUKI S. J. *Amer. Chem. Soc.* **80,** 2326 (1958).
13. SAUNDERS W. H., JR., ASPERGER S. and EDISON D. H. *Chem. & Ind. (Rev.),* 1417 (1957).
14. MISLOW S., BORČIĆ S. and PRELOG V. *Helv. Chim. Acta* **40,** 2477 (1957).
15. STEWART R., GATZKE A. L., MOCEK M. and YATES K. *Chem. & Ind. (Rev.)* 331 (1959).
16. DE BRUYNE J. M. A. and SMYTH C. P. *J. Amer. Chem. Soc.* **57,** 1203 (1935).
17. BELL R. P. and COOP I. E. *Trans. Faraday Soc.* **34,** 1209 (1938).
18. HALEVI E. A. *Trans. Faraday Soc.* **54,** 1441 (1958).
19. HALEVI E. A. and NUSSIM M. *Bull. Res. Council Israel* A**5,** 263 (1956);
20. Abstr. 16th Int. Cong. Pure Appl. Chem. II, 27 (1957).
21. HALEVI E. A., NUSSIM M. and RON A. To be published.
22. WELTNER W., JR. *J. Amer. Chem. Soc.* **77,** 3941 (1955).
23. ITO K. and BERNSTEIN H. J. *Canad. J. Chem.* **34,** 170 (1956).
24. ANDREWS L. J. *Chem. Rev.* **54,** 713 (1954).
25. PFEIFFER P. *Liebigs Ann.* **412,** 293 (1917).
26. HALEVI E. A. and NUSSIM M. *Bull. Res. Council Israel* A**7,** 230 (1958).
27. HALEVI E. A. and NUSSIM M. *Tetrahedron* **5,** 352 (1959).
28. PAUNCZ R. and HALEVI E. A. *Bull. Res. Council Israel* A**7,** 214 (1958).

OL.
7
59/60

International Journal of Applied Radiation and Isotopes, 1960, Vol. 7, pp. 198–206. Pergamon Press Ltd. Printed in Northern Ireland

Hydrogen Isotope Effects in the Photo- and Radiation Chemistry of Aqueous Solutions*

JOSHUA JORTNER and GABRIEL STEIN
Department of Physical Chemistry, Hebrew University, Jerusalem, Israel

(*Received* 26 *May* 1959)

The results obtained by various workers on hydrogen isotope effects in the radiation and photochemistry of aqueous solutions are surveyed. The reactions likely to lead to isotope effects are discussed.

LES EFFETS ISOTOPIQUES DE L'HYDROGÈNE DANS LA PHOTOCHIMIE ET LA CHIMIE DE RADIATION DES SOLUTIONS AQUEUSES

L'étude se fait des résultats qu'ont obtenus les différents chercheurs sur les effets isotopiques de l'hydrogène dans la chimie de radiation et la photochimie des solutions aqueuses. On discute les réactions qui sembleraient mener aux effets isotopiques.

ИЗОТОПНЫЙ ЭФФЕКТ ВОДОРОДА В ФОТО- И РАДИАЦИОННОЙ ХИМИИ ВОДНЫХ РАСТВОРОВ

Дается обзор работ, выполненных различными исследователями, по изотопному эффекту водорода в радиационной и фотохимии водных растворов. Обсуждаются возможные реакции, могущие вызвать изотопный эффект.

WASSERSTOFF-ISOTOPIE-EFFEKT IN DER PHOTOCHEMIE UND STRAHLENCHEMIE VON WÄSSERIGEN LÖSUNGEN

Ein Überblick über die Ergebnisse verschiedener Autoren über den Wasserstoff-Isotopie-Effekt in der Strahlen- und Photochemie von wässerigen Lösungen wird gegeben. Reaktionen, die wahrscheinlich Isotopie-Effekt herbeiführen, werden diskutiert.

VOL. 7 1959/

THE late Professor L. FARKAS was one of the small group of pioneers who laid the foundation of our knowledge of the properties of the light and heavy isotopes of hydrogen. He was amongst those who initiated the investigations of the kinetic isotope effect in the photochemistry of aqueous solutions. However the quarter of a century which elapsed since his pioneering investigations added surprisingly little to our understanding of the fundamental processes which cause the isotope effects observed. In photochemistry and in the recently rapidly developing field of radiation chemistry, the reactions which cause the isotope effects may well be the fundamental ones, and these effects may indicate the nature of the elementary processes likely to be involved.

PRIMARY PROCESSES IN THE PHOTO- AND RADIATION CHEMISTRY OF AQUEOUS SOLUTIONS

The action of ultraviolet light is selective. After the absorption process the whole energy of the absorbed light quantum is stored in the absorbing centre. The absorbing centre may be present at a low concentration in the solvent. The absorbing centre may

* Lecture delivered at the Tenth Farkas Memorial Symposium held on 29 December 1958 at Jerusalem.

consist of a molecule, a molecular complex, an ion pair, or a single ion with its solvation layer. The excitation energy is lost by light emission, thermal degradation or is utilized—wholly or partly—in a chemical reaction.

The energy loss of ionizing radiations is independent of the molecular structure, and results in ionization and excitation, caused by the energetic electrons. Eventually the electrons become thermalized. The reactions observed are thus those of electrons and of "radical ions" containing uneven numbers of electrons, in addition to the reactions of excited molecules.

The presence of the polar solvent will influence these reactions by:

(a) The possibility of the dissipation of excitation energy by collisions. Three body collisions in which the solvent molecules participate are favoured;
(b) The FRANCK–RABINOWITCH cage effect,[1] which will facilitate radical recombination and energy degradation;
(c) Solvation energy, which may supply the energy for processes which are endothermic in the gas phase, or modify the energy balance in other cases.

A kinetic isotope effect will be the result of reactions in which the solvent water participates, and in which a bond between H or D and the rest of a molecule is broken.

THE PRIMARY DEUTERIUM ISOTOPE EFFECT[2]

Bonds to D are more stable than bonds to H. The difference in zero-point energies causes a higher activation energy for the compound containing D. If the force constants are assumed to be identical, the mass effect on the bond stretching frequency will give for the difference in zero-point energy:

$$\Delta E^0 = E_H{}^0 - E_D{}^0 = A(K/M_H)^{1/2} \quad (1)$$

where K is the bond force constant, M_H is the mass of H, and

$$A = (h/4\pi c)(1 - 1/\sqrt{2}).$$

Assuming that the non-reacting bonds are unaffected during the reaction, the *maximum* value of the ratio of the rate constants (k_H/k_D) may be calculated. This maximum value corresponds to non-bonding of H or D in the activated complex. At relatively low temperature

$$(k_H/k_D) = \exp(\Delta E^0/RT). \quad (2)$$

This equation is a useful but not always sufficiently good approximation.[3] It would yield for example in the case of water,[2] where $\Delta E^0 = 1400$ cal between O–H and O–D, a ratio of 12·6 at 0°C, 10·6 at 25°C and 6·5 at 100°C. However the observed isotope effect is expected to be lower than this, since differences in zero-point energies in the activated complex may cancel part of the differences in the reactants, if bonding occurs in the activated complex. A reverse isotope effect may also occur, for example in the case of attack by H or D atoms. These are of course bound only in the activated complex.

When H and D occur in equivalent positions in the same molecule, their relative rates of reaction result in the intramolecular isotope effect. Measuring relative reaction rates of H and D in analogous compounds the intermolecular isotope effects are obtained.

There is apparently no difference in principle in the magnitude of the isotope effect for cleavage of H, H^+ or H^- from the molecule,[2] but the effects introduced by the magnitude of the bonding in the transition state may be very different in each case.

APPLICATION OF THE KINETIC ISOTOPE EFFECT TO PHOTO- AND RADIATION CHEMISTRY

Isotope effects may be investigated in solutions of low D content by measuring the isotopic separation factor, or the reaction rates may be compared in light and heavy water.

In the first case, reactions involving H or D bond rupture respectively will cause the

effect. In the second case charge transfer reactions may also show an isotope effect. Namely the interatomic distances within the primary hydration layer may be different in light and heavy water, when the activated state is formed prior to the electron transfer. MARCUS[4] interpreted the results of LANGE[5] on the isotopic effect on the heat of hydration as arising from differences in the atomic polarization of the dielectrically saturated primary solvation layer. These effects may well influence the rate of electron transfer processes in light and heavy water respectively.

No direct experimental chemical evidence can be obtained for the mechanism of the primary reactions in radiation and photochemistry. The yields of the radicals formed can be measured and their existence is manifested by their chemical reactions. Their primary yields are approximately independent of the solute. The reactions in these systems are generally of such high rate constants that under conditions of continuous irradiation conventional kinetic measurements will not lead to single rate constants. These can be derived in the case where a slow post irradiation reaction occurs, or when special flash and sector techniques are employed. Relative rate constants of radical reactions can be obtained by a study of competitive reactions. The importance of the application of the kinetic isotope effect to these systems lies in the fact that it presents the possibility of studying the primary reactions by the technique of competitive reactions. The isotope effect can also be applied to the study of the mechanism of radical reactions, which may proceed by electron or group transfer.

ISOTOPE EFFECTS IN PHOTOCHEMISTRY

The first investigation of the separation of the hydrogen isotopes in the photochemical liberation of hydrogen from aqueous solutions was carried out by FARKAS and FARKAS.[6] They investigated the separation of H and D liberated from a homogeneous solution under the action of ultraviolet light. Their results are shown in Table 1, S being the separation factor,

$$S = (\mathrm{D/H})l\,.\,(\mathrm{H/D})g.$$

TABLE 1. Isotope fractionation in photochemistry[6]

System	$\%D_2O$	S
0·05 N Na_2SO_3 in 1·0 N Na_2SO_3	15–75	10·6
0·05 N KI in 0·05 N HCl	15	3·7
	75	6·0
0·05 N NaI	64·8	6·8
0·05 N NaI in 0·05 N HCl	64·8	5·2
0·05 N $FeSO_4$ in 0·05 N H_2SO_4	15	3·8
	75	4·8
0·5 N $FeSO_4$ in 0·5 N H_2SO_4	50–75	3·8

These results show that in the photochemistry of the ferrous and iodide ions at low pH the separation factors are similar. The separation factor increases slightly in the case of iodide when at constant percentage D_2O, the pH of the solution increases; and also, when at a constant pH, the percentage D_2O is increased.

These results are consistent with our knowledge of the reaction steps leading to photochemical hydrogen evolution from aqueous ionic solutions. The absorption of the quantum results in the formation of an excited species, where the excited electron is bound in the field of the residual atom or ion and of the oriented water molecules. The solvation layer—according to the FRANCK–CONDON principle—is still in its ground state configuration as around the original ion. The primary step is thus

$$I^-\{aq\} \xrightarrow{h\nu} I\{aq^-\}$$

and

$$Fe^{2+}\{aq\} \xrightarrow{h\nu} Fe^{3+}\{aq^-\}$$

where {aq} denotes the oriented dielectric medium.[7,8,9] The excited state will have a very short lifetime, before returning to the ground state. There will be a certain

VOL. 7 1959/

probability that dissociative electron capture by one particular water molecule may occur, resulting in the formation of H, according to

$$I\{H_2O^-_{aq}\} \rightarrow I_{aq} + OH^-_{aq} + H$$
$$Fe^{3+}\{H_2O^-_{aq}\} \rightarrow Fe^{3+}_{aq} + OH^-_{aq} + H.$$

This reaction originally suggested by FRANCK and HABER[10] will be independent of pH and will lead to isotope fractionation by an intramolecular effect. Its contribution will be the greatest at high pH values, where the small residual quantum yield of H_2 will be mainly due to this process.[9]

However the main reaction leading to the evolution of H_2 is pH dependent.[9,11,12] FARKAS and FARKAS[6,13] already considered that electron transfer to a proton may be an efficient process, leading to the decomposition of the excited state according to

$$I\{aq^-\} + H^+_{aq} \rightarrow I_{aq} + H.$$

This view is supported by FRANCK and PLATZMAN.[7]

For the isotope effect in the reaction of the homogeneous proton discharge in solution

$$H_2DO^+ + e \rightarrow H_2O + D \text{ or } HDO + H$$

infrared evidence indicates that the zero-point energies of the O–H and O–D bonds should be closer in the hydroxonium ion than in H_2O. The infrared spectrum of the nitric acid monohydrate[14] was interpreted in analogy with the spectrum of the solid NH_3 by assigning the following values to the normal vibrations of the hydroxonium ion:

$$\nu_1 = 2650\ cm^{-1}, \quad \nu_2 = 1134\ cm^{-1},$$
$$\nu_3 = 3380\ cm^{-1}, \quad \nu_4 = 1670\ cm^{-1}.$$

An investigation of the infrared spectra of the oxonium halides[15] led to the following assignment of the vibrations:

$$\nu_2 = 1100\ cm^{-1}, \quad \nu_4 = 1700\ cm^{-1},$$
$$\nu_1\ (\nu_3) = 3200\ cm^{-1}, \quad \nu_3\ (\text{or } \nu_1) = 2600\ cm^{-1}.$$

The uncertainty of the assignment of ν_1 for the hydroxonium ion does not enable us to estimate the difference of the zero-point energies with certainty. However semi-empirical correlations of bond force constants with electronegativities and bond lengths[16] yielded for the force constant of the hydroxonium ion the value of $5{\cdot}96 \times 10^5$ dyn cm^{-1} (compared with the value of $7{\cdot}76 \times 10^5$ dyn cm^{-1} in H_2O[17]). If $\nu_1 = 3200\ cm^{-1}$ for the H_3O^+ ion then the analysis according to the standard methods[17] yields the value of $5{\cdot}55 \times 10^5$ dyn cm^{-1} for the force constant in good agreement with the semi-empirical correlation. Then we obtain $\Delta E^0 \sim 1200$ cal leading to the maximum value of approximately 7·5 for the isotope effect at 25°C. This effect is partly counteracted by the isotope effect on the hydration of the proton. The distribution of protons and deuterons between the isotopic water molecules and the hydroxonium ions is not random.[18,19] For solutions containing 15–75% D, the number of H atoms is 1·25–1·49 times greater than of D in the hydroxonium ions.[6] Thus altogether the proton discharge process may lead to a somewhat smaller fractionation effect than the dissociative electron capture process, which predominates in neutral solutions. These qualitative considerations on isotope effects are thus consistent with our knowledge of the mechanism of photochemical hydrogen evolution. The higher separation factor in the case of sulphite solutions is due to the chemical reactions following on the photochemical process, which add an isotope effect of their own to it.[6]

ISOTOPE EFFECTS IN RADIATION CHEMISTRY

In the radiation chemistry of dilute aqueous solutions, the energy is absorbed mainly by the solvent, water, and the chemical reactions observed are due to the chemically active intermediates formed from it. Free radical formation can be represented formally[20] as

$$H_2O \sim\!\!\!\rightarrow H + OH.$$

This overall process may be the result of either of two processes. LEA[21] proposed that ionization

$$H_2O \sim\!\!\!\rightarrow H_2O^+ + e$$

is followed by dissociation of the positive ion, utilizing the hydration energy according to

$$H_2O^+ \rightarrow H^+_{aq} + OH$$

and yielding the OH radical. The ejected electron will be captured

$$H_2O + e \rightarrow H_2O^-$$

and the negative ion will dissociate, utilizing the hydration energy:

$$H_2O^- \rightarrow H + OH^-_{aq}$$

yielding H atoms.

SAMUEL and MAGEE[22] however proposed that even in aqueous solution, the ejected electron will mainly recombine, according to

$$H_2O^+ + e \rightarrow H_2O^{\ddagger}$$

producing a highly excited water molecule which dissociates

$$H_2O^{\ddagger} \rightarrow H + OH.$$

Whilst charge recombination and dissociative radical formation from neutral, excited molecules may be of great importance in less polar solvents, the mechanism of SAMUEL and MAGEE was considered to be of much less importance in aqueous solution, where both the positive ion and the thermalized electron come under the strong influence of the dipolar solvent.[23] PLATZMAN and FROHLICH[24] calculated that the energy loss by the electron is a relatively slow process, and that the near-thermal electron will have sufficiently long lifetime to be captured according to the LEA mechanism. The mechanism leading to H atom formation which would occur in radiation chemistry according to the LEA mechanism is very similar to the process occurring in photochemical electron transfer, and a similar isotope effect would be expected. The SAMUEL–MAGEE mechanism however would yield a highly excited water molecule, with an energy content far exceeding that needed for the H—OH bond rupture. The charge recombination would yield some 12·6 eV, whilst only some 5 eV is needed for H formation. Thus in this case there will probably be little or no isotope fractionation, the available excess energy far exceeding any small differences in bond strengths.

In irradiated solutions in addition to the radical producing process, there are[15,26] processes leading directly to the formation of H_2 and H_2O_2. These molecular processes may be represented as

$$H_2O \sim\!\!\rightarrow H + \tfrac{1}{2}H_2O_2$$

and

$$H_2O \sim\!\!\rightarrow \tfrac{1}{2}H_2 + \tfrac{1}{2}H_2O_2.$$

The mechanism of these processes is not yet elucidated. It is possible to observe the isotope effect occurring in irradiated solution under conditions where all the H_2 gas evolved is due to the molecular process (by using acceptors which take up the radicals), or to obtain the total H_2 gas, most of which is due to the radical forming process. The results obtained by various workers are collected in Table 2.

TABLE 2. Separation factors in radiation chemistry

System	%D	S	Reference	Process
10^{-2} M $FeSO_4$ in 0·8 N H_2SO_4 de-aerated 200 kV X-rays	0·9	3·45	27	R + M
10^{-2} M $FeSO_4$ in 0·025 N H_2SO_4 de-aerated 200 kV X-rays	0·9	3·60	27	R + M
Methanol in D_2O solution de-aerated 200 kV X-rays	95	4·1	28	R
Cu^{+2} 0·02 Fe^{+2} 10^{-3} de-aerated 200 kV X-rays	84·5	3·1	28	M
10^{-3} M $FeSO_4$ in 0·8 N H_2SO_4 oxygen saturated 200 kV X-rays	0·9	1·90	27, 29	M
2 . 10^{-3} Ceric ammonium sulphate in 0·8 N H_2SO_4 de-aerated X-rays	0·9	1·94	27, 29	M
2 . 10^{-3} Ceric ammonium sulphate in 0·8 N H_2SO_4 Ra γ-rays	1·0	1·98	29	M
0·8 N H_2SO_4 oxygen saturated X-rays	1	1·92	29	M
$Po^{210}\alpha$ Fe^{+2} in 0·8 N H_2SO_4		2·2	30	M
$Po^{210}\alpha$ Ce^{+4} in 0·8 N H_2SO_4		1·9	30	M

VOL. 7 1959/6

TABLE 3a. Chemical yields in the radiation chemistry of aqueous solutions

Product	D_2O	H_2O
$(Fe^{3+})_{air}$	16·72[31] 17·06[32,31] 16·36[33] 18·6[34]	15·6
$(H_2O_2)_{air}$	1·24[31]	1·17
$(H_2)_{Br^-}$	0·38[31]	0·45

TABLE 3b. Radiation chemical primary yields in H_2O and D_2O

Cobalt γ-rays 0·4 N H_2SO_4[31]			X-rays[28] 0·1 N H_2SO_4		
	D_2O	H_2O		D_2O	H_2O
H	3·99	3·68	H	3·75	3·30
OH	3·14	2·96	OH	2·45	2·8
H_2O_2	0·81	0·81	H_2O_2	1·27	0·87
H_2	0·38	0·45	H_2	0·62	0·64
$-H_2O$	4·75	4·58	$-H_2O_2$	4·99	4·56

In experiments where the total yield due to molecular (M) and radical (R) intermediate processes is observed, and where the H_2 evolved is mainly due to the radical intermediate process, a separation factor of ~4 is obtained. This is similar to the factor obtained in photochemistry and would agree well with the LEA mechanism. The isotope effect would thus appear to provide additional evidence against the SAMUEL–MAGEE mechanism being the main process in aqueous solutions.

For the molecular yield alone, separation factors of ~2 are obtained at low deuterium content. It was suggested[27] that this value may be explained by assuming that the molecular yield results from the interaction of two excited water molecules. However the arguments on which this view was based were strongly criticized[28] and there is no valid mechanism yet to account for the experimental facts in this case.

The yield of the various primary products themselves will change. The yields obtained in light and heavy water are presented in Table 3a and b.

The viscosity of D_2O is ~20 per cent higher than that of H_2O. This will cause slower diffusion and recombination rates which increase the decomposition of heavy water.

ISOTOPE EFFECT IN SECONDARY PROCESS

The kinetic isotope effect, hitherto little investigated, shows promise in photochemistry and radiation chemistry, to serve as a valuable additional tool in elucidating the possible reaction mechanism and to indicate which one of the possible alternatives is the most likely one.

(a) *Interaction of the radicals with the solvent molecules*

The hydrogen atoms formed may react with the solvent molecules by the following reactions:

$$D + DHO \rightarrow H + D_2O$$
$$D + H_2O \rightarrow H + HDO \quad ;$$

another reaction involves isotopic exchange with hydroxonium ions

$$D + H_2DO^+ \rightarrow H + HD_2O^+$$
$$D + H_3O^+ \rightarrow H + H_2DO^+ \quad .$$

FARKAS and FARKAS[6] concluded that the reaction of D atoms with solvent is too slow to contribute to isotopic fractionation. For this reaction an activation energy in the gaseous phase of 16 kcal/mol was found.[35,36] It thus appears that the rate constant is of the order of magnitude of 1 sec^{-1}. It is likely that the activation energy for the reaction of D atoms with hydroxonium ions is of the same order of magnitude and it is not likely to be faster than the first process. The isotopic exchange reaction was investigated by FRIEDMAN and ZELTMAN[37] who found for this reaction a rate constant of about 2 sec^{-1} at pH = 2.

(b) *Interaction with solutes*

The reactions of hydrogen atoms will generally be divided into oxidation and reduction reactions.

One of the most interesting conclusions concerning the reaction of hydrogen atoms with ferrous ion is that in acid solution hydrogen atoms act as oxidizing agents.[38] This theory was recently proved experimentally by passing hydrogen atoms through aqueous solutions of ferrous ions.[39,40] It was also postulated that oxidation of the iodide ion may proceed by the action of hydrogen atoms in order to interpret the photochemistry[11] of this system at low pH.

The oxidation by hydrogen atoms may occur via one of the following mechanisms:

(a) $H_2^+{}_{aq}$ formation[38,41] followed by a charge transfer process

$$H + H^+{}_{aq} \rightleftharpoons H_2^+{}_{aq}$$

$$H_2^+{}_{aq} + Fe^{2+}{}_{aq} \rightarrow H_2 + Fe^{3+}{}_{aq}$$

(b) Oxidation by a ternary collision[40,42]

$$Fe^{2+}{}_{aq} + H + H^+{}_{aq} \rightarrow Fe^{3+}{}_{aq} + H_2$$

(c) Hydrogen atom transfer[43]

$$Fe^{2+}H_2O + H \rightarrow Fe^{3+}OH^- + H_2 \ .$$

The possibility of reaction (b) is probably excluded on the basis of the radiation-chemical experiments of ALLEN and ROTHSCHILD[44–46] who reported that the rate of oxidation of ferrous ion by atomic hydrogen did not change in accordance with it in the pH region 0·3–2·1. The results of BAXENDALE and HUGHES[28,47] on the competitive reactions of hydrogen atoms with ferrous ion and methanol showed that the ratio of the two reaction constants was unaffected by changing the acid concentration in the region 0·1–0·05 N, in agreement with the results of ALLEN and ROTHSCHILD.

It is interesting to investigate whether the isotope effect can help to decide between the remaining alternatives. It is clear that mechanism (c) should definitely involve an isotope effect which should not be pH dependent. This isotope effect, if occurring, would be in addition to the isotope effect obtained in the primary photochemical step. On the other hand mechanism (a) would show only a small isotope effect if any.

BAXENDALE and HUGHES[28,47] derive a value of 2·4 for the ratio of the constants of the reactions

$$Fe^{2+} + H \rightarrow Fe^{3+} + H_2 \text{ in } H_2O$$

$$Fe^{2+} + D \rightarrow Fe^{3+} + D_2 \text{ in } D_2O$$

but point out that the derivation of the rate constant in light water is not unambiguous. The investigation of the pH dependence is still required. BAXENDALE and HUGHES[28] pointed out that the observed rates of these reactions are consistent with a mechanism of hydrogen atom transfer. On the other hand an isotope effect of such order of magnitude may occur in a charge transfer mechanism, where the difference of the free energy of rearrangement of the primary ionic solvation layers in D_2O and H_2O may give rise to this effect. Thus these results do not exclude either of the two mechanisms.

Reduction reactions by hydrogen and deuterium atoms may occur by two mechanisms: electron transfer process

$$Cu^{2+}{}_{aq} + H \rightarrow Cu^+{}_{aq}$$

or by OH transfer from an ion pair

$$Fe^{3+}OH^- + H \rightarrow H_2O + Fe^{2+}{}_{aq};$$

both reactions should not show an isotope effect in agreement with the experimental results.[28]

Another interesting reaction is that between ferrous ion and hydroxyl radicals

$$Fe^{2+} + OH \rightarrow Fe^{3+} + OH^-.$$

This reaction may proceed through charge transfer or group transfer mechanism. Isotopic research may provide the final answer to this problem.

ISOTOPE EXCHANGE

The exchange of deuterium dissolved in water and exposed to γ-rays was investigated by GORDON and HART.[48] It was proposed that the exchange proceeds by the following mechanism

$$H_2O \sim\sim\sim\rightarrow H, OH, H_2, H_2O_2$$

$$H + D_2 \rightarrow HD + D$$

$$OD + D_2 \rightarrow HOD + D$$

$$2D \rightarrow D_2.$$

At steady state the yield of HD is equal to G_H while the yield of H_2 equals G_{H_2}. It was assumed by GORDON and HART that the hydrogen peroxide formed disappears by the reaction

$$D + H_2O_2 \rightarrow HOD + OH.$$

The pH dependence of the exchange reaction was investigated. The HD yield was approximately constant in the pH region 4–9. Above pH 9 a sharp drop was observed which was attributed to the dissociation of the hydroxyl radical.

$$OH \rightleftharpoons O^- + H^+$$
$$O^- + H \rightarrow OH^-$$
$$O^- + D \rightarrow OH^-$$

In the pH region 3–4 a rise in the HD yield is observed which may be attributed to the increase in the primary yield of hydrogen atoms. Below pH 3 a slight drop in the yield is observed. In their original work GORDON and HART considered the possibility that at low pH values H_2^+ is formed as postulated by RIGG *et al.*[41] decreasing the steady state concentration of hydrogen atoms and the rate of HD production. However recently[40] the absence of chain exchange reaction at low pH was taken to indicate that the exchange does not proceed by the possible mechanism

$$H^+ + D \rightarrow HD^+$$
$$HD^+ \rightarrow H + D^+.$$

The net result of this scheme will be

$$H^+ + D \rightarrow H + D^+.$$

D^+ formed would not participate significantly in the reverse reaction because of the high H^+ concentration. It was considered *a priori* that the rate of formation of H_2^+ is high, and thus the absence of an acid promoted exchange reaction was considered as evidence against the existence of H_2^+.

The work of GORDON and HART was confirmed and extended by FRIEDMAN and ZELTMAN.[37] The exchange reactions were treated by considering all the possible reactions in this system

$$H_2O \sim\sim\sim\sim\rightarrow H, OH, H_2H_2O_2$$

$$H + HD \rightarrow H_2 + D \quad (1)$$
$$H + D_2 \rightarrow HD + D$$
$$D + H_2 \rightarrow D_2 + H$$

$$H + H_2O_2 \rightarrow H_2O + OH \quad (2)$$
$$D + H_2O_2 \rightarrow HOD + OH$$

$$H_2 + OH \rightarrow H_2O + H \quad (3)$$
$$HD + OH \rightarrow H_2O + D$$
$$\hookrightarrow HOD + H$$
$$D_2 + OH \rightarrow HOD + D$$

$$2H \rightarrow H_2 \quad (4)$$
$$H + D \rightarrow D_2$$
$$2D \rightarrow D_2$$

$$H + OH \rightarrow H_2O \quad (5)$$
$$D + OH \rightarrow HOD$$

$$2OH \rightarrow H_2O_2 \quad (6)$$

$$D + H_2O \rightarrow HOD + H \quad (7)$$

Two alternative kinetic schemes were employed. Two sets of simplifying assumptions were made:

Mechanism *A*: $k_5 = k_6 = 0$

Mechanism *B*: $k_4 = k_6 = 0$

Mechanism *A* corresponds to the situation where all OH radicals react with hydrogen molecules. Mechanism *B* takes in to account the efficient recombination reaction between H and OH which is the chain terminating reaction. The actual mechanism is probably the intermediate case. But it was shown by FRIEDMAN and ZELTMAN that mechanism *A* is in better agreement with experimental data. The rate constant calculated for the exchange reaction (7) was found to be about 2 sec^{-1} at pH ~2 as mentioned above. This result puts a restriction on the possibility of efficient acid promoted exchange reaction between D atoms and water. If reaction (7) occurs by

$$H^+ + D \rightleftharpoons HD^+ \quad (8)$$

then $k_7 = k_8(H^+)$ and hence $k_8 \sim 200$ l. $mole^{-1}$ sec^{-1}.

The absence of an efficient acid-promoted exchange reaction is thus consistent with the

intermediate formation of H_2^+, if the rate of its formation is slow. That this indeed may be the case was recently shown in the reaction of H atoms in aqueous solutions.[49]

We see thus that evidence from isotope effects does not exclude the possibility of oxidation by H atoms acting in the form of $H_2^+{}_{aq}$ ions, and moreover indicates the necessary conditions which must be fulfilled to make this assumption possible.

Acknowledgements—We wish to thank Professor E. D. BERGMANN and the Israel Atomic Energy Commission for their interest and support.

REFERENCES

1. FRANCK J. and RABINOWITCH E. *Trans. Faraday Soc.* **30,** 120 (1934).
2. WIBERG K. B. *Chem. Rev.* **55,** 713 (1955).
3. BIGELEISEN J. and GOEPPERT-MAYER M. *J. Chem. Phys.* **15,** 261 (1947).
4. MARCUS R. A. *J. Chem. Phys.* **26,** 867 (1957).
5. LANGE E. *Z. Elektrochemie* **44,** 31 (1938).
6. FARKAS A. and FARKAS L. *Trans. Faraday Soc.* **34,** 1120 (1938).
7. PLATZMAN R. and FRANCK J. *Farkas Memorial Volume* p. 21. Research Council of Israel Special Publication No. 1, Jerusalem (1952); *Z. Phys.* **138,** 411 (1954).
8. STEIN G. and TREININ A. *Trans. Faraday Soc.* **55,** 1086, 1091 (1959).
9. JORTNER J. and STEIN G. To be published.
10. FRANCK J. and HABER F. *S.B. Preuss Akad. Wiss. Physik. Math. Kl.* 250 (1931).
11. RIGG T. and WEISS J. *J. Chem. Soc.* 4198 (1952).
12. RIGG T. and WEISS J. *J. Chem. Phys.* **20,** 1194 (1952).
13. FARKAS A. and FARKAS L. *Trans. Faraday Soc.* **34,** 1113 (1938).
14. BETHELL D. E. and SHEPPARD N. *J. Chim. Phys.* **50,** C72 (1953).
15. FERRISO C. E. and HORNIG D. F. *J. Chem. Phys.* **23,** 1464 (1955).
16. GORDY W. *J. Chem. Phys.* **14,** 305 (1946).
17. HERZBERG G. *Infrared and Raman Spectrum.* Van Nostrand, New York (1946).
18. BRESCIA F. *J. Amer. Chem. Soc.* **60,** 2811 (1938).
19. BRESCIA F. and LA MER V. K. *J. Amer. Chem. Soc.* **60,** 1962 (1938).
20. WEISS J. *Nature* **153,** 748 (1944).
21. LEA D. E. *Actions of Radiations on Living Cells.* Cambridge University Press (1947).
22. SAMUEL A. H. and MAGEE J. L. *J. Chem. Phys.* **21,** 1080 (1953).
23. STEIN G. *Disc. Faraday Soc.* **12,** 227, 289 (1952).
24. PLATZMAN R. and FROHLICH H. *Phys. Rev.* **92,** 1152 (1953).
25. ALLEN A. O. *J. Phys. Chem.* **52,** 479 (1948).
26. JOHNSON E. R. and ALLEN A. O. *J. Amer. Chem. Soc.* **74,** 4147 (1952).
27. KELLY P., RIGG T. and WEISS J. *Nature* **173,** 1130 (1954).
28. BAXENDALE J. H. and HUGHES G. *Z. Phys. Chem.* **14,** 323 (1959).
29. KELLY P., RIGG T. and WEISS J. *Chem. & Ind. (Rev.)* 1291 (1954).
30. MILLER N. *Rev. Pure Appl. Chem.* **7,** 123 (1957).
31. MAHLMAN H. A. and BOYLE J. W. *J. Amer. Chem. Soc.* **80,** 773 (1958).
32. HARDWICK T. J. PRCM-8 progress report (1956). Chemistry and Metallurgy Division Chalk River, Ontario, Canada, see ref. 31.
33. MCDOWELL W. R. ANL-5206, January (1954), see ref. 31.
34. TRUMBORE C. N. and ATEN A. H. W. *J. Amer. Chem. Soc.* **78,** 4179 (1956).
35. FARKAS L. and MELVILLE H. W. *Proc. Roy. Soc.* A**157,** 625 (1936).
36. FARKAS L. *J. Chem. Soc.* 26 (1936).
37. FRIEDMAN H. L. and ZELTMAN A. H. *J. Chem. Phys.* **28,** 878 (1958).
38. WEISS J. *Nature* **165,** 728 (1950).
39. CZAPSKI G. and STEIN G. *Nature* **182,** 598 (1958).
40. DAVIS T. W., GORDON S. and HART E. J. *J. Amer. Chem. Soc.* **80,** 4487 (1958).
41. RIGG T., STEIN G. and WEISS J. *Proc. Roy. Soc.* A**211,** 375 (1952).
42. ETHIER I. P. and HABER F. *Naturwissenschaften* **18,** 266 (1930).
43. URI N. *Chem. Rev.* **50,** 375 (1952).
44. ALLEN A. O. and ROTHSCHILD W. G. *Rad. Res.* **7,** 591 (1957).
45. ALLEN A. O., HOGAN V. D. and ROTHSCHILD W. G. *Rad. Res.* **7,** 603 (1957).
46. ALLEN A. O. and ROTHSCHILD W. G. *Rad. Res.* **8,** 101 (1958).
47. BAXENDALE J. H. and HUGHES G. *Z. Phys. Chem.* **14,** 306 (1958).
48. GORDON S. and HART E. J. *J. Amer. Chem. Soc.* **77,** 3981 (1955).
49. CZAPSKI G. and STEIN G. *J. Phys. Chem.* **63,** 850 (1959).

VOL. 7 1959/

International Journal of Applied Radiation and Isotopes, 1960, Vol. 7, pp. 207–216. Pergamon Press Ltd. Printed in Northern Ireland

The Radiation-induced Synthesis of the Insecticide "Gammexane"—I

Synthesis by Ultra-violet Light

P. R. HILLS, R. ROBERTS and M. W. SPINDLER
U.K. Atomic Energy Authority, Isotope Research Division, Wantage Radiation Laboratory, Wantage, Berks

(*Received* 15 *May* 1959; *in revised form* 6 *August* 1959)

The optimum conditions for the preparation of 1:2:3:4:5:6-hexachloro*cyclo*hexane by the photo-activated addition of chlorine to benzene have been established.

Quantum yields have been determined under a variety of conditions. In the absence of additives and without any pretreatment, a value of $1{\cdot}58 \times 10^3$ has been recorded, which has been increased to $8{\cdot}67 \times 10^3$ by modifying the experimental conditions. The addition of activators did not increase the gross yield of γ-isomer, but a comparison with published data shows that high chlorination yields have been achieved.

LA SYNTHÈSE INDUITE PAR LE RAYONNEMENT DE L'INSECTICIDE 'GAMMEXANE"—I. SYNTHÈSE À LA LUMIÈRE ULTRAVIOLETTE

Les meilleures conditions pour la préparation de l' 1:2:3:4:5:6-hexachloro*cyclo*hexane par l'addition photo-activée du chlore à la benzène ont été établies.

Les rendements par quantum ont été dosés pour des conditions variées. On a enregistré une valeur de $1{,}58 \times 10^3$ en l'absence de matières additives et sans aucun traitement préalable, valeur qui croît à $8{,}67 \times 10^3$ avec modification des conditions expérimentales. L'addition de matières activantes n'augmenta pas le rendement de l'isomer γ, mais une comparaison avec les données publiées indiquent que l'on a atteint de hauts rendements de chlorination.

РАДИАЦИОННЫЙ СИНТЕЗ ИНСЕКТИЦИДА "ГАММЕКСАН"—I. СИНТЕЗ ПРИ ПОМОЩИ УЛЬТРАФИОЛЕТОВОГО ОСВЕЩЕНИЯ

Установлены оптимальные условия получения 1:2:3:4:5:6-гексахлорциклогексана при помощи фото-активированного присоединения хлора к бензолу.

Квантовый выход определялся в различных условиях. В отсутствии добавок и без предварительной обработки было получено значение $1{,}58.10^3$, которое было затем доведено до $8{,}67.10^3$ путем изменения условий эксперимента. Добавление активатора не увеличило общий выход γ-изомера, но сравнение с опубликованными данными показывает высокий выход продукта хлорирования.

STRAHLUNGINDUZIERTE SYNTHESE DES INSEKTENVERTILGUNGSMITTELS "GAMMEXAN"—I. SYNTHESE MIT HILFE VON UV-LICHT

Optimale Bedingungen zur Herstellung von 1:2:3:4:5:6-Hexachloro*cyklo*hexan durch photo-aktivierte Aufnahme von Chlor in Benzol wurden festgestellt.

Die Ausbeute bei verschiedenen Bedingungen wurde bestimmt. Ohne Zusätze und ohne Vorbehandlung wurde eine Wert von $1{,}58 \cdot 10^3$ gefunden, welcher durch Veränderung der Versuchsbedingungen auf $8{,}67 \cdot 10^3$ erhöht wurde. Durch Zusatz eines Aktivators wurde die Ausbeute an γ-Isomeren nicht wesentlich gesteigert, aber ein Vergleich mit veröffentlichten Daten zeigt, dass eine höhe Chlorierung erzielt wurde.

1. INTRODUCTION

THE insecticide "Gammexane" is produced conventionally by the chlorination of benzene in a chain reaction initiated by ultra-violet light. Various methods for improving the yield have been reported. For comparison with an alternative method using γ-radiation it was desirable to establish the optimum yields from conventional methods.

The interaction of chlorine and benzene in sunlight was first studied by FARADAY[1] who, in 1825, isolated a crystalline product which was probably the α-isomer of 1:2:3:4:5:6-hexachloro*cyclo*hexane. MITSCHERLICH[2] later observed that the reaction velocity was greatly accelerated by sunlight, and in 1903, SLATOR[3] undertook a detailed study of the reaction kinetics. Unfortunately he overlooked the inhibitory effect of oxygen, later reported by LUTHER and GOLDBERG[4] and so reduced the value of this otherwise comprehensive examination. Hexachloro*cyclo*hexane exists in several isomeric forms and in 1912, VAN DER LINDEN[5] established the existence of four isomers. The discovery in 1945[6] that the γ-isomer was a potent insecticide encouraged further study of the preparation of this material.

In 1924, LOISEAU claimed in a patent[7] that X-rays were effective in initiating the reaction and some years later ALYEA[8] used the α-particles emitted by radon gas. Recently HARMER[9] has studied the reaction under the influence of cobalt-60 radiation. The reaction was effectively promoted by such radiation and *G*-values for the production of hexachloro*cyclo*hexane ranging between 11,000 and 124,000 were recorded.

The commercial production of Gammexane by ultra-violet light introduces certain technical difficulties. The mercury arcs used are not easy to maintain and the reaction vessels must be fitted with quartz windows to admit the radiation. If the light is strongly absorbed, reaction occurs in the layer nearest to the window and this is soon covered by a film of product that interferes with the further absorption of light. The use of penetrating radiation makes quartz windows unnecessary and the design of the reaction vessels is simplified. Absorption problems are less severe since high-energy radiation allows a more uniform energy deposition throughout the reacting volume; neither does separation of the product impair the absorption of further energy.

Commercially the required γ-isomer is formed in only a 10–12% yield. Several methods have been proposed for the improvement of the yield, generally by the inclusion of small amounts of additives in the reacting mixture. In the present work conventional yields have been established which can later be compared with other results using high-energy radiation.

2. EXPERIMENTAL

The equipment for carrying out the photoinitiated chlorination of benzene consisted of a source of filtered ultra-violet radiation and a reaction vessel containing benzene, which could be cooled. Chlorination was effected by passing chlorine gas into the benzene and irradiating for a suitable period. The product was isolated by steam distillation which removed the unchanged hydrocarbon. Pure 1:2:3:4:5:6-hexachloro*cyclo*hexane could be obtained by partial extraction of the product with iced methanol. The γ-isomer content was determined by derivative polarograph using a potassium chloride/sodium acetate buffer as recommended by DRAGT.[10] The light intensity, a value of which was necessary for the evaluation of the quantum yield, was determined with a uranyl oxalate dosimeter.[11,12]

Materials

Both chlorine and nitrogen were obtained from cylinders. Chlorine—Imperial Chemical Industries, 99·8 per cent contained 60 volumes per million oxygen after the release of 10 per cent of the total volume. Nitrogen—British Oxygen Company, contained 10 volumes per million oxygen. Benzene—Analar grade. It was shown that Analar

benzene contained small amounts of impurity and for some experiments the Analar material was subjected to additional purification by successive treatments with concentrated sulphuric acid and a 20% solution of sodium hydroxide. After thorough washing with water the material was fractionally distilled from sodium hydroxide.

The light source

Ultra-violet radiation was obtained from an Osram Black Glass lamp (125 W; ref. MWB/U). The lamp was housed in a vented aluminium box from which the light emerged through a planoconvex lens, so that the mercury arc was at its focal point.

The reaction vessel

A 100 ml round-bottomed flask was modified by the formation of two opposite flattened faces, 4·5 cm apart to reduce reflection losses. The reaction vessel was equipped with a gas inlet tube passing to the bottom of the flask and a thermocouple pocket. Exit gases were vented through a wide bore polythene tube.

Ancillary apparatus

All experiments were conducted in a darkened fume chamber. Chlorine was passed from its cylinder to a glass spiral which was surrounded by a thermostatted water bath held at 25°, before passing to a flowmeter and into a mixing chamber. Nitrogen was admitted to the mixing chamber through another similar flowmeter. Before admission to the reaction vessel, the gases were washed with concentrated sulphuric acid, to remove moisture and entrained particles from the gas cylinders, and saturated with benzene in a Dreschel bottle to reduce evaporation losses from the reacting benzene. The Dreschel bottle was housed in its own opaque container. Cooling water was circulated by a Stuart–Turner centrifugal pump, controlled by a Variac transformer. The coolant was directed on to the reaction vessel so that the flask was covered by a moving film of water. After collection, it returned to the reservoir. This method of cooling caused a variation in the amount of radiant energy absorbed which was less than the experimental error for the actinometer system.

Experimental procedure

Benzene (120 ml) was poured into the reaction vessel and the appropriate purging and presaturation carried out. The reaction vessel was then irradiated and the water flow varied to maintain an even temperature. After irradiation the reaction mixture was treated in darkness with an excess of 5% sodium hydrogen carbonate solution. The organic phase was separated, washed with water (3 × 100 ml) and steam distilled until all the benzene was removed. The crude *product* was separated by filtration and dried to constant weight over silica-gel and sodium hydroxide pellets.

Separation of 1:2:3:4:5:6-*hexachloro*cyclo*hexane*

The crude material (39·1 g) from several experiments, was powdered finely and extracted with iced methanol (60 ml) for 30 min. The extract was allowed to stand overnight and the crop of crystals (4·5 g) m.p. 77–108°C removed. This product was three times recrystallized from chloroform to afford γ-isomer m.p. 112·2–2·7°C. The melting point was unchanged when mixed with an authentic sample. The residue from the methanolic extraction was twice refluxed with carbon tetrachloride (60 and 50 ml) which deposited tabular crystals (7·31 and 8·12 g) respectively, m.p. 148·0–9·5°C. The first extract deposited more crystals (4·5 g) m.p. 155·0–5·5°C overnight. The first two products were combined and recrystallized twice from acetone and twice from carbon tetrachloride to give α-*isomer* m.p. 157–158°C. The residue from the carbon tetrachloride extractions (2·33 g) m.p. 294–311 5°C was twice recrystallized from acetone to give the β-*isomer* m.p. 309–10°C.

Determination of peroxides and hydroperoxides in benzene

Peroxides are able to oxidize ferrous to ferric iron. The ferric iron was determined spectrophotometrically via the intensely coloured compound ferric thiocyanate.[13] A stock solution was prepared from 1% ferrous

ammonium sulphate (50 ml), 1 N sulphuric acid (10 ml) and 0·1 N thiocyanate solution (10 ml). Aliquots (10 ml) of the stock solution were transferred to volumetric flasks containing the appropriate benzene sample (30 ml). The mixture was diluted to 50 ml and well shaken. After separation, the lower aqueous phase was removed for spectrophotometric measurement. An analogous blank was prepared from carbon tetrachloride. Optical densities were recorded at 4800 Å in 4 cm silica cells.

3. RESULTS AND DISCUSSION

(a) *Reaction without additives*

The aim of this series of experiments was to establish the optimum conditions for the chlorination of benzene under the influence of ultra-violet light alone. It was first necessary to establish that the reaction was completely dependent on the radiation used.

In the absence of radiation Analar benzene gave a hexachloro*cyclo*hexane yield of 1·363 $\times 10^{-2}$ moles per cent per hour while the corresponding figure for benzene purified by acid and alkaline washing was 1·386 $\times 10^{-2}$. Compared with results obtained later under the influence of ultra-violet light the relative yield was 0·04 per cent. As the dark reaction was negligible, it was possible to proceed to light-initiated reactions.

The optical transmission of pure benzene and benzene saturated with chlorine was measured at 3650 Å, the wavelength of the light emitted from the source, in 1 cm silica cells. Transmissions were respectively 99·4 and less than 0·5 per cent. It could therefore be assumed that all the radiant energy available was absorbed in the reaction vessel, and that the absorption was almost exclusively by the chlorine.

The effect of dissolved air on the reaction. In order to assess the magnitude of this effect, a series of experiments was conducted, in which various degrees of purging of the benzene were applied to remove dissolved air other than the small amount contained in the feed gases. The conditions employed were as follows, and are represented schematically in Fig. 1.

(1) A mixture of nitrogen and chlorine was passed into the hydrocarbon for 15 min, with irradiation for the whole period.

(2) As (1), but preceded by a nitrogen purge for 15 min.

(3) Benzene was purged with nitrogen for 15 min, then saturated with a stream of nitrogen and chlorine and finally irradiated for 15 min with the continued passage of the mixed gases.

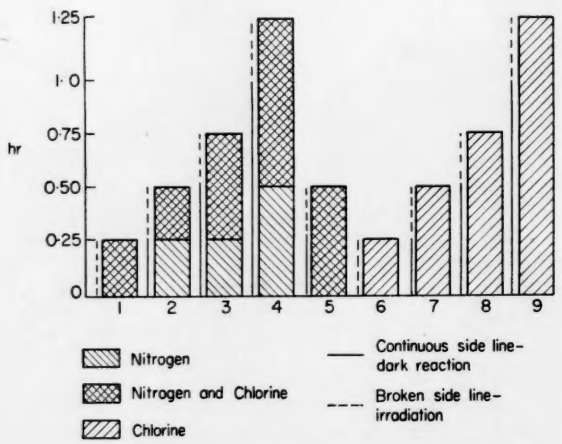

FIG. 1. Conditions for photo-initiated chlorinations.

The results of these and following experiments are set out in Table 1. Quantum yields were based on the number of chlorine molecules that had reacted. A preliminary purging improved the yield and an initial saturation with chlorine increased the yield still further.

Other conditions were employed as follows:

(4) The purging and saturation times were increased to 30 min each.

(5) The preliminary treatments were combined in a 15-min passage of chlorine and nitrogen together.

The extended purging did not afford a greatly increased yield and the combination of purging and saturation was moderately effective. The result of omitting the nitrogen purge altogether was then examined for four different saturation times, as follows:

(6) Chlorine was passed into the hydrocarbon for 15 min with irradiation.

(7,8,9) The benzene was saturated before irradiation by passing of chlorine for 15, 30 and 60 min respectively.

TABLE 1. The influence of conditions on chlorination yield

Condition	Yield (moles %)	Quantum yield	Average quantum yield
1	5·77	$1·48 \times 10^3$	$1·58 \times 10^3$
	6·58	$1·69 \times 10^3$	
2	12·31	$3·15 \times 10^3$	$3·14 \times 10^3$
	12·22	$3·13 \times 10^3$	
3	15·14	$3·88 \times 10^3$	$3·98 \times 10^3$
	15·97	$4·09 \times 10^3$	
4	16·43	$4·21 \times 10^3$	$4·31 \times 10^3$
	16·43	$4·21 \times 10^3$	
5	15·89	$4·08 \times 10^3$	$4·08 \times 10^3$
6	10·63	$2·72 \times 10^3$	$2·86 \times 10^3$
	11·70	$3·00 \times 10^3$	
7	14·49	$3·71 \times 10^3$	$3·63 \times 10^3$
	13·84	$3·54 \times 10^3$	
8	26·05	$6·67 \times 10^3$	$6·63 \times 10^3$
	25·70	$6·58 \times 10^3$	
9	33·69	$8·64 \times 10^3$	$8·67 \times 10^3$
	33·89	$8·69 \times 10^3$	

The extended presaturation times altered the yield quite favourably, but the trend of the figures indicated that saturation times in excess of 1 hr would produce relatively small increases in yield. Assuming that the velocity of the reaction was a function of the chlorine concentration, the omission of nitrogen would result in an increased chlorine concentration, and therefore, an elevated yield.

The effect of hydrocarbon purity on the reaction. In the foregoing experiments, it was observed that the agreement between duplicate runs improved as more stringent purification techniques were adopted. The irregular behaviour noted in the early experiments is not uncommon in the presence of chlorination inhibitors such as oxygen and some peroxy compounds. In later experiments it might be expected that all atmospheric oxygen would have been removed, but the possibility of combined oxygen still being present could not be excluded. Such an impurity might still be reducing the quantum yield in the later experiments.

The presence of peroxide-forming compounds. A sample of Analar benzene was subjected to vapour-phase chromatography to detect volatile impurities which might form peroxides or hydroperoxides. Using a dinitrodiphonic ester column, two peaks were recorded before the benzene peak. The more volatile component exhibited a shoulder which could have indicated the presence of another component. From the areas under the peaks, the two main constituents comprised 0·48 and 0·19 per cent of the Analar benzene. A chromatogram for chemically purified benzene was also made. The areas of the peaks and the component ratios are set out in Table 2.

The reduction of component *B* in the purified sample could be due to the removal of an unsaturated hydrocarbon by sulphuric acid.

The presence of peroxides. These impurities in the benzene might be able to form inhibitory peroxides or hydroperoxides. The

TABLE 2. Vapour-phase chromatography of Analar benzene

Sample	Component *A* Peak area	Component *B* Peak area	Ratio *A* : *B*
Analar	45 units	16 units	2·81 : 1
Purified	38 units	10 units	3·80 : 1

peroxide content of various benzene samples was determined spectrophotometrically. From the relative values of the peroxide content, indicated by the optical densities in Table 3, it was observed that Analar benzene contained an appreciable amount of peroxide. Purification reduced this amount to almost zero but when stored in air the peroxide content increased. Storage under nitrogen retarded the development of oxidizing materials while irradiation in air accelerated their formation.

Further chlorinations were conducted with purified and Analar benzene that had been refluxed for 30 min and distilled, in an atmosphere of nitrogen. The middle fraction was transferred to the reaction vessel in an oxygen-free atmosphere. This treatment should have destroyed all peroxides and prevented their re-formation. From the results in Table 4, it appeared that chemical purification had little effect on the eventual yield but that destruction of the peroxides by heating increased the yield slightly.

The formation of peroxides during the reaction. From the results obtained by vapour-phase chromatography and peroxide determination, it appeared that the impurities present might combine with residual oxygen photochemically, and inhibit the formation of hexachloro*cyclo*hexane. This effect was

TABLE 3. Relative peroxide content of various benzene samples

Sample	Optical density
Analar stored in air	0·107
Purified stored in air	0·033
Purified stored under nitrogen	0·007
Freshly purified	0·001
Irradiated in air	0·153

TABLE 4. Influence of hydrocarbon purity on chlorination yield

Condition	Quantum yield		
	Analar air stored	Purified air stored	Oxygen free
3	$3{\cdot}88 \times 10^3$	$4{\cdot}18 \times 10^3$	—
	$4{\cdot}09 \times 10^3$	$4{\cdot}48 \times 10^3$	—
8	$6{\cdot}67 \times 10^3$	$6{\cdot}39 \times 10^3$	$7{\cdot}71 \times 10^3$
	$6{\cdot}58 \times 10^3$	$6{\cdot}61 \times 10^3$	$7{\cdot}43 \times 10^3$
9	$8{\cdot}67 \times 10^3$	$8{\cdot}46 \times 10^3$	—
		$8{\cdot}51 \times 10^3$	—

studied by conducting experiments with Analar benzene that had been pre-irradiated in air. The hydrocarbon was irradiated for 30 or 60 min in air prior to the normal saturation with chlorine for 30 min in the dark, and then a light-induced reaction was carried out for 15 min. A 30-min pre-irradiation afforded duplicate quantum yields of 2·01 and $1{\cdot}99 \times 10^3$, while for a 60-min period the yield fell to $1{\cdot}11 \times 10^3$. In order to examine the connexion between atmospheric oxygen and the observed inhibition a sample of benzene was first purged with nitrogen for 15 min before pre-irradiation for 30 min. An improved quantum yield of $4{\cdot}55 \times 10^3$ was obtained. It was therefore apparent that residual oxygen when present inhibited the reaction.

Further chlorinations were carried out with the highly purified hydrocarbon. With a presaturation for 1 hr under standard conditions duplicate quantum yields of 8·46 and $8{\cdot}51 \times 10^3$ were obtained, which were comparable with the best average value of $8{\cdot}67 \times 10^3$ (Condition 9, Table 1).

It has been shown, by following the rise in temperature due to the exothermic solution of chlorine in benzene, that the hydrocarbon was saturated within 20 min. However, saturation times in excess of 20 min resulted in improved yields. These enhanced figures could not be due to increased chlorine concentration and could only be caused by the destruction of inhibitors during the prolonged saturation.

VOL. 7 1959/6

TABLE 5. Gross yield of γ-isomer under various conditions

Condition	$\phi \times 10^{-3}$	x	ϕx	Comparative yield
1	1·58 ± 0·10	14·08 ± 0·40	2224	0·19
2	3·14 ± 0·01	14·27 ± 0·22	4481	0·39
3	3·98 ± 0·10	14·34 ± 0·18	5707	0·50
4	4·31 ± 0·10	14·50 ± 0·71	6250	0·55
5	4·08 (1)	14·59	5953	0·52
6	2·86 ± 0·13	14·07 ± 0·12	4024	0·35
7	3·63 ± 0·09	12·86 ± 0·04	4668	0·41
8	6·63 ± 0·05	12·55 ± 0·34	8320	0·73
9	8·67 ± 0·02	13·17 ± 1·27(7)	11418	1·00
P 3	4·33 ± 0·15	13·71 ± 0·07	5936	0·52
P 8	6·50 ± 0·11	11·58 ± 0·16	7257	0·66
R 8	7·57 ± 0·14	12·05 ± 0·00	9121	0·80
P 9	8·49 ± 0·02	15·31 ± 1·06(3)	13451	1·18

P—Purified benzene. R—Redistilled benzene, transferred under nitrogen.

The production of the γ-isomer. In the foregoing account quantum yields were assessed on the total production of hexachloro*cyclo*hexane. The influence of these various conditions on the γ-isomer yield was next examined.

The samples of crude hexachloro*cyclo*hexane, obtained in the first series of experiments, were analysed polarographically for γ-isomer. These results are reported in Table 5. The product of the quantum yield, ϕ, and the γ-isomer percentage, x, is proportional to the total amount of γ-isomer produced in any experiment. The value for this quantity under the conditions that gave the best quantum yield was assigned an arbitrary value of unity and in the final column, the other values of ϕx are expressed comparatively. Unless otherwise indicated by a figure in parentheses the results were derived from duplicate runs.

The results in Table 5 indicated that no substantial improvement in the yield of γ-isomer was obtained throughout the various conditions. Several experiments were conducted at the best obtainable conditions to provide a realistic figure but the spread of results was certainly larger than the experimental error on the polarographic determination. There are indications that the use of purified benzene does result in a marginal improvement in the yield.

GUNTHER,[14] using a production method earlier described by another worker[15] found that extensive reaction afforded a product from which the γ-isomer was isolated in 42% yield. Prolonged chlorinations under the standard conditions were not effective in increasing the γ-isomer content (Table 6).

(b) *Reaction with additives*

Many additives have been suggested for the improvement of the γ-isomer yield.[16,17,18] Various additions were made to chlorination experiments under the standard conditions. In each case 1 g of additive was used either in solution or suspension. The results are collected in Table 7.

In no instance was the gross yield of γ-isomer improved. Where the actual γ-content had been increased the accompanying reduction in the total yield of hexachloro*cyclo*hexane cancelled this advantage.

FÜRST *et al.* have published several papers[19,20,21] related to the improvement of the yield of γ-isomer in the chlorination of benzene. One of these contributions[21] is

TABLE 6. The influence of prolonged chlorination on chlorination yields

Chlorination time (min)	γ-Content (%)
15	13·17 ± 1·27
30	13·87 ± 0·44
60	13·63 ± 0·50

TABLE 7. The influence of additives on the gross yield of γ-isomer

Additive	$\phi \times 10^{-3}$	x	ϕx	Comparative yield
Water	5·90 ± 0·10	11·78 ± 0·09	6950	0·61
Acetic acid	6·27 ± 0·03	17·38 ± 1·29	10897	0·95
Acetone	7·10 ± 0·25	16·11 ± 1·91(3)	11438	1·00
Ether	5·81 ± 0·13	14·95 ± 1·15	8686	0·76
Dioxan	4·42 ± 0·45	12·23 ± 0·05	5406	0·47
Alumina	4·86 ± 0·00	14·65 ± 0·64	7266	0·64
Activated charcoal	3·93 ± 0·36(5)	15·65 ± 1·46(5)	6150	0·54
Ferric chloride	0·00 (3)	—	0	0·00
Iodine	0·00 (3)	—	0	0·00
Cuprous chloride	4·32 ± 0·00	13·33 ± 0·95	5756	0·50
Phosphorus pentoxide	5·28 ± 0·35	12·77 ± 0·88	6743	0·59
Sodium sulphite	7·23 ± 0·60	15·00 ± 0·75	10845	0·95
Ammonium persulphate	6·70 ± 0·05	13·36 ± 0·49(3)	8951	0·78
Sodium thio-sulphate	4·78 ± 0·08(3)	12·81 ± 0·21	6128	0·54
Sodium dithionite	5·87 ± 0·17	13·12 ± 0·27	7701	0·67
Potassium permanganate	4·13 ± 0·05	14·79 ± 0·50(3)	6108	0·54
HCH*	4·51 ± 0·05	14·79 ± 0·23	6670	0·58

* Hexachloro*cyclo*hexane. Crude material first treated with methanol to reduce γ-isomer content. (Final content 4 per cent.)

concerned with the influence of inorganic substances on the reaction. In all, 150 compounds, selected from all groups of the periodic classification were examined. These workers chose as standard conditions the reaction of 100 g of benzene with a stream of chlorine, the flow of which oscillated between 4 and 6 l./hr. The period of each experiment was 90 min. Radiant energy was obtained from a 60 W/220 V incandescent lamp which gave an intensity of illumination "a quarter that of diffused daylight" when measured with a selenium photocell. No attempt was made to filter the light. Control experiments were carried out at 20°C and from the six results quoted, the average yield in grammes and the average γ-isomer content could be computed. The results were 9·0 ± 2·3 g and 19·9 ± 0·1% respectively. The large spread in the control yield, between 4·0 and 11·0 g was not surprising, since no attempt was made to remove oxygen at the commencement of each experiment. From the description of the various products, e.g. solid, soft or greasy, it would appear that the properties of the crude hexachloro*cyclo*hexane were not constant.

Of the 150 activators examined, results were quoted for twenty-six compounds that gave a γ-content in excess of 17 per cent, for thirteen compounds which gave a gross yield above 20 and for sixteen compounds which gave a negligible yield due to the almost complete inhibition of the reaction. A comparison of the results of FÜRST *et al.* and the results obtained in the present study are set out in Table 8. In both cases crude yields have been related to those derived from the appropriate light-initiated reaction in the absence of activator.

There are several reasons for the apparent lack of agreement in the results. FÜRST *et al.* have shown that the high polarographic values for the γ-isomer content are spurious.

VOL. 7 1959/

TABLE 8. Comparison of results with other published data

Additive	FÜRST *et al.*[18]		Current work	
	Yield	γ-Content	Yield	γ-Content
None	1·00	19·9	1·00	13·17
Ferric chloride	3·33	17·1	0·00	—
Iodine	0·26	37·0	0·00	—
Ammonium persulphate	5·33	15·5	0·77	13·36
Sodium thiosulphate	5·30	16·6	0·55	12·82
Sodium dithionite	2·37 3·04	20·8 18·7	0·67	13·12
Potassium permanganate	0·49	22·6	0·52	14·79
Magnesium oxide	0·11 5·47	22·0 16·1	—	—

They have proved that a tetrachloro*cyclo*hexane is produced as an intermediate, which contaminates the final product. This gives rise to a large increase in the apparent analytical value for the γ-isomer as measured by polarography. In fact, biological assay of some of their crude products indicated that the true content is less than that of typical commercial products. Under the mild experimental conditions employed by these workers it appears that the reaction does not go to completion, resulting in the formation of significant amounts of the tetrachloro*cyclo*hexane. The conditions applied in the present work are much more vigorous and the reaction will proceed to completion with the formation of hexachloro*cyclo*hexane. This was confirmed by analysing the chlorination products biologically and by their infrared absorption.

It may be assumed that the various activators employed in this reaction act as photosensitizers.

Chlorine absorbs light in two main spectral regions. One extends from 6430 Å to 2500 Å with a maximum at 3350 Å, and the other from 1900 Å to 1560 Å. The first band is continuous below 4785 Å and only in these regions does the absorption coefficient have any real magnitude.[22] Below this wavelength the chlorine molecule is dissociated.

Only light of wavelength less than 4785 Å will be effective in the induction of the benzene–chlorine reaction and the light wavelengths close to that of the absorption maximum will have the greatest effect. The output of a normal tungsten filament lamp (Fig.2) [23] extends from 3200 Å to 25,000 Å with its energy maximum at 10,500 Å, and only a minute part of its energy can be usefully absorbed by chlorine.

With tungsten illumination alone little overall reaction could be expected. However, in the presence of photosensitizers, such as the additives used by the German workers, complexes might be formed between the additive and chlorine, which could produce

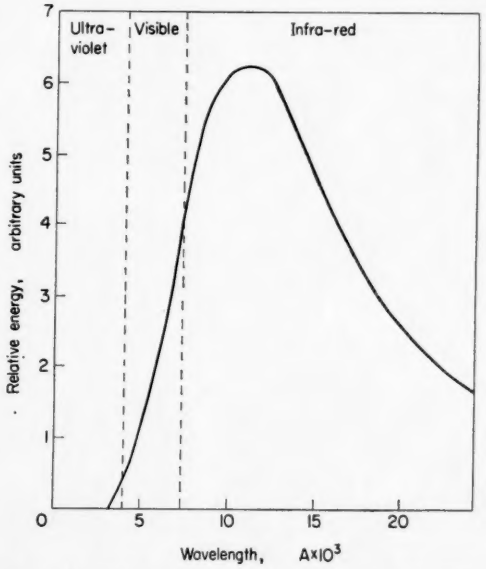

FIG. 2. Distribution of energy in the spectrum of tungsten filament lamp at 2750°K.

chlorine radicals when subjected to light of lower energy than that required to dissociate the chlorine molecule. Therefore it is reasonable that the use of photosensitizers results in enhanced yields. In the present work the light source used was sensibly monochromatic and the wavelength of 3650 Å employed was of maximum usefulness for the dissociation of chlorine. Under these conditions it is not surprising that the yields were not increased by the use of photosensitizers.

It is instructive to compare FÜRST's results with those obtained from the present work, in terms of the real yields expressed in moles per cent per hour. For the dark reaction, the figure is 5·074 moles per cent per hour, whereas our corresponding value is $1{\cdot}363 \times 10^{-2}$. The best conversion obtained in the earlier work was in the presence of magnesium oxide, under which conditions it can be computed that the yield was 6·908 moles per cent per hour. Yields of 33·79 moles per cent per hour have been noted in the current work in the absence of photosensitizers.

REFERENCES

1. FARADAY M. *Ann. Chim.* (*Phys.*) **29,** 269 (1825).
2. MITSCHERLICH E. *Ann. Physik. Chem.* **35** (2), 370 (1835).
3. SLATOR A. *Z. Phys. Chem.* **45,** 540 (1903).
4. LUTHER R. and GOLDBERG E. *Z. Phys. Chem.* **56,** 43 (1906).
5. VAN DER LINDEN L. *Ber. Dtsch. Chem. Ges.* **45,** 236 (1912).
6. SLADE R. E. *Chem. & Ind.* (*Rev.*), 314 (1945).
7. LOISEAU L. M. J. *Fr. Pat.* 565 356 (1924).
8. ALYEA H. W. *J. Amer. Chem. Soc.* **52,** 2743 (1930).
9. HARMER D. E. AECU Report 3077 (1955).
10. DRAGT G. *Analyt. Chem.* **19,** 7701 (1949).
11. PITTS J. N., MARGERUM J. A., TAYLOR R. P. and BRIM W. *Analyt. Chem.* **77,** 5499 (1955).
12. FORBES G. S. and HEIDT L. J. *J. Amer. Chem. Soc.* **56,** 2363 (1934).
13. WEISSBERGER A. *Technique of Organic Chemistry* Vol. 7, p. 315. Interscience Publishers, New York (1955).
14. GUNTHER F. A. *Chem. & Ind.* (*Rev.*), 399 (1946).
15. MATHEWS F. E. *J. Chem. Soc.* **59,** 165 (1891).
16. HAEN R. DE *Brit. Pat.* 694 405 (1953).
17. ORLOFF H. O. and WOREL C. V. *U.S. Pat.* 2691051 (1954).
18. POVENZ F. *Ger. Pat.* 873841 (1953).
19. FURST H., LANG J. and RAMMELT P-P, *Chem.-Tech.* (*Berlin*) **5,** 359 (1953).
20. LANGENBECK W., LOSSE G. and FÜRST H. *Chem.-Tech.* (*Berlin*) **4,** 247 (1952).
21. LANGENBECK W., LOSSE G. and FÜRST H. *Chem.-Tech.* (*Berlin*) **5,** 561 (1953).
22. HALBAN H. VON and SIEDENTOPF K. *Z. Phys. Chem.* **103,** 71 (1922).
23. Research Laboratories of the General Electric Company Ltd. *The Problem of Artificial Illumination* —V. G. E. C. Publicity Organisation (1939).

VOL.
7
1959/

International Journal of Applied Radiation and Isotopes, 1960, Vol. 7, pp. 217–224. Pergamon Press Ltd. Printed in Northern Ireland

The Radiation-induced Synthesis of the Insecticide "Gammexane"—II Synthesis by High-energy Radiation

P. R. HILLS, R. ROBERTS and M. W. SPINDLER
U.K. Atomic Energy Authority, Isotope Research Division, Wantage Radiation Laboratory, Wantage, Berks

(*Received* 15 *May* 1959; *in revised form* 6 *August* 1959)

A study of the preparation of 1:2:3:4:5:6-hexachloro*cyclo*hexane by radiation from cobalt-60 has shown that the Gammexane content of the crude material is independent of dose rate, benzene concentration and duration of the chlorination process. Small increases in the Gammexane content can be effected by low temperature chlorination.

When compared with the conventional photo-initiated reaction the radiation method exhibits a marginal improvement in Gammexane content but the efficiency of energy utilization is similar.

LA SYNTHÈSE INDUITE PAR LE RAYONNEMENT DE L'INSECTICIDE "GAMMEXANE"—II. SYNTHÈSE AU RAYONNEMENT DE HAUTE ÉNERGIE

La recherche sur la préparation de l'1:2:3:4:5:6-hexachloro*cyclo*hexane au moyen du rayonnement du cobalt 60 a montré que le titre de Gammexane dans la matière crue est indépendant du taux de dose, de la concentration de benzène et de la durée du procédé de chlorination. La chlorination à température basse peut achever de petites augmentations du titre de Gammexane.

Comparée avec la réaction photo-initiée conventionnelle, la méthode à rayonnement montre une amélioration marginale du titre de Gammexane mais l'efficacité d'emploi de l'énergie est pareille.

РАДИАЦИОННЫЙ СИНТЕЗ ИНСЕКТИЦИДА "ГАММЕКСАН"—II. СИНТЕЗ С ПОМОЩЬЮ ИЗЛУЧЕНИЯ ВЫСОКОЙ ЭНЕРГИИ

Исследование получения 1:2:3:4:5:6-гексахлорциклогексана при помощи излучения Co^{60} показало, что содержание гаммексана в неочищенном веществе не зависит от мощности дозы, концентрации бензола и продолжительности процесса хлорирования. Небольшое увеличение содержание гаммексана достигается низко-температурным хлорированием.

По сравнению с обычным фото-инициированием радиационный метод несколько увеличивает содержание гаммексана, но эффективность используемой энергии не меняется.

STRAHLUNGINDUZIERTE SYNTHESE DES INSEKTENVERTILGUNGSMITTELS "GAMMEXAN"—II. SYNTHESE DURCH HOCHENERGETISCHE STRAHLUNG

Eine Untersuchung der Herstellung von 1:2:3:4:5:6-Hexachloro*cyklo*hexan durch Strahlung von Co^{60} zeigt, dass der Gammexan-Gehalt im Rohmaterial von Dosisrate, Benzol-Konzentration und der Dauer des Chlorierungsprozesses unabhängig ist.

Im Vergleich mit der üblichen photosynthetischen Reaktion zeigt die Strahlungsmethode eine leichte Verbesserung des Gammexan-Gehaltes, aber die Wirksamkeit der Energieverwertung ist gleich.

1. INTRODUCTION

PART I of this paper[1] has described the initiation of the reaction by ultra-violet light when it was found impossible to increase the γ-isomer yield by the addition of various inorganic and organic materials. The yield of "Gammexane" obtained ranged from 12–16 per cent and under optimum conditions where the rate of halogenation was a maximum about 12–14 per cent of the product consisted of the γ-isomer.

The aim of the present work was to investigate the effect of dose rate, benzene concentration, temperature and degree of conversion on both the γ-isomer content and the overall yield of product for the high-energy radiation-initiated reaction.

2. EXPERIMENTAL

Radiation source

Radiation was obtained from a 700 c cobalt-60 source housed in a concrete shield, the design and operation of which has been described elsewhere.[2] The irradiation chamber was illuminated by a low-power ruby bulb in order to obviate any risk of photochemical initiation of the reaction.

Dosimetry

The ferrous sulphate system was used to measure the dose received by the contents of the reaction vessel. Experiments were carried out with the reaction vessel containing an amount of dosimeter solution equivalent to the charge used in the chlorination runs and with the cooling jacket filled with water.

The reaction vessel

This consisted of an inner cylinder of 100 ml capacity surrounded by an annular jacket through which cooling water could be passed. The inlet for chlorine and nitrogen extended to the bottom of the vessel and a thermo-couple well, terminating at the centre of the reaction volume, was included. The exit gases were discharged through a bulb surrounded by an ice–salt mixture. The bulb acted as a combined splash head and condenser from which spray and condensate drained back into the reaction vessel.

The gas train (Fig. 1)

The supply of nitrogen and chlorine was described in Part I of this paper. The gas train was protected by two surge bottles, one on either side of the wall of the shield through which the gases passed. As the passage of the dry gas mixture caused considerable

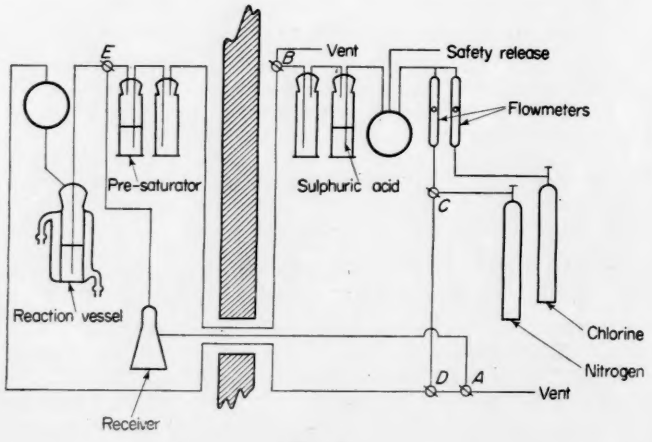

FIG. 1.

evaporation losses from the reaction vessel, the gases were passed through a pre-saturator whose contents were identical with those of the reaction vessel. It was found that the use of the pre-saturator and the partial condenser prevented any overall losses from the reaction vessel. The outgoing gases were passed to the atmosphere through a polythene tube connected to the splash head. Several three-way taps were incorporated to extend the usefulness of the system. Taps *A* and *B* could be opened to the atmosphere to avoid the "suck-backs" which otherwise occurred on interruption of the gas flow. Tap *B* could also be used to isolate the first stage of the system for testing the flow meters. The removal of the contents of the reaction vessel resulted in the copious liberation of chlorine even when these had been well purged with nitrogen, hence a product removal loop was essential. By applying a back pressure of nitrogen through taps *C* and *D* while tap *A* was closed, the product could be displaced through the gas delivery tube and tap *E* into the receiver. Any residual product was removed with additional solvent introduced through the inlet of the splash head and displaced as above.

OL.
7
59/60

The chlorination of benzene

Benzene or a mixture of benzene and carbon tetrachloride (80 ml) was added to the reaction vessel and chlorine passed for 1 hr to de-aerate and saturate the hydrocarbon. Previous work had indicated this to be the optimum period. The vessel was then irradiated for a given time, usually 15 min, and finally most of the excess chlorine was removed by the passage of nitrogen. During the reaction the supply of cooling water was adjusted periodically to maintain an even temperature. The product was then discharged into a receiver and isolated as before.

Separation of the isomers of 1:2:3:4:5:6-*hexachlorocyclohexane*

The products from several identical runs (80g) were combined, and separated as described in Part I of this paper.[1] There were obtained *γ-isomer* (5·38g), m.p. 112·5°C, unchanged when mixed with authentic material, *α-isomer* (17·02g), m.p. 157–157·5°C, and *β-isomer* (17·0g), m.p. 309°C.

Analysis of 1:2:3:4:5:6-*hexachlorocyclohexane-γ-isomer*

The polarographic method for the determination of γ-isomer has been referred to in Part I. It has been stated in the literature[3] that by-products of low chlorine content can give rise to spurious polarographic results. The presence of materials of low chlorine content was unlikely in the present work owing to the conditions used, but the validity of the polarographic technique was verified by two alternative methods.

Several analyses were conducted by a biological technique in which grain weevils—*Calandra granaria*—were incubated on filter paper impregnated with graded amounts of the samples under test. A similar control incubation was carried out with pure Gammexane. The response curve relating concentration of toxic material with percentage morality is of a sigmoid form and the necessary probit transformation and statistical evaluation of such results has been described by FINNEY.[4]

Biological evaluation of γ-isomer

A series of ten petri dishes each containing a closely fitting disc of filter paper was prepared for each sample and various amounts of an alcoholic solution of the sample were added to each plate so that the concentration range 20–200 mg/m² was covered in equal steps. The plates were then exposed to the atmosphere until the odour of the solvent had disappeared. A similar series was prepared with pure γ-isomer for the concentration range 2–20 mg/m². Another group of plates was treated with solvent only to act as a blank.

One hundred grain weevils were added to each of the plates which were then sealed with adhesive tape and incubated at 22°C for 24 hr. After incubation the insects were

removed to a warmed enamel dish and the living insects counted and removed with a suction bottle. The remaining insects were re-warmed and those which showed no movement after an individual examination of 5 sec were counted as dead.

From the relationship between the concentration at each level and the percentage mortality after correcting for the mortality observed in the blanks, the dose sufficient to kill half of the insects could be calculated—50% lethal dose (L.D.50). In later runs the probit transformation and the consequent statistical analysis was carried out on a Ferranti Mercury computer according to a programme which has been reported by Cooper.[6] The γ-isomer content of the test series was obtained by comparison with the L.D. 50s of the control experiments.

The results were consistent with those obtained polarographically although standard deviations of the order 3–5 per cent were obtained. These were attributed to several factors which could only be controlled in a laboratory fully equipped for biological evaluations of this type. It was observed, for instance, that the toxicity of a given material varied widely with the age of the insect and since some 7000 insects were used for the parallel estimation of each five samples, it was impractical to standardize the age of the insects used. The counting of the plated insects was a lengthy procedure both by reason of the numbers involved and the difficulty of deciding in a brief examination if an insect was dead or alive. As this decision was necessarily subjective it was essential to employ only one operator and to randomize the order in which the plates were examined. This imposed a considerable variation in the length of time the insects were in contact with the toxic material before counting and introduced a significant random variation to the results.

Some typical results were as follows:

Polarographic	13·3 ± 0·2%;	13·7 ± 0·2%;	13·7 ± 0·2%.
Biological	15 ± 3%;	11 ± 5%;	12 ± 3%.

Since further refinements of the biological evaluation were not possible in a general laboratory, an alternative method was used. Infra-red analysis, conducted according to the method of Hudson[5] gave the following results on three different samples obtained during the present work:

Polarographic	12·7 ± 0·2%	17·5 ± 0·3%	13·6 ± 0·2%
Infra-red	11·9 ± 1·8%	16·4 ± 1·3%	14·4 ± 1·9%

From these alternative procedures it was concluded that the polarographic method would be suitable for all further determinations.

VOL. 7 1959/6

3. RESULTS AND DISCUSSION

(a) *The influence of reaction conditions on γ-isomer content*

The effect of dose rate and benzene concentration. The γ-isomer yield was measured at several dose rates for various benzene–carbon tetrachloride mixtures as shown in Table 1. (Figures in parentheses indicate the degree of replication.) The results obtained

Table 1. γ-Isomer content at several dose rates and benzene concentrations

Benzene concentration (vol. %)	Dose rate (rads/hr)							
	$2{\cdot}33 \times 10^3$	$4{\cdot}05 \times 10^3$	$5{\cdot}56 \times 10^3$	$7{\cdot}06 \times 10^3$	$8{\cdot}22 \times 10^3$	$2{\cdot}09 \times 10^4$	$5{\cdot}13 \times 10^4$	Average
20	16·7	16·9	16·2	11·3	15·2 ± 2·5(2)	15·7	12·7	15·0 ± 2·2(8)
40	15·8 ± 10(2)	17·7	13·0	13·1	14·4	12·6	15·6	16·8 ± 1·8(8)
60	17·3	17·4	13·6	—	14·1	15·4	15·9	15·6 ± 1·6(6)
80	15·6 ± 1·2(3)	14·3 ± 0·3(3)	16·3 ± 0·4(2)	—	—	12·7	—	15·0 ± 1·4(9)
100	15·9 ± 0·9(8)	17·4	15·1	—	—	16·3	—	16·0 ± 1·0(11)
Average	15·9 ± 1·0(15)	16·1 ± 1·6(7)	15·1 ± 1·5(6)	12·2 ± 1·3(2)	14·7 ± 1·5(4)	14·5 ± 1·8(5)	14·7 ± 1·8(3)	15·3 ± 1·6(42)

TABLE 2. γ-Isomer content at several reaction temperatures

Temp. (°C)	Medium	Dose rate (rads/hr)	Gamma content (%)
−72	20% benzene–chloroform	$7{\cdot}03 \times 10^3$	$18{\cdot}1 \pm 0{\cdot}2$
25	20% benzene–chloroform	$7{\cdot}03 \times 10^3$	$16{\cdot}6 \pm 0{\cdot}1$
21	100% benzene	$7{\cdot}03 \times 10^3$	$16{\cdot}5 \pm 0{\cdot}4$
80	100% benzene	$7{\cdot}03 \times 10^3$	$13{\cdot}6 \pm 0{\cdot}2$

indicated no real change either with benzene concentration or dose rate.

The effect of temperature. The variation of the yield of γ-isomer with temperature was also studied between −72° and 80°C. At the lower temperature, mixtures of benzene and carbon tetrachloride could not be used since these solidified. By the determination of the freezing points of a number of benzene–chloroform mixtures, it was found that mixtures containing less than 40 per cent by volume of benzene were liquid at −72° and therefore a 20% solution of benzene in chloroform was chosen as the reaction medium. The reaction was carried out in a Dreschel bottle of dimensions similar to those of the water-jacketed flask used for runs at room temperature, using a mixture of solid carbon dioxide and alcohol as a refrigerant. Similarly a further series of experiments was conducted at the boiling point of benzene. The results are shown in Table 2. A comparison of the results at 25° and 21°C in benzene–chloroform and pure benzene indicates no change in the γ-isomer content due to the use of a different reaction medium.

From these results it could be seen that there was a marginal improvement in the percentage of γ-isomer obtained at −72°. However, this was of little practical significance since the overall yield was much reduced at this temperature.

The effect of increased reaction time. It has been reported[7] that exhaustive chlorination of benzene results in a crude product from which the γ-isomer may be isolated in a 42% yield. Accordingly the normal irradiation period of 15 min used in the current work was extended to 30 and 60 min. The results obtained for the yield of γ-isomer after various times were respectively 15 min, 16·1 per cent; 30 min, 15·2 per cent; and 60 min, 15·2 per cent. It appeared that the γ-isomer content was not improved by extending the irradiation period.

(b) *The influence of reaction conditions on the G-value*

The above experiments were chosen in order to find any variation in the γ-isomer content under different conditions. The constancy of the γ-isomer yield under these various conditions did not justify a further kinetic study of the system but from the data available it was possible to draw some conclusions about the behaviour of the radiation-induced reaction under various conditions.

Experiments carried out at constant dose rate and composition showed that the rate of product formation was linear with time. The line did not pass through the origin but had a positive intercept on the time axis. The positive intercept corresponded to the time of travel of the source.

The efficiency of the reaction was assessed in terms of the *G*-value for the formation of hexachloro*cyclo*hexane, i.e. the number of molecules of product formed for an energy absorption of 100 eV.

Data were available for the *G*-values at various dose rates for each concentration of benzene. When the sets of points were plotted logarithmically, linear relationships were indicated. Statistical regression lines of the log *G*-value y upon the log dose rate x for each concentration of benzene, are shown together with the experimental values in Table 3. The degree of correlation between the data and the calculated equations were assessed by the calculation of the correlation coefficient r and the associated probability level ascertained. The results were highly significant of a genuine linear relationship between the logarithm of the *G*-value and the dose rate. The standard deviations σ_b of the regression coefficients b were also calculated.

TABLE 3. The relationship between *G*-value and dose rate for several concentrations of benzene

Benzene concentration (mol. fraction)	*G*-value	Dose rate (ergs/l/hr)	Regression equation
0·2134	$7{\cdot}994 \times 10^{3}$	$6{\cdot}374 \times 10^{10}$	$y = 12{\cdot}37 - 0{\cdot}78x$
	$5{\cdot}454 \times 10^{4}$	$6{\cdot}539 \times 10^{10}$	
	$1{\cdot}034 \times 10^{5}$	$2{\cdot}663 \times 10^{9}$	$r = -0{\cdot}998$ $\rho = < 0{\cdot}001$
	$2{\cdot}080 \times 10^{5}$	$9{\cdot}000 \times 10^{8}$	$\sigma_b = \pm 0{\cdot}03$
	$2{\cdot}202 \times 10^{5}$	$1{\cdot}048 \times 10^{9}$	
0·4198	$1{\cdot}434 \times 10^{4}$	$5{\cdot}842 \times 10^{10}$	$y = 11{\cdot}05 - 0{\cdot}64x$
	$5{\cdot}501 \times 10^{4}$	$5{\cdot}994 \times 10^{9}$	
	$1{\cdot}050 \times 10^{5}$	$2{\cdot}441 \times 10^{9}$	$r = -0{\cdot}985$ $\rho = < 0{\cdot}01$
	$1{\cdot}790 \times 10^{5}$	$9{\cdot}605 \times 10^{8}$	$\sigma_b = \pm 0{\cdot}04$
	$4{\cdot}714 \times 10^{5}$	$2{\cdot}722 \times 10^{8}$	
0·6202	$1{\cdot}301 \times 10^{5}$	$5{\cdot}443 \times 10^{9}$	$y = 9{\cdot}32 - 0{\cdot}43x$
	$1{\cdot}696 \times 10^{5}$	$2{\cdot}217 \times 10^{9}$	
	$3{\cdot}400 \times 10^{5}$	$8{\cdot}720 \times 10^{8}$	$r = -0{\cdot}973$ $\rho = < 0{\cdot}01$
	$4{\cdot}162 \times 10^{5}$	$4{\cdot}279 \times 10^{8}$	$> 0{\cdot}001$
	$4{\cdot}364 \times 10^{5}$	$2{\cdot}472 \times 10^{8}$	$\sigma_b = \pm 0{\cdot}06$
0·8104	$1{\cdot}914 \times 10^{5}$	$2{\cdot}008 \times 10^{9}$	$y = 7{\cdot}96 - 0{\cdot}29x$
	$2{\cdot}715 \times 10^{5}$	$5{\cdot}341 \times 10^{8}$	
	$2{\cdot}732 \times 10^{5}$	$5{\cdot}341 \times 10^{8}$	$r = 0{\cdot}970$ $\rho = < 0{\cdot}01$
	$2{\cdot}697 \times 10^{5}$	$5{\cdot}341 \times 10^{8}$	$> 0{\cdot}001$
	$3{\cdot}298 \times 10^{5}$	$3{\cdot}981 \times 10^{8}$	$\sigma_b = \pm 0{\cdot}04$
1·0000	$1{\cdot}777 \times 10^{5}$	$1{\cdot}777 \times 10^{9}$	$y = 11{\cdot}64 - 0{\cdot}70x$
	$3{\cdot}731 \times 10^{5}$	$4{\cdot}728 \times 10^{8}$	
	$5{\cdot}641 \times 10^{5}$	$3{\cdot}464 \times 10^{8}$	$r = 0{\cdot}992$ $\rho = 0{\cdot}001$
	$7{\cdot}882 \times 10^{5}$	$1{\cdot}982 \times 10^{8}$	$\sigma_b = \pm 0{\cdot}05$

$$r = \frac{\Sigma(x-\bar{x})(y-\bar{y})}{((x-\bar{x})^2(y-\bar{y})^2)^{\frac{1}{2}}} \qquad \sigma_b^2 = \pm \Sigma(y-\bar{y})^2 - \frac{\Sigma(x-\bar{x})(y-\bar{y})}{\Sigma(x-\bar{x})^2} \Big/ (N-2)\Sigma(x-\bar{x})^2$$

Having established the nature of the individual lines it remained to examine the influence of the benzene concentration on the *G*-value. The slopes of the line appeared to vary regularly with the concentration but in view of the uncertainty indicated by the standard deviations of the slopes, these were compared by a method suggested by YATES.[8] For the 20% and 40% benzene dilutions it was found that the difference between the slopes was significant at the 0·05 probability level. For the 60% and 80% dilutions the probability was greater than 0·10. There was therefore insignificant evidence for the difference between the 60% and 80% slopes, and the case of the two lower concentrations was marginal. However, pooling the results for the 20% and 40% dilutions and the 60% and 80% dilutions gave two new lines for which the difference between slopes was significant at the 0·011 probability level, indicating that the results were not homogeneous.

In order to pursue this point a multiple regression was carried out. It was assumed that the data would best be represented by an equation of the form:

$$G\text{-value} = A[I]^{-b_1}\,[C]^{-b_2}$$

where A, b_1 and b_2 are constants, $[I]$ is the radiation intensity (ergs/litre/hour) and $[C]$ equals the molar fraction of benzene. The empirical equation derived from all the

VOL. 7 1959/6

TABLE 4. Multiple regression—analysis of variance

Source of variance	Sums of squares	Degrees of freedom	Mean squares	Variance ratio	Significance level (p)
Variation explained by $[I]$	4·0111	1	4·0111	294·9	0·001
Increment explained by addition of $[C]$	0·0290	1	0·0290	2·132	0·10
Total explained by $[I]$ and $[C]$ together	4·0401				
Residual	0·2311				
Total	4·2712				

experiments conducted in diluted benzene was:

$$G = A[I]^{-0\cdot64}\,[C]^{-0\cdot18}$$

The standard errors of b_1 and b_2 were $\pm 0\cdot04$ and $\pm 0\cdot13$ respectively. Since the standard error for b_2 was large, the significance of the concentration effect was examined further by an analysis of variance after a model described by BROWNLEE[9], shown in Table 4.

From this analysis it could be seen that the dose rate had a most marked effect on the G-value, significant at a probability level below 0·001, whereas the concentration effect was not significant. The result for the intensity exponent is consistent with the square root dependence often observed in radiation-induced chlorinations due to a biradical termination step in the reaction kinetics. From the differing slopes of the initial equations for each concentration of benzene there is a concentration effect but the nature of the data available does not allow this effect to be determined with the required accuracy. Further deductions from these data could only be speculative since the presence of benzene in the reaction mixture would introduce a marked protection effect on the radiation-initiated formation of radicals from the carbon tetrachloride.

(c) *Comparison of radiation and ultra-violet induced reactions*

In Part I of this paper[1] it was stated that the optimum γ-isomer content attained with ultra-violet irradiation was $13\cdot2 \pm 1\cdot3$ per cent. For the radiation-induced reaction at room temperature the mean value was $15\cdot3 \pm 1\cdot6$ per cent. An improvement can be obtained at lower temperatures but the increased γ-isomer content is accompanied by a lower gross yield of product which is not economically attractive. G-values of the order 10^5–10^6 have been recorded at dose rates of 10^3–10^4 rads per hour. The optimum quantum yield of $8\cdot67 \times 10^3$ for light of wavelength 3650 Å obtained in the ultra-violet experiments corresponds to a G-value of $4\cdot25 \times 10^4$. If the line for the 100% experiments is extrapolated to the absolute radiation intensity used in the ultra-violet runs, the calculated G-value is 427×10^4. There is therefore little difference in the efficiency of ultra-violet or γ-radiation for producing hexachloro*cyclo*hexane.

Acknowledgements—The authors are indebted to Mr. B. E. COOPER for the calculations carried out on the Ferranti "Mercury" computer, to Mr. P. J. FYDELOR for infra-red analyses, and to Dr. P. B. CORNWELL for providing the grain weevils used for the insecticide evaluations.

REFERENCES

1. Hills P. R., Roberts R. and Spindler M. W. *Int. J. Appl. Rad. Isotopes* **7,** 207 (1959).
2. Murray G. S., Roberts R. and Dove D. *Radioisotopes in Scientific Research* (Proc. 1st UNESCO Int. Conf., Paris, 1957). Pergamon Press, London (1958).
3. Furst H., Lang J. and Rummelt P–p *Chem.-Tech.* (*Berlin*) **5,** 319 (1953).
4. Finney D. J. *Probit Analysis.* Cambridge University Press (1952).
5. Hudson R. L. *Analyt. Chem.* **29,** (1957).
6. Cooper B. E. A.E.R.E. Report T/M 168.
7. Gunther F. A. *Chem. & Ind.* (*Rev.*), 399 (1946).
8. Yates F. *Proc. Roy. Soc. Edinb.* **59,** 184.
9. Brownlee K. A. *Industrial Experimentation.* H.M.S.O., London (1949).

VOL.
7
1959/

International Journal of Applied Radiation and Isotopes, 1960, Vol. 7, pp. 225–232. Pergamon Press Ltd. Printed in Northern Ireland

The Distribution and Radiation Dosimetry of Zinc-65 in the Rat

J. C. N. WAKELEY,* BRENDA MOFFATT,† ANN CROOK‡ and J. R. MALLARD‡

(*Received* 25 *April* 1959; *in revised form* 7 *July* 1959)

The concentration of radioactive Zn^{65} in fourteen organs and tissue has been measured for sixty-nine male rats over a period of 42 days. The results from the reproductive organs and pancreas compare favourably with those of other workers. The concentration of Zn^{65} in the prostate was ten times greater than that in any other organ. Calculation of the radiation dose however, indicated that for a dose of 80 rads to the prostate of the rat the rest of the body would receive approximately 50 rads. In man, such conditions seem hardly suitable for radiotherapy.

LA DISTRIBUTION DU ZINC-65 CHEZ LE RAT, ET LE DOSAGE DE SON RAYONNEMENT

On a mesuré la concentration du Zn^{65} radioactif dans 14 organes et dans le tissu de 69 rats mâles durant une période de 42 jours. Les résultats pour les organes de réproduction et pour le pancréas sont en bon accord avec ceux d'autres rechercheurs. La concentration du Zn^{65} dans le prostate fut dix fois plus forte que celle dans aucun autre organe. Cependant le calcul de la dose de rayonnement indiqua que, pour une dose de 80 rads au prostate du rat, le reste du corps recevrait environ 50 rads. Chez l'homme, de telles conditions semblent à peine convenables à la radiothérapie.

РАСПРЕДЕЛЕНИЕ И ДОЗИМЕТРИЯ ИЗЛУЧЕНИЯ Zn^{65} У КРЫС

Концентрация радиоактивного Zn^{65} в 14 органах и ткани 69 самцов крыс измерялась в течение 42 дней. Результаты, относящиеся с половым органам и поджелудочной железе, совпадают с результатами, полученными другими исследователями. Концентрация Zn^{65} в предстательной железе была в 10 раз большей, чем в любом другом органе. Расчет дозы облучения показал, однако, что при дозе облучения предстательной железы в 80 рад остальные части организма получают 50 рад. Для человека такие условия лучевой терапии вряд-ли пригодны.

VERTEILUNG UND STRAHLENDOSIMETRIE VON ZINK-65 IN RATTEN

Die Konzentration von radioaktivem Zink-65 wurde in 14 Organen und Geweben von 69 männlichen Ratten innerhalb eines Zeitraumes von 42 Tagen gemessen. Die Ergebnisse bezüglich Fortpflanzungsorganen und Pankreas stimmen gut mit denen anderer Autoren überein. Die Zink-65-Konzentration in der Prostata ist zehnmal höher als in allen anderen Organen. Berechnungen der Strahlungsdosis zeigen jedoch, dass bei einer Dosis von 80 rad auf die Ratten-Prostata der übrige Körper ebenfalls ungefähr 50 rad erhält. Diese Bedingungen sind daher ungeeignet für therapeutische Verwendung beim Menschen.

* Department of Surgery, Postgraduate Medical School, Hammersmith Hospital. Now in Urological Department, King's College Hospital.

† Department of Surgery, Postgraduate Medical School, Hammersmith Hospital. Now in Department of Urology, Francis Delafield Hospital, New York, U.S.A.

‡ Department of Physics, Hammersmith Hospital.

THE distribution of zinc in the various organs of the body has been widely studied over a number of years.[1–13] However the diversity of methods used by these various investigators made it very difficult to compare their results. More recently the use of Zn^{65} has made it possible to carry out a more detailed study of the zinc content in the experimental animal.[14–20] In a number of publications since 1951 MAWSON and FISCHER[13,17] have shown that there is a higher concentration of zinc in the male reproductive organs, especially the prostate gland, in the rat. The dorso-lateral lobe of the prostate contained about ten times as much as the coagulating glands, testis and seminal vesicles. It seemed reasonable therefore to study the distribution and excretion of the zinc in the rat and see if there was any correlation with the previous results, and whether Zn^{65} could be used as a therapeutic weapon in the treatment of carcinoma of the prostate. In order to estimate the therapeutic potentiality of Zn^{65} it is necessary to know the relative uptake and turnover of the isotope in the various organs of the body, so that the radiation dose may be determined.

MATERIALS

Animals

Male albino rats taken from stock were used. All were supplied with food (Diet 41, Dixons, Ware, Herts) and water ad lib. and were 12 weeks old when injected with radioactive zinc.

Zinc-65

This was obtained from the Radiochemical Centre, Amersham. It was present as the chloride, and had a specific activity of 1·4 mc/mg zinc.

METHODS

The radioactive zinc was diluted suitably to give a solution containing 100 μc/ml, and was sterilized and administered to the rats by intraperitoneal injection. All animals received 100 μc Zn^{65}, were kept together in large cages, and were taken at random from these cages for killing at varying intervals after injection.

In excretion studies, the rats were kept individually in metabolism cages, the urine and faeces being collected daily for 23 days. The activity over the site of injection was measured at intervals with an end-window Geiger counter (GM 4) for 22 days.

In turnover studies, the rats were killed by ether anaesthesia, the thorax opened quickly, and 2·0 ml blood withdrawn from the still-beating heart. Samples of lung, kidney, spleen, heart (ventricle), rectus abdominis muscle, shaft of femur, pancreas, liver, terminal part of ileum, epididymis, testis and seminal vesicle were taken, weighed, and put into 10% formolcalcium in separate containers. The whole intact dorso-lateral lobe of the prostate was dissected out, weighed, and also put into formol-calcium.

The radioactivity of all specimens was determined using either a well-type scintillation counter (Ekco N 550A; sensitivity 280,000 counts/min/μc Zn^{65}) for samples of low activity, or a multiple-tube Geiger–Müller counter equipment[20] (sensitivity 3200 counts/min/μc Zn^{65}) for samples of high activity. Standard solutions of Zn^{65} were counted at the same time as the specimens, to check the sensitivity of the counters. Corrections for decay of the isotope, background and resolving time were made and all results expressed as a percentage of the administered dose.

RESULTS

Absorption and excretion of radioactive zinc

Eight rats were used in this experiment, and kept in individual metabolism cages. On day 22, 15 per cent of the administered dose (A.D.) remained at the site of injection, and, apart from an initial rapid loss, the zinc left the injection site slowly throughout the period of observation (Fig. 1).

Very little Zn^{65} appeared in the urine—only a cumulative total of 2 per cent A.D. after 23 days of study. In contrast 55 per cent A.D. had been excreted in the faeces in the same time, the rate of excretion being rapid in the first two or three days, and much slower thereafter (Fig. 2).

Turnover of radioactive zinc by various body tissues

Animals were killed 1, 2, 4, 7, 14, 28 and 42 days after being injected. The groups of rats varied in number from eight to twelve.

VOL. 7 1959/

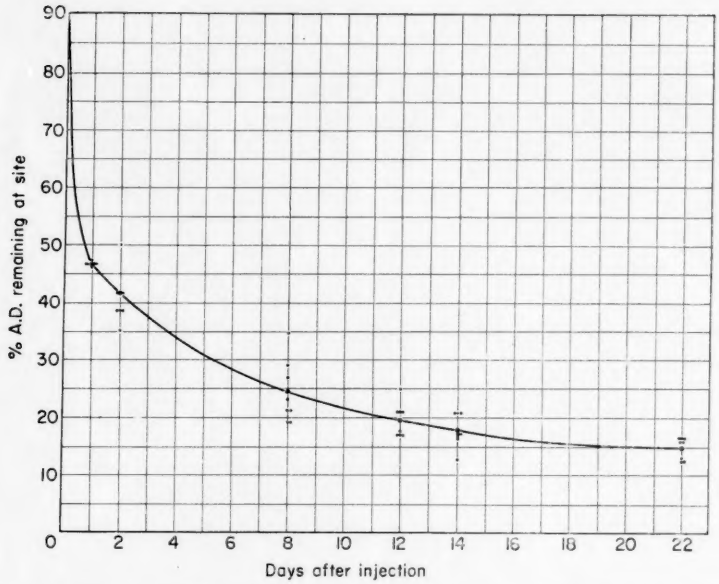

FIG. 1. Disappearance of Zn^{65} from site of injection. (Each point represents the mean from 8 rats.)

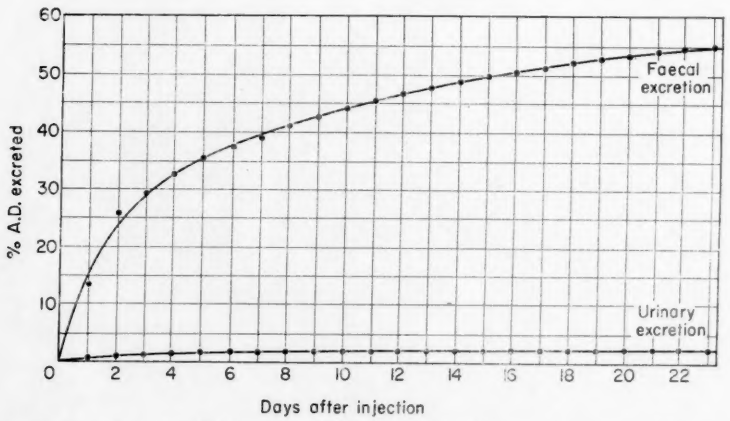

FIG. 2. Excretion of Zn^{65} in urine and faeces. (Each point represents the mean from 8 rats.)

The amount of radioactive zinc present in the various tissues studied is shown in Table 1.

The rate at which the Zn^{65} collects in and disappears from the different tissues falls into three groups:

(A) in which there is an initial rapid uptake followed by an exponential removal as seen in the prostate, seminal vesicle, rectus abdominis muscle, heart and lung;

(B) in which there is again an initial rapid uptake but the removal follows two exponential functions as in the liver, kidney, spleen, ileum and pancreas;

(C) in which there is a slow initial uptake, a period during which the concentration remains appreciably constant and a removal following a single exponential function as in the testis and femur.

TABLE 1. Turnover of Zn^{65}

	Day 1			Day 2			Day 4			Day 7			Day 14			Day 28			Day 42		
	Mean % A.D./g tissue or/ml blood	Standard deviation	Number of specimens measured	Mean % A.D./g tissue or/ml blood	Standard deviation	Number of specimens measured	Mean % A.D./g tissue or/ml blood	Standard deviation	Number of specimens measured	Mean % A.D./g tissue or/ml blood	Standard deviation	Number of specimens measured	Mean % A.D./g tissue or/ml blood	Standard deviation	Number of specimens measured	Mean % A.D./g tissue or/ml blood	Standard deviation	Number of specimens measured	Mean % A.D./g tissue or/ml blood	Standard deviation	Number of specimens measured
Ileum (terminal)	1·2	0·5	10	0·88	0·37	10	0·46	0·13	11	0·31	0·09	12	0·36	0·10	10	0·095	0·014	8	0·079	0·008	8
Pancreas	3·6	2·0	5	0·81	0·37	6	0·29	0·09	10	0·19	0·07	12	0·21	0·10	10	0·10	0·03	8	—	—	—
Liver	1·3	0·4	10	0·82	0·23	10	0·48	0·17	11	0·32	0·05	12	0·27	0·17	10	0·11	0·02	8	0·10	0·01	8
Kidney	0·67	0·24	10	0·53	0·09	10	0·34	0·11	11	0·27	0·06	12	0·23	0·19	10	0·088	0·016	8	0·072	0·018	8
Spleen	0·65	0·13	10	0·47	0·12	10	0·37	0·09	11	0·23	0·07	12	0·17	0·08	10	0·069	0·011	8	0·066	0·005	8
Lung	0·47	0·10	10	0·45	0·06	10	0·34	0·08	11	0·21	0·06	12	0·18	0·03	10	0·061	0·007	8	0·049	0·010	8
Heart	0·36	0·11	10	0·41	0·08	10	0·27	0·03	11	0·18	0·06	12	0·18	0·03	10	0·056	0·009	8	0·060	0·007	8
Rectus muscle	0·16	0·04	10	0·18	0·04	10	0·35	0·48	11	0·17	0·05	12	0·20	0·07	10	0·11	0·02	8	0·10	0·03	8
Testis	0·21	0·06	10	0·26	0·03	10	0·30	0·06	11	0·28	0·06	12	0·28	0·07	10	0·11	0·02	8	0·065	0·032	8
Epididymis	0·24	0·06	10	0·23	0·06	10	0·20	0·05	11	0·19	0·09	12	0·36	0·06	10	0·20	0·11	8	0·23	0·06	8
Seminal vesicle	0·27	0·09	10	0·23	0·05	10	0·21	0·05	10	0·15	0·04	12	0·14	0·03	10	0·050	0·02	8	0·079	0·077	8
Blood	0·11	0·02	10	0·087	0·015	10	0·072	0·024	11	0·072	0·012	12	0·082	0·011	10	0·036	0·006	8	0·028	0·002	8
Bone	0·37	0·11	10	0·40	0·04	10	0·40	0·12	11	0·44	0·08	12	0·46	0·08	10	0·31	0·06	8	0·14	0·03	8
D.L. prostate	1·6	0·8	10	1·9	1·0	10	1·7	0·6	11	1·3	0·6	12	1·5	1·6	10	0·83	0·23	8	0·81	0·18	8

VOL. 7 1959/60

The epididymis is unique in showing a secondary rise at the fourteenth day, preceded and followed by a decline in radioactivity. It is interesting to note that WETTERDAL[26] has reported a similar result.

The biological half-life of the isotope in the various tissues under investigation is given in Table 2.

DOSIMETRY

The radiation doses delivered to the various organs investigated have been calculated and the results are collected together in Table 3.

β-Ray dose

For the organs in Group A the β-ray dose is equal to

$$73{\cdot}8\ \bar{E}_\beta \times C_0 \times T_{\text{eff}}\ \text{rads},^{(22a)}$$

where $\bar{E}_\beta$ is the average β-ray energy (0·01 MeV), C_0 the extrapolated initial concentration in μc/g and T_{eff} the effective half-life of removal in days. The effective half-life was calculated from

$$\frac{1}{T_{\text{eff}}} = \frac{1}{T_{\text{biol}}} + \frac{1}{T_{\text{phys}}}$$

the value of T_{biol} being taken from the curve.

For Group B, the effective half-life and extrapolated initial concentration for each exponential term were determined from the curves. The β-ray dose is given by

$$73{\cdot}8\ \bar{E}_\beta\ [({}_1C_0 \times {}_1T_{\text{eff}}) + ({}_2C_0 \times {}_2T_{\text{eff}})]\ \text{rads}.^{(22b)}$$

For Group C it was assumed that the middle section was in fact constant, the β-ray dose being given by

$$51{\cdot}2\ \bar{E}_\beta \times C_t\ \text{rads}^{(22c)}$$

where C is the concentration which remained constant for a period of t days. Since t in each case was approximately 15 days the physical half-life of the isotope (250 days) was neglected. The dose during the period of uptake and removal is given by

$$73{\cdot}8\ \bar{E}_\beta \times C_0 T_{\text{eff}} \left[1 - \frac{T_{\text{up}}}{T_{\text{eff}}}\right] \text{rads}^{(22d)}$$

where T_{up} is the half period of uptake.

The γ-ray dose is made up of two contributions, one from the radioactivity localized within the organ itself and the other from the radioactivity distributed throughout the rest of the body. Owing to the shapes of the organs it is difficult to calculate the former dose but in the case of the prostate, which can be regarded as a sphere of radius 0·3 mm, the total γ-ray dose is

$$0{\cdot}034\rho k \times C_0 \times T_{\text{eff}} \times 3\pi R\ \text{röntgens}^{(22e,22f)}$$

where ρ is the density in g/cm^3, k is the dose rate in röntgens/hr at 1 cm from a point source of 1 mc of the isotope (for Zn^{65} $k = 2{\cdot}7$ cm^2.r/mc.hr), and R the radius of the organ in cm.

To get an estimate of the dose to different organs due to the total activity in the rest of the body, the rat was regarded as a cylinder of length $l = 15$ cm and radius $a = 3$ cm in which the radioactivity is uniformly distributed. The activity in the rest of the body at any time is equal to:

the injected dose − total activity excreted in the urine and faeces
− activity remaining at site of injection.

The dose at points of distance d cm from one end, along the axis of this cylinder was calculated from the following expression:

Total γ-ray dose at points on the axis

$$= \pi \times k \times 0{\cdot}034 \left[(l-d) \log_e \left\{ \frac{a^2}{(l-d)^2} + 1 \right\} + \right.$$
$$+ 2a \tan^{-1} \frac{(l-d)}{a} + d \log_e \frac{(a^2+1)}{d^2} +$$
$$\left. + 2a \tan^{-1} \frac{d}{a} \right] C_0 T_{\text{eff}}\ \text{röntgens}.^{(22a,22f,23)}$$

This expression ignores self absorption but the reduction for this at the centre will be no greater than 9 per cent.

A graph was plotted of the axial γ-ray dose as a function of distance along the axis from which an estimate of dose to the different organs was obtained.

DISCUSSION

The results of the excretion studies confirm the findings of other workers[1,7] that the vast majority of Zn^{65} is lost in the faeces, and only a small amount in the urine.

Table 2 shows that the turnover of zinc by the dorso-lateral lobe of the prostate is slower than that of any other tissues studied, with the exception of the rectus abdominis muscle.

TABLE 2. Biological half-life (in days) of Zn^{65} in the tissues studied

Group A		
Dorso-lateral prostate		27·5
Lung		9·5
Rectus muscle		40·0
Heart muscle		8·0
Seminal vesicle		13·5
Group B	*Initial rapid phase*	*Subsequent slower phase*
Pancreas	0·8	20
Ileum	2·0	13·5
Spleen	2·0	14·7
Kidney	1·7	15
Liver	1·25	17·5
Group C		
Testis		10·5 days preceded by 13·75 days almost constant content
Bone (femur)		15·35 days preceded by 15·25 days almost constant content

The long biological half-life for this muscle may be partially explained on the basis of it being contaminated with zinc which has been bound by protein near the site of injection.

The initial high uptake of Zn^{65} by the pancreas, and its rapid turnover have been noted by other workers[9,24] and it has been suggested that the pancreatic juice is the main route of zinc excretion.[9,25] This could account for the high excretion in the faeces.

Values for the turnover of Zn^{65} by the male reproductive organs in the rat have been obtained by WETTERDAL.[26] The values obtained are shown in Table 3 for comparison with those reported here. The agreement is seen to be satisfactory.

When the ability of the tissues to concentrate zinc is considered by calculating the ratio of Zn^{65}/g tissue to Zn^{65}/ml blood, it is at once obvious that the dorso-lateral lobe of the prostate is the only tissue which possesses this power to any degree, but this ratio is only of the order of twenty to twenty-five (see Fig. 3). It may be that bone is also able to effect a true concentration of zinc but to a much smaller degree.

TABLE 3. Biological half-life (in days) of Zn^{65} in the male reproductive organs

	Present study	WETTERDAL
Testis	10	12
Epididymis	First peak 1 approx. Second peak 14 approx.	First peak 3 Second peak 14 approx.
D-L prostate	27	6
Ventral prostate	—	6
Coagulating glands	—	6
Seminal vesicle	10	6

The measurement of radioactivity over the site of injection, though not very accurate, shows that the intraperitoneal route is not recommended for the administration of zinc because 15 per cent A.D. still remains at the injection site on the twenty-third day. This route was used, however, because of the low specific activity of the Zn^{65}, and the intention in subsequent experiments to give much larger doses of Zn^{65} which by any other route would have proved to be toxic.

These measurements suggest that as 45 per cent A.D. disappears from the injection site in the first 24 hr, 6·5 per cent A.D. in the next 24 hr, and thereafter a small, almost constant amount daily, some of the administered zinc is absorbed and rapidly carried away whilst the rest is bound by protein at the site of injection. The protein-bound zinc is released at a slow, fairly constant rate, which can be shown from the measurements to equal the loss of Zn^{65} in the faeces after the third day.

Up to and including the third day after injection, the disappearance of radioactive zinc from the injection site is greater than that lost in the faeces, but thereafter the two are approximately equal, indicating that equilibration of the administered Zn^{65} with the body's pool of zinc has occurred.

At the end of day 3, taking into account the Zn^{65} lost in the faeces and urine, or remaining at the site of injection, 33·5 per cent A.D. is distributed throughout the body. Since 1·5 mg Zn were injected, the total exchangeable body zinc must be 503 μg, and the daily bodily turnover of zinc is 15 μg because 1 per cent A.D. is lost daily in the faeces after equilibrium has been attained.

The radiation dosimetry is affected in two ways by the zinc which remains at the site of injection. First, the amount of zinc distributed throughout the body is smaller than that which would have occurred following

VOL. 7 1959/6

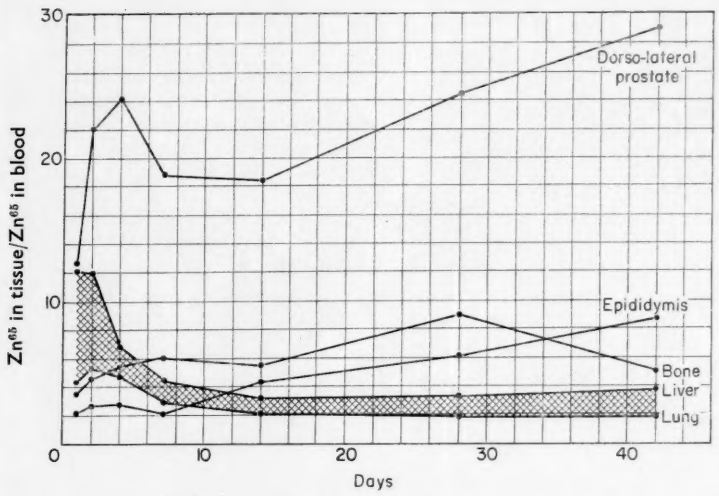

FIG. 3. Concentration of Zn^{65} by the various tissues compared with blood. (All other tissues investigated lie within the shaded area.)

an intravenous injection. As a result of this, the radiation doses would be somewhat larger than those quoted in Table 4 if the intravenous route were used. Secondly, there is a γ-ray dose contribution to neighbouring organs from the zinc localized at the site of injection. For the prostate, which is approximately 3 cm from the site of injection, this contribution is only 4 röntgens and it has been neglected in Table 4.

TABLE 4. Radiation doses delivered to the various organs and tissues

Organ	Group	Total β-dose (rads)	Own γ-dose (röntgens)	Gamma dose due to Zn^{65} in rest of body (röntgens)
Prostate	A	34	4	41
Epididymis	A	43	26	•40
Seminal vesicle	A	3		•41
Rectus abdominis muscle	A	5		•43
Heart	A	3		40
Lung	A	3		•40
Liver	B	7		44
Kidney	B	5		•44
Spleen	B	4		•44
Ileum	B	5		42
Pancreas	B	7		44
Testis	C	4	10	•33
Femur	C	9		•30

• These organs lie off the central axis of the body and the dose given is an overestimate. On the central plane perpendicular to the axis of the body the ratio of the surface dose to the central dose is 0·8 whilst at the end of the body it is 0·74. As a result, the correct dose to any of these organs cannot be less than 0·74 × the figure given above.

Average γ dose to whole body of rat = 22 röntgens.

The total dose to the prostate is approximately 80 rads whilst the total dose to other organs in the rat is approximately 50 rads. It is probable, therefore, that Zn^{65} has little use as a therapeutic weapon in man. One of the reasons for its unsuitability arises from the very low β-ray energy compared with the γ-emission for Zn^{65}. The possibility that Zn^{72} would be a much more favourable isotope has been considered but due to its short half-life (49 hr) the β-ray dose to the prostate would be only 20 rads.

On the other hand the curves of Fig. 3 show an average concentration factor of only 10 for the prostate relative to other organs so that even with a pure β-ray emitter the dose to the prostate will be, at the best, only ten times that to other organs. If similar conditions apply in man then in order to deliver a therapeutic dose of 5000 r one might give 500 r to most other organs; this seems hardly suitable for radiotherapy.

The possibilities of zinc radioisotope therapy seem to be remote particularly in view of the work of MAWSON and FISCHER[27] who showed that carcinometous prostate tissue has a significantly low total zinc content. However, DANIEL *et al.*[28] reported that in one of three patients measured the carcinometous prostate tissue relative to the blood

level was as high as forty. The concentration factor, however, may be such that localization studies could well be pursued, particularly since coincidence techniques may be possible with Zn^{65}. It may well be of value for demonstrating the position of secondary deposits from carcinoma of the prostate.

Acknowledgements—We wish to express our thanks to Mr. SELWYN TAYLOR for his help, interest and encouragement in this work and for the use of his laboratory facilities. Part of this work was undertaken on a British Empire Cancer Campaign Grant.

REFERENCES

1. SHELINE G. E., CHAIKOFF I. L., JONES H. B. and MONTGOMERY M. L. *J. Biol. Chem.* **147,** 409 (1943); **149,** 139 (1943).
2. VALLEE B. L., FLUHARTY R. G. and GIBSON J. G. *Acta Un. Int. Cancr.* **6,** 869 (1948).
3. FEASTER J. P., HANSARD S. L., MCCALL J. T., SKIPPER F. H. and DAVIES G. K. *J. Anim. Sci.* **13,** 781 (1954).
4. ROSENFELD I. and TOBIAS C. A. *J. Biol. Chem.* **191,** 339 (1951).
5. BANKS T. E., TUPPER R. and WORMALL A. *Biochem. J.* **47,** 466 (1950).
6. HEATH J. C. and LIQUIER-MILWARD J. *Biochem. Biophys. Acta* **5,** 404 (1950).
7. MONTGOMERY M. L., SHELINE G. E. and CHAIFOFF I. L. *J. Exp. Med.* **78,** 151 (1943).
8. LOWRY J. R., BALDWIN R. R. and HARRINGTON R. V. *Science* **119,** 219 (1954).
9. TUPPER R., WATTS R. W. E. and WORMALL A. *Biochem. J.* **50,** 429 (1952).
10. GIBSON J. G., VALLEE B. L., FLUHARTY R. G. and NELSON J. E. *Acta Un. Int. Cancr.* **6,** 1102 (1950).
11. EBAUGH F. G. and ROSS J. E. *Fed. Proc.* **11,** 413 (1952).
12. GUNN A., GOULD F. C., GINORI S. S. and MORSE J. G. *Proc. Soc. Exp. Biol., N.Y.* **88,** 556 (1955).
13. MAWSON C. A. *Nature* **176,** 317 (1955).
14. LUTZ R. E. *J. Industr. Hyg.* **8,** 177 (1926).
15. EGGLETON W. G. E. *Chin. J. Physiol.* **13,** 339 (1938); *Biochem. J.* **34,** 991 (1940).
16. VALLEE B. L. and ALTSCHULE M. D. *Physiol. Rev.* **29,** 370 (1949).
17. MAWSON C. A. and FISCHER M. I. *Nature* **167,** 859 (1951).
18. KEILIN D. and MANN T. *Biochem. J.* **34,** 1163 (1940).
19. FUJII T. *Nature* **174,** 1109 (1954).
20. TAYLOR S. *Nature* **179,** 585 (1957).
21. VEALL N. and BAPTISTA A. M. *Brit. J. Radiol. N.S.* **27,** 198 (1954).
22. LOEVINGER R., HOLT J. G. and HINE G. J. *Radiation Dosimetry* (Edited by HINE G. J. and BROWNELL G. L. (a) p. 828, (b) p. 835, (c) p. 830, (d) p. 839, (e) p. 857, (f) p. 861. Academic Press, New York (1956).
23. MAYNEORD W. V. *Brit. J. Radiol.* Suppl. 2, 151 (1950).
24. GILBERT I. G. F. and TAYLOR A. M. *Biochim. Biophys. Acta* **21,** 545 (1956).
25. BIRSTINGL M., STONE B. and RICHARDS V. *Amer. J. Physiol.* **186,** 377 (1956).
26. WETTERDAL B. *Acta Radiol., Stockh.* Suppl. 156 (1958).
27. MAWSON C. A. and FISCHER M. I. *Canad. J. Med. Sci.* **30,** 336 (1952).
28. DANIEL O., HADDAD F., PROUT G. and WHITMORE W. F. *Brit. J. Urol.* **28,** 271 (1956).

VOL. 7 1959/

International Journal of Applied Radiation and Isotopes, 1960, Vol. 7, pp. 233–243. Pergamon Press Ltd. Printed in Northern Ireland

Étude de l'Absorption Digestive de l'Eau chez les Malades Atteints de Cirrhose du Foie à l'Aide de Deux Indicateurs de l'Hydrogène

M. LAINÉ–BÖSZÖRMÉNYI* et P. FALLOT
Avec la collaboration technique de J. MASSON et P. CALVET
Service de Biologie du CEA, BP 2 Gif-sur-Yvette (S.-et-O.), France

(*Received* 15 *June* 1959)

Nous avons étudié chez quatre malades atteints de cirrhose du foie avec ascite, la vitesse d'apparition dans le sang périphérique de l'eau ingérée.

A cet effet, nous avons administré simultanément à nos malades de l'oxyde de deutérium par voie orale, et de l'eau tritiée par voie intraveineuse. Cette double épreuve permet de faire la part du phénomène de diffusion de l'indicateur hors des territoires vasculaires et de calculer les quantités absorbées par le tube digestif et transférées dans la circulation périphérique.

La vitesse d'absorption appréciée dans les conditions précédentes (1,2 pour cent par minute de la dose ingérée) s'avère notablement inférieure à celle observée par SCHOLER et CODE chez les sujets normaux (9 pour cent par minute de la dose ingérée).

Nous avons évoqué des hypothèses susceptibles de rendre compte des faits observés qui apportent une explication satisfaisante à l'opsiurie de GILBERT.

THE STUDY OF THE DIGESTIVE ABSORPTION OF WATER IN PATIENTS SUFFERING FROM CIRRHOSIS OF THE LIVER, BY USING TWO HYDROGEN TRACERS

We have studied the rate of appearance of ingested water in the peripheral blood of four patients suffering from cirrhosis of the liver with ascites.

For this purpose, oral administration of deuterium oxide and intravenous administration of tritiated water were made simultaneously. This double experiment enables the phenomenon of diffusion of the tracer outside the vascular regions to be observed and calculation to be made of the amounts absorbed by the digestive tract and transferred to the peripheral circulation.

The rate of absorption observed under the above conditions proves to be distinctly less (1·2% per minute of the ingested dose) than that observed by SCHOLER and CODE in normal subjects (9% per minute of the ingested dose).

Hypotheses are advanced which could account for the facts observed and which offer a satisfactory explanation of GILBERT's opsiuria.

ИЗУЧЕНИЕ С ПОМОЩЬЮ ДВУХ ТЯЖЕЛЫХ ИЗОТОПОВ ВОДОРОДА ПИЩЕВАРИТЕЛЬНОГО ВСАСЫВАНИЯ ВОДЫ У ПАЦИЕНТОВ, СТРАДАЮЩИХ ЦИРРОЗОМ ПЕЧЕНИ

Была изучена скорость появления выпитой воды в периферической крови четырех пациентов, страдающих циррозом печени и сопровождающей его водянкой брюшины.

Для этой цели одновременно вводились внутривенно тритиевая вода и per os тяжелая вода. Такой двойной эксперимент дает возможность наблюдать диффузию индикатора вне сосудистой системы и расчитать количества его, всасываемые пищеварительным трактом и передаваемые периферическому кровообращению. При указанных выше

* Attachée de recherches à l'Institut National d'Hygiène.

условиях скорость всасывания была значительно меньше (1,2% от всей проглоченной дозы в минуту), чем та, которую наблюдали Шолер и Код для нормальных индивидуумов 9% от всей проглоченной дозы в минуту).

Выдвигаются гипотезы, на основании которых можно истолковать полученные факты, а также дать достаточно удовлетворительное объяснение опсиурии Джильберта.

UNTERSUCHUNG DER VERDAUUNGSMÄSSIGEN AUFNAHME VON WASSER BEI LEBERCIRRHOSE PATIENTEN MIT HILFE ZWEIER WASSERSTOFF-INDIKATOREN

Wir untersuchten an 4 Lebercirrhosepatienten mit Ascites die Geschwindigkeit des Aufscheinens von dem mit der Nahrung aufgenommenen Wasser im peripheren Blut.

Zu diesem Zweck verabreichten wir unseren Patienten D^2-markiertes Wasser oral und T^3-markiertes Wasser intravenös. Diese doppelte Markierung gestattet die Beobachtung der Diffusion des Indikators ausserhalb des vaskulären Bereiches und die Berechnung der durch den Verdauungstakt aufgenommenen und in die periphere Zirkulation abgegebenen Mengen.

Die unter den vorliegenden Bedingungen aufgefundene Absorptionsgeschwindigkeit erwies sich bedeutend niedriger (1,2 Prozent der durch die Nahrung aufgenommenen Menge pro Minute), als sie von Scholer und Code bei Gesunden beobachtet wurde (9 Prozent pro Minute).

Eine der beobachteten Tatsachen Rechnung tragende Theorie wird angegeben, welche eine befriedigende Erklärung der Gilbert'schen Opsiurie liefert.

L'ABSORPTION digestive de l'eau chez les malades hépatiques n'a pas été étudiée jusqu'alors sur le plan expérimental bien que la possibilité de son ralentissement ait été pressentie depuis fort longtemps. VILLARET[1] dans son travail sur le syndrome d'hypertension portale, attire l'attention dès 1906 sur les lésions anatomiques de la muqueuse gastro-intestinale qui "suffisent à expliquer bien des troubles de l'absorption surtout aqueuse ainsi que l'opsiurie et l'anisurie." Ces troubles ne ressortissent certainement pas à ce seul mécanisme: l'augmentation des espaces de diffusion offerts à l'eau, le ralentissement de son excrétion rénale sous l'influence des facteurs neuro-endocriniens évoqué par CHABROL et COTTET[2] modifient de même la résponse à la diurèse provoquée.

Il est difficile de déterminer quelle est la part respective de ces différents facteurs incriminés à l'origine des perturbations hydriques. Nous nous proposons dans le présent travail de vérifier à l'aide des deux indicateurs de l'hydrogène s'il existe en effet chez les cirrhotiques une anomalie de l'absorption digestive de l'eau.

Avant l'emploi de la méthode des indicateurs nucléaires de nombreuses techniques ont été proposées pour mesurer la vitesse de passage de l'eau à travers le tube digestif chez l'animal, *in vitro* et *in vivo*.

Sur une paroi isolée séparant deux compartiments inégaux remplis d'une solution nutritive, on peut mesurer le flux net d'eau à l'aide d'une méthode microvolumétrique.[3] Le milieu doit être bien défini car sa composition influence fortement le transport d'eau. En effet, sur l'intestin grêle en survie, le métabolisme est altéré par l'absence d'apport nutritif, comme le montre l'adjonction de glucose au milieu que augmente le passage de l'eau et des électrolytes.[4,5]

On améliore les conditions physiologiques en opérant sur des anses intestinales extériorisées et perfusées à l'aide de solutions salines contenant une substance de masse moléculaire élevée (hémoglobine) les variations de la concentration de cette protéine qui ne traverse pas l'intestin indiquent la quantité de liquide absorbé ou secrété.[6]

Une autre méthode consiste à faire ingérer de l'eau à un animal qui est ensuite sacrifié: les différents segments du tube digestif sont prélevés entre deux ligatures, l'eau résiduelle est pesée et sa quantité déduite de celle administrée.[7] Cette technique entraîne des modifications consécutives à l'intervention qui perturbent le métabolisme de l'eau; par ailleurs elle ne permet pas de tenir compte du liquide intraluminal normal que certains évaluent à 12 pour cent de l'eau total de l'organisme.[8]

Pour se rapprocher encore des conditions normales en évitant les conséquences

VOL 7 1959/

immédiates du choc opératoire, on peut étudier l'absorption à l'aide d'une fistule intestinale.[9]

Chez l'homme le problème s'avère encore plus compliqué; il est difficile d'apprécier d'une façon certaine la disparition du liquide introduit dans la lumière intestinale ou mesurer son apparition dans le sang ce qui nécessiterait l'administration de quantités massives d'eau.

L'introduction en biologie de la méthode des isotopes rend possible la mesure, dans des conditions physiologiques chez l'animal et chez l'homme, du passage d'un indicateur de l'eau du tube digestif vers la circulation. Cependant pour connaître en valeur absolue la quantité d'eau marquée absorbée par unité de temps, la courbe sanguine établie par les dosages de la concentration isotopique du sang même à des intervalles de temps rapprochés ne suffit pas à elle seule, car l'indicateur de l'eau diffuse progressivement hors du territoire vasculaire dès son passage dans le sang. Pour cette raison, il est indispensable de mesurer cette vitesse de diffusion.

Dans ce but SCHOLER et CODE[10] ont suivi dans le sang artériel de sept sujets normaux la disparition de l'eau lourde (oxyde de deutérium) injectée par voie veineuse et ont établi une courbe moyenne de ce phénomène, celle-ci apporte les éléments nécessaires à la correction de la courbe sanguine obtenue après administration orale de l'indicateur et à la détermination, selon ces auteurs, de la quantité d'eau absorbée par l'estomac ou le duodénum par unité de temps.

L'application de cette méthode chez nos malades cirrhotiques nous a conduits à y apporter certaines modifications.

Pour éviter le danger des ponctions artérielles chez des malades hémorragiques nous avons effectué des prélèvements intraveineux. Or, même chez le sujet sain les courbes ainsi obtenues diffèrent sensiblement des courbes artérielles. De plus nous avons montré que chez les cirrhotiques, l'allure de la courbe veineuse de disparition de l'isotope diffère de la normale. Ces considérations interdisent donc l'emploi de la courbe moyenne de SCHOLER et CODE; aussi établissons nous pour chaque malade des courbes simultanées d'absorption et de diffusion; dans ce but nous avons recours à l'administration simultanée d'eau lourde (D_2O) par voie buccale, et d'eau tritiée (HTO) par voie veineuse.

PROTOCOLE EXPERIMENTAL

Cinq épreuves ont été pratiquées chez trois malades atteints de cirrhose du foie avec ascite et oedèmes. Voici succinctement résumée l'observation de ces malades.

Bad . . . (épreuve no. 2). Cirrhose hypertrophique au début chez un homme de 43 ans éthylique et gros mangeur. Présence d'une ascite abondante et d'oedèmes, sans syndrome hémorragique apparent.

Sa . . . (épreuves no. 4–5). Cirrhose hypertrophique chez une femme de 53 ans, avec fièvre, ascite, oedème, circulation collatérale et syndrome hémorragique. L'autopsie a révélé une pyléphlébite thrombosante et des plaques épiploiques de cytostéatonécrose. Une des deux épreuves a été pratiquée à la phase terminale de la maladie.

Spil . . . (épreuves no. 1–6). Cirrhose atrophique éthylique avec splénomégalie, ascite, oedèmes, subictère, circulation collatérale. Décès par hémorragie diffuse provenant de la muqueuse de la grosse tubérosité gastrique. Présence de varices oesophagiennes à l'autopsie.

Ces épreuves ont été réalisées chez les malades soumis au jeûne et à la suppression des liquides depuis la veille au soir. Nous leur administrons simultanément 75 à 80 ml d'oxyde de deutérium (D_2O) à 98, 99 pour cent par voie orale et 4 ml d'une solution physiologique contenant un millicurie de HTO, par voie veineuse. Le sang a été prélevé à la veine du pli du coude opposé à celui de l'injection, toutes les cinq minutes, pendant une heure à une heure et demie. Des ponctions veineuses ont été effectuées le lendemain matin chez les malades à jeun, puis pendant 8 à 10 jours encore quotidiennement.

MESURES DE CONCENTRATIONS ISOTOPIQUES

La mesure de la radioactivité spécifique de l'eau tritiée contenue dans les échantillons biologiques a été effectuée par scintillation liquide et la radioactivité mesurée par numération des photons lumineux produits par l'action des particules β de faible énergie sur une solution douée de propriété scintillante.[12,13]

A la suite de HAYES et GOULD qui ont été les premiers[11] à appliquer cette méthode à la mesure de l'eau tritiée, nous avons utilisé un mélange de 4 g ‰ 2-5-di-phényloxazole (PPO) de 0,1‰ de 1,4-di[2-(5-phényl-oxazolyle)] benzène (POPOP) dans le toluène distillé. La miscibilité de l'eau avec le toluène a été obtenue à l'aide d'éthanol absolue ajouté en quantité telle que la solution finale d'un volume de 15 ml demeure limpide par refroidissement. Ce mélange a été introduit dans une fiole en verre mince, et refroidie à $-10°C$ et placée entre les 2 photomultiplicateurs d'un spectromètre à scintillation liquide pour mesurer la radio-activité.

Dans nos conditions, le rendement de l'opération est de 5,8 pour cent par rapport au nombre théorique de désintégrations avec une précision de ± 3 pour cent (écart-type).

Pour obtenir l'eau à partir des échantillons biologiques (sang, urines) nous avons eu recours à l'entrainement par le toluène. Entre autres avantages, cette technique offre celui d'éviter l'introduction dans le liquide scintillant des nombreuses substances présentes dans les milieux biologiques qui entravent la production ou la transmission des photons lumineux. Ces substances ne sont que partiellement éliminées par la précipitation trichloracétique du plasma ou par la décoloration des urines à l'aide de charbon actif préconisé par LANGHMAN *et al.*[14] La méthode proposée offre les mêmes avantages que la sublimation décrite par COOPER[15] tout en étant plus facile à mettre en oeuvre.

La mesure de l'abondance isotopique en excès de deutérium a été effectuée par spectrométrie de masse selon une méthode antérieurement décrite par COURSAGET *et al.*[16] avec cette différence que la conversion de l'eau en hydrogène a été réalisée par le calcium.[17]

Cette technique de conversion qui est d'une exécution beaucoup plus aisée que la décomposition par le zinc ou l'uranium nous a conduit à effectuer des mesures relatives à une gamme d'étalonnage en raison de l'existence d'un effet de sélection isotopique. La précision des mesures a été de 2 pour cent pour les concentrations inférieures à 0,1 atomes pour cent en excès, et de 10 pour cent pour l'abondance isotopique normale.

VOL. 7 1959/

RESULTATS

Après administration perorale de D_2O

La Fig. 1 montre l'évolution de la concentration isotopique dans le sang veineux en fonction du temps. Les valeurs sont exprimées en fractions de la concentration à l'équilibre prise égale à l'unité. Cette concentration a été définie par la valeur limite vers laquelle tend la courbe des concentrations isotopiques, lorsque pendant un temps assez long, l'amplitude des oscillations ne la dépasse pas de ± 5 pour cent. D'autre part, l'extrapolation à zero de la courbe—en coordonnées semi-logarithmiques—de la période biologique, permet d'étayer par une autre méthode cette valeur à l'équilibre.

Chez les cirrhotiques il existe deux types de courbes comme chez le sujet normal. Parfois la courbe figurative dépasse notablement la valeur de l'équilibre entre la 10ème et la 25ème minute, parfois elle tend asymptotiquement vers cette valeur.

Après administration intraveineuse de HTO

La Fig. 2 montre l'évolution de la concentration isotopique dans le sang veineux en fonction du temps. La courbe moyenne présente une allure exponentielle et son analyse graphique permet d'obtenir la relation suivante:

$$C_{(\text{i.v.})_v t} = 12 \exp(-0{,}277\, t) + 0{,}81 \exp(-0{,}045\, t) + 1 \quad (1)$$

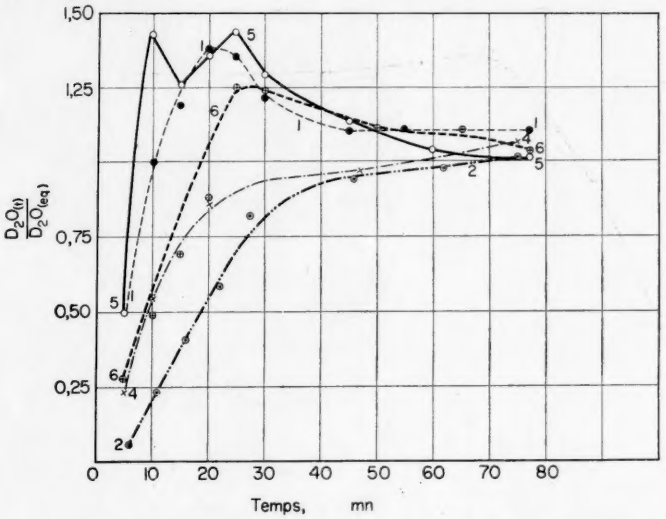

FIG. 1. Variations en fonction du temps de l'abondance isotopique en excès de D_2O de l'eau du sang veineux ($D_2O_{(t)}$) rapportée à sa valeur à l'équilibre ($D_2O_{(eq)}$) après administration orale d'eau lourde à des malades atteints de cirrhose du foie avec ascite.

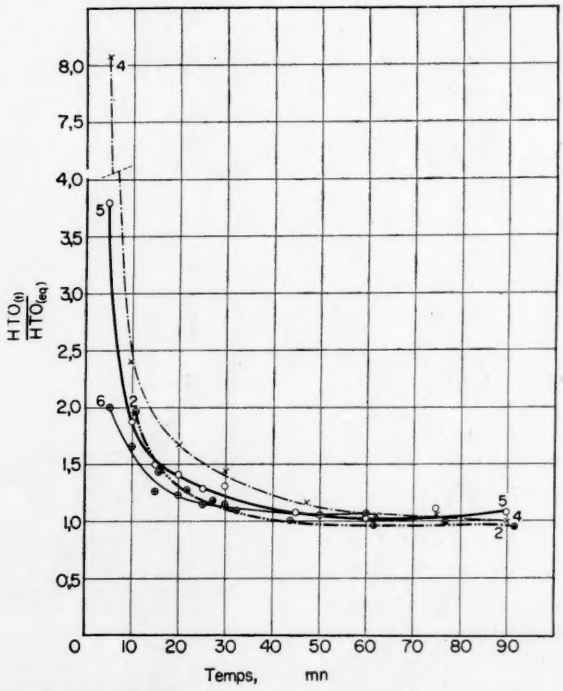

FIG. 2. Variations en fonction du temps de la concentration en HTO de l'eau du sang veineux ($HTO_{(t)}$) rapportée à sa valeur à l'équilibre ($HTO_{(eq)}$) après administration intraveineuse d'eau tritiée à des malades atteints de cirrhose du foie avec ascite.

OL.
7
59/60

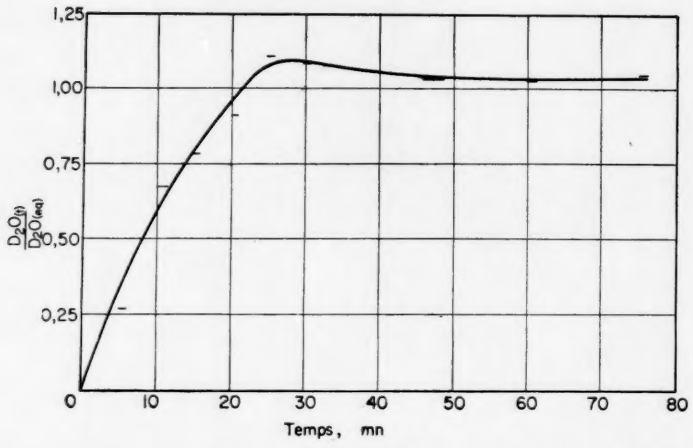

FIG. 3. Courbe moyenne des variations enregistrées en fonction du temps de l'abondance isotopique en excès de D_2O de l'eau du sang veineux ($D_2O_{(t)}$) rapportée à sa valeur à l'équilibre ($D_2O_{(eq)}$) après administration orale d'eau lourde à des malades atteints de cirrhose du foie avec ascite (2, 4, 5 et 6).

où $C_{(i.v.)_0 t}$ exprime la concentration isotopique au temps t (en minute) en fraction de la concentration à l'équilibre.

Les courbes artérielles de diffusion d'un groupe de sujets normaux établies par SCHOLER et CODE[10] d'une part, et par EDELMAN[18] d'autre part, sont respectivement représentées par les relations suivantes:

$$C_{(i.v.)_0 t} = 2{,}34 \exp(-0{,}21\, t) + 0{,}69 \exp(-0{,}035) + 1 \qquad (2)$$

$$C_{(i.v.)_0 t} = 2{,}42 \exp(-0{,}39\, t) + 0{,}73 \exp(-0{,}050\, t) + 1 \qquad (3)$$

La comparaison de ces résultats indique que l'utilisation des courbes obtenues chez les sujets normaux (équations (2) et (3)) entrainerait une erreur au cours de la correction des courbes d'absorption de nos malades atteints de cirrhose du foie.

Mesure de l'absorption digestive de l'eau lourde

Dans quatre épreuves les conditions techniques ont permis d'obtenir simultanément et pendant une période de temps assez longue des courbes d'absorption et de dilution avec un nombre de points suffisants (Epreuves 2, 4, 5 et 6). Nous avons établi la moyenne de ces points expérimentaux pour l'ensemble de ces 2 séries de courbes (Figs. 3 et 4).

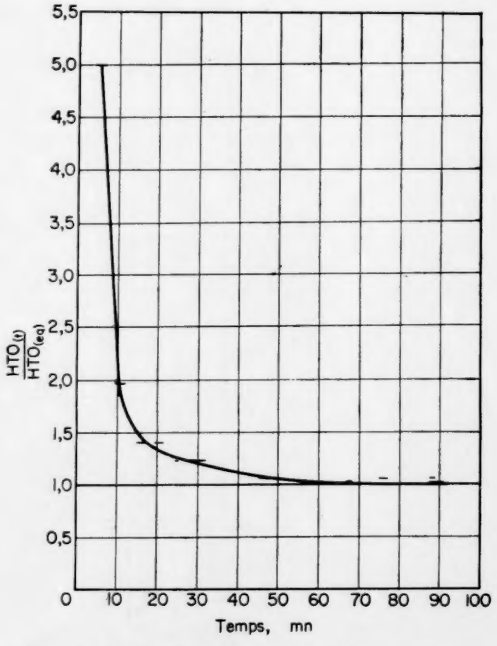

FIG. 4. Courbe moyenne des variations enregistrées en fonction du temps de la concentration en HTO de l'eau du sang veineux ($HTO_{(t)}$) rapportée à sa valeur à l'équilibre ($HTO_{(eq)}$) après administration intraveineuse d'eau tritiée à des malades atteints de cirrhose du foie avec ascite (2, 4, 5 et 6).

VOL. 7 1959/

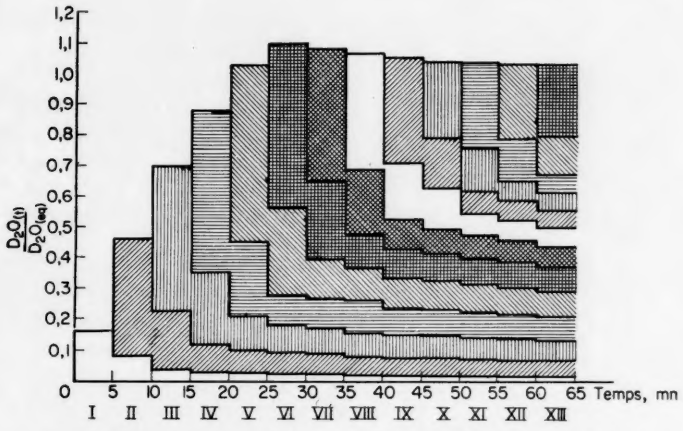

FIG. 5. Présentation graphique des résultats expérimentaux et de leur correction. Les surfaces hachurées montrent la disparition dans le sang de l'indicateur absorbé par le tube digestif pendant les intervalles de temps successifs.

Ainsi que nous l'avons signalé, les concentrations isotopiques sanguines obtenues après ingestion de l'eau marquée, doivent être considérées à tout moment comme traduisant l'existence de deux phénomènes simultanés:

Pénétration de l'indicateur du tube digestif vers le sang et fuite des quantités absorbée vers les espaces extra-vasculaires.

Cette fuite s'effectue dans un volume que l'on peut déterminer à l'aide de l'indicateur injecté par voie veineuse; ce volume est déduit des valeurs expérimentales de la concentration isotopique par la relation:

$$V_t = 100/C_{(\text{i.v.})_t} \qquad (4)$$

où V_t = le volume au temps t exprimé en pourcentage de sa valeur à l'équilibre;

$C_{(\text{i.v.})_t}$ = la concentration du sang veineux en eau tritiée après injection intraveineuse,

la valeur à l'équilibre de sa concentration étant prise égale à l'unité et correspond à un volume de dilution de 100 pour cent.

Divisons la durée de l'expérience en un certain nombre d'intervalles de temps successifs et égaux, désignons les par les caractères romaines I, II, III, . . . N.

Soit V_{I} le volume de distribution et $C_{\text{abs.I}}$ la concentration sanguine moyenne de l'indicateur absorbé (oxyde de deutérium), pendant le premier intervalle de temps, il est possible de calculer la quantité Q_{I} qui a traversé la paroi digestive pendant ce même intervalle. En effet:

$$Q_{\text{I}} = C_{\text{abs.I}}\, V_{\text{I}}. \qquad (5)$$

Ensuite, la dilution de Q_{I} se poursuit dans un volume croissant, donc sa concentration sanguine diminue progressivement (Fig. 5).

Pendant le deuxième intervalle de temps pris égal au précédent une quantité Q_{II} pénètre dans le sang, se dilue dans le volume V_{I} et contribue à l'augmentation de la concentration sanguine de l'oxyde de deutérium. Cette nouvelle quantité Q_{II} va subir sa propre dilution dans un volume croissant et dans le troisième intervalle de temps le volume V_{I} contiendra les quantités résiduelles de Q_{I}, de Q_{II} et la quantité Q_{III} absorbée pendant cet intervalle.

Tandis que Q_{I} poursuit sa dilution pendant les N intervalles égaux qui divisent la durée de l'expérience, Q_J se dilue pendant un temps égal à $(N–J)$, et Q_N pendant le dernier intervalle.

Connaissant la concentration sanguine de l'indicateur ingéré, le volume V_{I} et le facteur de dilution des quantités absorbées pendant

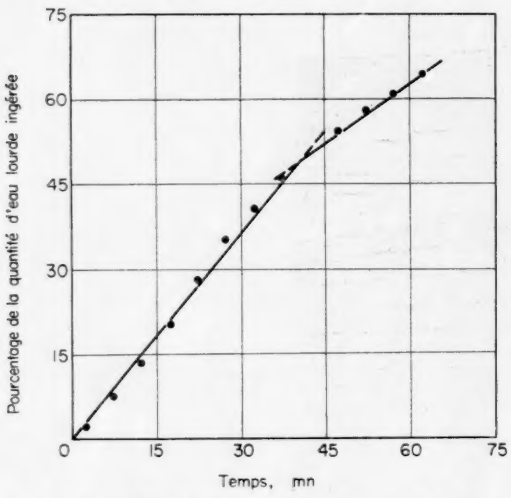

FIG. 6. Passage de l'eau lourde à travers la paroi digestive en fonction du temps.

les intervalles précédents, Q_J est donné par la relation:

$$Q_J = V_I[C_{(abs)} J - (C_{abs.I} (Ae^{-kt_J} + Be^{-k't_J} + 1) + C_{abs.II} (Ae^{-kt_{J-1}} + Be^{-k't_{J-1}} + 1) + \ldots C_{abs_{J-I}} (Ae^{-kt_{II}} + Be^{-k't_{II}} + 1)] \quad (5)$$

Partant de nos courbes moyennes de dilution et d'absorption, nous avons déterminé les quantités Q_I, Q_{II}, ... Q_N absorbées pendant les intervalles de temps de t_I à t_N: XIII intervalles de 5 minutes.

Ces quantités totales absorbées ont été exprimées en pourcentage de la quantité d'eau lourde ingérée à l'aide d'un facteur de correction (Fig. 6).

Portant ces valeurs en coordonnées cartésiennes en fonction du temps nous obtenons une courbe intégrée et nous pouvons calculer la vitesse moyenne d'absorption en traçant une droite qui correspond aux 40 premières minutes après l'ingestion. Nous reviendrons sur la signification des écarts observés entre la droite et les points expérimentaux. La vitesse moyenne calculée à partir de la pente de cette droite est de 1,2 pour cent par minute de la dose ingérée.

A la 40ème minute on observe une angulation de la courbe et les 5 derniers points expérimentaux sont alignés avec une pente moindre que la précédente correspondant à une vitesse d'absorption de 0,75 pour cent par minute.

L'absorption de 50 pour cent de l'eau lourde ingérée a eu lieu pendant 42,5 minutes et 67 pour cent pendant 67 minutes.

L'étude globale de la courbe montre qu'il n'existe aucune discontinuité dans l'absorption, mais son analyse révèle une allure sigmoïde avec un point d'inflexion se situant entre la 20ème et la 25ème minute.

Avant d'aborder la discussion de nos résultats, il convient de démontrer la validité de l'emploi des isotopes de l'hydrogène pour l'étude des mouvements de l'eau.

Malgré les différences des propriétés thermodynamiques du protium (^1_1H), du deutérium (^2_1H) et du tritium (^3_1H) on ne trouve pas d'écart significatif entre le comportement dans l'organisme animal de l'eau lourde (D_2O) et de l'eau tritiée (HTO). THOMSON et BALLOU[19] ont en effet montré que le rapport T/D du sang demeurait égal à 1, après administration simultanée par sonde gastrique chez le rat d'un mélange d'HTO et de D_2O.

GLASCOCK et DUNCOMBE[20] ont observé le même phénomène après injection intraveineuse des deux eaux marquées.

Enfin HSI WANG *et al.*[21] ont montré que le coefficient de diffusion dans l'eau était le même pour THO et DHO.

Partant de ces données il est légitime d'admettre que le protium se comporte comme ces isotopes.

La validité de l'emploi de ces indicateurs étant ainsi prouvée, il convient de rappeler leur signification dans les études de transfert. Ils traduisent un déplacement unidirectionnel et centrifuge de l'eau quand le compartiment de diffusion est infini par rapport à celui où l'indicateur a été introduit. S'il n'en est pas ainsi le retour de l'indicateur devient de plus en plus important à mesure que les valeurs s'approchent de l'équilibre mais peut être négligé au début de l'expérience.

Or on sait qu'il existe un passage incessant de l'eau dans les deux sens à travers la paroi intestinale, on est ainsi amené à définir un flux entrant, un flux sortant, et un flux net, somme algébrique des deux précédents.

VOL. 7 1959/6

Celui-ci est nul à l'état stationnaire, ou en l'absence de toute absorption ou secrétion, lorsque le volume d'eau intraluminale demeure constant. L'introduction d'un indicateur en quantité négligeable dans l'intestin permet alors de mesurer le flux sortant; la décroissance de la concentration isotopique de cette eau s'inscrit sur une courbe exponentielle. Cope *et al.*[22] ont déterminé la valeur de ce flux chez le chien porteur d'un petit estomac dans lequel le volume liquidien est demeuré constant ou a légèrement augmenté pendant la durée de l'expérience. Dans ces conditions, il fallait 20 minutes pour que 50 pour cent de la quantité initiale de l'indicateur soit transférée. Chez l'animal on peut aussi déterminer le flux entrant après injection de l'indicateur dans le sang et mesurer son apparition dans l'intestin extériorisé. La valeur de ces flux est inconnue chez l'homme.

Lorsque l'état stationnaire est détruit du fait de l'absorption d'une notable quantité d'eau (75 à 80 ml dans nos épreuves), la fuite de l'indicateur traduit en plus du renouvellement de l'eau, son transport vers la circulation. Si la quantité renouvelée est faible par rapport à celle absorbée et la vitesse d'absorption constante, la concentration isotopique ne varie pas dans la lumière de l'anse intestinale pendant la durée de l'absorption et la variation du volume d'eau résiduelle, en fonction du temps, s'inscrit sur une droite à pente négative.

Si l'on apprécie le phènomène dans un compartiment extra-intestinal, le sang périphérique en l'occurence, la variation de la concentration isotopique s'inscrit sur une courbe ascendante.

Après la correction que nous avons appliquée et qui tient compte de l'augmentation éventuelle (négligeable dans nos épreuves) du volume V_I due à l'absorption de l'eau lourde, l'allure de la courbe des concentrations isotopiques peut indiquer si le phénomène prédominant est le renouvellement de l'eau ou son absorption. Dans ce dernier cas l'on obtient une droite dont la pente mesure la vitesse d'absorption de l'eau ingérée. C'est effectivement ce qui résulte de la correction de nos courbes expérimentales.

Satisfaisante du point de vue théorique, la méthode utilisée peut néanmoins être entachée d'une erreur importante en raison des difficultés que pose la détermination exacte du premier volume de dilution V_I, dont la valeur figure dans les équations utilisées (5 et 6). Nous avons voulu diminuer cette erreur en établissant une courbe moyenne. Nous avons admis la validité de ce traitement pour des malades assez voisins du point de vue clinique chez lesquels les deux épreuves (HTO intraveineux et D_2O pérorale) ont été effectuées simultanément.

DISCUSSION DES RÉSULTATS OBTENUS

Considérant les données obtenues à l'aide de l'eau lourde comme représentatives des mouvements de l'eau ordinaire, nos résultats peuvent être interprétés en faveur d'un processus d'absorption, du moins en ce qui concerne les 40 premières minutes. L'allure sigmoide de la courbe peut s'expliquer par l'inégalité des quantités absorbées par unité de temps: elles passent par un maximum entre la 20ème et la 25ème minute. L'inégalité affecte surtout le premier intervalle de temps, pendant lequel une très faible quantité d'eau traverse la paroi digestive. En effet, Rittenberg et London[23] ont signalé chez le sujet normal un écart de plusieurs minutes entre le début de l'ingestion et le début de l'absorption.

L'angulation et la diminution de la pente (Fig. 6) entre la 40ème et la 60ème minute peuvent traduire soit un ralentissement de l'absorption, soit une part relativement accrue du phénomène de renouvellement. Le caractère linéaire de la courbe plaiderait en faveur de la première hypothèse.

La comparaison de nos résultats avec ceux obtenus par Scholer et Code[10] chez les sujets normaux, nous montre une diminution notable de la vitesse d'absorption des malades atteints de cirrhose du foie. Les valeurs observées par les auteurs américains étaient

respectivement 2,5 et 26 pour cent par minute de l'eau ingérée pour l'absorption duodénale et gastrique et le temps nécessaire pour l'absorption de 67 pour cent de l'eau administrée était de 34 et de 3,7 minutes pour ces deux groupes de sujets. Sans tenir compte du lieu d'absorption, HIGGINS *et al.*[24] et leurs collaborateurs donnent comme moyenne pour les sujets normaux un taux initial d'absorption de 9,5 pour cent par minute, or chez nos malades ce même taux était de 1,2 pour cent.

Quels mécanismes peut-on invoquer pour expliquer la diminution de la vitesse d'absorption de l'eau chez les malades porteurs d'une cirrhose du foie?

S'agit-il d'un retard du transit, d'une augmentation du fluide résiduel dans l'intestin, d'une imperméabilité de la muqueuse digestive ou d'un trouble circulatoire? Il est certes difficile de répondre à ces questions.

Le transit normal de l'eau dans le tube digestif est assez mal connu. Il est déterminé par les mouvements péristaltiques, l'état d'ouverture ou de fermeture du pylore: celui-ci est ouvert chez les sujets à jeun, mais les variations du pH, de la température et de la pression intragastrique modifient le jeu de ce sphinctor. La fermeture artificielle (ballonet ou ligature) ou pathologique du pylore rend possible la mesure de l'absorption purement gastrique. Pour introduire l'eau directement au contact de la muqueuse duodénale ou jéjunale, on peut opérer à l'aide d'une sonde sous contrôle radiologique, mais celle-ci perturbe la motricité locale et détermine une hypersécrétion aqueuse avec production de mucus.[25] Au cours de nos épreuves, nous avons voulu rester dans les conditions physiologiques de l'ingestion et étudier globalement l'absorption gastro-duodénale.

Un ralentissement du transit intestinal peut être observé dans les maladies du foie comme l'ont montré REYNELL et SPRAY[26] chez le rat intoxiqué par le tetrachlorure de carbone. Cependant il n'explique pas à lui seul le ralentissement de l'absorption de nos malades puisque selon SCHOLER et CODE l'absorption purement gastrique des sujets normaux est supérieure à celle de nos malades. D'ailleurs la Fig. 1 montre qu'il existe deux types de courbes chez les cirrhotiques qui correspondraient selon ces auteurs à l'absorption gastrique (courbes asymptotiques) et à l'absorption duodénale (courbes présentant un maximum).

L'augmentation du fluide résiduel de l'intestin peut exister même chez le sujet normal et introduire une cause d'erreur par la dilution de l'indicateur. Il est d'autant plus difficile d'en tenir compte que le volume de cette eau gastro-intestinale diffère d'un sujet à l'autre comme l'ont montré GOTCH *et al.*[27] ainsi que LIEBOWITZ *et al.*[28] Il y aurait donc intérêt à accroître le volume d'eau ingérée tout en respectant les conditions physiologiques.

Les solutions hypertoniques entraînent une sécrétion d'eau vers la lumière intestinale et pour les solutions iso ou hypotoniques la vitesse d'absorption aqueuse varie en raison inverse de la teneur en sels de la boisson d'expérience. C'est pourquoi nous avons eu recours à de l'eau lourde distillée qui s'absorbe facilement sans entraîner une augmentation de l'eau résiduelle.

Le fluide résiduel peut être augmenté chez les cirrhotiques qui sont plus souvent diarrhétiques qu'atteints de constipation, mais la teneur exagérée en eau des fèces peut provenir aussi bien d'une hypersécrétion colique que d'une diminution de la résorption aqueuse des selles liquides en provenance de l'intestin grêle.

Si la dilution n'a pas lieu dans la lumière intestinale, elle peut se produire au cours de la traversée de la paroi généralement oedématiée chez ces malades.

Par ailleurs, il existe chez les cirrhotiques une diminution de la surface d'absorption liée à une rétraction du mésentère qui raccourcit l'intestin grêle. Ce dernier facteur peut également intervenir dans le ralentissement de l'absorption.

Quant à la circulation portale, elle peut constituer le facteur limitant de la vitesse d'apparition de l'indicateur dans le sang périphérique.

Le rôle des facteurs circulatoires est d'autant plus important que la presque

VOL. 7 1959/

totalité de l'eau ingérée passe directement dans le système veineux mésentérique. A l'état normal, méme après ingestion d'une quantité considérable d'eau, ni le volume du sang circulant, ni la pression artérielle ne varient de façon significative. Cette régulation est assurée par la voie de dérivation du système porte qui peut retenir momentanément la majeure partie des liquides ingérés pour les libérer ensuite progressivement dans la circulation générale. L'indicateur peut donc apparaître avec un certain retard dans le sang périphérique (artériel ou veineux) où les mesures sont effectuées.

Ce retard est plus marqué chez les malades atteints de cirrhose du foie. L'étude histopathologique de cette affection montre, en effet, une congestion intense de la paroi digestive avec vascularisation exagérée et dilatation des veines sous muqueuses et sous séreuses. Dans une de nos observations la vérification anatomique révélait même un obstacle dans le tronc de la veine porte (pyléphlébite thrombosante).

Le retard à l'absorption peut donc relever de deux facteurs: ralentissement du transfert de l'eau à travers la paroi digestive ou ralentissement du passage de l'indicateur du système porte vers la circulation générale. Il est d'ailleurs probable que les deux phénomènes interviennent simultanément du fait de l'hypertension portale.

Quel que soit le mécanisme de ce trouble de l'absorption son résultat final se traduit par un retard à l'élimination rénale de l'eau. L'hypothèse de VILLARET concernant le rôle du système digestif dans l'opsiurie se trouve ainsi étayée par ces données expérimentales.

Remerciements—Les malades explorés étaient hospitalisés à l'Hôpital Lariboisiere, dans le Service du Docteur ROBERT WORMS, à qui nous adressons nos vifs remerciements.

BIBLIOGRAPHIE

1. VILLARET M. *Contribution a l'étude du syndrome d'hypertension portale. Les troubles du débit urinaire dans les affections hépatiques. Etude anatomique, expérimentale et clinique des territoires d'absorption et d'excrétion aqueuse.* G. Stainheil, Paris (1906).
2. CHABROL E. et COTTET J. *Paris Méd.* **39,** 220 (1949).
3. DURBIN R. P., FRANK H. et SOLOMON A. K. *J. Gen. Physiol.* **39,** 535 (1956).
4. FISCHER K. B. *J. Physiol.* **130,** 655 (1955).
5. SMYTH D. H. and TAYLOR G. B. *J. Physiol.* **136,** 632 (1957).
6. CURRAN P. F. and SOLOMON A. K. *J. Gen. Physiol.* **41,** 143 (1957).
7. FIESSINGER N. Congrès de la diurèse de Vittel, 3–8, Mai 1939.
8. GOTCH F., NADELL J. and EDELMAN I. S. *J. Clin. Invest.* **36,** 289 (1957).
9. BLICKENSTAFF D., BACHMANN D. M., STEINBERG M. E. et JOUMANS W. B. *Amer. J. Physiol.* **168,** 303 (1952).
10. SCHOLER J. F. et CODE C. F. *Gastroenterology* **27,** 565 (1954).
11. HAYES F. N. et GOULD, R. G. *Science* **117,** 480 (1953).
12. HAYES F. N. *Int. J. Appl. Rad. Isotopes* **1,** 45 (1956).
13. DAVIDSON J. D. et FEIGELSON P. *Int. J. Appl. Rad. Isotopes* **2,** 1 (1957).
14. LANGHMAN W. H., EVERSOLE W. J. HAYES F. N. et TRUJILLO T. T. *J. Lab. Clin. Med.* **47,** 819 (1956).
15. COOPER J. A. D., RADIN N. J. and BOWDEN A. *J. Lab. Clin. Med.* **52,** 129 (1958).
16. COURSAGET J., FALLOT P. et CHEVALLIER F. Troisième Congrès Médical International d'Evian, Sept. 1951.
17. FALLOT P., AEBERHARDT A. et MASSON J. *Int. J. Appl. Rad. Isotopes* **1,** 237 (1957).
18. EDELMAN I. S. *Amer. J. Physiol.* **171,** 279 (1952).
19. THOMSON R. C. et BALLOU J. E. *Arch. Biochem. Biophys.* **42,** 219 (1953).
20. GLASCOCK R. F. et DUNCOMBE W. G. *Biochem. J.* **53,** 440 (1954).
21. HSI WANG J., ROBINSON C. V. et EDELMAN I. S. *J. Amer. Chem. Soc.* **75,** 466 (1952).
22. COPE O., BLATT H. et BLATT M. R. *J. Clin. Invest.* **22,** 111 (1943).
23. RITTENBERG I. M. et LONDON D. *J. Biol. Chem.* **184,** 687 (1950).
24. HIGGINS J. A., LEE P. et SCHOLER J. F. *J. Clin. Invest.* **36,** 265 (1957).
25. OGAWA T. et NECHELES H. *Amer. J. Physiol.* **194,** 303 (1958).
26. REYNELL P. C. et SPRAY G. H. *Brit. J. Exp. Path.* **37,** 466 (1956).
27. GOTCH F., NADELL J. et EDELMAN I. S. *J. Clin. Invest.* **36,** 289 (1957).
28. LIEBOWITZ D., STONE H. H., LEVINE D., SCOTT K. G. et ALTHAUSEN T. L. *Gastroenterology* **32,** 265 (1957).

International Journal of Applied Radiation and Isotopes, 1960, Vol. 7, pp. 244–250. Pergamon Press Ltd. Printed in Northern Ireland

Beta-excited Characteristic X-rays as Energy Reference Sources

J. F. CAMERON and J. R. RHODES
Isotope Division, Atomic Energy Research Establishment, Harwell

(*Received* 8 *August* 1959)

The β-particles emitted from 1 mc of Kr^{85} sealed in a small nickel capsule were used to excite the characteristic K-X-rays of various elements. It was found that the best arrangement of source and target was with the source sandwiched between two thin foils of the target element. The use of these X-rays as energy references for the calibration of proportional and scintillation counters in the energy region 0 to 100 keV is illustrated. Since the energies of K-X-rays are known to about one part in 10^4 the accuracy of calibration depends only on the resolution of the instrument under test.

LES RAYONS-X CARACTÉRISTIQUES EXCITÉS AU RAYONNEMENT β COMME SOURCES D'ÉNERGIE DE REPÈRE

Les particules β émises par 1 mc de Kr^{85} scellé dans une petite capsule de nickel servirent à exciter les rayons-X-K de différents éléments. On découvra que le meilleur arrangement de source et cible fut où la source était serrée entre deux feuilles minces de l'élément servant de cible. On démontre l'emploi de ces rayons-X comme repères d'énergie pour l'étalonnage des compteurs proportionnels et ceux à scintillation dans la gamme d'énergie 0 à 100 keV. Les énergies des rayons-X-K étant connues à une exactitude d'environ 1 : 10^4, la précision de l'étalonnage dépend seulement de la résolution de l'instrument mis à l'essai.

ВОЗБУЖДЕННОЕ β-ЧАСТИЦАМИ ХАРАКТЕРИСТИЧЕСКОЕ РЕНТГЕНОВСКОЕ ИЗЛУЧЕНИЕ КАК ЭТАЛОННЫЙ ИСТОЧНИК ЭНЕРГИИ

β-частицы, испускаемые 1 mc Kr^{85}, помещенным в небольшой запаянный никелевый капсюль, применялись для возбуждения характеристического К-излучения различных элементов. Было найдено, что наилучшим расположением источника и мишени является такое, при котором источник помещается между двумя тонкими листками элемента мишени. Показано использование этого рентгеновского излучения в качестве эталона энергии для градуирования пропорциональных и сцинтиляционных счетчиков в област и энергий от I до 100 кэв. Так как энергия К-излучения известна с точностью приблизительно до 0,01%, то точность градуировки зависит только от разрешающей способности испытываемого прибора.

β-ANGEREGTE CHARAKTERISTISCHE RÖNTGENSTRAHLUNG ALS ENERGIE-REFERENZ-QUELLEN

β-Partikel von 1 mc K^{85}, verschlossen in einer kleinen Ni-Kapsel, wurden verwendet um die charakteristische K- und L-Strahlung verschiedener Elemente anzuregen. Die zwischen zwei dünnen Folien aus dem Targetmaterial gesandwichte Quelle erwies sich als günstigste Anordnung von Quelle und Target. Die Verwendung dieser Röntgenstrahlen als Energiereferenz zur Kalibrierung von Proportional- und Szintillationszählern im Energiebereich von 0–100 keV wird gezeigt. Da die Energien der K- und L-Strahlung bis auf eins in 10^4 bekannt sind, hängt die Genauigkeit der Kalibrierung nur vom Auflösungsvermögen des untersuchten Instrumentes ab.

1. INTRODUCTION

PROPORTIONAL and scintillation counters are now in widespread use for such purposes as radioactivation analysis and X-ray fluorescence spectroscopy. In most of these applications an accurate calibration of the energy scale is essential and this is generally accomplished by using a number of different sources emitting radiation of known energies. Characteristic X-rays excited by electromagnetic radiation from radioactive sources have been used[1] but because of the rapid variation in absorption cross-section with energy, several sources are required to cover the range of characteristic X-ray energies. A recent publication[2] has shown that β-excited characteristic X-radiation can also be used. Such a method provides a large number of calibration points with the use of only one radioactive source and consequently reduces the expense and possibility of contamination resulting from the use of a number of sources. A convenient isotope for this purpose is Kr^{85}. It was found that the β-particles from this source would excite characteristic X-radiation in the region 5–100 keV using elements from iron to thorium. Kr^{85} has a half-life of 10·6 years and decays by β-emission (maximum energy 0·67 MeV) in about 99·3 per cent of its disintegrations and by emitting a γ-ray of energy 0·52 MeV in 0·7 per cent of the disintegrations.[3] This γ-ray in no way interferes with the excitation of characteristic X-radiation and may be used to complete a calibration up to 500 keV. Furthermore Kr^{85} is relatively cheap and is an inert gas, so that any ingestion hazard in the event of source leakage is very small.

Three other sources of β-particles, Pm^{147}, Sr^{90}/Y^{90} and Tl^{204} were considered but found to be less suitable than Kr^{85}. The β-particles from Pm^{147} have a maximum energy of 0·22 MeV[3] and the proportion with energies sufficient to excite characteristic X-radiation from elements of high atomic number is small. The present commercial method of containing Pm^{147} and Sr^{90}/Y^{90} sources is in a silver matrix covered by thin silver foil. In the case of Pm^{147} this foil is thick enough to stop most of the β-particles and thus give a relatively large yield of silver characteristic X-rays. The high-energy β-particles from Sr^{90}/Y^{90} give a higher yield of interfering bremsstrahlung than those from the lower energy β-emitters. Tl^{204} emits β-particles of maximum energy 0·77 MeV[3] and in this respect is similar to Kr^{85}, but unfortunately about 2 per cent of the disintegrations result in the production of mercury characteristic X-rays (about 70 keV) by electron capture, with resulting complication of a calibration spectrum. In addition to the above disadvantages the potential contamination hazard from these necessarily thin-walled solid sources, especially Sr^{90}/Y^{90}, is higher than that from Kr^{85}.

2. SOURCE, DETECTORS AND SOURCE-DETECTOR DISTANCES

The source used in this investigation was 1 mc of krypton-85 sealed at atmospheric pressure in a nickel tube 1 cm long of 0·15 cm inside diameter with a wall thickness of 0·0025 cm. Sealing was accomplished by soft soldering the crimped ends of the tube. It was mounted, for ease of handling, by sandwiching between two films of 0·0025 cm nylon in the centre of a 5 cm diameter hole in a 7·5 cm square Perspex tray.

A xenon-filled proportional counter* 1·94 cm in diameter and 9·5 cm long, with a 1·2 cm × 0·5 cm beryllium window 0·05 cm thick, was used for measurements in the energy region 5 to 25 keV. For the energy range 20 to 100 keV a scintillation counter was used with a crystal of NaI(Tl), 3·81 cm in diameter by 2·54 cm thick which had an aluminium window 0·064 cm thick. These were used in conjunction with an amplifier† and a hundred-channel pulse-height analyser.

The scintillation counter was not used in the region below 20 keV because of the poor resolution attainable as compared with that

* Type PX28F, 20th Century Electronics Ltd. † Harwell Type No. 1430A.

of a proportional counter, and the proportional counter was not employed at energies above 25 keV because of the fall-off in detection efficiency.

A source to detector distance of 10 cm was used for all targets with the scintillation counter, and of 3 cm with the proportional counter. A krypton-85 source as small as 20 μc could be used if it were positioned 1 cm from the scintillation counter. In the case of the proportional counter a source strength of about 100μc would be required at this distance.

3. CHOICE OF TARGET AND OF SOURCE-TARGET DISPOSITION

The choice of target is determined by the energy of its characteristic K-radiation. Where possible, targets in the form of metal foils were used, but in some cases, for example in the rare earth series, foils were unobtainable and a suitable compound of the element was powdered and compressed into thin discs. Table 1 gives a list of the targets used, together with the energies[4] and relative intensities[5] of their principal characteristic K-lines. The choice of target thickness and of the geometrical arrangement used are governed by the considerations outlined below.

TABLE 1. Targets used with their characteristic K-energies and relative intensities

Target element	Atomic number	Form of target	K_{α_1}	K_{α_2}	K_{β_1}	K_{β_2}	Mean energy (keV)
			Relative intensities				
			100	50	21	5	
			Energies (keV)				
Fe	26	Metal foil	6·40	6·39	7·06	—	6·4
Ni	28	Nickel tube of source	7·48	7·46	8·26	8·33	7·5
Zr	40	Metal foil	15·77	15·69	17·67	17·97	15·7
Ag	47	Metal foil	22·16	22·00	24·94	25·45	22·1
Sn	50	Metal foil	25·27	25·04	28·48	29·11	25·2
Ce	58	Cerium nitrate discs	34·72	34·28	39·26	40·23	34·6
Ta	73	Metal foil	57·52	56·27	65·21	67·00	57·1
Pb	82	Metal foil	74·96	72·79	84·92	87·34	74·2
Th	90	Metal foil	93·33	89·94	105·59	108·67	92·2

VOL. 7 1959/

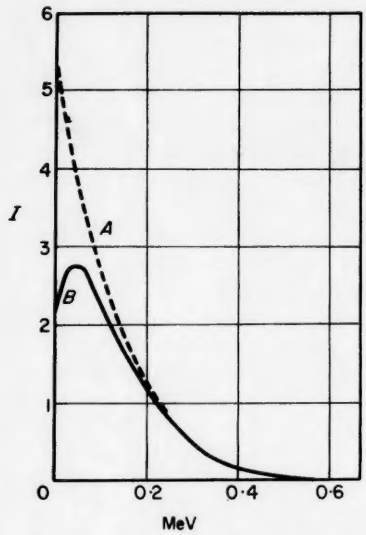

FIG. 1. Theoretical (*A*) and observed (*B*) bremsstrahlung spectra from Kr^{85}.

β-Particles, in addition to exciting characteristic X-radiation, give rise to a considerable amount of bremsstrahlung. The theoretical shape of the bremsstrahlung spectrum is almost independent of target atomic number.[6,7]

A theoretical energy distribution of the bremsstrahlung produced by the β-particles from Kr^{85} is shown by the dotted line in Fig. 1. The full line in Fig. 1 shows an experimental bremsstrahlung spectrum for an aluminium target using Kr^{85} and it is seen to have a broad peak between 20 and 100 keV. The shape of the low energy cut-off due to absorption in the target is determined by the atomic number of the target. With the targets used in this investigation the bremsstrahlung maximum varied from about 75 keV for thorium to about 40 keV for elements of atomic number 40 and below. For the elements cerium, tantalum, lead and thorium the characteristic X-rays more or less coincide with the bremsstrahlung peak and the former are thus less well-defined.

It was found that in all cases the target, source and detector arrangement shown in Fig. 2a with the target on the opposite side of the source from the detector was better from the point of view of exciting K-series photons than a transmission target. This is probably because bremsstrahlung is emitted mainly in the forward direction whilst characteristic radiation is isotropic.[8]

It was found that a filter (Fig. 2b) of the same material as the target considerably improved the definition of the characteristic X-ray peaks particularly where the characteristic radiation and bremsstrahlung were nearly coincident, and was used for all the elements considered, except cerium and nickel. Cerium, being in compressed disc form, was set up as in Fig. 2a, although this is not the best arrangement. The nickel capsule round the source was sufficient in itself to give a sharp K-peak. The main function of the filter in the case of iron is to cut out the nickel peak from the source capsule.

When the scintillation counter was used the aluminium window was sufficiently thick to stop all residual β-particles. The proportional counter, however, required for this

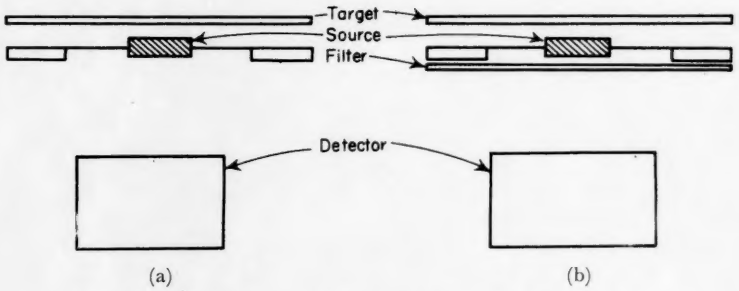

FIG. 2. Source–target–detector arrangements used (not to scale).

purpose a 250 mg/cm² aluminium absorber placed directly in front of the window. In both cases bremsstrahlung from the detector windows was found to make a negligible contribution to the experimental pulse-height distributions.

Since the energy of the characteristic radiation is just less than that at the K-X-ray absorption edge for the element, a filter of that element will transmit a high proportion of its own K-radiation, but will strongly absorb the incident radiation of energies just greater than that at the absorption edge. The same filtering effect takes place to a lesser extent for photons of energies below the K-X-ray energy. The filter itself produces characteristic radiation and bremsstrahlung from the incident β-particles, backscatters a proportion of the β-particles to produce more electromagnetic radiation in the target and re-emits as characteristic radiation some of the energy absorbed from the bremsstrahlung.

It is required to find the target thickness which gives maximum characteristic X-ray yield and the filter thickness giving the highest ratio of K-radiation to bremsstrahlung. These were found experimentally for silver and tantalum of which a large number of foils were available. The optimum target thickness depends on the relative efficiencies for production and self-absorption of characteristic radiation and bremsstrahlung. The efficiencies of producing bremsstrahlung and characteristic radiation both reach saturation at a thickness equal to that which stops the most energetic β-particles. Self-absorption also reaches a saturation value which depends on the absorption coefficient of the particular target for the energies of the two types of radiation. When using Kr^{85} as the source of β-particles it was found that the target thickness was not critical provided that it was greater than about 100 mg/cm². In all cases (except for nickel) the target thickness used was between 100 and 200 mg/cm². The filter thicknesses were more critical and the optimum thicknesses for silver and tantalum were found to be 45 mg/cm² and 170 mg/cm² respectively, and both represent a thickness such that the K-photons are attenuated by a factor of approximately 0·73. For the other targets used the range of foils was insufficient to enable the above figure to be verified with any accuracy but with the foils available it was evident that an attenuation factor of approximately 0·73 in the K-energy region did give optimum results. Table 2 shows filter thicknesses calculated on the basis of this figure and the thicknesses actually used.

The use of a filter for the K_β X-rays was investigated but the resultant improvement in peak width was small and did not warrant the additional complication.

VOL. 7 1959/6

4. EXPERIMENTAL RESULTS AND COMMENTS

Fig. 3 shows the experimental differential pulse-height distributions for the elements silver, tin, cerium, tantalum, lead and thorium using the scintillation counter. The peaks in this energy region obtained with Tm^{170} and Xe^{133} sources are shown for comparison. For clarity a complete curve is shown only for tin. The complete spectra for silver and tin show broad bremsstrahlung maxima at approximately 60 keV, but for tantalum, lead and thorium the bremsstrahlung maximum and K-peak are approximately coincident. Since the bremsstrahlung maximum is flat and filtration is taking place

Table 2. Thickness of filters used with foil targets

Target element	Ag	Sn	Ta	Pb	Tl
Approximate absorption coefficient at K-X-ray energy (cm²/g)	7·5	6·0	1·85	1·30	1·00
Calculated optimum filter thickness (mg/cm²)	42	52	170	240	314
Filter thicknesses used (mg/cm²)	40	50	168	288	288

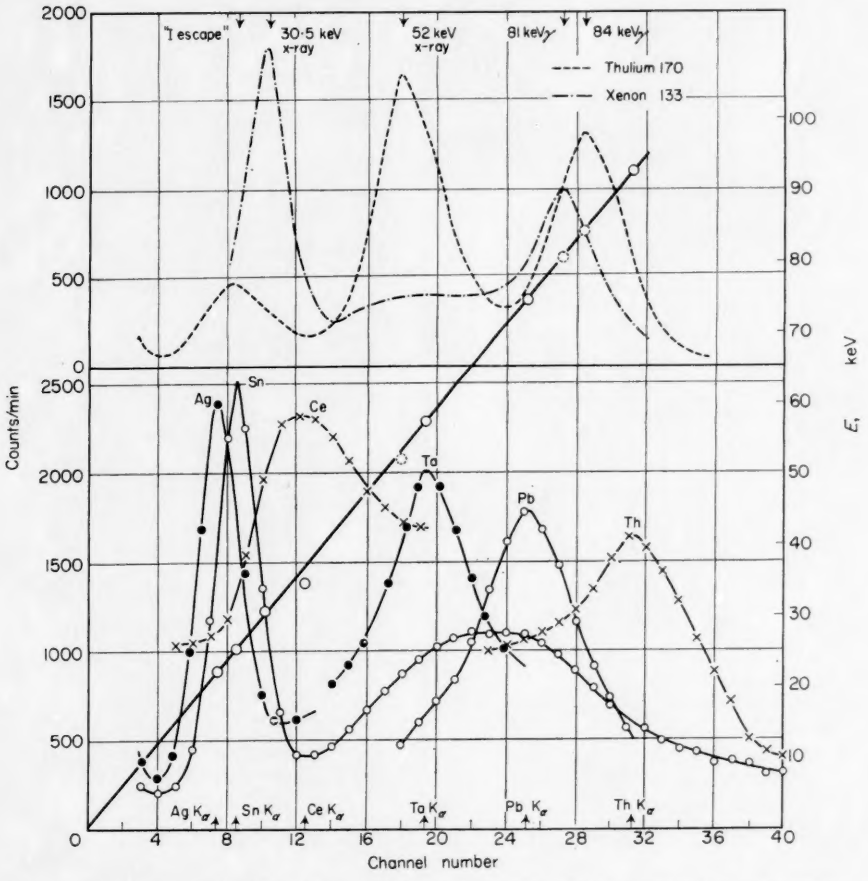

FIG. 3. Experimental differential pulse-height distributions using the scintillation counter.
(a) Tm^{170} and Xe^{133} calibration points.
(b) Characteristic radiation and bremsstrahlung from Ag, Sn, Ce, Ta, Pb and Th.

on each side of the K-peak, it was not found necessary to correct the latter by subtraction of the bremsstrahlung. However, in the case of cerium, where no filter is used, the distortion of the peak caused by bremsstrahlung, results in a shift of the maximum away from the K-X-ray energy unless a correction is made. The spectrum shown for thorium has been corrected for background due to radioactivity of the thorium itself. It is seen that the characteristic X-ray peaks are as suitable for calibration as the γ-ray peaks from the Tm^{170} and Xe^{133} sources.

On the same figure a graph of X-ray energy vs. pulse amplitude has been plotted, and the straight line so obtained shows that the overall response of the electronic equipment and sodium iodide crystal is linear in this energy region. The energies of the K-peaks were taken as the weighted arithmetic mean of the $K_{\alpha 1}$ and $K_{\alpha 2}$ energies ($\bar{E}$ in Table 1). Since the K_α lines were nearly resolved from the K_β lines the effect of the latter was to make the K-peak asymmetrical but not to move the position of the top of the peak. The fact that the point for 52 keV thulium-170 is not quite on the line is probably due to interference by the iodine

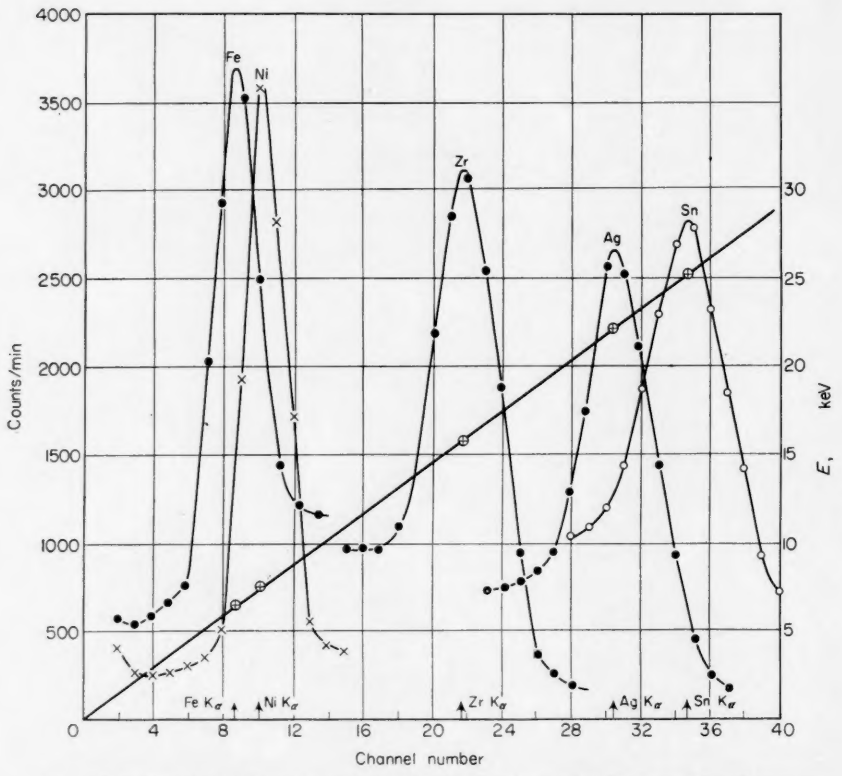

FIG. 4. Experimental differential pulse height distributions using the proportional counter.

escape peak at 55·5 keV from the 84 keV γ-ray.

Fig. 4 shows the experimental spectra for the elements iron, nickel, zirconium, silver and tin using the proportional counter. No appreciable bremsstrahlung is present in this energy region, and a graph of mean K-X-ray energy vs. pulse amplitude (Fig. 4) was again found to be linear over the range.

Conclusions

It has been shown feasible to use the characteristic X-rays excited by a low activity Kr^{85} β-source to calibrate proportional and scintillation counters in the energy region below 100 keV. Since the energies of K-lines for the elements are known to about one part in 10^4 the accuracy of calibration depends only on the resolution of the instrument.

REFERENCES

1. INSCH G. M. *Phil. Mag.* **41,** 857 (1950).
2. KEREIAKES J. G., KRAFT G. R., WEIR O. E. and KREBS A. T. *Nucleonics* **16** (1), 80 (1958).
3. ALLEN R. A., MILLETT R. J. and SMITH D. B. A.E.R.E. Report R.2938 (1959).
4. FINE S. and HENDEE C. F. *Nucleonics* **13** (3), 36 (1955).
5. BRAGG W. L. *Crystalline State* Vol. 1, Appendix II. G. Bell, London (1954)
6. LIDEN K. and STARFELT N. *Phys. Rev.* **97,** 419 (1955).
7. WU C. S. *Phys. Rev.* **59,** 481 (1941).
8. PRICE B. T., HORTON C. C. and SPINNEY K. T. *Radiation Shielding.* Pergamon Press, London (1957).

VOL. 7 1959/6

International Journal of Applied Radiation and Isotopes, 1960, Vol. 7, pp. 251–257. Pergamon Press Ltd. Printed in Northern Ireland

A Counter for Solid Samples Containing Labile Tritium

A. R. G. LANG and S. G. MASON
Physical Chemistry Division, Pulp and Paper Research Institute of Canada and Department of Chemistry, McGill University, Montreal, Quebec, Canada

(*Received* 6 *July* 1959)

The construction and operation of an apparatus for studying the exchange of tritium between cellulose and water by solid counting are described. It features a novel mechanism for manipulating the sample under high vacuum from a reaction chamber to a proportional counter. Counting characteristics, absorption of radiation by sample, gas and window, the time of reaction and contamination are discussed.

It is believed that the device may be used in other applications.

OL.
7
9/60

UN COMPTEUR POUR LES ÉCHANTILLONS SOLIDES CONTENANT DU TRITIUM LABILE

On décrit la construction et le fonctionnement d'un appareil destiné à l'étude de l'échange du tritium entre la cellulose et l'eau en comptant la radioactivité à l'état solide. Il montre un système inédit pour manoeuvrer l'échantillon hors de la chambre à réaction jusqu'au compteur proportionnel dans le vide poussé. On discute les caractéristiques du comptage, l'absorption du rayonnement par l'échantillon, par le gaz et par la fenêtre, le temps de réaction et la contamination.

Il est à croire que le dispositif servirait à d'autres applications.

СЧЕТЧИК ДЛЯ ТВЕРДЫХ ОБРАЗЦОВ, СОДЕРЖАЩИХ ЛАБИЛЬНЫЙ ТРИТИЙ

Описывается конструкция и работа счетчика твердых образцов для изучения обмена тритием между целлюлозой и водой. Прибор снабжен новым механизмом, позволяющим переносить образец из реакционного сосуда в пропорциональный счетчик без нарушения высокого вакуума. Обсуждаются характеристики счета, поглощение излучения образцом, газом и окошком, а также продолжительность реакции и степень загрязнения.

Автор полагает, что этот прибор может быть использован и в других случаях.

EIN ZÄHLER FÜR PROBEN IN FESTER FORM, WELCHE LABILES TRITIUM ENTHALTEN

Die Konstruktion und das Arbeiten einer Apparatur zur Untersuchung des Tr-Austausches zwischen Zellulose und Wasser durch Messung der festen Proben wird besprochen. Sie ermöglicht eine neue Technik des Hantierens der Probe unter Hochvakuum in der Reaktionskammer und in einem Proportionalzähler. Zählcharakteristiken, Absorption der Strahlung durch die Probe, im Gas und im Fenster, die Reaktionsdauer und die entstehende Verseuchung wird besprochen.

Es wird angenommen, dass dieses Gerät auch zu anderen Zwecken Verwendung finden kann.

INTRODUCTION

To investigate the exchange of tritium (H^3) between water vapour and cellulose sheets it was necessary to develop a device to carry out the exchange reaction and to measure the radioactivity of the sheets. The construction and operation of this counter are described in this paper. (Its application is considered elsewhere.[1]) A number of counters for measuring tritium in solid samples have been described,[2–9] but none was considered suitable for our purpose. The counter described here has a number of novel features which make it useful in various applications.

The principal difficulties encountered in counting tritiated samples arise from the weakness of the β-radiation involved. The maximum energy is only 18 keV, which corresponds to a thickness for complete absorption of about 1 mg/cm^2.[4,10] Thus absorption by the sample, counter, etc. can be appreciable and must be kept constant or corrections made. Surface irregularities of the samples may cause erratic results; however sources such as liquids[6] and shiny films[1] which have smooth surfaces, or those with reproducible surfaces may be counted satisfactorily.

The apparatus has provision for exposing the solid sample to tritiated water vapour, evacuating the system, and then measuring the radioactivity of the sample directly.

The apparatus was designed to meet the following requirements:

(1) Evacuation of the sample, after exposure to the water vapour, to a pressure of less than 1 μ Hg to reduce the adsorbed water to a negligible level of radioactivity.

(2) Separation of the exchange reaction chamber from the counter. (Preliminary experiments showed that tritiated water adsorbed on the counter walls could not be adequately removed by evacuation at room temperature, so that if the reaction and counting were done in one chamber an impracticably high contamination count resulted.)

(3) Exclusion of the atmosphere from the sample in the period between the completion of exchange and counting, to avoid the extremely rapid exchange between the sample and atmospheric water.[11]

(4) Placement of a thin conducting film at earth potential between the sample and the counter anode to prevent an electrostatic charge accumulating on the insulating surface of the sample.[12] This film will be called the "window," although its function is different from the window in a conventional end-window counter.

A preliminary apparatus was built in which a sample could be transferred from a reaction chamber to a counting chamber by rotating two matched plane plates which were sealed to one another with vacuum grease. Several greases were tried, but they always occluded sufficient active water to cause a large and irreproducible contamination of the counter. It was therefore abandoned for one using rubber O-ring vacuum seals.

DESCRIPTION

Vacuum transfer counter

The final apparatus is called a vacuum transfer counter (abbreviated to VTC) and is shown in Figs. 1 to 3.

As shown in Fig. 1, it consists essentially of a reaction chamber V and a counting chamber G bored into a cylindrical disc K. Both chambers are closed at the top by removable caps U and E, vacuum-sealed when in position by nitrile rubber O-rings in accurately machined grooves. An additional cap (not shown) fitted with a pirani gauge (Edwards, type MA-5) fits either chamber and is used for testing purposes.

The open bottom of each chamber matches a pocket L in the rotor N. The two pockets may be positioned beneath either chamber by rotating N with lever T. A spring-loaded indenting mechanism W maintains a gap between K and the rotor during this rotation, and ensures that the pockets are finally positioned concentrically with the

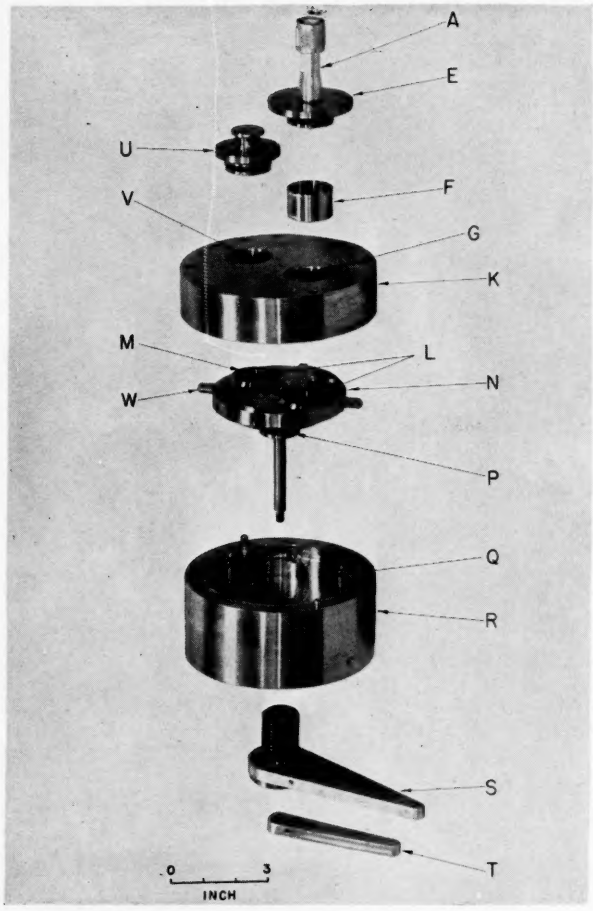

FIG. 1. Vacuum transfer counter. Exploded view. *A*—Amphenol plug; *E*—counter cap; *F*—insert; *G*—counter chamber; *L*—sample pockets: *N*—rotor; *P*—piston; *Q*—evacuation outlet; *S*—clamp; *T*—rotor positioning lever; *U*—reaction chamber cap; *V*—reaction chamber; *W*—indenting finger.

VOL.
7
59/60

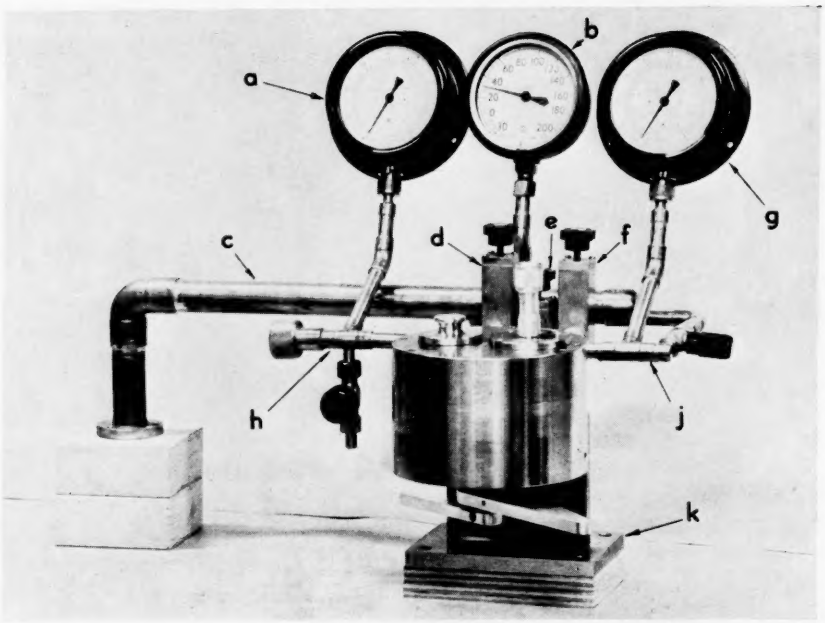

FIG. 3. Vacuum transfer counter and accessory apparatus. *a*—reaction pressure gauge; *b*—counting gas storage pressure gauge; *c*—vacuum manifold; *d*, *e* and *f*—vacuum valves; *g*—counting gas pressure gauge; *h*—inlet to reaction chamber; *i*—inlet to counter; *k*—stand.

VOL.
7
1959/

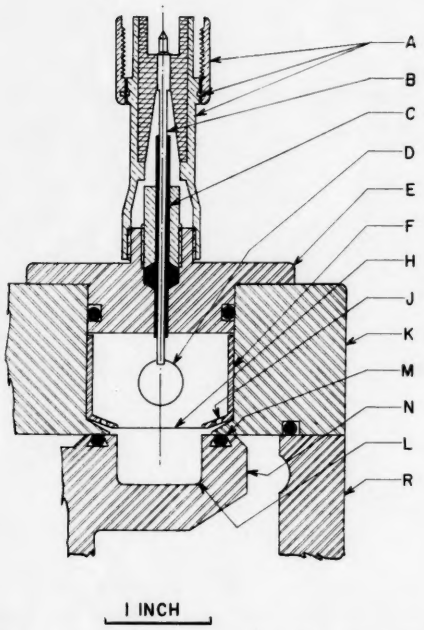

FIG. 2. Vacuum transfer counter. Section through counter chamber. *A*—Amphenol plug; *B*—anode rod; *C*—Teflon insulator and gasket; *D*—anode loop; *E*—cap; *F*—insert; *H*—gold plated plastic window; *J*—pressure equalizing holes; *L*—sample pocket; *M*—O-ring in trapezium groove; *N*—rotor.

chambers; the rotor can then be clamped to *K* by a screw device *S*, so that each pocket is vacuum-sealed to its chamber by an O-ring in a groove having a trapezium cross section (*M*, Fig. 2).

The rotor is totally enclosed by *R* (Fig. 1); vacuum seals are made around the periphery by an O-ring and at the moving joint *P* by a piston type O-ring system. Care was taken in the design to eliminate constricted volumes from which gas evacuation would be slow.

The volumes contained inside *R* and each chamber (*V* and *G*) may be evacuated separately through three corresponding 0·5 in. diameter outlets, which pass out of the back of the apparatus. *Q* is the outlet for *R*.

Fig. 2 shows the counting chamber in detail. The anode is a 1 cm diameter loop of 0·001 in. tungsten wire *D* attached to a 1/16 in. diameter rod of silver solder *B*, which passes into an Amphenol No. 82–804 plug *A*. The anode is insulated from the cap by a Teflon gasket *C*, which at the same time forms a vacuum seal between the rod and the cap *E*. An insert *F*, following the interior contour of the chamber, supports a thin 2 cm diameter window *H* of gold plated VYNS resin, prepared and calibrated by the method of PATE and YAFFE.[12] The superficial density of the films used for tritium measurements is between 10 and 20 $\mu g/cm^2$, but heavier films may be used for stronger emitters. Four 1/16 in. diameter holes *J* are drilled around the outside of the window to equalize the pressure on either side, and a hole is drilled in the side of the insert to match the evacuation outlet. The surface of the window is 0·055 in. from the lower surface of *K*.

The interior parts of the VTC are made from stainless steel, type 316, except for the brass indenting fingers, and the anode assembly.

Accessory apparatus

Fig. 3 shows a photograph of the accessory apparatus. The three outlets of the VTC are sealed by O-rings on to three 0·5 in. outer diameter pipes, which pass separately through Veeco high vacuum bellows sealed valves, type L50S (*d*, *e* and *f*), to a 1·125 in. outer diameter vacuum manifold *c*. A side inlet *j* allows counting gas to be metered into the counting chamber from a 3 liter storage cylinder (not shown). The pressure in the counting chamber is measured with an Edwards capsule dial gauge *g*, and in the storage cylinder with a compound bourdon type gauge *b*. Vapours are led from a suitable storage vessel (not shown) into the reaction chamber through another side inlet *h*. The pressure in the reaction chamber is measured with a second Edwards capsule

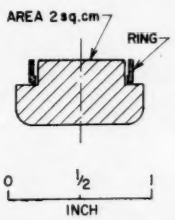

FIG. 4. Aluminium sample holders.

dial gauge *a*, or, at low pressure, with the pirani gauge mounted in the cap (not shown). The copper or brass pipes and fittings are soldered or screwed together.

To evacuate the system a mechanical pump, a two-stage oil diffusion pump and a liquid-air trap are used.

Fig. 4 shows an aluminium sample holder on which experimental samples, e.g. cellulose film, are held in place by a ring.

The counter is connected through a linear preamplifier to a conventional scaler with a resolving time of 15 μsec. A stabilized high voltage supply provides the polarization voltage for the counter.

EXPERIMENTAL PROCEDURE

To illustrate the use of the apparatus, the measurement of the tritium exchange between cellulose and water is described.

Infinitely thick samples were used: the superficial densities of the samples were greater than 1 mg/cm^2, the maximum range of tritium β-particles.[4,10] A film such as regenerated cellulose was mounted on the holder (Fig. 4), which was then passed down through the reaction chamber into the pocket of the rotor, and the cap replaced. The other pocket contained a blank holder. The rotor was then clamped against *K* (Fig. 1), valve *d* (Fig. 3) was closed to isolate the reaction chamber, and the water vapour having a tritium activity of 1·2 μc/mg was expanded into it by opening a valve to a tube containing 0·26 g of activated charcoal, which had been saturated with tritiated water. Exchange now occurred between the cellulose hydroxyl hydrogens and the hydrogens of the water.[1] After reacting for 1 hr, the gaseous and adsorbed water were removed from the reaction chamber by evacuating for 20 hr with all other parts of the VTC isolated from the vacuum line to prevent radioactive contamination. The rotor was then unclamped and the whole apparatus evacuated for a further 5 hr.

The sample was next transferred while under vacuum to the counting position, and again clamped in position. Methane gas (c.p.), previously dried by being passed over activated silica gel at −78°C, was slowly added to an absolute pressure of 9 cm Hg and the radioactive count rate was measured.

The apparatus was now re-evacuated, the blank holder clamped beneath the counting chamber, methane gas added, and the radioactivity measured. The second count rate was used to make a correction for the contamination of the counter, as will be described later.

PERFORMANCE OF APPARATUS

Counter plateau

The counter was operated in the proportional region. A source of benzidine with tritium incorporated by the method of WILZBACH,[13] placed in the position normally occupied by the sample, was used to determine the plateaus of the counter at various discriminator bias potentials. From these were chosen the operating conditions of a polarization voltage of 1·4 kV and a discriminator bias of 5V. At these conditions the plateau (Fig. 5) had a slope of 2·3 per cent per 100 V for 400 V, and the count rate varied linearly with the discriminator bias at a rate of 0·42 per cent per volt.

Absorption of radiation

The number of tritium β-particles which enter the counter depends upon the mass of gas per unit area through which they pass, and the superficial density of the window. For reproducible results these quantities must be constant, or corrections applied.

The mass of gas per unit area was kept constant by fixing (a) the distance between the sample and the window and (b) the methane pressure. Table 1 shows the operating values and tolerances with the corresponding experimental reproducibilities.

The superficial densities of the gold-plated plastic films used as windows have

VOL. 7 1959/6

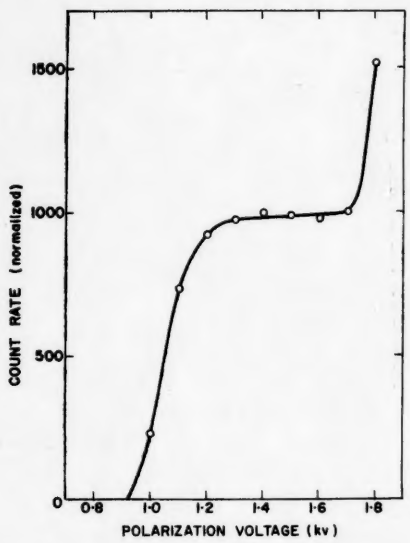

FIG. 5. Counter plateau curve at a discriminator bias of 5V.

been related experimentally to the observed count rates. All observed count rates were corrected to an arbitrary film density of 15 μg/cm^2 by using the factor given by the empirical equation:

$$W = -0{\cdot}0154\sigma + 1{\cdot}231$$

where σ is the superficial density of the film (μg/cm^2) and W is a factor such that

$$\text{(Observed count rate)} = W \times \text{(count rate for } \sigma = 15\text{)}$$

This equation fits the experimental data between 10 and 20 μg/cm^2 to within 0·4 per cent.

All these absorption effects will, of course, be less for stronger β-emitters.

TABLE 1. Effect of sample position and methane pressure on the count rate

Quantity	Operating value	Tolerance	Reproducibility of count rate (%)
Distance between sample and window	2·4 mm	±0·1 mm	±2·5
Methane gas pressure	9·0 cm	±0·05 cm	±0·2

Leakage of apparatus

The ability of the apparatus to hold a vacuum was most important, particularly in the reaction chamber, which must be isolated for the duration of the reaction. The reaction chamber after evacuation and isolation leaked at the rate of 0·08 μ Hg/min; the rest of the apparatus could be maintained at 0·5 μ with continuous pumping.

It was found that the rubber O-rings contained at least 8 per cent by weight of volatile material. In normal O-ring applications this is probably of minor importance since the cross section of rubber which is exposed to the vacuum is small. However, in the case of the two O-rings M in the rotor of the VTC a large surface area of rubber was exposed at some stages. Therefore, to hasten the initial degassing of the VTC, all O-rings were separately pre-evacuated while heating.

Contamination of counter

To prevent excessive radioactive contamination of the counter, it was found necessary (a) to replace the O-rings in the face of the rotor after each experiment and (b) after the reaction, to evacuate the reaction chamber for 20 hr, and then to separate the rotor from K (Fig. 1) and evacuate the entire VTC for 5 hr.

A correction was applied for the contamination which remained after this evacuation by assuming that the count rate resulting from contamination in the presence of the treated cellulose sample was the same as that from a similarly treated blank sample holder. This correction was not always constant, but as it was related to the count rate of a second, untreated holder always included in the VTC, this was used as a reference for applying the correction. The relation between the count rates of the untreated and treated blank holders was determined as follows: Two blank sample

holders were put into the pockets of the rotor. One of these was treated with active water vapour as if it were a sample; the other was not treated. At the completion of the reaction and the subsequent evacuation, the count rate of the treated holder was measured. The apparatus was evacuated again, then the untreated sample holder was moved to the counting position and counted. Fig. 6 shows the relationship found between the two count rates. For the cellulose samples used,[1] the contamination count was determined from Fig. 6 by setting the value for the blank, untreated holder on the abscissa and using the linear graph to read the corresponding value from the ordinate. This value was subtracted from the count rate of the cellulose sample. The correction was normally between 10 and 20 per cent of the sample count.

The correction curve would, of course, have to be redetermined for any other radioactive gas used.

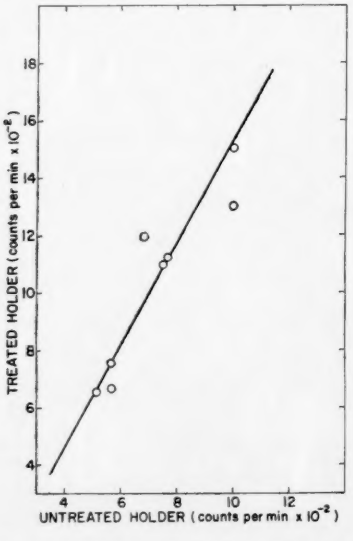

FIG. 6. Correction curve for contamination of counter.

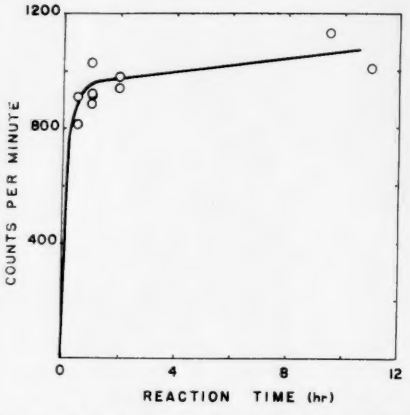

FIG. 7. Variation of count rate with time of reaction of cellulose film with tritiated water.

Reaction time

Samples of regenerated cellulose film were exchanged with tritiated water in the VTC at 95 per cent relative humidity and 25°C for 0·5, 1·2, 9·5 and 11 hr, and then counted. Fig. 7 shows that at first the count rate increased rapidly with time, but after 1 hr it rose by only 1 per cent/hr. One-hour reactions were therefore used since this ensured adequate replication of conditions. The slow increase (1 per cent/hr) in the extent of the reaction after 1 hr was not reported elsewhere,[11,14] and was probably caused by the time necessary for diffusion in the VTC to re-establish isotopic equilibrium throughout the water in the various parts of the apparatus after the exchange decreased the activity in the vicinity of the sample.

Reproducibility

Similar samples of cellulose film were reacted with tritiated water vapour in the VTC for 1 hr and counted. The results were 9200, 10300, 8900 and 9200 counts per min with a mean value of 9400 $\pm$ 7 per cent. Stronger emitters would yield better reproducibility.

DISCUSSION

The procedure described gave relative values of the radioactivity in the samples. If necessary these values may be made absolute by calibration of the VTC with a sample of known activity.

The VTC had excellent counting

characteristics with none of the irregularities previously found in the direct counting of solid tritium-labelled samples,[6] and could be operated under high vacuum conditions. The reproducibility with cellulose film was very good when the inherent difficulties of directly counting tritium in solids are considered, and using such a notorious radioactive contaminant as tritiated water. These advantages of the VTC could probably be used more generally to study other systems.

Acknowledgements—The authors are indebted to J. A. LAPOINTE, C. K. T. WEBB and Dr. L. YAFFE for valuable advice and assistance in the design and construction of the counter. This work was supported by the award of a Frank J. Sensenbrenner Fellowship and National Research Council of Canada Studentships.

REFERENCES

1. LANG A. R. G. and MASON S. G., forthcoming publication.
2. BEISCHER D. E. *Nucleonics* **11** (12), 24 (1953).
3. CALKINS G. D., POBERESKIN M., YOUNG V. E. and NOWACKIZ L. J. *Nucleonics* **13** (2), 76 (1955).
4. EIDINOFF M. L. and KNOLL J. E. *Science* **112,** 250 (1950).
5. GRAY I., IKEDA S., BENSON A. A. and KRITCHEVSKY D., *Rev. Sci. Instrum.* **21,** 1022 (1950).
6. JACKSON F. L. and LAMPE H. W. *Analyt. Chem.* **28,** 1735 (1956).
7. JENKINS W. A. and YOST D. M. *J. Chem. Phys.* **20,** 538 (1952).
8. JENKINS W. A. *Analyt. Chem.* **25,** 1477 (1953).
9. RYDBERG J. *Acta Chem. Scand.* **12,** 399 (1958).
10. LIBBY W. F. *Analyt. Chem.* **19,** 2 (1947).
11. ALMIN K. E. *Svensk Papp-Tidn.* **55,** 767 (1952).
12. PATE B. D. and YAFFE L. *Canad. J. Chem.* **33,** 15 (1955).
13. WILZBACH K. E. *J. Amer. Chem. Soc.* **79,** 1013 (1957).
14. MANN J. and MARRINAN H. J. *Trans. Faraday Soc.* **52,** 481 (1956).

OL.
7
9/60

technical notes

The Use of Irradiated Extraction Replicas to Identify Inclusions and Precipitates in Metals: A Preliminary Note

(*Received* 10 *September* 1959; *in revised form* 18 *September* 1959)

THE identification of the material present in precipitates and inclusions in metals is an extremely difficult problem. Radioisotopes have often been used to help to identify specific components. Frequently a particular component is made radioactive and is then added to the melt. A specimen is cast and prepared for metallographic examination. Autoradiographs taken at this stage are then compared with micrographs.[1] In favourable circumstances it is possible to eliminate the addition of activity to the melt and to irradiate only the small sample prepared for metallography.[1]

Both these techniques involve handling up to 1 mc of active material and more frequently, where the second method is not possible, active material has to be used in furnaces and put through rollers where contamination is undesirable. Also if autoradiographs with good resolution are to be attained with penetrating radiation it is essential that thin sections should be prepared and their direct grinding is laborious.

This note describes the application of the extraction replica technique,[2,3] as used in the preparation of electron microscope replicas, to the identification of inclusions and precipitates. The specimen is first prepared for metallographic examination in the usual way and micrographs are taken. The specimen is then etched with an etchant which is suitable for the specimen in use, that is one which will attack the edges of the inclusions or precipitates and leave them relatively loose.[4] A solution of formvar in chloroform is spread over the surface of the specimen and when this has dried a further strengthening layer of about 1×10^{-3} in. of collodion in acetone is applied. After these layers have dried the part of the film to be removed is marked out with a sharp razor blade. One corner is gently raised with the razor blade and the replica is peeled off with forceps. At this stage, the replica is inspected under a microscope and compared with the original specimen and micrograph.

The replicas are then irradiated with neutrons in a reactor. Irradiation of formvar–collodion replicas is limited to $<3{\cdot}4 \times 10^{17}$ n/cm^2 as they become brittle at higher levels of irradiation.

The irradiated extraction replica is mounted by placing it on a drop of collodion in acetone on a clean subbed glass slide.[5] The size of the drop is chosen to ensure that a thin protective layer of collodion is spread over the replica besides the thicker layer beneath which attaches it to the slide. When the replica and mount are quite dry they are covered with autoradiographic stripping film, mounted with the emulsion in contact with the thin collodion layer now covering the replica. After exposure in a dry atmosphere, as a further precaution against chemical attack of the stripping film by the replica, the autoradiograph is developed and fixed. The autoradiograph and replica remain in contact and can now be viewed under the microscope with transmitted light; a considerable advantage as compared with the difficult procedure of viewing an opaque specimen through the autoradiograph with reflected light.

Other replicas taken from the same specimen and irradiated for the same time can be studied to find the γ-spectrum, decay constants and β-absorption coefficients of the radiations. These techniques should also be applied to control replicas to make sure that impurities in the collodion and formvar do not contribute to the results. With these data it should be possible to identify the radioisotopes causing the blackening at particular places on the replica. It should also be possible to identify more than one kind of radioactive inclusion or precipitate by using several different radiation and decay times before the autoradiographs are taken.

Fig. 1 shows a replica of a stainless steel specimen with the autoradiograph attached. The autoradiograph was produced by Mn^{56} radiation. The specimen was etched in 10% nital for 1 min and the replica was irradiated for 12 hr in a neutron flux of 10^{12} n/cm^2/sec (total $4{\cdot}3 \times 10^{16}$ n/cm^2). Fig. 2 shows a replica taken from the surface of uranium

VOL. 7 1959/6

OL.
7
9/60

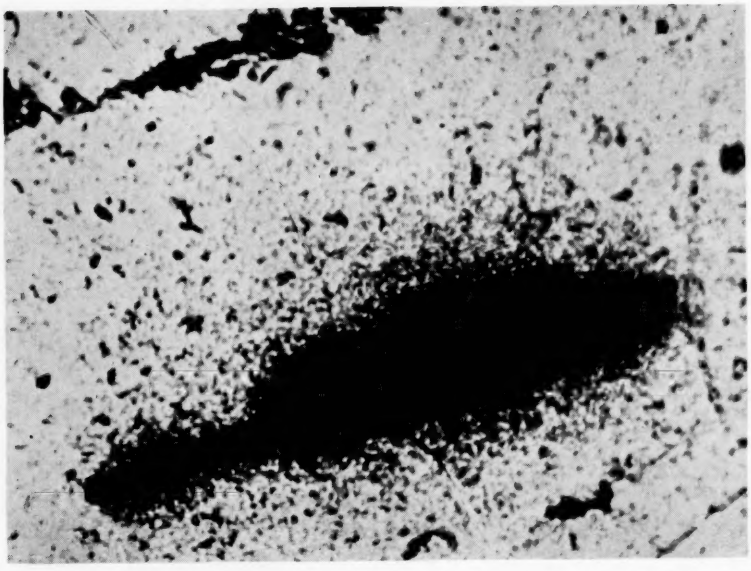

FIG. 1. Replica and autoradiograph of Mn^{56} in an inclusion in steel ($\times 660$).

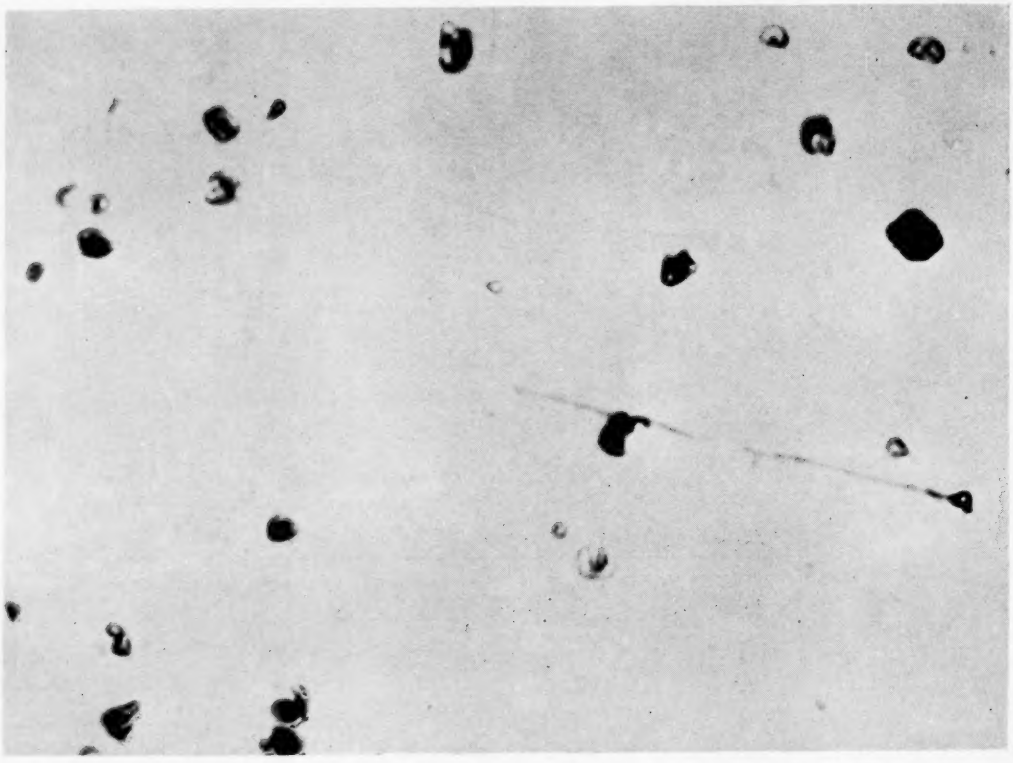

FIG. 2. Replica and autoradiograph of an α-track from an inclusion in uranium (×2660).

VOL.
7
1959/

etched for 2 min in 50% HNO_3. The autoradiograph attached to the replica (which was not irradiated in this case) shows an α-track coming from one of the extracted inclusions. An exposure of 5 days was used. The preliminary work reported in this Technical Note will be described in detail in a later publication.

S. M. MAKIN

Isotope Research Division
Atomic Energy Research Establishment
Harwell

OL.
7
59/60

References

1. KOHN A. *Proceedings 2nd Radioisotope Conference Oxford, July* 1954. Vol. 2, p. 68.
2. BOOKER G. R. and NORBURY J. *Brit. J. Appl. Phys.* **8,** 109 (1957).
3. BOOKER G. R. and NORBURY J. *Brit. J. Appl. Phys.* **9,** 361 (1958).
4. GREAVES R. H. and WRIGHTON H. *Practical Metallography*. Chapman and Hall, London (1957)
5. BERRIMAN R. W., HERTZ R. H. and STEVENS G. W. W. *Brit. J. Radiol.* **23,** 472 (1950).

Tracing of Water Flow by Means of Radioactive Isotopes and Scintillation Counters

(*Received* 4 *September* 1959)

In connection with the paper on "Tracing of water flow by means of radioactive isotopes and scintillation counters" by Ljunggren *et al.*,[1] I would like to comment on some advantages of using Geiger counters in such work that are generally overlooked.

When someone says "high-sensitivity counter," most people immediately respond "scintillation counter, naturally," even as our Swedish friends have done. But the twenty- to fifty-fold higher sensitivity of scintillation counters usually cited is on the basis of unit volume. This may be valid for comparing a 1-in. scintillation crystal with a 1-in. end-window counter. But when the amount of sample is unlimited, as in the present case, a much larger (but less expensive) Geiger tube can be and should be used. Further, several identical Geiger tubes can be wired together in parallel to the same voltage source and amplifier.

We have used this type of detector for measuring radioactivity in rivers to determine their flow rates by the total-count method.[2,3] We find that a bundle of four 1- by 12-in. counter tubes is as sensitive, when immersed in a large volume of solution of 1-MeV γ-emitting isotope, as the scintillation counter described by Dr. Ljunggren and his colleagues. The bundle is but little larger than their probe, and it operates at the end of a 100-ft cable without a preamplifier.

The resolution of Geiger tubes is also enhanced by the parallel arrangement. While one tube is discharged, the others remain sensitive, so that the effective dead time is reduced from 200 to 50 μsec. This allows counting rates up to 2000 counts/sec without making a correction greater than 10 per cent. This is still much inferior to the speed of scintillation counters, which are preferable whenever very fast counting rates are encountered.

A valuable advantage of Geiger counters over scintillation counters is their quantitative equivalence. One tube may be replaced by another in a fixed-voltage circuit without changing the sensitivity more than 1 per cent. A similar exchange of scintillation probes might change the counting rate 20 per cent to 50 per cent, or even more, depending upon the spectrum of γ-radiation measured. Careful adjustment of the voltage would reduce this, but it could hardly be hoped to equal the reproducibility of Geiger tubes inherent in their flat plateau region.

Table 1

	Scintillation counter	Geiger counter
Sensitivity $\left(\frac{\text{counts/min}}{\mu c/m^3}\right)$	450	400
Background (counts/sec)	0·8	2·7
Maximum dilution (m^3/c)	15×10^6	20×10^6
Maximum counting rate (counts/sec)	100,000	2000
Maximum temperature (°C)	35	100
Dimensions (in.)	2×11	$2\frac{3}{4} \times 20$
Interchangeability (%)	± 20	± 1
Cost ($)	700	600

Some of the factors that influence the choice of one counter or the other are compared quantitatively in Table 1. Another natural advantage of Geiger tubes is their operability at higher ambient temperatures. The probe and ratemeter used by Dr. Ljunggren is only slightly more costly than our tube bundle with a battery-operated scaler. A scaler for the scintillation counter would cost considerably more. The maximum dilution detectable with our counter is based on twice the standard deviation of 1-min counts at background.

The conclusion I would like to press is that, although scintillation counters excel in some features and Geiger tubes in others, they do not differ greatly in sensitivity with large samples. The belief that scintillation counters are always preferable to Geiger counters for high sensitivity applications is a myth which should be dispelled.

D. E. Hull

California Research Corporation
Richmond Laboratory
576 *Standard Avenue*
Richmond, California

References

1. Ljunggren K., Erwall L.-G., Rennerfelt J. and Westermark T. *Int. J. Appl. Rad. Isotopes* **5,** 204 (1959).
2. Hull D. E. *Int. J. Appl. Rad. Isotopes* **4,** 1 (1958).
3. Hull D. E. and Macomber M. *Proceedings of the Second International Conference on the Peaceful Uses of Atomic Energy Geneva*, 1958. Vol. 19, p. 324. United Nations, New York (1958).

VOL. 7 1959/

International Journal of Applied Radiation and Isotopes, 1960, Vol. 7, pp. 261–272. Pergamon Press Ltd. Printed in Northern Ireland

Biological Fractionation of Isotopes

H. J. M. BOWEN
Isotope Research Division, Wantage Radiation Laboratory,
Grove, Berks, England

(*Received* 4 *August*; *in revised form* 29 *August* 1959)

The fractionation of isotopes occurs in numerous biological processes, but the effects are always small except in a few cases involving hydrogen and deuterium. Fractionations may be caused by differences in rates of reaction or diffusion, or by differences in equilibrium constants. Very little systematic research has been published on this subject, but all the observed data agree with the hypothesis that light isotopes travel more quickly than heavy ones through metabolic pathways. There is a marked need for experiments in which the isotopic abundances in the growth medium, dissected organism and its excreta are recorded.

Among the more interesting observations which have received special attention are the lethal effect of deuterium on most organisms, the use of C^{12}/C^{13} ratios in inferring the biogenic origin of carbon in ancient rocks, O^{18}/O^{16} ratios for determining the temperature of prehistoric seas and S^{32}/S^{34} ratios for deciding the date of evolution of sulphur bacteria.

LE FRACTIONNEMENT BIOLOGIQUE DES ISOTOPES

Le fractionnement des isotopes prend lieu en bien des procédés biologiques, mais les effets en sont toujours petits sauf en quelques cas entraînant l'hydrogène et le deutérium.

Les fractionnements peuvent être à cause des différences dans les taux de réaction ou de diffusion, ou des différences dans les constantes d'équilibre. Sur ce sujet très peu de recherche systématique a paru, mais toutes les données observées accordent avec l'hypothèse que les isotopes légers parcourent les voies métaboliques plus rapidement que les isotopes lourds. Il y a un besoin particulier d'expériences dans lesquelles sont constatées les abondances isotopiques dans le moyen de croissement, dans l'organisme disséqué et dans ses excréments.

Parmi les observations plutôt intéressantes qui ont reçu une attention particulière se trouvent l'effet funeste du deutérium sur la plupart des organismes, l'emploi des rapports C^{12}/C^{13} pour déduire l'origine biogénique du carbone dans les anciens rochers, des rapports O^{18}/O^{16} pour caractériser la température des mers préhistoriques et des rapports S^{32}/S^{34} pour constater l'époque d'évolution des bactéries au soufre.

БИОЛОГИЧЕСКОЕ РАЗДЕЛЕНИЕ ИЗОТОПОВ

Разделение изотопов происходит в большом числе биологических процессов, но эффекты всегда малы, за исключением нескольких случаев, когда разделяются водород и дейтерий. Разделение изотопов может быть обусловлено различием как в скоростях реакции или диффузии, так и в константах равновесия. По этому вопросу опубликовано очень мало систематических исследований, но все полученные результаты согласуются с предположением о том, что легкие изотопы быстрее перемещаются путем обмена веществ, чем тяжелые. Представляет интерес проведение опытов в которых регистрируется изотопный состав как окружающей среды, в которой происходит рост организма, так и самого организма и его выделений. Среди наиболее интересных наблюдений, которые можно считать достоверными, особенно привлекают внимание: летальное действие дейтерия на большинство организмов, использование отношения концентраций C^{12}/C^{13} для доказательства биогенного происхождения углерода в древних горных породах, отношения концентраций O^{18}/O^{16} для определения температуры доисторических морей и отношения концентраций S^{32}/S^{37} для установления времени эволюционного развития серобактерий.

OL.
7
9/60

1

BIOLOGISCHE ISOTOPENTRENNUNG

Isotopentrennung tritt bei zahlreichen biologischen Prozessen auf, jedoch sind diese Effekte fast immer sehr klein, ausgenommen einige wenige Fälle, bei denen es sich um Wasserstoff und Deuterium handelt. Trennungen können durch Unterschiede der Reaktionsgeschwindigkeit oder durch Diffusion entstehen oder durch Unterschiede der Gleichgewichtskonstanten. Nur wenige systematische Untersuchungen wurden auf diesem Gebiet veröffentlicht, aber alle Beobachtungen stimmen mit der Hypothese überein, dass die leichteren Isotope sich schneller auf den Stoffwechselbahnen fortbewegen als die schweren. Ein ausgesprochener Mangel an experimentellen Untersuchungen herrscht bezüglich der Isotopenhäufigkeit im wachsenden Medium, in den einzelnen Teilen des Organismus und in seinen Ausscheidungen.

Von den interessantesten Beobachtungen auf dem Gebiet, welche spezielle Beachtung gefunden haben seien folgende erwähnt: Die tödl. Wirkung von Deuterium auf die meisten Organismen, die Verwendung des C^{12}/C^{13} Verhältnisses für den Beweis des biogenetischen Ursprunges von Kohlenstoff in alten Gesteinen, das O^{18}/O^{16} Verhältnis zur Bestimmung der Temperatur in prähistorischen Meeren und das S^{32}/S^{34} Verhältnis zur Datierung der Entwicklung von Schwefelbakterien.

INTRODUCTION

THE majority of elements possess more than one stable isotope, but in biochemical work it is generally assumed that all the isotopes of a given element behave in a similar fashion. In some cases, however, there are small differences in their behaviour which can lead to partial fractionation and are of general interest. Research on these fractionation effects has been largely academic and our present state of knowledge is far from complete. It is, however, important that all biologists using radioactive tracers should know how accurately that tracer represents the behaviour of the natural element. In addition, suggestions have recently been made that biological fractionation of isotopes might be a useful preliminary to other methods of separation on an industrial scale. A critical review of this field is therefore needed, since other reviews are now incomplete.[1–3]

VOL. 7 1959/

THEORY

All separation processes depend on mass differences, as a lighter isotope has less inertia than a heavy one, but the functional dependence on mass is often complicated. Only two such processes contributing to fractionation will be considered here, chemical reaction and diffusion.

The rate constant of a chemical reaction involving the transfer of a single atom is a complex function of temperature which is inversely proportional to the square root of the effective mass of the atom transferred[4]; hence the ratio of rate constants for two isotopes of masses m_1 and m_2 is given by

$$\frac{k_1}{k_2} = \left(\frac{m_2}{m_1}\right)^{1/2} F(T)$$

where $F(T)$ is a ratio of partition functions which is theoretically calculable from spectroscopic data. UREY and GRIEFF[5] were the first to work out actual values of $F(T)$ for simple gaseous reactions, and hence to calculate equilibrium constants. They showed that the fractionation of isotopes in chemical reactions should be most efficient at low temperatures, and this has been confirmed by experimental work described below. It should be noted that the fractionation of isotopes at equilibrium is not predicted by classical physics, though it is by quantum mechanics.[6,7] Further information on rate constants for isotopic reactions may be obtained from BIGELEISEN[8,9] and on equilibrium constants from UREY.[10]

A detailed exposition of the factors affecting isotopic separation by diffusion has been given by SENFTLE and BRACKEN.[11]

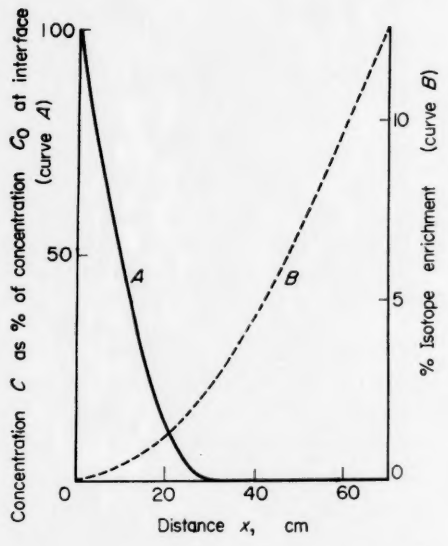

FIG. 1. Concentration and isotope enrichment as a function of distance x from interface: from SENFTLE and BRACKEN[11].
Assumptions: k 0·0154, m_1 103, m_2 105, t 120 days.

These workers were concerned only with isotope fractionation in geological processes, but their results are applicable to any system involving diffusion from one phase into another. If we consider diffusion from a liquid into a solid phase, the concentration C at a distance x inside the solid is given by

$$C = C_0\left(1 - \operatorname{erf} kx\sqrt{\left(\frac{m}{t}\right)}\right)$$

where C_0 is the concentration at the interface,
k is a constant for any pair of phases,
m is the mass of the diffusing species,
t is the time.

From this expression we can calculate the percentage isotope enrichment as a function of distance inside the solid, which is

$$100(C_1C_{2,0}/C_{1,0}C_2 - 1)$$

for two isotopes 1 and 2. The graphs of these two functions of x are shown in Fig. 1.

Near the interface very little fractionation takes place, but the farther inside the element penetrates, the greater is the enrichment in the lighter isotope. Hence, while it is theoretically possible to obtain big enrichments by diffusion processes, in practice the amount of highly enriched material is vanishingly small. Some compromise must be accepted for practical separations involving lower enrichment factors but larger amounts of material. In chromatography, for example, the initial fraction of eluate should be enriched while the final fraction should be depleted in the lighter isotope. The fractions in which isotopic separation can be experimentally demonstrated are extremely small, and the bulk of the material has a normal isotopic composition.

Table 1 lists the square roots of the ratios of the masses of the heaviest to the lightest stable isotope for a number of elements of biological interest.

This table shows the unique position occupied by the isotopes of hydrogen with respect to fractionation processes. The square roots of the masses of protium and deuterium differ by 41 per cent while all other differences recorded are under 10 per cent and are generally much less. This is the order of magnitude of almost all experimentally determined fractionation factors for elements other than hydrogen.

Heavy elements are not necessarily less liable to isotopic fractionation than light ones.

TABLE 1. $\sqrt{(m_2/m_1)}$ for isotopes of biological interest

Element	m_1	m_2	$\sqrt{(m_2/m_1)}$
H	1	2	1·4142
Li	6	7	1·0801
B	10	11	1·0488
C	12	13	1·0409
N	14	15	1·0351
O	16	18	1·0606
Mg	24	26	1·0409
S	32	34	1·0308
Cl	35	37	1·0281
K	39	41	1·0254
Ca	40	48	1·0954
V	50	51	1·0100
Fe	54	58	1·0364
Cu	63	65	1·0158
Zn	64	79	1·0459
Mo	92	100	1·0426
U	234	238	1·0085

This is because many heavy elements have more stable isotopes than do light ones, so that the relative differences in mass between the heaviest and lightest may be surprisingly large. For example $\sqrt{(m_2/m_1)}$ for the isotopes of molybdenum Mo^{92} and Mo^{100} is larger than that quoted for carbon or nitrogen in the table.

TECHNIQUES

The measurement of isotopic abundance has recently been reviewed in a monograph.[12] The only satisfactory method applicable to every element is mass spectrometry.[13,14] For hydrogen and some light elements it is possible to use thermal conductivity or density determinations,[12] spectrometry[15,16] and certain nuclear reactions for isotopic analysis.[17,18] Mass spectrometry is certainly the most accurate method for determining isotope ratios; the precision attainable depends to some extent on the natural abundance of the rarer isotope, but is in the region of 0·1 per cent in the figure quoted for the ratio. Early measurements have lower precision.

ISOTOPE FRACTIONATION BY SINGLE CELLS

If a simple cell is suspended in an aqueous medium, both organic and inorganic substances are taken up and metabolized within the cell, and other products are excreted. The mechanism of uptake is little understood but in the case of ions it takes place against a big concentration gradient and is quite likely to involve organic chelating agents which carry the ions across the cell membrane into the cytoplasm.[19,20] From theoretical considerations developed above the lighter isotope would be expected to move into a cell faster than a heavy one, and to move out faster in excretory processes. The best conditions for fractionation require a small percentage uptake (or a short time of uptake) from the medium, a small percentage excretion (if the element concerned is excreted), or a series of chemical changes during metabolism in which the rate determining process has a large fractionation factor. Enough is known to say that these conditions often occur in simple cells and are still more frequent in multicellular organisms. Fractionation would not be expected when there is a large percentage uptake or excretion, or in cyclical processes where enriched material is constantly fed back into the main metabolic stream.

Hydrogen

Isotopic fractionation of hydrogen has been demonstrated in two unicellular organisms. Cloud *et al.*[21] reported a marine bacterium capable of producing hydrogen gas from a saline glucose medium, and that this hydrogen was depleted in deuterium by a factor of 20 over the medium. Augood[22] showed that when *Chlorella* was grown intensively in culture solutions, the alga preferentially absorbed light water leaving the mother liquor enriched in deuterium. Both workers suggested the possibility of adapting their discoveries for the large scale production of water enriched in deuterium oxide.

The two to one ratio in mass between hydrogen and deuterium can lead to some remarkable isotope effects on the rates of enzymic reactions and hence on water uptake and living processes generally. Thorn[23] has shown that succinic oxidase oxidizes succinic acid at a rate which depends on the number of deuterium atoms substituted at the methylene groups. Tetradeuterated succinic acid is oxidized at only 40 per cent of the rate of the unsubstituted material. The alga *Chlorella pyrenoidosa* takes up D_2O and T_2O respectively, 50 per cent and 45 per cent as rapidly as H_2O.[24,25] In this organism deuterium is found to enter into fats faster than into proteins or carbohydrates. With such large retarding factors as these, it is scarcely surprising that *Chlorella* grows much more slowly or even dies in water enriched in deuterium oxide.[26,30] Horwitz[31] suggests that this is caused by the inhibition of one of the dark reactions of photosynthesis.

VOL. 7 1959/6

TAYLOR and HARVEY[32] found a similar retardation in the rate of respiration of yeast cells grown in high concentration of D_2O. It appears that concentrations of D_2O exceeding 30 per cent kill the alga, unless it is allowed an adaptation period with gradually increasing amounts of heavy water, in which case adapted cultures tolerant of up to 98 per cent D_2O can arise. Thirty per cent D_2O has also been shown to be toxic to cereal seedlings[33–35,101] and to cause sterility in male mice.[36] The interesting observation that D_2O causes an increase in cell size in *Chlorella*[25] has recently been confirmed for mammalian cells.[37] Cell division is presumably retarded more by the isotope effect than is cell expansion.

Lithium

BOWEN[38] grew *Saccharomyces cerevisiae* in media containing lithium citrate and glucose. Lithium was found to enter the cell and largely replace potassium, but lithium rich cells incubated in media containing potassium rapidly lost their lithium again. After short periods of uptake the Li^6/Li^7 ratio inside the yeast was increased about 2 per cent above that of the medium, but it dropped to normal when the yeast became saturated with lithium. If potassium salts were then added, the ratio inside the yeast dropped below the value for the medium, showing that Li^6 enters and leaves cells faster than does Li^7.

Carbon

UREY[39] quotes a 3 per cent discrimination against C^{13} by algae. This order of result was also obtained by BUCHANAN *et al.*,[40] who made a detailed survey of carbon isotope ratios during the growth of *Scenedesmus obliquus* in sealed containers containing radioactive $C^{14}O_2$. They found a 4·33 per cent discrimination against C^{13} and a 10·35 per cent discrimination against C^{14}.

Comparable figures for discrimination against C^{13} have been found for *Chlorella pyrenoidosa* by WEIGL[41] and by VAN NORMAN and BROWN,[42] but these authors found much greater discrimination against C^{14} (24 per cent and 15 per cent respectively). The enzyme urease has been shown to hydrolyse C^{12}-urea 10 per cent faster than C^{14}-urea at 37°C.[43] Theoretically the discrimination against C^{14} should be twice that against C^{13}[8,9] but a larger difference is always found experimentally, even in chemical work,[44] which has not yet been explained.

Oxygen

The enrichment of O^{16} during bacterial respiration was first shown by DOLE *et al.*,[45] and has since been confirmed by LANE and DOLE.[46] The fractionation reported varied from 0·8 per cent to 2·9 per cent for different organisms. It has been suggested that fractionation occurs largely through the activity of metallo-enzymes since fractionation factors of about 1 per cent have been found for cytochrome oxidase and tyrosinase.[47] Marine phytoplankton do not fractionate oxygen in photosynthesis[107] but the carbonates secreted by certain marine algae are enriched in O^{16}.[106]

Sulphur

In a series of papers, THODE and co-workers[48–53] have summarized much data on the natural fractionation of sulphur isotopes. The bacterium *Desulphovibrio desulfuricans* is capable of reducing sulphate

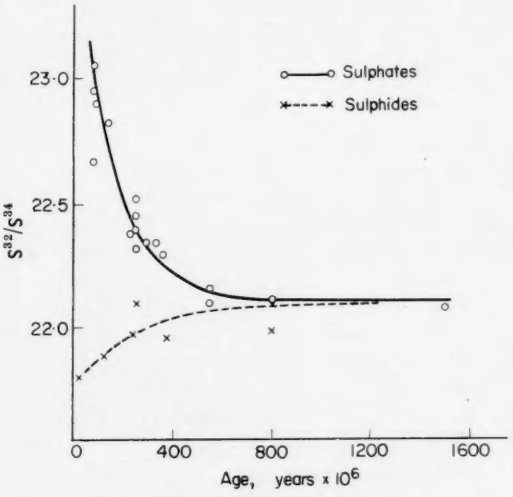

FIG. 2. S^{32}/S^{34} ratios in sulphides (—o—) and sulphates (—x—) as a function of age: from THODE *et al*[51].

to sulphide and the sulphide produced is enriched in S^{32} from 0 to 2·5 per cent. Extensive studies have shown that fractionation is more efficient at low temperatures,[50,53] at high sulphate concentrations and low rates of reaction[53,54] as predicted by theory. At low rates of reaction the rate controlling step is the primary reduction to sulphite leading to marked enrichment in S^{32}, but at high rates the uptake of sulphate ions through the cell wall appears to determine the rate and this has a low fractionation factor.[53] The bacterium *Thiobacillus thiooxidans* which oxidizes elemental sulphur to sulphate has not been proved to fractionate the isotopes.[54]

THODE *et al.*[51] have drawn attention to the S^{32}/S^{34} ratios in sedimentary sulphides and sulphates of different geological ages: their data are shown in Fig. 2.

Samples over 800 million years old have all about the same S^{32}/S^{34} ratio, but from that date S^{32} has become increasingly enriched in sulphides and correspondingly depleted in sulphates. These results suggest that sulphur bacteria evolved about 800 million years ago and have been increasingly responsible for catalysing the reaction:

$$HS^{32}O_4^- + HS^{34-} = HS^{34}O_4^- + HS^{32-}$$

However, AULT[97] claims that further determinations of S^{32}/S^{34} ratios do not confirm THODE's contention, and that sulphur bacteria have probably been active for at least 2000 million years.[104]

ISOTOPE FRACTIONATION BY HIGHER PLANTS

The three major metabolic changes occurring in higher plants are photosynthesis, respiration and translocation. Photosynthesis involves the uptake of atmospheric CO_2 by the leaves with the concomitant release of oxygen, while respiration has the opposite over-all effect. Translocation implies the uptake of water and salts by the roots and their dispersal throughout the plant: the water is subsequently lost by transpiration through the leaves and the salts remain behind. All three processes could thoeretically lead to isotope fractionation.

Photosynthesis

In photosynthesis we would expect the carbon dioxide taken up to be somewhat enriched in C^{12}, while the oxygen given out should be depleted in O^{18}. Both these expectations have apparently been confirmed by direct experiment. Leaves of barley (*Hordeum vulgare*) take up $C^{13}O_2$ at about 96 per cent of the rate they take up $C^{12}O_2$[42] and discriminate still more strongly against $C^{14}O_2$.[42,55,56] The pondweed *Elodea canadensis* gives off photosynthetic oxygen which has a density 8·1 p.p.m. lower than the bicarbonate oxygen which it uses for growth according to VINOGRADOV and TEIS.[57] On the other hand DOLE and JENKS[58] using *Chlorella*, *Helianthus* and *Coleus* found this density to be 1·2 p.p.m. higher in their experiments. Further work has revealed some underlying complications to this simple picture.

A number of workers have investigated the C^{12}/C^{13} ratio in plant tissues.[40,59–63] The results have been reviewed[64,65] and agree remarkably well, though some of WICKMAN's theoretical conclusions[62] have been justly criticized.[64] Terrestrial plants are enriched in C^{12} by about 1·8 per cent compared with atmospheric CO_2, though there is some evidence that the figure is lower for gymnosperms than for angiosperms. Aquatic plants are generally less strongly enriched, and this is particularly marked for the marine plants analysed, which were mostly multicellular algae: they are enriched in C^{12} by only 0·5 per cent. It appears that marine plants and many terrestrial aquatics obtain their carbon from dissolved bicarbonate rather than atmospheric carbon dioxide, and the former is known to be relatively poor in C^{12}. SILVERMAN and EPSTEIN[98] claim that marine sediments can be distinguished from other sediments by their lower C^{12}/C^{13} ratio. It would be useful to measure C^{12}/C^{13} ratios in different chemical fractions of plant

VOL. 7 1959/

extracts, but this does not appear to have been done. RANKAMA[65,66] has suggested that carbon in ancient sedimentary or metamorphic rocks can be classified as biogenic or not depending on its C^{12}/C^{13} ratio, and has used this criterion to support the identification of the pre-Cambrian fossil *Corycium enigmaticum*. On this basis petroleum, natural methane and certain graphites are biogenic, whereas other graphites and diamonds are not. It will be shown later on that limestones and biogenic carbonates are exceptions, as they are depleted in C^{12}.

The isotopic composition of atmospheric oxygen has still not been adequately explained.[67–9] This oxygen is unaccountably enriched in O^{18} (it has a density 6·6 p.p.m. higher than oxygen from fresh water) and one possible contributory reason for this is advanced below: an explanation not involving biological processes has been suggested by ROAKE and DOLE.[70] These authors point out that in the equilibrium between gaseous carbon dioxide and liquid water the CO_2 is preferentially labelled with O^{18}. If this CO_2 were then broken down by ultra-violet light in the stratosphere it might exchange oxygen atoms with molecular oxygen, as noted in electric discharges. It is generally accepted that atmospheric oxygen has been and is being produced by green plants, and further observations have shown that photosynthetic oxygen comes entirely from plant water and not from atmospheric carbon dioxide.[71–73]

Hence the work VINOGRADOV and TEIS[57] and DOLE and JENKS[58] described above does not give a complete analysis of the situation. KAMEN and BARKER,[72] DOLE[74] and EPSTEIN[99] have summarized our present state of knowledge of this point.

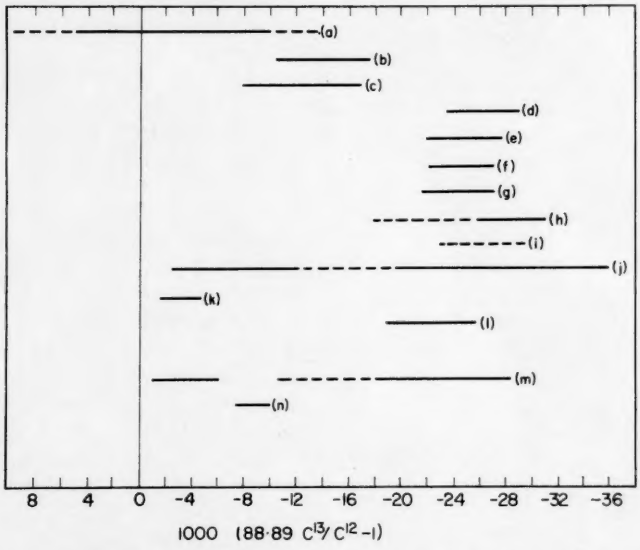

FIG. 3. Differences in C^{13} content from an arbitrary standard: from CRAIG[63].
(a) Limestones. (b) Marine invertebrates. (c) Marine plants. (d) Land plants. (e) Recent wood. (f) Fossil wood. (g) Coal. (h) Sediments. (i) Petroleum. (j) Graphites. (k) Diamonds. (l) Igneous rocks. (m) Natural CO_2: Natural CH_4 from Yellowstone Park, U. S. A. (n) Atmospheric CO_2.

Respiration

Recent work tends to confirm that there is little or no fractionation of oxygen isotopes in photosynthesis.[105,107] Isotope effects in respiration have scarcely been investigated, though BAERTSCHI[75] found no fractionation in the respired carbon dioxide from bean seeds sprouted in the dark. RAKESTRAW *et al.*[76] showed that the enrichment of O^{18} in dissolved ocean air was highest at depths

where there was least oxygen present (cf. Fig. 4), and concluded that O^{16} must be preferentially respired by marine animals and plankton. Oxygen in respired carbon dioxide comes largely from water, and not from atmospheric oxygen.[108]

Translocation

The translocation of water by plants is a one-way process in which isotope fractionation might be expected. One would predict that transpired water would be depleted in the heavy isotopes D and O^{18}, with a corresponding enrichment in the soil or

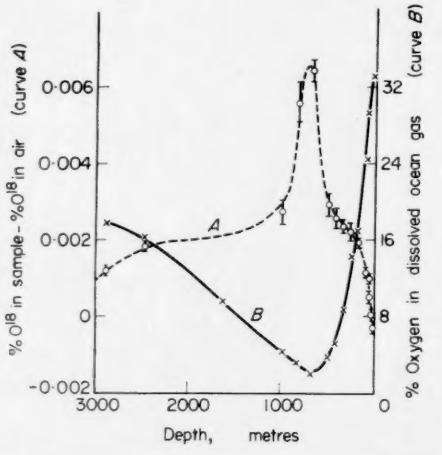

FIG. 4. Oxygen content and O^{18} content of dissolved gases in the ocean as a function of depth: from RAKESTRAW *et al*[176].

culture solution water when most of this had been used up. The water in the plant itself might be expected to occupy an intermediate position. Many early investigators relied on determinations of the density of water, which does not distinguish the effects caused by deuterium and O^{18}, e.g. WASHBURN and SMITH[77]; these measurements have been summarized by KAMEN[1] who concludes that, contrary to expectation, plant water is denser than natural surface water by a factor of 0–3·8 p.p.m. Plant carbohydrates also give water slightly denser than normal on combustion.[78] CARLBOM *et al.*[79] percolated growing barley plants with tap water and obtained quite large enrichments of deuterium in the residual water. No measurements of the O^{18} or D content of transpired water have been made, though these would place our knowledge of isotope effects on a sounder footing.

A hypothesis which explains the fragmentary data is the following. Plants lose water by transpiration as fast as they take it up, but we assume that the isotope effect is much greater in transpiration than it is in uptake. Hence plant water becomes enriched in both deuterium and O^{18}, and the fact that photosynthetic oxygen comes from plant water[71] might explain in part why atmospheric oxygen is unexpectedly heavy.[67] From this hypothesis we would predict relatively little fractionation in the uptake of simple inorganic ions (e.g. Li^+, Cl^-), but would not exclude the possibility of measurable fractionation of elements which combine chemically with cellular constituents (e.g. B, N, Cl, S). The only evidence we have on the uptake of ions is some early work by BREWER and BAUDISCH[80,81] and by JACQUES[82] on Li^6/Li^7 and K^{39}/K^{41} ratios in plant tissues. The potassium fractionation reported by these workers could not be confirmed by COOK[83] using a more accurate technique of isotopic analysis. Later work by MULLINS and ZERAHN[84] has shown that the K^{40} content of potassium in wood, bone and various minerals is constant to $\pm 0{\cdot}5$ per cent, so if any fractionation exists in this element it is undetectable by present-day techniques. Nitrogen is the only non-metal for which isotope effects have been sought. HOERING[85] found the N^{15}/N^{14} ratio varied between limits differing by 1·5 per cent in various plant samples, and PARWEL *et al.*[86] found N^{14} slightly enriched in wood with respect to atmospheric nitrogen. Unfortunately the ratio was not measured in the source of nitrogen on which the plants grew, so the results are not definitive. However, it is noteworthy that HOERING found clover the most strongly enriched in N^{14} with respect to the atmosphere, since this plant obtains most of its nitrogen from the air. The fact that petroleum oil and chile nitrate are both enriched in N^{14} is hardly good evidence for their organic origin.

VOL. 7 1959/

ISOTOPE FRACTIONATION BY ANIMALS

The possibilities of isotope fractionation by animals, with their more complicated patterns of metabolism and excretion, would appear to be more extensive than those in plants. Animals differ from plants in that their primary mode of ingestion is very unlikely to cause fractionation, though subsequent diffusion through the walls of the stomach and intestine might be expected to concentrate lighter isotopes.

Animals also have a far larger percentage excretion than do plants. Excretory products from plants are practically limited to water, CO_2 and oxygen lost from the tissue surfaces. These losses are also found in animals, but they are of minor importance compared with metabolic waste products excreted in the urine, and other waste (including much material which cannot be metabolized) in the faeces. We would expect to find enrichment of light isotopes in urine, if anywhere, but this appears to have been seldom sought and never found. This enrichment might be swamped in the case of elements which are readily absorbed (e.g. H, N, Cl, Br, K, S) and therefore appear in larger amounts in the urine than in the faeces. Polyvalent elements like Ca, Mn, Fe, Cu and Zn, of which more than 5 per cent is seldom metabolized, might be expected to show more marked enrichment of their light isotopes in urine. Actual measurements of isotope ratios in animals are few in number and virtually confined to two phyla, molluscs and vertebrates.

Molluscs

In molluscs, several workers[40,59,63] independently found that the organic carbon of the mollusc was enriched in C^{12} relative to the calcium carbonate of the shell. CRAIG found this enrichment to be of the order of 1·0–1·5 per cent for two marine gastropods and also for other marine organisms secreting lime (two echinoderms, one coral and five calcareous algae). BUCHANAN *et al.* grew fresh water molluscs in a sealed aquarium containing C^{14}, and showed that the specific activity of the shell carbonate was 6 per cent higher than the molluscan animals. DE VRIES[87] has confirmed the order of magnitude of CRAIG's figures for C^{13}, but finds that wild snails may now have a higher specific C^{14} activity in the flesh than in the shell. He attributes this to recent fluctuations in atmospheric C^{14} caused by atomic explosions. The C^{14} specific activity in shells is known to be higher than in wood and other plant material.[102,103] It seems clear that C^{13} is removed faster than C^{12} from the oceans by sedimentation as organically produced carbonate, while C^{12} concentrates in the soft tissues. N^{14} was depleted below atmospheric nitrogen in a single specimen of clam tissue.[85]

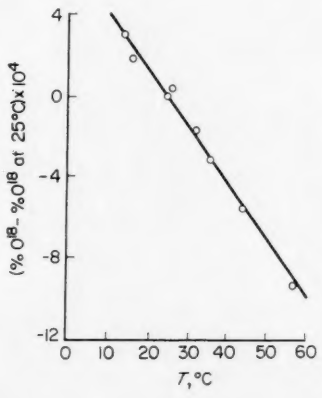

FIG. 5. O^{18} content of $CaCO_3$ as a function of the temperature of precipitation: from MCCREA[88].

Some of the most interesting observations of biological fractionation have been those of O^{18}/O^{16} ratios in recent and fossil mollusc shells.[39,88,89,90,100] MCCREA[88] calculated a decrease of $2{\cdot}75 \times 10^{-5}\%$ O^{18} in oxygen per degree rise in temperature for the precipitation of calcium carbonate from water. Fig. 5 shows the observed changes in O^{18} content as a function of temperature; the slope of this line is $2{\cdot}94 \times 10^{-5}\%$ $O^{18}/°C$.

From these and other results it has proved possible to estimate the temperature at which fossil molluscs once existed from their O^{18} content. The sensitivity of the method is sufficient to record cyclical variations in the O^{18} content across transverse sections of

belemnites, corresponding to annual growth rings over a small temperature range.[89]

Vertebrates

In vertebrates, much early work failed to distinguish between fractionation of hydrogen and oxygen.[1,12] THOMPSON and BALLOU fed mixed deuterium and tritium to rats but could find no isotope effect in the body water nor in the liver, pelt or carcass.[91,92] They did, however, find a 6–7 per cent enrichment of deuterium relative to tritium in muscle, fat and brain. In similar experiments EIDINOFF *et al.*[93] found deuterium enriched relative to tritium by 8 per cent in rat liver glycogen and by 18 per cent in liver fatty acid, and GLASCOCK and DUNCOMBE[94] have shown that tritium is used less readily than deuterium in lipid metabolism of unweaned rats. These observations imply corresponding enrichment in protium in the tissue studied, though this has not been found by direct experiment. Complete hydrogen/deuterium balance experiments have yet to be carried out on animals.

In the same way, observations on the fractionation of nitrogen by vertebrates are incomplete, though proteins from blood, milk and several soft tissues appear to be depleted in N^{14} by about 0·5 per cent.[85] We would expect urine to be correspondingly enriched in N^{14}. Earlier measurements on amino acids failed to detect any difference from standard N^{14}/N^{15} ratios.[95] SWENDSEID *et al.*[96] found rat tissue to be generally enriched in C^{12} compared with mineral sources, but the rat diet was not specified. The lighter isotope of sulphur is also enriched in human hair and in avian eggs.[49] Finally, rats which breathe oxygen enriched in O^{18} produce carbon dioxide depleted in this isotope[109], and since respiratory CO_2 is in isotopic equilibrium with body water[110] the fractionation must take place during the reduction of molecular oxygen.

VOL. 7 1959/

REFERENCES

1. KAMEN M. D. *Bull. Amer. Mus. Nat. Hist.* **87,** 105 (1946).
2. THODE H. G. *Research* **2,** 154 (1949).
3. INGERSON E. *Bull. Geol. Soc. Amer.* **64,** 301 (1953).
4. GLASSTONE S., LAIDLER K. J. and EYRING H. *The Theory of Rate Processes.* McGraw Hill, New York (1941).
5. UREY H. C. and GRIEFF L. J. *J. Amer. Chem. Soc.* **57,** 321 (1935).
6. WALDMANN L. *Naturwissenschaften* **31,** 205 (1943).
7. BIGELEISEN J. and MAYER M. G. *J. Chem. Phys.* **15,** 261 (1947).
8. BIGELEISEN J. *Science* **110,** 14 (1949).
9. BIGELEISEN J. *J. Chem. Phys.* **17,** 675 (1949).
10. UREY H. C. *J. Chem. Soc.* 562 (1947).
11. SENFTLE F. E. and BRACKEN J. T. *Geochim. et Cosmoch. Acta* **7,** 61 (1956).
12. KIRSHENBAUM I. *Physical Properties and Analysis of Heavy Water.* McGraw Hill, New York, (1951).
13. ASTON F. W. *Mass Spectra and Isotopes.* E. Arnold (1942).
14. DUCKWORTH H. E. *Mass Spectroscopy.* Cambridge University Press (1958).
15. THORNTON V. and CONDON F. E. *Analyt. Chem.* **22,** 690 (1952).
16. BRODY J. K., FRED M. and TOMKINS F. S. *Spectrochim. Acta* **6,** 383 (1954).
17. HAIGH C. P. *Nature* **172,** 359 (1953).
18. HERR W. *Z. Naturf.* **8** A, 305 (1953).
19. EPSTEIN E. *Nature* **171,** 83 (1953).
20. SUTCLIFFE J. F. *Symp. Soc. Exp. Biol.* **8,** 325 (1954).
21. CLOUD P. E., FRIEDMAN I., SISLER F. D. and DIBELER V. H. *Science* **127,** 1394 (1958).
22. AUGOOD D. R. *Industr. Chem. Mfr.* **30,** 585 (1954).
23. THORN M. B. *Biochem. J.* **49,** 602 (1951).
24. WEINBERGER D. and PORTER J. W. *Science* **117,** 636 (1953).
25. WEINBERGER D. and PORTER J. W. *Arch. Biochem. Biophys.* **39,** 395 (1954).
26. REITZ O. and BONHOEFFER K. F. *Z. Phys. Chem.* **174** A, 424 (1935).
27. MEYER H. *Naturwissenschaften* **24,** 346 (1936).
28. CRAIG F. N. and TRELEASE S. E. *Amer. J. Bot.* **24,** 232 (1937).
29. MOSES V., HOLM-HANSEN O. and CALVIN M. *Biochem. Biophys. Acta* **28,** 62 (1958).
30. WALKER J. R. and SYRETT P. J. *Nature* **183,** 1193 (1959).
31. HORWITZ I. *Plant Physiol.* **29,** 215 (1954).
32. TAYLOR G. W. and HARVEY E. N. *Proc. Soc. Exp. Biol.*, N.Y. **31,** 954 (1937).

33. Pratt R. and Curry J. *Amer. J. Bot.* **24,** 412 (1937).
34. Polyakov Y. A. *Pochvovedenie* **7,** 25 (1953).
35. Badenova K. *Fiziol. Rast.* **3,** 43 (1956).
36. Hughes A. M. and Calvin M. *Science* **127,** 1445 (1958).
37. Katz J. J., Crespi H. L., Hasterlik R. J., Thompson J. F. and Finkel A. J. *J. Nat. Cancer Inst.* **18,** 641 (1957).
38. Bowen H. J. M. *J. Nuclear Energy* **2,** 255 (1956).
39. Urey H. C. *Science* **108,** 489 (1948).
40. Buchanan D. L., Nakao A. and Edwards G. *Science* **117,** 541 (1953).
41. Weigl J. W. UCRL 590 (1950).
42. van Norman R. W. and Brown A. H. *Plant Physiol.* **27,** 691 (1952).
43. Rabinowitz J. L., Sall T., Bierly J. N. and Oleksyshyn O. *Arch. Biochem. Biophys.* **63,** 437 (1956).
44. Stevens W. H., Pepper J. M. and Lounsbury M. *J. Chem. Phys.* **20,** 192 (1952).
45. Dole M., Hawkins R. C. and Barker H. A. *J. Amer. Chem. Soc.* **69,** 226 (1947).
46. Lane G. A. and Dole M. *Science* **123,** 574 (1956).
47. Feldman D. E., Yost H. T. and Benson B. B. *Science* **129,** 146 (1959).
48. Thode H. G., Macnamara J. and Collins C. B. *Canad. J. Res.* B **27,** 361 (1949).
49. Szabo A., Tudge A. P., Macnamara J. and Thode H. G. *Science* **111,** 464 (1950).
50. Thode H. G., Kleerekoper H. and McElcheran D. *Research* **4,** 581 (1951).
51. Thode H. G., Macnamara J. and Fleming W. H. *Geochim. et Cosmoch. Acta* **3,** 235 (1953).
52. Thode H. G., Wanless R. K. and Wallouch R. *Geochim. et Cosmoch. Acta* **5,** 286 (1954).
53. Harrison A. G. and Thode H. G. *Trans. Faraday Soc.* **53,** 84 (1957).
54. Jones G. E. and Starkey R. L. *Appl. Microbiol.* **5,** 111 (1957).
55. Weigl J. W. and Calvin M. *J. Chem. Phys.* **17,** 210 (1949).
56. Weigl J. W., Warrington P. M. and Calvin M. *J. Amer. Chem. Soc.* **73,** 5058 (1951).
57. Vinogradov A. P. and Teis R. V. *Dokl. Akad. Nauk SSSR* **33,** 490 (1941).
58. Dole M. and Jenks G. *Science* **100,** 409 (1944).
59. Nier A. O. and Gulbransen E. A. *J. Amer. Chem. Soc.* **61,** 697 (1939).
60. Murphey B. F. and Nier A. O. *Phys. Rev.* **59,** 771 (1941).
61. Rankama K. *J. Geol.* **56,** 199 (1948).
62. Wickman F. E. *Geochim. et Cosmoch. Acta* **2,** 243 (1952).
63. Craig H. *Geochim. et Cosmoch. Acta* **3,** 53 (1953).
64. Craig H. *J. Geol.* **62,** 115 (1954).
65. Rankama K. *Geochim. et Cosmoch. Acta* **5,** 142 (1954).
66. Rankama K. *Bull. Geol. Soc. Amer.* **59,** 389 (1948).
67. Dole M. *J. Amer. Chem. Soc.* **57,** 2731 (1935).
68. Dole M. *J. Chem. Phys.* **4,** 268 (1936).
69. Morita N. and Titani T. *Bull. Chem. Soc. Japan* **11,** 36 (1936).
70. Roake W. E. and Dole M. *J. Amer. Chem. Soc.* **72,** 36 (1950).
71. Ruben S., Randall M., Kamen M. D. and Hyde J. L. *J. Amer. Chem. Soc.* **63,** 877 (1941).
72. Holt A. S. and French C. S. *Arch. Biochem. Biophys.* **19,** 429 (1948).
73. Kamen M. D. and Barker H. A. *Proc. Nat. Acad. Sci. Wash.* **31,** 8 (1945).
74. Dole M. *Chem. Rev.* **51,** 263 (1952).
75. Baertschi P. *Helv. Chim. Acta* **36,** 773 (1953).
76. Rakestraw N. M., Rudd D. P. and Dole M. *J. Amer. Chem. Soc.* **73,** 2976 (1951).
77. Washburn E. W. and Smith E. R. *J. Res. Nat. Bur. Stand.* **12,** 205 (1934).
78. Morita N., Goto K. and Titani T. *Bull. Chem. Soc. Japan* **13,** 99 (1938).
79. Carlbom L., Nielsen N. and Skjöldebrand R. *Nature* **177,** 988 (1956).
80. Brewer A. K. *J. Amer. Chem. Soc.* **58,** 365 (1936).
81. Brewer A. K. and Baudisch O. *J. Amer. Chem. Soc.* **59,** 1578 (1937).
82. Jacques A. G. *J. Gen. Physiol.* **23,** 741 (1940).
83. Cook K. L. *Phys. Rev.* **64,** 278 (1943).
84. Mullins L. J. and Zerahn K. *J. Biol. Chem.* **174,** 107 (1948).
85. Hoering T. *Science* **122,** 1233 (1955).
86. Parwel A., Ryhage R. and Wickman F. E. *Geochim. et Cosmoch. Acta* **11,** 165 (1957).
87. de Vries H. *Science* **128,** 250 (1958).
88. McCrea J. M. *J. Chem. Phys.* **18,** 849 (1950).
89. Urey H. C., Lowenstam H. A., Epstein S. and McKinney C. R. *Bull. Geol. Soc. Amer.* **62,** 399 (1951).
90. Epstein S., Buchsbaum R., Lowenstam H. A. and Urey H. C. *Bull. Geol. Soc. Amer.* **62,** 417 (1951).
91. Thompson R. F. and Ballou J. E. *Arch. Biochem. Biophys.* **42,** 219 (1953).
92. Thompson R. F. and Ballou J. E. *J. Biol. Chem.* **206,** 101 (1954).
93. Eidinoff M. L., Perri G. C., Knoll J. E., Marano B. J. and Arnheim J. *J. Amer. Chem. Soc.* **75,** 248 (1953).
94. Glascock R. F. and Duncombe W. G. *Biochem. J.* **51,** *Suppl.* 40 (1952).
95. Schoenheimer R. and Rittenberg D. *J. Biol. Chem.* **127,** 285 (1939).

96. Swendseid M. E., Barnes R. H., Hemingway A. and Nier A. O. *J. Biol. Chem.* **142,** 47 (1942).
97. Ault W. U. in Abelson P. H. *Researches in Geochemistry*. John Wiley, New York (1959).
98. Silverman S. R. and Epstein S. *Bull. Amer. Ass. Petrol. Geol.* **42,** 998 (1958).
99. Epstein S. in ref. (97).
100. Lowenstam H. A. and Epstein S. *J. Geol.* **62,** 207 (1954).
101. Crumley H. A. and Meyer S. L. *J. Tenn. Acad. Sci.* **25,** 171 (1950).
102. Anderson E. C. and Libby W. F. *Phys. Rev.* **81,** 64 (1951).
103. Kulp J. L., Feely H. W. and Tryon L. E. *Science* **114,** 565 (1951).
104. Kulp J. L., Ault W. U. and Feely H. W. *Nat. Res. Coun. Pub.* No. 400, 45 (1956).
105. Ulubekova M. V. *Dokl. Akad. Nauk SSSR* **112,** 772 (1957).
106. Lowenstam H. A. and Epstein S. *J. Geol.* **65,** 364 (1957).
107. Vinogradov A. P., Kutiurin V. M., Ulubekova M. V. and Zadoroshnyi I. K. *Dokl. Akad. Nauk SSSR* **125,** 1151 (1959).
108. Vartapejyan B. B. and Kursanov A. L. *Dokl. Akad. Nauk SSSR* **104,** 272 (1955).
109. Day J. N. E. and Sheel P. *Nature, Lond.* **142,** 916 (1938).
110. Lifson F., Gordon G. B., Visscher M. B. and Nier A. O. *J. Biol. Chem.* **180,** 803 (1949).

VOL.
7
1959/6

International Journal of Applied Radiation and Isotopes, 1960, Vol. 7, pp. 273–286. Pergamon Press Ltd. Printed in Northern Ireland

Continuous Measurement of Specific Activity of $C^{14}O_2$ in Expired Air*

GEORGE V. LEROY, GEORGE T. OKITA, EDWARD C. TOCUS and DONALD CHARLESTON
Argonne Cancer Research Hospital, The University of Chicago

(*Received* 29 *August* 1959)

The majority of carbon compounds of metabolic interest ultimately are degraded to carbon dioxide and urea which are excreted. Following the administration of a tracer dose of a C^{14}-labeled metabolite, there is assumed to be a pattern of elimination of $C^{14}O_2$ which is characteristic for the healthy state, and which is distorted in disease. This pattern is represented by the time-course of specific activity of $C^{14}O_2$ in expired air. Metabolic studies in human subjects and in animals are facilitated by the apparatus described in this report which permits the continuous measurement of radioactive $C^{14}O_2$ in expired air. The apparatus consists of an air-collection system, a ventilation meter, a $C^{12}O_2$ (infrared) analyzer, a 4π G–M counter with anti-coincidence circuitry, and a ratio analyzer to compute C^{14}/C^{12}. Analog data are printed out on a four-channel recording millivoltmeter at the rate of four items per minute on each channel. The data are in such a form that they can be converted readily to digital information for processing in a high-speed computer. Rapid estimates of the size and kinetics of the carbon dioxide pool are possible when labeled bicarbonate is used as the tracer.

OL.
7
9/60

LA MESURE CONTINUE DE L'ACTIVITÉ SPÉCIFIQUE DU $C^{14}O_2$ DANS L'AIR EXPIRÉ

La plupart des composés de carbone ayant un intérêt métabolique se dégradent enfin jusqu'au bi-oxyde de carbone et à l'urée, lesquels sont excrétés. On suppose que, suivant l'administration d'une dose indicatrice d'un métabolite marqué de C^{14}, il existe un modèle de l'élimination du $C^{14}O_2$ qui est particulier à l'état de santé et qui est déformé par la maladie. Ce modèle se montre par la variation, au cours du temps, de l'activité spécifique du $C^{14}O_2$ dans l'air expiré. Les études métaboliques chez les sujets humains et chez les animaux sont rendues plus faciles par l'appareil qu'on décrit dans cette communication, lequel permet la mesure continue du $C^{14}O_2$ dans l'air expiré. L'appareil comprend un système pour encaisser l'air, un compteur de ventilation, un analysateur à $C^{12}O_2$ (infrarouge), un compteur G–M à 4π ayant des circuits contre la coincidence et un analysateur pour obtenir le rapport C^{14}/C^{12}.

Les données analogues sont imprimées par un millivoltmètre enregistreur à quatre voies à une vitesse de quatre articles par minute dans chaque voie. Les données sont de telle forme qu'on peut les convertir facilement en renseignement digital afin de les passer par un calculateur de grande vitesse. On peut atteindre des estimations rapides de la kinétique du bi-oxyde de carbone en employant comme indicateur le bicarbonate marqué.

НЕПРЕРЫВНЫЕ ИЗМЕРЕНИЯ УДЕЛЬНОЙ АКТИВНОСТИ $C^{14}O_2$ В ВЫДЫХАЕМОМ ВОЗДУХЕ

Большинство соединений углерода, участвующих в обмене веществ, в конечном итоге превращается в выделяемые организмом двуокись углерода и мочевину. Используя введение в организм метаболитов, меченых C^{14}, принимается, что выделяемое количество $C^{14}O_2$ является характерным индикатором на состояние организма. Это количество представляется временной зависимостью удельной активности выдыхаемого $C^{14}O_2$. Исследование обмена веществ у человека и животных облегчается применением

* This research was supported by the United States Atomic Energy Commission.

аппарата, описанного в данном сообщении, который позволяет производить длительные измерения радиоактивного $C^{14}O_2$ в выдыхаемом воздухе. Аппаратура состоит из собирающей воздух системы, измерителя скорости воздуха, инфракрасного анализатора CO_2 счетчика 4π-Гейгера-Мюллера, работающего по схеме антисовпадений, и анализатора, предназначенного для определения соотношений C^{14}/C^{12}. Аналогичные данные регистрировались также на 4-х канальном автоматическом милливольтметре со скоростью четырех записей в минуту по каждому каналу. Полученные на этом приборе данные могут быть легко переведены в числовые значения для обработки на высоко-скоростном счетчике. Быстрая оценка количества и кинетики двуокиси углерода становится возможной, когда в качестве индикатора употребляется меченый бикарбонат.

KONTINUIERLICHE MESSUNGEN DER SPEZIFISCHEN AKTIVITÄT VON $C^{14}O_2$ IN DER ATEMLUFT

Die Mehrzahl der für den Stoffwechsel wichtigen Kohlenstoffverbindungen werden letzten Endes zu CO_2 und Harnstoff abgebaut und ausgeschieden. Es wird angenommen, dass nach Verabreichung einer geringen Menge eines C^{14}-markierten Stoffwechselproduktes, die Abgabe von $C^{14}O_2$ in einer für den Gesundheitszustand ganz charakteristischen Weise vor sich geht, welche bei Auftreten von Erkrankungen gestört wird. Diese Abgabe wird durch die zeitliche Veränderung der spezifischen Aktivität der ausgeatmeten Luft wiedergegeben. Die in diesem Bericht beschriebene Apparatur, welche eine kontinuierliche Messung des radioaktiven $C^{14}O_2$ in der ausgeatmeten Luft gestattet, vereinfacht Stoffwechseluntersuchungen am Menschen und am Versuchstier. Diese Apparatur besteht aus einem Luftsammelgerät, einem Strömungsmesser, einem $C^{14}O_2$ (infrarot) Analysator, einem 4π-Geiger-Zählrohr mit Antikoinzidenzschaltung und einem Analysator, welcher das Verhältnis C^{14}/C^{12} bestimmt. Analoge Werte werden von einem 4-Kanal-Millivoltmeter-Registriergerät aufgezeichnet und zwar werden 4 Messpunkte pro Minute in jedem Kanal registriert. Die Messergebnisse werden in einer Form geliefert, welche seicht in Informationen für eine elektronische Rechenmaschine von hoher Leistungsfähigkeit umgewandelt werden kann. Rasche Bestimmungen von Menge und Kinetik von Kohlendioxyd sind auf diese Weise möglich, wenn als Indikator markiertes Bicarbonat verwendet wird.

VOL. 7 1959/6

THE majority of chemical compounds of interest in the study of metabolism can be labeled with carbon-14. In spite of the devious pathways involved in intermediary metabolism, most carbon-containing substances are converted ultimately to carbon dioxide. An examination of the time-course of the specific activity (SA) of expired air following the administration of C^{14}-labeled material should provide valuable information on biochemical events occurring in the intact human or animal subject. Dissatisfaction with the conventional procedure of collecting separate samples of expired air for radiochemical analysis led us to develop the apparatus described in this paper.* Our primary objective was to obtain the SA–time curve for $C^{14}O_2$ during a suitable period of time after the administration of tracer substances labeled with carbon-14. As an aid in the interpretation of such curves, we needed a reliable estimate of the kinetics of the carbon dioxide pool, e.g. the size of the pool, and its rate of turnover. To make this estimate, it was necessary to measure the amount of carbon dioxide exhaled in the period during which a SA–time curve was obtained following a tracer dose of $NaHC^{14}O_3$.

The apparatus, which is shown in use in Fig. 1, consists of the following elements:

(a) Air collection system
(b) Ventilometer
(c) Carbon dioxide ($C^{12}O_2$) analyzer
(d) Radiation detector
(e) Ratio analyzer for C^{14}/C^{12}
(f) Recording millivoltmeter.

A block diagram of the apparatus is shown in Fig. 2. Descriptions of the individual elements follow:

* The same considerations that led us to the development of our device for the continuous measurement of SA of $C^{14}O_2$ in expired air, also motivated B. M. TOLBERT and his colleagues at the Radiation Laboratory, University of California. Working independently, and apparently concurrently, their apparatus was described in 1956.[1]

OL.
7
9/60

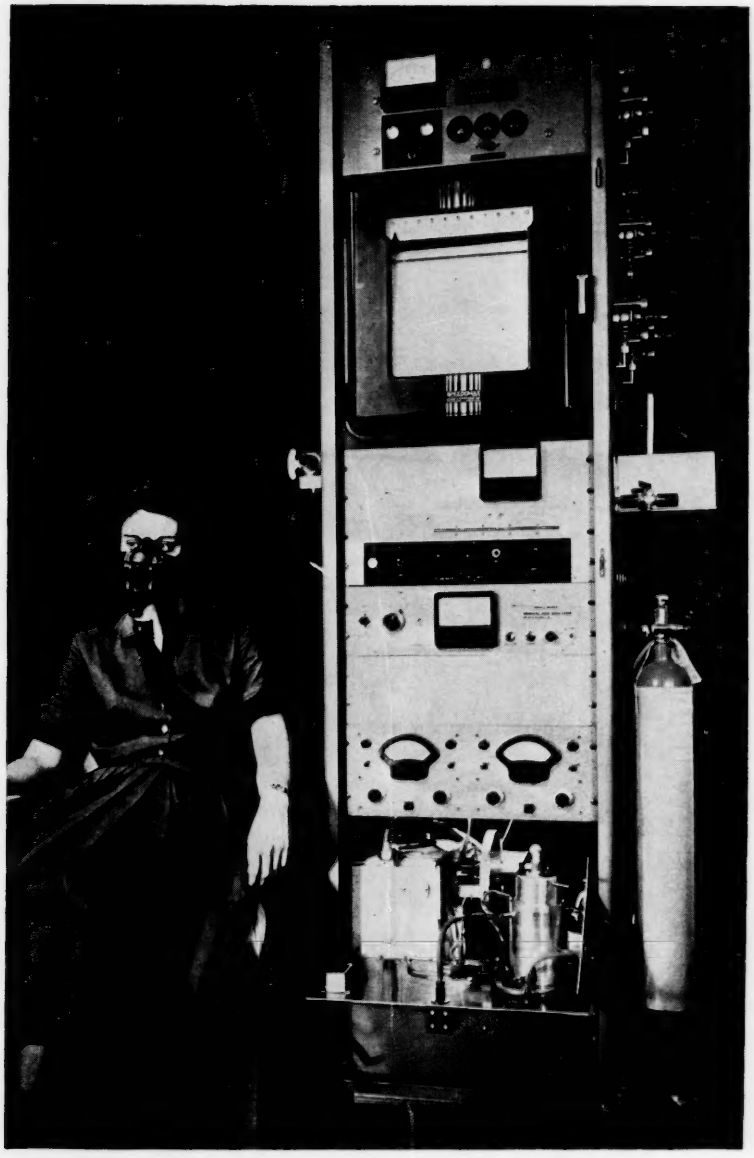

FIG. 1. Continuous carbon-14 dioxide analyzer in operation. This subject is wearing the modified aviation-type face mask. The 4π counter is on the shelf in the lower right hand corner of the apparatus.

VOL
7
1959/

70L.
7
59/60

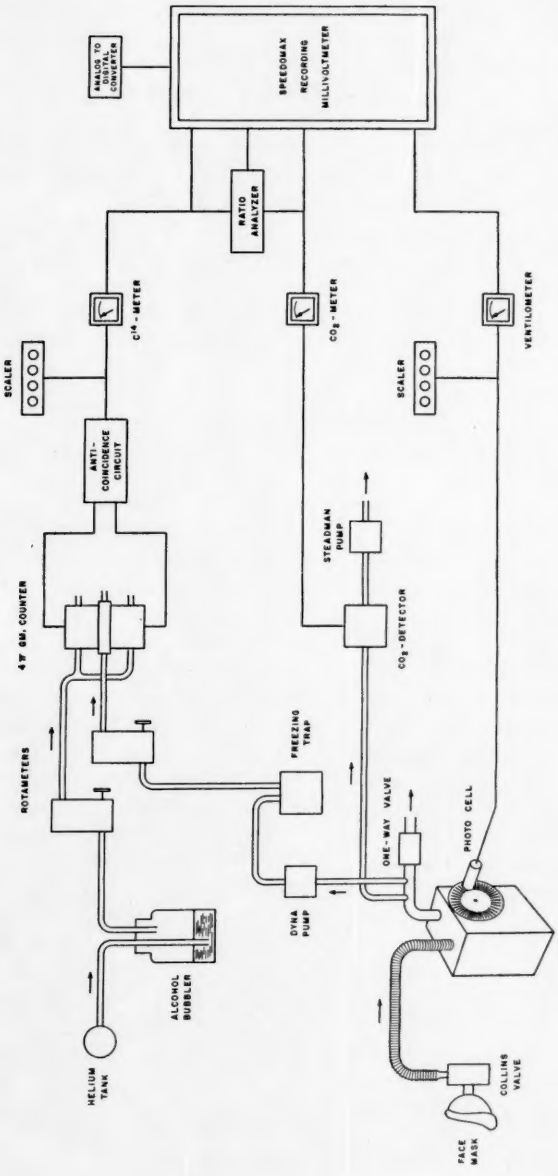

FIG. 2. Block diagram of the components of the apparatus.

(a) *Air-collection system*

The air-collection system currently preferred consists of a face mask of the type used in anesthesia. We have experimented with the standard BMR mouthpiece and nose clip, but found it uncomfortable for use over long periods of time. An aviation face mask has also been used satisfactorily for subjects whose facial configuration and size is appropriate. In some cases, an unpredictable amount of leakage occurred due to a poor fit, and for this reason it is not used routinely. Consideration was given to a "space helmet" type of air-collection system, but this was rejected since it increased the dead space in the system, and required a forced air intake which was difficult to adjust to the changing minute volume of ventilation.

The primary considerations in the air-collection system were comfort, minimal resistance to exhalation and minimal dead space. The combination of the anesthesia face mask and a Collins, type J, valve is the most satisfactory arrangement that we have tested up to this time. The data (see below) on the response time of the entire instrument indicate that this air-collection system is satisfactory with respect to minimizing the dead space. Resistance to exhalation in the system and the ventilometer is reduced by the application of negative pressure at the exit-fitting sufficient to transfer approximately 1 l. of air per minute to the carbon dioxide analyzer. The measured resistance at the mouthpiece is 2–3 mm of H_2O, and the maximum air flow through the entire system is in excess of 25 l/min.

(b) *Ventilometer*

Average volume of ventilation (l/min) and total volume of ventilation is determined with a ventilometer developed in our laboratory. Expired air passes through the Collins valve and a 1 in. corrugated tube to a standard dry-test gas meter (Phipps and Bird, No. 70–851) modified for our purpose. The mechanical output of the meter results in rotary motion of a shaft to which is attached the liter-per-revolution pointer, and the train of gears actuating the cumulative recording dials. To obtain a continuous record of average ventilation per minute, it was necessary to translate the rotary motion into electrical information suitable for a rate meter. To accomplish this, a slotted disk was attached to the output shaft of the gas meter, and was used to interrupt a collimated beam of light between a lamp and a photoelectric cell. Appropriate circuitry was designed to accept the range of pulse widths generated by the motion of the slotted disk. These variations in pulse width resulted from non-uniformity of the velocity of expired air—and hence of the speed of rotation of the disk—throughout successive cycles of exhalation. Relatively rapid motion of the disk occurs early in expiration, and the movement declines toward zero as the subject stops exhaling and inhales for the start of another cycle. The use of an aluminum disk, and well-lubricated bearings reduced the inertia and friction of the mechanism. The slow rate of air movement at the end of exhalation required the use of many interrupting slots in order to gain sufficient *bits* of information when the disk was moving slowly. The aluminum disk contains 150 radial slots, so that one complete revolution of the shaft, which results from the transit of 1 l. of air, should produce 150 pulses. Between the end of one exhalation, and the start of the succeeding one, the rotation of the slotted disk is slowed to a rate equivalent to 1 l/min (i.e. the amount of air removed by the sampling pumps), and this "dead time" determined the minimum time constant for the pulse-rate meter actuated by the electrical pulses generated by the interrupted light beam. It was found empirically that an 80-sec time constant smoothed out the record of the ventilometer, and allowed enough sensitivity to detect even small (i.e. less than 0·5 l/min) changes in the rate of breathing. The pulses generated by the slotted disk pass to a pulse-rate meter, the output of which is recorded on the Speedomax chart. The pulses also pass to a scaler and register, which totalizes the volume of ventilation over any period of time.

Since the volume of air per revolution of the shaft is known (i.e. 1 l.) and since the pulses produced per revolution are counted,

VOL. 7 1959/

the output of the rate meter, or the reading of the scaler can be converted readily into units of volume. The ventilometer was calibrated in two ways: using a wet-test gas meter and a Tissot spirometer. The reference instruments were compared with each other by pumping air from the Tissot through the wet-test meter at a steady rate of approximately 7 l/min. The indicated volumes were identical within the accuracy of reading the instruments. The ventilometer was then connected to the wet-test meter and room air was drawn through both at several rates and for several periods of time. The results are shown in Fig. 3. The response of the ventilometer is linear over the range 1–10·3 l/min. Using a filled Tissot spirometer, air was displaced from it and through the ventilometer at a steady rate, and intermittently to simulate normal respiration. The total volumes recorded by the ventilometer were the same as those measured by the spirometer (Fig. 3). Finally, the Collins valve of the air-collection system was connected to a filled Tissot spirometer and the total volume breathed over a long period was recorded. The ventilometer total was in good agreement with the Tissot. A calibrating factor, 148 pulses/l. was obtained from these tests. Since the slotted disk could

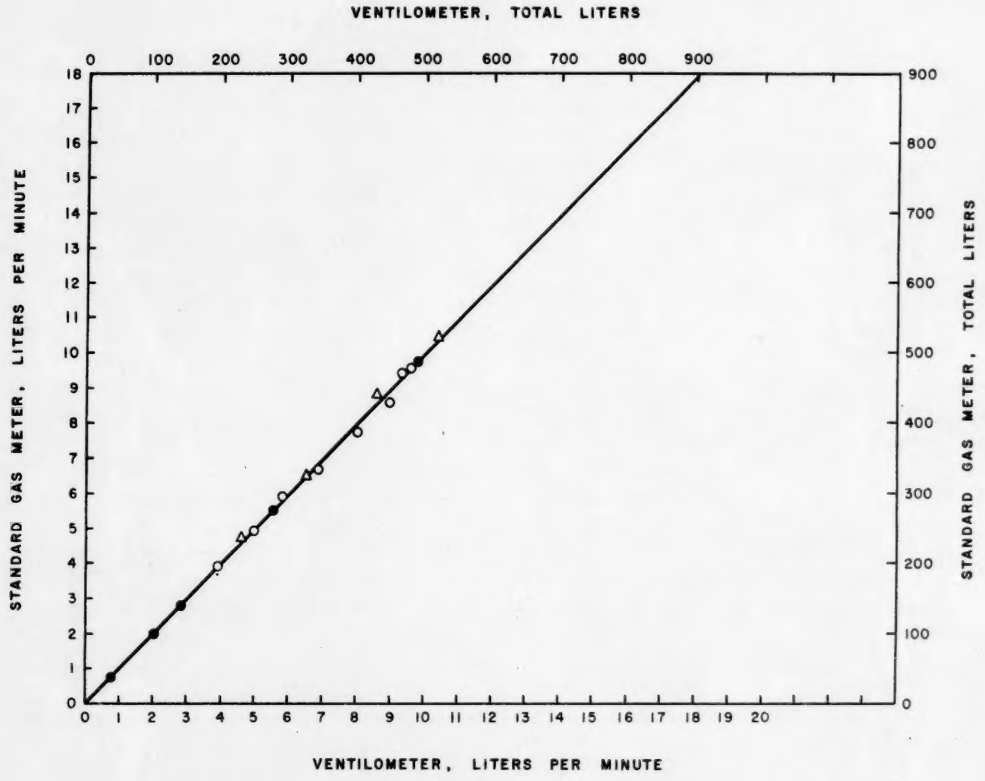

FIG. 3. Calibration of the ventilometer.

○ indicate liters per minute from the wet-test meter vs. liters per minute from the reading of the rate meter. ● indicate total liters of ventilation from the wet-test meter vs. total liters from the scaler register which totalizes the pulses from the ventilometer. △ indicate total liters from the Tissot spirometer vs. total liters from the scaler register. The correction factor used for the ventilometer was 148 pulses = 1 liter.

generate 150 pulses per revolution (or per liter), the overall efficiency of this air-metering system is 98·6 per cent. The pulse-rate meter and the scaler of the ventilometer system are provided with calibrating signals of 1800 and 3600 pulses/sec.

(c) *Carbon dioxide* ($C^{12}O_2$) *analyzer*

At the output fitting of the gas meter, approximately 250 ml/min of mixed expired air is removed and pumped through the micro-catheter cell of a Spinco–Beckman, Model LB-1 medical gas analyzer, the circuitry of which has been modified. As supplied by the manufacturer, the Model LB-1 has an electrical output which is at a voltage level above ground. The unit was modified so that it provided an analog output signal with reference to ground. This modification was necessary because of the input circuitry of the recorder, to be explained in detail below. The CO_2 analyzer is responsive to rapid changes in percentage CO_2 and tends to fluctuate during a breath cycle in spite of the large dead space (or mixing volume) afforded by the mask, tubing and gas meter. Such fluctuation was undesirable since the output of the CO_2 meter (i.e. percentage CO_2) is multiplied by the output of the ventilation rate meter (i.e. liters exhaled per minute) to obtain total volume of CO_2 exhaled at any time. For this reason, a long time-constant was introduced into the metering circuit, by the addition of a suitable capacitator, to average out the unwanted excursions. The output of the LB-1 unit is not designed to be more than an approximate linear function of the CO_2 content. The drift of the instrument causes a deviation from linearity over many hours of operation that may be as great as 1 per cent/hr; but which does not compromise an experiment of 2–4 hr duration. Nevertheless, the lack of linearity requires calibration before each clinical trial. This is done by means of a gas-switching manifold which permits the operator to select any one of several analyzed mixtures of CO_2 in oxygen. The test gas is passed through the CO_2 analyzer at the same rate as the sample of expired air, so that the analog voltage equivalent respectively to 2, 3 and 4 per cent CO_2 is recorded.

(d) *Radiation detector*

The radioactivity of $C^{14}O_2$ is measured with a specially-designed Geiger–Müller counter, the geometry of which approaches 4π. Expired air, at the rate of approximately 1 l/min is obtained at the outlet of the gas meter–ventilometer assembly by means of a Dyna pump. The positive action of the pump moves the air first through a freezing trap (ethanol–dry ice) to remove water vapor. The air then moves to a rotameter which permits regulation of flow through the G–M counter so that the rate is identical with rate of flow of the counting gas. This equalization of pressures is necessary to protect the Mylar windows of the counter, and to minimize diffusion through the windows.

The 4π counter* is shown schematically in Fig. 2. It consists of two 3-in. (or 4-in.) hemispheres of aluminum which face one another separated by a 1-in. spacing ring of clear Lucite. Each hemisphere has a window of aluminized plastic, Mylar, the density of which is approximately 0·95 mg/cm². The Mylar windows and the Lucite spacer define the active volume of the counter, which is approximately 116 ml, and through which dried air is pumped at approximately 1·0 l/min. The counting gas which permits operation in the Geiger region is helium bubbled through ethanol at 0°C. The resulting characteristic Geiger-region plateau is approximately 300 V in length with a slope of 5 to 6 per cent, as shown in Fig. 4.

The physical geometry of the 4π counter suggested the possibility of reducing background by anti-coincidence (a-c) counting. Such a circuit reduced background by approximately 30 per cent. The a-c circuit is designed primarily for reliability, and has a

* The prototype of this counter was designed in collaboration with Mr. Charles Soderquist of the Central Shops of the Research Institutes, The University of Chicago. Current models are produced by the Instrument and Development Company of Chicago.

VOL. 7 1959/

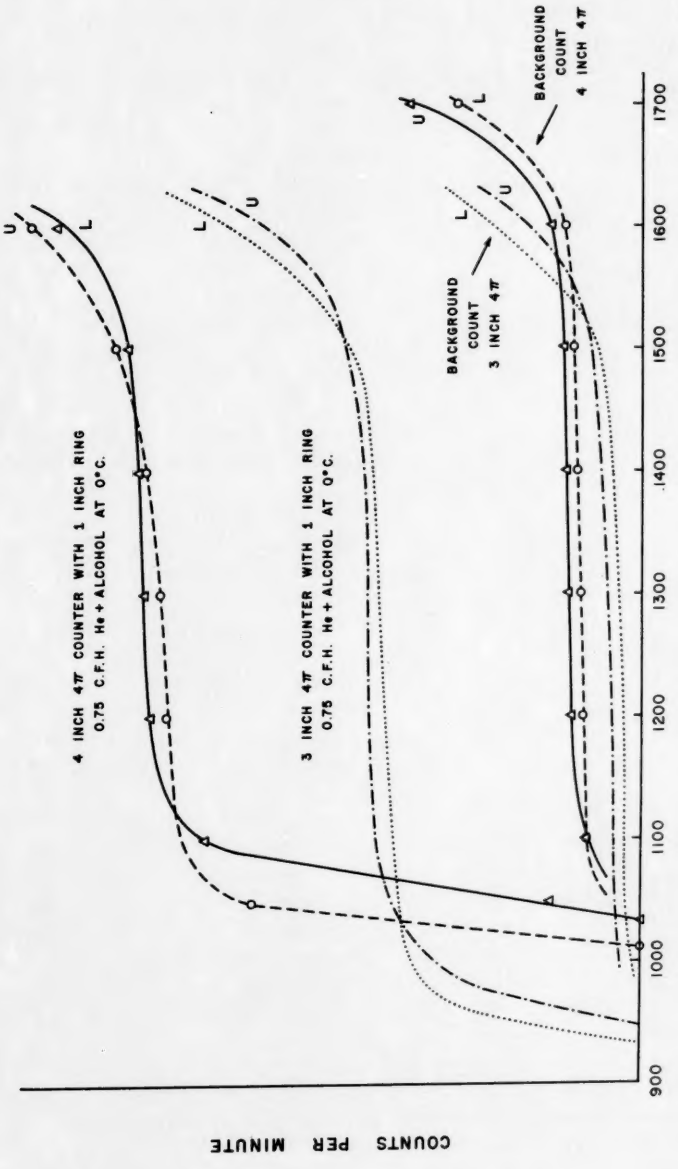

FIG. 4. Performance characteristics and plateaus of representative examples of the 3-in. and the 4-in. 4π counter. Curves labeled "U" designate data from the upper counter, those labeled "L", from the lower counter of the pair.

resolving time which permits it to count as rapidly as 10,000 per sec. The output of the a-c circuit goes to a count-rate meter, and also to a scaler, the register of which totalizes the radioactivity counted in the total volume of air expired during an experiment. A tabulation of data from tests of a 3-in. 4π counter with an active volume of 116 ml is given in Table 1. These data led

TABLE 1. Performance of 4π G–M counter, operating in anti-coincidence

Conditions	Background, unshielded (counts/min)	Gas mixture containing $C^{14}O_2$ at 1·0 l/min (counts/min)
A. *Old windows*		
Upper counter	109	229
Lower counter	112	258
Upper + lower	221	487
Upper + lower + anti-coincidence	166	431
Number of coincidence counts eliminated	55	56
B. *New windows*		
Upper counter	83	221
Lower counter	87	228
Upper + lower	170	459
Upper + lower + anti-coincidence	116	402
Number of coincidence counts eliminated	54	57

to further investigation of what appeared to be an excessive background despite the a-c feature. It can be seen from the data that the a-c circuit seems to be consistently effective in rejection of what appears to be the "cosmic background", but the non-coincident activity remained excessive. It was found that the Mylar windows retained (or adsorbed) some $C^{14}O_2$ and contributed a fairly constant "background" to each side of the counter. A maximum amount of carbon dioxide is attained in a very short time, and no further increase is seen over long periods of operation. The data in Table 1 were obtained with a 4π counter that had been in use for 6 months. When new Mylar windows were installed, the background dropped from an average of 110 counts/min to an average of 85 counts/min. Within 48 hr of exposure to $C^{14}O_2$ at the usual concentrations, the counter had returned to its former background rate, approximately 110 counts/min.

The 4π counter is calibrated in two ways; first, in the course of an experiment; and second, by means of a standard gas mixture containing $C^{14}O_2$. In either case, the reference measurement of radioactivity is made with a vibrating reed electrometer, the output voltage of which is converted to disintegrations per minute (dis/min). The conversion factor for the electrometer is obtained with $C^{14}O_2$ released from a standard sample of $NaHC^{14}O_3$ supplied by the National Bureau of Standards.

Calibration in the course of an experiment is accomplished by collecting several 5-min samples of air from the outlet of the gas meter using a plastic Douglas bag. The volume of air collected is passed through an absorption tower containing 1 N NaOH, and then through a wet-test gas meter. Triplicate 10-ml samples of $NaOH–Na_2CO_3$ are analyzed manometrically for total CO_2. The gas extracted is transferred in the vacuum line to a 250 ml ionization chamber for measurement of radioactivity by the vibrating-reed electrometer. We thus obtain specific activity (SA) expressed as dis/min per mM, and the total radioactivity expressed as dis/min per liter, for comparison with the counts per minute from the 4π detector. Over the range of radioactivity encountered in typical experiments, the relationship between dis/min and net counts/min is linear, as shown in Fig. 5. For this particular counter, the overall efficiency (net counts/min per dis/min) was 27 per cent. This value is an overall correction factor which includes self-absorption and geometry, and which can be applied to radioactivity per liter, and to specific activity (SA) or radioactivity per mM.

The foregoing procedure is obviously a tedious way to determine the efficiency of the radiation detection system. For routine use, a gas mixture containing 3 per cent CO_2, 97 per cent O_2, and a known amount

VOL. 7 1959/

of $C^{14}O_2$ approximately 12,000 dis/min per liter is pumped through the counter at the same rate as expired air. This calibration is performed before any experiments are done, and at the conclusion of each test. The or both of the channels of the anti-coincidence circuit. This provides a check on the operation and calibration of the anti-coincidence circuit, the count-rate meter, and the scaler that totalizes the radioactivity

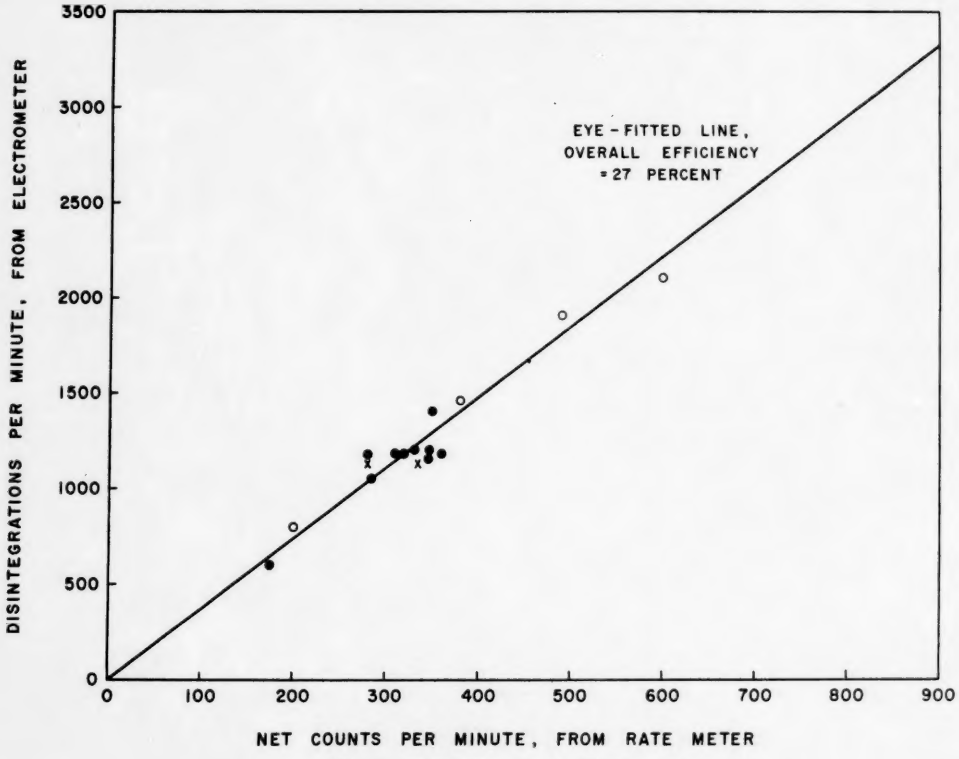

Fig. 5. Calibration of a 4π $C^{14}O_2$ counter.

○ dis/min per liter in Douglas bag samples, vs. count-rate meter reading as net counts/min per liter. ● dis/min per mM in Douglas bag samples, vs. specific activity reading of the ratio analyzer, expressed as net counts/min per mM. × dis/min per liter in the calibrating gas mixture vs. net counts/min per liter at the start and finish of a typical experiment.

overall efficiency factor obtained with the standard gas mixture is the value used in the mathematical treatment of the data.

The performance of the electronic circuits associated with the 4π counter can be tested by means of internal calibration signals which closely approximate the input pulses received from the counter. A binary count-down circuit supplies pulse rates of 350, 900, 1800 and 3600 counts/min from the 60 cycle line voltage (Fig. 6). Any one of these count rates can be switched into either in expired air. The ratio analyzer circuit (see below) can also be checked by a simple calculation when a calibrating pulse is supplied to the count-rate meter while the output of the CO_2 analyzer is kept at a predetermined value. The count-rate meter is provided with three time constants: 1 sec, 10 sec, and 50 sec. In ordinary operation the 50-sec time constant is used, since we are interested principally in the SA of expired air. When $NaHC^{14}O_3$ or rapidly metabolized material is used, the time constant

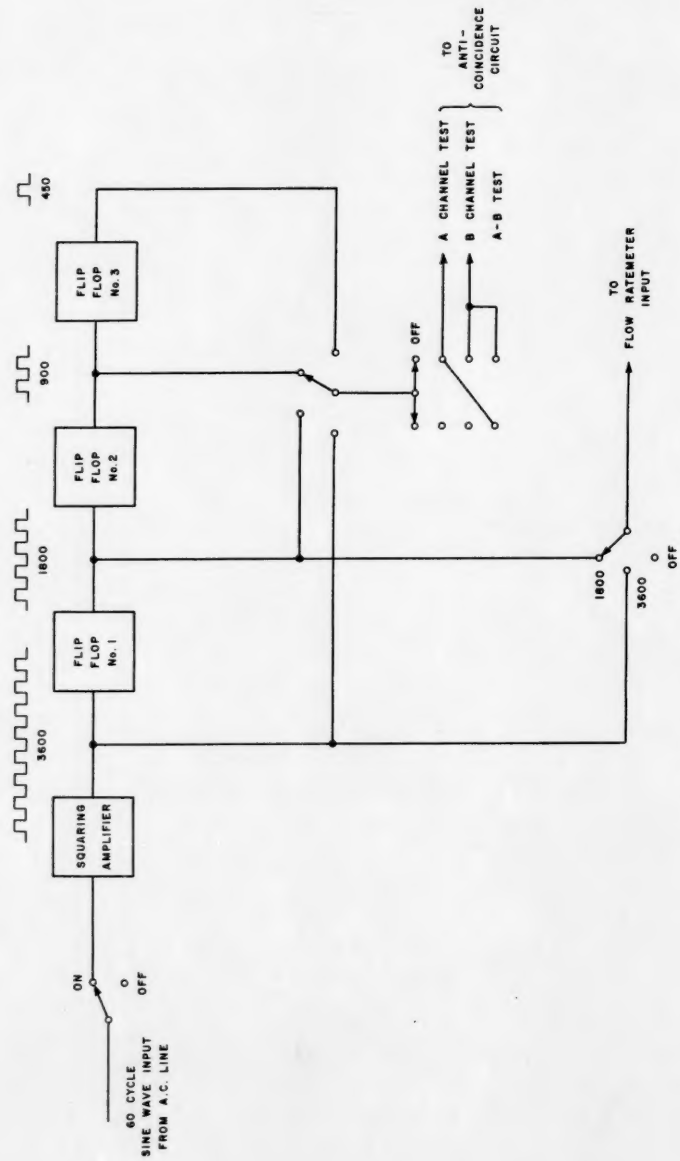

Fig. 6. Diagram of internal calibration signal system.

VOL.
7
1959/

is set at 10 sec prior to intravenous injection of the tracer. The shorter time constant permits rapid response during the early portion of the SA–time curve when the radioactivity of expired air is high. When the die-away curve is established, the time constant is switched to 50 sec.

(e and f) *Ratio analyzer and recorder*

A Leeds and Northrup Speedomax Model G, 10-mV, multiple-point recorder was modified to plot the four analog functions: rate of ventilation, radioactivity counting rate, percentage CO_2, and specific activity. All input connections were made in a straightforward manner with the exception of the SA measurement. Specific activity is defined here as the ratio: C^{14}/CO_2. A technique devised by TOLBERT *et al.*[1] was employed to compute the function within the recorder and thus eliminate the need for an external ratio analyzer. The modification involved the addition of a multi-position, multi-gang switch linked to the main camshaft of the Speedomax and wired in such a way that the standard reference voltage is switched out of the circuit, and the output voltage representing percentage CO_2 is substituted for it during the ratio-print cycle. In addition to this, the self-calibrating automatic current adjuster of the Speedomax was disabled to avoid the possibility of calibrating all points against the substitute voltage. Internal calibration of the recorder is accomplished by a semi-automatic current adjuster involving a push-button type of operation which need be done only once before each test to assure precise interval calibration.

DISCUSSION

Response time

The response time of the instrument is defined as the time required for either of the rate meters (ventilation or radioactivity) to react to abrupt changes in operating conditions. It is convenient to express the results as the "50 per cent time", and the "90 per cent time". In the case of the startup of the ventilometer (see Fig. 7), the 50 per cent time is 120 sec and the 90 per cent time 210 sec, when the level of ventilation is 10 l/min. When the ventilation shifts suddenly from, say 7 l/min to 10 l/min (Point A, Fig. 8), the 90 per cent response time is less than 30 sec. In the case of the radioactivity-rate meter, the rapid rise following injection of labeled bicarbonate reached a peak in 60 sec (Fig. 7). A better estimate of response time for the C^{14} detection system is possible from inspection of Fig. 8. In this experiment at Point A, the subject whose expired air contained $C^{14}O_2$ transferred the mask to another person whose expired air contained no radioactivity. The latter person ventilated more rapidly (10 l/min vs. 7·5 l/min) than the first subject. Under these conditions the 50 per cent time for the radiation-detection unit was 140 sec, and the 90 per cent time was 300 sec. Referring again to Fig. 8, at Point B, the mask was traded back to the person exhaling $C^{14}O_2$, and the startup of the detector is shown. The 50 per cent response time for the startup was 180 sec, and the 90 per cent was 330 sec. The time constants of the rate meters for these trials were set at the normal value of 50 sec in the case of the C^{14} meter, and 80 sec in the case of the ventilometer. The values for response time are considered to be suitable for recording physiological events occurring in the human circulatory–respiratory system.

Sensitivity

The sensitivity of the instrument refers to the smallest amount of $C^{14}O_2$ that can be detected in expired air under ordinary experimental conditions. Assuming a background of 110 counts/min, a net counting rate of 55 counts/min can be measured reliably. Applying the overall efficiency factor of 0·27, this becomes 200 dis/min in the active volume of the counter—116 ml—or 1·7 dis/min per ml of expired air. This amount of radioactivity is equivalent to 8×10^{-4} μc/l. Since mixed expired air contains about 1·5 mM of CO_2 per liter,

the limit of measurement of specific activity is approximately 5×10^{-4} μc/mM. This sensitivity permits the use of tracer doses of $NaHC^{14}O_3$ of the order of 0·05 to 0·1 μc per kg, and doses of glucose-C^{14} (for example) of the order of 0·5 to 1 μc per kg.

minute on the Speedomax chart. Any point, multiplied by the count-rate scale factor, and divided by 148 is converted to liters per minute. The reading of the ventilation-scaler register, divided by 148, gives the total ventilation in liters for the period of the test.

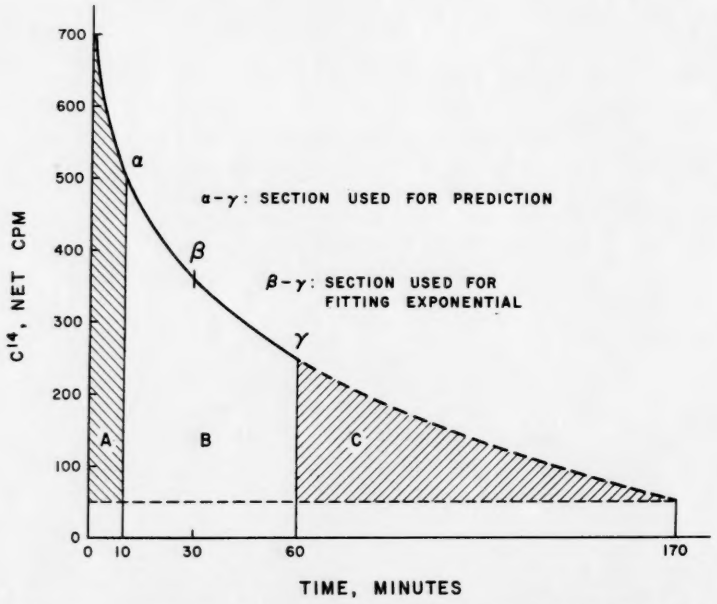

Fig. 9. Schematic curve for the die-away of SA of $C^{14}O_2$ in expired air following a single intravenous dose of $NaHC^{14}O_3$. The portion of the curve: β–γ is used for fitting an exponential to predict the tail of the curve, and also to determine the y-intercept.

Processing of the analog data

Processing of the analog data depends upon the design of the experiment, the type of information desired and the computing facilities that are available. In this section, a brief summary is presented to demonstrate the operations necessary to convert the analog points into a specific activity–time curve for use in an estimate of the size and kinetic behavior of the carbon dioxide pool. An example of the original record for such a study is shown in Fig. 7. For convenience, the SA data are shown diagrammatically in Fig. 9, with a conventional x-axis. The steps involved in data processing follow:

(1) *Output of carbon dioxide.* The ventilation-rate data are recorded as counting rate per

The concentration of carbon dioxide in expired air, as determined by the infrared analyzer, is printed on the Speedomax chart in arbitrary units, designated $\alpha(t)$. These points are converted into percentage CO_2 by the empirically determined calibration factor β according to equation 1.

$$\text{Percentage } CO_2 = \beta \times \alpha(t) \qquad (1)$$

Gas volumes are corrected to s.t.p. by a single factor E. The output of $C^{12}O_2$, in moles per hour, is then given by equation 2.

$$\text{M/hour} = \frac{V}{148} \times \frac{60}{1} \times \frac{\text{Percentage } CO_2}{22{\cdot}4 \times E} \times \frac{1}{100} \qquad (2)$$

59/60
VOL. 7

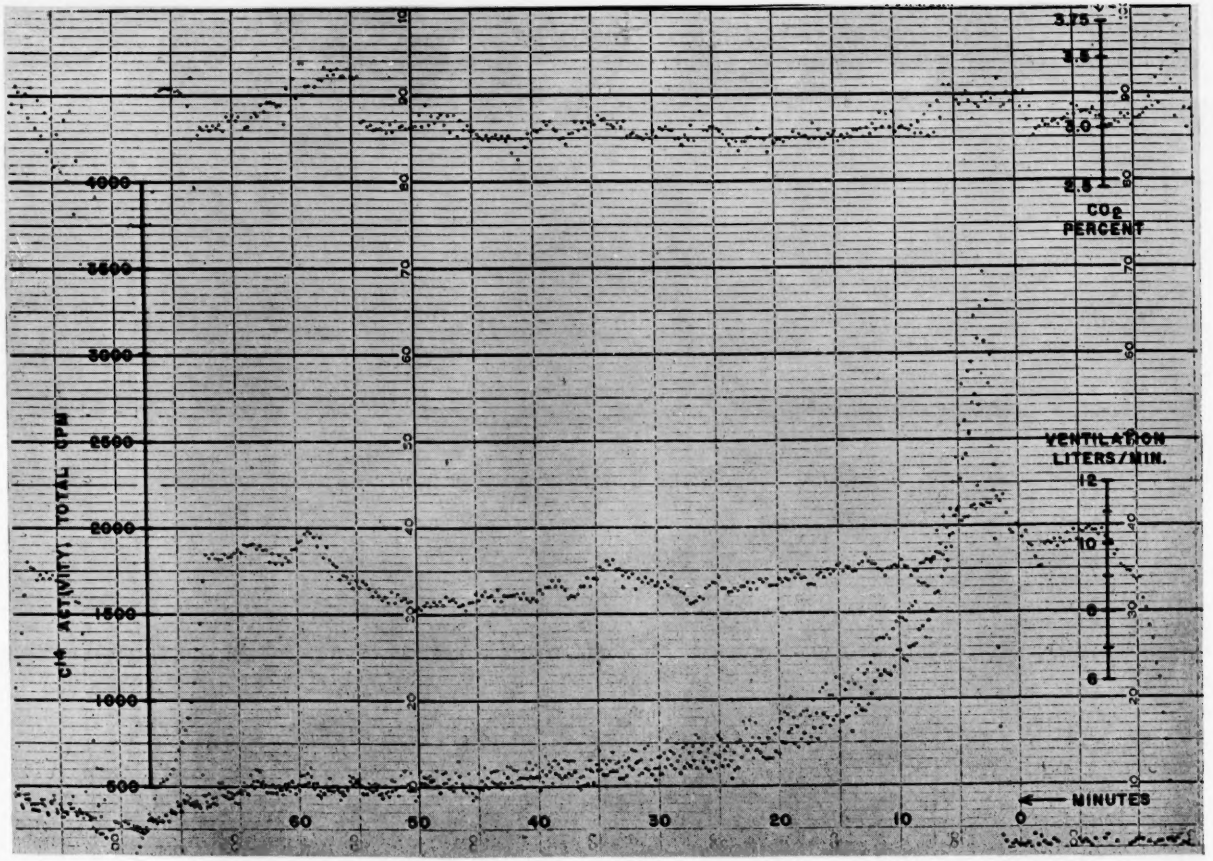

Fig. 7. Reproduction of an original record of data obtained following the intravenous injection of 10 μc of $NaHC^{14}O_3$ at 0 min. The subject donned the face mask at —16 min, and the points on the ventilometer record demonstrate the response time of the startup of this unit. In the original record, radioactivity is printed in blue, and specific activity in red. In this reproduction, the red points appear grey, and lie parallel to and just above the radioactivity curve.

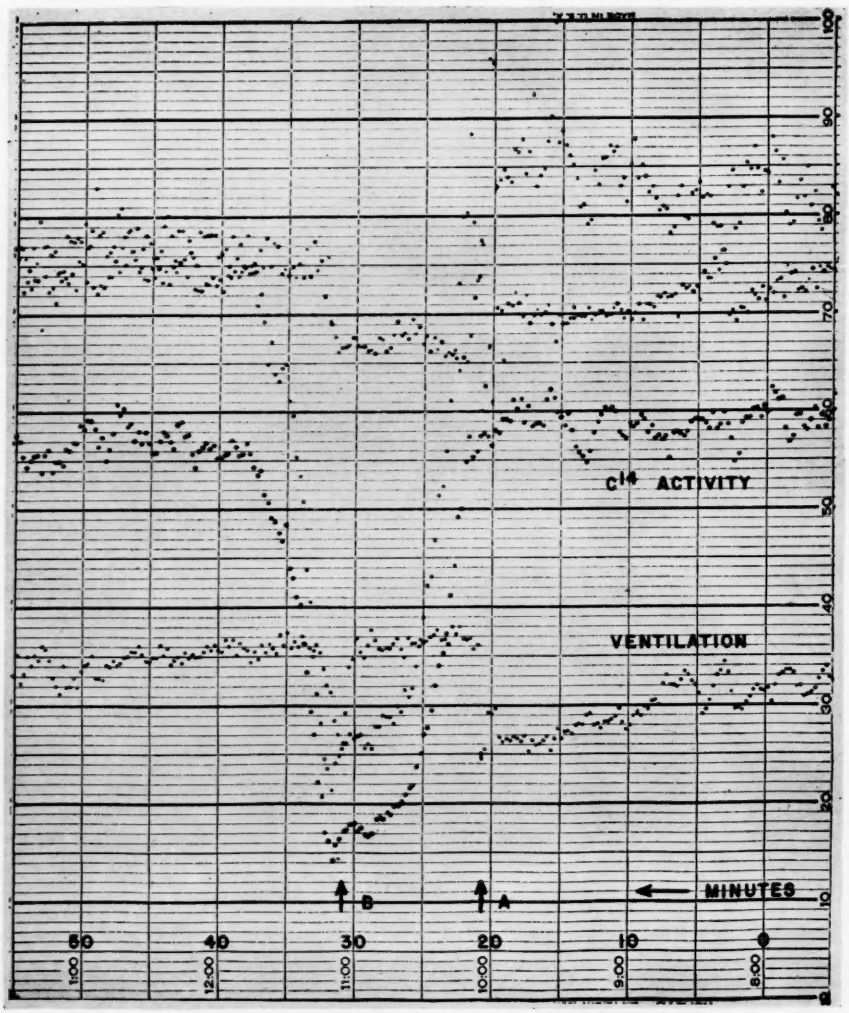

Fig. 8. Reproduction of an original record to demonstrate response time of radioactivity meter. The series of points are—from top to bottom—specific activity, percentage CO_2, radioactivity, and ventilation. At A, the subject who was exhaling $C^{14}O_2$ transferred the mask to another person whose expired air contained no radioactivity. The rate of ventilation of these two individuals differed by approximately 33 per cent, but note the rapid response of the ventilometer to the new rate. At B, when the radioactivity record had returned to the background level, the mask was transferred back to the original subject. The series of points demonstrate the rate of response of the system during startup.

VOL.
7
1959/

where V is the reading of the ventilation meter in counts/min, and percentage CO_2 is determined by equation (1).

(2) *Radioactivity data.* All counting rates are corrected to net counts/min by subtraction of the average background rate. The same correction is applied to the total counts read from the scaler-register at any time during the experiment.

(3) *Specific activity.* The output of the ratio-analyzer which is printed on the chart consists of the ratio: (analog voltage supplied by the radioactivity count-rate meter) ÷ (analog voltage of the CO_2 analyzer). This datum is designated by $y(t)$. To obtain specific activity (C^{14}/C^{12}), $y(t)$ must be multiplied by a conversion factor, γ:

$$\gamma = \frac{100 \times 22{\cdot}4 \times E \times (7{\cdot}07 \times 10^{-12})}{\text{Eff.} \times \text{Vol.} \times \beta} \quad (3)$$

where $7{\cdot}07 \times 10^{-12}$ is the activity-mass coefficient for carbon-14; Eff. is the overall efficiency of the G–M counter determined by calibration with the gas mixture containing $C^{14}O_2$; and Vol. is the active volume of the counter in ml.

If the appropriate assumptions regarding mixing are valid, with this information the principles of isotope dilution can be applied to determine the size and turnover rate of the carbon dioxide pool, either by fitting an exponential to the die-away curve, or by using the Stewart–Hamilton procedure.[2]

(4) *Turnover or flow in carbon dioxide pool.* The result of handling the analog data as described above gives a curve of SA from T_0 to T_t following a single intravenous injection of $NaHC^{14}O_3$. In order to estimate pool size and turnover, assumptions must be made about the nature of the curve for the time beyond $T = 64$ min,* in addition to the usual assumptions about the mixing of a solute in body fluids. It was found that the latter part of the observed SA–time curve appeared to follow fairly closely an exponential form (Fig. 9) and it was decided to project the curve beyond $T = 64$ min by extrapolating according to an exponential law. The exponential used to predict the tail of the SA–time curve (and also to determine the y-intercept) was found by fitting a straight line to values for SA at 30, 45 and 60 min after the injection of the tracer. In general, the amount of tracer C^{14} represented by the area under the predicted portion of the curve was 10–20 per cent of the amount of C^{14} recovered during the period T_0 to $T_t = 64$ min.

In experiments where SA was measured for several hours, we observed progressive deviation from the exponential form. Our analysis makes the assumption that such deviation reflects secondary reactions in which CO_2 is utilized, such as biosynthesis and exchange with bone carbonate. The further assumption is made that relatively little of the CO_2 involved in such secondary reactions returns to the pool during 1 hr. Over longer periods, an increasing amount of such CO_2 returns to the pool, where—if labeled—it can be detected and counted in expired air. With these assumptions, the area under the SA–time curve plus the area under the fitted exponential tail multiplied by the rate of expiration of $C^{14}O_2$ equals the amount of tracer C^{14} which traverses the carbon dioxide pool. This amount includes $C^{14}O_2$ entering secondary reactions, but includes little or no $C^{14}O_2$ returned to the pool from such reactions. This value for turnover, or flow, may be compared to the measured excretion of CO_2 in expired air. The size of the CO_2 pool, and its turnover rate may be estimated by the standard Stewart–Hamilton analysis, or by a standard isotope-dilution calculation using the y-intercept of the exponential.

As would be expected, the value for turnover (or flow) determined by isotope dilution—and expressed in moles per hour—is always greater than the value for the output of carbon dioxide in expired air. The ratio of these two values: (moles per hour in expired air) ÷ (moles per hour flowing through the pool) provides a correction factor which can be applied to measured values for the fraction of any C^{14}-labeled

* The choice of $T = 64$ min was based upon reports that transit time for biosynthesis of compounds for which CO_2 is a precursor is of the order of 1 hr. The actual value—64 min—was chosen for convenience in the machine computation.

substance excreted as carbon dioxide per unit time. The corrected value is, then, a reliable expression of the percentage of dose oxidized to carbon dioxide per unit time.

SUMMARY

The instrument shown in Fig. 1 has been in almost constant use for 18 months up to the time this report was prepared. It was transported to the Second International Conference on the Peaceful Uses of Atomic Energy in Geneva, and operated there daily as a part of the Technical Exhibit. Maintenance has not been a major problem except in the case of the carbon dioxide analyzer. An analog-to-digital convertor will be added to facilitate the processing of data. Prior to the installation of this unit, the graphic record is transcribed to punch cards for machine analysis using either the IBM-650, or the Univac.

The advantages of a continuous measurement of C^{14} radioactivity, and of the total amount of CO_2 in expired air can be summarized briefly:

(1) The procedure is no more disturbing to the subject than is the intermittent collection of single samples of expired air for analysis by conventional radiochemical methods. The average subject soon becomes accustomed to the mask, and appears to remain in a fairly steady state throughout.

(2) With suitable calibration, the overall reliability of data obtained with the continuous instrument should be comparable to data obtained by collecting, as a series of individual samples, all the air expired during the period of the experiment. If smaller samples are taken at longer intervals, the reliability is less. Moreover, if the air obtained as individual samples is assayed as $BaCO_3$, the reliability is considerably less than when the continuous instrument is used.

(3) The volume of data for use in analysis is much greater than when an experiment is performed using a series of samples of expired air. The instrument can be set to print out any information channel as often as four times a minute. The response-time is such that it is possible to conduct experiments during which the rate of appearance of $C^{14}O_2$ varies widely over relatively short periods of time. It is also possible to perform experiments involving changing levels of activity where the rate of ventilation and the excretion of carbon dioxide vary over a wide range.

(4) The information generated by the instrument is available for machine computation, thus making the analysis of data nearly as rapid as the collection of it.

(5) The saving in the time devoted to radiochemical and mathematical analysis more than offsets the initial cost of such an instrument.

Acknowledgements—The authors are indebted to Mr. JOHN STUPKA, director of the Machine Shop of the Argonne Cancer Research Hospital, for his help on many aspects of the development of the instrument. They are also grateful for the assistance of Mr. PAUL MEIER, Associate Professor of Statistics, in the design of the experimental procedure and in the method for analysis of the data.

REFERENCES

1. TOLBERT B. M., KIRK M. and BAKER E. M. *Amer. J. Physiol.* **185,** 269 (1956).

2. MEIER PAUL and ZIERLER K. L. *J. Appl. Physiol.* **6,** 731 (1954).

VOL. 7 1959/

International Journal of Applied Radiation and Isotopes, 1960, Vol. 7, pp. 287–298. Pergamon Press Ltd. Printed in Northern Ireland

Investigation of Distribution and Excretion of C^{14} Tagged Triethylene Thiophosphoramide following Injection by Various Routes*

JEANNE C. BATEMAN, HARRY N. CARLTON, RALPH C. CALVERT and GORDON E. LINDENBLAD
The Departments of Surgery of the Garfield Memorial Hospital and The Washington Hospital Center, Washington, D.C.

(*Received* 3 *August* 1959)

The hematologic depressant action of alkylating agents has been a limiting factor in their usefulness as anti-cancer drugs. Clinically it appears that injection of drug into tumor sites is associated with greater hematopoietic tolerance than is intravenous administration. Due to patient variability this study was planned so that C^{14} labelled N, N′, N″ triethylene thiophosphoramide would be injected first by the intravenous route and at a later date by the intratumor route in the same patient, in a series of eleven advanced cancer cases. Serial blood and urine samples were collected for comparative study of blood levels and urinary excretion rate.

It was observed that higher radioactive blood levels were obtained earlier when satisfactory intravenous injection was achieved than when local injection was given. This probably accounts for the more severe hematologic effect encountered following the former route. More prolonged elevation of serum radioactivity followed local injection suggesting slower delivery of compound. In general, 25 per cent of the first 24 hr C^{14} excretion was achieved in 3 hr and 50 per cent in 6 hr following injection.

Gas-flow scanning of electrophoretic patterns on blood serum revealed all of the isotope to be associated with the protein fractions. Loose chemical association or adsorption phenomena was assumed.

RECHERCHE SUR LA DISTRIBUTION ET L'EXCRÉTION DE LA THIOPHOSPHORAMIDE DE TRIÉTHYLÈNE MARQUÉE AU C^{14} SUIVANT L'INJECTION PAR DIFFÉRENTS CHEMINS

L'action dépressante hématologique des agents alcoylateurs a imposé une limite sur leur utilité comme drogues contre le cancer. À l'aspet clinique il paraît que l'injection d'une drogue dans les sites des tumeurs entraîne une tolérance hématopoïétique plus grande que ne fait l'administration intraveineuse. Vu la variabilité des malades, on a projeté cette recherche de sorte que la N, N′, N″ thiophosphoramide d'éthylène marquée au C^{14} serait injectée d'abord par la voie intraveineuse et ensuite par la tumeur dans le même malade, dans une série de onze cas de cancer avancé. Des échantillons de sang et d'urine furent pris à la série afin de faire la comparaison des niveauz dans le sang et des taux d'excrétion urinaire.

On observa dans le sang des taux de radioactivité plus élevés, et qui parurent plus tôt, lorsqu' on acheva une injection intraveineuse efficace que lorsqu'on fit une injection locale. Ceci donne probablement la raison pour l'effet hématologique plus grave que l'on trouve à la suite de l'emploi du premier chemin. Une augmentation plus prolongée de la radioactivité du sérum suivait l'injection locale, ce qui suggère une livrée plus lente du composé. En générale,

* Aided by Atomic Energy Commission Grant (AT-(30-1)1781) and The District of Columbia Division, American Cancer Society (Doris Speck Fund).

25 pour cent de l'excrétion du C^{14} des premières 24 heures s'acheva en 3 heures, et 50 pour cent en 6 heures, suivant l'injection.

L'examen à l'écoulement de gaz des modèles électrophorétiques produits dans le sérum de sang montra que tout l'isotope s'associait avec les fractions protéiniques. On y supposa une association chimique légère ou des phénomènes d'adsorption.

ИССЛЕДОВАНИЕ РАСПРЕДЕЛЕНИЯ И ВЫДЕЛЕНИЯ ТРИЭТИЛЕНА ТИОФОСФОАМИДА, МЕЧЕНОГО C^{14} И ВВОДИМОГО ПОСЛЕДОВАТЕЛЬНО РАЗЛИЧНЫМИ ПУТЯМИ

Применение алкилирующих агентов как антиканцерогенных лекарств ограничивается тем, что они изменяют картину крови. Клинически доказано, что введение лекарства непосредственно в опухоль обуславливает большую стабильность кровотворения, чем введение внутривенно. Изменчивость кровотворения изучалась введением меченного C^{14} И, И′, И″триэтилентиофосфоамида одним и тем же пациентам (2 случаев запущенных форм рака) сначала внутривенно, а затем непосредственно в опухоль. Пробы крови и мочи собирались для сравнительного определения концентрации вводимого вещества в крови и скорости выделения с мочой. Было показано, что наиболее высокую радиоактивность крови удается достигнуть быстрее при удачном внутривенном введении, чем при местной ин'екции. Вероятно, это об'ясняется более резким нарушением состава крови, которое наблюдается при внутривенном введении. Замедленное повышение радиоактивности сыворотки крови после местной ин'екции свидетельствует о более медленном всасывании вводимого соединения. Было найдено, что 25% от всего выделяющегося в течение первых 24 часов количества C^{14}, получается через 3 часа и 50%—через 6 часов после ин'екции. Было показано, что вся радиоактивность сосредоточена в белковых фракциях сыворотки крови, разделенных электрофоретически. Предполагается, что радиоактивный препарат присоединяется адсорбционно или слабой химической связью.

UNTERSUCHUNG DER VERTEILUNG DER AUSSCHEIDUNG VON C^{14}-MARKIERTEN TRIETHYLENTHIOPHOSPHORAMID NACH INJEKTION IN VERSCHIEDENE BAHNEN

Infolge der hämatologisch schädigenden Wirkung von alkalisierenden Mitteln sind deren Verwendbarkeit als Anti-Krebs-Medikamente begrenzt. Klinisch zeigte sich, dass die Injektion dieser Mittel in das Tumorgebiet hämatopoätisch besser vertragen wird als intravenöse Verabreichung. Wegen der Verschiedenartigkeit des Patientenmaterials wurden diese Untersuchungen in der Weise vorgenommen, dass bei 11 fortgeschrittenen Krebsfällen N,–N′,–N″-Triäthylenthiophosphoramid zuerst auf intravenösem Wege und dann auf intratumoralen Wege jeweils dem Patienten verabreicht wurde. Serienproben von Blut und Harn wurden gesammelt, um Vergleichswerte der Konzentration im Blut und der Ausscheidungsgeschwindigkeit durch den Harn zu bestimmen.

Es wurde beobachtet, dass bei intravenöser Injektion höhere radioaktive Konzentrationen im Blut früher anzutreffen waren, als nach lokaler Injektion. Dies ist wahrscheinlich die Ursache, warum auf dem ersteren Wege ungünstige hämatologische Wirkungen auftreten. Der verlängerte Anstieg der Serumaktivität nach lokaler Injektion deutet auf langsamere Anlieferung der Verbindung. Im allgemeinen wurden 25 Prozent der C^{14}-Ausscheidung der ersten 24 Stunden bereits 3 Stunden und 50 Prozent 6 Stunden nach der Injektion erreicht.

Gas-Durchfluss-Scanning von elektrophoretisch behandeltem Blutserum zeigte, dass die gesamte Menge des Radioisotopes in Verbindung mit der Proteinfraktion zu finden ist. Es wird angenommen, dass lose chemische Bindungen oder Absorptionsphänomene vorliegen.

VOL. 7 1959/6

THE antitumor activity of N, N′, N″ triethylene thiophosphoramide (Thio-TEPA) against a variety of animal[1–4] and human[5–9] neoplasms has been demonstrated. Its almost complete lack of clinical toxicity and its adaptability to a variety of routes of therapy has increased the desirability of this compound in the chemotherapy of solid tumors. However, like other radiomimetic chemotherapeutic agents Thio-TEPA is a bone marrow depressant. Undesirable hematologic effects, especially following the intravenous administration of Thio-TEPA have been described.[10,11] In

an effort to increase therapeutic effectiveness and decrease these unfavorable side effects various routes of administration have been employed. Clinically it has appeared that larger doses of drug could be given with less hematopoietic depression when Thio-TEPA was injected at the tumor site than when it was given by the intravenous route.[12] It seemed desirable therefore to investigate the blood level of the drug, its rate of excretion and localization in tissue following different routes of administration. Isotopic labelling offered a method for such a study. It was further hoped that such a procedure might throw some light on the manner in which Thio-TEPA was transported and excreted.

Earlier experiments[13] in patients given labelled compound indicate that there was a considerable variation in serum levels between patients given similar doses of drug by the same route. Factors such as age, sex, weight, type, extent and duration of disease as well as renal reserve made the pairing of human patients almost impossible. It was, therefore, decided in this study to use the patient as his own control whenever possible. Serial blood and urine samples were analyzed for levels of radioactivity following administration of labelled drug. In order to investigate possible changes in the serum protein components following administration of C^{14} tagged Thio-TEPA, paper electrophoresis studies were done on a selected number of specimens. As a control serial samples of normal serum treated with varying amounts of labelled Thio-TEPA were also analyzed. Chromatograms were made on a limited number of urine specimens obtained from the treated patients. An attempt was made to locate C^{14} distribution in both serum and urine specimens.

Study of tissue localization of the labelled drug in these patients will be reported separately.

OL.
7
9/60

MATERIALS AND METHODS

Eleven patients with advanced neoplastic disease were studied. There were six females and five males. In all cases diagnosis had been made from histopathologic specimens obtained at biopsy or surgery. The diagnoses of these cases were: embryonal carcinoma of the testes 2, mammary carcinoma 1, carcinoma of the large bowel 3, bronchogenic carcinoma 1, carcinoma of the larynx 1, carcinoma of the pancreas 1, lymphoma 2. Table 1 lists the data pertinent to each case. Nine patients received C^{14} labelled Thio-TEPA by the intravenous and intratumor routes; in one of these it was also possible to repeat the study following intragastric instillation of drug. Two patients expired before a second study could be achieved. Unless already hospitalized the patient was admitted on the day preceding the start of a study. Breakfast was withheld on the morning of the study. However, subsequent nourishment was permitted. The patient was maintained on bed rest. As soon as a preinjection specimen of blood was drawn the C^{14} labelled Thio-TEPA was injected either into a vein on the opposite arm or into a selected tumor site. Serial blood collections were then made. Blood specimens were centrifuged and serum decanted as soon as possible. Serum specimens were then refrigerated. Immediately prior to injection of drug the patient's bladder was emptied by voiding or catheterization. Where full co-operation was impossible an indwelling catheter was left in during the study period. Urine volumes were measured; 15 ml aliquots were refrigerated.

For comparison serial blood samples were collected on three fasting untreated normal adults. Following collection of blood during the first hour of study the normal individuals were allowed to eat as had been the patients and also to resume their normal activity. Collection of blood was continued through a total of 12 hr in this group.

N, N′, N″ triethylene thiophosphoramide in crystalline form, in which all the carbons were labelled with carbon-14, was obtained through the courtesy of Dr. W. H. Langham[14] of the Los Alamos Laboratories and the Thio-TEPA prepared was found to contain 5·71 μc/mg of C^{14} radioactivity.

TABLE 1. Diagnosis, history, date and route of administration of C^{14} labelled Thio-TEPA in eleven patients

Case	Age	Sex	Diagnosis and history	Date	Route	Remarks
1	45	F	Reticulum cell sarcoma ovaries, broad ligament. 1952 hysterectomy and post op. X-ray. Jan. 1954 X-ray to jaw. April 1955 chylous effusion, X-ray to chest. July 1955 began chemotherapy.	7 March '58 17 March '58	I.V. Scalp nodule	NPN 38 NPN 47
2	23	M	Embryonal ca. testicle, pulmonary metastases. July 1957 orchiectomy. August 1957 began chemotherapy.	4 November '57 11 November '57	I.V. Rt. neck node	Expired 1 February '58
3	38	F	Mammary ca. Dec. 1951 rt. radical mastectomy, post op. X-ray and castration. Feb. 1957 osseous metastases to cervical and lumbar spine, metastases to left breast, axilla and brain. April 1957 began chemotherapy.	28 October '57	Intrathecal	Expired 3 November '57
4	38	F	Adenoca. sigmoid, metastases to uterus, ileum and nodes. Oct. 1954 int. resection. Nov. 1956 abd. recurrence, pul. metastases, severe anemia. Began chemotherapy.	28 May '57 3 June '57	I.V. Abd. tumor	Expired 10 June '57
5	29	M	Embryonal ca. testicle. June 1957 orchiectomy. July 1957 laparotomy, partial resection tumor, rt. ureteral ligation. Aug. 1957 began chemotherapy.	3 September '57 4 September '57	I.V. Abd. tumor	NPN 65 24 October '57 Expired 27 October '57
6	33	M	Adenoca. ascending colon metastatic to 18/35 nodes. July 1957 resection August 1957 began chemotherapy.	23 August '57 5 September '57 21 January '58	Intra-abd. I.V. Gastric	
7	48	F	Undiff. bronchogenic ca. metastatic to brain. April 1957 X-ray to pulm. lesion. Oct. 1957 expl. craiotomy, began chemotherapy.	4 November '57 8 November '57	I.V. Intrathecal	Expired 14 November '57
8	55	F	Hodgkins Disease, Abd. mass. preauricular, submandibular, cervical, axillary nodes. April 1957 began chemotherapy.	7 March '58 11 March '58	I.V. Cerv. node	Veins sclerosed
9	71	M	Squam. ca. larynx. Jan. 1955 biopsy then X-ray. June 1955 larygectomy and left radical neck dissection. April 1957 X-ray to ant. upper sternum and left supraclavicular area for recurrence. May 1957 began chemotherapy.	24 May '57 8 June '57	I.V. lt. arm. Lt. neck mass	Expired 12 June '57
10	66	M	Adenocarcinoma pancreas Sept. 1957 Biopsy pancreatic tumor, cholecystojejunostomy, ant. gastrojejunostomy. Oct. 1957 began chemotherapy.	8 January '58	I.V.	Expired 11 January '58
11	34	F	Adenocarcinoma ascending colon. March 1957 rt. hemicolectomy. June 1957 colostomy. July 1957 began chemotherapy.	8 November '57	Abd. tumor	Expired 14 November '57

VOL. 7 1959/

Each milliliter of prepared compound gave an average of $1{\cdot}79 \times 10^6$ counts/min. The radiochemical purity of the compound was assayed at the Los Alamos Laboratories. A solution containing 10 mg of labelled Thio-TEPA per ml of pyrogen free distilled water was used in this study. With only one exception 20 mg of compound were administered per dose. One patient received a single dose of 50 mg of Thio-TEPA given by the intratumor route.

A Model No. 314 Tri-Carb liquid scintillation spectrometer was employed for detecting radioactivity in serum and urine samples. The optimal efficiency calibration point for counting C^{14} was ascertained by counting serial dilutions of the labelled Thio-TEPA. All specimens of serum and urine represented 0·05 ml quantities which were obtained with standardized micro-pipettes of 0·05 ml capacity with a measurement of error of less than 1·0 per cent for 0·005 ml. Each specimen was added to 10·0 ml of scintillator solution which was made by the addition of 7·0 ml of 2,5-diphenyloxazole, 300·0 mg per cent in toluene, to which was added 3·0 ml of 100% ethanol. In these proportions serum was found to be soluble. Five dram low potassium content vials were used for counting samples. The latter were placed in a deep freeze for a minimal time of 10 min, then shaken vigorously before being counted. A 30 min average background count was taken. Each sample of urine or serum was counted for a period of 3 min, and an average taken for the count per minute. The background count was deducted from the latter figure.

Serum protein partition was studied by a closed strip method of paper electrophoresis,[15] in which a barbiturate buffer was employed. Bromphenol Blue was used to dye the dried strips. Densitometry and integration of pattern densities then were accomplished. Gas-flow scanning of the electrophoretic patterns demonstrated very low radioactivity levels when the patterns were scanned following the dye and acid washing procedures. After it became apparent that the radioactivity on the strip was largely lost during the dye and washing steps, gas-flow counting was done prior to these procedures.

Urine chromatograms were made by spotting 0·1 ml samples of urine on Whatman No. 3 and No. 52 papers. The system for chromatography was carried out in a saturated atmosphere (acetone 1 part, distilled water 3 parts) in a constant temperature assembly at 80°F. The radioactivity levels were ascertained by continuous gas-flow counting.

OBSERVATIONS

Serum levels of radioactivity

Table 2 gives the serum levels of radioactivity following intravenous and local administration of 20 mg of C^{14} labelled triethylene thiophosphoramide. For technical reasons it was not possible to get complete studies on all of the patients.

Each patient was given the first dose of drug by the intravenous route except in cases 3, 6, 10 and 11. Patient No. 10 expired before a second dose (intravenous) of drug could be given. In patient No. 11 local injection only was employed and in this case 50 mg of the drug were injected into a huge recurrent tumor involving the right half of the abdomen.

Radioactivity was detectable within 30 sec of administration in all except three studies (cases 4, 6 and 9). In case 6 following administration of C^{14} tagged Thio-TEPA by stomach tube, no counts were obtained prior to the 2-min sample following which there was a slow increase up to the 10-min sample with a subsequent decline. In case 4, following administration of tagged drug into a hard abdominal tumor, radioactivity could not be demonstrated in serum at any time. This also happened when drug was injected into the left antecubital vein in case 9. The latter patient had a massive recurrent tumor of the left neck following treatment for squamous cell carcinoma of the larynx. Therapy had consisted of primary irradiation, then laryngectomy and a left radical

TABLE 2. Serum levels of radioactivity following intravenous and local administration of 20 mg of C^{14} labelled Thio-TEPA. Counts per minute per 0·05 ml sample

Case	Route	30 sec	1 min	2 min	3 min	4 min	5 min	6 min	7 min	9 min	10 min	12 min	15 min	30 min	1 hr	3 hr	6 hr	9 hr	12 hr	24 hr
1	Intravenous	52	227	—	223	165	140	—	151	150	157	133	112	81	92	82	60	—	58	47
	Scalp nodule	43	—	84	—	100	117	118	161	210	190	187	172	328	140	103	102	89	78	44
2	Intravenous	164	184	—	228	251	241	—	—	—	223	—	193	—	—	169	177	—	148	142
	Cervical node	140	142	144	134	144	154	—	—	—	161	—	251	—	240	188	182	—	228	157
3	Intravenous	771	746	—	615	559	510	—	—	—	—	—	338	—	330	—	—	—	210	—
	Intrathecal	129	—	131	142	142	174	—	—	—	226	—	235	—	—	308	—	—	—	—
4	Intravenous	76	268	306	114	108	128	—	—	—	105	—	106	—	84	104	81	—	88	79
	Abdominal tumor	LB	LB	LB	LB	LB	LB	—	—	—	LB	—	LB	—	LB	LB	LB	—	LB	LB
5	Intravenous *	61	69	—	—	—	—	—	—	—	—	—	131	—	92	—	53	—	53	60
	Abdominal tumor	43	65	49	—	—	64	—	—	—	52	—	77	—	86	74	78	—	46	59
6	Intravenous	64	60	96	96	—	152	—	—	—	75	—	—	—	112	100	100	—	124	60
	Intraperitoneal	LB	LB	LB	—	LB	LB	—	—	—	35	—	35	—	29	33	LB	—	LB	LB
	Gastric tube	LB	LB	LB	—	15	47	—	—	—	135	—	65	—	55	56	41	—	40	31
7	Intravenous	60	55	79	127	108	—	—	—	—	193	—	—	—	193	175	162	—	158	104
	Intrathecal	111	120	—	144	—	152	168	—	—	150	—	142	171	206	251	—	—	—	211
8	IV-Hand vein *	37	42	—	43	—	46	—	66	—	46	52	—	43	50	43	46	—	44	41
	Cervical node	40	42	32	30	40	30	—	32	34	50	54	158	46	70	40	20	—	LB	LB
9	Intravenous †	LB	LB	LB	LB	LB	LB	—	—	—	LB	—	LB	—	LB	LB	LB	—	LB	LB
	Left neck tumor †	87	109	99	73	—	103	—	—	—	52	—	60	68	77	80	70	—	77	52
10	Intravenous *	34	62	57	52	64	100	—	—	—	96	—	91	—	83	67	53	—	78	33
11	Abdominal tumor ‡	140	126	168	218	—	296	—	—	—	408	—	605	—	504	315	215	—	206	158

LB Counts below background.
* Marked sclerosis of veins secondary to multiple venipunctures.
† Alteration vascular structures left neck and upper chest due to extensive tumor and post-radiation fibrosis.
‡ 50 mg tagged Thio-TEPA injected.

neck dissection and subsequently another course of X-ray therapy to the left supraclavicular area and upper sternum. Although no autopsy was done it was presumed that the vascular pattern was so deranged by surgery, X-ray and tumor that drug was trapped in the left upper extremity.

An initial high peak at 1 min was followed in cases 1, 4 and 7 by a second peak which probably represented recirculation. In case 3 an intravenous study was done subsequent to intrathecal injection of labelled drug. High serum levels of radioactivity were maintained in this patient and were associated with low levels in the urine (Table 3). The patient was in a terminal state and presumably was excreting very little drug. In cases 5, 8 and 10 sclerosis of veins secondary to multiple venipunctures was considered responsible for the initial low counts and slow rise to maximum levels.

An attempt was made in each case to inject drug into an accessible tumor site in order to obtain studies comparable to those following intravenous treatment. In case 1 a scalp nodule was injected; in cases 2 and 8 metastatic cervical nodes were used. In cases 3 and 7, in whom multiple metastases were present, the tagged drug was injected intrathecally at the time of a spinal tap. Three patients received injection of drug into large abdominal tumors; one into a large neck tumor. In one patient (case 6) drug was given by the intraperitoneal route and subsequently through a stomach tube.

The serum level of radioactivity following local administration of drug appeared to be related to the vascularity of the site of injection. The rapid delivery of radioactivity into the blood following intrathecal injection was striking. In only one instance following local injection could no serum activity be demonstrated. The recurrent abdominal tumor in this patient (case 4)

VOL. 7 1959/

TABLE 3. Urine levels of radioactivity following administration of C^{14} labelled Thio-TEPA. Total counts excreted per collection interval

Case	Route injection	15 min	30 min	1 hr	3 hr	6 hr	9 hr	12 hr	18 hr	24 hr	48 hr
1	Intravenous	—	—	34,960	4,515,000	6,783,000	—	10,626,000	—	1,176,000	—
	Scalp nodule	—	—	2,269,000	3,226,440	19,570,000	—	7,864,000	—	1,392,000	4,216,000
2	Intravenous	—	—	—	8,660,000	13,800,000	—	11,950,000	—	6,500,000	—
	Cervical node	—	—	—	14,000,000	9,650,000	8,650,000	4,630,000	—	1,240,000	—
3	Intravenous	36,400	—	26,840	—	347,000	—	3,620,000	—	2,217,600	2,816,000
	Intrathecal	—	—	21,920	9,736,000	—	—	7,323,200	—	3,080,000	—
4	Intravenous	271	8,803	138,104	637,468	1,074,416	425,944	1,487,640	517,040	1,152,220	—
	Abdominal tumor	2,200	8,900	29,500	66,000	120,600	168,420	128,000	25,000	168,000	—
5	Intravenous	—	—	4,335,600	25,562,000	12,014,800	—	—	—	5,082,700	—
	Abdominal tumor	—	—	308,040	5,325,600	8,271,200	—	5,331,200	—	7,947,600	—
6	Intravenous	—	—	3,042,000	6,450,000	13,738,200	—	8,870,000	—	6,020,000	—
	Intraperitoneal	58,500	—	1,111,600	10,040,800	11,304,000	—	—	—	8,989,200	—
	Gastric tube	—	711,680	1,712,600	6,191,600	9,689,000	5,737,500	3,796,040	3,039,000	2,289,040	—
7	Intravenous	—	2,121,000	—	6,779,500	8,025,600	—	7,380,000	—	3,494,400	—
	Intrathecal	122,400	48,160	74,400	9,178,620	2,527,600	10,405,200	6,351,900	—	11,393,400	—
8	Intravenous	—	18,500	2,125,500	3,498,600	4,921,400	—	6,580,000	—	3,672,000	—
	Cervical node	43,200	268,180	84,960	4,410,000	4,218,800	—	17,792,000	—	4,400,000	—
9	Intravenous	—	—	15,600	170,100	758,200	—	136,000	LB	LB	LB
	Neck tumor	—	1,124,720	893,200	1,893,200	2,586,040	—	322,400	726,000	870,000	—
10	Intravenous	—	618,800	7,021,500	16,104,000	15,660,000	—	20,791,000	—	14,257,600	—
11	Abdominal tumor	—	—	6,480	88,400	5,001,600	2,915,100	265,320	—	10,339,140	—

was found at autopsy to be relatively avascular. The injected drug probably remained localized or entered the general circulation at a level lower than background counting.

In general, higher earlier peaks of radioactivity in serum were noted following satisfactory intravenous injection than following local administration of drug (Fig. 1). There was a tendency for a more prolonged elevation of serum radioactivity following the latter route, however. In all but two patients (cases 2 and 7) who received the standard dose and in the one case (11) who received a larger dose, the serum activity had dropped to a fairly low level by 24 hr. In case 2 post mortem examination revealed a right hydronephrosis. Patient 7 was in poor condition following an exploratory craniotomy and expired within a few days following these studies. Although renal function studies were not done, gross impairment can be assumed and considered responsible for delayed excretion in the two latter cases.

Urine excretion of radioactivity

The urine levels of radioactivity following injection of C^{14} labelled triethylene thiophosphoramide in eleven patients are given in Table 3 as total counts per time interval. Each count represents the total amount of C^{14} excreted from the last previous specimen to the time indicated for the specimen being counted.

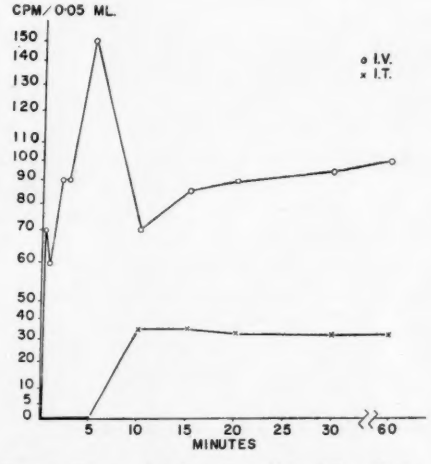

FIG. 1. Serum levels of radioactivity from C^{14} labelled Thio-TEPA in case 6 following intravenous and intratumor injection. Logarithm of counts/min 0·05 ml serum plotted against time.

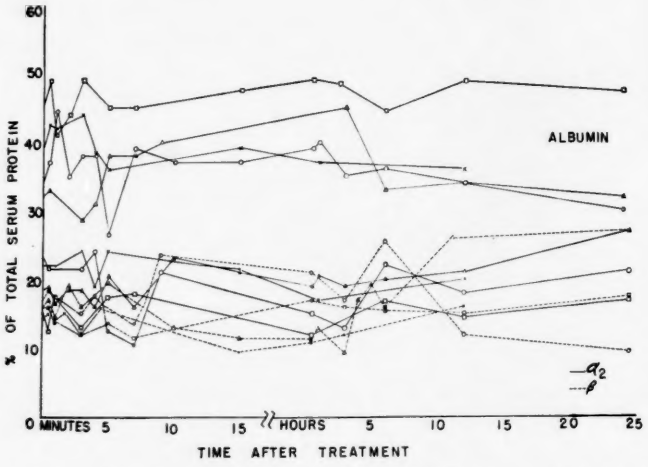

FIG. 2. Percentage of total serum protein for albumin, α_2- and β-globulin plotted against the time following intravenous administration of C^{14} labelledThio-TEPA.

Except in two cases (7 and 9) very little isotope was excreted by 30 min. Counts of 2×10^6 or over were obtained by 1 hr in five patients (5, 6, 7, 8 and 10) who received labelled drug by the intravenous route and in two instances (1 and 9) following local injection of the drug. In one case (case 6) in which tagged drug was administered through a stomach tube there was also an early high count. A comparative 30-min urine count was not made in this case following intravenous injection. It was undetermined, therefore, if an equivalent amount of isotope was excreted as when drug was given by the intragastric route. At 1 hr the total excreted tag was greater following intravenous injection than following intragastric administration in this patient and least following intraperitoneal injection. In the majority of cases excretion of isotope diminished after the first 6 hr following administration. In two instances (cases 1 and 3) in which urine collections were made for the second 24-hr period isotope excretion was relatively low. In case 1 who had received tagged drug into a scalp nodule, the second 24-hr urinary excretion was 11 per cent of that excreted in the first 24 hr. Patient 3 who maintained a high serum level of radioactivity following intravenously injected drug excreted 30 per cent as much tag during the second 24 hr as during the first. It was assumed that delayed excretion was attributable to the patient's terminal state. Case 9 is of interest because of the low excretion of isotope following intravenous administration of drug. This was the patient in whom no blood levels were demonstrable and in whom it was assumed that drug was trapped and largely fixed in tissues peripheral to tumor and scar which blocked return circulation.

Serum electrophoretic studies

Serum electrophoretic studies were obtained on serially collected blood specimens in four patients (cases 2, 3, 7 and 10) who had been given C^{14} labelled Thio-TEPA by the intravenous and in three patients (cases 2, 3 and 11) by the intratumor route. The changes following the intravenous injection of drug are illustrated in Fig. 2. Percentage of protein for albumin, α_2 and β-globulin are plotted against time. Changes following intratumor injection showed a similar trend and therefore are not illustrated. The data from the normal untreated group are presented in Fig. 3.

The lability of the serum protein components was an unexpected finding. It was first considered possible that it was related

VOL. 7 959/

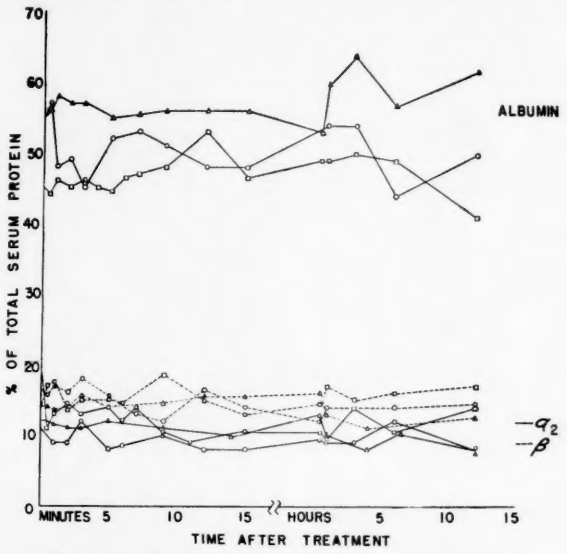

FIG. 3. Percentage of total serum protein for albumin, α_2- and β-globulin plotted against time following institution of serial bleedings in normal untreated adults.

to the injection of a highly reactive chemical compound. An early effect might be expected and there did appear to be a suggestive decrease in β- and a slight increase in α_2-globulin in the first 20 min. However, statistical analysis of these data* showed no significant difference in the treated patients other than the lower percentage of serum albumin as compared to that in normal individuals. Subnormal levels of serum albumin are a frequent finding in the blood of cancer patients. It might be pointed out that the rather marked drop noted in one normal person (Fig. 3) occurred in an individual who exhibited considerable apprehension when subjected to veni-puncture. The other two normal individuals were unmindful of the procedure.

In an effort to obtain further information related to the electrophoretic changes in human serum following contact with C^{14} labelled Thio-TEPA a series of *in vitro* studies were done on serum obtained from healthy individuals. Each series was represented by an untreated control and two separate specimens of serum treated with tagged Thio-TEPA in quantities representing 100 and 200 times the usual dose of drug expected to reach an equivalent amount of serum following intravenous injection of 20 mg of Thio-TEPA. The serum in each case was placed in a test tube fitted with a revolving "paddle" type stirring rod and kept at a constant temperature of 37·5°C. Samples were withdrawn prior to addition of drug at $\frac{1}{2}$, 1, 3, 5, 7, 9, 12, 15, 30 and 60 min thereafter. An electrophoretic study was then made on each sample.

A separate graph was made for each serum on which the albumin fraction for specimens with no added drug, specimens containing 100 times the standard dose and with 200 times the standard dose were plotted against time. Fig. 4 represents the study on one serum. Because the percentage of the various proteins were correlated, if there existed an effect at all it should have shown up in the albumin fraction. On analysis of the data* from this study the addition of 100 and 200 times the usual dose

* Kindly done by Doctors E. Gehan, M. Schneiderman and J. McKeon of the National Institutes of Health, Bethesda, Maryland.

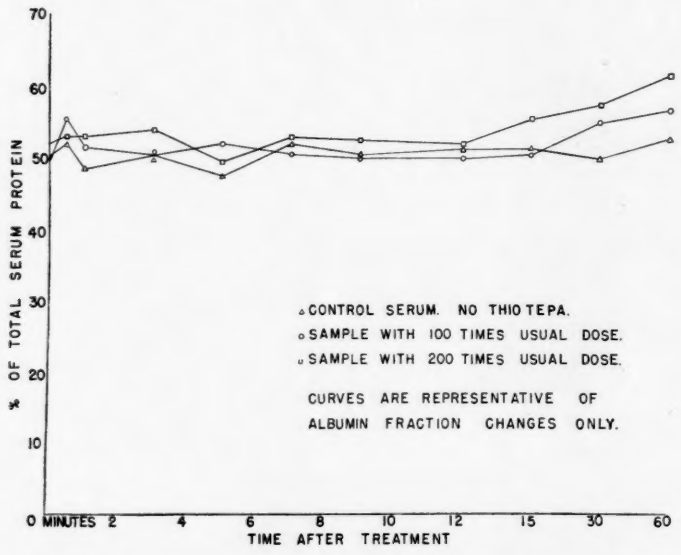

FIG. 4. Percentage of total serum protein for albumin plotted against time in normal serum, normal serum treated with 100 times usual dose C^{14} labelled Thio-TEPA and normal serum treated with 200 times usual dose C^{14} labelled Thio-TEPA and maintained at 37·5°C.

VOL. 7 1959/6

of C^{14} labelled Thio-TEPA to normal serum appeared to have no effect on the protein partition.

Gas-flow counting of the electrophoretic patterns (done prior to the dyeing procedure) revealed the degree of radioactivity to be in close approximate intensity with the percentage amount of protein present on the dyed pattern. The recorded levels of radioactivity found to exist between protein bands was no greater than the background activity. It would seem from this finding that the C^{14} was attached only to protein material rather than being dispersed over the entire pattern.

Electrophoretic studies done on C^{14} labelled Thio-TEPA alone employing identical factors as for serum protein separations showed that there was less than 0·5 in. migration of the 0·01 ml sample. This finding further confirmed the impression that C^{14} tagged Thio-TEPA, while in the blood stream, was attached in some way to the protein components of the serum.

Urine chromatography

Chromatograms were made from a total of fifty serially collected urine specimens obtained over a period of 24 hr from twelve patients, four of whom received labelled C^{14} Thio-TEPA by the intravenous route and eight by local injection. Levels of radioactivity from two to fifteen times the recorded background were found at R_f values of 0·45, 0·68, 0·72, 0·87 and 0·95. The radioactive level observed at R_f values of 0·68 and 0·87 represented the most consistently found peaks, an incidence of twenty-four occurrences each for the fifty chromatograms evaluated. The peak at 0·87 probably represented unchanged drug; the other peaks were not identified. Chromatograms of C^{14} tagged Thio-TEPA alone in an identical solvent system were characterized by a single peak at R_f 0·87. The presence or absence of these radioactive levels bore no relation to the time following the injection of isotopically labelled compound or to the level of radioactivity observed in the specimen. In addition to the observed peaks, a low level of radioactivity of one to one and one half times background was dispersed over the entire chromatogram. This was in

contrast to the observation on serum where radioactivity was found to be associated only with protein fractions.

Discussion

Rapid disappearance of radioactivity of isotopically labelled alkylating agents from the blood in cancer patients and animals has been reported by SMITH *et al.*[16] NADKARNI[17] observed removal of over 90 per cent of injected isotopically labelled triethylene melamine, triethylene phosphoramide and myleran within 2 to 3 min. Appreciable levels of radioisotope were observed in human plasma up to 12 hr following injection of C^{14} tagged N′-(oxapentamethylene)-N′, N″-diethylene thiophosphoramide by MALLER *et al.*[18]

No attempt was made in this study to calculate the total persisting dose of labelled drug in the circulating plasma, extracellular fluid or total body water at any one time. It was felt that such determinations either would have necessitated unwarranted assumptions regarding body fluids which were deranged in advanced debilitating disease or would have involved application of a number of tests impractical at the time of study. The use of the same individual for two studies, i.e. administration of drug by two different routes, at fairly close intervals, was intended to compensate for the individual physiologic variability which tends to confuse clinical experimentation of this type.

From the observations in this study it is apparent that numerous factors determine not only the height but the duration of the blood level of an agent such as Thio-TEPA following administration to human patients. Of primary importance is the accessibility of the drug to the general circulation. Should some block be present in the path of an injected vein, and this is not infrequent in patients who have been subjected to many procedures, drug may reach the general circulation very slowly. On the other hand, injection of a very vascular local site, such as the scalp or a vascular tumor, may result in rapid entrance into the general circulation with early high levels. Injection of hard, sclerotic tumor will delay appearance of drug in the blood stream and, as in one case herein reported, completely prevent detectable amounts of drug from entering the blood stream.

Blood levels of drug appear also to be affected by rate of urinary excretion. High blood levels were seen in a patient whose urinary output was low. The terminal state of the patient at the time of the study was probably responsible for poor renal function. This would substantiate clinical observations that azotemic patients do not tolerate alkylating drugs in the same doses as do patients with satisfactory renal function.

The rapid delivery of the drug into the general circulation following intrathecal injection precludes the existence of a blood brain barrier to this alkylating agent. This fact may be of some clinical importance in the treatment of primary brain tumors or of intracranial metastatic lesions provided that these neoplasms are themselves at least relatively vascular.

The rapid absorption of drug following gastric instillation in one case was interesting. However, it should be pointed out that the drug was administered in solution and not in a tablet or capsule form.

Crosslinking of bovine serum albumin incubated with the compounds nitrogen mustard and myleran, resulting in an increase in molecular weight, has been reported.[19] The possibility that a similar effect on the serum of human patients following injection of Thio-TEPA might be responsible for the lability of the resulting electrophoretic patterns seen in this study was considered. However, the change in serum protein pattern occurring in some untreated normal individuals following venipuncture as well as the stability of the serum protein pattern following exposure *in vitro* to large doses of Thio-TEPA suggests other mechanisms. The possibility that such events may be mediated by the adrenals in response to stress alone and/or the direct effect of the alkylating agent on the adrenal gland must be considered. Preliminary studies on mice and autopsy material obtained from patients included in this study* suggest that there is

* To be reported later.

considerable localization of labelled Thio-TEPA in the adrenals. Apparently C^{14} tagged Thio-TEPA is either adsorbed by the serum proteins or is loosely bound to them. None was found free in the serum. However, such was not the situation in the urine where diffuse dispersion of radioactive tag was encountered.

SUMMARY AND CONCLUSIONS

(1) N, N′, N″ triethylene thiophosphoramide isotopically labelled with carbon-14 was administered by intravenous and by local routes to a series of far-advanced cancer patients. In eight individuals it was possible to give the drug by both routes: in one additional patient drug was also administered by intragastric instillation; two individuals were treated by one route alone.

(2) Higher blood levels of C^{14} were obtained earlier when satisfactory intravenous injection of tagged drug was achieved than when local injection was given. A more prolonged elevation of serum isotope followed administration by the latter route. In all cases serum activity had dropped to a fairly low level by 24 hr except in two patients assumed to have depressed renal function and in a third who received a large single dose of drug into a sclerotic tumor.

(3) In general, 25 per cent of the first 24 hr excretion of drug was achieved in 3 hr and 50 per cent in 6 hr. Only a small percentage of tag appeared to be excreted during the second 24 hr following administration.

(4) Delivery of the drug into the general circulation after intravenous administration was markedly slowed in the presence of venous sclerosis proximal to the site of injection. Local injection into the highly vascular area resulted in prompt general circulation of drug.

(5) Changes in serum protein pattern following administration of labelled Thio-TEPA were marked but variable. They appeared to be related to some factor other than a direct effect of an alkylating agent. A stress factor was postulated.

(6) Scanning of electrophoretic patterns on blood serum revealed all of the isotope to be associated with protein fractions. A loose chemical association or adsorption phenomena was assumed.

(7) Scanning of serial urine chromatograms revealed a low general dispersion of isotope in addition to irregular concentrations at seven peaks.

VOL. 7 1959/6

REFERENCES

1. Crossley M. L., Allison J. B., Parker R. P., Kuh E. and Seegar D. R. *Proc. Soc. Exp. Biol., N.Y.* **83,** 438 (1953).
2. Personeus G., Halliday S. L., McKenzie D. and Williams J. H. *Proc. Soc. Exp. Biol, N.Y.* **81,** 614 (1952).
3. Shay H., Gruenstein M. and Atwater J. *Proc. Amer. Assoc. Cancer Res.* **11,** 1 (1953).
4. Sparks S. J., Stevens M. L., Landes M. J., Halliday S. L., McKenzie D. and Williams J. H. *Blood* **8,** 653 (1953).
5. Bateman J. C. *New Engl. J. Med.* **252,** 879 (1955).
6. Bateman J. C. and Carlton H. N. *J. Amer. Med. Assoc.* **162,** 701 (1956).
7. Bateman J. C. and Winhip T. *Surg. Gynec. Obstet.* **102,** 347 (1956).
8. Shay H. and Sun D. C. H. *Cancer* **8,** 498 (1955).
9. Smith N. J., Rosello S., Chile S. and Shay H. *J. Pediat.* **46,** 493 (1955).
10. Olson K. *Ann. N.Y. Acad. Sci.* **68,** 1018 (1958).
11. Ultmann J. E., Hyman G. A. and Gelhorn A. *Ann. N.Y. Acad. Sci.* **68,** 1007 (1958).
12. Bateman J. C. *Ann. N.Y. Acad. Sci.* **68,** 1057 (1958).
13. Bateman J. C. Unpublished data.
14. Langham W. Personal communication.
15. Block R. J., Durrum E. L. and Zweig G. *A Manual of Paper Chromatography and Paper Electrophoresis.* Academic Press, New York (1957).
16. Smith P. K., Nadkarni M. V., Trams E. G. and Davison C. *Ann. N.Y. Acad. Sci.* **68,** 834 (1958).
17. Nadkarni M. V., Trams E. G. and Smith P. K. *Proc. Amer. Assoc. Cancer Res.* **2,** 235 (1957).
18. Maller R. K., McIver F. A. and Heidelberg C. *Cancer Res.* **17,** 287 (1957).
19. Stacy K. A., Cobb M., Cousens S. F. and Alexander P. *Ann. N.Y. Acad. Sci.* **68,** 682 (1958).

International Journal of Applied Radiation and Isotopes, 1960, Vol. 7, pp. 299–305. Pergamon Press Ltd. Printed in Northern Ireland

Iodine–131 Thyroid Uptake Study of Endemic Goiter Patients in Taiwan

TIEN-CHENG KAO, KUANG-CHU WANG, SHEH-FANG YANG and JUI-SAN CHEN

College of Medicine, National Taiwan University, Taipei, Taiwan

(*Received* 3 *February* 1959)

A study of thyroid uptake in the endemic goiter area of the Hsin-Chu district in Taiwan indicates that more than half the patients showed an iodine-131 uptake of more than 50 per cent. Eighty-eight persons with goiter were examined, half of them adults and half of them school children. In general the children had a higher uptake than the adults, but the adults showed signs and symptoms of hypothyroidism not found in the children.

ÉTUDE DE L'ABSORPTION DE L'IODE-131 PAR LA GLANDE THYROÏDE CHEZ DES TAIWANNAIS SOUFFRANTS DU GOITRE ENDÉMIQUE

Une étude de l'ablation thyroïde faite dans la région de goitre endémique du pays Hsin-Chu au Taiwan indique que plus de la moitié des malades montraient une ablation d'iode-131 de plus de 50 pour cent. On a examiné quatre-vingt-huit souffrants du goitre, dont la moitié adultes et la moitié enfants écoliers. Pour la plupart les enfants présentaient une ablation supérieure à celle des adultes, mais les adultes portaient des indications et des symptômes de l'hypothyroïdisme qui étaient absents chez les enfants.

ИССЛЕДОВАНИЕ УСВОЯЕМОСТИ I^{131} ЩИТОВИДНОЙ ЖЕЛЕЗОЙ ПРИ ЗАБОЛЕВАНИИ ЭНДОМИЧЕСКИМ ЗОБОМ НА ТАЙВАНЕ

Изучение усвоения иода-131 щитовидной железой в районах эндемического зоба на Тайване показало, что больше половины пациентов усваивают иод-131 более чем на 50%. Проводились набдюдения над 88 больными зобом, половина из которых были взрослые, а вторая половина—дети школьного возраста. Дети обладали большей усвояемостью чем взрослые, но только у взрослых обнаруживались симптомы пониженной функции щитовидной железы.

UNTERSUCHUNGEN ÜBER DIE J-131 AUFNAHME DER SCHILDDRÜSE BEI ENDEMISCHEN KROPF-PATIENTEN IN TAIWAN

Eine Untersuchung der Schilddrüsen-Funktion in dem endemischen Kropfgebiet im Hsin-Chu-Bezirk in Taiwan ergab, dass mehr als die Hälfte aller Patienten eine über 50 prozentige J-131-Aufnahme zeigten. 88 Kropfpatienten wurden untersucht die Hälfte davon waren Erwachsene, die andere Hälfte Schulkinder. Im allgemeinen zeigten die Kinder eine höhere Aufnahme als die Erwachsenen, hingegen zeigten die Erwachsenen Symptome von Hypothyroidismus, der bei den Kindern nicht aufgefunden wurde.

INTRODUCTION

GOITER is exceedingly common in Taiwan. MAXWELL[1] records that in certain mountain villages almost all the inhabitants have the disease. Affected areas include the Ying-Ko area of Taipei district in the north, the Tachia neighborhood in the west, and the areas of Pinan and Dainan in Taichung district in the eastern part of the island.

TABLE 1. Prevalence of goiter in Taiwan

Author	Area	Persons examined	With goiter	Incidence in per cent
Kawaishi	Entire island	318,116	26,979	8·5
Hashimoto and Kyo	Ying-Ko	23,463	6,200	26·4
Hashimoto and Sha	Pinan and Dainan	4,060	745	18·3
Chen *et al.*	Liu-Chia	2,186	1,104	52·3

Surveys of prevalence formerly have been made by KAWAISHI and his co-workers[2], and recently by CHEN and his co-workers[3]. Table 1 indicates the prevalence of goiter in Taiwan.

Insufficient iodine intake may be the main cause of goiter in Taiwan. KAWAISHI, however, suggests that iodine deficiency is not entirely responsible and that geochemical and climatic factors that raise the demand for iodine must also be taken into account.

The uptake of iodine by the thyroid of the patient with endemic goiter is usually found to be greater than normal. This was recognized long ago from a study performed with stable iodine and has been amply confirmed by the more direct measurement made with I^{131}.

A project was started for I^{131} thyroid uptake study of endemic goiter patients on this island. This I^{131} uptake study was made in these areas where iodized salt had not been supplied. The first area was Liu-Chia area of Hsin-Chu district. This area is located about 40 miles south of Taipei, and is in the northwestern part of Taiwan. This paper reports the I^{131} uptake. Conversion ratio and urinary discharge problems will be published later.

VOL. 7 1959/

MATERIALS AND METHOD

One hundred patients in the Liu-Chia endemic-goiter area were selected for I^{131} thyroid uptake measurement. Clinical examination was performed and the basal metabolic rate was measured in every patient. Iodine-131 uptake measurement was made on eighty-eight patients out of the 100; twelve did not come back for counting.

The uptake measurement was made 24 hr after administration of 25 μc (Radiocaps I^{131}, Abbot Laboratory) and the ORINS standard neck phantom was used for 100 per cent standard measurement. The measurements were taken by a scintillation counter with a $3/4 \times 3/4$-in. NaI crystal, and collimation. We used the ORINS standard method,[4,5] "A" and "B" filters, and the 10-in. distance from the crystal center to the neck surface.

RESULTS OF I^{131} UPTAKE AND CLINICAL FINDINGS

Criteria for the classification of the degrees and kinds of endemic goiter are as follows:

Group I Persons with palpable goiters. The slightly diffuse, enlarged gland is not visible with the head in the normal position but is readily palpable.

Group II Persons with visible goiters. The gland is moderately diffusely enlarged and readily visible with the head in the normal position.

Group III Persons with conspicuously enlarged goiters.

Group IV Persons with diffusely huge goiters.

Group V Uninodular goiter of small size (SUN).

Group VI Uninodular goiter of moderate size (MUN).

TABLE 2. Iodine-131 uptake in schoolboys with endemic goiter

No.	Age	Goiter	Uptake (%)	BMR (%)	Symptoms	Signs
1	7	I	71	+15	—	—
2	7	II	62	+14	—	—
3	7	I	65	+10	—	—
4	7	I	38	+2	—	—
5	8	I	55	−15	—	—
6	8	I	63	+9	—	—
7	8	I	28	+17	—	—
8	9	I	77	+8	—	—
9	9	II	71	+9	—	—
10	9	I	78	−12	—	—
11	10	II	71	+4	—	—
12	10	II	67	+15	—	—
13	10	II	48	−7	—	—
14	10	I	67	+17	—	—
15	10	I	64	+30	—	—
16	11	V (SUN)	58	+14	—	—
17	12	I	27	+4	—	—
18	14	V (SUN)	49	−13	—	—

Group VII Uninodular goiter of large size (LUN).

Group VIII Multinodular goiter (Mul N).

Observations on these patients have been classified by these signs and symptoms of hypothyroidism:

Signs: puffy face, dry skin, coarse skin, and nonpitting edema.

Symptoms: general weakness, dizziness, headache, fear of cold, lumbago, and numbness of extremities.

For purposes of comparison of age and sex, the patients with endemic goiter have been divided into four groups: schoolboys, schoolgirls, men, and women.

Eighteen schoolboys were examined. Thirteen boys showed an I^{131} uptake of more than 50 per cent. The BMR values were in the normal range except in one. None of the boys had any of the signs or symptoms of hypothyroidism (Table 2).

Twenty-six schoolgirls were examined. Eighteen girls showed an I^{131} uptake of more than 50 per cent. The BMR values were in the normal range except in one. Signs or symptoms of hypothyroidism were not detected in these girls (Table 3).

Eleven men were examined. Eight showed an I^{131} uptake of more than 50 per cent. The BMR values of eight men were in the normal ranges; the values for two men were below normal and for one the BMR was above normal. Nine men showed symptoms of hypothyroidism and six men showed signs of hypothyroidism (Table 4).

Thirty-three women were examined. Nineteen showed an I^{131} uptake of more than 50 per cent. The BMR values of thirty women were in the normal range; the values for two women were above normal, and for one the BMR was below normal. Twenty-eight women showed symptoms of hypothyroidism and twenty-six showed signs of hypothyroidism.

DISCUSSION

In this series, most of these patients were euthyroid with normal BMR and showed heavy concentration of I^{131} in the thyroid gland. In the adult group, there were more cases with hypothyroidism and nodular goiter, but there was no obvious hypothyroidism in the groups of school children. The thyroid I^{131} uptake was rather higher, especially in the younger group.

Fig. 1 shows the thyroid I^{131} uptake of all

TABLE 3. Iodine-131 uptake in schoolgirls with endemic goiter

No.	Age	Goiter	Uptake (%)	BMR (%)	Symptoms	Signs
1	5	I	58	+10	—	—
2	6	II	50	−3	—	—
3	7	II	39	+16	—	—
4	7	I	53	+12	—	—
5	7	I	47	+10	—	—
6	7	II	77	−9	—	—
7	7	III	66	+3	—	—
8	8	III	62	+16	—	—
9	8	I	33	+7	—	—
10	9	I	43	+18	—	—
11	9	II	70	+27	—	—
12	9	II	66	+3	—	—
13	10	V (SUN)	78	−1	—	—
14	10	II	64	+10	—	—
15	10	II	37	+5	—	—
16	10	V (SUN)	92	+5	—	—
17	10	II	49		—	—
18	10	VIII (Mul N)	58	+3	—	—
19	10	II	68	+9	—	—
20	10	I	69	+6	—	—
21	12	II	79	+1	—	—
22	12	II	79	+9	—	—
23	12	II	79	−2	—	—
24	12	I	30	+15	—	—
25	13	VI (MUN)	30	+14	—	—
26	14	VIII (Mul N)	52	0	—	—

TABLE 4. Iodine-131 uptake in men with endemic goiter

No.	Age	Goiter	Uptake (%)	BMR (%)	Symptoms	Signs
1	15	II	62	+14	+	−
2	16	II	64	−9	++	+
3	17	III	56	−7	−	−
4	29	II + V	72	+16	+	−
5	30	III	45	−11	+	−
6	31	III	65	+1	−	−
7	35	III	46		++	+
8	55	VI (MUN)	41	+17	++	+
9	57	IV	53	+17	++	+
10	65	VIII (Mul N)	67	+27	+	+
11	68	VII (LUN)	52	−18	+	+

patients, comparing with their BMR. A histogram of the frequency of thyroid I^{131} uptake of eighty-eight patients with endemic goiter (Hsin-Chu) is shown in Fig. 2. It is compared with the histogram of the frequency of thyroid I^{131} uptake of 103 patients with endemic goiter in the Andean province of Mendoza in Argentina, drawn by NUNEZ[6]. The superimposed curve represents the normal distribution curve of thyroid I^{131} uptake in the area of Boston (U.S.A.) given by Skanse in STANBURY *et al.*[7].

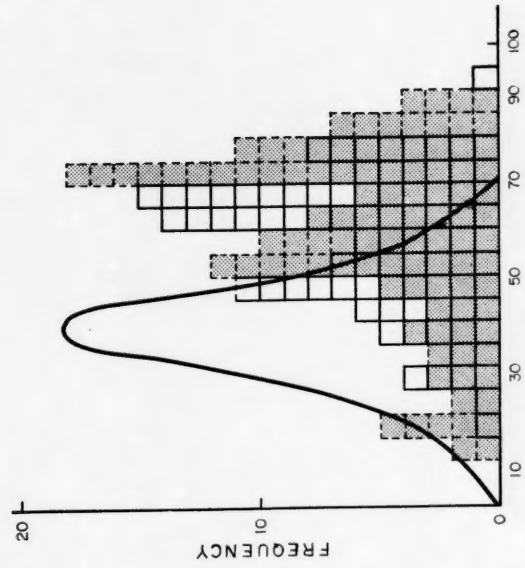

FIG. 2. Histogram of the frequency of I^{131} thyroid uptake in Hsin-Chu endemic goiter area, Taiwan, compared with that of the Mendoza area, Argentina (shaded area) and distribution curve for normal subjects in the area of Boston, U.S.A. (curve).

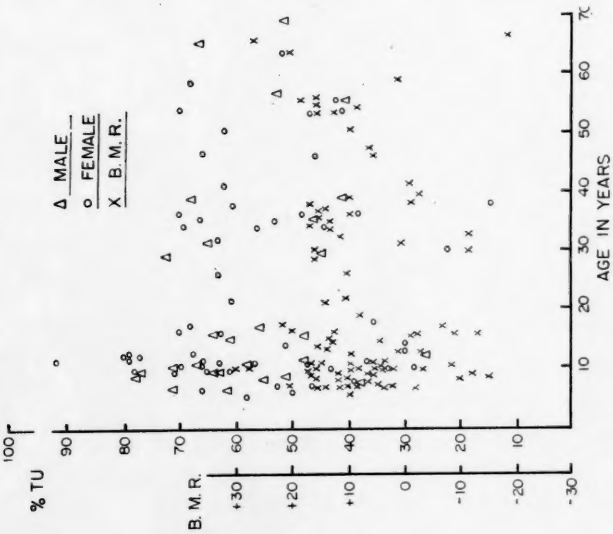

FIG. 1. Comparison of I^{131} uptake with BMR.

TABLE 5. Iodine-131 uptake in women with endemic goiter

No.	Age	Goiter	Uptake (%)	BMR (%)	Symptoms	Signs
1	16	II + V (SUN)	63	−2	−	+
2	16	III + V (SUN)	70	+13	−	−
3	17	III	68	+20	−	−
4	18	V (SUN)	36	+22	+	−
5	19	V (SUN)	49	+8	−	−
6	21	II	61	+14	+	−
7	22	VI (MUN)	32	+16	+	−
8	26	VII (LUN)	64	+11	+	+
9	30	III	23	−16	+	+
10	32	II	63	+12	+	−
11	33	III	56	+11	+	+
12	34	II	68	+16	+	+
13	34	IV + V (SUN)	44	+13	+	+
14	35	III	66	+13	+	+
15	35	II	45	+15	+	+
16	36	II	70	+15	+	+
17	36	IV	48	+10	+	+
18	36	III	39	+9	+	+
19	37	III	61	+14	+	+
20	38	IV	15	+17	+	+
21	38	III	53	−1	+	+
22	39	III	68	+10	+	+
23	39	II	41	−2	+	+
24	41	III	62	−1	+	+
25	46	III	46	+6	+	+
26	47	II	66	+7	+	+
27	50	III	62	+10	+	+
28	53	IV + V (SUN)	48	+17	−	+
29	53	IV + V (SUN)	42	+13	+	+
30	54	II	75	+9	+	+
31	55	III	43	+19	+	+
32	58	IV + V (SUN)	68	+2	+	+
33	62	V (SUN)	52	+21	+	+

We are now investigating PBI^{131}, conversion ratio, and urinary I^{131} discharge. This preliminary study in the Hsin-Chu endemic area apparently shows a high thyroid uptake of I^{131} in the adult group and still higher in the younger group. This also indicates that iodine hunger is more prominent in the children than the adult in Hsin-Chu endemic area and that hypothyroidism is developed in later ages.

SUMMARY

(1) Eighty-eight cases with endemic goiter in Hsin-Chu area were examined with administration of 25 μc of I^{131} and a standard measuring system.

(2) Thyroid I^{131} 24-hr uptake results were as follows:

Eighty-eight persons with endemic goiter were examined.

Fifty-eight showed an I^{131} uptake of more than 50 per cent.

In the forty-four school children with endemic goiter, thirty-one showed an I^{131} uptake of more than 50 per cent.

In the forty-four adults with endemic goiter, twenty-seven showed an I^{131} uptake of more than 50 per cent.

VOL. 7 1959/

REFERENCES

1. Jefferys W. H. and Maxwell J. L. *Diseases of China including Formosa and Korea* (2nd Ed.) J. L. Maxwell, London (1929).
2. Kawaishi K. and Hashimoto Y. *Ann. Surg.* **113,** 481 (1941).
3. Chen K. P. *Mem. Coll. Med. Taiwan* **5,** Nos. 1–2, 97 (1958).
4. Brucer M., Oddie T. H. and Edridge J. S. Thyroid Uptake Calibration. I. Mock-iodine, a Radioactive Iodine Gamma-Ray Standard. U.S. Atomic Energy Commission Report ORINS-14, July 25, 1956. [Available from the Office of Technical Services, Department of Commerce, Washington, D.C. Price 50 cents.]
5. Brucer M. Thyroid Radioiodine Uptake Measurement. A Standard System for Universal Intercalibration. U.S. Atomic Energy Commission Report ORINS-19. [Available from the Office of Technical Services, Department of Commerce, Washington 25, D.C. Price $3.50.]
6. Nunez C. The use of artificial radioisotopes in diagnostic, therapeutic and clinical research in Argentina. *Proceedings of the First United Nations Conference on the Peaceful Uses of Atomic Energy Geneva*, 1955. Vol. 10, p. 226. United Nations, New York (1956).
7. Stanbury J. B., Brownell G. L., Riggs D. S., Perinetti H., Itoiz J. and del Castillo E. B. *Endemic Goiter: The Adaptation of Man to Iodine Deficiency*, p. 44. Harvard University Press, Cambridge, Mass. (1954).

OL.
7
9/60

International Journal of Applied Radiation and Isotopes, 1960, Vol. 7, pp. 306–310. Pergamon Press Ltd. Printed in Northern Ireland

Detection and Determination of Tritium Labelled Compounds on Paper Chromatograms

P. A. OSINSKI*

(*Received* 27 *July* 1959; *in revised form* 1 *October* 1959)

Tritium labelled compounds on paper chromatograms are detected, localized and the ratios of their activities determined precisely with a windowless scanner. Filter paper strip is pulled, by a wheel driven by a synchronous motor, between two windowless, flow, Geiger–Müller counters. The flow of argon saturated with propanol vapour provides an air-lock. Pulses from the Geiger tubes are fed to a precision, linear ratemeter and recorder with chart speed equal to that of the filter paper strip. The efficiency of counting tritium is low. The sensitivity limit lies around 3 mμc/cm^2 of Whatman No. 1 filter paper.

VOL. 7 1959/6

LA DÉTECTION ET LE DOSAGE DES COMPOSÉS MARQUÉS AU TRITIUM SUR LES CHROMATOGRAMMES EN PAPIER

Au moyen d'un scanner à échantillon interne, il est possible de détecter, de localiser et de déterminer avec précision le rapport des activités de composés tritiés chromatographié sur papier filtre. Une roue entrainée par un moteur synchrone fait passer la bande de papier filtre entre deux compteurs Geiger–Müller à échantillon interne. Un courant d'argon saturé de vapeur de propanol empêche l'entrée d'air. Les pulsations des tubes Geiger sont captées par un intégrateur lineaire de precision raccordé à un registreur, dont le papier se deroule a la même vitesse que le chromatogramme. L'efficacité du comptage de tritium est basse. La limite inférieure de sensibilité se situe aux environs de 3 mμc/cm^2 du papier filtre Whatman No. 1.

ОБНАРУЖЕНИЕ И ОПРЕДЕЛЕНИЕ СОЕДИНЕНИЙ, МЕЧЕНЫХ ТРИТИЕМ, С ПОМОЩЬЮ БУМАЖНОЙ ХРОМАТОГРАФИИ

Метод бумажной хроматографии позволяет разделять соединения, меченные тритием, и определять отношения их активностей на безокошечных счетчиках. Полоска фильтровальной бумаги протягивалась с помощью колеса, вращающегося от синхронного мотора, между двумя безокошечными проточными счетчиками Гейгера–Мюллера.

Аргон, насыщенный парами пропилового спирта, подавался через воздухонепроницаемый затвор. Импульсы от трубки Гейгера поступали на прецезионный линейный измеритель скорости и записывались на диаграммную ленту со скоростью, равной скорости движения полоски фильтровальной бумаги. Коэффициент полезного действия счета трития мал. Чувствительность лежит в пределах около 3 mμc/см^2 на фильтровальной бумаге Ватман № 1.

BESTIMMUNG TRITIUM-MARKIERTER VERBINDUNGEN AUF PAPIERCHROMATOGRAMMEN

Tritium-markierte Verbindungen auf Papierchromatogrammen werden mit Hilfe eines fensterlosen Scanners nachgewiesen lokalisiert und ihre Aktivitätsrate genauestens bestimmt.

* Chercheur agré de l'Institut Interuniversitaire des Sciences Nucléaires. Laboratoire de Recherches, Service du Prof. J. P. Hoet, Hôpital St. Pierre, Louvain.

Ein Filterpapierstreifen wird über ein durch einen Synchronmotor angetriebenes Rad zwischen 2 fensterlosen Durchfluss-GM-Zählern hindurchgezogen. Ein Strom von Propylalkohol-gesättigtem Argon verhindert den Zutritt von Luft. Die Impulse der Geigerzähler werden von einem linearen Präzisionsratemeter-Gerät mit angeschlossenem Schreiber registriert, dessen Papierrolle mit der gleichen Geschwindigkeit wie der Filterpapierstreifen bewegt wird. Die Nachweisempfindlichkeit für Tritium ist gering: ihre untere Grenze liegt bei 3 mμC/cm^2 für Whatman No. 1 Filterpapier.

TRITIUM labelled compounds on paper chromatograms can be detected either by autoradiography, or by cutting the chromatograms into strips, eluting and estimating the activity by one of the usual methods. The former procedure is very slow and the latter, while yielding quantitative data, is often very laborious and does not provide precise localization.

In the course of work with tritium labelled adrenal steroids, the problem of locating and measuring the activity on paper chromatograms has been solved by the construction of a windowless scanner.

1. DESCRIPTION

The filter paper strip is passed between two windowless, flow, Geiger–Müller counters. The shallow groove in which the strip slides provides the only outlet for the counter gas, thus preventing air contamination of the Geiger tubes (Fig. 1). The body of the apparatus is made of brass and the Geiger tubes are cylindrical, 20 mm in diameter and 40 mm long. Slits 8 × 30 mm are cut parallel to the anode wires, which are of tungsten and are 0·075 mm in diameter. The sides of the cylinder are closed with polyethylene stoppers which are painted black as the tubes appear to be somewhat photosensitive.

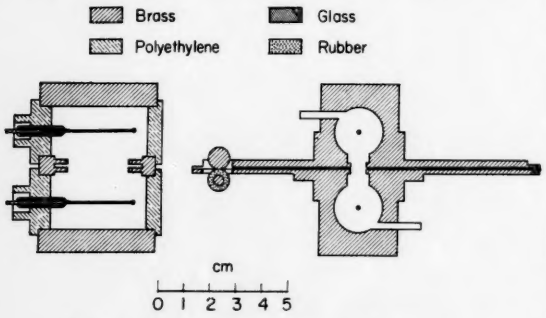

FIG. 1. Windowless scanner for filter paper chromatograms.

The 0·3 × 35 mm groove protrudes 55 mm on either side of the Geiger tubes.

A dented brass wheel, driven by a synchronous motor is used to pull the chromatogram strip. The wheel diameter was chosen to make the rate of advance of the filter paper identical with the recorder chart speed, namely 1 cm/min. Strips of any length, varying in thickness from cellophane film to Whatman No. 3 MM filter paper and in width from 6 to 35 mm can be scanned.

Argon saturated with propanol vapour at mains water temperature is used as the counter gas. The flow rate of 150 cm^3 of gas/min provides an effective air-lock even in a draughty room. The counter requires no preamplifier; it is connected by 1 ft of cable to a precision linear ratemeter and a chart recorder. The plateau of the counter starts at 1275 V and the usual working voltage is 1400 V. At this voltage the background rate with blank filter paper is around 100 counts/min. The limit of sensitivity for tritium determination appears to be somewhat below 3 mμc per cm^2 of Whatman No. 1 filter paper.

The whole assembly is shielded by 1 in. of lead.

2. RESULTS

Before reporting the performance of the scanner, some of its working principles will be discussed. The thickness of Whatman No. 1 filter paper is about 150 μ. The

maximum range of tritium β-particles in water is about 8 μ and although in a very porous material such as filter paper the maximum distance of penetration will be slightly greater, it can be assumed that particles will be detected only from a thin layer on either side of the strip. Thus the efficiency for counting tritium in this system is very low, of the order of 1 per cent. The slits in the Geiger–Müller tubes have purposely been made quite large in order to increase sensitivity which is achieved, however, at the expense of some resolving power. On theoretical grounds it may be predicted that two substances on the chromatogram will be well resolved if separated by a distance at least equal to the slit width. Another effect of a wide slit is a broadening of the recorded peaks; a point source will be recorded as a peak with base width equal to slit width. Both predictions have been verified experimentally using a short time constant (0·5 sec) on the ratemeter and with high count rates. At low count rates however, it is necessary to use longer time constants, up to 10 sec, which results in further broadening of the peaks and loss of resolution due, in this case, to delayed response of the measuring circuits. Another feature worth mentioning is the accumulation of electric charges on a thick non-conducting source.[1] This phenomenon is well known in windowless counters and results in a slow decrease of the counting rate. It is very apparent in our system on stationary filter paper (Fig. 2) but it is much less so when the strip is moving. Nevertheless this can be a source of serious error, but only at high counting rates. Another error to be expected at high count rates, is a coincidence loss of two kinds, due first to the dead time of the Geiger counters and second to the connection of the counters in parallel which means that two discharges occurring within the resolving time are registered as a single pulse by the ratemeter.

All the work reported below was done with Whatman No. 1 filter paper strips, 30 mm wide.

At an early stage it was found that mere spotting of the strip with radioactive substances leads to unsatisfactory results. It is necessary to equilibrate and run the chromatogram to ensure an even distribution of substance through the paper and along it. As radioactive compounds, cortisol (-1:2 -H^3(Δ^4-pregnene-11 β:17 α:21-triol-3:20-dione) and some of its derivatives[2] are being used as a matter of routine. The chromatograms were run in the Bush C system[3] as well as in the formamide–chloroform/benzene systems described by ZAFFARONI.[4] Visual localization of α–β unsaturated ketones was made by contact photography in u.v. light. Fig. 3 shows the recording of four chromatograms, run with 1, 5, 10 and 20 μg of cortisol-1:2-H^3 (specific activity: 30 mμc/μg) in 100 μg of inactive cortisol. The areas under the peaks were determined by cutting out the areas and weighing. The areas expressed in milligrams are plotted vs. quantity in micrograms in Fig. 4. Another

TABLE 1

Inactive cortisol (μg)	Peak areas			
	1st day	2nd day	3rd day	Average
0	79·0	86·5	90·7	85·4
50	78·1	86·5	80·6	81·7
100	86·0	87·9	78·6	84·8
200	74·9	80·5	79·0	78·1

TABLE 2

Sample No.	Scanning No.	Peak areas		
		Cortisol	Cortisone	Cortisone / Cortisol
1	1	76·2	149·7	1·96
	2	78·5	157·0	2·00
2	1	69·4	142·3	2·05
	2	80·0	156·0	1·95
3	1	81·3	160·9	1·98
	2	90·2	176·8	1·96

VOL. 7 1959/

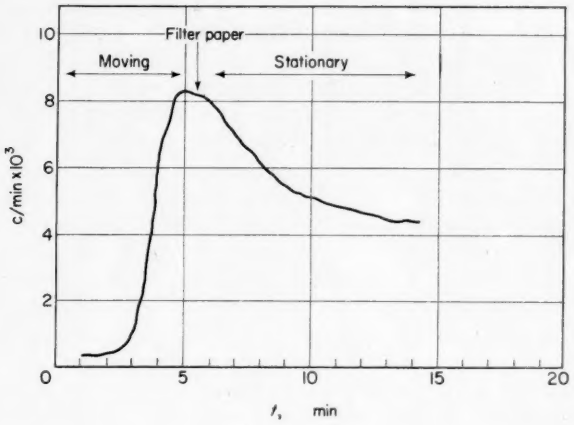

FIG. 2. The influence on count rate of the accumulation of electric charges on the stationary filter paper.

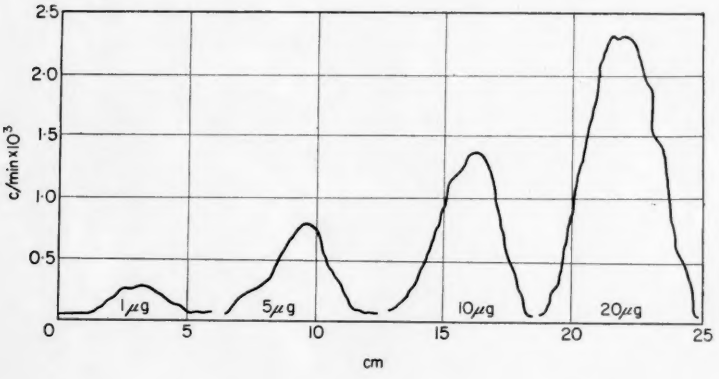

FIG. 3. Recording of four chromatograms, run with 1, 5, 10 and 20 μg of cortisol-1:2-H^3 in 100 μg of inactive cortisol.

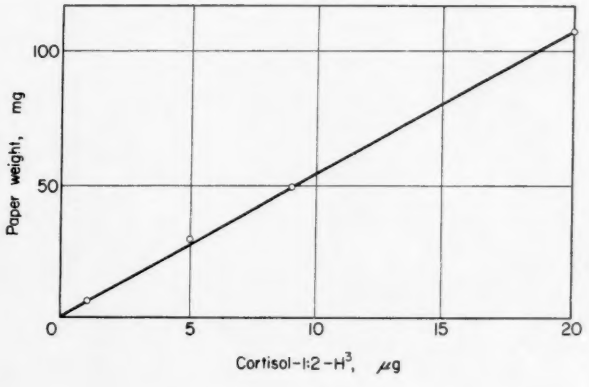

FIG. 4. Surface areas under peaks (expressed in milligrams of paper weight) plotted versus quantity in μg of cortisol-1:2-H^3.

group of four chromatograms were run with 10 μg of cortisol-1:2-H^3, and 50, 100 and 200 μg of inactive cortisol were added to the second, third and fourth chromatogram. It was found that there is a broadening of the peaks with increasing quantity of substance, but the surface areas remain almost constant. Table 1 shows the results of scanning the four chromatograms on 3 consecutive days. The influence of dilution appears negligible in the range investigated, but day-to-day reproductibility is not good and differences of over 10 per cent were found. The main reason seems to be variable room temperature. Further measurements were made to investigate the relative precision and reproductibility of our instrument. Three chromatograms were run spotted with a solution containing cortisol-1:2-H^3 and twice as much cortison-1:2-H^3, both of identical specific activity. The results of two scannings are shown in Table 2. One can conclude that this instrument provides an easy way of detecting and localizing tritium labelled compounds of reasonably high activity on filter paper strips. Absolute activity measurements cannot be made since too many variables are involved, but relative activities can be estimated fairly precisely.

Acknowledgements—The author wishes to thank Prof. Dr. M. DE VISSCHER for the loan of a ratemeter and a recorder. The work of Mr. C. SIEGERTSZ in scanner construction is gratefully acknowledged.

REFERENCES

1. VERLY W. G., BRICTEUX-GREGOIRE S., KOCH G. and DERNY E. *Proceedings of the Second United Nations Conference on the Peaceful Uses of Atomic Energy, Geneva*, 1958. p. 121. United Nations, New York.
2. OSINSKI P. A. and VANDERHAEGHE H. In preparation.
3. BUSH I. E. *Biochem. J.* **50,** 370 (1952).
4. ZAFFARONI A. *Recent Progr. Hormone Res.* **7,** 255 (1953).

VOL 7 1959/

International Journal of Applied Radiation and Isotopes, 1960, Vol. 7, pp. 311–316. Pergamon Press Ltd. Printed in Northern Ireland

Use of Radioactive Isotopes of Arsenic and Niobium for Investigations on Metallurgical Reactions

M. L. SAZONOV and L. A. SCHWARZMAN
Institute of Metal Physics, Moscow, Central Ferrous Metallurgy Institute

Methods for investigation of arsenic and niobium distribution between iron and slag by means of radioactive isotopes of these elements (As^{76} and Nb^{95}) are studied. Special emphasis is placed on the technique used for the removal of radioactive admixtures and for the identification of radioactive isotopes. Thermodynamic data characteristic of the oxidation of arsenic and niobium dissolved in liquid iron are given.

L'EMPLOI DES ISOTOPES RADIOACTIFS D'ARSENIC ET DE NIOBIUM DANS LES RECHERCHES SUR LES RÉACTIONS MÉTALLURGIQUES

On étudie des méthodes pour la recherche sur la distribution de l'arsenic et du niobium entre le fer et la scorie au moyen des isotopes radioactifs de ces éléments (As^{76} et Nb^{95}). On donne une insistance particulière sur la technique par laquelle se fait l'enlèvement des mélanges radioactifs ainsi que l'identification des isotopes radioactifs. On présente les données thermodynamiques particulières à l'oxydation de l'arsenic et du niobium délayés dans le fer liquide.

ИСПОЛЬЗОВАНИЕ РАДИОАКТИВНЫХ ИЗОТОПОВ МЫШЬЯКА И НИОБИЯ ДЛЯ ИЗУЧЕНИЯ МЕТАЛЛУРГИЧЕСКИХ РЕАКЦИЙ

В статье описываются методы изучения распределения мышьяка и ниобия между железом и шлаком с использованием радиоактивных изотопов этих элементов—As^{76} и Nb^{95}. Особое внимание уделяется описанию применявшихся способов очистки радиоактивных препаратов от радиоактивных примесей и идентификации изотопов. Приводятся данные, характеризующие термодинамические условия окисления мышьяка и ниобия, растворенных в жидком железе.

DIE VERWENDUNG VON RADIOAKTIVEN ARSEN- UND NIOBISOTOPEN FÜR UNTERSUCHUNGEN VON METALLURGISCHEN REAKTIONEN

Methoden zur Untersuchung der As- und Nb-Verteilung in Eisen und Schlacke wurden mit Hilfe der Radioisotope dieser Elemente (As^{76}, Nb^{95}) studiert. Besonderer Wert wurde auf die Technik der Abtrennung der radioaktiven Beimengungen und der Identifizierung der Radioisotope gelegt. Thermodynamische Daten, charakteristisch für die Oxydierung von As und Nb, verdünnt in flüssigem Eisen, werden angegeben.

VOL. 7 59/60

RADIOACTIVE isotopes have been widely used in investigations on metallurgical reactions in recent years. In particular, they have been applied to investigations on the distribution of elements between liquid iron and slags of various composition.

The sampling method involving continuous metal–slag contact maintained until the establishment of equilibrium, with subsequent withdrawal and analysis of samples, was conventionally used for studying the distribution of elements between iron and slag.

A consecutive saturation method has recently been proposed.[1] It consists essentially in feeding small portions of slag containing the element being distributed on to the surface of liquid iron. Upon melting

and interaction with the metal the slag is removed from the reaction zone by absorption on crucible walls. Equilibrium can be considered to be established when, after the introduction of a certain amount of slag, the concentration of the element in metal becomes constant. In both methods the distribution ratio L at equilibrium is the ratio of the element concentration in slag to that in metal.

The application of isotopes permits investigations on the distribution of elements at very low concentrations that are not detectable by chemical analysis, and makes these investigations considerably less time-consuming, the L value being determined from the metal and slag activities.

A necessary condition for successful application of isotopes is that the preparations used be free of radioactive admixtures. In ordinary metallurgical laboratories identification of the metal and slag activities can be made by simple procedures, viz. by measuring the half-life periods and also by determining the nature of absorption of the radiation emitted by these materials. Moreover, in some cases, means are available for removing active admixtures from the preparations.

This paper is concerned with methods for investigations on the distribution of niobium and arsenic between iron and slag, making use of the Nb^{95} and As^{76} isotopes. The preparations used contained active admixtures. Consequently special attention had to be paid to the technique of their purification, and to the identification of isotopes.

DISTRIBUTION OF NIOBIUM

Niobium is one of the most important alloying elements. Under conditions of metallurgical melting processes the introduction of the niobium alloy into liquid steel would result in a partial loss of niobium by oxidation. Thus investigations on the thermodynamics of the reaction between niobium dissolved in liquid iron and the oxidizing slag would be of considerable interest.

The radioactive niobium used was available as an aqueous solution of niobium oxalate. According to the specification the preparation contained about 0·5 per cent of active admixtures. The half-life period of Nb^{95} is 35 days, it emits electrons of a maximum energy of 0·15 MeV, and 0·764 meV γ-quanta.[2] In investigations carried out by the consecutive saturation method activity was introduced into the slag.

For this purpose slag powder contained in an iron crucible was soaked with an aqueous solution of $Nb_2^{95}(C_2O_4)_5$, then subjected to slow heating in an induction furnace in order to remove the water and decompose the oxalate, and after that melted. This slag, usually defined as initial, was ground to powder and then used in experiments on niobium distribution.

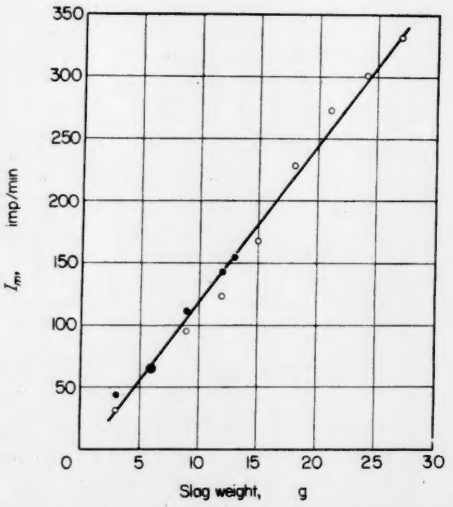

FIG. 1. Metal activity against weight of the added slag.

The initial slag powder was portioned by 3 g. Each portion was slowly fed to the liquid metal surface, and a metal sample was then withdrawn. Fig. 1 shows the results of two experiments carried out at 1600°C plotted as the activity of the standard metal sample (I_m imp/min) against the weight of added slag. As can be seen from the figure, the activity of metal samples did not tend to

a limit but continuously increased with the addition of new slag portions. This indicated that the element being distributed had a strong tendency towards transfer from slag to metal, its distribution ratio being correspondingly very low. This is obviously incompatible with the known properties of niobium. The strong oxygen affinity of the latter would cause its preferable concentration in the oxidizing slag, i.e. the L value ought to be high. Indeed, parallel experiments carried out by the sampling method

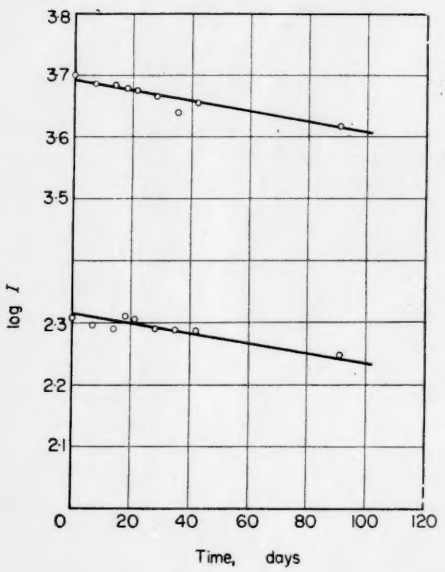

FIG. 2. Counting rate logarithm against time.

have shown that $L_{Nb} > 1000$. An explanation of this contradiction might be furnished by the assumption that the substance transferred from slag to metal is not niobium, but rather some other active admixture readily reducible with iron. Identification of the activity transferred from slag to iron was carried out in order to verify this suggestion. The half-life period was estimated in the first place. Fig. 2 shows the results obtained in corresponding measurements as a plot of the standard sample counting rate logarithm against time. The lower curve represents the results of measurements making use of an aluminium filter 4 mm thick. The top curve represents counting rate measurements carried out in the absence of a filter. Both lines can be seen to correspond to a practically identical half-life period of about 300 days. It can also be seen that the aluminium filter attenuated radiation by a factor above 20. The strong absorption indicates that radioactive decay is accompanied by either β-radiation of an energy above 2 MeV, or γ-radiation of a low energy. In determining the radioactive isotope responsible for this radiation consideration should be given to its chemical properties, as well as to the fact that, together with Nb^{95}, it is recovered from U^{235} fission products. All this appears to be in favour of the suggestion that the active admixture is Ru^{106}. Ru has a low oxygen

TABLE 1

Weight of slag (mg)	Activity of the metal samples (imp/min)
500	2·4
500	2·0
500	2·0
500	2·1
500	2·1
	Mean value 2·1 ± 0·2

affinity and practically does not oxidize from a solution in iron. The half-life period of Ru^{106} is 365 days and its decay is accompanied by low-level β-radiation with the formation of short-lived Rh^{106} emitting β-particles of high energy and γ-quanta of moderate energy. These data permit the development of a technique for removal of active admixtures from radioactive niobium. This technique involves a sufficiently prolonged contact between the initial slag and the iron, Nb^{95} essentially remaining in the slag, and the active admixtures being transferred to the metal. The slag purified in this way was separated from the metal and used in experiments. Table 1 is an example of the results obtained in experiments on determination of the niobium distribution ratio by the consecutive saturation method.

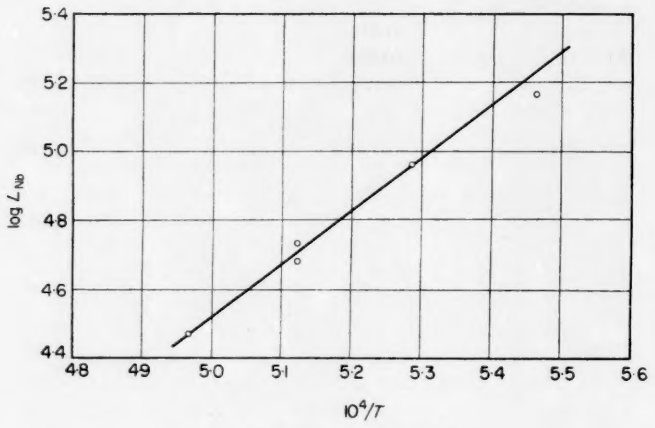

FIG. 3. log L_{Nb} against $1/T$.

The initial slag radioactivity was 10,400 imp/min and consequently

$$L_{Nb} = \frac{104{,}000}{2{\cdot}1} = 4{\cdot}9 \times 10^4.$$

The niobium equilibrium concentration in metal can be seen to be attained immediately after the addition of 500 mg of slag. This concentration is very low. Thus to obtain more reliable results determination of the L_{Nb} value was repeated several times, whilst the metal sample activities were measured within 20–40 min. Determination of the niobium content in iron at such high L_{Nb} values would require a very high concentration of slag with respect to Nb_2O_5. Thus for diluted solutions the only possible means of studying the distribution of niobium between iron and the oxidizing slag would be the tracer method. If the slag composition is constant, the temperature dependence of L_{Nb} will be determined by the equation[3]:

$$\frac{d \ln L_{Nb}}{dT} = \frac{\Delta H}{RT^2}. \qquad (1)$$

Upon integration it becomes

$$\log L_{Nb} = -\frac{\Delta H}{4{\cdot}575\,T} + B \qquad (2)$$

where ΔH is the enthalpy change in the reaction and B is a constant value.

The results of experiments carried out within the range of 1535–1740°C shown in Fig. 3 as a plot of log L_{Nb} against $1/T$ seem to confirm the validity of (2). The equation for the straight line of Fig. 4 will be

$$\log L_{Nb} = \frac{70{,}500}{4{\cdot}575\,T} - 3{\cdot}18. \qquad (3)$$

It follows that the oxidation of one gramme-atom of niobium dissolved in iron is accompanied by the liberation of 70,500 cal. This value is in fair agreement with that calculated from the heats of formation of solid FeO and Nb_2O_5.

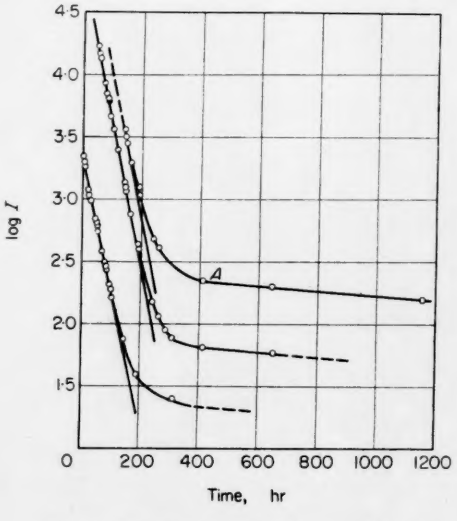

FIG. 4. Counting rate logarithm against time.

DISTRIBUTION OF ARSENIC

Arsenic is an impurity detrimental to iron. Thus it would be essential to find out if it could be removed from liquid metal by means of slag. As the arsenic concentration in steel is usually low, it would be feasible to study its distribution between metal and slag by means of radioactive isotopes.

Radioactive As^{76} emits electrons of an energy from 1·1 to 2·7 MeV. Its half-life period is 26·7 hr.[2,4,5] Thus the presence of even small amounts of active admixtures of a longer half-life period would lead to considerable errors. The relative concentration of such admixtures would naturally increase with time upon decomposition of As^{76}.

The presence of active admixtures was determined by the half-life period of arsenic dissolved in iron. Since in the first set of measurements the activity of As was very high, a filter was used in measurements of the metal sample counting rate. With decay of As^{76} the filter thickness was being correspondingly diminished and the last measurements were made without a filter. The results of these measurements are shown in Fig. 4 as a plot of the counting rate logarithm against time. The lower and middle curves represent measurements carried out with an aluminium filter 4 and 1 mm thick respectively. The top curve represents measurements in the absence of a filter. The straight-line parts of the curve can be seen to correspond to the tabulated half-life period of As^{76}. A marked deviation from linear dependence is observed after the completion of 6–7 half-life periods. Practically no As^{76} was left in the sample after the lapse of a time corresponding to 10–12 half-life periods, and the subsequent counting rate decrease is apparently accounted for by decay of the active admixtures. The half-life periods of the latter can be determined from the straight-line part of the upper curve starting from point *A*. The value obtained appears to be about 60 days.

A special set of runs was carried out in order to find out the effect of active admixtures on the accuracy of L_{As} determinations. Slag was fed on to liquid iron containing active As. After the system was left to stand at a constant temperature the slag was separated from metal by freezing it on a steel rod. A new portion of slag was then fed on to the metal surface and again removed after standing. This procedure was repeated seven times. Activities of the seven slag samples were then determined as a function of time, within 300 hr. The results of these measurements are plotted in Fig. 5 as the counting rate logarithm against time. The straight line corresponds to the tabulated

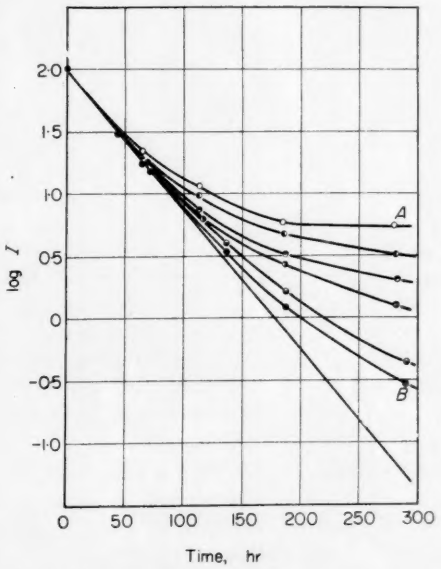

FIG. 5. Counting rate logarithm against time (for seven different slag samples).

half-life period of As^{76}. The half-life periods of activities contained in all slag samples can be seen to differ from the tabulated value. The deviations gradually diminish from the first (upper curve) to the last sample. This may be due to the fact that the active admixture distribution ratio is higher than that of arsenic and consequently the latter would concentrate mainly in the slag.

Thus the use of successive slag portions would lead to gradual removal of the active admixtures that are present along with arsenic. The results obtained permit quantitative evaluation of the error that would

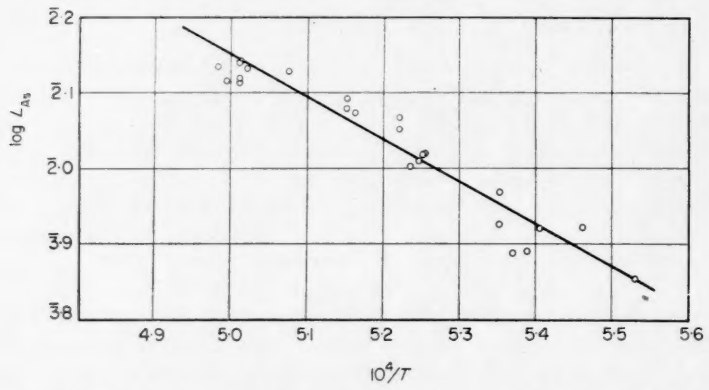

FIG. 6. log L_{As} against $1/T$.

take place if the active admixtures were not accounted for. It may be assumed to a first approximation that there is almost no decay of active admixtures during the time of experiment (300 hr). In this case, for example in 280 hr after the first activity measurements (point *A*) when the decay of As^{76} would be practically completed, the counting rate would be accounted for only by admixtures. As can be seen from Fig. 5 this value appears to be 5·5 per cent of the counting rate obtained in the first measurements. It will be noted that in the next slag samples the fraction of active admixtures becomes smaller. Thus for the seventh sample it attains only 0·36 per cent after 280 hr (point *B*). It follows that active admixtures can be completely removed from active arsenic contained in iron by the simple procedure of introducing oxidizing slag. This procedure was used prior to investigations on the distribution of arsenic between iron and slag.

The results of experiments with slag consisting of iron oxides alone are given in Fig. 6 as a plot of log L_{As} vs. $1/T$.

Experimental evidence can be seen to be in good agreement with (2) that will be written as

$$\log L_{As} = -\frac{26{,}500}{4{\cdot}575T} + 1{\cdot}05. \qquad (4)$$

It follows that the oxidation of one gramme-atom of arsenic dissolved in iron is accompanied by absorption of 26,500 cal. This value is in fairly good agreement with the one obtained from thermodynamic data on the heats of formation of solid FeO and As_2O_3.

Special experiments carried out at constant temperature have shown that the L_{As} value does not depend on the concentration of arsenic in iron. This leads to the conclusion that arsenic is contained in slag as a cation As^{+++}, rather than as As_2O_3 molecules.

As can be seen from (4) the L_{As} values are very low. Thus at 1600°C $L_{As} = 0{\cdot}01$. For that reason investigations on the distribution of arsenic between iron and slag are made possible only by the application of radioactive isotopes. Moreover, it can be inferred from the evidence obtained that the removal of arsenic from liquid iron by means of slag would not be effective.

REFERENCES

1. SOUROV V. F., TRAVIN O. V. and SCHWARZMAN L. A. Novy metod izuchenya ravnovesya v systeme metal-shlak. *Problemy metallovedenya i fiziki metallov*. 4 Sbornik trudov. Metallurgizdat (1955).
2. BOCHKAREV V., KEIRIM-MARKUS N., LVOVA M. and PROUSLIN YA. *Izmerenya aktivnosti istochnikov beta- i gamma-izlouchenya*. Izd. Akad. Nauk SSSR (1953).
3. TOMILIN I. A. and SCHWARZMAN L. A. *Izv. Akad. Nauk SSSR, Otdel. Techn. Nauk*, No 10 (1956).
4. GOUSEV N., MASHKOVICH V. and OBVINTZEV G. *Gamma-izlouchenie radioactivnykh izotopov prodouktov delenya*. Gos. Izd. Fiz.–Mat. Liter., Moskva (1958).
5. SPITZYN V. N., KODOCHIGOV P. N., GOLOUTVINA M. M., KOUZINA A. F. and SOKOLOVA Z. A. *Metody raboty s primeneniem radioactivnykh indikatorov*. Izd. Akad. Nauk SSSR (1955).

VOL. 7 1959/6

International Journal of Applied Radiation and Isotopes, 1960, Vol. 7, pp. 317–322. Pergamon Press Ltd. Printed in Northern Ireland

The Synthesis of Non-random Copolymers by the Gamma Irradiation of Emulsion Systems—II

P. HAYDEN and R. ROBERTS
Technological Irradiation Group, Isotope Research Division, Atomic Energy Research Establishment, Harwell, England*

(*Received* 10 *July* 1959)

Non-random copolymers have been synthesized by irradiation of vinyl monomers emulsified in polymeric latices. In particular, the synthesis of copolymers of polytetrafluoroethylene is described.

The reaction products were resolved by either fractional precipitation or fractional solution.

LA SYNTHÈSE DES COPOLYMÈRES NON AU HASARD PAR L'IRRADIATION DES SYSTÈMES D'ÉMULSION

On a achevé la synthèse des copolymères non au hasard par l'irradiation des monomères vinyliques émulsifiées en réseaux polymériques. Surtout décrit-on la synthèse des copolymères du polytetrafluoroéthylène.

La résolution des produits de réaction se fit soit par la précipitation fractionnelle soit par la solution fractionnelle.

СИНТЕЗ УПОРЯДОЧЕННЫХ СОПОЛИМЕРОВ ПРИ ГАММА-ОБЛУЧЕНИИ ЭМУЛЬСИОННЫХ СИСТЕМ

Сравнительно упорядоченные сополимеры синтезировались облучением винильных мономеров, эмульгированных в полимерных латексах. В частности, описывается синтез политетрафторэтилена. Продукты реакции очищались фракционным осаждением или фракционным растворением.

DIE SYNTHESE VON NICHT-STATISTISCH VERTEILTEN COPOLYMEREN DURCH γ-BESTRAHLUNG VON EMULSIONSSYSTEMEN

Durch Bestrahlung von Vinylmonomeren, emulgiert in Polymergittern, wurden nicht statistisch verteilte Copolymere hergestellt. Besonders die Synthese von Copolymeren des Polytetrafluoräthylens wird beschrieben.

Die Trennung der Reaktionsprodukte wurde entweder durch fraktionierte Fällung oder durch fraktionierte Lösung erreicht.

COMPARATIVE radical yields from polymers and monomers, on exposure to high energy radiation, suggest that irradiation of chosen polymer and monomer mixtures would result in both non-random copolymerization and homopolymerization of the monomer. The relative yields of the two processes should depend, not only on their initiation rates from the polymer and monomer respectively, but also on their respective kinetic coefficients of propagation, transfer and termination. (The kinetic coefficients

* The U.K.A.E.A. Isotope Research Division is now at Wantage Radiation Laboratory, Wantage, Berks.

of a chain growing from a polymer may differ slightly from those of the homopolymerization reaction, especially in the case of polytetrafluoroethylene copolymers.) Several authors[1–6] have described the application of this technique, using various polymer–monomer combinations. The ability of monomers to dissolve or swell polymeric materials varies considerably. Consequently, products obtained by this method vary between two extremes, classed as surface or matrix copolymers, depending on whether the monomer has copolymerized only on the surface or throughout the bulk of the polymeric material. The success of this technique in synthesizing homogeneous samples of non-random copolymers, presupposes adequate diffusion of monomer into the polymer during irradiation and in general high rates of conversion cannot be used.

High reaction rates and conversions are obtainable with vinyl polymerizations in aqueous emulsion systems, without the difficulties encountered in bulk reactions caused by increases in reaction media viscosities. Efficient reactant mixing is also considerably simplified. The synthesis of non-random copolymers by the γ-irradiation of emulsion systems has been described in a previous paper.[7] Monomer is imbibed into a latex of the polymer and the mixture irradiated at room temperature.

This communication describes other examples of the use of this method. In particular, various vinyl monomers have been copolymerized with polytetrafluoroethylene.

EXPERIMENTAL

Materials

Commercial monomers were freed from inhibitors by washing with dilute aqueous solutions of sodium hydroxide, followed by washing with water and drying with anhydrous sodium sulphate. For preparative purposes this purification was sufficient. Further purification by low-vacuum distillations in a nitrogen atmosphere had no significant effect on the relative yields of copolymer and homopolymer.

Dispersions of polytetrafluoroethylene, under the trade name of "Fluon" Dispersion G.P.I., were obtained from Imperial Chemical Industries Ltd.

Source

Irradiations were performed in cobalt-60 γ-radiation sources, at a dose rate of $8{\cdot}8 \times 10^4$ rads/hr as measured with the ferrous dosimeter with $G_{Fe}^{+++} = 15{\cdot}5$.

Method

The details of the method have been described previously,[7] consequently only a brief summary is included here with special mention of details pertinent to the present systems.

Normally the polymer latex was prepared by irradiating an emulsion of its monomer for 4 to 5 hr, thereby providing a sample free of any residual catalyst or other additive. It usually contained 20% polymeric material. Traces of unchanged monomer were removed by bubbling a stream of nitrogen through the latex.

For copolymerizations of polytetrafluoroethylene, a commercially supplied dispersion was used.

Purified monomer (one part) was thoroughly mixed with the polymer latex (five parts). This mixture was irradiated until more than 90 per cent of the monomer had polymerized. This usually required up to 5 hr. No polymerization of the added monomer could be detected prior to irradiation, even on standing for 2 days.

The products were coagulated by slowly pouring the latex into stirred boiling methanol, except in cases of copolymers containing vinyl acetate or ethyl acrylate components when boiling dilute aqueous solutions of sodium sulphate were used. After drying and reprecipitation, the reaction products were resolved by fractional precipitation using the techniques described in the first paper.

Fractional precipitations were impossible with products resulting from reaction with

VOL. 7 1959/

polytetrafluoroethylene, due to the insolubility of the latter in common solvents under normal conditions. However, this inert behaviour rendered fractional solution particularly facile in extracting the homopolymer formed.

EXAMPLES

1. *Polyvinyl acetate–acrylonitrile*

A latex, formed by mixing monomeric acrylonitrile (one part) with polyvinyl acetate latex (five parts), was irradiated for 4 to 5 hr at room temperature (12°C). Product coagulation and partial removal of adsorbed emulsifying agent was effected by pouring the latex into dilute aqueous sodium sulphate solution containing 20% methanol. On drying, further purification was accomplished by reprecipitation from a 1% solution in dimethylformamide into a 20% aqueous solution of methanol. Subsequently, a 1% solution in dimethylformamide was fractionally precipitated using a mixture of methanol and water (2 : 1, by volume) as non-solvent. A trace of calcium chloride (0·2 per cent), dissolved in this mixture, aided the coagulation of the precipitates.

Fractional precipitation resolved the reaction product into three distinct molecular species, namely polyacrylonitrile (formed by homopolymerization of the added monomer), unchanged polyvinyl acetate and a component containing both acrylonitrile and vinyl acetate. During the fractionation, subsequent to the early precipitation of polyacrylonitrile, the copolymer was held as a colloidal sol causing a marked turbidity. Repeated shaking, stirring and centrifuging failed to cause any separation in the solid form, except further traces of 95% pure acrylonitrile. Continued addition of the non-solvent mixture caused the sudden flocculation of the colloidal sol, leaving a clear solution after centrifuging. Further addition of non-solvent finally precipitated the polyvinyl acetate. A second fractionation on the copolymer fraction again resolved into three parts as before, but with vastly decreased quantities of the two homopolymers. Repeated fractionations achieved no further resolution, but it is interesting to note that a turbidity appeared after the addition of that fraction of non-solvent that normally precipitated polyacrylonitrile. On fractionating solutions containing known quantities of the copolymer and two homopolymers, each component was recovered about 95% pure after two precipitations. The composition of the fractions was measured by elemental analysis.

The integrated result of two successive fractionations on a single sample of reaction product is shown in Fig. 1.

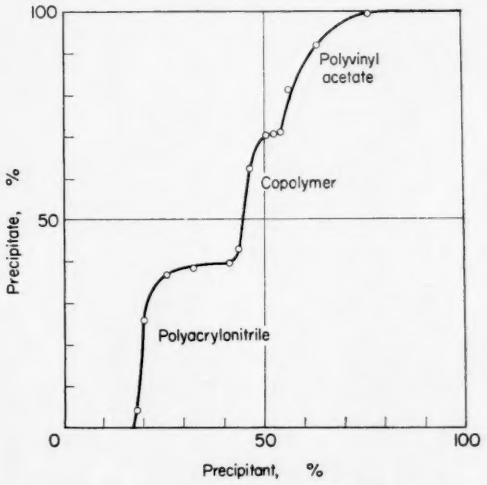

FIG. 1. Fractional precipitation of the reaction products from the polyvinyl acetate and acrylonitrile irradiations.

2. *Polymethyl methacrylate–acrylonitrile*

Polymethyl methacrylate latices were prepared by irradiation of 20% aqueous emulsions of the monomer.

A mixture of this latex (five parts) with monomeric acrylonitrile (one part) was irradiated for 4 hr at room temperature. Purification was by coagulation and precipitation as before, with the exception that pure methanol was used as precipitant.

Fractional precipitation, using dimethyl formamide as solvent and methanol as precipitant, resolved the reaction product

into the two homopolymers and a copolymer. The integrated results of two consecutive fractionations on a single sample of product are shown in Fig. 2. The fractions were characterized by elemental analysis. Resolution efficiencies were about 93–97 per cent after two consecutive fractionations.

3. *Copolymers of ethyl acrylate and methyl methacrylate*

Non-random copolymers of ethyl acrylate with methyl methacrylate have been synthesized in two ways. Firstly, by irradiation of a polyethyl acrylate latex mixed with monomeric methyl methacrylate: and

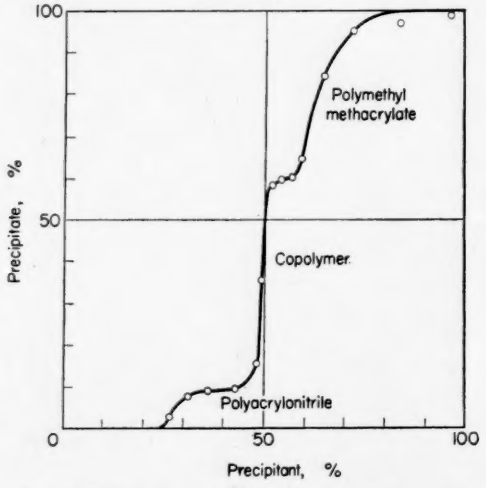

FIG. 2. Fractional precipitation of the reaction products of the polymethyl methacrylate irradiations.

secondly, vice versa, i.e. using a polymethyl methacrylate latex mixed with monomeric ethyl acrylate. Normally, one part of monomer was mixed with five parts of latex containing 20% polymeric material.

Purification, to remove surface active agents, was accomplished by coagulation and reprecipitations (from 2% chloroform solutions) in excesses of methanol containing 20% water.

Fractional precipitation, by a method based on that by SCHMETS and SMETS,[8] resolved the reaction product into three components. Polymethyl methacrylate was precipitated from a 1% solution in chloro-

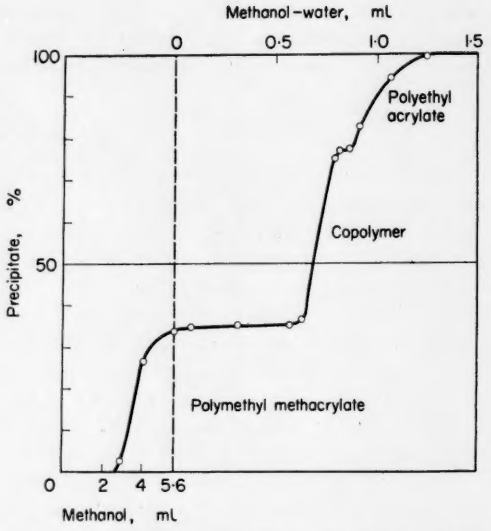

FIG. 3. Fractional precipitation of the products resulting from the irradiation of polyethyl acrylate with methyl methacrylate.

form by the addition of methanol. Figs. 3 and 4 show that the precipitation of this component began when 1·3 ml of methanol per ml of original polymer solution had been added. Continued addition of methanol

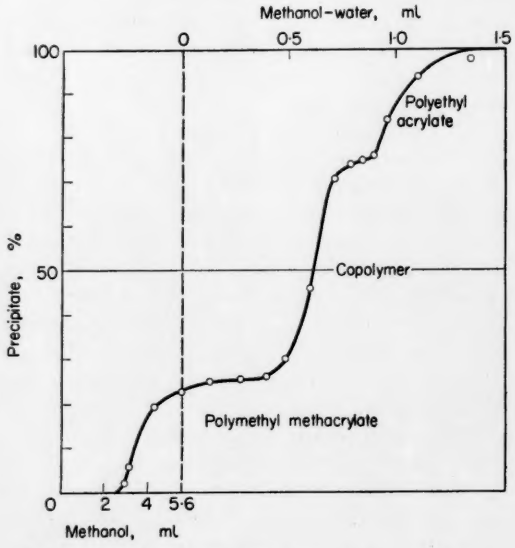

FIG. 4. Fractional precipitation of the products resulting from the irradiation of polymethyl methacrylate with ethyl acrylate.

VOL 7 1959/

gradually precipitated more polymer, found to be 80–85% pure polymethyl methacrylate in each case. After the addition of 5·6 ml of methanol per ml of original polymer solution, a mixture of methanol and water (3 : 1) was used as precipitant. The copolymers were flocculated at differing stages, depending on their respective methods of synthesis. Finally, after the addition of 0·9 ml of the second precipitant per ml of original chloroform solution, polyethyl acrylate was precipitated. A second fractional precipitation achieved further resolution and Figs. 3 and 4 show the integrated results of two consecutive runs on single samples of the products. No further resolution was obtained by repeated fractional precipitations. Infra-red spectroscopic analysis, although not favourable in this case, showed that the average composition of the combined first fraction was 93% pure polymethyl methacrylate whilst the final fraction was 98% pure polyethyl acrylate. The composition of the copolymer depended on the method of synthesis. For instance, the copolymer arising from the reaction of equal weights of polymethyl methacrylate and monomeric ethyl acrylate contained 50% ethyl acrylate, whereas equal weights of polyethyl acrylate and monomeric methyl methacrylate reacted to form a copolymer containing 75% ethyl acrylate and 25% methyl methacrylate.

4. *Copolymerizations with polytetrafluoroethylene*

A commercially supplied "Fluon" Dispersion was used as the polymer latex. To avoid high final concentrations of polymeric material, these dispersions were diluted with water prior to mixture with monomer. The final recipe contained 26·3%PTFE with 9·1% monomer.

Copolymerizations were achieved with a variety of monomers including methyl methacrylate, butyl methacrylate, ethyl acrylate, vinyl acetate and styrene.

These systems were notable for the facility with which the vinyl homopolymers were extracted from the unchanged PTFE and copolymer by washing in hot or cold benzene for 2 days. Experiments demonstrated that homopolymers mixed with the copolymer–PTFE fraction were completely recoverable using this procedure. The copolymer–PTFE mixtures were characterized by infra-red spectroscopy.

TABLE 1. The copolymerization of vinyl monomers with polytetrafluoroethylene dispersion at various temperatures
(Dose rate, 8·8 × 10^4 rads/hr. Irradiation time, 4 hr)

Monomer	Temperature (°C)	% Vinyl component in the mixture after	
		A. Coagulation	B. Extraction
Styrene	12	25	Trace
	55	25	6
	58	26	7·5
	80	25	8
Methyl methacrylate	12	22	0
	55	23	3
	80	23	5
Butyl methacrylate	13	23	0
	55	25	8
Ethyl acrylate	13	24	0
	55	25	7
Vinyl acetate	12	23	0
	30	24	2
	55	24	6

In each case, the relative yield of copolymer to homopolymer was markedly dependent upon the reaction temperature. Table 1 shows that little or no copolymerization occurred at room temperature. At 55°C, some of the monomer entered into a copolymerization reaction, the remainder forming homopolymer.

Qualitative experiments on the direct thermal polymerization in the absence of radiation showed that, although the overall rate of polymerization increased from a negligible value at room temperature, no copolymer could be detected after 6 hr reaction at 70°C.

In no case was any polytetrafluoroethylene detected in the soluble fractions of the reaction products.

DISCUSSION

Non-random copolymerization between addition polymers and vinyl monomers in emulsion systems were discussed previously.[7] The present results conform with the conclusions reached there, namely that polymers with large *G*-values for crosslinking or dislinking reactions act as good substrates for copolymerization reactions.

The observations on the copolymerization of vinyl monomers with polytetrafluoroethylene deserve consideration. Unfortunately since the experimental conditions were not well defined, in that air and unknown commercial additives were present, no rigorous mechanism can be elucidated. The outstanding feature is the marked temperature dependence of the relative yields of copolymer and homopolymer, the antithesis of the behaviour observed in grafting styrene to polybutyl methacrylate.

Kinetic analysis[9] shows that the rate of an emulsion polymerization may be written in the general form

$$R = K[I]^n[M]^m[S]^s$$

where R is the polymerization rate, K is a composite term of elementary velocity coefficients, I is the initiation rate and $[M]$ and $[S]$ are the concentrations of monomer and emulsifier respectively. The values assumed by the exponents n, m and s depend on experimental conditions. Assuming, as a first-order approximation, that the propagation and termination velocity coefficients of homopolymeric and copolymeric radicals are equal, the comparative yield of the two species will depend on their relative initiation rates. Transfer reactions must play but minor roles producing copolymer, as none is formed by thermal activation alone. The *G*-values of the dislinking reaction in PTFE and radical yields of monomers are largely independent of temperature. Random copolymerization studies show that the addition of vinyl monomers to PTFE radicals is more favourable than their addition to vinyl radicals. Initiation by direct action would therefore not lead to the observed effect of temperature. An indirect action, by radicals generated by the radiolysis of the aqueous phase diffusing into the latex particles and attacking both the polymer and monomer, as in reactions (1) and (2), might be expected to be temperature dependent.

$$R_{\dot{w}} + \text{—}CF_2\text{—}CF_2\text{—} \rightarrow \text{—}CF_2R_w + \text{—}CF_2\cdot \xrightarrow{M} \text{—}CF_2M\cdot \quad (1)$$

$$R_{\dot{w}} + CH_2{:}CHX \rightarrow R_w\text{—}CH_2\text{—}CHX\cdot \xrightarrow{M} R_w\text{—}CH_2\text{—}CHX\text{—}M\cdot \quad (2)$$

Conclusion

From the variety of polymeric and monomeric species used in these reactions, the method appears to be capable of widespread application in the synthesis of non-random copolymers.

Acknowledgements—The authors' thanks are due to Mr. P. G. Garratt who did much of the experimental work, and Mr. P. J. Fydelor for carrying out the infra-red absorption measurements.

REFERENCES

1. Ballantine D. S. *et al. J. Polymer Sci.* **19,** 219 (1956).
2. Ballantine D. S. *Mod. Plast.* **35,** 171 (1957).
3. Sabban-Danon J. *J. Polymer Sci.* **29,** 367 (1958).
4. Chapiro A. *J. Polymer Sci.* **34,** 481 (1959).
5. Restaino A. J. and Reed W. N. *J. Polymer Sci.* **36,** 499 (1959).
6. Angier D. J. and Turner D. T. *J. Polymer Sci.* **28,** 265 (1958).
7. Hayden P. and Roberts R. *Int. J. Appl. Rad. Isotopes* **5,** 269 (1959).
8. Schmets J. and Smets G. *Bull. Soc. Chim. Belg.* **63,** 59 (1954).
9. Medvedev S. S. *Czech. Chem. Comm.* **22,** 174 (1957).

VOL. 7 1959/

International Journal of Applied Radiation and Isotopes, 1960, Vol. 7, pp. 323–326. Pergamon Press Ltd. Printed in Northern Ireland

Dosimétrie des Rayonnements au Moyen de Matières Plastiques–I

Détermination de la Dose Point par Point dans une Enceinte Irradiée aux Rayons Gamma du Radiocobalt

M. LEFORT et X. TARRAGO
Laboratoire de Physique Nucléaire de la Faculté des Sciences de Paris, Orsay

(*Received* 4 *September* 1959)

On expose la méthode utilisant la variation d'absorption à 3000 Å induite par les rayons γ dans le polymethacrylate transparent pour déterminer la dose reçue en chaque point d'une enceinte.

On donne des résultats obtenus sur l'uniformité de la dose dans un volume irradié par des sources de radio-cobalt disposées tout autour sur un anneau.

PLASTICS RADIATION DOSIMETRY. DETERMINATION OF DOSE RATES FOR A KILOCURIE RADIOCOBALT GAMMA RAYS SET

The radiation induced absorption at 3000 Å in transparent methyl methacrylate is used for measuring radiation doses at each point of a volume irradiated by six radiocobalt sources. Results are given on the uniformity of dose in this volume.

ДОЗИМЕТРИЯ ИЗЛУЧЕНИЯ ПЛАСТМАСС. ОПРЕДЕЛЕНИЕ ДОЗЫ ГАММА-ОБЛУЧЕНИЯ ДЛЯ КИЛОКЮРИ РАДИОАКТИВНОГО КОБАЛЬТА

Поглощение света при 3000 Å, вызванное облучением прозрачного метилметакрилата, используется для измерения распределения доз по об'ему, облучаемому шестью источниками радиокобальта. Приведены результаты измерения, характеризующие однородность распределения доз по этому об'ему.

DIE VERWENDUNG VON PLASTIK ZUR STRAHLUNGSDOSIMETRIE. BESTIMMUNG DER γ-DOSIS-RATE IN EINER KILOCURIE Co^{60} BESTRAHLUNGSANLAGE

Die Veränderung der Absorption bei 3000 Å in transparentem Methylmetacrylat wird verwendet um die Dosis in jedem Punkt eines mit 6 Co^{60}-Quellen bestrahlten Volumens zu bestimmen. Ergebnisse über die Gleichförmigkeit der Dosis innerhalb des Volumens werden gegeben.

L'AUGMENTATION de l'absorption dans la région du proche ultraviolet à la suite de l'irradiation aux rayons ionisants de diverses matières plastiques, a été observée depuis plusieurs années. DAY et STEIN ont proposé en 1951[1] l'utilisation de cet effet en dosimétrie. Plus récemment BOAG *et al.*[2] ont obtenu des résultats très satisfaisants et montré que l'on pouvait mesurer au moyen de Plexiglas (methacrylate de methyle) des doses allant de 10^5 à 2×10^8 rads. Nous avons utilisé cette technique pour déterminer la dose reçue en divers points d'un volume d'environ 1 l. soumis à l'irradiation de six

sources de radiocobalt. Les mesures ont été faites par petits volumes élémentaires de moins de 1 cm³ et on a pu ainsi tracer une carte à trois dimensions de la dose reçue dans l'enceinte.

ETALONNAGE DU DOSIMETRE

Spectre d'absorption

Nous avons utilisé des plaquettes de Plexiglas de 3 mm d'épaisseur de 15 mm de long et de 6 mm de large. Ces plaquettes étaient montées sur un support spécial à la place du porte cuve dans un spectrophotomètre Jobin et Yvon. Nous avons trouvé un spectre d'absorption analogue à celui de Boag *et al.*, avec un fort accroissement dès que la longueur d'onde devient inférieure à 3100 Å. La reproductibilité vérifiée entre plusieurs échantillons est à 5 pour cent, à condition de sélectionner le Plexiglas non rayé.

L'étalonnage de l'accroissement de densité optique en fonction de la dose absorbée dans le Plexiglas de 3 mm d'épaisseur a été fait en irradiant l'échantillon dans un emplacement où la dose absorbée a été déterminée avec beaucoup de soin au moyen d'une solution de sulfate ferreux.

La différence entre les spectres du Plexiglas irradié et du Plexiglas témoin présente un maximum très net à 2990 Å comme on le voit sur la Fig. 1 et c'est à cette longueur d'onde que nous avons fait ensuite toutes les mesures. Pour l'étalonnage on a vérifié que la différence de densité optique était bien homogène en tous les points de la plaquette

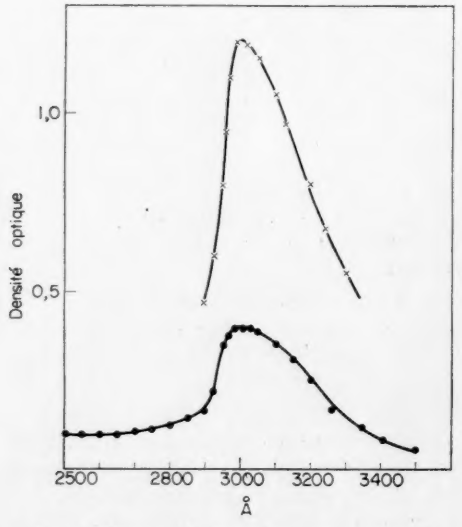

Fig. 1. Spectre d'absorption par rapport à un temoin non irradié.
× après 3 h d'irradiation.
● après 8 h d'irradiation.

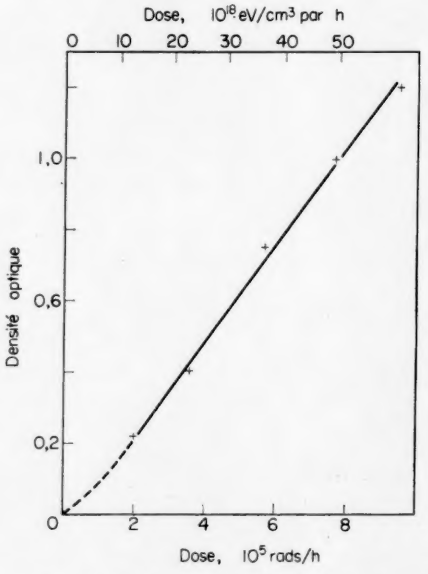

Fig. 2. Étalonnage du dosimètre plastique.

et que la dose reçue était par conséquent bien la même que celle mesurée par la solution de sulfate ferreux. La courbe de la Fig. 2 indique la différence de densité optique mesurée à 2990 Å dans le Plexiglas en fonction de la dose qui serait absorbée au même point dans 1 g d'eau mesurée au moyen des ions ferriques. On sait, en effet, que le rendement d'oxydation des ions ferreux en ions ferriques dans une solution (0,8 N H_2SO_4) est égal à 15,5 $\pm$ 0,1 ions par 100 eV absorbés. Nous avons déterminé la dose de cette façon avec une erreur maximum de 1 pour cent en faisant un grand nombre de mesures.

VOL. 7 1959/

Comme on le voit sur la Fig. 2 la diminution de transparence dans le Plexiglas n'est proportionnelle à la dose, qu'à partir d'une dose d'environ 10^5 rads. Cette période d'induction où le rendement est plus faible a été observée également par BOAG *et al.*[2]

MESURE DE LA DOSE EN CHAQUE POINT D'UNE ENCEINTE

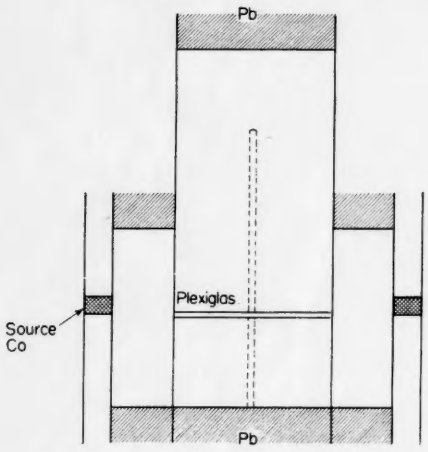

FIG. 3. Coupe verticale du dispositif d'irradiation.

Notre dispositif d'irradiation au radiocobalt,[3] comporte six sources de 130 c placées sur un anneau de 16 cm de diamètre. Sur cet anneau on a prévu six canaux d'irradiation en position entre deux sources. Mais on peut également descendre au centre un cylindre de 9 cm de diamètre et 20 cm de hauteur (voir Fig. 3).

Les sources de radiocobalt sont des petits cylindres de 1 cm de haut sur 16 mm de diamètre et leur base est à 5 cm au-dessus du fond du cylindre. Nous désirions connaître le degré d'uniformité de la dose dans cette enceinte. On a d'abord exploré les variations de dose selon les diamètres dans une section de 3 mm d'épaisseur placée soit au fond du cylindre, soit au niveau des sources (Fig. 3). Pour cela un disque de Plexiglas était divisé en petits rectangles de 15 mm sur 6 et on mesurait la densité optique en plusieurs points de chacun de ces

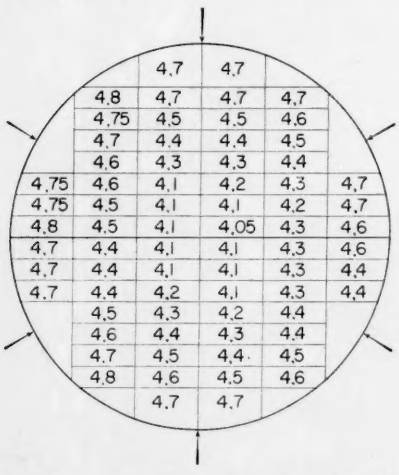

FIG. 4. Coupe horizontale du volume irradié au niveau des sources.
Doses exprimées en 10^{18} eV cm^{-3} h^{-1}.

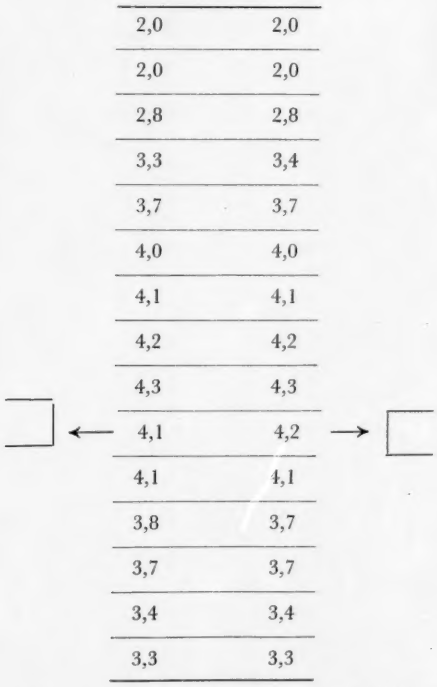

FIG. 5. Coupe verticale du volume irradié.
Doses en 10^{18} eV cm^{-3} h^{-1}.
(Les fiches représentent le niveau des sources.)

rectangles. On reconstituait le disque en rassemblant l'ensemble et on le plaçait à irradier. Les mesures de densité optique aux mêmes points que précédemment permettent alors d'obtenir 22 déterminations de dose sur un diamètre de 9 mm. On constate ainsi qu'au fond du cylindre l'uniformité est presque parfaite puisque toutes les doses sont comprises entre 2,8 et 3,0 $\times$ 10^{18} eV par hr et par cm^3 d'eau soit un écart de 3,3 pour cent.

La Fig. 4 représente schématiquement les résultats obtenus au niveau des sources; les bords placés près des sources reçoivent 4,8 $\times$ 10^{18} eV/cm^3 tandis que la dose au centre n'est que de 4,05. L'écart atteint ici un peu moins de 20 pour cent; ce qui reste satisfaisant.

Les variations de dose selon la hauteur sont représentées dans la Fig. 5 obtenue en plaçant une série de plaquettes de Plexiglas au centre du cylindre. On peut voir, par exemple, qu'un échantillon de 9 cm de diamètre et de 6 cm de haut placé à 4 cm du fond reçoit une dose uniforme à 20 pour cent près. Ces diverses mesures semblent illustrer l'intérêt des multisources disposées annulairement lorsqu'on veut obtenir des doses à la fois élevées et uniformément distribuées sur un volume assez important.

Au cours d'une deuxième étude nous nous proposons d'utiliser cette méthode de dosimétrie pour déterminer l'énergie transférée au cours du ralentissement du faisceau de protons de 150 MeV du synchrocyclotron d'Orsay par des épaisseurs variables de substances.

BIBLIOGRAPHIE

1. Day M. J. et Stein G. *Nature* **168,** 644 (1951).
2. Boag J. W., Dolphin G. W. et Rotblat J. *Rad. Res.* **9,** 589 (1958).
3. Lefort M. et Tarrago X. *J. Phys. Radium* **19,** 61 A (1958).

VOL. 7 1959/6

International Journal of Applied Radiation and Isotopes, 1960, Vol. 7, pp. 327–329. Pergamon Press Ltd. Printed in Northern Ireland

Radioactive Ion Exchange Surfaces, Versatile Radiation Sources

ALBERT E. JOHNSON, JR. and ALVIN S. BLUM

The Radioisotope Laboratory, Research Department, Veterans Administration Hospital, Coral Gables, Florida, and the University of Miami School of Medicine, Coral Gables, Florida

(*Received* 14 *September* 1959)

A sheet plastic material has been developed which has uniform ion exchange properties restricted to a thin layer of a single surface. With this material it is possible to obtain an infinitely thin source of radioactivity by simply immersing in an appropriate solution of radioactive isotopes.

DES SURFACES RADIOACTIVES À ÉCHANGE D'IONS, DES SOURCES DE RADIATION VERSATILES

On a achevé un matériel plastique en forme de feuille ayant des propriétés d'échange d'ions uniformes et limitées à une mince couche d'une seule surface. Avec ce matériel on peut obtenir une source de radioactivité infiniment mince en le trempant tout simplement dans une solution convenable d'isotopes radioactifs.

ИОННО-ОБМЕННЫЕ ПОВЕРХНОСТИ РАДИОАКТИВНЫХ ЧАСТИЦ-ПЕРСПЕКТИВНЫЕ ИСТОЧНИКИ ИЗЛУЧЕНИЯ

Изготовлена листовая пластмасса с равномерно распределенными ионно-обменными свойствами, сосредоточенными в тонком слое у поверхности. Такой материал дает возможность получения бесконечно тонкого радиоактивного слоя путем простого погружения в соответствующий раствор радиоактивных изотопов.

RADIOAKTIVE IONENAUSTAUSCHENDE OBERFLÄCHE: EINE VIELSEITIG VERWENDBARE STRAHLENQUELLE

Eine Plastikfolie wurde entwickelt, welche die Eigenschaft eines gleichförmigen Ionenaustauschers, jedoch beschränkt auf eine dünne Schichte einer Fläche, besitzt.

Mit diesem Material erhält man ganz besonders dünne Strahlenquellen einfach durch Eintauchen der Folien in eine geeignete Radioisotopenlösung.

A SUCCESSFUL therapeutic application of artificial radioisotopes has been the irradiation of surface lesions by planar radioactive sources. Strontium-90 applicators are convenient and easy to use in the treatment of eye and skin tumors[1–2]; however, they suffer from a lack of flexibility and consequently are available only in fixed sizes and shapes and cannot be expected to conform to the particular lesion to be irradiated. When the applicator is larger than the lesion, excessive normal tissue is destroyed; if the applicator is too small, overlapping of radioactive fields will result in non-uniform irradiation and excessive destruction of tissue. These problems were resolved by LOW-BEER[3–4] who dried phosphorus-32 on blotting paper, which was cut to fit the individual lesion.

It is difficult to get uniform or reproducible

deposition of an isotope by drying in a porous medium. In the case of soft betas, there may be appreciable self-absorption by the medium, resulting in a considerably altered distribution of the β-energies at the surface of the medium.

OBJECTIVES

To make more effective use of the variety of isotopes that are available, we have attempted to prepare a flexible sheet medium which would have the following properties:

(1) Absorb radioactive ions only at a designated surface when immersed in a solution of radioactive isotope.

(2) Have a sufficient capacity for these ions to give effective radiation doses.

(3) Have sufficient thickness to absorb β-rays coming from the activated surface through the back of the sheet.

Having such a material available, the therapist could cut and shape it to fit the lesion. He could then dispense the requisite amount of an isotope having the desired range of radiation for a particular depth of tissue. By immersing the pre-cut piece of sheet material into the solution of isotope, he would automatically plate the isotope on the surface, producing a radiation source with intensity, shape and energy designed for that particular situation.

The commercial ion exchange resins have a great ion holding capacity, but absorption of the desired ions is uniform throughout and cannot be applied as an infinitely thin layer on the surface.

PREPARATION AND PROPERTIES

Controlled sulfonation or amination of rigid and flexible epoxy, polyester or styrene–divinylbenzene resins gave products having ion exchange properties restricted to the desired surface. However, these resins did not lend themselves well to a uniform, flexible medium. A further disadvantage was the rapidity with which the ions were leached from the surface of the resin on prolonged contact with moisture.

We found that the three desired properties for this medium were best met by the commercial plastic cellulose tetranitrate (Pyroxylin, Parlodion). Parlodion obtained from Mallinckrodt Chemical Works is soluble in 25 parts of a solution of ethanol, 1 vol.; ether, 3 vol. From this solution, thick (relative to the range of β-rays) flexible sheets can be cast. An isotonic NaCl solution containing I^{131} showed an adsorption of 0·0024 $\mu c/cm^2$ of cellulose tetranitrate. Since there are appreciable amounts of carrier I^- as well as large amounts of Cl^- and bisulfate anion competing for the anion exchange groups of the resin, this adsorption of the desired I^{131} can be greatly increased, using carrier-free iodide in a low ionic strength solution. (Most anion exchange resins show their preferential adsorption only at low ionic strength.) The chromate-51 anion has a greater affinity for the ion exchange groups than iodide, and samples of Parlodion adsorbed 0·001 $\mu c/cm^2$ of this isotope. The chromate-51 used in this case was of low specific activity, 23 mc/g in an HCl, saline solution, indicating a minimum of 0·0001 mg/cm^2 surface absorption excluding Cl^-.

The examples given were carried out on untreated Parlodion; a greater adsorption per square centimeter can be obtained by amination of the nitro groups.

Untreated Parlodion has no cation exchange properties.

Cellulose tetranitrate may be conveniently given cation exchange properties by sulfonation of the desired surface, using concentrated sulfuric acid. If the surface of Parlodion is exposed to concentrated sulfuric acid at 25°C for 1 min (or 10% fuming sulfuric at 0° to 10° for 1 min), washed free of unreacted acid, a product is obtained having good cation exchange properties. The depth of the cation exchange groups, using these conditions, is extremely thin. This is demonstrated by sulfonating both surfaces of a sheet of Parlodion, immersing

VOL.
7
1959/

VOL.
7
59/60

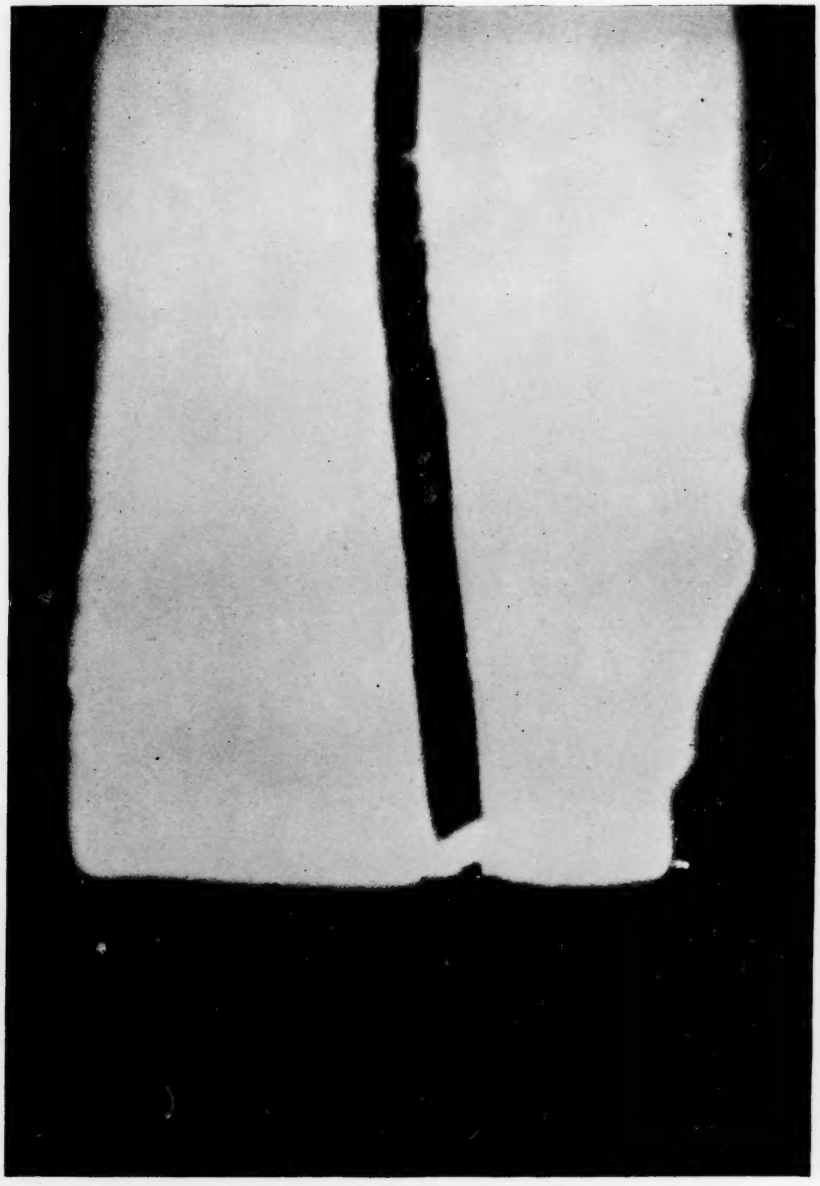

FIG. 1. Enlarged autoradiograph of section through plastic sheet having ion exchange properties on both surfaces, after immersion in Ni^{63}. Non-radioactive edge placed in contact with film.

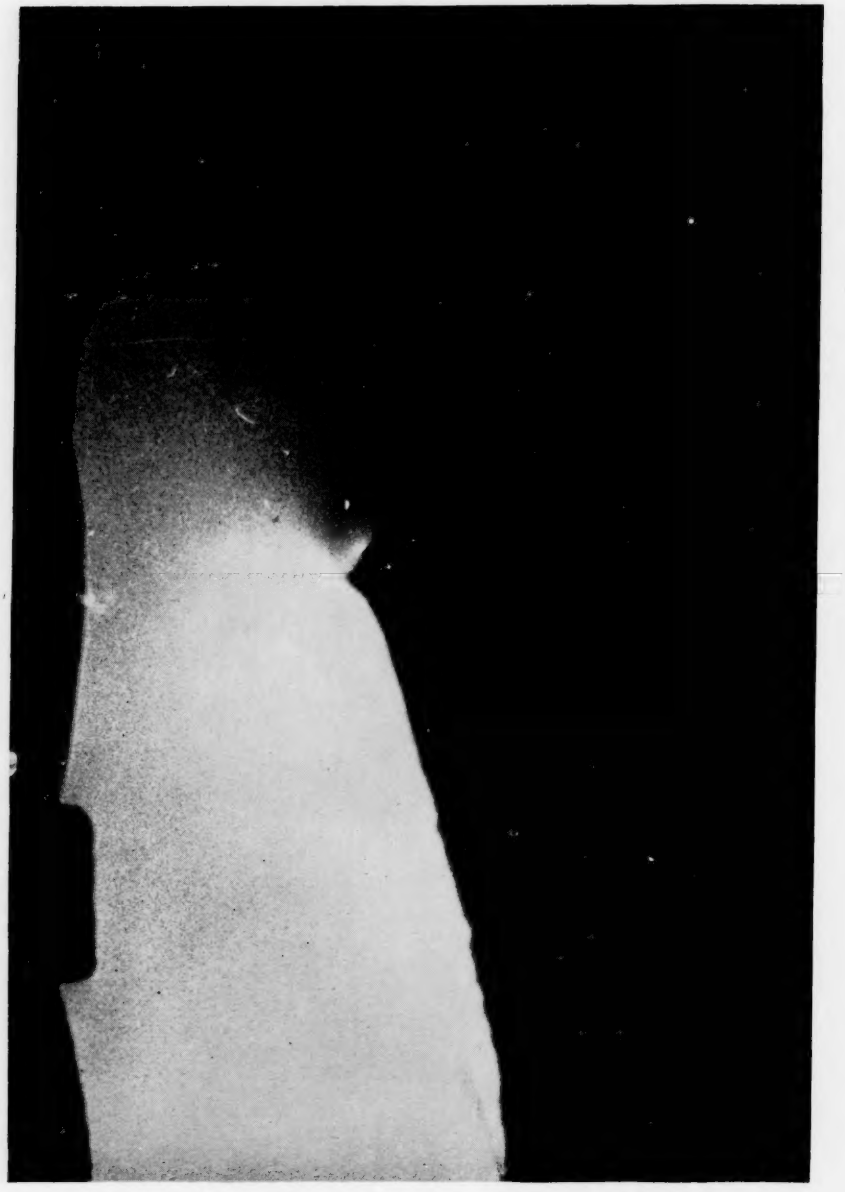

FIG. 2. Enlarged autoradiograph of section through plastic sheet having ion exchange properties restricted to a single surface, after immersion in Ni^{63}. Non-radioactive edge placed in contact with film.

VOL
7
1959/

OL.
7
59/60

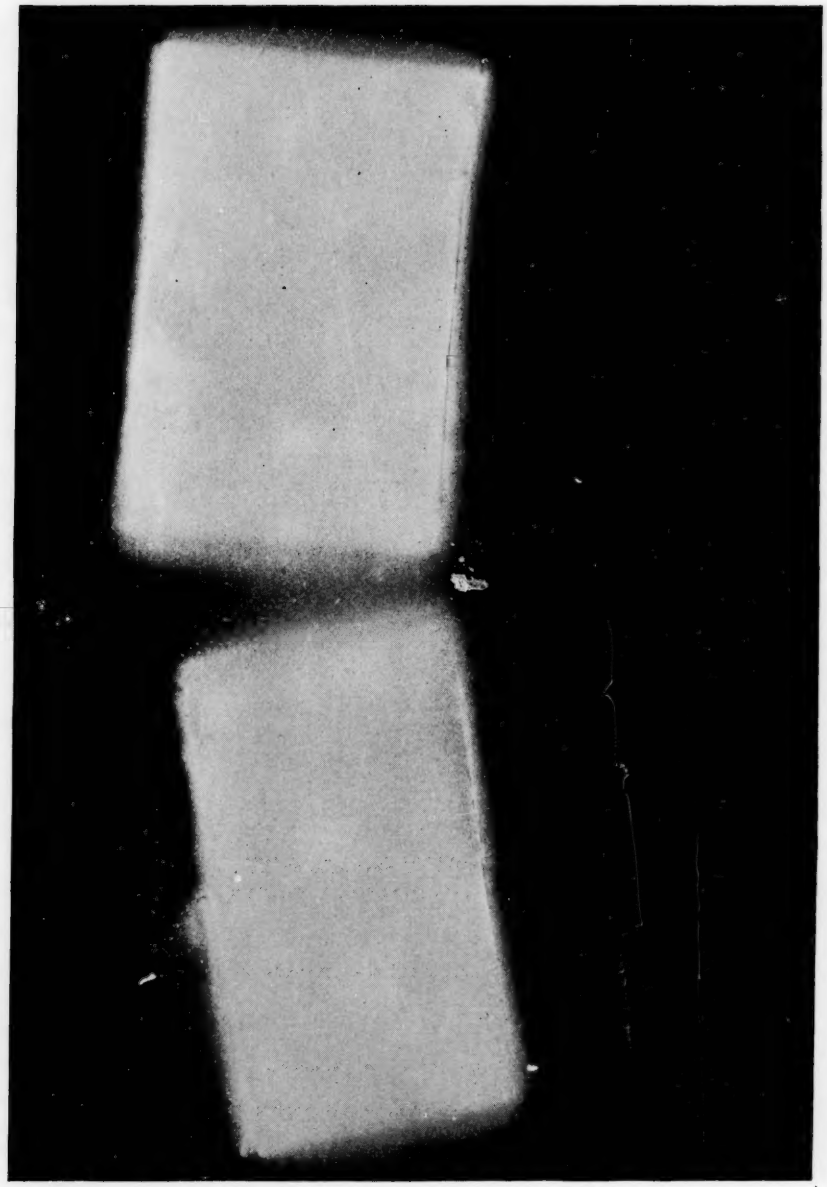

FIG. 3. Enlarged autoradiograph of plastic sheet with one ion exchange surface after immersion in Pm^{147}. Radioactive surface in contact with film.

VOL.
7
1959/

in a solution of $Ni^{63}Cl_2$, and making an autoradiograph by placing the unsulfonated edge against sheet film (Fig. 1). The spacing between the two sharply defined lines represents Parlodion that did not absorb Ni^{63}. This distance, within our limits of measurement, (plus or minus 0·02 mm) is equal to the actual thickness of the sulfonated sheet. The distance between the lines in the autoradiography is actually smaller than the distance between ion exchange surfaces by twice the range of the β-ray. Ni^{63} was selected for its short range in plastic.

Cation exchange groups may be placed selectively on any portion of the sheet plastic by simply protecting the undesired portion by painting with paraffin before exposing to sulfuric acid. This is readily demonstrated by the autoradiograph in Fig. 2. Prior to sulfonation, all surfaces of this sample except for a single surface were protected with wax. The wax was removed and the sample immersed in Ni^{63} solution, then rinsed. The sample was placed edgewise on the film.

To demonstrate the uniformity of distribution of an isotope on the surface, an autoradiograph using the short range of Pm^{147} was made with the active surface placed in contact with the film (Fig. 3).

The total amount of ions captured by the ion-exchange groups is minute (micro equivalents) and as many competing ions as possible must be eliminated.

Dorche and Costet[5] have shown that sufficient ions are leached from glass by solutions standing for a period of time, to interfere with many reactions. The use of polyethylene containers is recommended for storage of these materials.

The total capacity for a given exchange surface is readily measured by immersion in a solution of known specific activity and calculation from the amount of isotope absorbed.

With this method, we estimate that Parlodion has a capacity of 0·00045 mg ferric ion per cm^2 or 0·0001 mg chromate ion per cm^2. In order to adsorb sufficient isotope on the surface of the medium for therapeutic application, a solution of high specific activity is required. If Na^{24} were available carrier free, we calculate, on the basis of the adsorption of Fe^{59}, that it would be possible to obtain a surface having a capacity of 1·3 c/cm^2 and for Pm^{147}, 140 μc/cm^2.

When a 7 cm^2 plate of sulfonated Parlodion was immersed in 8 cm^3 solution of Pm^{147} containing 30 μc/cm^3, 66 per cent of the isotope adsorbed immediately on the surface. This adsorption of isotopes is quite firm. All measurements of capacity were made after serial washing of the surface with ion-free water. Continuous washing over a period of 24 hr results in the slow removal of ions from the surface.

If these radioactive surfaces are placed in direct contact with the skin, some exchange of the radioactive ions and the skin ions (e.g. Na) may result. This can be eliminated by the use of a thin (10 micra) impermeable plastic membrane.

It is understood that this technique of radioisotope application is not limited to examples and conditions discussed, but may find wide and varied uses in medicine (e.g. a thin flexible tubing, having a uniform coating of isotopes on its inner surface. This tubing might be then sewn into tumors for therapeutic irradiation). This method may also be used in the physical sciences as a means of coating various materials with a thin, permanent layer of radioactive material.

REFERENCES

1. Hahn, Paul. *Therapeutic Use of Artificial Radioisotopes*. John Wiley, New York (1956).
2. Tracerlab, Inc. *Tracerlog* p. 6, June (1952).
3. Low-Beer B. V. A., *Radiology* **47,** 213 (1946).
4. Low-Beer B. V. A., *Amer. J. Roentgenol.* **58,** 4 (1947).
5. Dorche J. and Costet C. *Bull. Soc. Pharm. Bordeaux* **94,** 18 (1955).

technical notes

Dose Distribution of Gamma Radiation in Cylindrical Volumes of Water

(*Received* 7 *October* 1959)

FOR the industrial application of γ-rays it is important to use an arrangement which does not cause the dose rate to vary too much throughout the irradiated volume. To obtain some information on dose-rate distribution we have made some rough preliminary measurements in cylindrical volumes of water with linear γ-ray sources. (In practice the objects to be irradiated will have certain empty spaces between them, but the packing fraction will be different in each case.)

As it is practical to arrange the objects to be irradiated in a regular pattern we have used four or three cylinders surrounding one source. It is evident that such a pattern can be extended to contain as many sources and cylinders as required, all occupying equivalent positions (except those at the edges).

Our results are given in Table 1. We suppose that the cylinders would be rotated and therefore we compare the average value of the dose rate at the circumference to that at the centre and half-way between the centre and the edge.

TABLE 1. Dose-rate distribution in cylinders of water surrounding a linear γ-source. Measurements have been normalized to a value of the dose rate = 1 at the edge of the cylinder (the counter being just inside the water)

Number of cylinders surrounding γ-source	Diameter of each cylinder (cm)	Dose rate measured at	Radionuclide	
			Co^{60}	Cs^{137}
4	56	Half-way	0·45	0·42
		Centre	0·32	0·31
3	56	Half-way	0·41	0·39
		Centre	0·30	0·25
4	35	Half-way	0·63	0·72
		Centre	0·52	0·53
3	35	Half-way	0·49	0·50
		Centre	0·43	0·42

"Half-way" indicates the average dose rate at a distance from the centre equal to half the radius.

It is seen that the dose-rate distribution with Cs^{137} is not very different from that with Co^{60}. (This can be understood from the greater penetration of the Co^{60} γ-rays in combination with the greater build-up[1] in the case of Cs^{137}.) In all cases the dose rate at the centre is so much smaller than the average value at the edge as to give rise to very serious problems in practical use. Cylinders of 35 cm diameter are much better than those of 56 cm and four cylinders around the γ-source are better than three, at least in the case of the narrower cylinders.

Experimental

The water cylinders (in steel drums) and the γ-sources (vertical glass tubes containing a solution) were 41 cm high. (Measurements with much higher —essentially infinitely long—cylinders and sources would have had more meaning, but the experimental difficulty involved would have been too large.) A slight error may have been introduced by the fact that the cylinders did not quite touch. The fact that there were no other cylinders behind those surrounding the source probably had very little influence on the average dose rate, as the main contribution is from the parts nearest the γ-source.

Dose-rates were measured by means of thick-walled chromium steel Geiger counters. The counting rate gives an approximate measure of the dose rate, but the accuracy is not high.[2]

Acknowledgement—This investigation was performed as part of the program of the Foundation for Fundamental Research of Matter (FOM) with the financial support of the Organisation for Pure Research (ZWO).

Institute for Nuclear Physics Research
Amsterdam

A. H. W. ATEN JR.
A. C. PIETERSE*

References

1. EVANS R. D. *The Atomic Nucleus* p. 733. McGraw Hill, New York (1955).
2. MAYNEORD W. V. *Brit. J. Radiol.* Suppl. **2,** p. 175 (1950).

* Present address: Reactor Centrum Nederland, Petten (North Holland).

VOL. 7 1959/6

Isotope Labelling by Means of Electrical Gaseous Discharges

(*Received* 1 *September* 1959;
in revised form 23 *October* 1959)

WILZBACH has shown[1] that tritium in gaseous form in contact with (mainly) organic substances gives compounds labelled unspecifically with tritium. TURTON[2] has shown that β-radiation from Kr^{85} induces reactions of similar kinds. The reactions take days or even weeks. It is generally agreed[1] at present that ionizing radiation is a "catalyser" even if the mechanism is not known. In order to reduce the reaction times and investigate operational procedures that render possible mechanism studies, we have looked for radiation-like ("radiomimetic") agents and will report here on the use of radio and microwave discharges.

Principles

The formation of short-lived gaseous ions, excited states, free radicals and other energetic entities may be said to characterize the action of ionizing radiation. Such entities are also formed, however, in gaseous discharges. The similarity between radiation chemistry and reactions in electric discharges can be traced back at least to LIND's classical monograph.[3]

From these points of view, electric discharges should generally be suitable for speeding up the Wilzbach labelling procedure. Several ways of doing this, including the use of d.c. discharges and various types of a.c. discharges[4,5] are possible.

In order to compare the gain using electrical discharge in comparison with ionizing radiation, we shall discuss the energy input, i.e. the power and related properties. We first express the β-radiation in watts and then compare it with electrical discharges.

The power P of a radioactive source (strength C c and average energy/disintegration $\bar{E}$ (MeV)) (see for instance ref. 10, p. 230) is

$$P = C \times \bar{E} \times 5{\cdot}93 \times 10^{-3}\ \text{W}.$$

(Some losses due to radiation absorption in walls have to be considered if the pressure and dimensions are small.)

We assume a source of 10 c of T_2 or the equivalent of Kr^{85} (roughly 0·3 c). This corresponds to $0{\cdot}34 \times 10^{-3}$ W (since $\bar{E} = 5{\cdot}7$ keV[11]).

If a gaseous discharge is applied to the system from some electrical device, we may consider part of the energy absorbed in the system to be equivalent to that of ionizing radiation. The energy absorbed will be used to excite molecules electronically and to ionize and break chemical bonds, thus forming entities having high potential energies i.e. excited molecules, gaseous ions and free radicals. Suppose that the electrical energy input is P (watts) and that the efficiency of yielding the exciting input is η_r. Then the "radiomimetic" power P_r is

$$P_r = P\eta_r$$

To take an example, we apply a microwave signal to a bulb of gas. The microwave power may be 200 W (see below) but the efficiency η_r is not known. However, a reasonable guess might be a few per cent. Suppose that only 1 W is left as the radiomimetic power. The gain in power as compared with the 10 c bulb is $1/0{\cdot}3 \times 10^{-3}$ i.e. about 3000. A Wilzbach treatment that takes one week could therefore be made in a few minutes if the yield increases linearly with the power. This latter condition means, in other words, that the total energy, Pt (t time in sec) is the relevant measure of the extent of the reaction, a thing which is not known at present. If the concentration of activated molecules is limited due to recombination, then the gain will rise more slowly.

The dose rate in pure T_2 (far from walls) is a constant and about 34,000 rad/sec. Suppose that a gaseous discharge occurs. The equivalent dose rate is, in general,

$$\frac{dD}{dt} = \frac{P_r \cdot 10^5}{m}\ \text{rad/sec}$$

where m is the mass of gas in grammes. If 1 W radiomimetic power is absorbed in a gas bulb 10 cm^3 in volume at 10 mm T_2 the corresponding equivalent dose rate in this example is as high as about 3000 Mrad/sec. Tritium alone would give about a 100,000 times lower dose rate.

Electrical discharge types

The choice between the multitude of electric discharge types[5] should be governed by several practical factors. The energy input should be as high as possible in order to reduce the time required for reaction. The equivalent ion "temperature" should be low because it is felt that radiation or radiomimetic damage might be connected with this property. The presence of metals or other conductors does not seem so attractive because catalytic processes may occur. Electrical arcs with their extremely high electrode temperatures would be unsuitable. A low working pressure is a limitation. The Wilzbach procedure does not have this limitation, nor do any radiation catalyzed processes. Experience in the

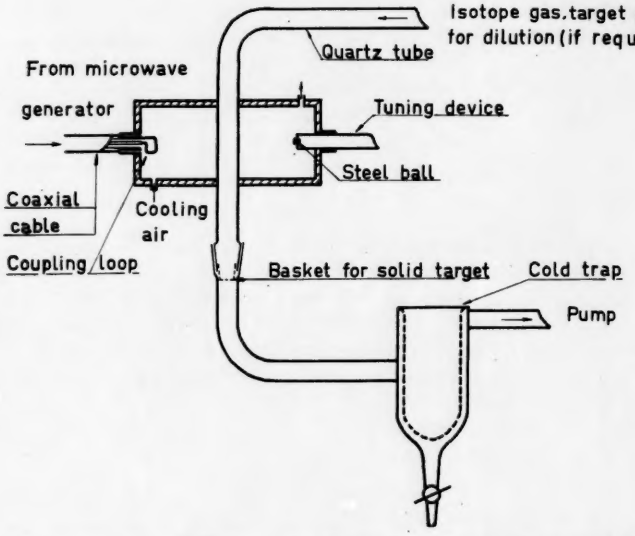

FIG. 1. Apparatus for microwave discharge treatment of gaseous or solid target substances with isotope labelling gases.

discharge field shows that, among electrode-less discharges a high frequency is to be preferred. Radio waves are one possibility and microwaves (a special case) another for instance. From published data,[5] it is evident that pressure of the order of 100 mm Hg can be achieved. The choice between microwaves and radio waves will be governed by practical factors. At present, microwaves seem preferable. If low ion temperature turns out to be an important property (see above), microwaves are superior. We have studied the use of a Tesla leak detector and a microwave generator.

Tesla work

A unit used by us (Model T 2, high frequency leak tester, Edwards High Vacuum Ltd, Crawley, England) operates at a few megacycles/second and gives a very high field strength which facilitates the passage through glass walls (in comparison with testers of lower frequencies). The active power is estimated to be about 0·1 W. The discharge cannot be made in a reproducible manner without special precautions.

The microwave approach

Two generators were tested, one at 25 W and one at 200 W (Siemens Radartherm). Both operate at 2425 Mc/sec and are generally used for muscle therapy and beauty treatment. The commercial units are provided with antennae of various kinds in which a glass bulb with appropriate gas mixture can be placed. From the microwave point of view, the use of a resonance cavity would be a better approach. The microwave energy will be used more efficiently in such a case and the field strength in the gas will be higher, thus making possible a higher working pressure. Fig. 1 shows a cavity used successfully. The diameter (D) was calculated from the resonance criterion when the TM_{010} mode is used:

$$f_0 = \frac{c \times 2{\cdot}405}{D\pi}$$

(c velocity of light).

The diameter should be 94·6 mm in this case. The coupling between the cable and the cavity can be varied by turning the loop at the left side of the figure and the resonance condition can be found by varying the position of the steel ball.

There are two ways of performing isotope labelling using this unit. A sealed bulb with the "isotope gas" and the "target gas" (or liquid or solid target) can be treated in the cavity for a certain time and the labelling result investigated. Another way is to have the gas mixture or only one of the gases streaming through a tube in the cavity (cf. Fig. 1). In this case, one might have the advantage of being able to elucidate the mechanism of the procedure. If gaseous ions are the main entities responsible for the reaction, one can easily extract them with an electric field across the tube situated downstream from the plasma zone and before the target zone. Studies with and without the ion filter should show in what respect ions play a role in the isotope labelling reaction. It

VOL. 7 1959/

should be possible also to distinguish between the parts played by positive and negative ions.

We think it justified to predict that the excitation (in the sense described above) of the isotope gas alone in a streaming system of the type considered above would minimize the destruction of the target molecules which always takes place in radiation induced reactions. The reaction taking place, viz. ion–molecule reactions[7,12] or whatever it may be, probably leads to some destruction which cannot be avoided in this type of rather violent labelling. It is possible that a high specific activity can be achieved if fresh, undiluted isotope gas is steadily fed into the reaction zone.

Some examples

H_2–D_2O *exchange* (*June* 1958). 1 ml D_2O was placed in a glass bulb and, after evacuation, H_2 was fed into the bulb (volume 10 cm^3) to a pressure of 5 mm. A treatment of the gas with the Tesla unit was performed for about 2 hr at 0°C. The proton signal from the heavy water was measured by a nuclear magnetic resonance spectrometer. The signal in relative units was significantly increased above the level before treatment so that the result was qualitatively quite evident. The conditions of the experiment were not exact enough to permit a quantitative treatment.

*Tritium labelling of PAS.** An ampoule of 1 cm^3 T_2 at 5 mm pressure containing 100 mg para-amino-salicylic acid (PAS) in powder form was treated for a little less than 5 min by the microwave generator. The PAS was purified by HANNGREN using the technique developed by him and RYDBERG[6] and the specific activity was measured. The result was 0·1 μc/mg for the purified product.[8] This should be compared with a figure of 0·1 μc/mg PAS after Wilzbach tritiation for 60 min at 300 mm pressure. It should be pointed out that this experiment was only an introductory one and was certainly not made at the optimum conditions.

Applicability

It should be pointed out that the method would have a wide applicability, i.e. it could be used for all radioactive or stable isotopes which can be put into the gaseous state at workable temperatures. (The liquid state might be accessible with special techniques.) Virtually all cases accessible with Wilzbach tritiation and the Turton technique should be within the grasp of the method. Deuteration carried out in a suitable manner might yield complete D-substitution of certain compounds e.g. C_6D_6 or reactor moderators and coolants of polycyclic type. Many other applications are evident, e.g. treatment of hydrocarbons with $S^{35}O_2$ which might yield radioactive sulphonic acids, etc. In addition, surface labelling of covalent solid matter, e.g. plastics, might be possible.

Another advantage is that the electric discharge method does not involve any large amount of radioactive matter since the energy is taken from the electrical mains and not from radioactive sources (e.g H^3, Kr^{85}). Actually, only a moderate excess might be necessary and it may be unimportant to recover unused gases. Even if H^3 is not very hazardous, large quantities of it require some precautions in handling which can now be largely avoided even when the streaming method is used. This fact has, moreover, some economic merits.

Acknowledgements—The authors are indebted to Professor O. LAMM for his kind co-operation, and to Dr. S. FORSÉN for his suggesting the nuclear resonance method for the H-analyses and for performing analyses in this way. At the Geneva exhibition (Sept. 1958), one of us (T. W.) had useful discussions with Dr. K. E. WILZBACH on the method. This work has been supported by the Swedish Cancer Society and the Swedish Atomic Committee.

Addendum

After this manuscript was completed, the paper by R. M. LEMMON *et al.* (*Science* **129,** 1740 (1959)) appeared. Their ideas seem to be rather similar, in principle, to ours. They have selected, however, the so-called silent discharges for speeding up the tritium labelling procedure. Judging from the figures, it seems that this type of discharge uses the electrical energy less efficiently. At the same time DORFMAN and WILZBACH (*J. Phys. Chem.* **63,** 799 (1959)) have published tritiation speeded up by Tesla discharge. This approach is very similar to ours. The destruction observed might be due to local heating in the arcs mentioned. The results confirm the general discussion given in our paper and it seems clear that the η_r is much more than 1 per cent guessed above.

TORBJÖRN WESTERMARK
HANS LINDROTH
Division of Physical Chemistry
BENGT ENANDER
Division of Electronics
Royal Institute of Technology
Stockholm 70, *Sweden*

References

1. WILZBACH K. E. *J. Amer. Chem. Soc.* **79,** 1013 (1957).

* In collaboration with Dr. Å. HANNGREN. Details will be reserved for a special publication.

2. TURTON C. N. *Int. J. Appl. Rad. Isotopes* **2,** 182 (1957); *Proceedings of the Second United Nations International Conference on the Peaceful Uses of Atomic Energy, Geneva* 1958. Paper P/284. United Nations, New York.
3. LIND S. C. *The Chemical Effects of Particles and Electrons*. American Chemical Society Monograph Series No. 2, New York (1928). (See especially Chapter 17.)
4. THOMAS C. L., EGLOFF G and MORELL J. C. *Chem. Rev.* **28,** 1 (1941).
5. *Encyclopaedia of Physics*, Volume 22, Gasentladungen II, especially BROWN S. C. Breakdown in gases. Alternating and high-frequency fields.
6. RYDBERG J. and HANNGREN Å. *Acta Chem. Scand.* **12,** 332 (1958).
7. STEVENSON D. P. and SCHISSLER D. O. *J. Chem. Phys.* **23,** 1353 (1955); Ibid. **24,** 926 (1956) and other works by these authors.
8. HANNGREN Å. *Acta Radiol. Stockh.*, Supplementum 175 (1959). (Dissertation, see especially the note on p. 19 on electrical discharge labelling.)
9. WESTERMARK T., LINDROTH H. and ENANDER BENGT. Swedish Patent Application No. 1936/59, Feb. 28, 1959.
10. WHITEHOUSE W. J. and PUTMAN J. L. *Radioactive Isotopes*. Clarendon Press, Oxford (1953).
11. RIESZ P. and WILZBACH K. E. *J. Phys. Chem.* **62,** 6 (1958).
12. GORDUS A., SAUER M. and WILLARD J. E. *J. Amer. Chem. Soc.* **79,** 3284.

VOL
7
1959/

book reviews

DANIEL BLANC: **Détecteurs de Particules. Compteurs et Scintillateurs. Mécanisme et Realisation.** Masson, Paris, 1959. 324 pp. 3.900 fr.

DANS un livre de trois cent pages, Monsieur BLANC expose l'essentiel de nos connaissances sur les compteurs de la physique nucléaire. Son plan passe en revue tous les types de détecteurs: chambres d'ionisation et compteurs proportionnels en trois chapitres, compteurs Geiger–Müller en quatre chapitres fort détaillés: citons l'étude des compteurs "Maze" à coque de verre, et des compteurs à vapeur polyatomique pure. Deus chapitres sont ensuite consacrés à des appareils spéciaux: compteurs à étincelles et détecteurs par conduction électrique; ce dernier constitue une bonne monographie d'un sujet bien délimité.

Viennent ensuite les détecteurs "optiques": un court chapitre sur les photomultiplicateurs, un autre sur les compteurs Čerenkov et deux sur les scintillateurs. Le livre se termine par deux chapitres technologiques: l'un sur la réalisation des compteurs—et essentiellement des compteurs Geiger–Müller, le second sur le coefficient de température des détecteurs. Les compteurs de neutrons et de photons ne sont pas oubliés: ils viennent en additif à chacun des types d'appareils. Une trentaine de tables de valeurs numériques, et quinze cent références bibliographiques complètent ce livre.

Cet ouvrage est la rédaction d'un cours du troisième cycle de l'enseignement supérieur français. Il s'adresse à des physiciens avertis, et suppose connus, les éléments de la physique nucléaire. C'est avant tout un ensemble de leçons sur l'instrumentation, et l'on regrette qu'il y soit peu question des méthodes de mesure. On connait en effet, la richesse de ces méthodes (spectrométrie, coïncidences, rétrodiffusion, angle solide défini . . .) et l'ingéniosité qu'elle permet aux expérimentateurs. Monsieur BLANC a d'ailleurs donné de temps à autre, des exemples de ces méthodes, en particulier à propos des compteurs Čerenkov mais sans leur donner le développement qu'elles méritent.

La place prédominante a été donnée aux compteurs Geiger–Müller, dont l'auteur est spécialiste. L'exposé en est clair et très détaillé. En revanche, l'auteur a limité volontairement l'étude des scintillateurs, ce qui donne une idée inexacte du développement actuel de la technologie.

Certains chapitres annexes sont des mises au point bibliographiques: l'appareillage y est analysé à la lumière d'une bibliographie importante, et l'exposé manque un peu de synthèse.

La présentation de l'ensemble est bonne, et les tables numériques nombreuses. Seules quelques négligences dans les légendes de figures, et quelques anglicismes (maximum permissible, collectage) nuisent un peu à l'ensemble.

Au total c'est un livre intéressant et dense.

J. CHÂTELET

L. V. GROSHEV, V. N. LUTSENKO, A. M. DEMIDOV and V. I. PELEKHOV: **Atlas of Gamma-ray Spectra from Radiative Capture of Thermal Neutrons** (Translated from the Russian by J. B. SYKES). Pergamon Press, London, 1959. 198 pp. £7.

THE *Atlas* is a compilation of γ-ray spectra arising from radioactive neutron capture (the n, γ reaction), and nuclear energy levels and spins. The authors are one of the two leading groups of physicists working in this field. The other group has also independently published a very similar compilation (G. A. BARTHOLOMEW and L. A. HIGGS: Compilation of Thermal Neutron Capture Gamma Rays. CRGP-784. Atomic Energy of Canada Ltd, 1958) which contains a little less detailed information than the *Atlas* and does not include the nineteen sets of previously unpublished results by GROSHEV *et al.*

The first part of the book consists of a table of stable isotopes and lists their percentage abundance, thermal neutron radioactive capture cross-section (erroneously labelled "thermal neutron capture cross-section" in the table heading and only explained correctly in small print), half-life of the product nucleus and angular momentum and parity data for the target and product nuclei. The binding energy of the neutron in the product nucleus is also given.

The principal part of the book gives details of γ-spectra arising from neutron capture in sixty-seven elements. The results are clearly presented, usually as a table and two graphs. One of these shows the plotted spectrum from the magnetic Compton spectrometer used by the authors and the other illustrates the spectrum corrected for the variation of spectrometer efficiency with energy and for the absorption of radiation in the specimen. This seems

to be unnecessary duplication and the inclusion of the experimental plot could well have been limited to previously unpublished results. It is not explained that the γ-ray energies shown in the spectra are obtained by extrapolating the high energy edge of the peak to the axis and are not represented by the peak maximum. A diagram shows nuclear energy levels and spins in the product nucleus.

Two short appendices include the spectra of internal conversion electrons emitted in thermal neutron capture (for Cd, Sm and Gd only) and the γ-rays from radioactive decay from some short-lived product nuclei. Both appendices consider very few elements and are of limited interest.

The *Atlas* is well printed with a few exceptions (the P^{32} and Ca graphs, and the small superscripts in the first table) and should prove a useful reference book for physicists, reactor engineers, and all those interested in neutron reactions.

D. B. SMITH

Radiocarbon Supplement: American Journal of Science. Edited by R. A. FLINT and E. S. DEEVEY, Jr., Yale University. Vol. 1, May 1959. 218 pp. $2.50 (To be published annually: Subscription $4.50).

COINCIDING as it does with the establishment of the International Agency for ^{14}C Determination at Charlottenlund, Denmark, and of the Radiocarbon Dates Association Inc. at Andover, Mass., U.S.A., the publication of this supplement by the *American Journal of Science* represents another valuable step in integrating research in the field of carbon dating.

The *Supplement* is a forum for the publication of natural radiocarbon measurements from all parts of the world and this first issue contains contributions from thirteen laboratories distributed over Europe and North America, covering measurements of samples collected from representative areas all over the world. The fact that many of these reports are numbered parts of a series indicates that leading laboratories which have published elsewhere have adopted the *Supplement* as their reporting medium.

Although papers on measuring and processing techniques are not specifically ruled out, it is evident that the emphasis will be on the reporting of results and the first issue certainly devotes most of its space to such reports. These are couched in the pithy, informative style which has now become normal for radiocarbon results. Each entry gives laboratory of measurement, exact location of sample, its substance, name of collector and identifier of the specimen. The estimated age is quoted with the accumulated standard error of measurement and comments are usually added which compare results with other relevant dates, draw attention to any special treatment of samples and sometimes outline the archaeological significance of results. Entries average about 10 lines and include references to other published data.

At the end of this issue, a 15-page classified bibliography of radiocarbon dating gives references to lists of dates, methods of processing and measurement and interpretation of results. It is followed by a list of laboratories (with addresses) known to have been engaged in radiocarbon measurements.

The *Supplement* is written by specialists for specialists and as such is undoubtedly excellent. It could commend itself more to the interested, general reader, however, by a more informative method of titling the separate papers. Nearly all the papers in this issue have the same title, preceded or followed by the name of a different laboratory. The title of the second paper alone makes it clear that interest is centred on the dating of peats. A later paper entitled "Lamont Radiocarbon Measurements VI" is entirely devoted to the assay of modern carbon samples of precisely known age and shows the significance of modern disturbances in the isotopic constitution of atmospheric CO_2. In the list of contents, however, it is almost indistinguishable from the first paper, which has a similar title, but is concerned with archaeological and geological dating. It is to be hoped also that in future issues, separate papers describing new developments in radiocarbon dating techniques may be included.

The publication of the *Supplement* will be most welcome to all those engaged in radiocarbon dating and related fields.

J. L. PUTMAN

VOL. 7 1959/

OL.
7
59/60